

**FEDERAL UNIVERSITY OF SÃO CARLOS
EXACT SCIENCE AND TECHNOLOGY CENTER
CHEMISTRY DEPARTMENT
GRADUATE PROGRAM IN CHEMISTRY**

**FLOW CHEMISTRY APPLIED TO HAZARDOUS
REACTIONS, AND FLUOROPHORES SYNTHESIS WITH
PHOTOPHYSICS STUDIES**

Juliana Maria de Souza

Thesis presented as part of the requirements to obtain the title of DOCTOR IN SCIENCE, concentration area: ORGANIC CHEMISTRY.

Advisor: Prof. Dr. Kleber Thiago de Oliveira

Scholarship: CNPq (Brazil) and M4ALL/VCU (USA)

**São Carlos – SP
2020**

I dedicate this work to my family for always being by my side at all times. Also, to every single person who motivates me to become a better person and chemist.

“Once you stop learning, you start dying.”

Albert Einstein

Acknowledgments

I thank God, essential in my life, for the people He has placed in my path. Some of them inspire me, help me, challenge me, and encourage me to better myself each day. My journey of victories and defeats has made me see the true meaning and beauty of life. My personal and professional growth would not be possible without God's presence in every step I take.

To my family, especially my parents, Marly and Reginaldo, who made every effort to help me complete this stage of my life. They are present at all times, whether they be times of happiness or of sadness. Thanks also to my dear sisters, Renata and Tatiana, who are essential for my wellbeing.

To my fiancé, Matthew Robey, for all the love and support and for making me believe in my potential every day. For always encouraging me in the moments when I thought I had no more strength to keep doing my best.

To Professor Kleber T. de Oliveira for the guidance since 2011. Words are not enough to express how grateful I am for the opportunity to be part of the Bioorganic Chemistry Laboratory (LQBO). For the trust in allowing me to study abroad for one year and a half; it was a dream that came true. For the friendship and for not letting me get discouraged in the face of difficulties over the past years. He is undoubtedly the person I admire the most.

To Professor Timothy J. Brocksom for the excellent advice given during the development of this work.

To all my friends from the LQBO for their friendship, suggestions during the group meetings and all the moments of laughter and fun. A special thanks to Aloisio Bartolomeu and Vinicius Wellington. They showed me that real friends can be by your side even across the world.

To all DQ/UFSCar faculty and staff for all their services and help.

Acknowledgments

To CNPq for the scholarship granted for the development of part of this project and to FAPESP for their financial support.

To the Coordenação de Aperfeiçoamento de Pessoal de Nível Superior – Brasil (CAPES) Finance Code 001 – that partially financed this work.

To UFSCar for providing the infrastructure and the opportunity to undertake and develop this work.

To Professor D. Tyler McQuade for the opportunity to be at M4ALL Institute. It was undoubtedly one of the biggest challenges I have ever faced. I will always be very grateful for the confidence and everything I have learned from him and the 3TC team.

To Dr. David Snead for all conversations and assistance throughout M4ALL. He showed a constant concern in making me become a better professional every day.

To Claire Fuller and Otto Euller for their kindness during my first months in the USA.

To Amy Miner, our incredible M4ALL laboratory manager, who is always willing to help the entire team with anything.

To Virginia Commonwealth University (VCU) and Medicines for All Institute, for their financial support and for treating me so well the past year and a half. Also, to Bill & Melinda Gates Foundation for believing and investing in M4All's causes.

Finally, I thank all who contributed directly and indirectly in my formation and in the accomplishment of this work.

LIST OF ABBREVIATIONS

- 3TC – Lamivudine
ACQ – Aggregation-caused quenching
AIDS – Acquired Immunodeficiency Syndrome
AIE – Aggregation-induced Emission
API – Active Pharmaceutical Ingredient
AY – Assay Yield
BCH-189 – Racemic 2'-deoxy-3'-thiacytidine
BPR – Back-pressure Regulator
CFL – Compact Fluorescent Lamp
DBU – 1,8-Diazabicyclo(5.4.0)undec-7-ene
DCM – Dichloromethane
DKR – Crystallization-induced Dynamic Kinetic Resolution
DMA – Dimethylacetamide
DMF – Dimethylformamide
DNA – Deoxyribonucleic Acid
EDG – Electron donating group
EWG – Electron withdrawing group
FDA – Food and Drug Administration
FTC – Emtricitabine
HBV – Hepatitis B Virus
HIV – Human Immunodeficiency Virus
HOMO – Highest Occupied Molecular Orbital
I.D. – Inner Diameter
ISC – Intersystem crossing
IY – Isolated Yield
KDM – Kornblum-DeLaMare
LC-MS – Liquid Chromatography-Mass spectrometry
LED – Light-emitting diode
LUMO – Lowest Unoccupied Molecular Orbital
M4ALL – Medicines for All Institute
MB – Mass Balance

List of abbreviations

MW – Microwave
NCS – N-Chlorosuccinimide
NMR – Nuclear Magnetic Resonance
NPW – Novel Process Windows
O.D. – Outer Diameter
OY – Overall Yield
PC – Photocatalyst
PDT – Photodynamic Therapy
PFA – Perfluoroalkoxy
PI – Processes Intensification
PPE – Personal Protective Equipment
PTFE – Polytetrafluoroethylene
PTSA – *p*-Toluenesulfonic acid
 R_f – Retention Factor
RIR – Restriction of intramolecular rotation
ROS – Reactive Oxygen Species
rt – room temperature
SET – Single Electron Transfer
SI – Supporting Information
SM – Starting material
SOMO – Singly Occupied Molecular Orbital
TEA – Triethylamine
TLC – Thin-Layer Chromatography
TMSI – Trimethylsilyl iodide
TPP – *meso*-Tetraphenylporphyrin
UCLA – University of California, Los Angeles
USA – United States of America
UV – Ultra-violet
VCU – Virginia Commonwealth University
YM – Ylidenemalononitriles

LIST OF TABLES

PART 1

Table 1. Checking of TPP loading at 1.0 mL.min ⁻¹ (Pump A).....	38
Table 2. Checking of TPP loading at 0.5 mL.min ⁻¹ (Pump A).....	39
Table 3. Checking of TPP loading at 0.25 mL.min ⁻¹ (Pump A).....	40
Table 4. Influence of different diene 53 concentrations.....	41
Table 5. Scope for the developed protocol.....	45
Table 6. Variation of the vinyl acetate addition time – 4 g scale reaction.....	61
Table 7. Initial results for sulfenyl chloride 114 formation in continuous conditions.....	64
Table 8. End-to-end approach of continuous synthesis of compound 115 from thiol 113	67
Table 9. Comparison between DCM in toluene in steady state conditions.....	75
Table 10. Variation of SO ₂ Cl ₂ number of equivalents – reaction in toluene.....	78
Table 11. Optimization of reaction in toluene and steady state conditions.....	79
Table 12. Scale-up experiments in steady state conditions.....	80

PART 2

Table 1. Photophysical properties of 8d-e , 10d , 8g and 8o-p in DCM in ambient conditions.....	238
Table 2. Photophysical properties of 18g , 18h , 18j , and 18m in DCM in ambient conditions.....	247

LIST OF FIGURES

PART 1

Figure 1. Comparison of batch and continuous flow processes.....	03
Figure 2. General representation of a continuous flow setup.....	04
Figure 3. Surface to volume ratio - difference between continuous conditions and batch reactors.....	05
Figure 4. Simplified representation of a steady state condition during a continuous process.....	07
Figure 5. Electromagnetic spectrum of light and associated energies.....	09
Figure 6. Photocatalysis cycles representation – oxidative, reductive and energy transfer.....	11
Figure 7. Simplified orbitals diagram of the oxygen molecule.....	16
Figure 8. Production of ¹ O ₂ by the action of a photocatalyst.....	19
Figure 9. Lamivudine (29) and Cytidine chemical structures.....	22
Figure 10. Silica gel bottle used as the reactor body.....	29
Figure 11. Main materials used in the photoreactor construction.....	30
Figure 12. Step-by-step batch photoreactor assembly.....	31
Figure 13. Setup for photochemical batch reactions.....	31
Figure 14. Construction of photochemical reactor for continuous flow reactions.....	32
Figure 15. Final assembly of the photochemical reactor and PFA tubular reactor.....	33
Figure 16. Simplified representation of a tube-in-tube reactor.....	34
Figure 17. Tube-in-tube reactor built in our group.....	35
Figure 18. Final setup for photooxygenations and KDM rearrangement in continuous flow conditions.....	43
Figure 19. Oxygenation of the solution containing the TPP + diene – batch experiments.....	44
Figure 20. EasyMax HFCal runs – Reaction performed under N ₂ atmosphere. a) Addition of 2.2 equiv. SO ₂ Cl ₂ addition over 30 min b) 2.0 equiv. vinyl acetate over 30 min.....	57
Figure 21. Comparative chart of the heat released in common exothermic reactions.....	58

Figure 22. Initial system to study sulfenyl chloride 114 synthesis in continuous conditions.....	63
Figure 23. Change in color when sulfenyl chloride 114 is formed.....	64
Figure 24. End-to-end approach to perform compound 115 synthesis under continuous conditions – initial experiments.....	66
Figure 25. ¹ H NMR analysis of the crude mixture of reaction of thiol 113 with SO ₂ Cl ₂	69
Figure 26. Continuous flow setup for the steady state experiments – Vapourtec E-Series to pump solutions A and B and Chemyx syringe pump for vinyl acetate.....	74
Figure 27. Variation of dichloro acetate 115 yield over time.....	77
Figure 28. Final continuous flow setup used to scale-up the reaction.....	81
Figure 29. EasyMax 102 from Mettler Toledo used to carry out batch experiments.....	182
Figure 30. Dichloro-acetate 115 crystallization in DCM/hexanes.....	184
Figure 31. X-ray crystallography of the compound 115a	185
Figure 32. ¹ H NMR of byproduct 119 in the crude reaction mixture: a) vinyl acetate; b) vinyl acetate after reaction with SO ₂ Cl ₂ ; c) Crude reaction mixture in DCM.....	186
Figure 33. Use of 1,2,3-trichloropropane as NMR internal standard for the steady state studies. a) Crude mixture + 1,2,3-trichloropropane/ steady state (¹ H NMR right after fraction was collected); b) Same sample with no extraction with NaHCO ₃ (¹ H NMR overnight).....	187

PART 2

Figure 1. General concepts regarding molecular organic photochemistry.....	218
Figure 2. Absorption and emission of light by fluorophores.....	219
Figure 3. Jablonski Diagram – difference between fluorescence and phosphorescence.....	219
Figure 4. Matlaline, the fluorescent substance in the wood of the tree <i>Eysenhardtia polystachya</i>	220
Figure 5. Compound 5 X-ray crystallography.....	229

Figure 6. Compound 6 X-ray crystallography – obtained from reaction of 1 with NCS.....	230
Figure 7. Compound 3a X-ray crystallography.....	231
Figure 8. Change of emission color from cyan/green to yellow by R ₁ and R ₂ variation and comparison with previous work.....	236
Figure 9. Compound 8c X-ray crystallography.....	237
Figure 10. YM 13 planarity representation.....	241
Figure 11. ¹ H NMR of amidine 8g and pyridine 18g obtained after aromatization.....	243
Figure 12. Pyridine 18g X-ray crystallography.....	243
Figure 13. Crystalline samples of 18i under A) ambient light and B) 365 nm excitation.....	248
Figure 14. Pyridine 18i X-ray crystallography – hydrogen bond interaction between amino group (NH) and nitrile (CN).....	249
Figure 15. Pyridine 18i fluorescence in different solvents – A and B) EtOH, EtOAc, MeCN, DCM, toluene (left to right); C) Mesitylene, toluene, pentane and hexanes; D) Same as in C, after addition of EtOAc.....	250
Figure 16. Emission spectra of 18i in a solution of toluene (from 100% to 70%) and DCM (from 0% to 30%).....	251
Figure 17. YM containing PEG (R ₂ position) increased solubility in water; A) 3f in THF /BnNH ₂ (1:1); B) 3f in H ₂ O/BnNH ₂ (1:1); C) 3f in THF/H ₂ O/BnNH ₂ (1:1:1).....	283
Figure 18. Normalized absorption spectra of 8d , 8e and 10d in DCM.....	284
Figure 19. Normalized emission spectra of 8d , 8e and 10d in DCM ($\lambda_{\text{ex}} = 405$ nm).....	285
Figure 20. Emission decays for 8d , 8e and 10d in DCM ($\lambda_{\text{ex}} = 405$ nm, $\lambda_{\text{em}} =$ emission maximum).....	285
Figure 21. Normalized absorption and emission spectra of 8d in DCM ($\lambda_{\text{ex}} = 405$ nm).....	286
Figure 22. Normalized absorption and emission spectra of 8e in DCM ($\lambda_{\text{ex}} = 405$ nm).....	286
Figure 23. Normalized absorption and emission spectra of 10d in DCM ($\lambda_{\text{ex}} = 405$ nm).....	287
Figure 24. Normalized absorption spectra of 8g , 8o and 8p in DCM.....	287

Figure 25. Normalized emission spectra of 8g , 8o and 8p in DCM ($\lambda_{\text{ex}} = 405$ nm).....	288
Figure 26. Emission decays for 8g , 8o and 8p in DCM ($\lambda_{\text{ex}} = 405$ nm, $\lambda_{\text{em}} =$ emission maximum).....	288
Figure 27. Normalized absorption and emission spectra of 8g in DCM ($\lambda_{\text{ex}} = 405$ nm).....	289
Figure 28. Normalized absorption and emission spectra of 8o in DCM ($\lambda_{\text{ex}} = 405$ nm).....	289
Figure 29. Normalized absorption and emission spectra of 8p in DCM ($\lambda_{\text{ex}} = 405$ nm).....	290
Figure 30. Normalized absorption spectra of 18g , 18h , 18j , and 18m in DCM.....	290
Figure 31. Normalized emission spectra of 18g , 18h , 18j , and 18m in DCM ($\lambda_{\text{ex}} = 405$ nm).....	291
Figure 32. Emission decays for 18g , 18h , 18j , and 18m in DCM ($\lambda_{\text{ex}} = 405$ nm, $\lambda_{\text{em}} =$ emission maximum).....	291
Figure 33. Normalized absorption and emission spectra of 18g in DCM ($\lambda_{\text{ex}} = 405$ nm).....	292
Figure 34. Normalized absorption and emission spectra of 18h in DCM ($\lambda_{\text{ex}} = 405$ nm).....	292
Figure 35. Normalized absorption and emission spectra of 18j in DCM ($\lambda_{\text{ex}} = 405$ nm).....	293
Figure 36. Normalized absorption and emission spectra of 18m in DCM ($\lambda_{\text{ex}} = 405$ nm).....	293
Figure 37. Relationship between emission peak intensity and the percentage of toluene.....	294
Figure 38. Emission decays for 18i in a solution of toluene (from 100% to 70%) and DCM (from 0% to 30%). ($\lambda_{\text{ex}} = 405$ nm, $\lambda_{\text{em}} =$ emission maximum).....	294
Figure 39. Compound 3a X-ray cristallography.....	295
Figure 40. Compound 3c X-ray crystallography.....	296
Figure 41. Compound 3d X-ray crystallography.....	297
Figure 42. Compound 3e X-ray crystallography.....	298
Figure 43. Compound 3g X-ray crystallography.....	299

Figure 44. Compound 3h X-ray crystallography.....	300
Figure 45. Compound 3r X-ray crystallography.....	301
Figure 46. Compound 5 X-ray crystallography.....	302
Figure 47. Compound 6 X-ray crystallography.....	303
Figure 48. Compound 8c X-ray crystallography.....	304
Figure 49. Pyridine 6b X-ray crystallography – R ₂ = Cl.....	305
Figure 50. Pyridine 11a X-ray crystallography – R ₂ = Ph.....	306
Figure 51. Pyridine 18d X-ray crystallography – R ₂ = S-Alkyl.....	307
Figure 52. Pyridine 18g X-ray crystallography – R ₂ = S-Aryl.....	308
Figure 53. Pyridine 19f X-ray crystallography – R ₂ = H.....	309

LIST OF SCHEMES

PART 1

Scheme 1. Synthesis of a Rosuvastatin intermediate (2) under continuous flow and batch conditions.....	12
Scheme 2. Synthesis of Irinotecan [®] intermediate (6) under continuous flow.....	13
Scheme 3. Artemisinin synthesis (9).....	14
Scheme 4. Stephenson syntheses involving photo-redox and Flow Chemistry processes.....	14
Scheme 5. First uses of singlet oxygen in organic synthesis.....	16
Scheme 6. Some methods to produce ¹ O ₂ through chemical reactions.....	18
Scheme 7. Kornblum-DeLaMare rearrangement – peroxides and endoperoxides.....	20
Scheme 8. A) Method of choice for the industrial production, B) Previous literature for 3TC and FTC synthesis.....	25
Scheme 9. Stabilization of 45 by anchimeric assistance.....	26
Scheme 10. Crystallization-induced dynamic kinetic resolution (DKR).....	27
Scheme 11. Diene 53 photooxygenation and Kornblum-DeLaMare rearrangement – Flow/Batch setup to initial studies.....	37
Scheme 12. Continuous KDM rearrangement optimizations. A) by using a 250µL microchip; B) by using a 16 mL stainless steel coil reactor.....	42
Scheme 13. End-to-end setup for photooxygenation followed by KDM rearrangement.....	43
Scheme 14. Continuous end-to-end assembly to furans synthesis and probable mechanism of furan formation.....	51
Scheme 15. Further rearrangements of KDM products at different temperatures.....	52
Scheme 16. M4ALL developed new route to lower cost 3TC/FTC production.....	54
Scheme 17. Comparison between M4ALL and Whitehead routes to 3TC.....	55
Scheme 18. Late-stage functionalization approach – minimizing L-menthol (33) loss.....	56
Scheme 19. Possible pathways involving vinyl acetate - A: Reaction with sulfenyl chloride 114 to form 114a ; B: Reaction with SO ₂ Cl ₂ leading to byproduct 119	59

Scheme 20. Vinyl acetate addition prior to SO ₂ Cl ₂ and byproduct 120 formation.....	60
Scheme 21. Initial setup for sulfenyl chloride 114 synthesis.....	62
Scheme 22. New setup including vinyl acetate addition step.....	65
Scheme 23. Initial setup and reaction conditions for steady state studies.....	68
Scheme 24. Proposed intermediate 121 as a possible precursor of sulfenyl chloride 114	70
Scheme 25. First stage reaction of thiol 113 with SO ₂ Cl ₂ working as a thiol “protecting group”.....	70
Scheme 26. Simultaneous mixing of solutions A, B and neat vinyl acetate.....	71
Scheme 27. Modified setup – insertion of a separated mixing point for solutions A and B.....	72
Scheme 28. Simplified setup for initial steady state studies.....	73
Scheme 29. Possible side reactions of toluene with sulfuryl chloride.....	76
Scheme 30. Improved flow setup for dichloro acetate 115 synthesis.....	77
Scheme 31. Final flow setup for the reaction scaling-up - 1/8" O.D. PFA tube.....	79

PART 2

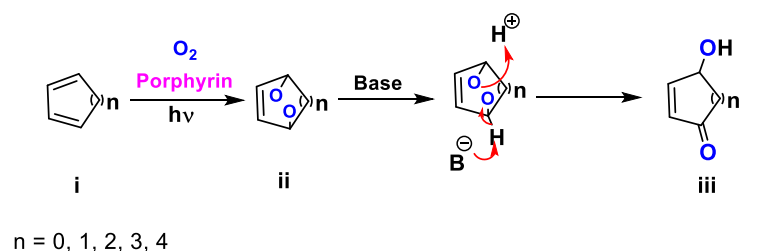
Scheme 1. Previous reports overview.....	222
Scheme 2. Overview of different substitutions of YM and their position once cyclized.....	223
Scheme 3. Main methodologies described in the literature to produce 3-cyano-2-aminopyridines.....	225
Scheme 4. Substituted pyridines.....	225
Scheme 5. Recent literature of addition of NCS and Aryl-S-Cl to enamines.....	228
Scheme 6. Exploratory experiments - Better understanding of new substrates behavior under conditions previously established by our group.....	229
Scheme 7. General reaction and scope of sulfur-ylidenemalononitriles substrates.....	232
Scheme 8. “Turn-on” reaction of ylidenemalononitrile enamines (II) with primary amines to yield fluorescent molecules.....	234

Scheme 9. Green and yellow fluorescent molecules obtained from reaction of benzylamine with ylidenemalononitriles (varying R ₁ and R ₂).....	235
Scheme 10. YMs reaction with benzylamine – understanding how R ₁ and R ₂ affect the cyclization rates.....	240
Scheme 11. Facile synthesis of highly substituted pyridines from YMs.....	242
Scheme 12. Obtention of pyridine 18g from sulfur-substituted YMs 3g	243
Scheme 13. Proposed mechanism to amino-pyridines formation - Dimroth rearrangement mechanism.....	244
Scheme 14. Amino-pyridines obtained from YMs with varying R ₁ and R ₂ groups.....	245
Scheme 15. Aggregation of different types of molecules ant its relation to fluorescence.....	248

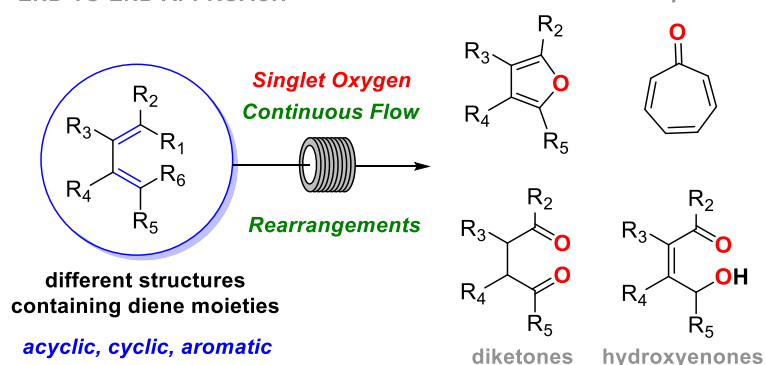
Abstract

FLOW CHEMISTRY APPLIED TO HAZARDOUS REACTIONS, AND FLUOROPHORES SYNTHESIS WITH PHOTOPHYSICS STUDIES

In Part 1 two distinct cases of continuous flow conditions applied to hazardous reactions are described. The first example consists of the continuous photooxygenation of a series of dienes (**i**) that yields endoperoxides (**ii**), and/or which are potentially explosive intermediates. All reactors used for photooxygenation were built by our group and the details for their construction are discussed. End-to-end approaches involving endoperoxidation, Kornblum-DeLaMare rearrangement (KDM) and additional hydroxyenone (**iii**) rearrangements are comprehensively described with scope. Thus, significant organic building blocks, such as hydroxyenones, furans and diketones are obtained (Scheme i).

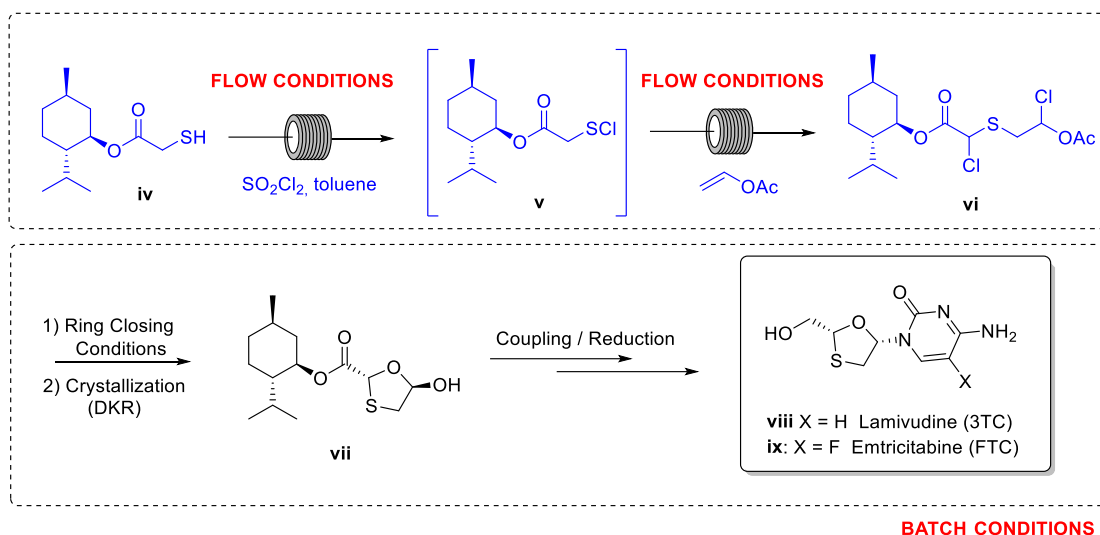


END-TO-END APPROACH



Scheme i. Overview of the developed photooxygenation in continuous flow conditions and further rearrangements.

In the second example the development of a flow setup to perform two hazardous steps in the synthesis of Lamivudine (3TC – HIV drug) is described (Scheme ii, from **iv** to compound **vi**). The route described is under development by the Medicines for All Institute (M4ALL), an American startup within Virginia Commonwealth University (VCU).



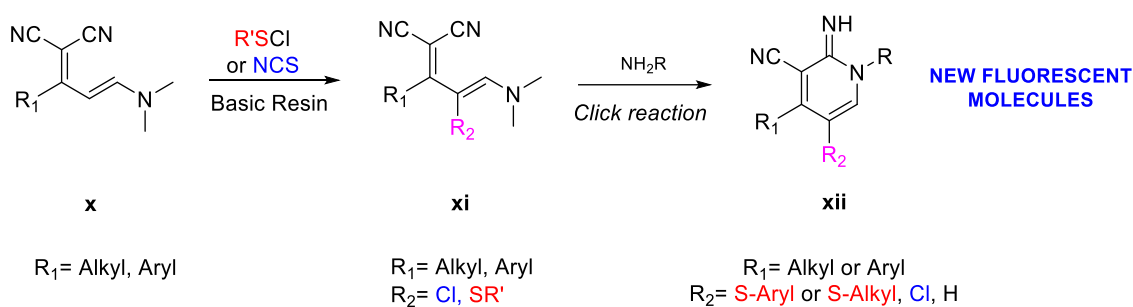
Scheme ii. M4ALL's route to Lamivudine (3TC) synthesis.

The above step consists of the reaction between thiol **iv** and sulfuryl chloride (SO_2Cl_2 , toxic and an extremely reactive reagent), which yields sulfenyl chloride **v**, a highly electrophilic species (Scheme ii). It is followed by the addition of vinyl acetate, generating an intermediate that is readily consumed by the remaining SO_2Cl_2 , then forming dichloro acetate **vi**. The reactions involving SO_2Cl_2 and vinyl acetate are exothermic and the chlorination generates toxic gases HCl and SO_2 . Preliminary experiments showed rapid reagent addition has a role decreasing byproduct formation. Seeking high-scale production, a safer and more efficient process would be necessary, justifying the use of continuous conditions.

In Part 2 we developed the synthesis of sulfur-ylidenemalononitriles **xi** (Scheme iii). Ylidenemalononitriles (YMs) are versatile intermediates in the synthesis of multi-substituted heterocycles (pyridines and pyrones) and fluorescent amidine-based probes. The literature lacks an efficient methodology to perform YM's R_2 -position

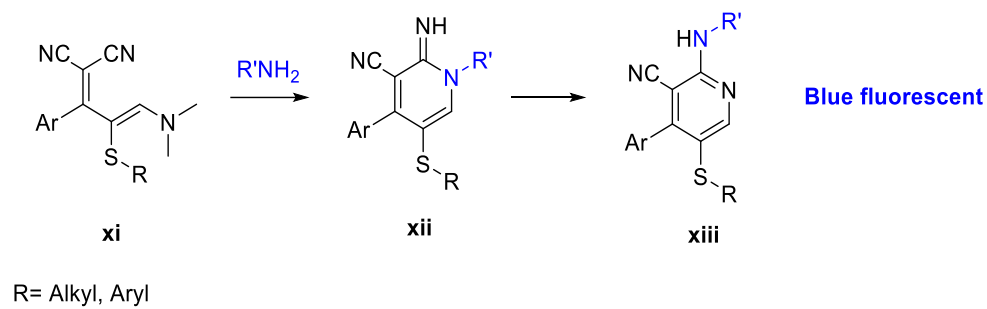
functionalization. All previous attempts experimented by our group failed. Several electrophilic species were utilized without any success.

Having the reaction between vinyl acetate and sulfenyl chloride (3TC route) as inspiration, we decided to use sulfenyl chloride as the electrophilic species towards reaction with YM. As result, an efficient methodology leading to the desired sulfur-YMs **xi** in high yields was achieved. We also demonstrated that the resulting R₂-substituted YMs cyclize forming amidines **xii** (Scheme iii). The obtained cyclic amidines **xii** are fluorescent. Their color can be tuned from different shades of green to yellow through the variation of R₁ and R₂ groups, yielding different λ_{\max} , as shown in the photophysic studies of some of the synthesized molecules.



Scheme iii. YMs functionalization at R₂-position followed by cyclization to fluorescent amidines.

While performing a substrate scope study, all of the YMs produced the expected amidine, but some of them were unstable and produced a single product of reduced polarity. It revealed a blue fluorescent color that turned out to be aminopyridine. Herein, we present these results in details, demonstrate a new method for producing multi-substituted pyridines. We also provide an example where one of the products exhibits aggregation-induced emission (AIE), a trait that can have optoelectronic and biological applications (Scheme iv).

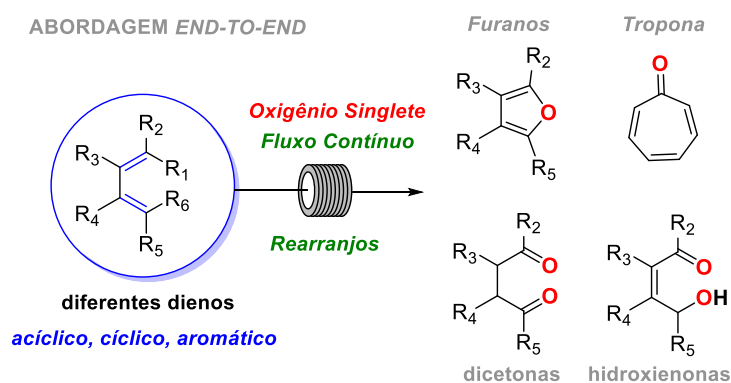
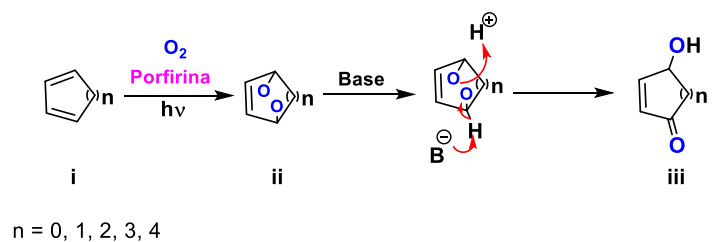


Scheme iv. Amino-pyridines (**xiii**) synthesis from amidines **xii**.

Resumo

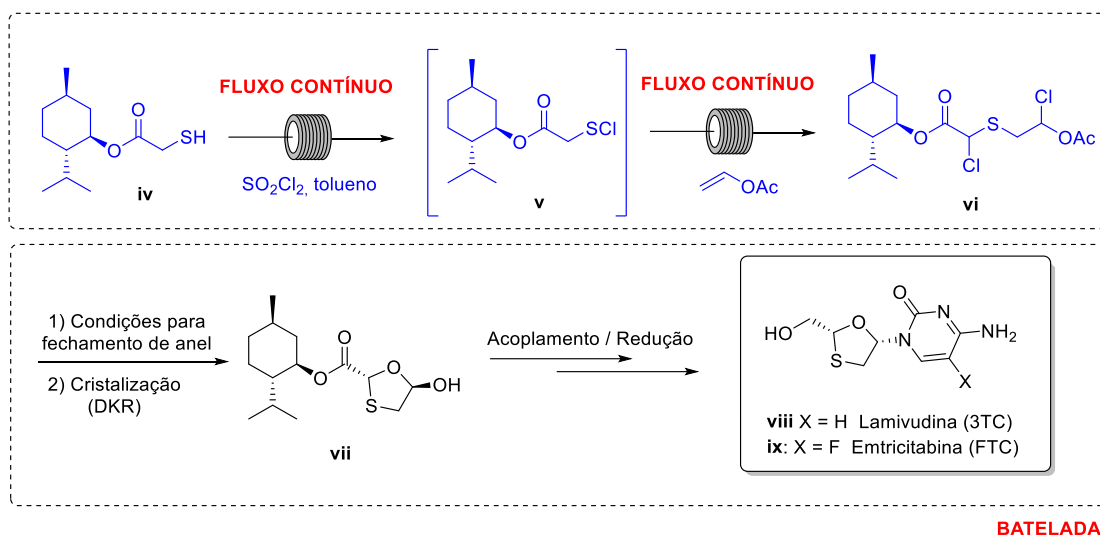
FLUXO CONTÍNUO APLICADO A REAÇÕES PERIGOSAS, E SÍNTESE DE FLUORÓFOROS COM ESTUDOS FOTOFÍSICOS

A Parte 1 apresenta dois casos distintos de aplicação de fluxo contínuo na realização de reações perigosas. O primeiro exemplo consiste na foto-oxigenação contínua de uma série de dienos (**i**), que resulta em endoperóxidos (**ii**), intermediários potencialmente explosivos. Outros rearranjos, envolvendo as hidroxienonas **iii**, também são discutidos. Todos reatores utilizados para foto-oxigenação foram construídos por nosso grupo e os detalhes para sua construção também são discutidos. As abordagens *end-to-end* envolvendo endoperoxidação, rearranjo Kornblum-DeLaMare (KDM) e rearranjos adicionais são descritas de maneira abrangente com prova de escopo. Dessa forma, importantes blocos construtores, tais como hidroxienonas, furanos e dicetonas são obtidos (Esquema i).



Esquema i. Visão geral das foto-oxigenações e subsequente rearranjos em condições contínuas.

O segundo exemplo mostra o uso de fluxo contínuo para executar duas etapas de risco na síntese de Lamivudina (3TC), um importante medicamento para o tratamento de HIV/AIDS (Esquema ii, **iv** ao composto **vi**). A rota descrita está sendo desenvolvida pelo *Medicines for All Institute (M4ALL)*, iniciado na *Virginia Commonwealth University (VCU)*.



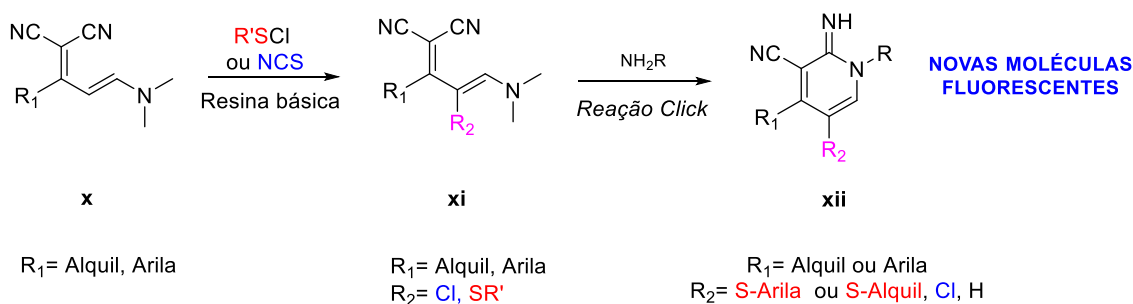
Esquema ii. Rota desenvolvida pelo M4ALL para a síntese de Lamivudina (3TC).

A etapa estudada consiste na reação do tiol **iv** com cloreto de sulfurila (SO_2Cl_2 , tóxico e extremamente reativo), resultando no cloreto de sulfenilo **v**, espécies altamente eletrofílicas (Esquema ii). Esta etapa é seguida pela adição de acetato de vinila, a qual gera um intermediário que é rapidamente consumido pelo restante de SO_2Cl_2 , levando ao composto **vi**. As reações com SO_2Cl_2 e acetato de vinila são exotérmicas e a cloração gera gases tóxicos, HCl e SO_2 . Nós observamos que a rápida mistura de reagentes tem um importante papel na diminuição de subprodutos. Para a produção em larga escala, é necessário o desenvolvimento de um processo mais seguro e eficiente, justificando o uso de condições contínuas.

A Parte 2 exhibe a síntese de enxofre-ilidenomalononitrilos **xi** (Esquema iii). Ilidenomalononitrilos (IMs) são intermediários versáteis na síntese de heterocíclicos multisubstituídos (piridinas e pironas) e sondas fluorescentes à base de amidina. Falta à literatura uma metodologia eficiente para executar funcionalização de IMs na posição R_2 .

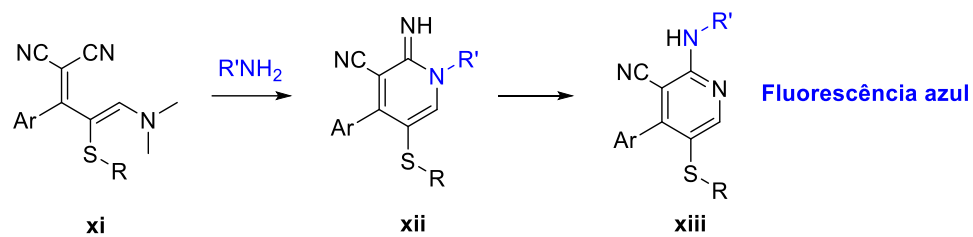
Todas as tentativas anteriores experimentadas por nosso grupo falharam e várias espécies eletrofílicas foram utilizadas sem sucesso.

Tendo a reação entre acetato de vinila e cloreto de sulfenilo (rota 3TC) como inspiração, decidimos utilizar o cloreto de sulfenilo como espécies eletrofílicas para a reação com IM. Como resultado, desenvolvemos uma metodologia eficiente capaz de produzir IMs substituídos com enxofre, **xi**, em rendimentos satisfatórios. Também demonstramos que os IMs substituídos na posição R₂ podem ciclizar na presença de uma base primária formando amidinas fluorescentes **xii** (Esquema iii). A fluorescência das amidinas cíclicas **xii** podem ter suas cores variadas desde diferentes tons de verde ao amarelo, simplesmente através da variação dos grupos R₁ e R₂, produzindo moléculas com diferentes λ_{\max} , como mostrado pelos estudos fotofísicos.



Esquema iii. Funcionalização de IMs na posição R₂ seguida de ciclização e formação de amidinas fluorescentes.

Durante a expansão do escopo reacional, praticamente todos os IMs produziram a amidina esperada, mas algumas eram extremamente instáveis sendo convertidas a um produto majoritário de menor polaridade. Tal produto apresenta fluorescência na região do azul e após caracterização, descobrimos que se tratava de amino-piridinas. Apresentamos esses resultados em detalhes, demonstrando um novo método para produzir piridinas multisubstituídas. Também fornecemos um exemplo em que um dos produtos exibe emissão induzida por agregação (AIE), com possíveis aplicações optoeletrônicas e biológicas (Esquema iv).



R= Alquil, Arila

Esquema iv. Síntese de amino-piridinas (xiii) a partir de amidinas xii.

SUMMARY

PART 1

1. Introduction.....	03
1.1. Hazardous Reactions in Continuous Conditions.....	03
1.1.1. A Brief Overview: Flow Chemistry.....	03
1.1.2. Important Parameters and Steady State.....	06
1.1.3. Safe Processes: Performing Hazardous Reactions in Flow.....	07
1.1.4. Photochemical Reactions.....	08
1.1.5. Reactions with Singlet Oxygen ($^1\text{O}_2$).....	15
1.1.6. Kornblum-DeLaMare Rearrangement.....	19
1.2. New Routes toward Lamivudine (3TC).....	21
1.2.1. Medicines for All Institute Goals.....	21
1.2.2. Lamivudine Synthesis.....	21
2. Objectives.....	28
3. Results and Discussion.....	29
3.1. Reactors.....	29
3.1.1. Building the Photochemical Reactor.....	29
3.1.2. Tube-in-tube Reactor.....	33
3.2. Continuous Endoperoxidation Followed by Rearrangements in End-to-end Approaches.....	36
3.2.1. Development of the Methodology.....	37
3.2.2. End-to-end Approach.....	42
3.2.3. Methodology Application – Reaction Scope.....	44
3.2.4. Partial Conclusions.....	52

3.3. Continuous Synthesis of a New Intermediate for Lamivudine and Emtricitabine Production.....	53
3.3.1. A Brief Overview of Ongoing M4ALL Routes to 3TC.....	53
3.3.2. Lamivudine Synthesis by M4ALL.....	56
3.3.3. Continuous Flow Experiments, System Design and Considerations.....	62
3.3.4. Surveying Reactor Configurations.....	62
3.3.5. Steady-State and Reactor Output.....	67
4. Conclusions.....	77
5. Experimental Section.....	79
5.1. Photooxygenation Reactions and Kornblum-DeLaMare Rearrangement (KDM).....	80
5.1.1. Batch Protocol to <i>cis,cis</i> -1,3-cyclooctadiene (53) Photooxygenation Followed by KDM Rearrangement.....	80
5.1.2. General Procedure for Dienes Photooxygenations Followed by KDM Rearrangement in Continuous End-to-end Experiments.....	80
5.1.3. General Procedure for Dienes Photooxygenations Followed by KDM Rearrangement to Obtain Furans in a Continuous End-to-end Approach.....	81
5.1.4. NMR – Product characterization.....	82
5.1.5. NMR Spectra.....	93
5.2. Continuous Synthesis of a New Intermediate for Lamivudine and Emtricitabine Production.....	180
5.2.1. Experimental Procedure – Batch Experiments.....	180
5.2.2. Experimental Procedure – Continuous Conditions Experiments.....	182
5.2.3. Crystallization of the Dichloro Acetate 115	184
5.2.4. Reaction of Vinyl Acetate with SO ₂ Cl ₂	186
5.2.5. 1,2,3-trichloropropane as the NMR Internal Standard.....	186
5.2.6. NMR – Product Characterization.....	188
5.2.7. NMR Spectra.....	191

PART 2

1. Introduction.....	218
1.1. Fluorophores Synthesis with Photophysics Studies.....	218
1.1.1. Basic Concepts.....	218
1.1.2. A Brief History Regarding Fluorescence.....	220
1.1.3. Applications of Fluorescent Molecules.....	221
1.1.4. Synthesis of Ylidenemalononitriles (YMs).....	222
1.1.5. Synthesis of Pyridines from Ylidenemalonitriles.....	224
2. Objectives.....	226
3. Results and Discussion.....	228
3.1. Increasing Scope of Clickable Fluorophores: Electrophilic Substitution of Ylidenemalononitriles.....	228
3.2. Demonstrating the Scope.....	231
3.3. Cyclization to Amidine.....	234
3.4. Photophysical Observations and Measurements.....	235
3.5. Cyclization Rate with Primary Amines.....	238
3.6. Pyridine Synthesis from YMs.....	241
4. Conclusions.....	252
5. Experimental Section.....	254
5.1. General Information.....	254
5.2. General Procedure for Alkylidene Malononitrile Preparation.....	254
5.3. General Procedure for Enamine Preparation.....	255
5.4. Procedure for Enamine 1 Reaction with NCS.....	255
5.5. Pinner Conditions for Cyclization of Compound 3a	256

5.6.	General Procedure for Enamine Reaction with R-S-Cl.....	256
5.7.	General Procedure for Cyclization with Primary Amines.....	257
5.8.	General Procedure for Pyridines Synthesis from YMs.....	257
5.9.	NMR - Product Characterization.....	258
5.10.	Enamine 3f Increased Solubility in H ₂ O.....	283
5.11.	Photophysical Studies.....	283
5.12.	X-ray Crystallography.....	295
5.13.	NMR Spectra.....	310
6.	References.....	426

PART 1

FLOW CHEMISTRY APPLIED TO HAZARDOUS REACTIONS

“Results and Discussion” and “Experimental Section” are reproduced with permission from **DE SOUZA, J. M.**; BROCKSON, T. J.; MCQUADE, D. T.; DE OLIVEIRA, K. T. “Continuous Endoperoxidation of Conjugated Dienes and Subsequent Rearrangements Leading to C–H Oxidized Synthons” *J. Org. Chem.* **2018**, *83*, 7574–7585. Copyright 2018 American Chemical Society.

and

DE SOUZA, J. M.; BERTON, M.; SNEAD, D. R.; MCQUADE, D. T. “A Continuous Flow Sulfuryl Chloride Based Reaction – Synthesis of a Key Intermediate in a New Route Toward Emtricitabine and Lamivudine” *Org. Process. Res. Dev.* **2020**, *24*, 10, 2271–2280. Copyright 2020 American Chemical Society.

INTRODUCTION

1. Introduction

1.1. Hazardous Reactions in Continuous Conditions

1.1.1. A Brief Overview: Flow Chemistry

The concept of “flow chemistry”, also referred to as “continuous flow chemistry” is present in any chemical process that occurs in a continuous flowing stream. This is unlike batch operations where the reaction volume remains static in the vessel throughout the process. Continuous flow processes conventionally take place in a reactor with constant reagent input and product output (Figure 1). It is a very well-established technique that has been used in the industry for years to manufacture large amounts of material. Flow chemistry has garnered considerable attention over the past two decades due to its application in laboratory scales by academic research groups as well as the pharmaceutical industry.¹

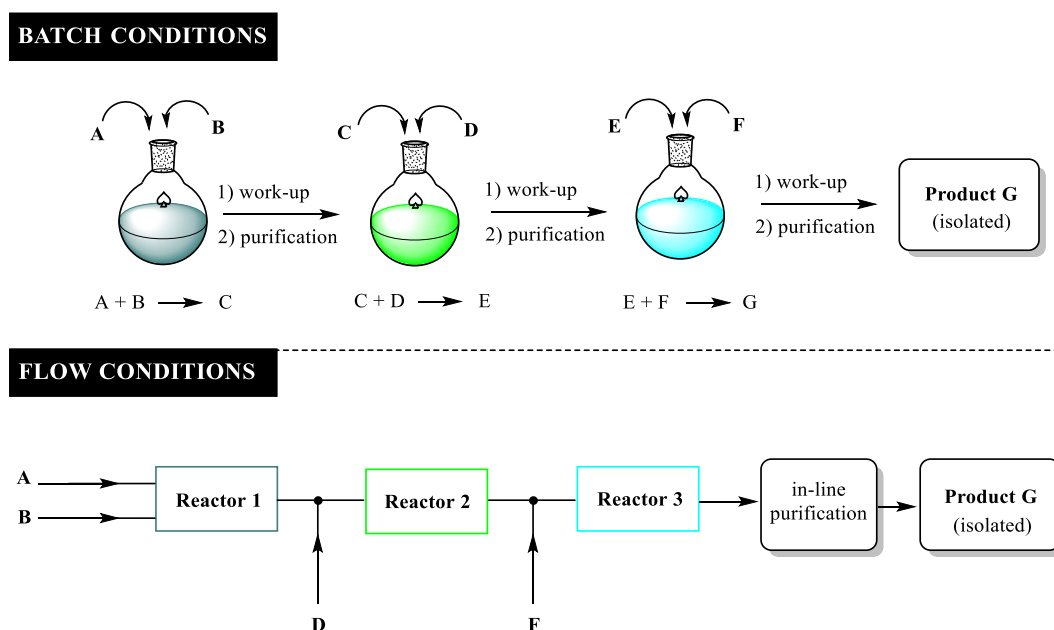
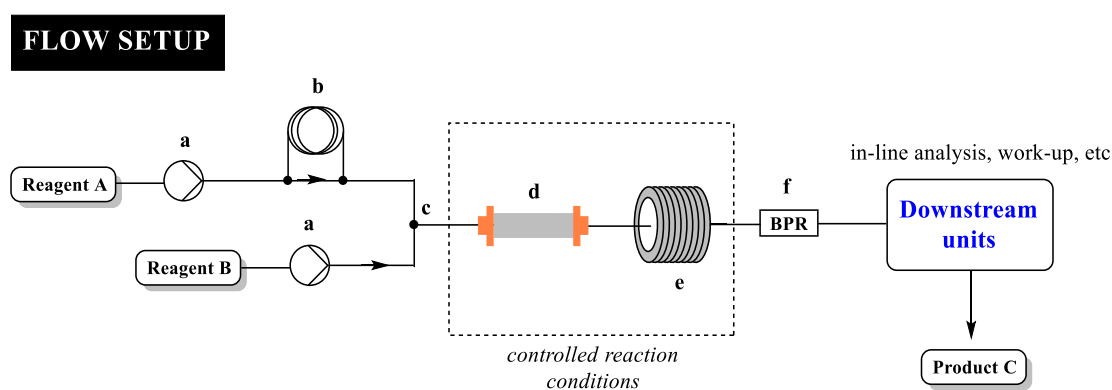


Figure 1. Comparison of batch and continuous flow processes.

The application of flow chemistry relies on the technique of pumping reagents using different reactors types (plug flow,² columns,³ gas,⁴ for slurries,⁵ photochemical,⁶ trickle

bed reactors (TBRs),⁷ etc) to perform specific reactions. The pumps inject the reactive materials into a tube and different reagents can be added in different points of the system in a continuous manner. The simplest flow setup makes use of a T-piece followed by a tube and commercial pieces of equipment. These include pumps, reactors, back-pressure regulators (BPRs), valves, tubing (stainless steel, perfluoroalkoxy (PFA), polytetrafluoroethylene (PTFE), among others), and downstream units (Figure 2). Upon scale-up, a series of modifications needs to be considered due to the larger dimension of the final setup. For instance, the T-piece and tubing may be replaced by a static mixer and jacketed coil, respectively, leading to a more cost-effective reactor.



- (a) **Pumps:** delivery of solvent and reagents (piston, peristaltic, syringe or gear pumps)
(b) **Loop:** introduction of small volumes of reagent
(c) **T-piece:** mixing point - reagents streams are combined
(d) **Column:** packed with solid reagents, catalysts or scavengers
(e) **Coil reactor:** where the reaction takes place
(f) **BPR:** Back-pressure regulator

Figure 2. General representation of a continuous flow setup.

Nowadays, continuous flow technologies have become increasingly popular, offering solutions for engineering and/or chemical problems.⁸ The small dimensions of a flow reactor and its large surface area/volume has numerous advantages (Figure 3). These improvements include mixing, mass and heat transfer, temperature control, residence time, photon-flux in photochemical reactions, process automation and intensification, and easy scale-up by increasing the number of reactors (numbering up) or the reactor dimensions. In addition, once the reaction is completed it leaves the system, avoiding

sustained exposure to conditions that would eventually lead to side reactions, byproducts or impurities formation.⁹

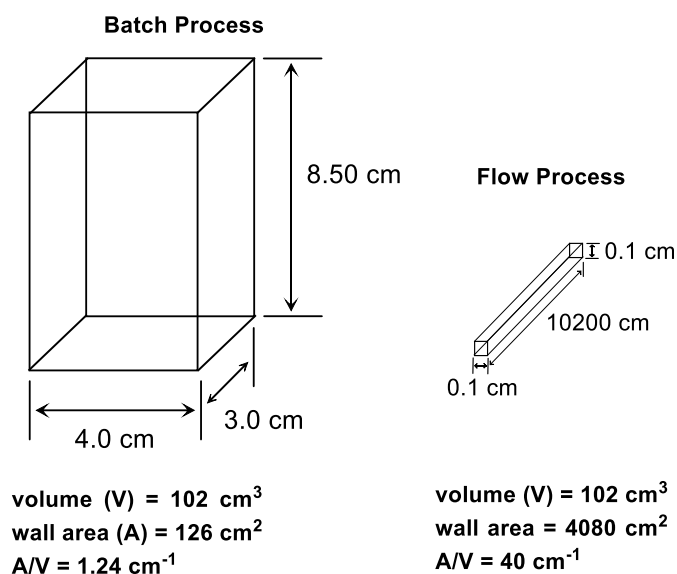


Figure 3. Surface to volume ratio – difference between continuous conditions and batch reactors.

Continuous flow should be seen as a utility for all synthetic chemists. It does not refer to a single technology but an effective toolbox containing distinct alternatives for a reactional system. Even the most technologically advanced alternative does not eliminate the classic way of making synthesis in batch conditions however. On the contrary, they are complementary techniques. There are numerous reactions that work absolutely well in batch without reason to transpose them under flow conditions. Several transformations do have serious limitations. In these cases, continuous conditions may provide the solution.

1.1.2. Important Parameters and Steady State

While running reactions under continuous conditions, a series of parameters must be taken in consideration such as the reaction time, reagents stoichiometry and flow rates of each solution injected into the reactor. In a given reaction in batch conditions, the stoichiometry is easily defined by the molar ratio of the reagents present in this transformation. In a continuous process, however, stoichiometry is defined by the applied flow rates and reagents molarity.

Unlike batch processes where the reaction time is given by the total period the reagents are stirred in the reactor, flow processes define the residence time by the ratio of the reactor volume and the reaction's overall flow rate, $\tau = V/q$. The variable τ corresponds to the residence time, V is the volume of the reactor, and q is the system total flow rate. The residence time can be varied either by changing the flow speed or the length/volume of the flow path (size of the reactor).

Steady state is among one of the most relevant concepts in continuous processes. It determines a condition where all the parameters of the system remain unchanged (steady) while the reaction takes place in the reactor zone. In other words, in a steady state condition, all state variables are constant even in the face of ongoing processes that can change them (turbulence, exothermicity or endothermicity, and others). During a flow process it is necessary to wait until steady state conditions are achieved in order to obtain constant and reproducible data. For instance, it is not completely reliable to report overall conversion/yield of a reaction carried out in a continuous way. This kind of report represents the entire reaction mixture collected and analyzed/isolated. Under continuous flow conditions the reaction mixture in the extremities (“tails”) does not present constant conditions, especially due to the dilution of the original prepared solution (Figure 4).^{10,11}

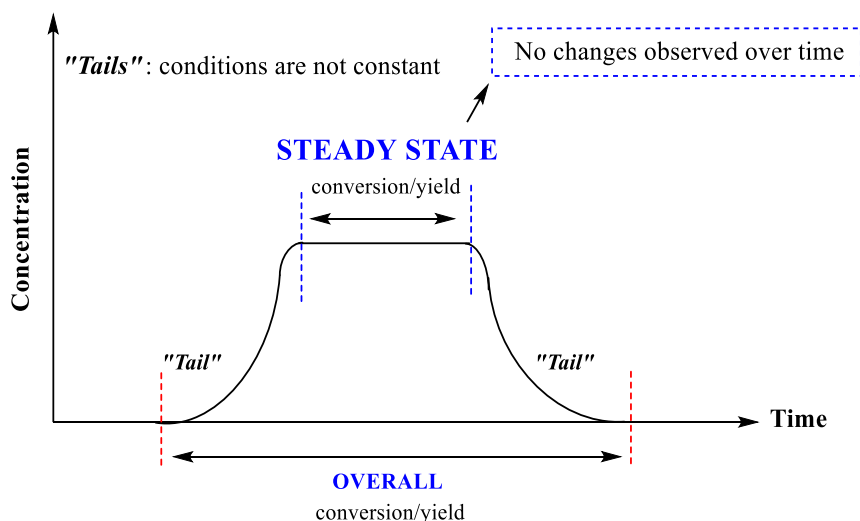


Figure 4. Simplified representation of a steady state condition during a continuous process.

1.1.3. Safe Processes: Performing Hazardous Reactions in Flow

Continuous conditions negate the need to store unstable intermediates or handle toxic, explosive and reactive reagents, thus providing safety to hazardous transformations.¹² Some examples of dangerous reactions/reagents in which the use of continuous flow systems can provide better results and safety are shown below:

- *Organometallic reactions*: fast and exothermic reactions (organolithium, Grignard reagent).¹³
- *Diazo compounds*: toxic, carcinogenic and explosive (*e.g.* diazomethane can cause DNA methylation, presents high volatility (bp: $-23\text{ }^{\circ}\text{C}$), sensitivity to heat, light, mechanical shock and explosive decomposition).¹⁴
- *Diazonium compounds*: thermal instability.¹⁵
- *Azides*: short shelf-life, toxic and highly explosive properties, potential to generate hydrazoic acid in acidic conditions which is harmful for the respiratory system.
- *Nitration*: fast and highly exothermic reactions and nitrated compounds can violently decompose at higher temperatures and are potentially explosive.
- *(Iso)cyanides*: extremely volatile and possess malodor (*e.g.* hydrogen cyanide is highly toxic).
- *Phosgene*: Highly poisonous and volatile (bp: $8.3\text{ }^{\circ}\text{C}$).

▪ *Halogenation*: reagents can be corrosive and toxic (e.g. F₂ is known to be highly toxic and reactive and it is not compatible with silicon and quartz. Fluorination reactions with this gas usually are fast and exothermic to the point of being explosive).¹⁶

The heat generated during fast and highly exothermic reactions can result in hot spots formation and increase the occurrence of runaway reactions, thus reducing the overall selectivity of the process. Under heat conditions, byproducts can be easily obtained due to the formation and decomposition of unstable intermediates. For these reasons, processes such as nitration, halogenation and organometallic reactions can be reasonably difficult to handle, especially due to the safety concerns. A variety of continuous flow technologies enables the fulfillment of many before impracticable reactions, mainly on large scale.

Enabling technologies can go even further than improving the types of reactions aforementioned. Micro-processes and processes intensification (PI) can increase heat and mass transfer in reactions with known kinetics. Nevertheless, Novel Process Windows (NPWs) technologies act offering extreme reactional conditions in order to accelerate the reaction rates. The application of this concept drastically reduces the reaction time by utilizing superheated and pressurized systems. Thus, not only reactions that occur on an explosive regime, but also high pressures (p), high temperatures (T), high concentrations (c) or solvent-free transformations can be safely explored.^{17, 18, 19} As a result, the process productivity increases by altering the reactivity of the substrates. However, the obtention of an acceptable level of selectivity must be taken in consideration.²⁰

1.1.4. Photochemical reactions

Application of light sources to perform photoinduced transformation of organic molecules was described for the first time in 1834 by Hermann Trommsdorf, when he depicted how crystals of α -santonin – a sesquiterpene lactone used as febrifuge and isolated from *Artemisia* plants – would turn yellow and “burst” when exposed to the sunlight. Through the use of a prism, he studied the dependence of the crystal decomposition with varied wavelength.²¹ However, the mechanism of crystal to crystal transformation of α -santonin was explained only a few years ago.²² Besides being the oldest documented solid-state photochemistry for an organic compound, α -santonin was the first drug to be formulated in the United States (Pfizer and Erhart).²³

Many chemists invested efforts to obtain a better understanding of this chemistry over several years. Among the renowned photochemistry pioneers, Cannizzaro, Paternó, Ciamician and Silber must be cited. The first investigated α -santonin photodegradation.²⁴ The others acquired their knowledge about this chemistry while working with Cannizzaro as his disciples. Giacomo Ciamician and Paolo Silber have an important role in the development of modern photochemistry. Their main study topics cover the investigation of photoreductions, photocycloadditions and α - and β -cleavage of ketones.²⁵

Giacomo Ciamician is considered one of the first photochemistry promoter. In his work published in 1912, he highlighted the world's need for an alternative and renewable source of energy different than coal. He envisioned the possibility of utilizing solar energy and photochemical devices to produce fuels.²⁶

Initiation of organic reactions by the use of visible light is attractive due to the lack of visible light absorbance by organic molecules (absence of highly conjugated systems). In other words, higher selectivity can be achieved, reducing side reactions (byproducts formation) and material degradation, often associated with photochemical reactions performed with high energy UV radiation (Figure 5).

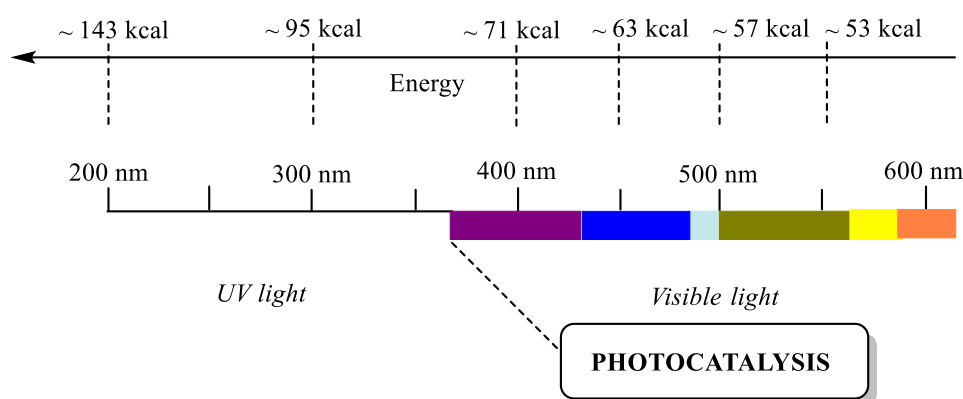


Figure 5. Electromagnetic spectrum of light and associated energies.

UV lamps present many drawbacks such as high cost, poor efficiency and health risks, besides their poor reaction selectivity, which render them impractical for large scale reactions. The use of visible light (43% of solar Energy) as a “reagent” for chemical transformations presents numerous advantages. It provides energy to drive chemical

reactions, can be selectively applied, used in large excess and leaves no trace, easy to generate (CFL, LEDs, sun), safe and non-toxic.

The use of sun light to execute large-scale chemical reactions in industries is still unusual. One of the main reasons is the difficulty of efficiently harvesting solar energy. The solar radiation is irreproducible since it presents fluctuating nature, especially due to the different geographical areas and weather changes. Nevertheless, significant advances have been recently reported by Noël's group on the implementation of continuous flow reactors for solar photochemistry.²⁷

Since only a small number of organic molecules are capable of absorbing visible-light, researchers conceived the idea of using light-harvesting molecules, the so-called photocatalysts. An approach that has been receiving attention recently and makes use of the catalytic activation of organic substrates is the visible light photocatalysis: Photoinduced Single Electron Transfer (SET) – reduction and oxidation – and Photoinduced Energy Transfer.

SET reactions exploit the ability of a photocatalyst to absorb visible light and either remove an electron from or donate an electron to a simple organic substrates after the excitation process (Figure 6).²⁸ The photoredox and photocatalysis research field changed dramatically 10 years ago, largely due to the independent research works accomplished by the MacMillan,²⁹ Yoon,³⁰ and Stephenson groups.³¹

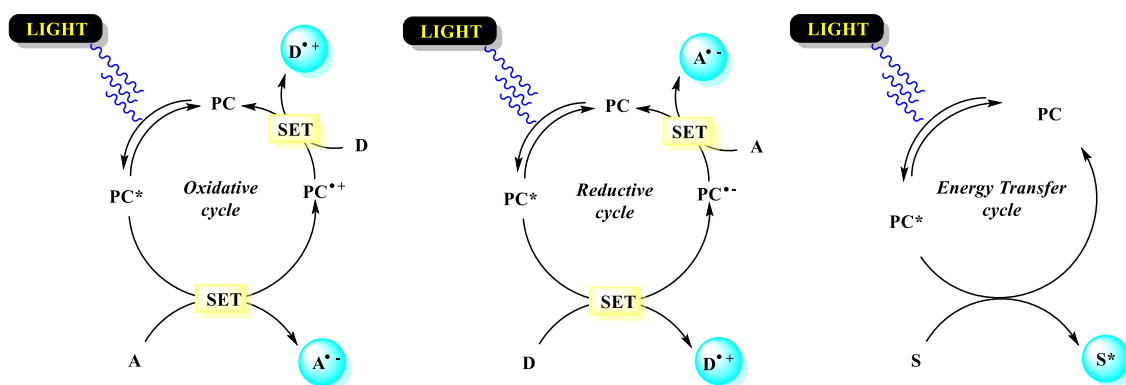


Figure 6. Photocatalysis cycles representation – oxidative, reductive and energy transfer.

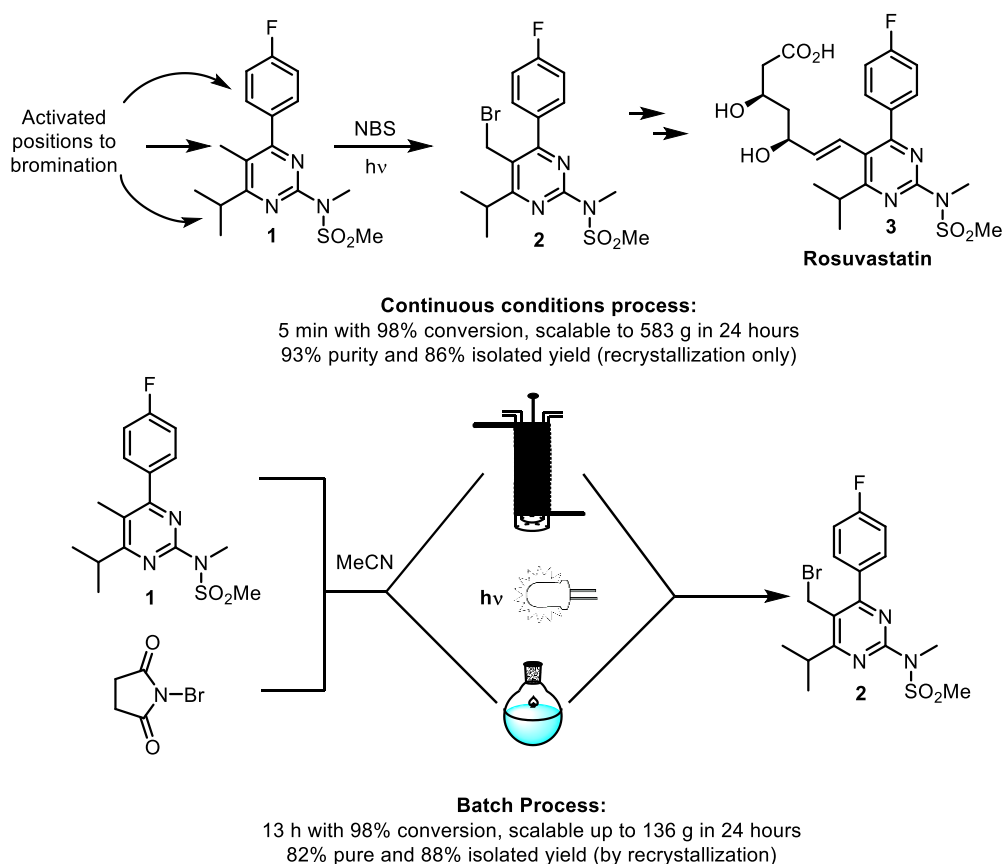
One of the ever-present limitations of photochemical processes (reactions and photocatalysis) is scaling-up. Whether by the use of UV light or part of the visible radiation, there is always the issue of low light penetration in the reaction systems which, according to the Lambert-Beer Law, decreases exponentially with the optical path. Recent works mention that up to 50% of light irradiation is absorbed in the first 500 μm of the optical path (conventional glassware).³² Thus, only a small part of the system is under the desired reaction conditions. In addition, it is difficult to precisely control reaction times. This implies part of the transformed product becomes excessively irradiated and degradation and formation of byproducts may occur.

In this context, the use of continuous flow technologies has revolutionized the field of photochemical and photocatalyzed reactions.³³ It can solve several technical problems inherent to these reactions ranging from high dilution and even efficiency in promoting molecules to the excited state. The large surface area-to-volume (A/V) ratio in microreactors and tubular reactors allows for a fast and efficient transfer of light energy to the reaction content by placing virtually all of the contents under identical excitation conditions. This efficiency in irradiation avoids excess light, time and most importantly, the occurrence of many side reactions. Also, eventual cooling needs of the reaction mixture are facilitated allowing greater reaction control.³⁴

Essentially, the two main strategies used to scale up photochemistry in flow have been: running reactions for longer amounts of time and numbering up reactors in parallel. The first strategy is limited to mg/g scale, useful for initial stages of drug discovery or to

screen new material properties. Generally, when higher productivity is required the scaling-out approach is chosen.

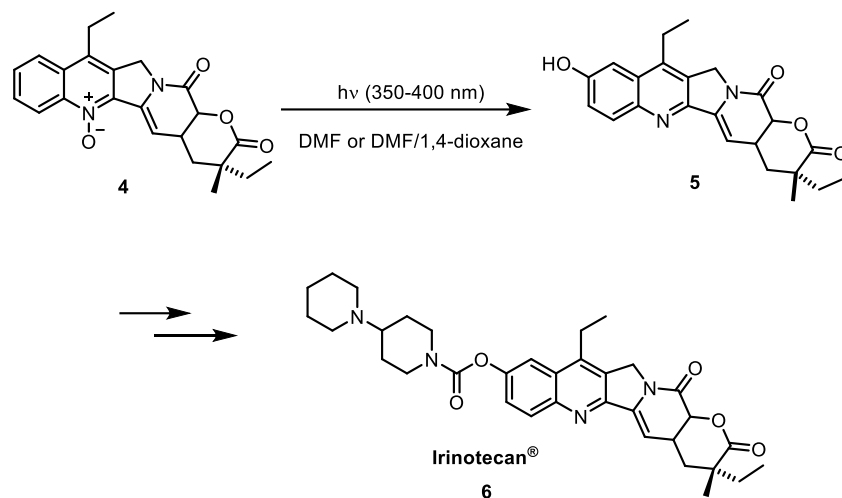
An example of the improvements that continuous flow technology can bring is showcased in the synthesis of intermediate **1** (Scheme 1) that allows the production of Rosuvastatin (**3**).³⁵ In this case the use of continuous conditions allowed a four-fold increase in scaling up compared to the batch reaction (24 h).³⁴



Scheme 1. Synthesis of a Rosuvastatin intermediate (**2**) under continuous flow and batch conditions.

Another relevant example is the production of intermediate **5** (Scheme 2), a precursor in the synthesis of the anti-cancer drug Irinotecan[®] with a worldwide demand of 1 t/yr by the pharmaceutical industry.³⁶ This reaction was initially developed in batch involving a dilution six times higher than the current continuous flow process. The use of continuous conditions resulted in 90% yield against 50% obtained in batch mode. The

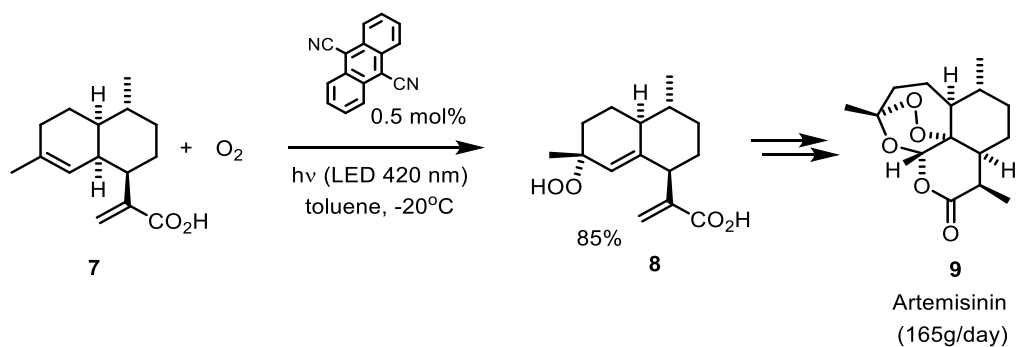
actual production capacity of this single plant is 2 kg/day, thus supplying almost all the annual demand of this input if operated 360 days in a row (720 kg).



Scheme 2. Synthesis of Irinotecan[®] intermediate (6) under continuous flow.

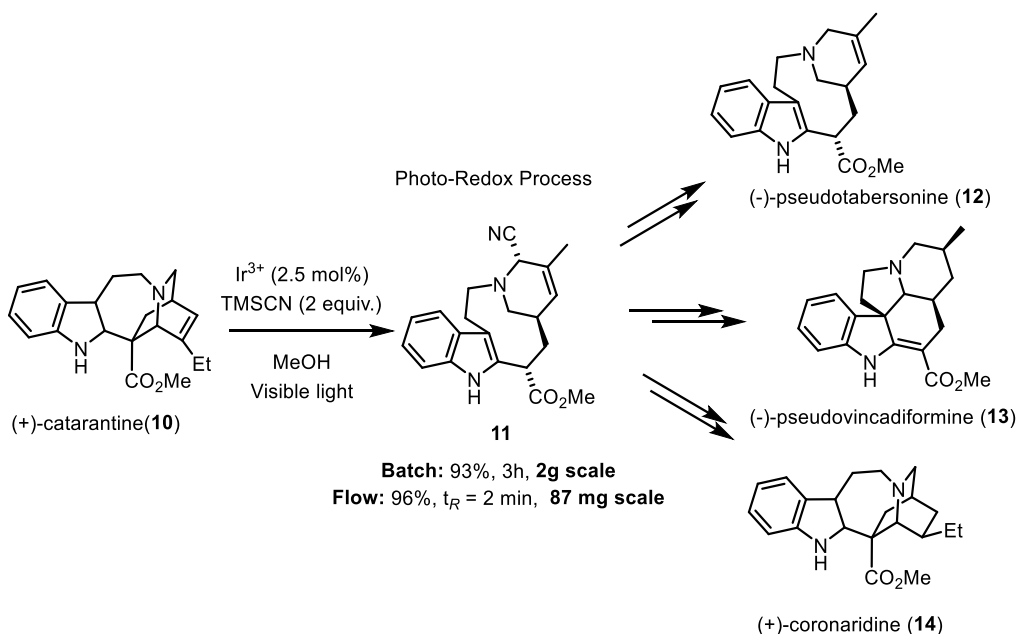
The most commonly used photoreactors are tubular types. These are easily constructed with polymer tubes (*e.g.* PFA and PTFE) inert and transparent to UV-Vis sources of light. It is possible to use tubes of high lengths and internal diameter around 1 mm, proving an efficient contact of the reaction mixture with multidirectional light sources (UV, CFL or LED).³⁷ An additional advantage of having small irradiated volumes is the guarantee that potentially explosive intermediates such as peroxides will be generated in small quantities, thus improving process safety.^{32,37}

As mentioned above, tubular reactors have been efficiently used in photochemical reactions and have clear advantages over microchips or parallel plates, such as easy reaction scaling-up and the low cost.³⁸ For instance, Seeberger (Max Planck - Germany)³⁹ has shown the synthesis of artemisinin (9) through reactions with singlet oxygen generated under continuous conditions (Scheme 3).



Scheme 3. Artemisinin synthesis (**9**).

Stephenson demonstrated one of the first total syntheses involving continuous flow reactions consisting in a photo-redox processes in a tubular system (Scheme 4). Three natural products could be synthesized from the common intermediate **11**. This work not only raises the possibility and real use of continuous flow photo-redox reactions, but also points out to a weakness still present in many works, the real scale-up. The steady-state reactions work more efficiently, yet the authors could not perform it on a multigram scale given the precariousness of the photoreactor they used (see SI from original publication⁴⁰).



Scheme 4. Stephenson syntheses involving photo-redox and Flow Chemistry processes.

The examples cited above are just a few cases selected in order to exemplify the benefits of PhotoFlow. Other scenarios have required production of new reactor systems to attain large quantities of material. Recently, McQuade's group published a review covering some of the latest examples of photoreactors exclusively applied in pharma industries in large scale production.⁴¹

1.1.5. Reactions with Singlet Oxygen ($^1\text{O}_2$)

Photocatalyzed reactions involving singlet oxygen ($^1\text{O}_2$) in organic synthesis have been documented for more than 70 years.⁴² Nevertheless, the nature of this transformation was not initially well recognized. It is noteworthy that studies on this excited state of molecular oxygen, albeit highly unstable, were a landmark for better understanding of the photooxygenation reactions⁴³ as well as their applications in the synthesis of natural products and drugs.⁴⁴

Although molecular oxygen ($^3\text{O}_2$) is the most abundant and readily accessible oxidizing agent, to serve as a convenient reagent for mild and selective oxy-functionalization, it must be electronically excited to its first singlet state ($^1\text{O}_2$). In its triplet ground state, this oxidant is not particularly useful in organic synthesis due to the lack of selectivity in its characteristic radical-type reactions.⁴⁵ Singlet oxygen is more electrophilic than molecular oxygen. It acts as a mild oxidizing agent in chemical transformations and can transfer energy to other molecules in a process called physical quenching.

In its ground state, molecular oxygen has two electrons with parallel spins occupying π -antibonding orbitals (π^*). After furnishing a specific amount of energy, these two electrons can be paired. In this case, the spin quantum number is zero and the molecule is called singlet oxygen (multiplicity is given by $2S + 1 = 1$, when $S = 0$) (Figure 7).⁴⁵

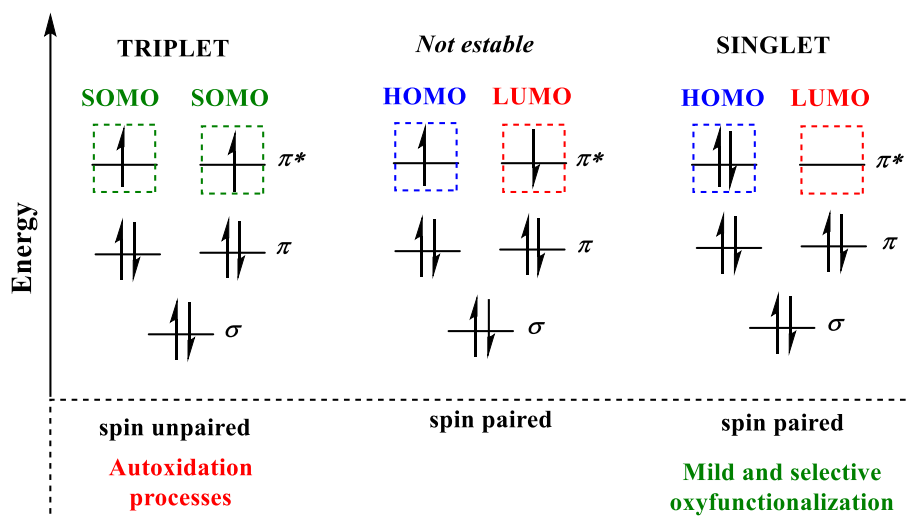
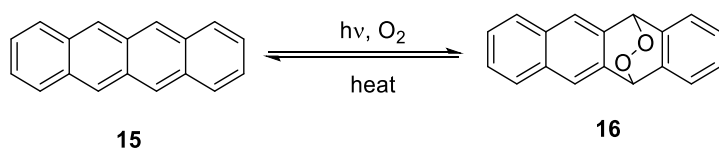


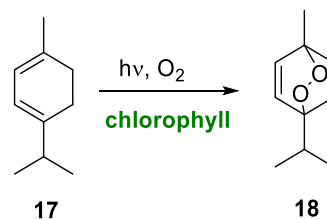
Figure 7. Simplified orbitals diagram of the oxygen molecule.

The earliest description of $^1\text{O}_2$ was made by Fritzsche in 1867, who noticed the formation of a crystalline material when a solution of naphthacene (**15**) was exposed to light and heat. At that time neither the structure of the product nor the nature of the process as a self-sensitized singlet oxygen [4+2] cycloaddition was recognized (Scheme 5A).⁴⁶ The first evidence for the existence of a metastable and highly reactive form of oxygen was reported later by Kautsky and coworkers in 1931.⁴⁷ In 1944, Schenck and Ziegler showed the first use of singlet oxygen in organic synthesis by conducting the oxidation of α -terpinene (**17**) in the presence of chlorophyll (from spinach) and sunlight leading to the formation of a bicyclic monoterpene, (\pm)-ascaridole (**18**) (Scheme 5B).⁴⁸

A) Fritzsche, 1867



B) Schenck and Ziegler, 1944



Scheme 5. First uses of singlet oxygen in organic synthesis.

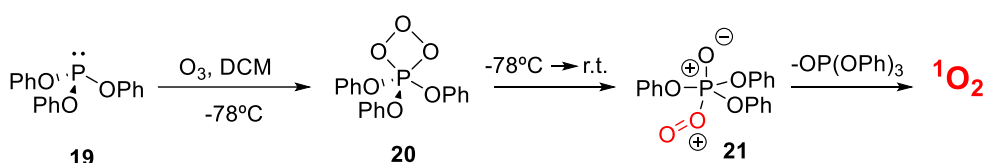
Christopher Spencer Foote was the most influential expert in reactive oxygen species, with singlet oxygen his main pursuit. He accomplished many studies involving this reactive intermediate, which provided an important theoretical base and helped to disseminate the $^1\text{O}_2$ use in organic synthesis.⁴⁹ Despite its short lifetime and reactivity, $^1\text{O}_2$ participates in many selective reactions, some of them synthetically useful. An example is its reaction with dienes yielding endoperoxides.

Singlet oxygen is involved in processes that result in the neoplastic cell death. This phenomenon forms the basis for photodynamic therapy (PDT), a contemporary and non-invasive form for cancer treatment.⁵⁰ Likewise, the feared aging process involves extremely reactive oxygen species (ROS), generated via cellular metabolism as well as by respiratory pathways. The toxic effects of oxygen radicals on cellular components results in oxidative damage which is responsible for the cellular dysfunction with age.⁵¹

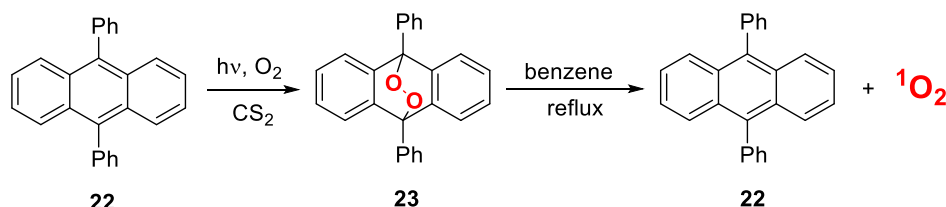
Singlet oxygen reaction is a useful tool in the synthesis of oxygenated structures such as hydroperoxides, endoperoxides, dioxetanes, peroxides and sulfoxide. It promotes carbon-oxygen and heteroatom-oxygen bonds formation in addition to the high atom-economy and low cost.⁵² In this context, [4+2] and [2+2] cycloadditions, ene reactions and heteroatom oxidations can be performed.⁵³

There are at least three main methods to generate $^1\text{O}_2$ by chemical reactions: (i) Murray Method, a thermal process to decompose ozone-phosphite adducts; (ii) Thermal decomposition of endoperoxides and (iii) Decomposition of hydrogen peroxide with bleach (Scheme 6).⁵⁴

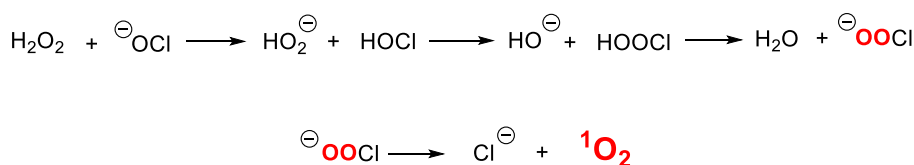
A) Murray Method: thermal decomposition of ozone-phosphite



B) Thermal decomposition of aromatic endoperoxides



C) Decomposition of hydrogen peroxide



Scheme 6. Some methods to produce $^1\text{O}_2$ through chemical reactions.

Dye-sensitized photoexcitation of triplet oxygen ($^3\text{O}_2$) employing porphyrinoid compounds is already well established.⁵⁵ It is among the most efficient organic photocatalysts capable of generating *in situ* singlet oxygen ($^1\text{O}_2$) in photooxygenation reactions. In the presence of a light source, porphyrin derivatives can absorb energy and promote one electron to a more energetic orbital (LUMO, S^* - singlet excited state) (Scheme 8). From this point the reaction follows one of two different pathways. The electron can lose energy and decay to its ground state in a process called fluorescence or to its excited triplet state (T^*), in this case by intersystem crossing (ISC) through a spin inversion process. While in its T^* state, the photocatalyst can, again, decay to its ground state, losing energy by phosphorescence or simply transferring this energy to others molecules, for instance, the molecular oxygen. It is during this process that singlet oxygen is generated (Figure 8).⁵⁶

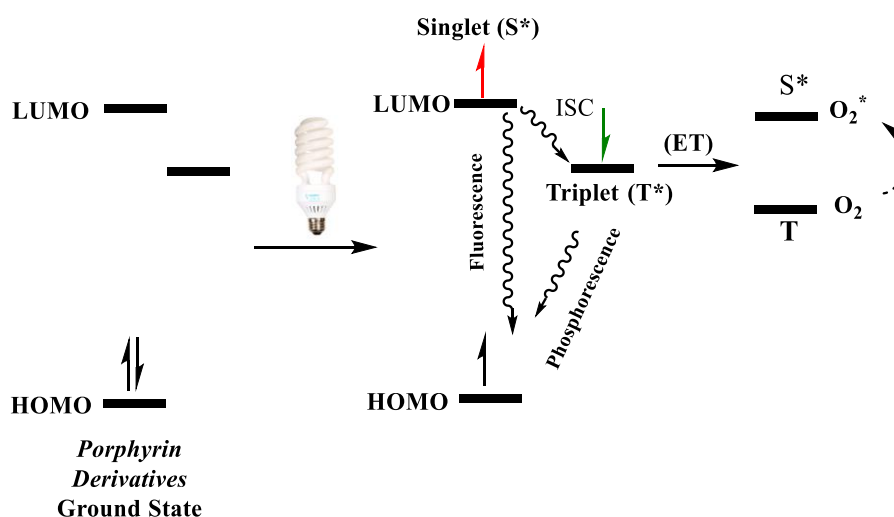


Figure 8. Production of $^1\text{O}_2$ by the action of a photocatalyst.

There are some experimental limitations regarding the potential hazards of flammable solvent-oxygen mixtures. The same holds true for reactions involving explosive intermediates such as endoperoxides. Continuous flow approaches have revolutionized the photochemical transformations with $^1\text{O}_2$.^{57,58}

1.1.6. Kornblum-DeLaMare Rearrangement

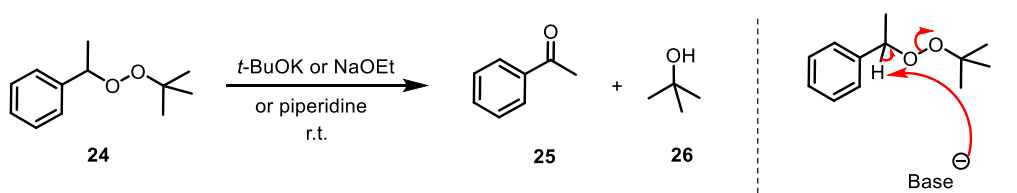
Organic peroxides can rearrange to produce different compounds depending on the reaction conditions. They can be carried out using acid or basic catalysts or via radical processes. The Baeyer-Villiger, Criegee and Hock reactions, the Kornblum–DeLaMare rearrangement, Dakin, and Elbs oxidation are examples where the reaction key steps present peroxides rearrangements.⁵⁹

The Kornblum-DeLaMare rearrangement (KDM) consists of the rearrangement of organic peroxides into ketones and alcohols, including γ -hydroxy enones **28** in the case of endoperoxides **27** (Scheme 7B).⁶⁰ It is performed mainly under base-catalyzed conditions, although acid conditions can also promote the rearrangement.⁶¹ The latter is not commonly found in the literature, nor are the asymmetric approaches for this rearrangement.⁶² First described in 1951,⁶³ Kornblum and DeLaMare observed that the treatment of 1-phenylethyl *tert*-butyl peroxide (**24**) with KOH, NaOEt, or pyridine

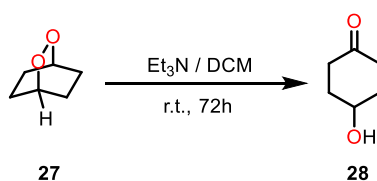
resulted in the decomposition of **24** in acetophenone (**25**) and *tert*-butanol (**26**) (Scheme 7A).

This rearrangement consists in three steps occurring presumably in a concerted manner. The reaction starts with a base-mediated α -hydrogen abstraction from **24**, which decomposes to form the anion *tert*-butoxide and acetophenone (**25**). The protonation of the *tert*-butoxide anion results in *tert*-butanol (**26**) (Scheme 7A).

A) Kornblum-DeLaMare observations



B) Rearrangements starting from endoperoxides



Scheme 7. Kornblum-DeLaMare rearrangement – peroxides and endoperoxides.

KDM rearrangement is a very versatile transformation in organic synthesis which allows an *umpolung* modification on endoperoxide structure, but with serious restrictions of use due to safety issues and difficulties to scale up the reactions.⁶⁴ Nevertheless, literature lacks studies using endoperoxide transformations and the use of continuous flow conditions to overcome safety issues related to this reaction – endoperoxides are potentially explosive.

1.2. New Routes toward Lamivudine (3TC)

1.2.1. Medicines for All Institute Goals

The Medicines for All Institute (M4ALL) was created in July of 2017 within Virginia Commonwealth University (VCU) with the financial support of the Bill & Melinda Gates Foundation. Located at Richmond, Virginia's State capital in USA, M4ALL's main goal is to reduce the costs of expensive pharmaceutical products and to improve access to effective, safe and affordable medicines.

With the rising prices of important medicines, innovators and generic manufacturers are not motivated to reduce manufacturing costs. With M4ALL's novel chemical process technologies, hopefully, this scenario may be changed. The expected effect is that these processes will expand patient access to existing medication as well as new, more affordable alternatives. M4ALL's manufacturing process possesses the potential to disrupt the pharmaceutical supply chain, mainly for the generic manufacturers. The competitive generic market presents narrow margins and high barriers to the entry of new competitors, especially the manufacturers of global health treatments.⁶⁵

1.2.2. Lamivudine Synthesis

Lamivudine and Emtricitabine (3TC and FTC, respectively) are essential components of widely prescribed anti-HIV multi-drug regimens.⁶⁶ Both nucleosides analogs are high dosage/high demand drugs and manufactured in large volumes (>10⁶ kg/yr). Though the active pharmaceutical ingredient (API) price (~\$100/kg), the API cost is the major cost driver for these global health medicines. Procurers (governments and non-governmental organizations) are placing downward pressure on the medicine prices. This pressure places manufacturers between a rock and a hard place. The Medicines for All Institute (M4ALL) seeks find a middle ground by creating low cost API routes that enable procurers to receive lower medicine prices and manufacturers to continue

receiving margins that support their needs. M4ALL has been working a new route to the oxathiolane core that serves as a key intermediate for the synthesis of both 3TC and FTC.

Although a permanent cure for HIV remains elusive, the current medications designed to treat HIV help lower the patients viral load, fight infections, and improve their quality of life. These medicines are capable of controlling the virus' growth, improving immune system efficiency, reducing symptoms, and consequently preventing transmission to others. The FDA has approved more than two dozen antiretroviral drugs to treat HIV. Lamivudine (**29**), commonly called 3TC (trade name Epivir) (Figure 9)⁶⁷ is one such drug. It is a nucleoside analogue similar to cytidine (**32**).⁶⁸

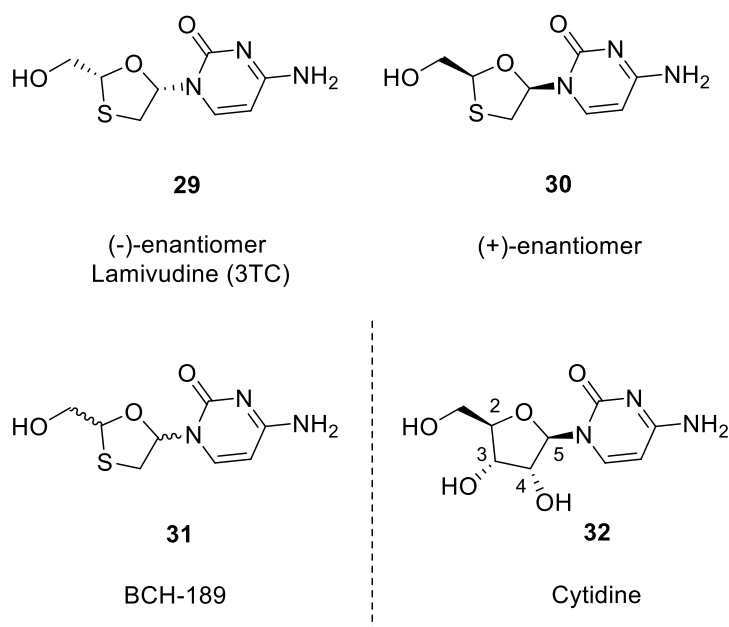


Figure 9. Lamivudine (**29**) and Cytidine chemical structures.

BCH-189 (**31**) is known as a mixture of four possible isomers of Lamivudine (*cis* and *trans*). Among them, the β -L-(-)-enantiomer (3TC, **29**) is considerably less toxic than other three corresponding ones (Figure 9).⁶⁹ Numerous methods for the optical resolution of *cis*-BCH-189 by biological enzymes have been reported.⁷⁰

The racemic mixture **31** was discovered by Bernard Belleau and Nghe Nguyen-Ba in 1988 and the (-)-enantiomer isolated in 1989.⁷¹ In 1995, it was approved for use in the United States and it is on the World Health Organization's List of Essential Medicines.

Lamivudine has proven to be one of the most successful medications for the treatment of HIV/AIDS as well as chronic Hepatitis B (HBV). It is typically used in conjunction with other antiretrovirals. 3TC is capable of inhibiting both types (1 and 2) of HIV and Hepatitis B virus reverse transcriptase. It is phosphorylated by intracellular kinases into active metabolites that compete for incorporation into viral DNA. This process produces Lamivudine 5'-triphosphate, the active anabolite that prevents the replication of HIV-1 and HBV. They inhibit the HIV reverse transcriptase enzyme competitively, acting as a chain terminator of DNA synthesis. The absence of a 3'-OH group in the incorporated nucleoside analogue prevents the formation of the 5' to 3' phospho-diester linkage essential for the elongation of the DNA chain, and therefore, the viral DNA growth is interrupted.⁷²

Until a few years ago, only nucleosides containing the natural β -D-configuration were studied as chemotherapeutic agents due to their accessibility. The discovery of 3TC sparked tremendous interest in the synthesis of β -L-nucleosides since several viruses can accept them as substrates for their own replication, leading to stalled synthesis of their DNA.

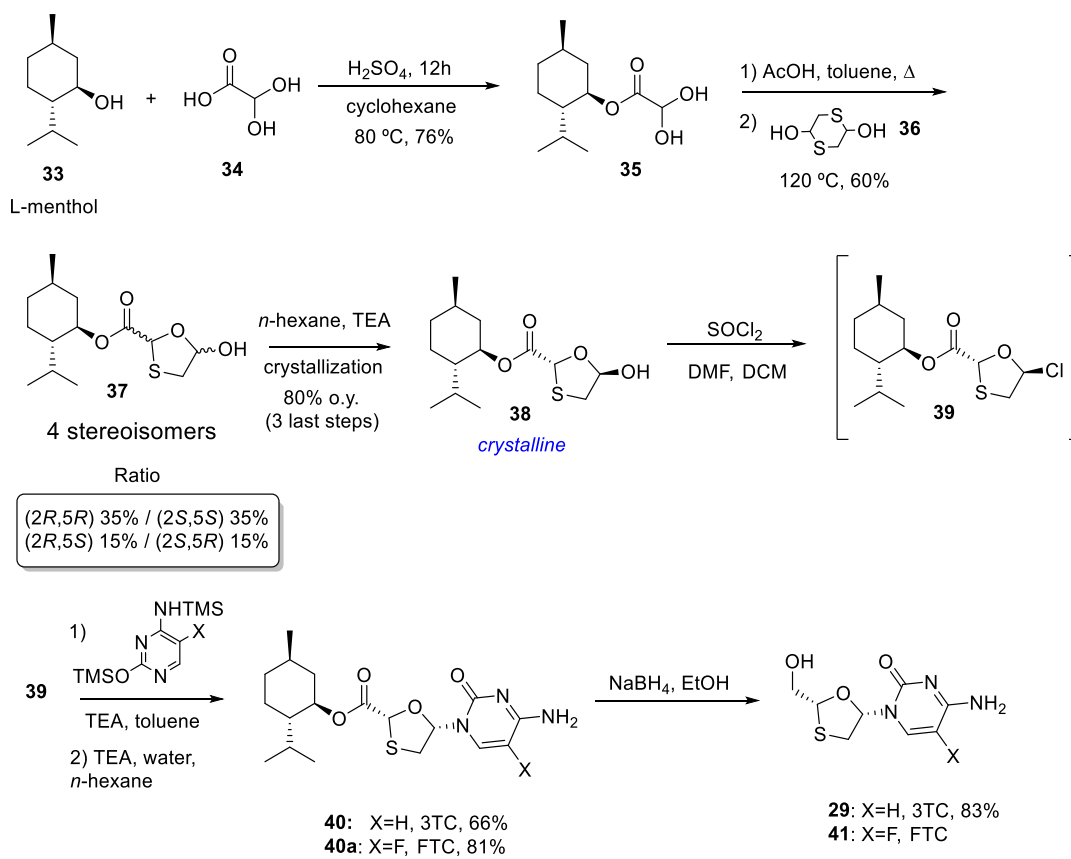
A method of efficiently obtaining bulk quantities of 3TC is of key interest, as mass demand is predicted. There are several reported methods to synthesize Lamivudine.⁷³ Formation of a mixture of D and L-nucleosides is a common occurrence during the synthesis of Lamivudine (**29**). Separating racemic mixtures is challenging and affects the yield. Enantioselective synthesis of Lamivudine was first reported by Chu and co-workers.⁷⁴ Most methods obtain the desired chiral 1,3-oxathiolane core by either crystallizing the correct isomer from a racemic mixture by kinetic resolution process (50% maximum yield)⁷⁵ or by crystallization-induced dynamic kinetic resolution (DKR).⁷⁶ Processes involving enzymatic hydrolysis/acetylation of the other stereoisomers are also described.⁷⁷

Although diastereo and enantioselective synthesis of Lamivudine is already documented, for the large-scale synthesis of 3TC, *N*-glycosidation approaches are preferred due to their lower cost.⁷⁸ In spite of its structural simplicity, the synthesis of the oxathiolane core in the 3TC molecule has presented a major synthetic challenge, mainly due to two factors: (a) the need of an efficient stereochemical control of two potentially epimerizable stereocenters (positions 2 and 5) and (b) the need for stereoselective *N*-

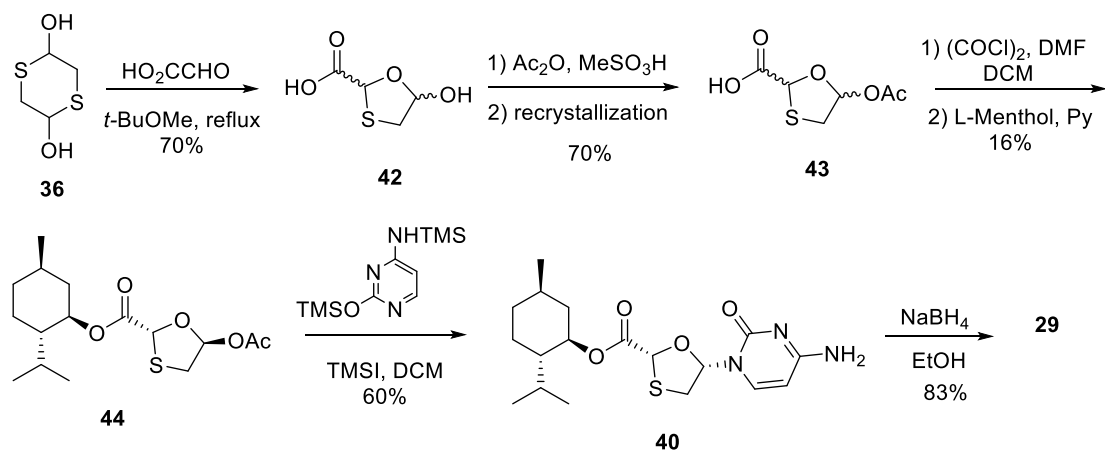
glycosidation methodologies when no adjacent directing groups are present in the glycosidation site.

One choice method for the industrial production of 3TC and FTC (**41**) follows the procedure suggested by Whitehead et al. which involves the coupling reaction between L-Menthyl ester **39**, prepared from 5-hydroxyoxathiolane **38**, and the presilylated cytosine or 5-fluorocytosine. Compound **38** with defined stereocenter at position 2 and 5 (*2R,5R*) can be isolated via crystallization in TEA and hexanes (DKR). The final *2R,5R* configuration at the oxathiolane ring is obtained through chlorination reaction at the position 5 with SOCl_2 in catalytic DMF. These conditions allow the reaction to take place with retention of the starting material stereochemistry at position 5, leading to nucleoside precursors **40** and **40a** in acceptable yields (**40**: 66%; **40a**: 81%) and anomeric selectivity (**40**: $\alpha:\beta = 10:1$ and **40a**: not given) (Scheme 8A).⁷⁹ The reduction of these intermediates with sodium borohydride provides 3TC and FTC. This approach is a convenient alternative to the previous methodology by Tse et al.,⁸⁰ which used the more unstable and expensive (although more efficient) trimethylsilyl iodide (TMSI) to perform a Vorbrüggen reaction to promote the desired *N*-glycosidation (**40**: 75%, $\beta:\alpha = 23:1$; **40a**: 91%, $\beta:\alpha = 28:1$) (Scheme 8B).

A) Whitehead et al. Method

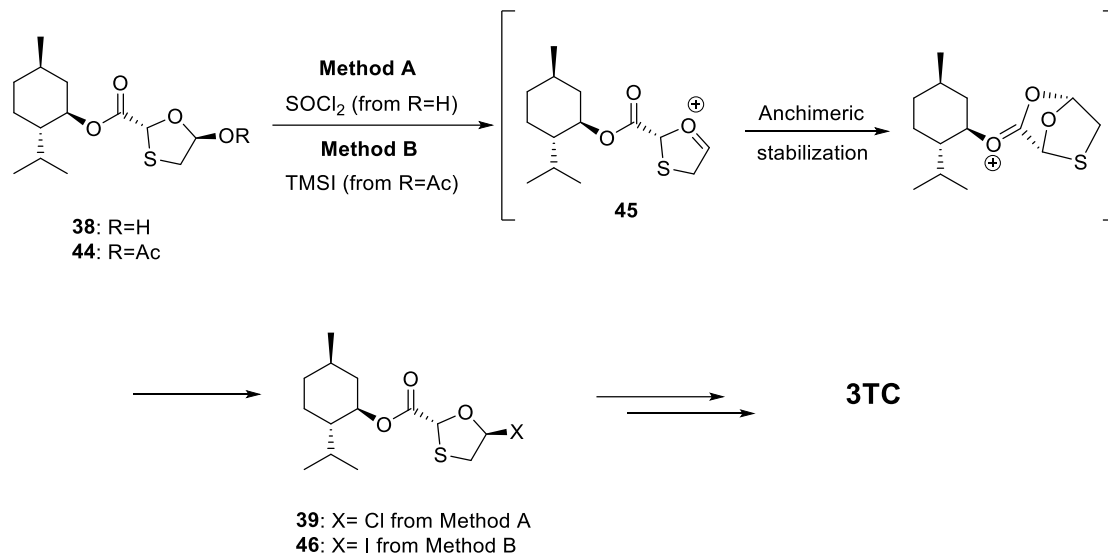


B) Previous reports



Scheme 8. A) Method of choice for the industrial production, B) Previous literature for 3TC and FTC synthesis.

It is worth mentioning that in both cases the high β -selectivity is due to formation of oxonium ion **45**, stabilized through anchimeric assistance by the menthyl ester function (Scheme 9).

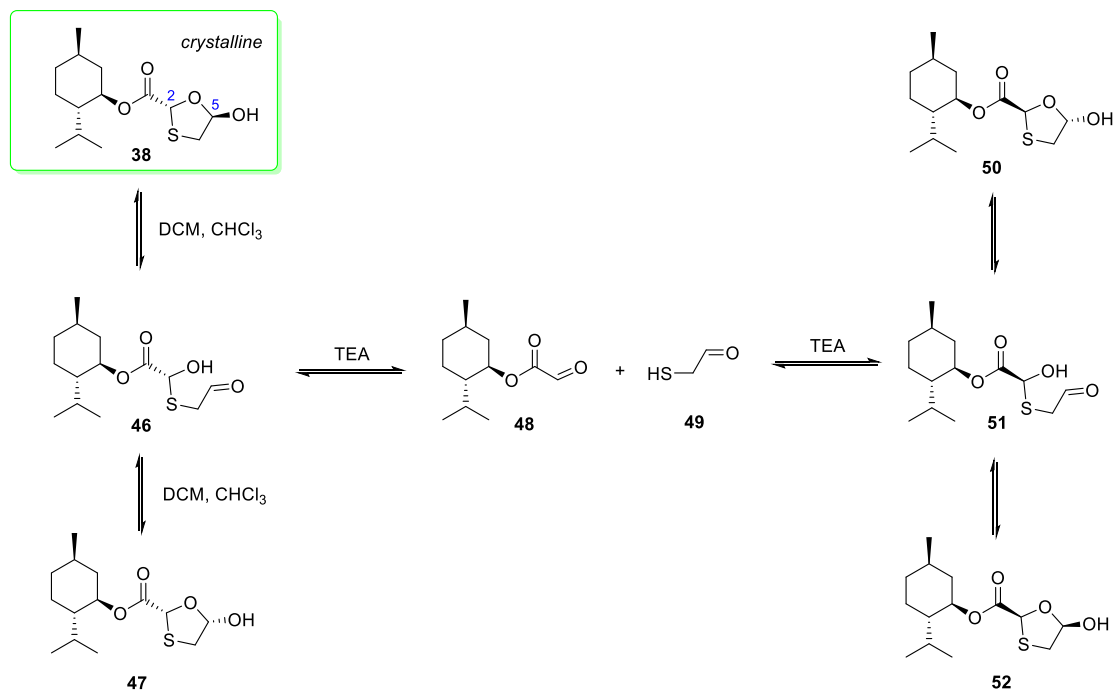


Scheme 9. Stabilization of **45** by anchimeric assistance.

The use of crystallization-induced dynamic kinetic resolution (DKR) during 3TC synthesis is essential to improve yields of compound **38**. It was discovered that in certain solvents, such as DCM or CHCl_3 , rapid equilibration at C-5 produced a mixture of β and α isomers **38** and **47**, yet no epimerization at C-2 is observed. Whitehead et al. suggested that this equilibrium could be further distorted via cleavage of the hemithioacetal **46** to give menthyl glyoxalate **48** and mercaptoacetaldehyde **49**. The union of these two equilibria should then provide a method of transforming the undesirable diastereoisomers into desirable ones. These would be removed from the equilibrium via crystallization (Scheme 10). A number of bases were evaluated for this purpose; Py gave only a small amount of interconversion whereas TEA caused rapid interconversion. Only a catalytic amount of TEA (1–10%) is needed to achieve rapid interconversion and selective precipitation/crystallization of **38** in 80% yield (Scheme 8A).

Many research groups have been studying different alternatives to decrease the overall cost of 3TC production.⁸¹ Nevertheless, most manufacturers still believe the

methodology developed by Whitehead and co-workers, published more than a decade ago, is most practical. Advances in this area are needed in order to produce a new and cheaper route with a competitive cost.



Scheme 10. Crystallization-induced dynamic kinetic resolution (DKR).

2. Objectives

Herein, we describe two different examples of hazardous reactions that can have their outcome and safety improved by applying continuous conditions. In the first case, we develop a methodological study on endoperoxidation reactions of different diene classes followed by KDM rearrangement and other transformations in a continuous flow regime with step-by-step or by end-to-end approaches. Variables evaluated are photocatalyst loading, substrate concentration, oxygen pressure, flow rate and rearrangement temperature. The construction of a homemade photochemical reactor and a gas-liquid flow reactor (tube-in-tube) to perform these reactions is achieved using basic accessible materials.

In the second example we showcase two hazardous steps in the synthesis of an important intermediate toward Lamivudine (3TC – HIV drug) in continuous conditions. The route displayed is under development by the Medicines for All Institute (M4ALL). These two steps consist of a series of highly exothermic transformations and toxic gases releases such as HCl and SO₂. Preliminary experiments suggested rapid reagent addition and mixing decreased byproduct formation. With high scale production and process safety in mind, we devised an efficient flow setup.

RESULTS AND DISCUSSION

3. Results and Discussion

3.1. Reactors

3.1.1. Building the Photochemical Reactor

To perform the photochemical reactions in batch and continuous flow regime, we built homemade reactors with simple and affordable materials. Herein we provide the necessary details for their reproduction by any research group worldwide.

Batch endoperoxidation experiments were carried out in a photoreactor assembled by our research group. The reactor body was made from a silica gel bottle marketed by Merck, as shown in Figure 10. A circular cut was made on its top in order to set a cooler fan to avoid temperature increase during the reaction period due to the LED's heat. The bottom was also cut from all four sides, leaving space for air circulation and consequent cooling of the LEDs.



Figure 10. Silica gel bottle used as the reactor body.

Aluminum plates were attached to the bottle walls on its inside using a double-sided tape, and the LEDs were carefully inserted into the metal support shown in Figure 11, 12 and 13. The LED wiring was welded (*ca.* 7.5 cm) with SnPb 60/40 solder. Liquid electrical tape was applied on top of the solder some liquid electrical tape to protect it (Figure 11).

Each side of the photoreactor has 10 LED set strips (*ca.* 12 cm) associated in series, totaling four sets of 20 W each, attached separately on its walls. A duplicate set

was crafted for a separate 100 W reactor. However, this additional strip was placed on top of the magnetic stirring plate, illuminating the flask at its bottom (Figure 12 and 13).

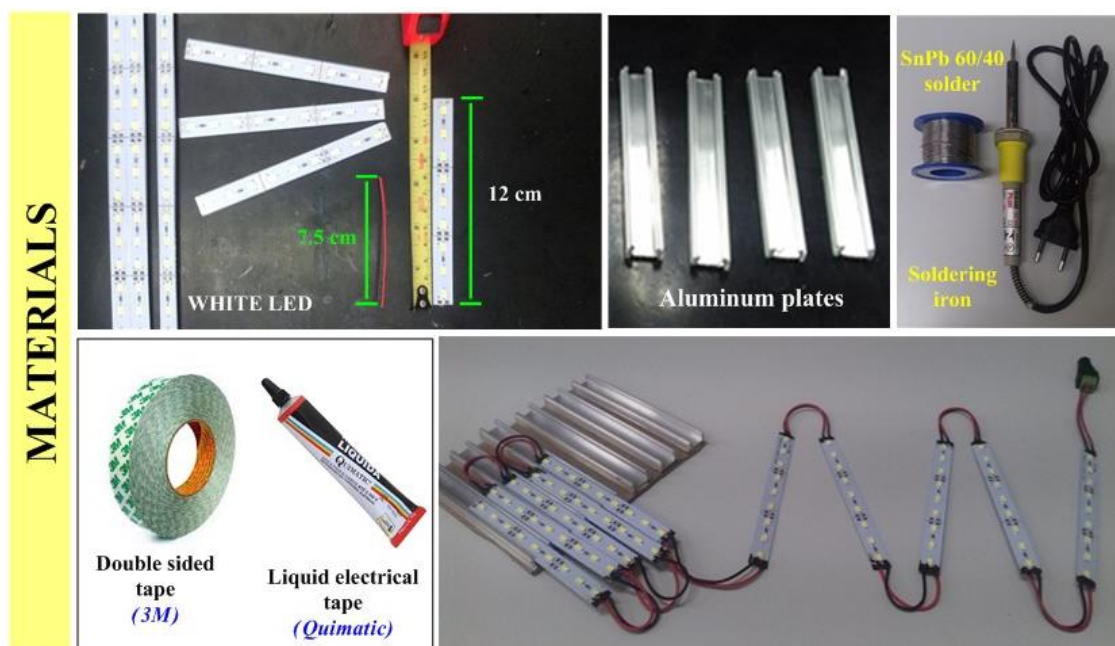


Figure 11. Main materials used in the photoreactor construction.

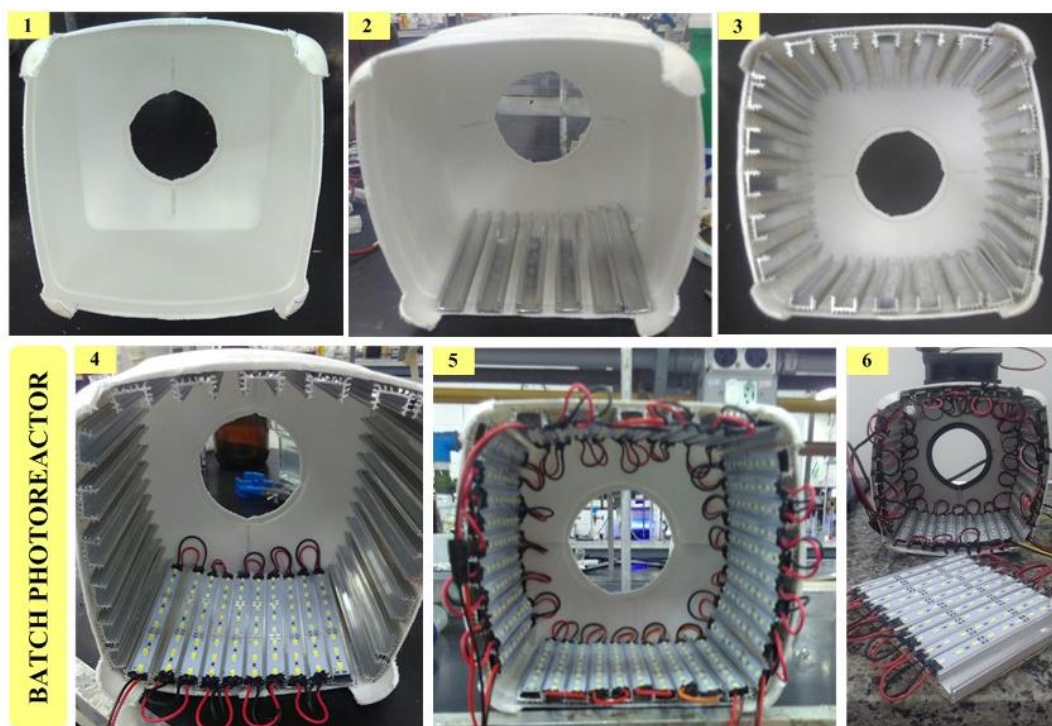


Figure 12. Step-by-step batch photoreactor assembly.

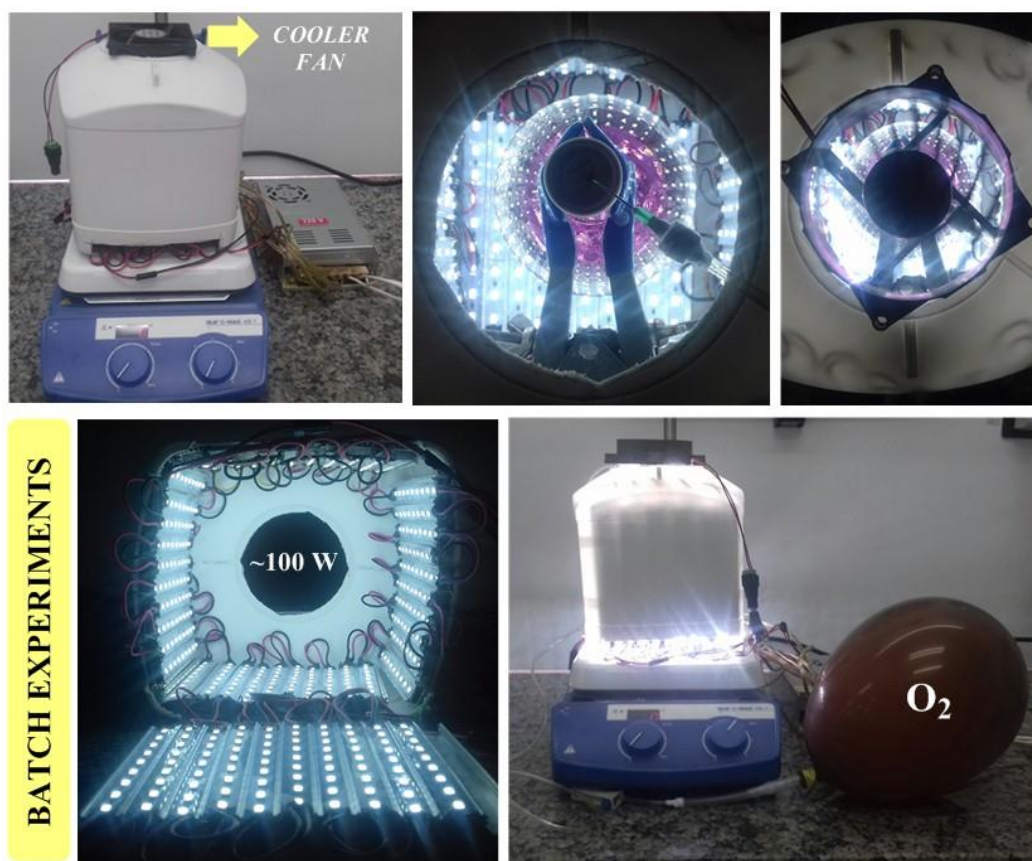


Figure 13. Setup for photochemical batch reactions.

The flow photoreactor was constructed from a reagent packaging can from Sigma-Aldrich (approximately 30 cm in length and 16 cm radius, Figure 14). The black pieces attached to it support and centralize the tubular reactor. Furthermore, two holes were drilled into the can for a PFA tubing inlet and outlet, and a lamp nozzle and computer fan were fastened to the bottom. In addition to the central LED lamp, aluminum-based LEDs tapes were also matched to the reactor walls, totalizing 100 W of power (30 W central lamp and 70 W side LEDs).



Figure 14. Construction of photochemical reactor for continuous flow reactions.

A glass cylinder wrapped with PFA (perfluoroalkoxy polymer) tubing (12 m, I.D.:0.065 in and O.D.: 0.125 in - Volume 23 mL) was positioned therein. To avoid heating of the system, one additional cooler fan was placed on top of the photoreactor. This ensured the photooxygenation would be performed at room temperature (Figure 15).

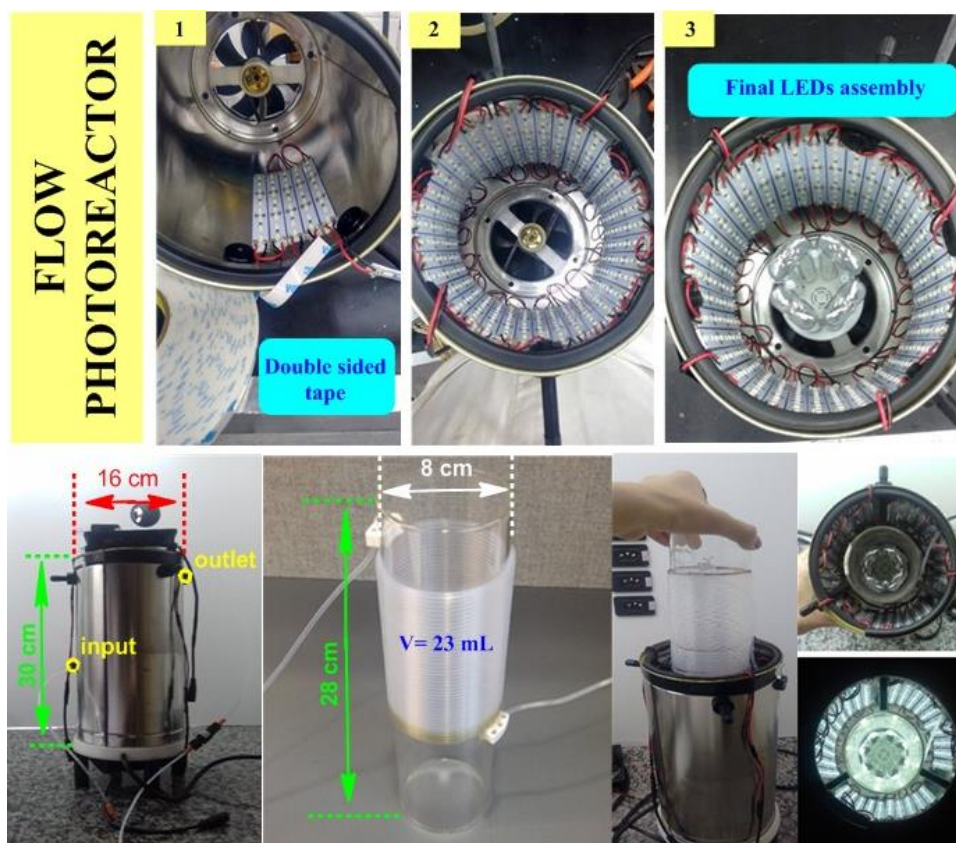


Figure 15. Final assembly of the photochemical reactor and PFA tubular reactor.

3.1.2. Tube-in-tube Reactor

Tube-in-tube reactors have been utilized in several organic transformations under continuous flow conditions with reactive gases.⁸² It is basically a tube inside another tube (Figure 16). The inner tube is made of a semi-permeable membrane and the outer tube commonly of PFA or PTFE. Usually, the former contains the solution of reagents and the latter, the gas. The use of permeable membranes facilitates the transport of gases in the liquid current, making possible to use highly toxic and dangerous gases in a controlled, safe and reliable way.

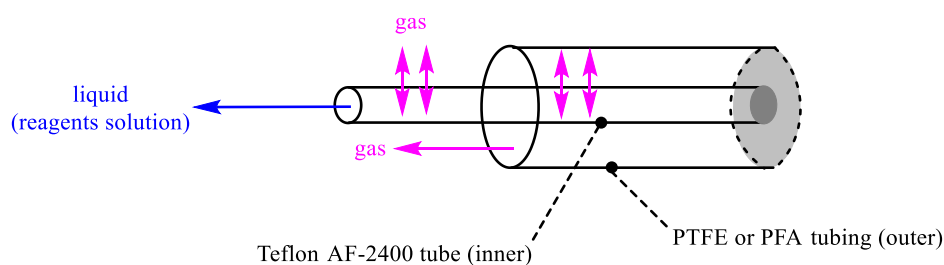


Figure 16. Simplified representation of a tube-in-tube reactor.

To perform the oxygenation of the solution containing the diene and the photocatalyst, we constructed a simple tube-in-tube reactor with inexpensive materials. It was based on the model developed by the Steven Ley group.^{82e} In our design, an acrylic sheet was used as a support for the manometer and tubular reactor, the latter made of PFA external tube (1.4 m) and a TeflonAF-2400[®] (1.0 mm O.D. and 0.8 mm I.D.) porous inner tube (1.5 m) (Figure 17). The assembly of this reactor involves some modifications in relation to the original one by Steven Ley, especially the tightening and connections.

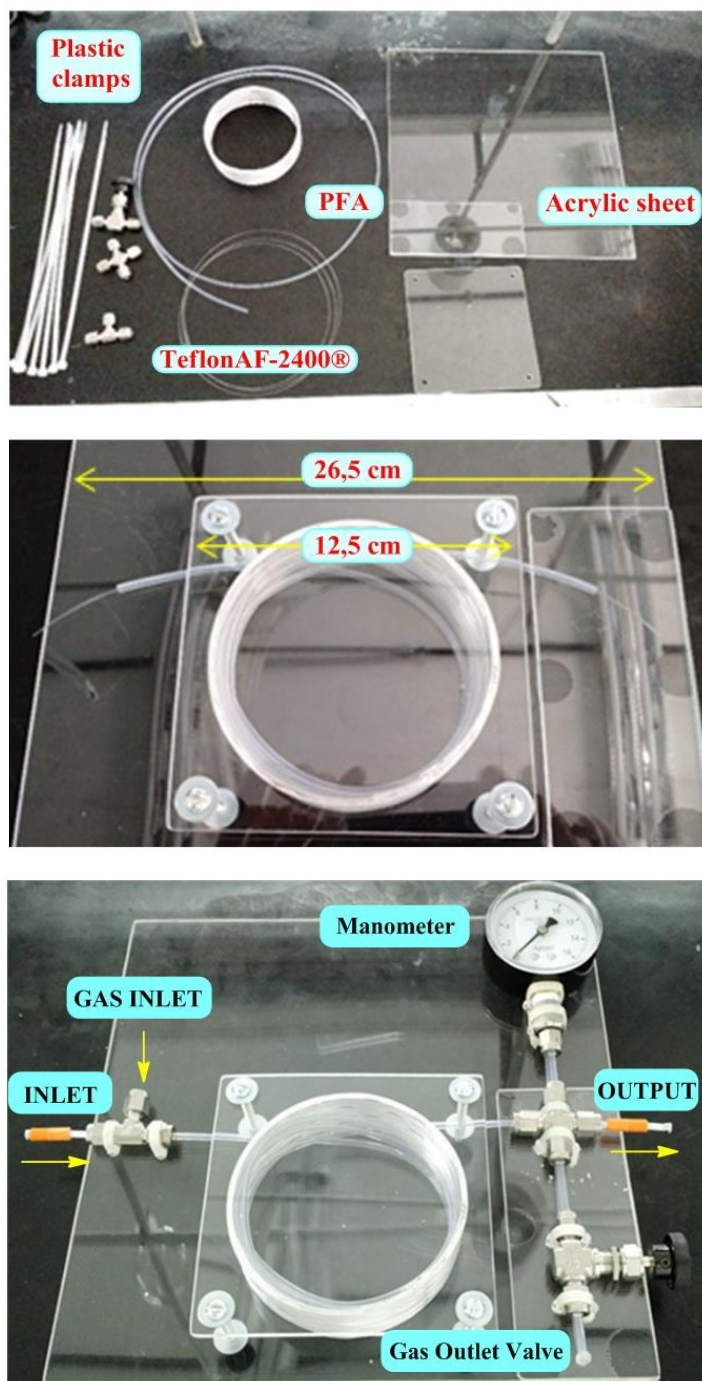


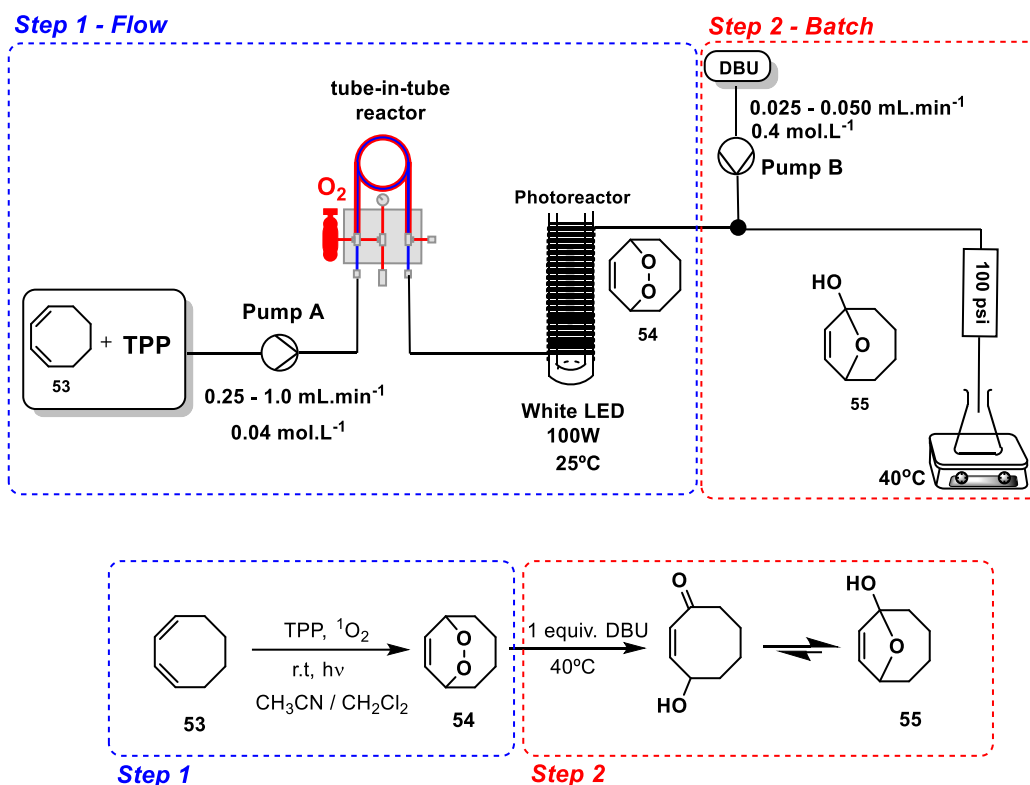
Figure 17. Tube-in-tube reactor built in our group.

3.2. Continuous Endoperoxidation Followed by Rearrangements in End-to-end Approaches

The studies were initiated by the evaluation of endoperoxidation conditions of *cis,cis*-1,3-cyclooctadiene (**53**) (Scheme 11). Diene **53** was selected for methodology development due to its well-known endoperoxide stability, enabling the evaluation of a series of variables and reaction conditions.

Our research group has been working for many years with the synthesis of porphyrins and their derivatives. We elected TPP as the photocatalyst for the photooxygenation reactions. It can be easily obtained in large amounts with methodologies developed by our group.⁸³ In previous experiments, we noticed when TPP is employed together with white LED as light source instead of FLC, higher yields and lower residence times were obtained. This observation relies on the fact the broad emission spectra of the white LED (480–700 nm) coincides with the porphyrin absorption bands (500–670 nm).^{58f}

After some exploratory tests in batch, continuous flow studies began using the assembly shown in Scheme 11. Pump A was used to inject the solution containing diene **53** and *meso*-tetraphenylporphyrin (TPP) in CH₃CN:DCM (2:1) through the tube-in-tube reactor pressurized with O₂.



Scheme 11. Diene **53** photooxygenation and Kornblum-DeLaMare rearrangement – Flow/Batch setup to initial studies.

3.2.1. Development of the methodology

We decided to carry out the photooxygenation (Step 1) under continuous flow conditions and study the KDM rearrangement (Step 2) in batch simultaneously by reacting the endoperoxide **54** after collection. A syringe pump (Pump B) was used to slowly inject a DBU solution (1 equiv.) to simulate future end-to-end transformation experiments. In this setup, a 100 psi BPR was also adapted at the end of the photochemical reactor, thus enabling the reaction of endoperoxidation in a pressurized medium with high amounts of dissolved oxygen (*ca.* 1:1 v/v).

Three flow rates (0.25, 0.50 and 1.0 mL.min⁻¹) were evaluated (Tables 1–3) in order to find the best residence time for the endoperoxidation step. For the batch KDM rearrangement (Step 2), a 0.4 mol.L⁻¹ DBU solution at reduced flow (0.025–0.05 mL.min⁻¹) was employed, keeping the batch transformation at 40 °C; DBU flow rate was

maintained ten times lower in relation to the diene flow rate solution in order to avoid a very large dilution during the rearrangement. After collecting the reaction content, the reaction was warmed from room temperature to 40 °C for 45 min in all experiments until all the endoperoxide **54** were consumed.

The results obtained at 1.0 mL.min⁻¹ flow rate (Pump A) are depicted in Table 1. From 0.1 to 0.5 mol% of **TPP** no significant differences in the yields were obtained (21–36%) with the best productivity (9.6 g.day⁻¹) and yield (36%) as shown in entry 4 (Table 1). However, given the low residence time into the photochemical reactor, in all the conditions the starting material **53** was partially recovered.

Table 1. Checking of **TPP** loading at 1.0 mL.min⁻¹ (Pump A).

Entry ^{a,b,c}	TPP (mol%)	Yield (55) (%)	STY ^e (g/day)
1	0.1	21	5.5
2	0.2	29	7.5
3	0.3	34	9.1
4	0.4	36/35 ^d	9.6/9.3 ^d
5	0.5	33	8.6

^a 3 mmol of the substrate **53** in a mixture CH₃CN/DCM (2:1), 75 mL at 0.04 mol.L⁻¹

^b 1 equiv. of DBU for the batch rearrangement step (Step 2)

^c photoreactor residence time = 23 min

^d double checked experiment for reproducibility confirmation

We decided to test a flow rate at 0.5 mL.min⁻¹ (Table 2) and obtained significant yield increases (37–62%) with a throughput 7.7 g.day⁻¹ for **TPP** at 0.4 mol% (Entry 4) as the best result balancing both yield, throughput and the lower **TPP** loading.

Table 2. Checking of **TPP** loading at 0.5 mL.min⁻¹ (Pump A).

Entry ^{a,b,c}	TPP (mol%)	Yield (55) (%)	Throughput (g/day)
1	0.1	37	4.9
2	0.2	44	5.8
3	0.3	53	7.0
4	0.4	56/59 ^d	7.4/7.7 ^d
5	0.5	62	8.2

^a 3 mmol of the diene **53** in a mixture CH₃CN/DCM (2:1), 75 mL at 0.04 mol.L⁻¹

^b 1 equiv. of DBU for the batch rearrangement step (Step 2)

^c photoreactor residence time = 46 min

^d double checked experiment for reproducibility confirmation

Once the flow rate was adjusted to 0.25 mL.min⁻¹ significant improvements in yields were observed (60–78% – Table 3), although with lower productivity compared to the previous flow at 0.5 mL.min⁻¹. As such, we selected the conditions of Entry 4, Table 2 as the optimal setup.

Table 3. Checking of **TPP** loading at 0.25 mL.min⁻¹ (Pump A).

Entry ^{a,b,c}	TPP (mol%)	Yield (55) (%)	Throughput (g/day)
1	0.1	60	4.0
2	0.2	67	4.4
3	0.3	72	4.8
4	0.4	74/77 ^d	4.9/5.0 ^d
5	0.5	78	5.1

^a 3 mmol of the diene **53** in a mixture CH₃CN/DCM (2:1), 75 mL at 0.04 mol.L⁻¹

^b 1 equiv. of DBU for the batch rearrangement step (Step 2)

^c photoreactor residence time = 92 min

^d double checked experiment for reproducibility confirmation

Two additional variables were analyzed in order to check the influence of diene **53** concentration (Table 4), as well as the influence of O₂ pressure in the tube-in-tube reactor. For the evaluated conditions, the increase of the diene **53** concentration decreases both the yields and throughput, therefore we selected 0.04 mol.L⁻¹ as the optimum concentration of starting material. It is important to note that in entries 3–7 (Table 4), precipitation of the photocatalyst **TPP** was observed. However, even under conditions where **TPP** remained solubilized (Entry 6, Table 4) the results were not higher than those of Entry 2, Table 4, which are identical to those of Entry 4, Table 2 as previously optimized.

Finally, the influence of different oxygen pressures was evaluated by using all the previous optimized conditions and keeping the pressure into the tube-in-tube membrane reactor at 4, 6 or 8 bar. With no significant changes in yields (54–58%) we decided to keep 6 bar as the optimum pressure of O₂ (56%).

Table 4. Influence of different diene **53** concentration.

Entry ^{a,b}	[53] ^c (mol.L ⁻¹)	Yield (55) (%)	Throughput (g/day)
1	0.02	50	6.6
2	0.04	56/59 ^d	7.4/7.7 ^d
3	0.08	47 ^e	6.1
4	0.08	49 ^f	6.5
5	0.12	38 ^{e,f}	5.0
6 ^g	0.12 ^g	40 ^g	5.2 ^g

^a 1 equiv. of DBU for the batch rearrangement step (Step 2)

^b photoreactor residence time = 46 min and flow rate at 0.5 mL.min⁻¹ (Pump A)

^c using CH₃CN/DCM (2:1) mixture as solvent and 0.4 mol% of **TPP**

^d double checked experiment for reproducibility confirmation

^e it was observed a partial **TPP** precipitation

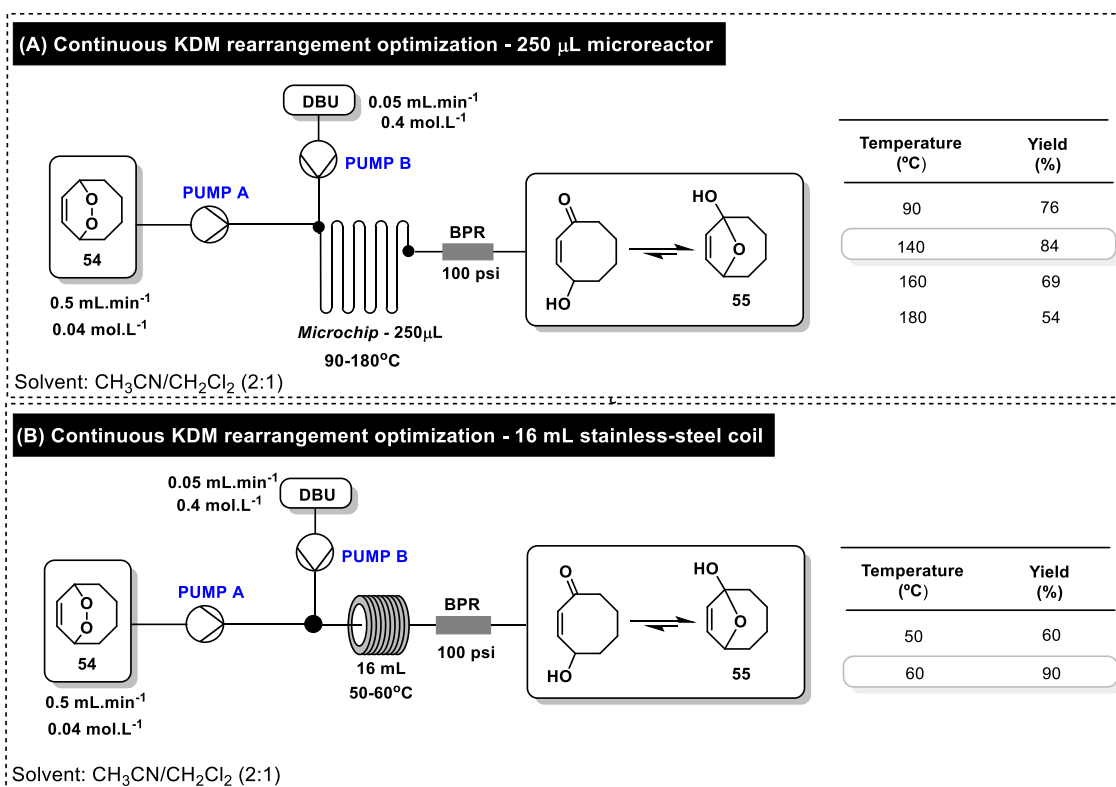
^f 1:1 CH₃CN/DCM mixture was used to avoid **TPP** precipitation.

^g carried out in DCM.

The Kornblum-DeLaMare rearrangement is often assisted by basic catalysis and heating, but always after the endoperoxide preparation. It is noteworthy that this rearrangement has not been thoroughly explored due to the instability of the formed intermediates which may be explosive. To date, there are no reports on continuous flow studies or even scaled up protocols. Our results show the initial endoperoxidation of diene **53** in the presence of DBU (catalyst for second step) does not occur. This is likely due to the photochemical quenching that the DBU causes in **TPP**, thus preventing the formation of singlet oxygen. The integration of separated steps was necessary for having the end-to-end protocol.

Hence, integration studies of the continuous end-to-end photooxygenation and KDM rearrangement were initiated using a 250 μ L microchip (Scheme 12A). For the rearrangement optimization under continuous flow conditions, the purified endoperoxide **54** was used to evaluate separately how it is processed, without any losses caused by byproducts from photooxygenation stage.

The flow rate of **53** + **TPP** and temperature of the KDM rearrangement were the same as previously optimized ($0.5 \text{ mL}\cdot\text{min}^{-1}$ and $40 \text{ }^\circ\text{C}$). However, at $40 \text{ }^\circ\text{C}$ the endoperoxide **54** was not completely converted in **55**. Rearrangement temperatures were raised to $90\text{--}180^\circ\text{C}$ (Scheme 12A). The best result was obtained at $140 \text{ }^\circ\text{C}$ (84% yield). Despite the success of these results, the microchip reactor became noticeably clogged. To address this problem the KDM rearrangement was also performed using a 16 mL tubular stainless-steel reactor ($1/8''$ O.D.) (Scheme 12B) giving the compound **55** in 90% yield at $60 \text{ }^\circ\text{C}$ in a more robust and reproducible manner.

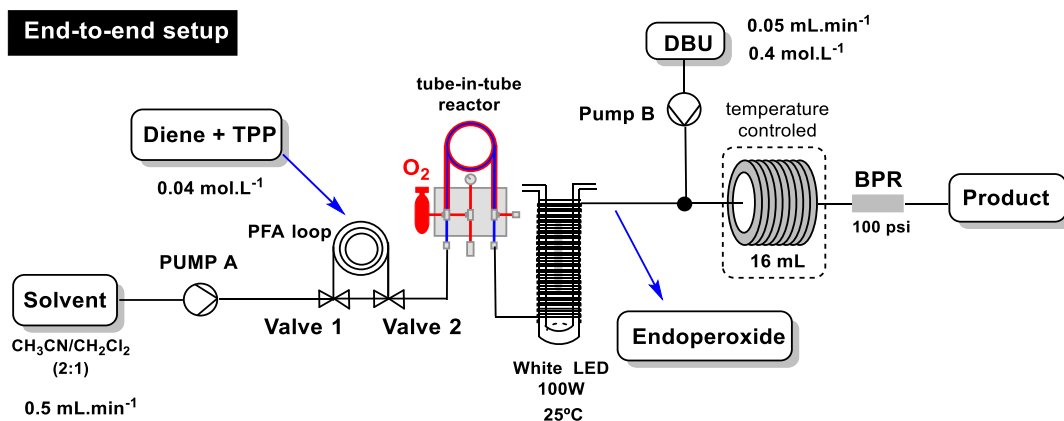


Scheme 12. Continuous KDM rearrangement optimizations. A) by using a $250 \mu\text{L}$ microchip; B) by using a 16 mL stainless steel coil reactor.

3.2.2. End-to-end Approach

The telescoping of all the steps was performed (Scheme 13) with an additional loop in the beginning of the setup to avoid direct reagent contact with the pump. The first end-to-end experiment using all the previous optimized steps (Scheme 13 and Figure 18)

yielded the compound **55** in 55% (isolated yield). Compared to the yields of the independent steps (59% and 90%, thus 53% overall yield), the overall yield was slightly higher, confirming the efficiency of the setup.



Scheme 13. End-to-end setup for photooxygenation followed by KDM rearrangement.

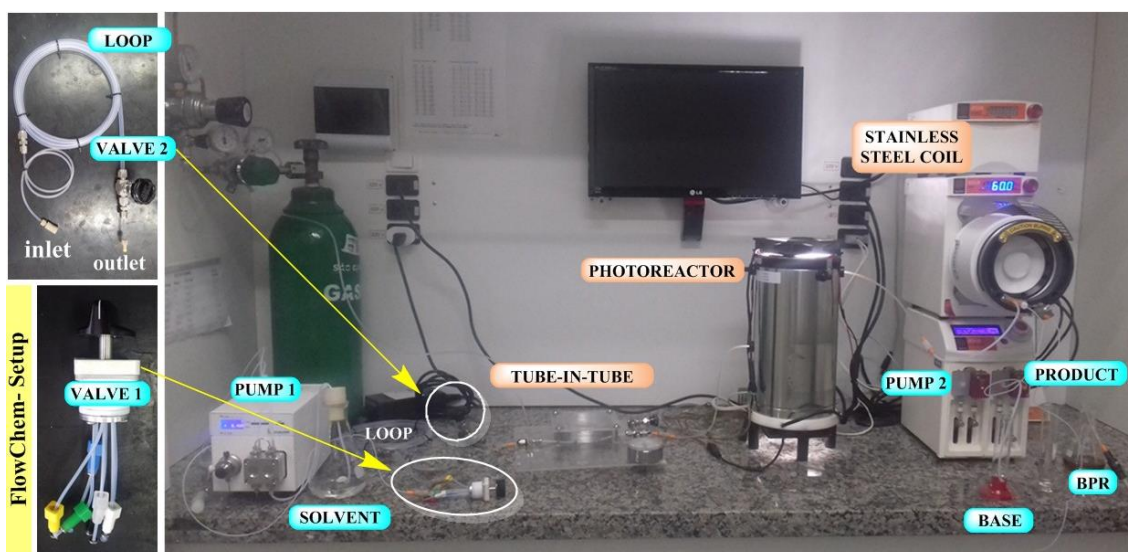


Figure 18. Final setup for photooxygenations and KDM rearrangement in continuous flow conditions.

We have tested the process intensification of this end-to-end protocol in a long-run experiment (9 h). The scale-up from 3 mmol to 10 mmol was accomplished giving the product **55** in 63% overall yield (*ca.* 1.0 g), that is, almost 80% per step.

In order to compare the efficiency of our flow setup, we chose the optimum conditions to obtain **55** continuously (End-to-end approach, Scheme 13), and repeated the exact same reaction using our photochemical batch reactor instead (100 W). The oxygenation of the solution containing TPP and diene was carried out by bubbling oxygen onto it using a simple latex balloon (1 atm), which was maintained throughout the reaction time (Figure 19). After keeping the mixture reacting in a conventional vessel for 46 and 32 min (Photooxygenation step and KDM rearrangement, respectively), **55** was obtained in 16% overall yield. The developed continuous setup delivers 55% more of the desired product without increasing the reaction time.

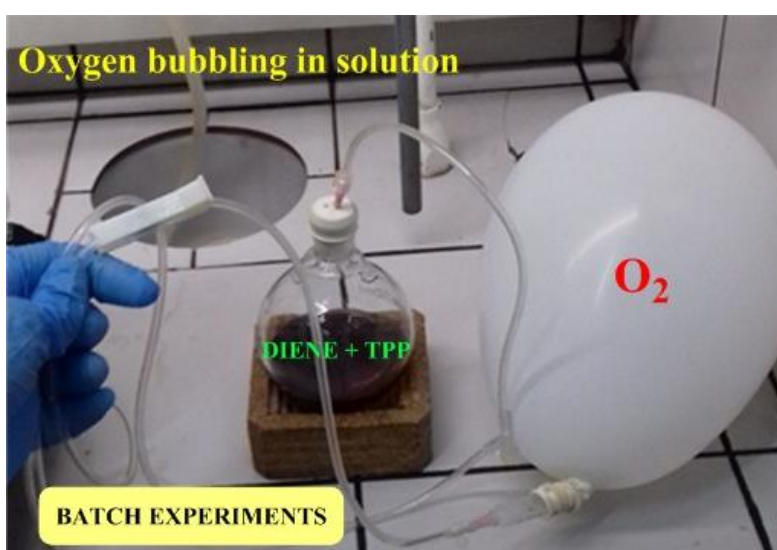
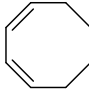
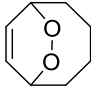
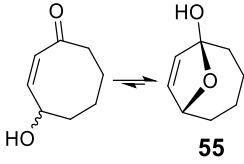
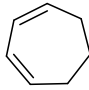
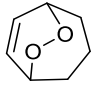
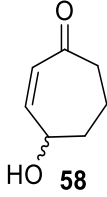
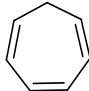
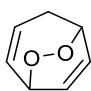
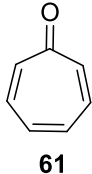
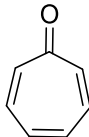
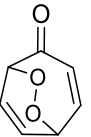
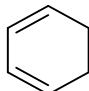

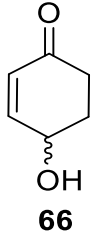
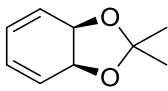
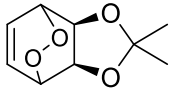
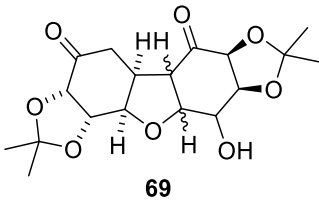


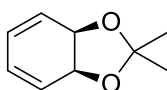
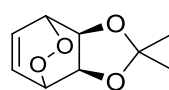
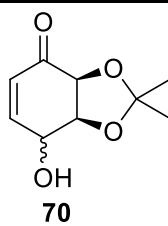
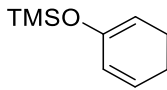
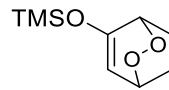
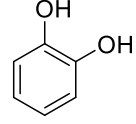
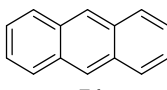
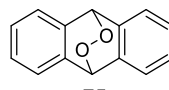
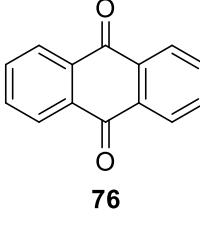
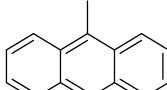
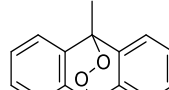
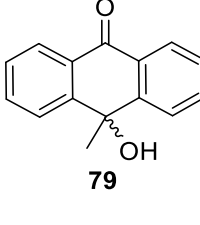
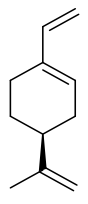
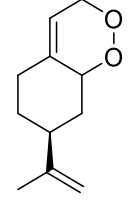
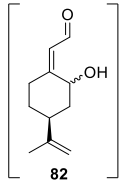
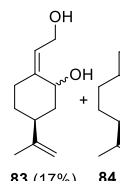
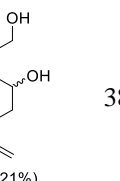
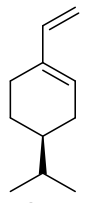
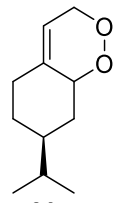
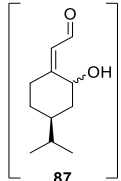
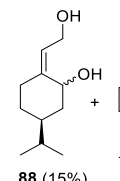
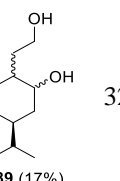
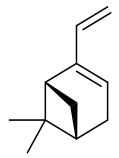
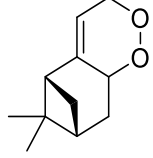
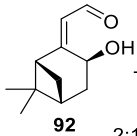
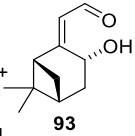
Figure 19. Oxygenation of the solution containing the **TPP** + **diene** – batch experiments.

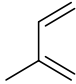
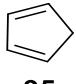
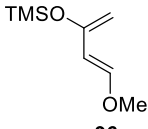
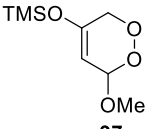
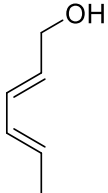
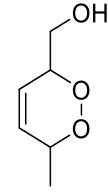
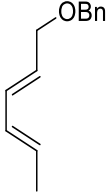
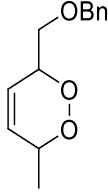
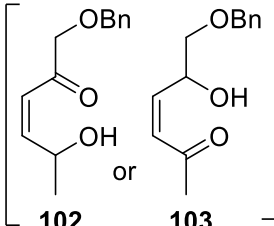
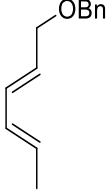
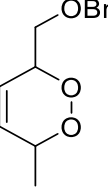
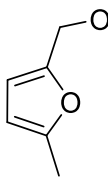
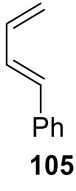
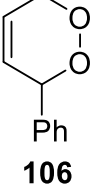
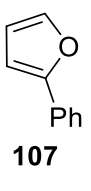
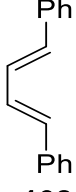
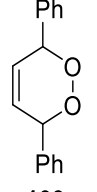
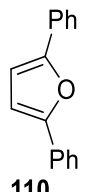
3.2.3. Methodology Application - Reaction Scope

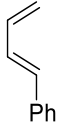
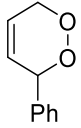
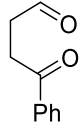
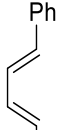
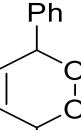
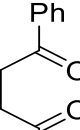
The substrates below were used to explore different reactivities, instabilities of the endoperoxide intermediates, tolerance of functional groups, and possible applications of the rearranged products (Table 5).

Table 5. Scope for the developed protocol.

Entry	Diene	Endoperoxide	Base	T(°C)	KDM reaction product	Overall Yield (%) ^a
1	 53	 54	DBU	60	 55	55
2	 56	 57	DBU	60	 58	92
3	 59	 60	DBU	25	 61	36
4	 61	 63 (62%)	DBU or Et ₃ N		Complex mixture	-
5	 64	 65	DBU	60(80)	 66	29(67) ^b
6	 67	 68	DBU	25	 69	10 ^c

7			Et ₃ N	25(0)		13(29) ^d
8			DBU	25		15
9			DBU	60		74 ^e
10			DBU	60		96
11			DBU	80		38
						83 (17%)
						84 (21%)
12			DBU	80		32
						88 (15%)
						89 (17%)
13			DBU	60		22
						93
					2:1	

14		Complex mixture	-	-	-	-
	94					
15		Complex mixture	-	-	-	-
	95					
16			DBU or Et ₃ N	25	Complex mixture	-
	96	97				
17			DBU or Et ₃ N	25	Complex mixture	-
	98	99 (57%)				
18			Et ₃ N	60		-
	100	101			102 or 103	
19			Et ₃ N and after, PTSA	60		42 ^f
	100	101			104	
20			Et ₃ N and after, PTSA	0		29 ^g
	105	106			107	
21			Et ₃ N and after, PTSA	0		58 ^f
	108	109			110	

22	 105	 106	Et ₃ N	25	 111	42
23	 108	 109	Et ₃ N	60	 112	80

^a isolated yield after purifications by chromatography.

^b 29% yield with the rearrangement temperature at 60 °C and 67% yield at 80 °C.

^c in the presence of DBU only the dimer **69** is formed.

^d The KDM rearrangement performed in the presence of Et₃N yielded exclusively the hydroxyenone **70** at 25 °C (13% yield) and at 0 °C the yield was improved to 29%.

^e the reaction was performed in DCM due to the precipitation of anthraquinone (**76**) in CH₃CN, which caused clogging.

^f in this case the reaction was performed starting from a solution of diene at 0.04 M and 0.4 mL.min⁻¹ (Pump A). Et₃N solution (0.4 M) was pumped at 40 μL.min⁻¹ (Pump B), and PTSA solution (0.05 M) was pumped at 0.4 mL.min⁻¹. It was necessary for complete starting material consumption in the photooxygenation step.

^g in this case the reaction was performed starting from a solution of diene at 0.04 M and 0.25 mL.min⁻¹ (Pump A). Et₃N solution (0.4 M) was pumped at 0.025 mL.min⁻¹ (Pump B), and PTSA solution (0.05 M) was pumped at 0.25 mL.min⁻¹. It was necessary to completely consume the starting material in the photooxygenation step.

As expected, some modifications in the methodology were needed for some substrates as highlighted in Table 5. These small changes, especially in the KDM rearrangement temperatures, were carried out only when necessary. During the accomplishment of the scope studies, exploratory experiments of isolated steps under continuous conditions were carried out to verify the total consumption of the substrates, endoperoxide formation and rearrangements.

For Entry 2 it was possible to apply the standard optimized conditions and convert the diene **56** to the hydroxyenone **58** in 92% overall yield. The cycloheptatriene (**59**) was efficiently photooxygenated, and the endoperoxide **60** was converted to the corresponding hydroxyenone (entry 3), and after water elimination, tropone (**61**) was obtained in 36% overall yield. This result is quite relevant due to the number of steps performed and the lack of more efficient methodologies in the literature for the production of this important synthetic intermediate.⁸⁴ The use of tropone (**61**) as the diene (Entry 4) did not yield any rearrangement product that could be isolated, although we isolated the corresponding endoperoxide **63** (58%) in an exploratory photooxygenation experiment.

At Entry 5, the product **66** was obtained starting from **64** in 29% yield when the rearrangement step was carried out at 60 °C, however, when the rearrangement temperature was adjusted to 80 °C the compound **66** was obtained in 67% yield.

The photooxygenation of the diene **67** was monitored in an experiment under continuous flow conditions to evaluate the occurrence of endoperoxidation under the optimized methodology parameters. Total consumption of the starting material was observed. By using DBU (Entry 6) for the rearrangement step only traces of the product **70** were observed, with preferential formation of dimer **69** (10%). On the other hand, by using Et₃N (Entry 7), the dimer **69** was undetected. Preferential formation of **70** in 13% yield was attained by holding the rearrangement temperature at 25 °C, or 29% at 0 °C. Compound **70** is considered an important intermediate in the synthesis of *myo*-inositol.⁸⁵

The reaction of diene **71** yielded the catechol (**73**) in 15% overall yield (Entry 8). Loss of the TMS protective group and aromatization were observed. There are examples in the literature in which silicon protections can be removed in the presence of DBU.⁸⁶

Reactions of derivatives **74** and **77** (entries 9 and 10) efficiently yielded products **76** and **79** in 74 and 96% yield, respectively. In the case of substrate **74** an additional stage of oxidation of the hydroxy-ketone intermediate was observed since only anthraquinone **76** was efficiently isolated (74% yield).

Some derivatives with acyclic or with at least one exocyclic double bond such **80**, **85**, **90** and **94** were also tested and are shown in entries 11–14. At entries 11 and 12, two naturally occurring dienes **80** and **85** were tested. In both cases, there was complete consumption of dienes, and stable and isolable endoperoxides were observed. However, attempts to isolate the KDM rearrangement products to obtain **82** and **87** were unsuccessful. Due to the possibility of degradation of aldehydes **82** and **87**, we reacted the crude reaction mixture with NaBH₄ (2 equiv.). This allowing the isolation of corresponding **83** (17%) and **84** (21%) diols (Entry 11), and **88** (15%) and **89** (17%) (Entry 12). Similarly, the reaction of diene **90** yielded a stable endoperoxide intermediate **91** (52%). An end-to-end experiment gave the compounds **92** + **93** (2:1) in 22 % yield (Entry 13).

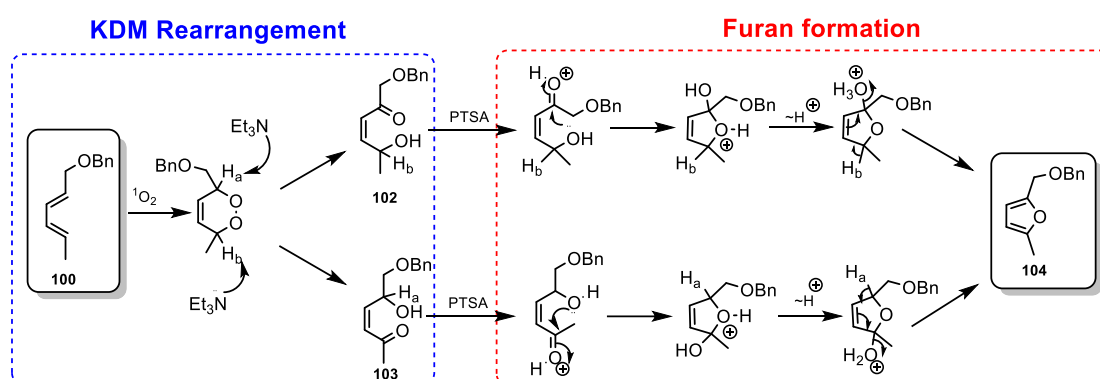
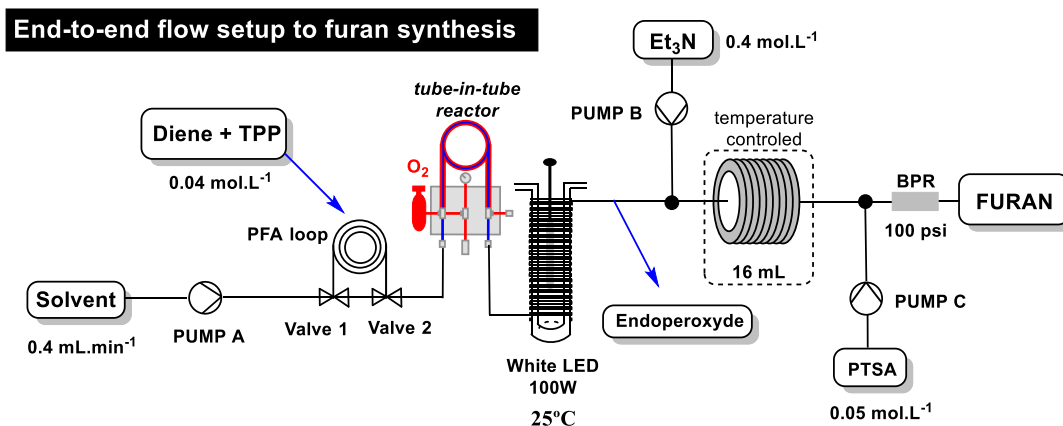
As expected, isoprene (**94**) (Entry 14) and cyclopentadiene (**95**) (Entry 15) yielded complex mixtures in the first step. This is likely due to the occurrence of various organic

peroxides and [2 + 2] cycloaddition products with singlet oxygen or endoperoxide thermal rearrangements at room temperature.⁸⁷

Dienes **96** and **98** (entries 16 and 17) yielded the respective endoperoxides **97** and **99** during the exploratory experiments of the photooxygenation step. In the end-to-end processes however only complex mixtures were obtained.

As shown in Entry 17, endoperoxide **99** was efficiently prepared and isolated in 57% yield in exploratory experiments, though a very complex mixture occurred in the rearrangement step. In an attempt to circumvent this problem, the alcohol **98** was protected with a benzyl group, which yielded diene **100**. Photooxygenation of **100** (Entry 18) similarly yielded the corresponding endoperoxide. The KDM rearrangement in the presence of Et₃N or DBU (end-to-end protocol) resulted in the formation of a relatively polar major product (possible keto-alcohols **102** or **103**). When we tried to characterize **102/103** by ¹H NMR in CDCl₃ we confirmed the formation of furan **104**. TLC of the reaction product before and after NMR analysis was different. Probably, **102/103** rearranged to furan **104** in CDCl₃ (acid catalysis). To confirm, a sample of reaction mixture (**102/103**) was treated with PTSA (1.2 equiv. to neutralize the DBU and keep the medium slightly acid) in batch, which confirmed our suspicion. With the significance of this multistep transformation, we decided to adapt the flow setup with an in-line workup containing PTSA (Scheme 14) and the diene **100** was efficiently converted into furan **104** in 42% overall yield (Entry 19).

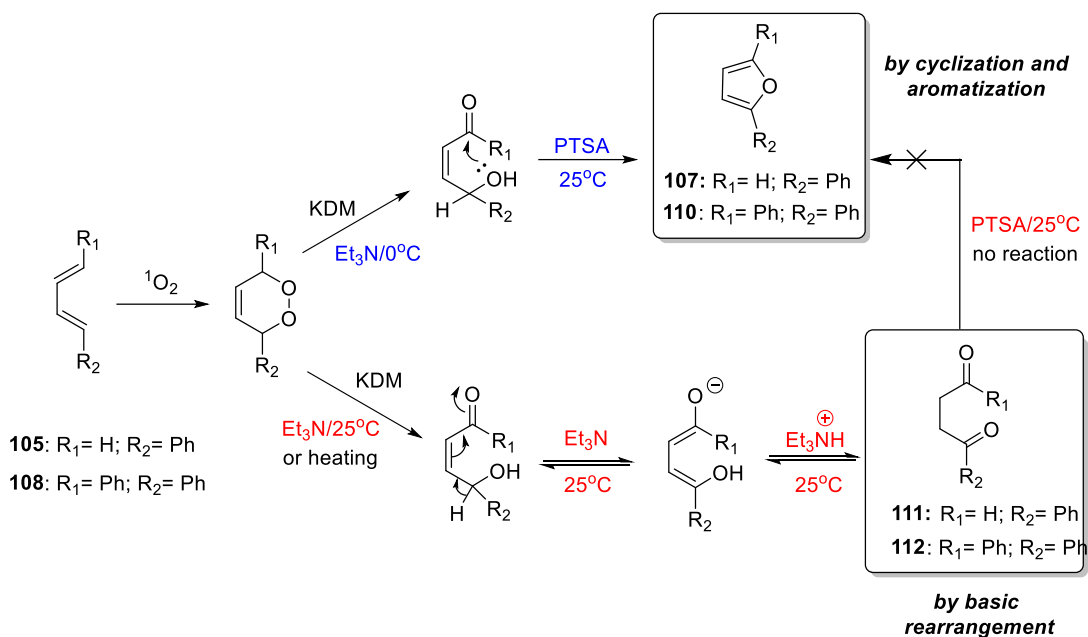
Dienes **105** and **108** were also submitted to the end-to-end reaction conditions of Scheme 14 and generated **107** (29%) and **110** (58%), respectively. This demonstrated the possibility of continuous end-to-end production of different substituted furans (entries 20 and 21). Similar results involving furan chemistry have been reported in the literature, but never under continuous conditions or even in an end-to-end protocol.^{88, 89}



Scheme 14. Continuous end-to-end assembly to furans synthesis and probable mechanism of furan formation.

Relevant results were observed starting from diene **105** and **108** in which the respective furans **107** (29% yield) and **110** (58% yield) are obtained if the KDM rearrangement is carried out at 0 °C with further in-line treatment with PTSA (entries 20 and 21). Only the respective dicarbonyl compounds **111** (42% yield) and **112** (80% yield) are isolated at 25 °C and 60 °C (entries 22 and 23, respectively) even after further acid treatment at the same temperature.

These results indicate that at 0 °C the keto-alcohol intermediates are produced and easily converted into the furan derivative under acid catalysis (Scheme 15). At higher temperatures there is an additional proton rearrangement yielding more stable dicarbonyl products that are more resistant to in-line transformation into the respective furans (Scheme 15).



Scheme 15. Further rearrangements of KDM products at different temperatures.

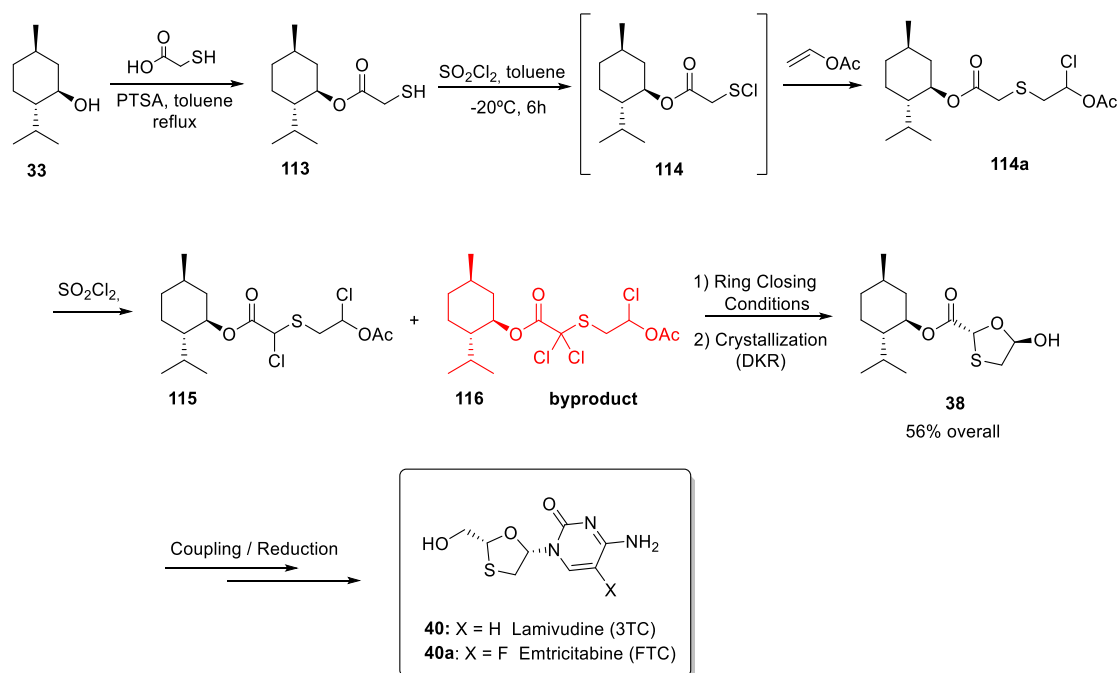
3.2.4. Partial Conclusions

The photooxygenation studies allowed us to explore a series of transformations in diene moieties involving a safe photooxygenation step with singlet oxygen to obtain endoperoxides followed by different rearrangements in a continuous approach. Relevant results were found, highlighting the ability of the setup to perform safe, reproducible and scalable multi-step transformations with multiple C-H oxidations. These studies open up a series of possibilities for the continuous scaled-up production of important intermediates, and serve as a proof of concept for several other synthetic methodologies seeking substituted furans and 1,4-dicarbonyl derivatives.

3.3. Continuous Synthesis of a New Intermediate for Lamivudine and Emtricitabine Production

3.3.1. A Brief Overview of Ongoing M4ALL Routes to 3TC

M4ALL has been working on two main routes to 3TC, herein called Route 1 (Scheme 16) and Route 2. They will not be described in detail since they are ongoing projects led by different members of the M4ALL team. Route 1 begins with a Fischer Esterification between L-menthol (**33**) and thioglycolic acid. The menthyl thioglycolate (**113**) is then treated with SO_2Cl_2 to produce the sulfenyl chloride intermediate **114**. Its reaction with vinyl acetate and SO_2Cl_2 , respectively, yields compound **115**. The dichlorinated intermediate **115** is submitted to specific cyclization conditions developed by our group in order to obtain oxathiolane **38**. The following steps to 3TC consist of the same reactional conditions described by Whitehead et al. (Scheme 16).⁹⁰



Scheme 16. M4ALL developed new route to lower cost 3TC/FTC production.

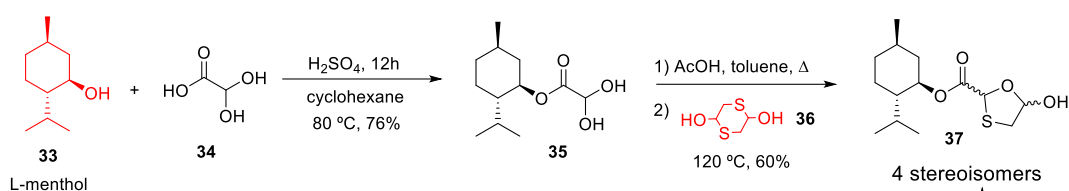
Synthesis of ester **113** is described in the literature.⁹¹ Compound **115** is unprecedented however, as well as its usage in the formation of the oxathiolane core. One of the main reagents responsible to inflate the price of 3TC is L-menthol, which constitutes around 35% of the synthesis' total cost. In theory the easiest way to reduce the price would be to replace the chiral auxiliary. In practice this does not prove to be a simple task. Not only does L-menthol (**33**) act as a chiral auxiliary, but its crystallinity is essential for the DKR process after formation of the hydroxyoxathiolane (**38**).

Efforts were invested toward finding a cheaper alternative. The main requirement of our goal was to find a chiral auxiliary to provide crystallinity to the oxathiolane. Most of the esters obtained with different auxiliaries were not crystalline. M4ALL team was able to find only one distinct chiral auxiliary, a lactate derivative, with similar characteristics to L-menthol.⁹² In addition to this route recently published, an alternative route has been explored and will be discussed in the next section. It is expected to be concluded mid-2020.

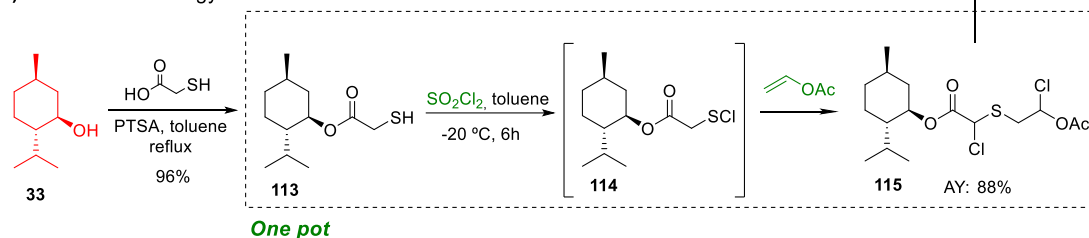
Although this route still makes use of L-menthol, its final cost is lower than the route currently used in the pharma industries, representing a victory for the M4ALL team. Besides L-menthol, 1,4-dithiane-2,5-diol (**36**) also presents an elevated price (Scheme 17). Instead of using **36**, M4ALL made use of a one pot step from **113** to **115**, the precursor of **37**. It utilizes cheaper reagents such as SO₂Cl₂ and vinyl acetate. Costs were further reduced by cutting solvent amount and catalysts loads.

L-menthol may be recovered at the end of the process. After completion of the reduction step with NaBH₄, the reaction mixture is quenched with dilute hydrochloric acid, adjusting the pH to 4–4.5. In this condition the 3TC and FTC are present in the salt formed in the aqueous layer. Washing the final solution with toluene and diethyl ether allows recovery of the menthol, which is then purified by further solvent washings.⁹³ The problem to this approach is that the recovery process is costly.

A) Whitehead et al. Methodology

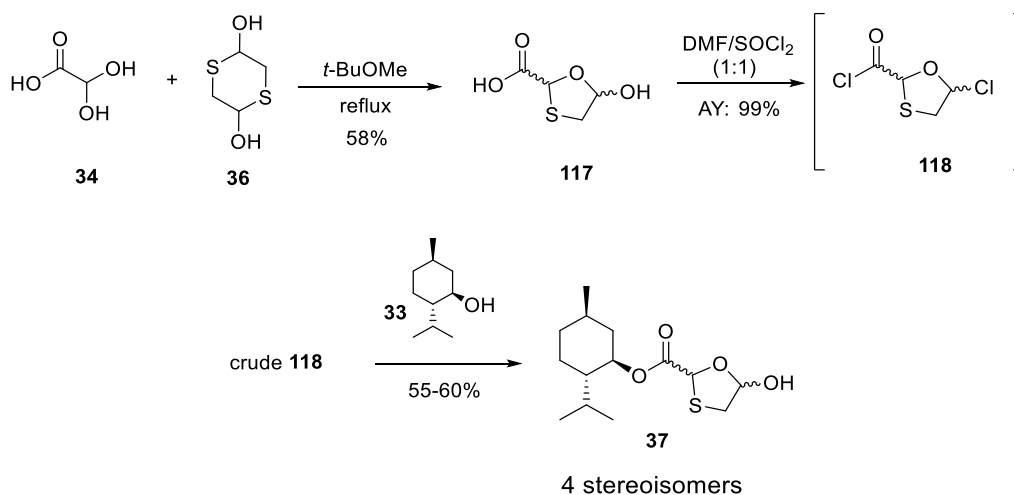


B) M4ALL Methodology



Scheme 17. Comparison between M4ALL and Whitehead routes to 3TC.

L-menthol (**33**) is always used at the beginning of the route, meaning a considerable percentage of the initial amount is lost during the steps taken to create the final drug. To minimize L-menthol (**33**) loss, M4All tried a late-stage menthol functionalization. Unfortunately, our first attempts did not result in the desired outcome, especially due to the lower menthol ester (**37**) yields (55–60%) (Scheme 18). The main reason for this unsuccessful approach is the sensitivity of the oxathiolane **117** to acidic media. Reaction of carboxy-oxathiolane **117** with thionyl chloride (SOCl_2) to form acyl chloride **118**, produces HCl. Despite all attempts, we were unable to remove the acid from the reaction in an efficient manner. The M4ALL team is still searching alternatives to replace 1,4-dithiane-2,5-diol (**36**) in the step to obtain the carboxy-oxathiolane **117** and investigating new conditions for cost-effective steps in this route.



Scheme 18. Late-stage functionalization approach – minimizing L-menthol (**33**) loss.

3.3.2. Lamivudine Synthesis by M4ALL

The reaction between thioglycolate **113** and SO_2Cl_2 is exothermic along with the reaction with vinyl acetate. In addition to the dichlorinated specie **115** that is shown in Scheme 16, a trichloride byproduct **116** can be formed. We hypothesized that a continuous approach would enable the achievement of a safe scale-up for these steps and improve their selectivity towards compound **115**.

Sulfuryl chloride reacts vigorously with thiols.⁹⁴ After addition of SO_2Cl_2 , the colorless solution of thiol **113** becomes yellow, indicating the sulfenyl chloride **114** formation (Scheme 16). The rate of temperature rise was enough to prompt a study of both the SO_2Cl_2 and vinyl acetate reactions using heat flow calorimetry. For the batch experiments we used EasyMax 102 for better temperature control during the course of the reaction, especially during reagent addition. Figure 20 shows the output of EasyMax HFCal runs.

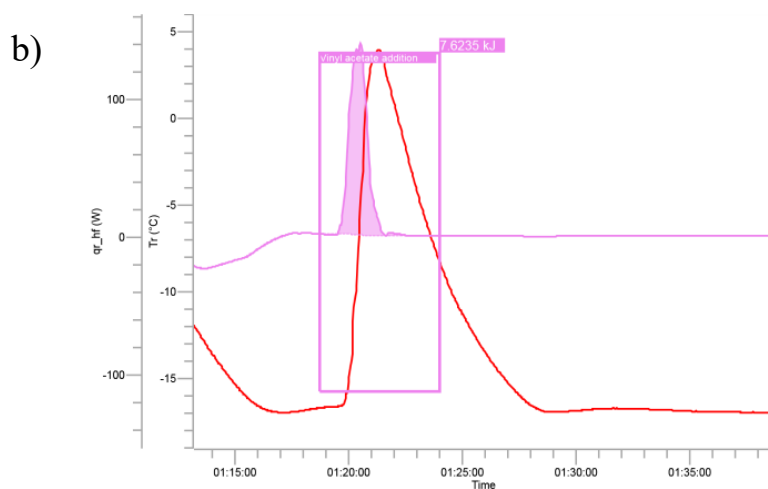
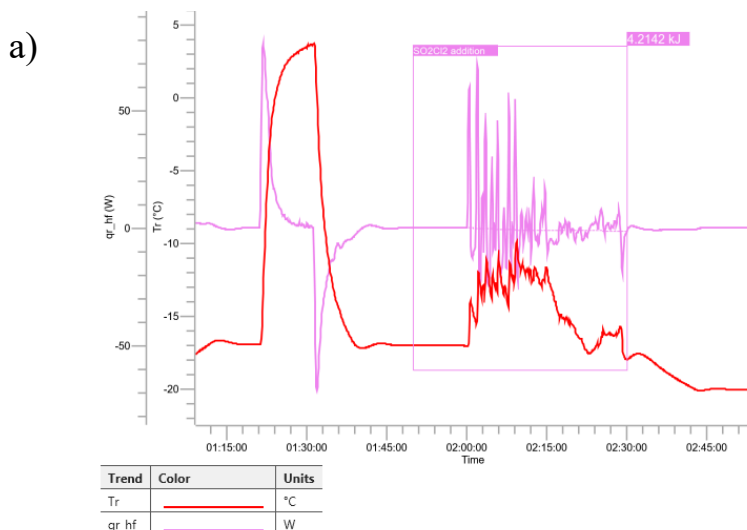
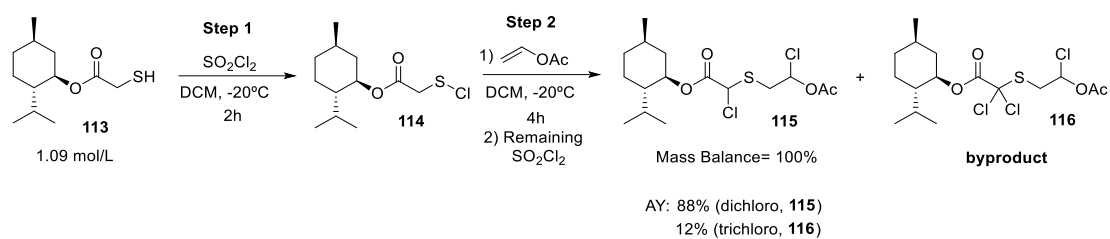


Figure 20. EasyMax HFCal runs – Reaction performed under N₂ atmosphere. a) Addition of 2.2 equiv. SO₂Cl₂ over 30 min; b) 2.0 equiv. vinyl acetate over 10 min.

Batch optimization experiments revealed that 2.2 equiv. of SO₂Cl₂ produced the best yields and selectivity. Two equivalents are necessary to support the multiple chlorinations (Step 1 and 2, Figure 20) and we presume the 10% excess is due to reagent decomposition. The heat released during the formation of sulfenyl chloride **114** (Step 1)

is 242 kJ/mol. The vinyl acetate addition (Step 2) involves both the sulfenyl chloride **114** addition to vinyl acetate and the chlorination of the alpha position to the ester **114a** to yield the desired dichloride **115**. For this sequence of reactions, the generated heat is 438 kJ/mol. We predict this translates to an adiabatic temperature rise of 102–133 °C for the Step 1 and 138–207 °C for Step 2, if the reaction is carried out in toluene. These highly energetic exotherms require either changing the reactor modality, slowing the reagent's addition or active cooling strategies (Figure 20).

Figure 21 displays the range of heat released during common exothermic reactions in kJ/mol.⁹⁵ Step 1 is comparable to nitration or Grignard reactions and Step 2 to hydrogenation of nitro compounds.

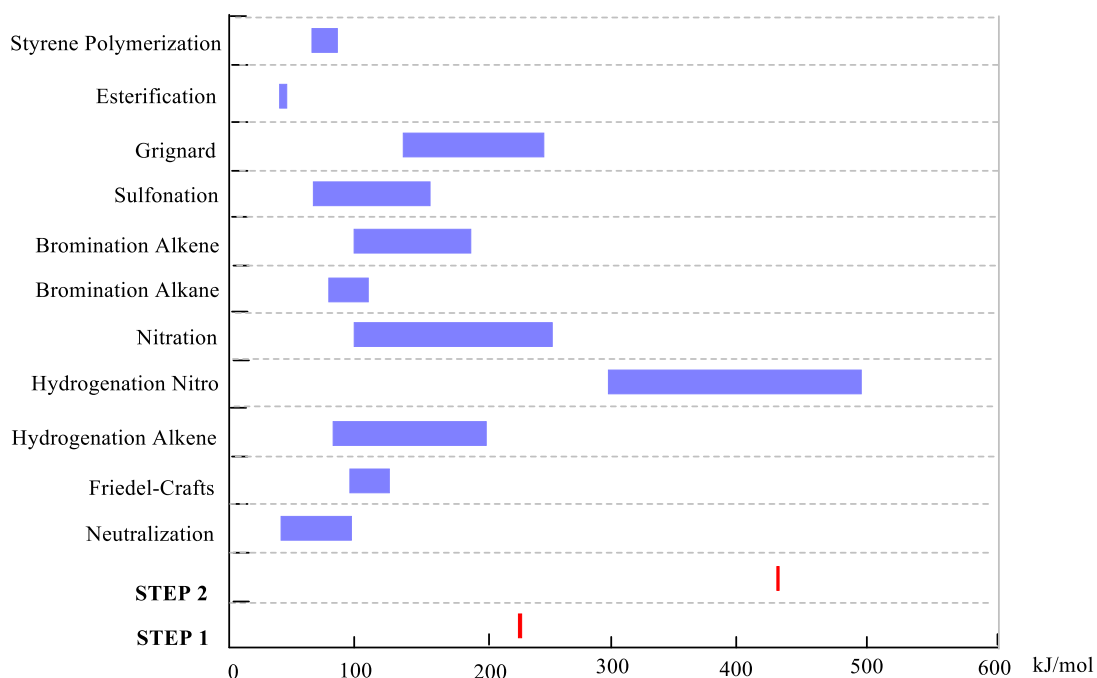
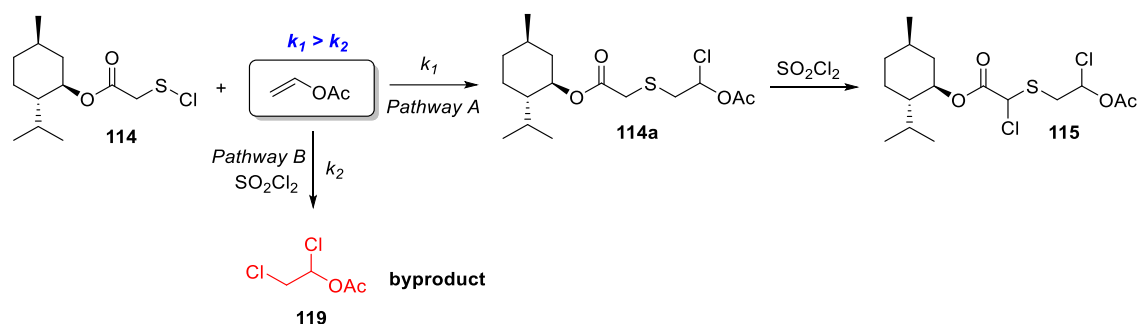


Figure 21. Comparative chart of the heat released in common exothermic reactions.

Vinyl acetate can also react with SO_2Cl_2 and form byproduct **119**. Although this reaction is not as favorable as the reaction with **114a**, traces of **119** are always detected in the final crude mixture (Scheme 19).



Scheme 19. Possible pathways involving vinyl acetate – A) Reaction with sulfenyl chloride **114** to form **114a**; B) Reaction with SO_2Cl_2 leading to byproduct **119**.

In order to acquire more information about these chemical transformations we performed a series of experiments with varying parameters such as temperature, reagent addition rate, and adding vinyl acetate before or after SO_2Cl_2 addition.

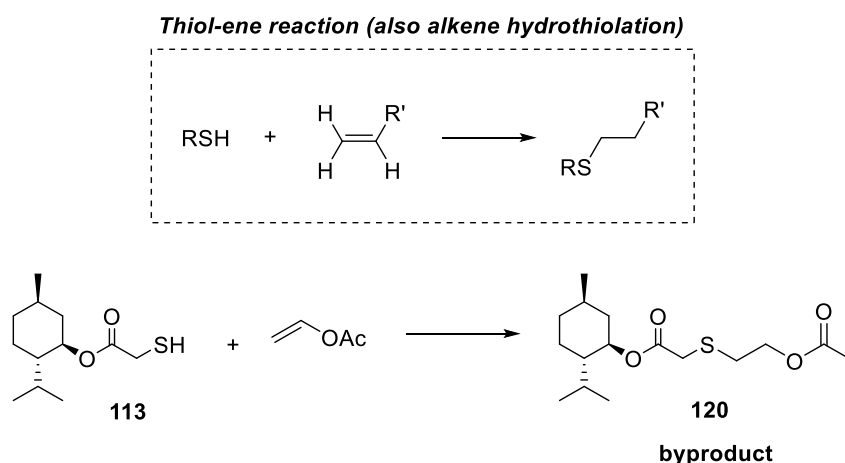
The formation of sulfenyl chloride **114** can be monitored by ^1H NMR. The reaction typically presents AY ranging from 95–100%. Increasing the temperature of Step 1 from $-20\text{ }^\circ\text{C}$ to $0\text{ }^\circ\text{C}$ or room temperature while Step 2's temperature is kept at $-20\text{ }^\circ\text{C}$ does not result in change in the final yield of compound **115**. In DCM, **115** was formed in AY= 88%. Toluene, a greener option, resulted in lower yields (AY= 78%). Choosing a green solvent to perform reactions with SO_2Cl_2 is complicated due to the lack of chemical compatibility of the reactive reagent with common organic solvents. Reactions in different solvents than chlorinated are scarcely found in the literature, with dichloromethane and chloroform being the most common.

The increase in temperature in Step 2 from $-20\text{ }^\circ\text{C}$ to $-5\text{ }^\circ\text{C}$ did not result in a different outcome. When the addition of vinyl acetate was performed at room temperature, lower yields as well as inferior mass balance were obtained.

During reaction optimization, we observed that reactions carried out under autogenous pressure provided better results. Small perturbations to the system headspace such as sampling the reaction by opening the reactor decreased yields at least 10%. The reaction produces a number of gaseous byproducts including HCl and SO_2 . We observed that **115** is more stable under acidic solutions, which may indicate HCl loss in the headspace can affect the yield. It appears lower reaction temperatures for Step 2 increases reaction tolerance to pressure changes. This is likely due to higher amounts of HCl gas

dissolving in the reaction mixture. The combination of exotherm and “pressure sensitivity” suggest a continuous flow approach might be an ideal modality to run this reaction sequence.

Regarding the order of addition of vinyl acetate, we noticed that when performed prior to the SO_2Cl_2 addition, considerably lower yields of **115** were obtained (AY= 57%). In this case, byproduct **120** was formed from the reaction of thiol **113** with vinyl acetate, confirmed by ^1H NMR analysis. This transformation is already described in the literature and corresponds to a click thiol-ene reaction also known as alkene hydrothiolation. Thiols can react with alkenes via a radical mechanism, which can be easily initiated in the presence of light.⁹⁶ Consequently, the addition of vinyl acetate must be performed only after all thiol **113** is converted to the sulfenyl chloride **114** (Scheme 20).



Scheme 20. Vinyl acetate addition prior to SO_2Cl_2 and byproduct **120** formation.

Since temperature changes did not result in any significant effect in Step 1, we fixed the addition time of SO_2Cl_2 in 15 min and $-20\text{ }^\circ\text{C}$ for both steps. We varied only vinyl acetate (2 equiv.) addition time (5, 15 and 60 min), analyzing the crude reaction right after completion of a four-hour period starting from the exact moment when the first volume of vinyl acetate was added to the EasyMax reactor containing the sulfenyl chloride **114a** solution. We noticed a direct relation between the addition time and the final amount of trichloro acetate **116** obtained from the over-reaction of **115** with SO_2Cl_2 (Table 6).

Table 6. Variation of the vinyl acetate addition time – 4.0 g scale reaction.

Entry	Vinyl acetate Add. time (min)	T (°C) increase ΔT	Monochloro 114a (%)	Dichloro 115 (%)	Trichloro 116 (%)	MB (%) After 6h
1	5	24	0	88	11	99
2	15	13	0	73	26	99
3	60	1.5	1	63	36	100

Byproduct **116** increases from 11% to 31% when vinyl acetate is added in a period of 5 and 60 min, respectively (Table 6, entries 1 and 3). The increase in temperature during the five-minute addition in Entry 1 is $\Delta T = 24$ °C, while the slower addition, Entry 3 (60 min), is $< \Delta T = 2$ °C. This is evidence that **116** formation is not associated with the higher temperature reached during the fast addition. Indeed, Entry 1 recovers its original temperature (-20 °C) in a matter of 10–15 min after vinyl acetate addition. It is safe to consider that Entry 3 presents a constant temperature during the whole process since the increase in temperature is small (< 2 °C). If trichloro acetate **116** formation was associated with the temperature increase, Entry 1 would contain a higher percentage of **116** compared to Entry 3.

These observations indicate that faster addition of vinyl acetate can lead to better yields of compound **115** and byproduct **116** formation can be suppressed. Performing such rapid additions in batch reactors can be troublesome. Dealing with exothermic reactions, especially during scale-up, is not an easy task. The safety risk is one of the main factors that must be taken into account.

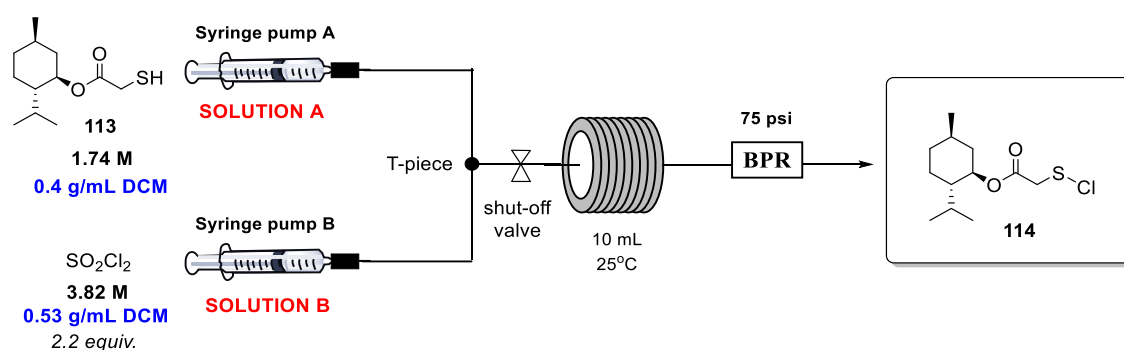
Although addition time is not important in Step 1, SO_2Cl_2 is an extremely reactive reagent with both corrosive and toxic properties. Its reaction with thiols leads to potentially harmful gases such as HCl and SO_2 . All these key observations created a perfect scenario where a continuous flow approach for both steps became imperative for the following reasons: i) increase safety to perform exothermic transformation in large scale; ii) work in pressurized system and avoid loss of gas intermediates; iii) fast addition can be achieved safely and reaction can be completed in reduced residence time.

3.3.3. Continuous Flow Experiments, System Design and Considerations

The two stages reaction between sulfonyl chloride and menthyl thioglycolate **113** and then vinyl acetate generates both SO₂ and HCl, as mentioned before. Resistant fluoropolymer tubing such as PFA or PTFE were considered for the reactor material as well as chemical resistant pumps and syringes. Due to the gas evolution, back-pressure regulators (BPR) were also utilized for the setup construction.

3.3.4. Surveying Reactor Configurations

As performed for the photooxygenations reactions with ¹O₂, we also analyzed this sequence of transformations step-by-step. The formation of sulfenyl chloride **114** in flow conditions was the first step to be studied. Chemyx syringes pumps were used to pump the reagents solutions, thiol **113** (1.74 M, 0.4 g/mL in DCM, Solution A) and SO₂Cl₂ (3.82 M, 0.53 g/mL in DCM, 2.2 equiv., Solution B). Two stainless-steel syringes from Harvard Apparatus (8 mL each) were used (Scheme 21 and Figure 22). Such syringes are intended for high pressure applications with strong resistance to the most aggressive liquids.



Scheme 21. Initial setup for sulfenyl chloride **114** synthesis.

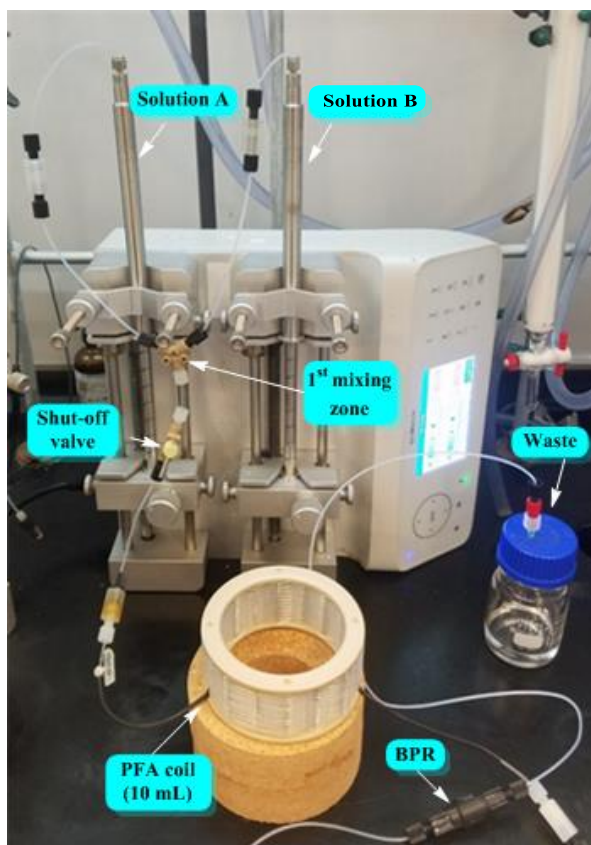


Figure 22. Initial system to study sulfenyl chloride **114** synthesis in continuous conditions.

The setup shown in Scheme 21 was built with PFA tubing (1/16" O.D.) and the reactor consists in a 10 mL coil from Vapourtec, with the same material and internal diameter. We used small diameter tubing to eliminate any mixing issues that a larger diameter could potentially enlist. Mixers were not used, only a simple T-piece. Due to the intense gas release, a 75 psi BPR was added at the end of the system to pressurize the reactor content (Scheme 21 and Figure 22). In addition, a shut-off valve was placed before the reactor to facilitate the swap of the two 8 mL syringes by a 50 mL containing solvent to push the material through the system. At the moment solutions A and B met each other in the T-piece, it is possible to observe change in the solution color from colorless to yellow, indicating the reaction between thiol **113** and SO_2Cl_2 to form **114** (Figure 23).

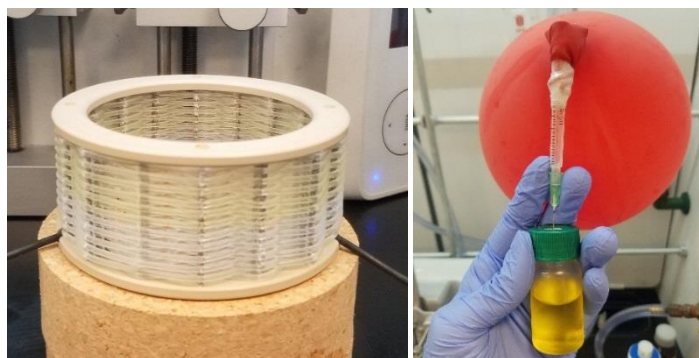


Figure 23. Change in color when sulfenyl chloride **114** is formed.

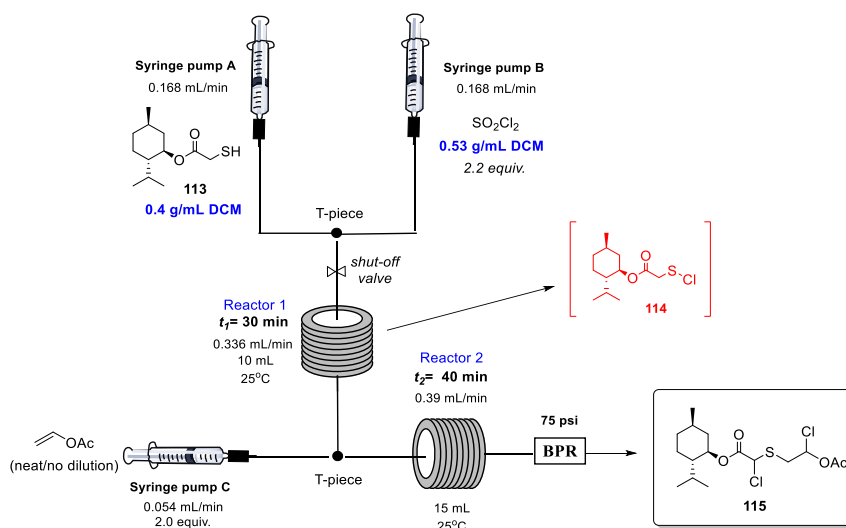
When a total flow rate of $0.336 \text{ mL}\cdot\text{min}^{-1}$ was applied at room temperature, **114** was obtained in 92% AY and no starting material remained (Entry 1, Table 7). At the same flow rate and residence time, lower temperature ($0 \text{ }^{\circ}\text{C}$) slows the reaction down, as expected, yielding **114** in 80% AY and 15% of thiol **113** remains unreacted (Entry 2). By cutting the residence time in a half, a similar outcome is observed (Entry 3). The mass balance inferior to 100% was a concern, because it was not clear what would cause mass loss in this process. Entry 1 was repeated several times and assay yields ranging 92 to 100% were observed. We then realized the chosen internal standard for NMR analysis, mesitylene, was reacting with the remaining excess of SO_2Cl_2 , and probably was the culprit of the fluctuating yields. Indeed, it is described in the literature that aromatic compounds can be chlorinated by sulfuryl chloride.⁹⁷

Table 7. Initial results for sulfenyl chloride **114** formation in continuous conditions.

Entry	Scale (mg)	Flow rate ($\text{mL}\cdot\text{min}^{-1}$)	Reactor Vol. (mL)	Residence time (min)	T ($^{\circ}\text{C}$)	Compound 113 (%)	Product 114 (%)	MB (%)
1	400	0.336	10	30	25	0	92	92
2	400	0.336	10	30	0	15	80	95
3	400	0.336	5	15	25	12	82	94

For the assay yields shown on Table 7, the entire volume of reagents injected in the reactor was collected and mesitylene was added in a 1:1 ratio relative to starting material **113** at room temperature. To obtain reliable NMR data, we took extra precautions before preparing the NMR sample. For instance, the crude mixture were collected in a flask with DCM in order to dilute the solution exiting the reactor. In addition, a low temperature bath ($-78\text{ }^{\circ}\text{C}$) was used to minimize side reactions. The internal standard was added only after the collection of the entire volume of the crude mixture. A small aliquot was then diluted in CDCl_3 for NMR analysis. These small changes during sample preparation provided the desired product **114** in an average of 98% AY (triplicate experiments).

After obtaining satisfactory yields of **114** and reproducible data, we moved to the Step 2. Sulfenyl chloride **114** is extremely reactive and moisture sensitive. Thus, this intermediate must be readily consumed. The same configuration used to obtain compound **114** under continuous conditions (Figure 2) was applied as well as the conditions that led to the best yield (30 min of residence time, $0.336\text{ mL}\cdot\text{min}^{-1}$ total flow rate, AY= 98%). A second reactor, 15 mL PFA coil (Vapourtec), and a third syringe pump for vinyl acetate injection were added to the original setup. A T-piece connects both reactors and the BPR was moved to the end of the system (Scheme 22 and Figure 24). Neat vinyl acetate was used and its flow rate adjusted to pump 2 equiv. relative to the starting amount of the compound **113**.



Scheme 22. New setup including vinyl acetate addition step.

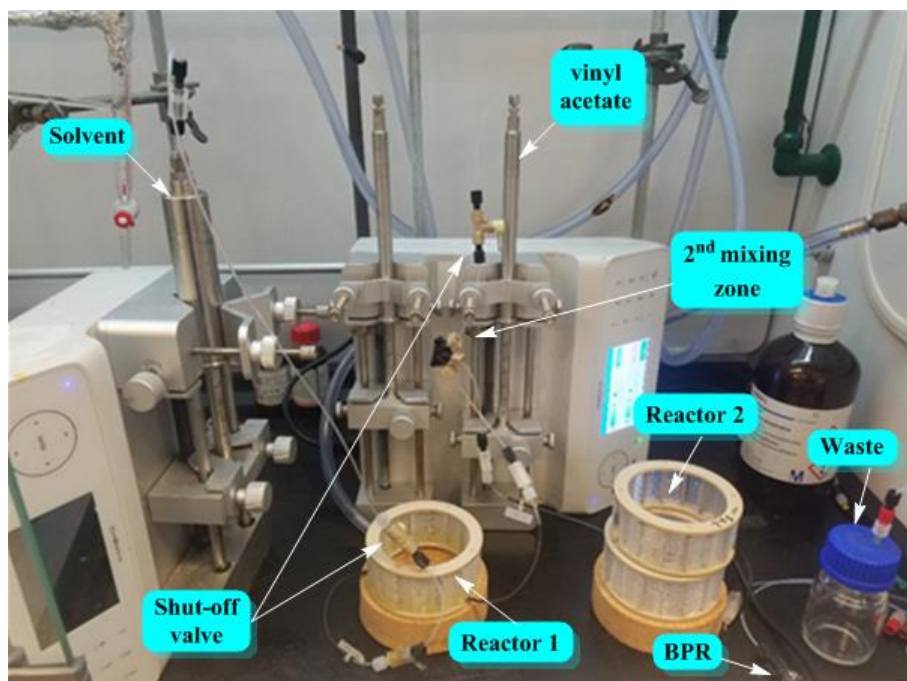


Figure 24. End-to-end approach to perform compound **115** synthesis under continuous conditions – initial experiments.

The residence time in the Reactor 1 was fixed in 30 min for all experiments and changes to the reactor size were adjusted as necessary. A first run using this setup yielded 85% AY of **115** and 13% of byproduct **116**, with a 98% mass balance that is similar to the results obtained in the batch approach (Table 8, Entry 1). Decreasing residence time in a half from 40 to 20 min produces **115** in 92% AY and **116** in 6% (Entry 2). Further reduction in residence time, however, does not provide adequate time for the full consumption of **114**. Seeking better reagent mixing, we kept the higher flow rate of $1.17 \text{ mL}\cdot\text{min}^{-1}$ and doubled the reactor size from 15 to 30 mL to obtain full conversion of the sulfenyl chloride **114**. In 26 min of residence time, **115** was obtained in 99% AY and byproduct formation considerably decreased (Entry 4). Triplicate experiments were performed and results are reproducible.

Table 8. End-to-end approach of continuous synthesis of compound **115** from thiol **113**.

Entry	Reactor Vol. (mL)	Flow rate (mL.min ⁻¹)	Residence time (min)	T (°C)	Dichloro 115 (%)	Trichloro 116 (%)	MB (%)
1	15	0.390	40	25	85	13	98
2	15	0.780	20	25	92	8	100
3	15	1.170	13	25	84	3	99*
4	30	1.170	26	25	99	1	100

* 2% mono chloro and 10% sulfenyl chloride left

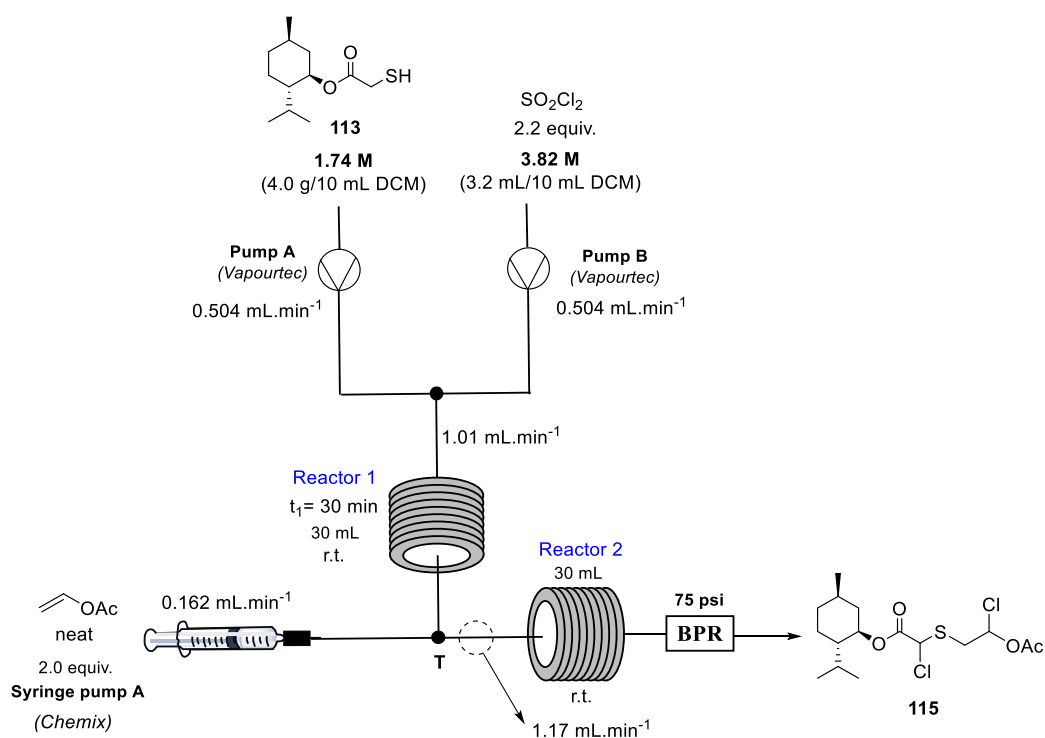
To perform the experiments on Table 8, the total volume of reagent solutions pumped into the system was inferior to the capacity of the reactor (< 1/4 of the reactor maximum volume). Since the purpose of these experiments was to gather information about the system, the reactions were carried out on a small, 400 mg scale. The entire amount collected for analysis was a single fraction with no disposal of the “tails”. The data shown on Table 8 provided a reasonable starting point for the steady state studies. From this point on, all flow experiments were conducted utilizing reagent solutions with at least two volumes relative to the total reactor volume (*e.g.* if a 20 mL reactor is used, at least 40 mL of solution of reagents are pumped into the system). AY corresponds to average yields from “*n*” fractions collected from the steady state, the point where the reactor parameters are all constant.

3.3.5. Steady-State and Reactor Output

To pump larger volumes of reagents, we chose Vapourtec E-Series pumps.⁹⁸ They are high-pressure precision peristaltic pumps, capable of pumping at up to 10 bar, with flow rates from 0.10 to 10.0 mL.min⁻¹. They are resistant to strong acids, bases and organometallic reagents, as well as a range of gases. A standard peristaltic pump gives significant flow rate fluctuations. This is especially important when pumping solutions to

perform reactions that are stoichiometry-sensitive; if these flow fluctuations were out of phase there would be huge swings in the reaction stoichiometry resulting in no reliable/reproducible data. This is aggravated when delivering reagent solutions against high back-pressures. E-Series has a nonlinear rotor system that can adjust its rotation rate while the tubing is being compressed, thus maintaining a constant flow rate. A standard peristaltic pump works at a steady rotational speed. E-Series holds two types of color-coded fluoropolymers tubing (red and blue) crimped end connectors, which present remarkable chemical compatibility with a broad range of substances.

The new setup illustration is shown in Scheme 23. Two Chemyx syringe pumps were replaced by E-Series V-3 pumps (Solution A and B). For the vinyl acetate injection, we kept one of the syringe pumps to precisely inject the smaller volume of vinyl acetate (its flow rate is about 6 times slower than Solution A and B summed).



Scheme 23. Initial setup and reaction conditions for steady state studies.

Because we increased the flow rate of solutions A and B (1.01 mL.min⁻¹), we expected that the 30 mL reactor for the sulfenyl chloride **114** synthesis shown in Scheme 23 would not be necessary. A 30-minute residence time is needed to fully convert **113**

when a total flow of $0.336 \text{ mL}\cdot\text{min}^{-1}$ is applied, as displayed in Table 7. Multiplying the flow rate by 3 improves mixing efficiency and may reduce residence time, considering an inefficient mixing can slow down the reaction. We reduced the residence time of Step 1 by switching the 30 mL (30 min) reactor for a 10 mL (10 min) and observed an unexpected occurrence in the ^1H NMR. In addition to the expected singlet for **114** methylene group $-\text{CH}_2-\text{S-Cl}$ (4.17 ppm), a broad singlet appears in 4.02 ppm. When the residence time was increased, the integral value of this signal decreased inversely with product **114** (Figure 25). Initially, we believed the signal at 4 ppm belonged to the thiol **113** $-\text{CH}_2-$ group (3.3 ppm) and the strong acidity in the mixture caused the $-\text{CH}_2-$ chemical shift and altered the coupling pattern (See Experimental Section / Part 1 for detailed NMR analysis).

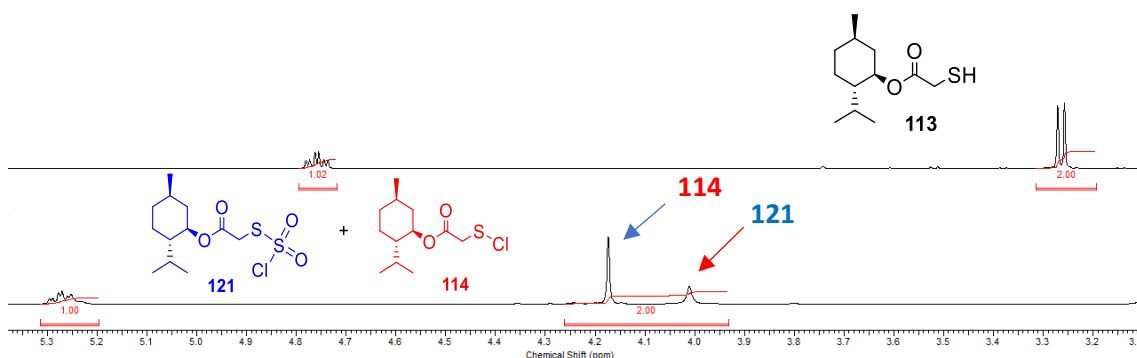
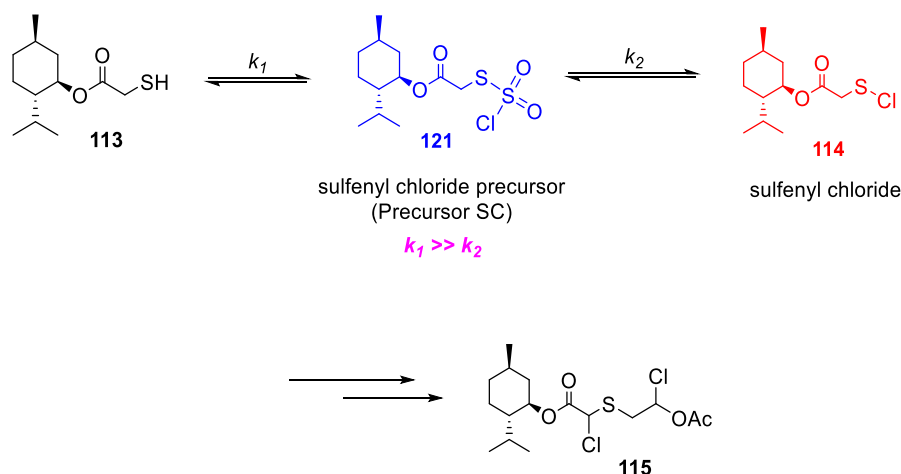


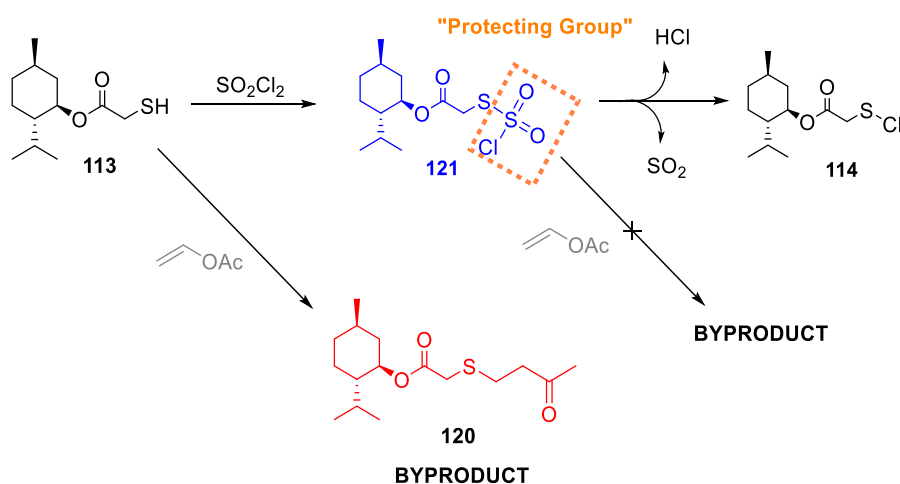
Figure 25. ^1H NMR analysis of the crude mixture of reaction of thiol **113** with SO_2Cl_2 .

We hypothesized thiol **113** rapidly reacted with SO_2Cl_2 leading to the intermediate **121**, which was stable enough to be detected by ^1H NMR. Our experiments suggested **121** immediately forms when SO_2Cl_2 is added and HCl and SO_2 are gradually released to form sulfenyl chloride **114** (Scheme 24). Several references showing this type of intermediate produced from reaction of alcohols with SO_2Cl_2 is prevalent in the literature.⁹⁹ The reaction with thiols however only has a single scientific reference.¹⁰⁰ Although not widely studied, this literature precedent supports our hypothesis.



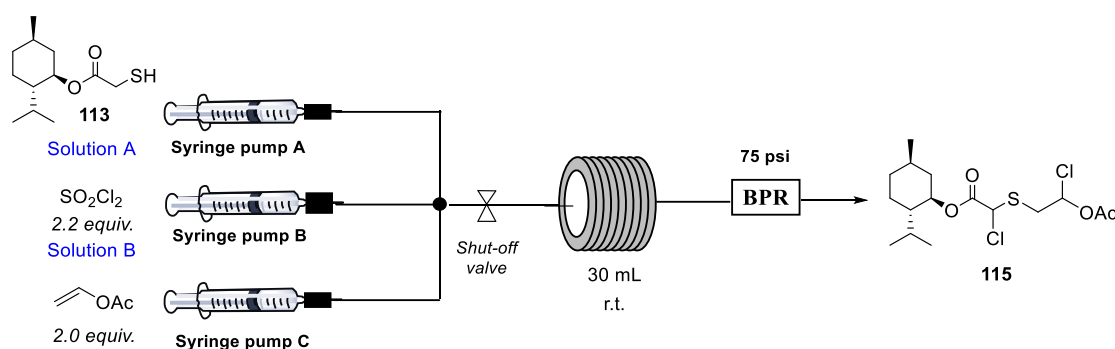
Scheme 24. Proposed intermediate **121** as a possible precursor of sulfenyl chloride **114**.

Considering intermediate **121** is formed rapidly and does not present any reactivity with vinyl acetate, this first reaction stage of **113** with SO_2Cl_2 works as a thiol “protecting group”. It avoids compound **113**'s undesired reaction leading to byproduct **120** (Scheme 25). The most probable reaction pathway for intermediate **121** is the release of HCl and SO_2 resulting in the sulfenyl chloride **114**. If this holds true, the final setup size can be reduced as there would be no need to use Reactor 1.



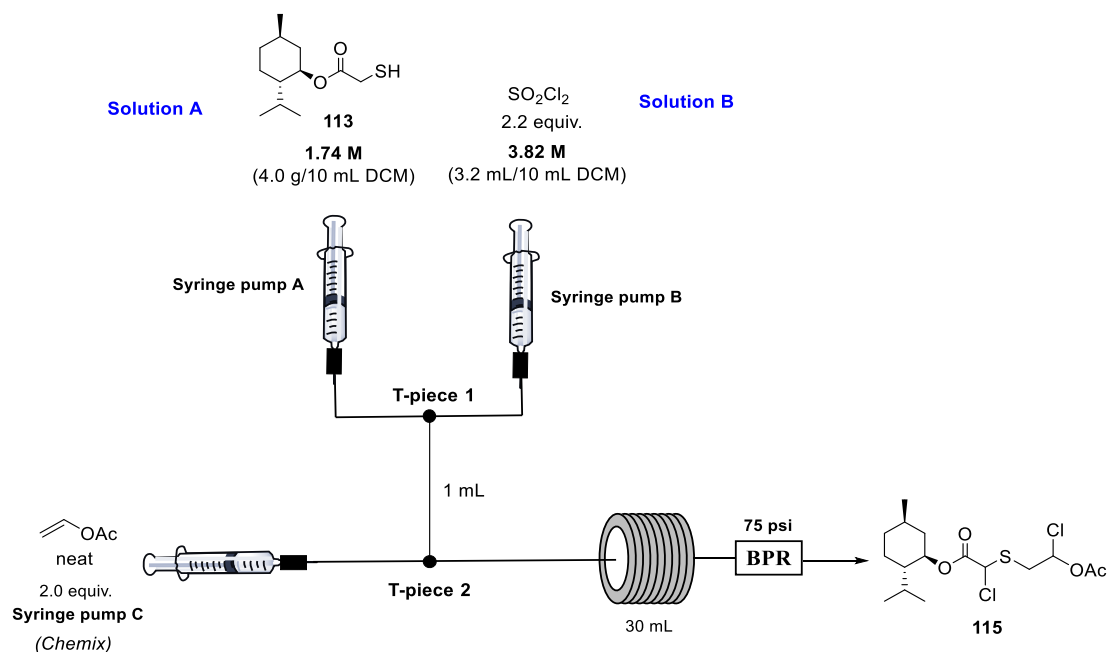
Scheme 25. First stage reaction of thiol **113** with SO_2Cl_2 working as a thiol “protecting group”.

To test our hypothesis, we performed the reaction in small scale (1.0 g) using a new setup with three Chemyx syringe pumps as displayed in Scheme 26. Solutions A, B and vinyl acetate were mixed simultaneously. The ^1H NMR analysis of the crude mixture showed higher amounts of byproducts **119** and **120** than observed in previous experiments. Dichloro acetate **115** yield drops significantly from 99% to 57% AY and monochlorinated species **114a** is not entirely consumed – 20% remains unreacted due to a fraction of SO_2Cl_2 reacting with vinyl acetate, yielding byproduct **119**.



Scheme 26. Simultaneous mixing of solutions A, B and neat vinyl acetate.

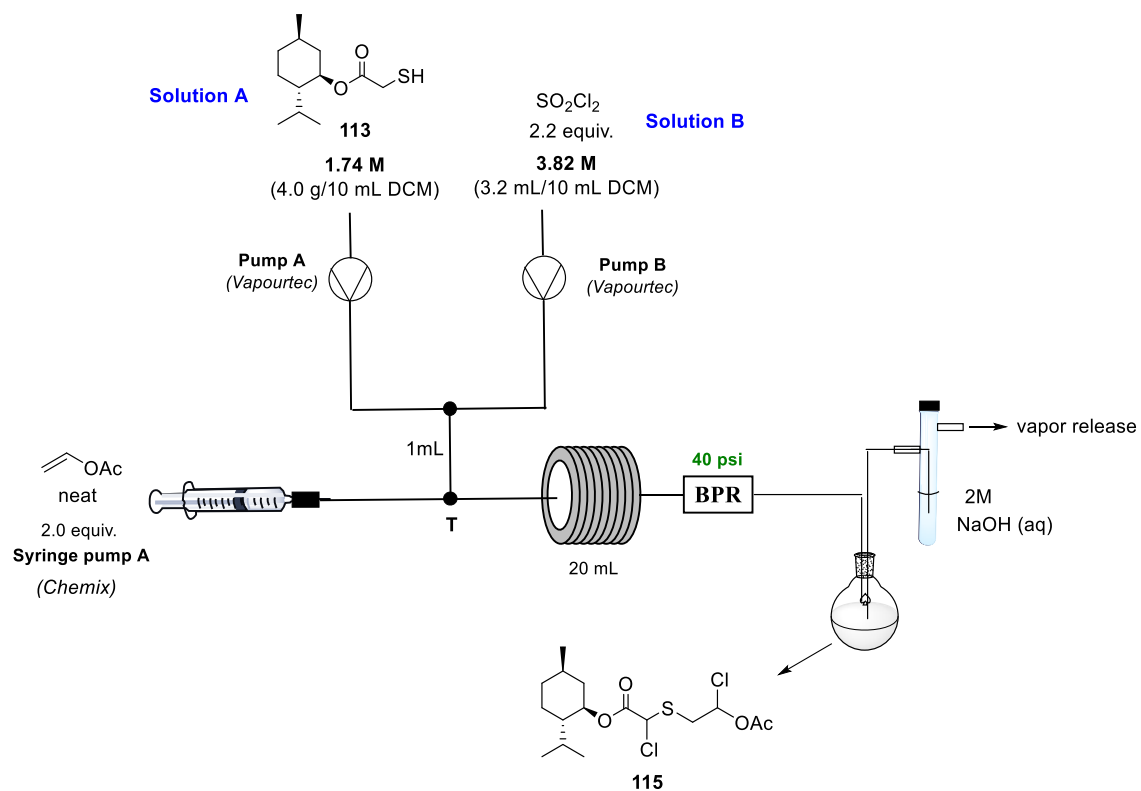
We continued searching for an efficient and compact setup. Scheme 27 shows our final attempt. Instead of mixing A, B and vinyl acetate simultaneously, a small piece of PFA tubing (1 mL) was placed between T-piece 1 and 2. At the first mixing point, thiol **113** was quickly consumed. When the resulting mixture met the second mixing point, there was no remaining thiol **113**, only intermediate **121**. Such modification eliminates byproduct **120** formation.



Scheme 27. Modified setup – insertion of a separated mixing point for solutions A and B.

When operating the two syringes pumps A and B at $0.504 \text{ mL}\cdot\text{min}^{-1}$ each and syringe pump C with vinyl acetate at $0.162 \text{ mL}\cdot\text{min}^{-1}$ ($1.17 \text{ mL}\cdot\text{min}^{-1}$ total), the configuration described in Scheme 27 yields **115** in 95% AY in 26 min residence time. In this case, the reaction was performed in 1.0 g scale and the whole volume of reagents injected was collected for the assay yield. Trichloro acetate **116** was formed in 5% AY. This result confirms the validity of our hypothesis regarding intermediate **121**.

With these results in hand, steady state initial studies were conducted using a simplified setup with E-Series pumps for solutions A and B (Scheme 28 and Figure 26). In addition, the reactor volume was fixed at 20 mL for all experiments.



Scheme 28. Simplified setup for initial steady state studies.

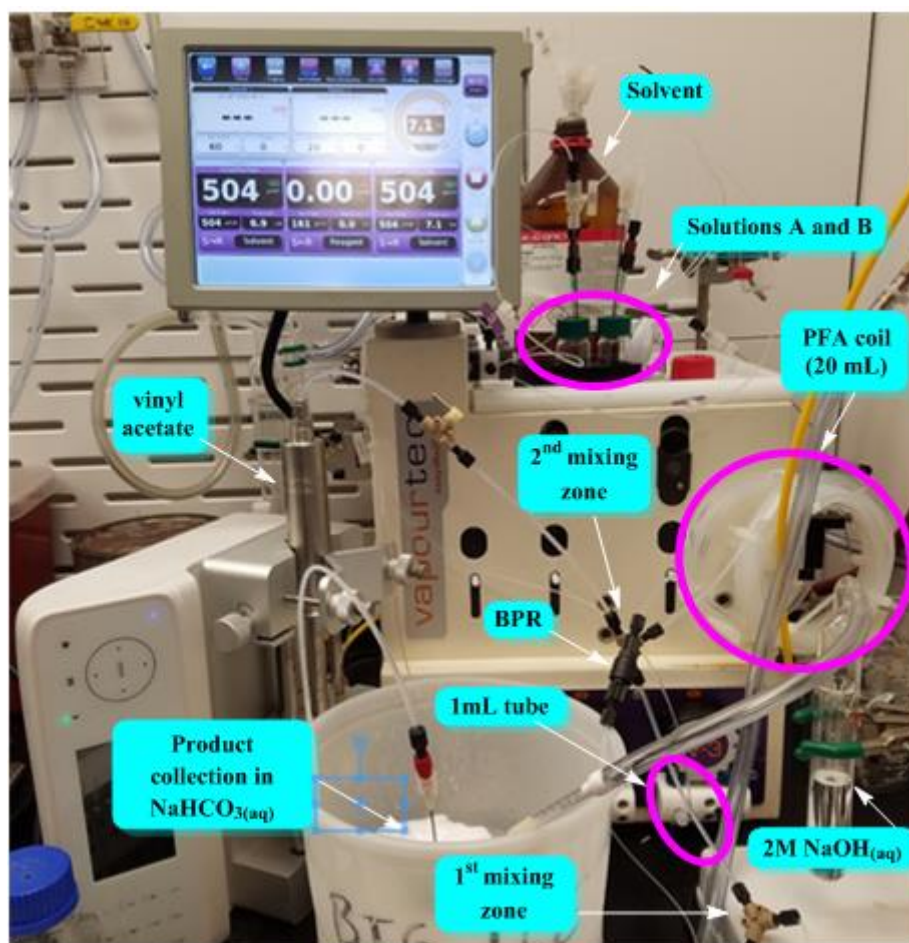


Figure 26. Continuous flow setup for the steady state experiments – Vapourtec E-Series to pump solutions A and B and Chemyx syringe pump for vinyl acetate.

Several issues were encountered during the transition from syringe to peristaltic pumps (E-Series). Vapourtec pumps stopped working properly and the injected volume of solutions A and B was constantly varying. We also noticed once the reactor is filled with reagents, the pressure inside the system increases from 5 up to 8 or 9 bar, which is uncomfortably close to the equipment's maximum operating pressure (10 bar). We suspected this was the cause of the unexpected behavior of the pumps. Besides checking the pumps calibration, the 75 psi BPR was replaced with a 40 psi to decrease back-pressure in the system (Scheme 28 and Figure 26).

The setup displayed in Scheme 28 was used for the steady state studies. The best condition obtained from the small-scale experiments was used as the starting point

(pumps A and B at 0.504 mL.min⁻¹ each and syringe pump C with vinyl acetate at 0.162 mL.min⁻¹, 1.17 mL.min⁻¹ total in a 20 mL reactor).

We noticed that during long runs, mesitylene was reacting with SO₂Cl₂. Many NMR internal standards were tested with no success. Most of them was incompatible with SO₂Cl₂, leading to the formation of unwanted chlorinated species. We sought to select not only an inert internal standard but also one with high boiling point. Gas release after the BPR is very intense and volatile standards would be easily lost during samples collection, resulting in not reliable assay yields. Based on our previous observation that most reactions with SO₂Cl₂ are carried out in chlorinated solvents, we searched for suitable chlorinated molecules possessing high boiling points. Among the selected molecules, 1,2,3-trichloropropane (bp 157 °C) was the only option that did not react with SO₂Cl₂. Thus, it was successfully applied as the NMR internal standard for the assay yields.

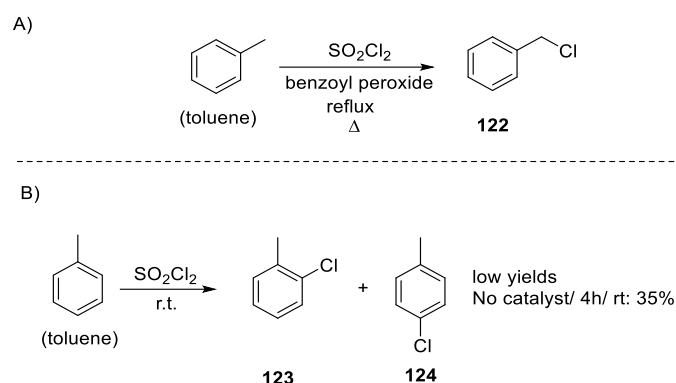
The updated setup was finally tested. Steady state conditions in DCM yielded 97% AY of compound **115** and 3% of **116** (Table 9, Entry 1). The isolated yield for this entry after extraction with NaHCO_{3(aq)} and chromatographic column produced **115** and the byproduct **116** at 88% and 3% yield, respectively. In steady state, toluene is equally viable as DCM (Table 9, Entry 2).

Table 9. Comparison between DCM in toluene in steady state conditions.

Entry	Solvent	Flow rate (mL/min)	Residence time (min)	Monochloro 114a (%)	Dichloro 115 (%)	Trichloro 116 (%)	MB (%)
1	DCM	1.17	17	0	97	3	100
2	toluene	1.17	17	0	96	4	100

As observed with mesitylene, we were concerned toluene would react with SO₂Cl₂. There is existing literature supporting the occurrence of toluene chlorination (Scheme 29). In the first case, Scheme 10A, toluene reacts only under very specific conditions: reflux and with addition of a chain initiator, benzoyl peroxide, to produce compound **122**.¹⁰¹ It also reacts at room temperature yielding a mixture of *ortho*- and

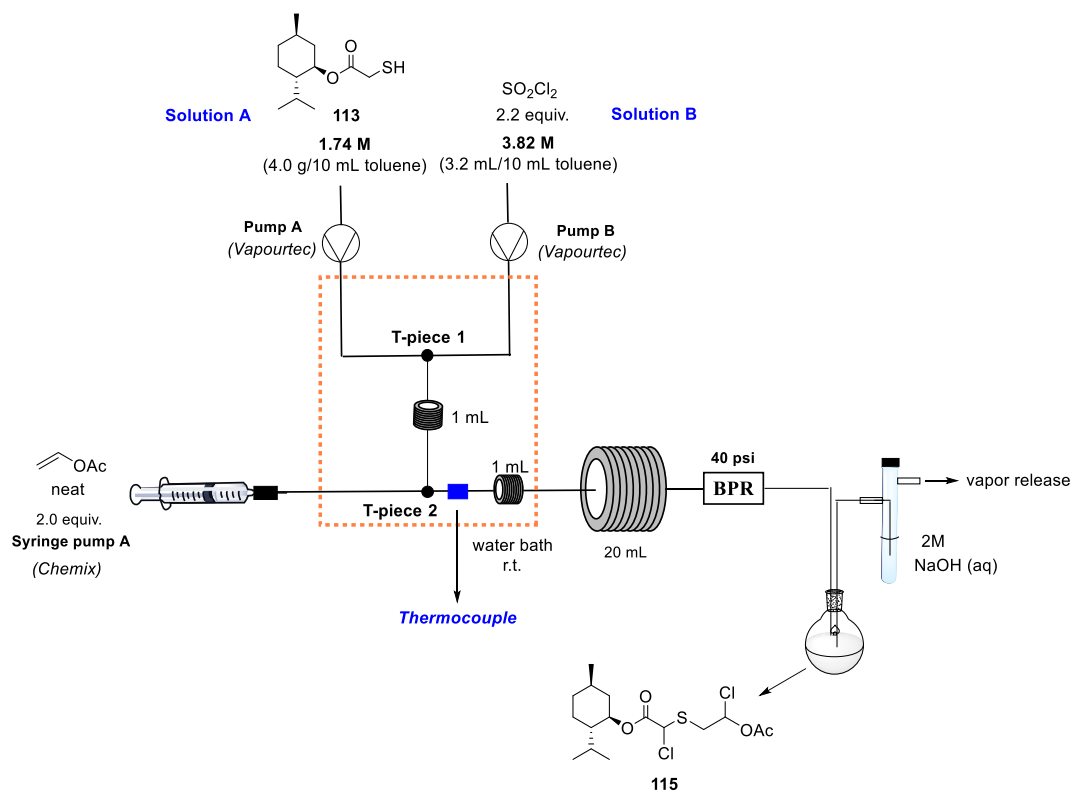
para-substituted aromatic ring, **123** and **124**, yet in low yields, around 35% after 4 h.¹⁰² Compounds **123** and **124** were not detected in our reaction mixture. Considering industrial production of compound **115** using our developed conditions, it would be inadvisable to prepare large amounts of SO₂Cl₂ solution in toluene, but rather use it immediately upon preparation.



Scheme 29. Possible side reactions of toluene with sulfonyl chloride.

Performing the reaction in large scale not only increased the amount and intensity of gas released, but also increased the temperature mainly in the second mixing zone (T-piece 2). To ensure this was not affecting the steady state, a thermocouple was inserted inside the tubing right after the second mixing zone. In addition to the 1 mL coil placed between T-piece 1 and 2, a second coil of same volume was placed after T-piece 2 (Scheme 30). This part of the system was submerged in a water bath at room temperature to provide superior heat dissipation.

The reaction condition displayed in Entry 2 (Table 9) was repeated in an extended time run (70 min) and using the improved setup. Nearly 100 mL of solutions A and B (*ca.* 5 reactor volumes) were pumped into the reactor (Scheme 30). Approximately 50 samples were collected over the total experiment time. The steady state is reached around the initial 5 minutes and the yield average is 98% AY of **115** (Figure 27).



Scheme 30. Improved flow setup for dichloro acetate **115** synthesis.

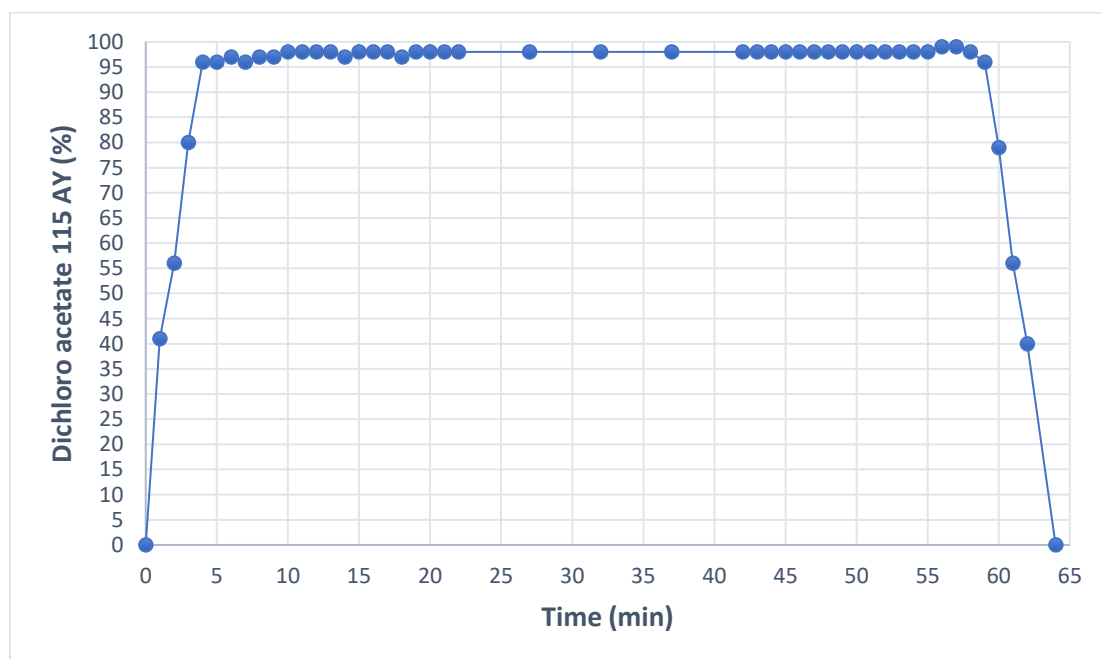


Figure 27. Variation of dichloro acetate **115** yield over time.

A temperature rise of 2 °C was observed right after the T-union 2, remaining constant through the entire experiment run in this point of the system. After confirming the temperature increase in the mixing zone was not affecting the steady state, the reaction in toluene was optimized before scaling-up the process. The number of SO₂Cl₂ equivalents were decreased. The absence of remaining sulfonyl chloride would maximize compound **115** yield. Results displayed in Table 10 affirms this is not true. Entries 1 and 2, where 2.0 and 2.1 equiv. were utilized still present a small percentage of **116** as well as unreacted mono-chlorinated specie **114a**. We opted to keep 2.2 equiv. SO₂Cl₂ for the scale-up runs to ensure **114a** is completely consumed.

Table 10. Variation of SO₂Cl₂ number of equivalents – reaction in toluene.

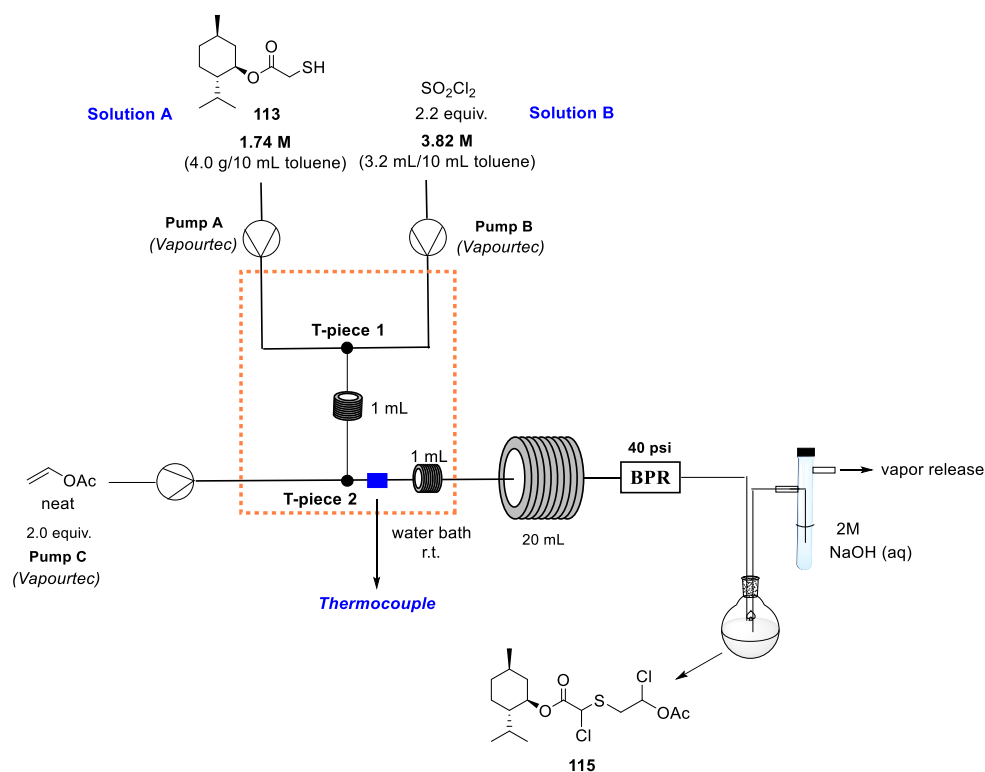
Entry	SO ₂ Cl ₂ (equiv.)	Flow rate (mL/min)	Residence time (min)	Monochloro 114a (%)	Dichloro 115 (%)	Trichloro 116 (%)	MB (%)
1	2.0	1.17	17	7	90	3	100
2	2.1	1.17	17	4	95	1	100
3	2.2	1.17	17	0	97	3	100

The 20 mL reactor was employed for all experiments. Only the flow rates were varied, and consequently the residence time. We expected with flow rate improvements, better mixing would eliminate byproduct **116** formation altogether. Increasing the total flow rate from 1.17 up to 2.11 mL.min⁻¹ (17 and 9 min residence time, respectively) does not change the yield of compound **115** (96–97% AY in all cases) (Table 11). Since the yields described in the table below are very similar, we chose Entry 2 as the optimized condition for scale-up with 97% AY of **115** and no **114a** remaining. We were convinced that a small amount of trichloro acetate **116** would always be formed. Byproduct formation had been suppressed around 10% under continuous flow conditions, proving that better selectivity was achieved over our previous batch approach for synthesis of compound **115**.

Table 11. Optimization of reaction in toluene and steady state conditions.

Entry	Solvent	Flow rate (mL/min)	Residence time (min)	Monochloro 114a (%)	Dichloro 115 (%)	Trichloro 116 (%)	MB (%)
1	toluene	1.17	17	0	96	4	100
2	toluene	1.40	14	0	97	3	100
3	toluene	1.76	11	1	96	3	100
4	toluene	2.11	9	1	97	2	100

One final modification was necessary to scale-up the reaction setup for continuous flow conditions. The syringe pump for vinyl acetate was replaced with a third E-Series pump, to inject larger volumes of the reagent in an interrupted manner during long-run experiments. A 1/8" O.D. PFA tube was used in lieu of 1/16" O.D. (all system tubing and the 20 mL reactor) to test scaling-up the system by doubling the tubing diameter (Scheme 31).



Entry 2 (Table 11) was repeated using the final flow setup with nearly the same outcome. This proves that replacing the syringe pump with a third V-3 E-Series and increasing the tube diameter does not disturb the system (Entry 1, Table 12). The 1.40 mL.min⁻¹ flow rate was increased five times (7.00 mL.min⁻¹) and a run starting from a total of 20 g of thiol **113** was achieved (Entry 2, Table 12). Once more, no alteration in the final yield of **115** was observed. Entry 3 (Table 12) corresponds to the longest run performed thus far (158 g of starting material). Reaction mixture fractions were collected in steady state over 1.5 h every six minutes. The operation was extremely stable and no yield fluctuations were observed. Considering **115** can be obtained at 98% AY (Entry 3), the product **115** throughput would be 141 g/h.

Table 12. Scale-up experiments in steady state conditions.

Entry	Scale (g)	Flow rate (mL/min)	Residence time (min)	Monochloro 114a (%)	Dichloro 115 (%)	Trichloro 116 (%)	MB (%)
1	8	1.40	14	0	98	2	100
2	20	7.00	14	1	97	2	100
3	158	7.00	14	0	98	2	100

The setup used for scaling-up the reaction is shown in Figure 28. The only difference is that a third V-3 pump from E-Series is used to inject vinyl acetate into the reactor. Since the total flow rate was increase five times (1.4 to 7.0 mL.min⁻¹), reactor volume was increased from 20 to 100 mL to maintain the same residence time as the smaller scale (Figure 28).

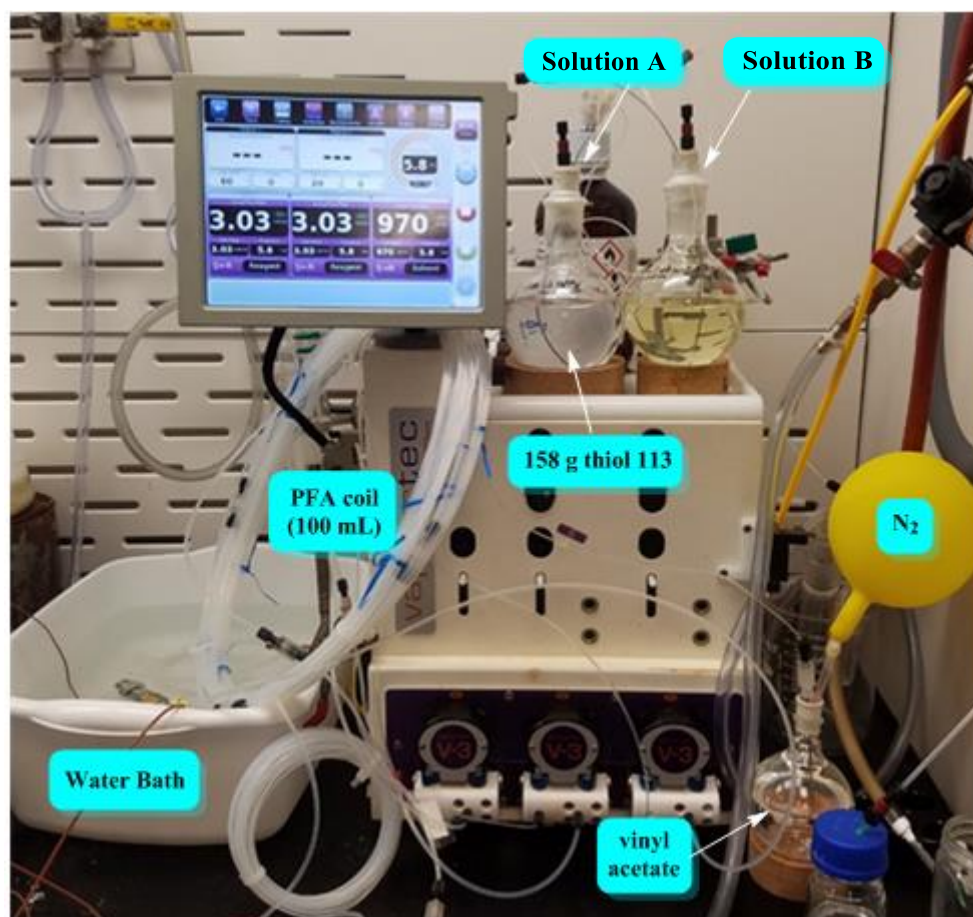


Figure 28. Final continuous flow setup used to scale-up the reaction.

4. Conclusions

Herein we discussed two cases where continuous conditions were applied for hazardous reactions. The results clearly prove the improvement obtained for both processes overall in comparison to batch.

In the first example we accomplished the photooxygenation of different diene moieties resulting in endoperoxides, which are potentially explosive intermediates. Photochemical transformations have several limitations when conducted in conventional batch conditions, namely long reaction times, high dilution, and low light penetration in the reaction vessel. The continuous flow setup developed by our group proved efficient, considerably minimizing the aforementioned issues. In addition to the photooxygenations, the KDM rearrangement of endoperoxides and further hydroxyenone rearrangements were also studied in flow conditions. These studies open up a series of possibilities for the continuous scale-up of important synthetic intermediates, such as substituted furans and 1,4-dicarbonyl derivatives.

In the second case, continuous conditions were used to improve a two-step sequence of reactions in a new route developed by M4ALL to produce Lamivudine and Emtricitabine (3TC and FTC, respectively), important HIV drugs. These reactions are exothermic and release toxic gases (HCl and SO₂). Higher selectivity of the desired product was achieved, minimizing byproduct formation by about 10%. To move this route forward to the pilot scale, it is extremely important to reduce material losses. We demonstrated a stable flow system that can be scaled-up and able to deliver compound **115** in high yields (98 ± 2%). The final run produced around 260 g of **115** with a throughput of 141g/h. These data suggest that a continuous production strategy is feasible for producing the dichloro acetate **115** and the designed setup provided increased safety to the process.

In summary, the two cases outlined in Part 1 showcase how useful and efficient enabling technologies can be. The development of “problematic” transformations using continuous flow conditions results in a series of improvements such as decreased reaction times, higher selectivity, and safety.

EXPERIMENTAL

SECTION

- *PART 1* -

5. Experimental Section

The starting materials were purchased from Sigma-Aldrich and were used without further purification except for compounds **14**¹⁰³, **27**¹⁰⁴, **32**¹⁰⁵, **47**¹⁰⁶, which were prepared as described in the literature. For thin layer chromatography (TLC) we used 60 F₂₅₄ (0.25 mm) silica gel and for column chromatography silica gel (pore size 60 Å, 70–230 mesh, 63–200 µm).

¹H NMR and ¹³C NMR spectra were recorded in a Bruker Avance 400 operating at 400.15 MHz and 100.62 MHz, respectively, at room temperature using CDCl₃ or C₆D₆ or acetone-d₆, when necessary. Chemical shifts were assigned in δ (ppm) relative to tetramethylsilane (TMS) or to the residual solvent peak as a reference and the coupling constants (*J*) are given in Hertz (Hz). The multiplicity is presented as follows: singlet (*s*), broad singlet (*br. s.*), doublet (*d*), broad doublet (*br. d*), triplet (*t*), quadruplet (*q*), octet (*oct*), double doublet (*dd*), double triplet (*dt*), double double doublets (*ddd*), triple doublets (*td*), multiplet (*m*).

The melting points of the solids were determined in a *Microquimica* MQAPF-301 apparatus and were not corrected. HRMS analyses were recorded on a Bruker micrOTOF-Q II mass spectrometer equipped with electron spray ionization - time of flight (ESI-TOF), operating in positive mode. IR analysis was recorded on an IR-Prestige-21 Fourier transform infrared spectrophotometer - SHIMADZU, with the absorption frequencies expressed in cm⁻¹. The solid samples were analyzed on KBr pellets and oil samples as a liquid film on KBr cells.

NMR data was processed using the ACD Labs software and the names of all products were generated using the PerkinElmer ChemDraw Ultra v.12.0.2 software package. Some intermediate compounds were not isolated during end-to-end approaches. Continuous flow experiments were carried out using Syrris equipment (Asia modules) such as the syringe pump (500 µL and 1000 µL), stainless steel coil (16 mL) and microchip reactor (250 µL). The back-pressure regulators (BPR – 100 psi) were acquired from Upchurch Scientific Inc. KNAUER HPLC pumps (AZURA P 4.1S) were also used. All capillary tubing and fittings were purchased from Swagelok, and materials for the photoreactor construction were procured locally.

5.1. Photooxygenation reactions and Kornblum-DeLaMare rearrangement (KDM)

5.1.1. Batch Protocol to *cis,cis*-1,3-cyclooctadiene (**53**) Photooxygenation Followed by KDM Rearrangement

In a round-bottom flask 7.38 mg of **TPP** (0.4 mol%, 0.012 mmol) was added, which was dissolved in 25 mL of DCM. Subsequently, *cis,cis*-1,3-cyclooctadiene (**53**) (381.1 μL , 3 mmol) was added and then 50 mL CH_3CN . The photochemical batch reactor (white LED ~ 100 W) was used, maintaining the irradiation and magnetic stirring of this mixture for 46 min. Then, 457.8 μL of DBU (3 mmol) was added, submitting the reaction to heating at 60 °C in a convectional oil bath for 32 min. Compound **55** was obtained in 16% yield (0.48 mmol; 67.5 mg) after purification by silica gel chromatography (DCM/MeOH (9:1)).

CAUTION: Endoperoxides are potentially explosive intermediates. Always use PPEs and handle reactive compounds in the laboratory fume hood. While running the reaction make use of a blast shield. Avoid exposing peroxides to heat, friction, mechanical shock or contamination with incompatible materials.

5.1.2. General Procedure for Dienes Photooxygenations Followed by KDM Rearrangement in Continuous End-to-end Experiments

All the methodology was developed with 3 mmol of substrate/75 mL of solvent (0.04 mol.L⁻¹), and the scope with 1 mmol/25 mL of solvent. **TPP** (2.46 mg; 0.004 mmol; 0.4 mol%) was dissolved in 8 mL of DCM, and after, 1 mmol of the diene in 17 mL of CH_3CN was mixed giving a diene concentration at 0.04 mol.L⁻¹. The resulting solution was then transferred to the PFA loop (25 mL), which was subsequently connected to the system and then protected from light.

Operation 1. Before connecting the PFA loop to the system, valve 2 (Scheme 3) must be closed, and the flow of the solvent mixture ($\text{CH}_3\text{CN}/\text{DCM}$ (2:1)) from pump A (Knauer) (0.5 mL.min⁻¹ flow rate) must be directed into the loop to pressurize it until 6 bar. After

reaching this pressure, valve 1 must also be closed to the pressurized loop, and then opened in the reactor's direction. The whole setup is pressurized with oxygen (6 bar) until its stabilization (~v/v 1:1 gas/solvent after 100 psi BPR).

Operation 2. Simultaneously with Operation 1, a solution of DBU or Et₃N (1 equiv.; 0.4 mol.L⁻¹) is injected with a syringe pump (Syrrix) (pump B) at 50 μL.min⁻¹ into the temperature controlled coil at 60 °C (stainless steel reactor, 16 mL – Syrris), where the DBU solution encounters the endoperoxide-containing reaction mixture.

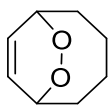
Operation 3. After setup stabilization, Valve 2 must be opened and pumped. A solvent flow should be redirected to the loop, using Valve 1 in order to allow the input of **diene** + **TPP** into the reactors.

After collecting the entire reaction volume, it was concentrated under reduced pressure at 30 °C. The crude residue was then purified by column chromatography over silica gel. Changes in the purification process are shown for each case where necessary.

5.1.3. General Procedure for Dienes Photooxygenations Followed by KDM Rearrangement to Obtain Furans in a Continuous End-to-end Approach

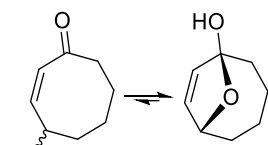
All operations 1, 2 and 3 previously described were performed to synthesize furans. Additionally, a new pump (pump C) was inserted into the setup after the stainless steel reactor output, where the KDM product-containing mixture encounters a PTSA solution also in CH₃CN/DCM (2:1) (0.05 mol.L⁻¹; flow rates at Table 5) in a T-Mixer (Scheme 14).

5.1.4. NMR – Product Characterization

**54**

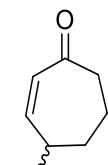
7,8-dioxabicyclo[4.2.2]dec-9-ene (54).¹⁰⁷ It was obtained after

purification by silica gel chromatography using DCM as eluent (6–21% yield, degradation during purification in silica gel). Endoperoxide **54** is a pale-yellow oil: ¹H NMR (400 MHz, CDCl₃): δ_H 6.13–6.18 (m, 2H), 4.74–4.77 (m, 2H), 2.07–2.14 (m, 2H), 1.70–1.90 (m, 4H), 1.56–1.63 (m, 2H); ¹³C NMR (100 MHz, CDCl₃): δ_C 128.1, 76.5, 33.1, 24.0.

**55**

9-oxabicyclo[4.2.1]non-7-en-1-ol (55). It was obtained as a white

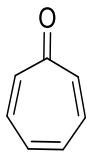
solid after purification by chromatography over silica gel (DCM/MeOH (9:1)) (yields available on Tables 1–4): m.p. 93–95°C (lit.¹⁰⁸ 93–94°C); ¹H NMR (400 MHz, C₆D₆): δ_H 5.48 (dd, *J* = 5.7, *J* = 1.2 Hz, 1H), 5.43 (dd, *J* = 5.7, *J* = 1.9 Hz, 1H), 4.73–4.75 (m, 1H), 2.99 (s, 1H), 2.07–2.14 (m, 1H), 1.72–1.84 (m, 2H), 1.48–1.63 (m, 2H), 1.23–1.41 (m, 2H), 1.07–1.14 (m, 1H); ¹³C NMR (100 MHz, CDCl₃): δ_C 134.4, 132.6, 111.4, 81.6, 39.0, 33.4, 23.7, 23.0. FT-IR (KBr pellet, cm⁻¹): 3400, 3302, 1618, 1438, 1419, 1203, 1180, 1130, 1097, 1062, 1043.

**58**

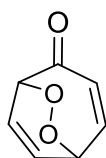
4-hydroxycyclohept-2-en-1-one (58).¹⁰⁹ It was obtained as a yellow oil after

purification by chromatography over silica gel (DCM/MeOH (9.5:0.5)) in 92% overall yield (0.92 mmol; 116 mg): ¹H NMR (400 MHz, C₆D₆): δ_H 6.27 (ddd, *J* = 12.6, *J* = 3.1, *J* = 1.2 Hz, 1H), 5.86 (ddd, *J* = 12.6, *J* = 2.3, *J* = 1.0 Hz, 1H), 4.01–4.06 (m, 1H), 2.52 (br. s, 1H), 2.25–2.32 (m, 1H), 2.10–2.17 (m, 1H), 1.67–1.75 (m, 1H), 1.41–1.50 (m, 1H),

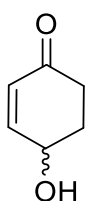
1.15–1.37 (m, 2H); ^{13}C NMR (100 MHz, C_6D_6): δ_{C} 202.8, 150.0, 130.1, 70.6, 43.4, 35.5, 18.7.



61 Cyclohepta-2,4,6-trienone (**61**).¹¹⁰ Tropone (**61**) was obtained as a yellow-orange oil after purification by chromatography over silica gel (EtOAc/hexanes (7:3)) in 36% overall yield (0.36 mmol; 38.2 mg): ^1H NMR (400 MHz, CDCl_3): δ_{H} 7.07–7.15 (m, 2H), 7.00–7.05 (m, 2H), 6.96–6.99 (m, 2H); ^{13}C NMR (100 MHz, CDCl_3): δ_{C} 188.3, 142.2, 136.2, 134.8.

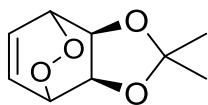


63 6,7-dioxabicyclo[3.2.2]nona-3,8-dien-2-one (**63**).¹¹¹ It is obtained as a yellow oil after purification by flash chromatography over silica gel employing DCM as eluent. Starting from 0.5 mmol of **61** and using optimal photooxygenation conditions (P_{O_2} = 6 bar, 0.5 mL.min⁻¹ flow rate) endoperoxide **63** was isolated in 62% yield (0.31 mmol; 43.0 mg): ^1H NMR (400 MHz, CDCl_3): δ_{H} 7.00–7.07 (m, 2H), 6.48–6.53 (m, 1H), 6.01 (ddd, J = 10.9, J = 2.2, J = 0.7 Hz, 1H), 5.08 (t, J = 7.4 Hz, 1H), 4.99 (br. d, J = 7.8 Hz, 1H); ^{13}C NMR (100 MHz, CDCl_3): δ_{C} 195.1, 144.8, 138.1, 131.4, 123.2, 85.6, 75.4.



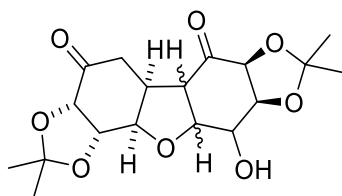
66 4-hydroxycyclohex-2-enone (**66**).¹¹² It was obtained as a yellow oil after purification by chromatography over silica gel (DCM/MeOH (9:1)) in 67% overall yield (0.67 mmol; 74.8 mg) at 80 °C and 29% (0.29 mmol; 32.6 mg) at 60 °C (see Table 5): ^1H NMR (400 MHz, C_6D_6): δ_{H} 6.50 (ddd, J = 10.2, J = 2.3, J = 1.7 Hz, 1H), 5.78 (ddd, J = 10.2, J = 2.0, J = 1.0 Hz, 1H), 3.87–3.99 (m, 1H), 2.64 (br. s, 1H), 2.27 (dt, J = 16.7, J = 4.5 Hz, 1H), 1.83–1.92 (m, 1H), 1.72–1.79 (m, 1H), 1.54–1.64 (m, 1H); ^{13}C NMR (100

MHz, C₆D₆): δ_C 198.6, 153.7, 129.2, 66.4, 35.9, 32.9; FT-IR (KBr, thin film, cm⁻¹) ν : 3431, 2960, 2879, 1658, 1209, 1066, 972, 943, 866.

**68**

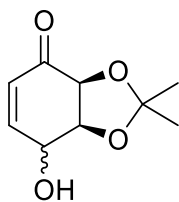
(3*aR*,7*aS*)-2,2-dimethyl-3*a*,4,7,7*a*-tetrahydro-4,7

epidioxobenzo[d][1,3]dioxole (**68**)⁹⁶. The crude photooxygenated residue was concentrated under reduced pressure (30 °C) and then dissolved in an ice-cold hexane/EtOAc (8:2) mixture, stirred with activated carbon, and then filtered through a Celite[®] plug. The endoperoxide appears as a slightly purple solid due to TPP contamination. Purification by chromatographic column leads to endoperoxide degradation (exploratory experiments): m.p. 115–118 °C (lit. not available); ¹H NMR (400 MHz, CDCl₃): δ_H 6.55–6.56 (m, 2H), 4.87–4.90 (m, 2H), 4.56–4.57 (m, 2H), 1.33–1.34 (m, 6H); ¹³C NMR (100 MHz, CDCl₃): δ_C 130.5, 110.3, 71.8, 71.5, 25.6, 25.4.

**69**

Decahydrodibenzofurans **69**.⁹⁶ It was obtained as

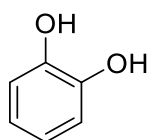
diastereoisomeric mixture (yellow oil), after purification by chromatography over silica gel (Hexane/EtOAc (9:1)) in 10% overall yield (0.10 mmol; 36.8 mg): See NMR spectra.

**70**

7-hydroxy-2,2-dimethyl-7,7a-dihydrobenzo[d][1,3]dioxol-4(3aH)-one

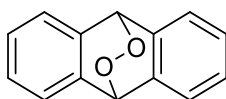
(**70**).⁹⁶ It was obtained as a slightly yellow oil, after purification by chromatography over silica gel (Hexanes/EtOAc (6:4), (1:1)), in 13% (0.13 mmol; 24.3 mg) at 25 °C and 29% (0.29 mmol; 52.8 mg) at 0 °C, overall yield, when Et₃N (1 equiv.) is used in the KDM rearrangement step. Compound **70** is not stable at room temperature (hydroxyl group

must be protected to avoid aromatization): ^1H NMR (400 MHz, CDCl_3): δ_{H} 6.83 (ddd, $J = 10.3$, $J = 3.4$, $J = 0.9$ Hz, 1H), 6.05–6.09 (m, 1H), 4.52–4.54 (m, 1H), 4.40–4.44 (m, 2H), 2.36 (br. s, 1H), 1.36–1.38 (m, 6H); ^{13}C NMR (100 MHz, CDCl_3): δ_{C} 193.8, 147.7, 128.6, 110.6, 79.4, 74.2, 67.2, 27.3, 25.7; FT-IR (KBr, thin film, cm^{-1}): 3435, 1734, 1679, 1637, 1382, 1224, 1080.

**73**

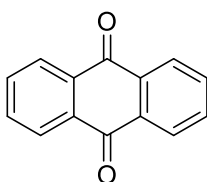
*Pyrocatechol (20)*¹¹³. It was obtained after purification by chromatography

over silica gel (DCM/MeOH (9:1)) as a brown solid in 15% yield (0.15 mmol; 16.3 mg): m.p. 97–100 °C (lit.¹¹⁴ 104 °C); ^1H NMR (400 MHz, CDCl_3): δ_{H} 6.82–6.89 (m, 4H), 5.22 (s, 2H); ^{13}C NMR (100 MHz, CDCl_3): δ_{C} 143.5, 121.2, 115.5.

**75**

*9,10-dihydro-9,10-epidioxyanthracene (75)*¹¹⁵. It was obtained as a

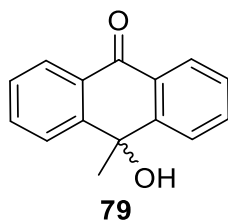
white solid. After removing part of the solvent mixture containing the crude photo-oxygenated compound under reduced pressure (30 °C), endoperoxide **75** was precipitated and filtered off (exploratory experiment): m.p. 155–158 °C (lit.¹⁰⁸ 156 °C); ^1H NMR (400 MHz, CDCl_3): δ_{H} 7.42–7.44 (m, 4H), 7.29–7.31 (m, 4H), 6.04 (s, 2H); ^{13}C NMR (100 MHz, CDCl_3): δ_{C} 138.0, 127.9, 123.6, 79.3; FT-IR (KBr pellet, cm^{-1}): 3023, 2345, 1460, 1172, 769, 621.

**76**

*Anthracene-9,10-dione (76)*¹⁰⁸. Anthraquinone presents low solubility

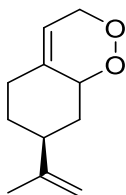
and precipitates during the solvent concentration. The precipitate was filtered and washed with a small amount of DCM to remove **TPP** traces and remaining solvent was concentrated under reduced pressure (30 °C). The recovered product was purified by chromatography over silica gel (Hexane/EtOAc (7:3)). Compound **76** was obtained as

off-white solid in 74% overall yield (0.74 mmol; 154.8 mg): m.p. 284–287 °C (decomposition) (lit. 284–286 °C); ^1H NMR (400 MHz, CDCl_3): δ_{H} 8.31–8.34 (m, 4H), 7.80–7.84 (m, 4H); ^{13}C NMR (100 MHz, CDCl_3): δ_{C} 183.2, 134.1, 133.5, 127.2; FT-IR (KBr pellet, cm^{-1}): 1676, 1573, 1328, 1280, 935, 806, 692.



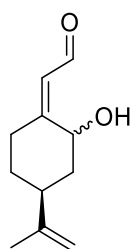
10-hydroxy-10-methylanthracen-9(10H)-one (**79**)¹¹⁶. It was

obtained as a pale-yellow solid in 96% yield (0.96 mmol; 214.4 mg) after purification by chromatography over silica gel (DCM/hexane (9:1)): m.p. 156–159 °C (lit.¹¹⁷ 159–161 °C); ^1H NMR (400 MHz, CDCl_3): δ_{H} 8.14 (dd, $J_1=7.90$, $J_2=1.35$ Hz, 2H), 7.90–7.94 (m, 2H), 7.62–7.68 (m, 2H), 7.41–7.46 (m, 2H), 2.75 (br. s, 1H), 1.68 (s, 3H); ^{13}C NMR (100 MHz, CDCl_3): δ_{C} 183.5, 148.7, 133.8, 129.6, 128.0, 127.0, 125.9, 70.0, 36.9; FT-IR (KBr pellet, cm^{-1}) ν : 3433, 1649, 1598, 1580, 1460, 1385, 1322, 1283, 1082, 1028, 929, 761, 687.



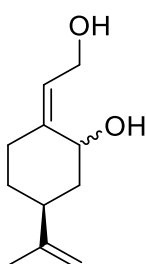
7-(prop-1-en-2-yl)-3,5,6,7,8,8a-hexahydrobenzo[c][1,2]

dioxine (**81**). The endoperoxide, a colorless oil, was obtained as a mixture of diastereoisomers after purification by chromatography over silica gel (DCM/hexane (3:7)) in 31% yield (0.31 mmol; 56.6 mg): ^1H NMR (400 MHz, CDCl_3): δ_{H} 5.56–5.65 (m, 1H), 4.64–4.98 (m, 4H), 4.27–4.36 (m, 1H), 2.00–2.45 (m, 4H), 1.72–1.86 (m, 3H), 1.15–1.50 (m, 2H); ^{13}C NMR (100 MHz, CDCl_3): δ_{C} 148.3, 145.2, 138.4, 137.6, 116.1, 115.5, 111.4, 109.5, 78.9, 75.8, 70.4, 70.2, 42.7, 38.6, 34.6, 31.8, 31.4, 31.2, 28.3, 27.3, 22.5, 20.6 (diastereoisomers mixture – duplicate signals). FT-IR (KBr, thin film, cm^{-1}): 1645, 1438, 1049, 894.

**82**

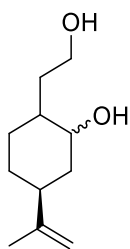
(*Z*)-2-((4*S*)-2-hydroxy-4-(prop-1-en-2-yl)cyclohexylidene)

acetaldehyde (**82**). It was obtained as a mixture of the diastereoisomeric aldehydes (0.25:1). Overall yields are low (<10%) and not reproducible due to the aldehyde instability during purification by chromatography.

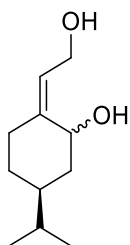
**83**

(*Z*)-2-(2-hydroxyethylidene)-5-(prop-1-en-2-yl)cyclohexanol (**83**). It was

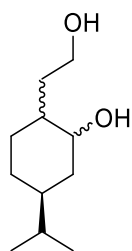
obtained after reduction of the reaction mixture containing the intermediate diastereoisomeric aldehydes by stirring the collected solution with NaBH₄ (2 equiv.) for 2 h (batch procedure) at room temperature and purifying the diol **83** by chromatography over silica gel (EtOAc/hexanes (7:3)). Compound **83**, a pale-yellow solid, was isolated in 17% overall yield (0.17 mmol; 30.2 mg): m.p. 69–72 °C; ¹H NMR (400 MHz, CDCl₃): δ_H 5.48 (t, *J* = 6.7 Hz, 1H), 4.64 (br. s, 2H), 4.26 (dd, *J* = 11.6, *J*₂ = 4.4 Hz, 1H), 4.17 (d, *J* = 6.7 Hz, 2H), 3.57 (br. s, 1H), 2.20 (dt, *J* = 13.5, *J* = 3.6 Hz, 1H), 1.96–2.15 (m, 3H), 1.69–1.76 (m, 1H), 1.65 (s, 3H), 1.41 (q, *J* = 11.9 Hz, 1H), 1.14–1.24 (m, 2H); ¹³C NMR (100 MHz, CDCl₃): δ_C 148.5, 146.1, 120.6, 109.1, 73.5, 58.3, 43.9, 42.3, 36.0, 32.6, 20.8. FT-IR (KBr pellet, cm⁻¹): 3329, 1643, 1439, 1001.



84 2-(2-hydroxyethyl)-5-(prop-1-en-2-yl)cyclohexanol (**84**). Identical experimental procedure described above for **83** syntheses. It was obtained as a complex mixture of diastereoisomers from further reduction of compound **83**, in 21% overall yield (0.21 mmol; 39.5 mg), dark-yellow oil: Complex NMR data (see NMR spectrum); FT-IR (KBr, thin film, cm^{-1}): 1643, 1438, 1087, 1001, 881.

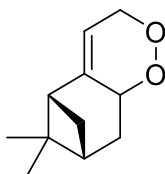


88 (*Z*)-2-(2-hydroxyethylidene)-5-isopropylcyclohexanol (**88**). It was obtained after reduction of the crude mixture containing the diastereoisomeric aldehydes by stirring the collected solution with NaBH_4 (2 equiv.) for 2 h (batch procedure) at room temperature. Diol **88**, a pale-yellow solid, was isolated in 15% overall yield (0.15 mmol; 27.7 mg) after purification by chromatography over silica gel (EtOAc/hexane (7:3)): m.p. 59–63°C; ^1H NMR (400 MHz, CDCl_3): δ_{H} 5.51 (t, $J = 6.1$ Hz, 1H), 4.21–4.28 (m, 3H), 2.22 (dt, $J = 13.5$, $J = 3.5$ Hz, 1H), 1.95–2.05 (m, 2H), 1.72 (br d, $J = 12.1$ Hz, 1H), 1.49 (oct, $J = 6.7$ Hz, 1H), 1.19–1.38 (m, 3H), 0.89 (d, $J = 1.04$ Hz, 3H), 0.87 (d, $J = 1.04$ Hz, 3H). ^{13}C NMR (100 MHz, CDCl_3): δ_{C} 146.7, 120.1, 73.6, 58.2, 42.8, 40.7, 36.0, 32.2, 30.7, 19.9, 19.8; FT-IR (KBr pellet, cm^{-1}): 1646, 1444, 1120, 1006, 985.

**89**

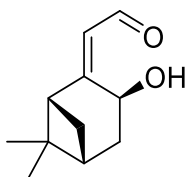
2-(2-hydroxyethyl)-5-isopropylcyclohexanol (89). Same experimental

procedure described above for **88**. It was obtained as a complex mixture of diastereoisomers from further reduction of compound **83**, in 21% overall yield (0.21 mmol; 39.5 mg), yellow oil: Complex NMR data (see NMR spectrum); FT-IR (KBr, thin film, cm^{-1}) ν : 3412, 2931, 1029, 983.

**91**

6,6-dimethyl-3,5,6,7,8,8a-hexahydro-5,7-

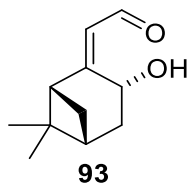
*methanobenzo[c][1,2]dioxine (91)*¹¹⁸. It was obtained in 52% overall yield (0.52 mmol; 94.0 mg) as a slightly yellow oil after purification by chromatography over silica gel (DCM/hexane (1:1)). ¹H NMR (400 MHz, CDCl_3): δ_{H} 5.39–5.43 (m, 1H), 5.29–5.35 (m, 1H), 4.90 (dt, $J = 15.9, J = 2.5$ Hz, 1H), 4.47 (ddd, $J = 15.9, J = 3.0, J = 1.9$ Hz, 1H), 2.63–2.69 (m, 2H), 2.37–2.45 (m, 1H), 2.07–2.12 (m, 1H), 1.55 (ddd, $J = 13.9, J = 6.6, J = 2.3$ Hz, 1H), 1.04–1.06 (m, 1H), 1.30 (s, 3H), 0.98 (s, 3H); ¹³C NMR (100 MHz, CDCl_3): δ_{C} 143.8, 114.1, 75.0, 71.4, 50.4, 41.6, 39.7, 37.1, 30.2, 27.0, 23.8.

**92**

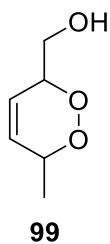
(Z)-2-(3-hydroxy-6,6-dimethylbicyclo[3.1.1]heptan-2-

ylidene)acetaldehyde (92). It was obtained as a yellow oil in 14% overall yield (0.14 mmol; 25.7 mg) after purification by chromatography over silica gel (Hexane/EtOAc (8:2)): ¹H NMR (400 MHz, CDCl_3): δ_{H} 9.70 (d, $J = 3.3$ Hz, 1H), 5.99 (dd, $J = 3.3, J = 1.1$ Hz, 1H), 4.82 (d, $J = 8.6$ Hz, 1H), 4.00 (br. s, 1H), 2.58 (t, $J = 5.4$ Hz, 1H), 2.38–2.51 (m, 2H), 2.09–2.13 (m, 1H), 1.98 (ddd, $J = 14.6, J = 4.0, J_3 = 1.6$ Hz, 1H), 1.71 (d, $J = 10.1$ Hz,

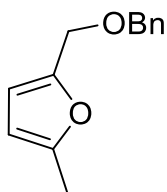
1H), 1.32 (s, 3H), 0.70 (s, 3H); ^{13}C NMR (100 MHz, CDCl_3): δ_{C} 191.8, 171.8, 124.5, 62.6, 52.9, 41.1, 39.8, 34.3, 27.3, 25.8, 22.5; FT-IR (KBr, thin film, cm^{-1}): 3433, 1673, 1629.



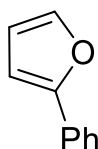
(*Z*)-2-((1*R*,3*R*,5*R*)-3-hydroxy-6,6-dimethylbicyclo[3.1.1] heptan-2-ylidene)acetaldehyde (**93**). It was obtained as a yellow oil in 8% overall yield (0.08 mmol; 12.7 mg) after purification by chromatography over silica gel (Hexanes/EtOAc (8:2)): ^1H NMR (400 MHz, CDCl_3): δ_{H} 9.95 (d, $J = 8.0$ Hz, 1H), 6.06 (d, $J = 8.0$ Hz, 1H), 3.60 (t, $J = 5.4$ Hz, 1H), 2.49–2.58 (m, 1H), 2.35–2.42 (m, 1H), 1.98 (ddd, $J = 14.7$, $J = 4.2$, $J = 1.0$ Hz, 1H), 1.87 (d, $J = 10.3$ Hz, 1H), 1.39 (s, 3H), 0.73 (s, 3H) ^{13}C NMR (100 MHz, CDCl_3): δ_{C} 190.8, 171.1, 128.1, 67.7, 45.1, 41.9, 39.7, 34.6, 26.8, 26.1, 22.3; FT-IR (KBr, thin film, cm^{-1}): 3435, 1652, 1629.



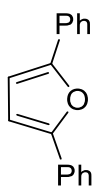
(6-methyl-3,6-dihydro-1,2-dioxin-3-yl)metanol (**99**)¹¹⁹. It was obtained as a yellow oil in 57% overall yield (0.57 mmol; 73.7 mg) after purification by chromatography over silica gel (DCM/MeOH (9:1)): ^1H NMR (400 MHz, CDCl_3): δ_{H} 5.97 (dt, $J = 10.3$, $J = 1.7$ Hz, 1H), 5.84–5.88 (m, 1H), 4.78–4.83 (m, 1H), 4.41–4.45 (m, 1H), 3.86 (dd, $J_1 = 12.3$, $J_2 = 7.75$ Hz, 1H), 3.70 (dd, $J = 12.3$, $J = 3.1$ Hz, 1H), 2.28 (br. s, 1H), 1.20 (d, $J = 6.8$ Hz, 3H); ^{13}C NMR (100 MHz, CDCl_3): δ_{C} 131.3, 123.0, 79.7, 74.3, 63.2, 17.5.

**104**

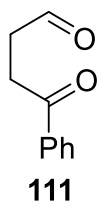
2-((benzyloxy)methyl)-5-methylfuran (**104**)¹²⁰. It was obtained as a yellow oil in 42% overall yield (0.42 mmol; 85.3 mg) after purification by chromatography over silica gel (Hexane/EtOAc (7:3)): ¹H NMR (400 MHz, CDCl₃): δ_H 7.26–7.37 (m, 5H), 6.20 (d, *J* = 3.0 Hz, 1H), 5.90–5.93 (m, 1H), 4.55 (s, 2H), 4.42 (s, 2H), 2.29 (s, 3H); ¹³C NMR (100 MHz, CDCl₃): δ_C 152.6, 149.8, 138.0, 128.3, 127.9, 127.6, 110.4, 106.1, 71.7, 63.9, 13.6.

**107**

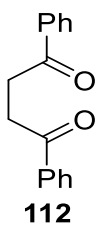
2-phenylfuran (**107**)¹²¹. It was obtained as colorless oil in 29% overall yield (0.29 mmol; 41.9 mg) after purification by chromatography over silica gel (Hexane/EtOAc (9.8:0.2)): ¹H NMR (400 MHz, CDCl₃): δ_H 7.69–7.68 (m, 2H), 7.50 (d, *J* = 2.0 Hz, 1H), 7.45–7.40 (m, 2H), 7.30–7.28 (m, 1H), 6.69 (d, *J* = 3.2 Hz, 1H), 6.52 (dd, *J* = 3.2 Hz, *J* = 2.0 Hz, 1H); ¹³C NMR (100 MHz, CDCl₃): δ_C 154.2, 142.4, 131.0, 128.7, 127.3, 123.9, 111.7, 105.2.

**110**

2,5-diphenylfuran (**110**)¹²². It was obtained as pale-yellow solid in 58% overall yield (0.58 mmol; 128.5 mg) after purification by chromatography over silica gel (Hexane/EtOAc (9.5:0.5)): m.p. 85–88 °C (lit.¹²³ 86–88 °C); ¹H NMR (400 MHz, acetone-*d*₆): δ_H 7.87–7.81 (m, 4H), 7.48–7.41 (m, 4H), 7.34–7.27 (m, 2H), 6.97 (2H, s); ¹³C NMR (100 MHz, acetone-*d*₆): δ_C 154.2, 131.7, 129.8, 128.4, 124.5, 108.6.

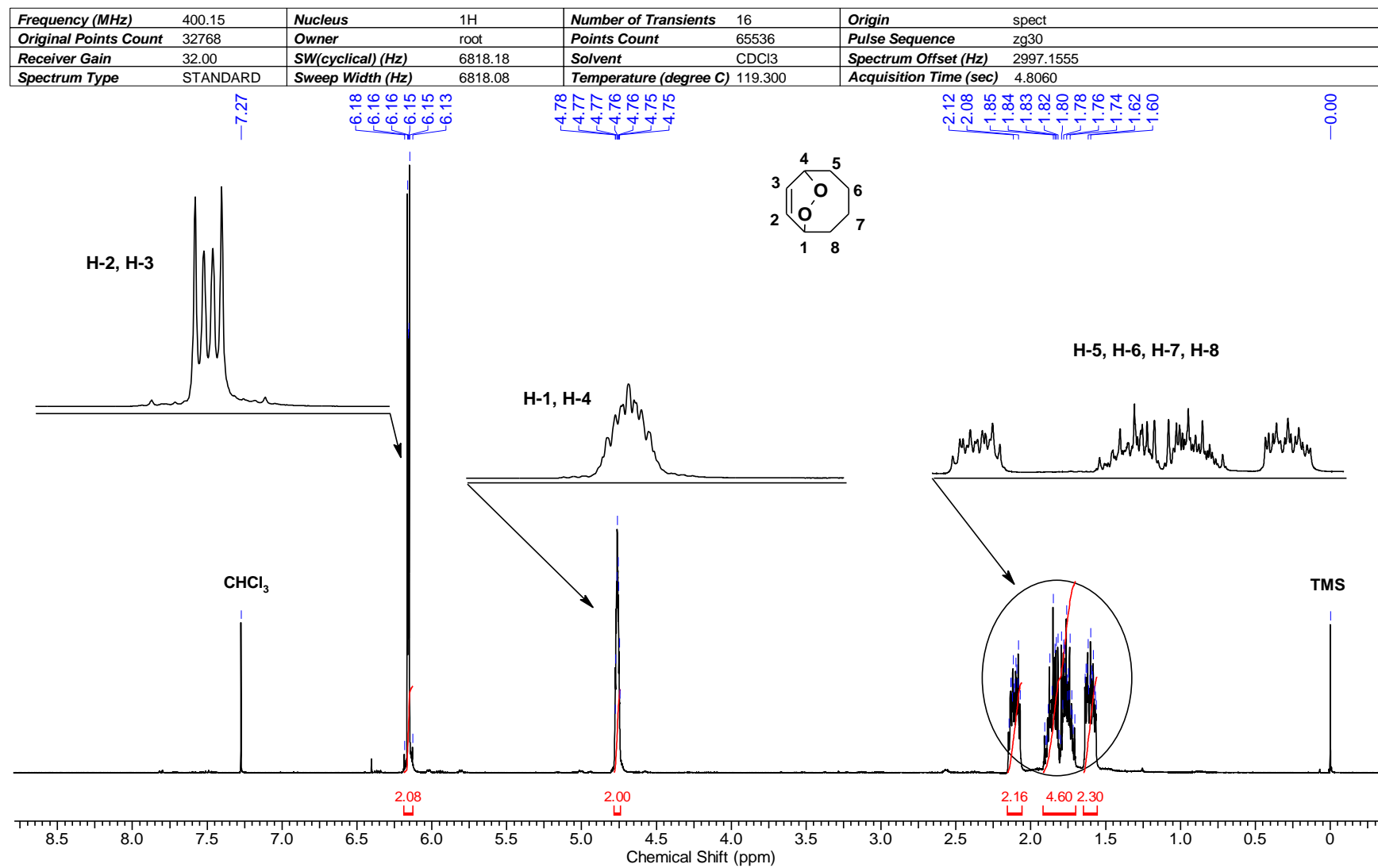


*4-oxo-4-phenylbutanal (III)*¹²⁴. It was obtained as a colorless oil in 42% overall yield (0.42 mmol; 67.6 mg) after purification by chromatography over silica gel (Hexane/EtOAc (7:3)): ¹H NMR (400 MHz, CDCl₃): δ_H 9.90 (t, *J* = 0.7 Hz, 1H), 8.00–7.96 (m, 2H), 7.60–7.54 (m, 1H), 7.49–7.44 (m, 2H), 3.32 (t, *J* = 6.2 Hz, 2H), 2.92 (td, *J* = 6.2, *J* = 0.6 Hz, 2H); ¹³C NMR (100 MHz, CDCl₃): δ_C 200.6, 197.8, 136.3, 133.2, 128.6, 128.0, 37.5, 30.9.

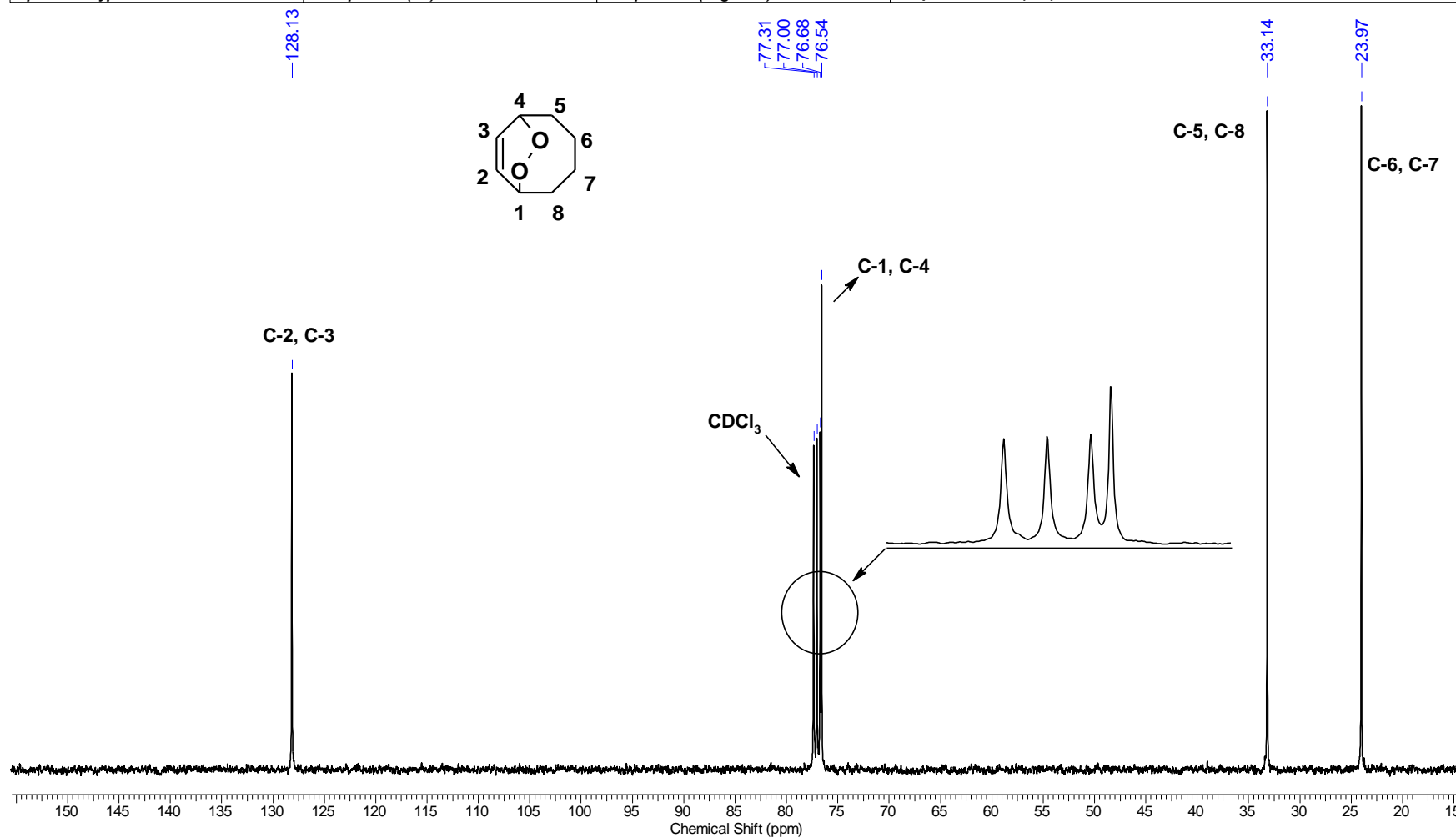


*1,4-diphenylbutane-1,4-dione (59)*¹²⁵. After removing part of the solvent mixture under reduced pressure (30 °C), dione **59** precipitates as a white solid (soluble in acetone). It was filtered-off and the remaining product solution was concentrated and purified by chromatography over silica gel (Hexane/EtOAc (8:2)). It was obtained in 80% overall yield (0.80 mmol; 191.3 mg): m.p. 143–145 °C (lit.¹²⁶ 142–143 °C); ¹H NMR (400 MHz, acetone-d₆): δ_H 8.09–8.05 (m, 4H), 7.67–7.61 (m, 2H), 7.57–7.51 (m, 4H), 3.48 (s, 4H); ¹³C NMR (100 MHz, acetone-d₆): δ_C 199.0, 138.1, 133.9, 129.6, 128.9, 33.2. FT-IR (KBr pellet, cm⁻¹) ν: 3066, 2914, 2835, 1718, 1683, 1448, 1240, 756, 690.

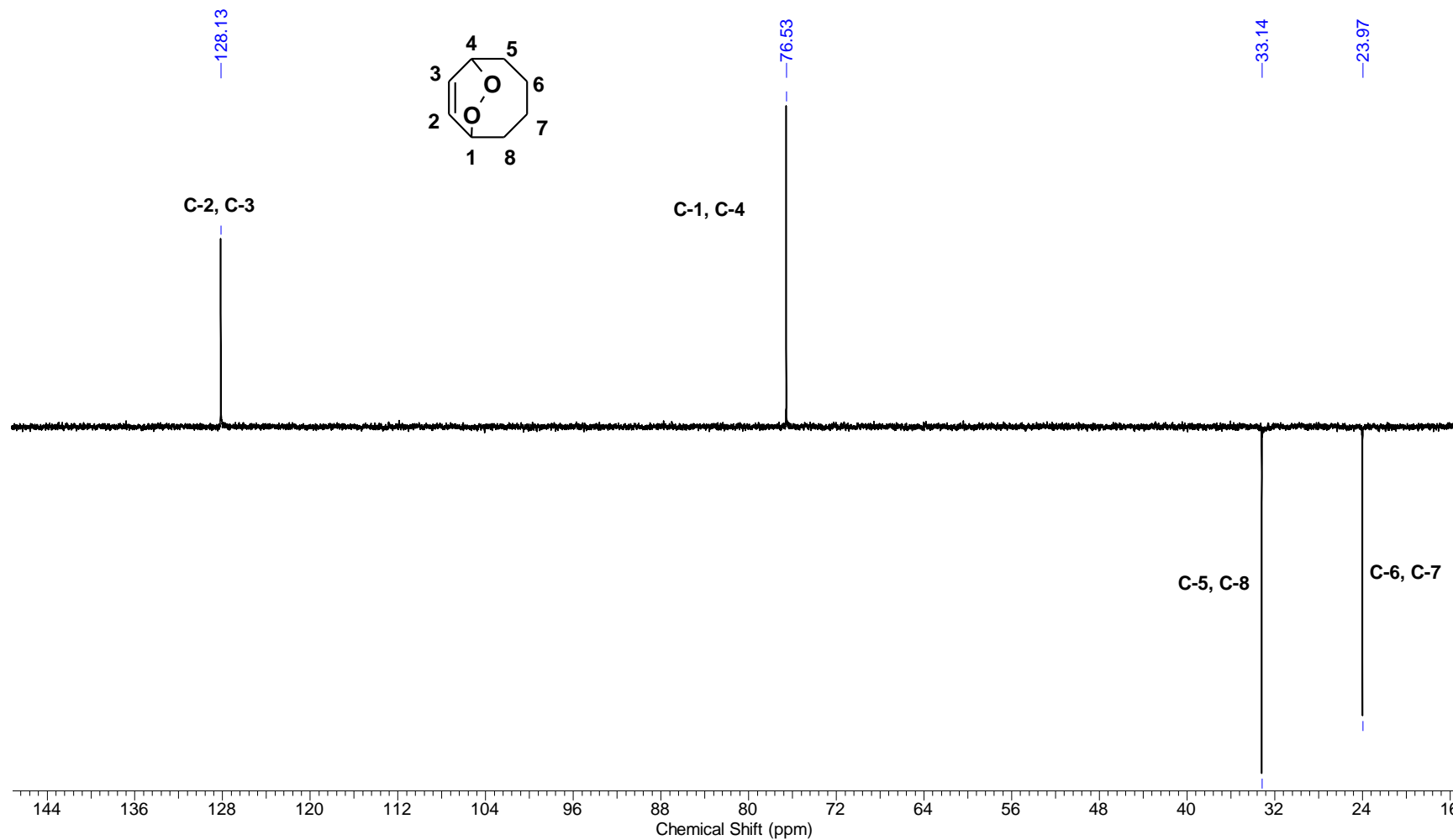
5.1.5. NMR Spectra



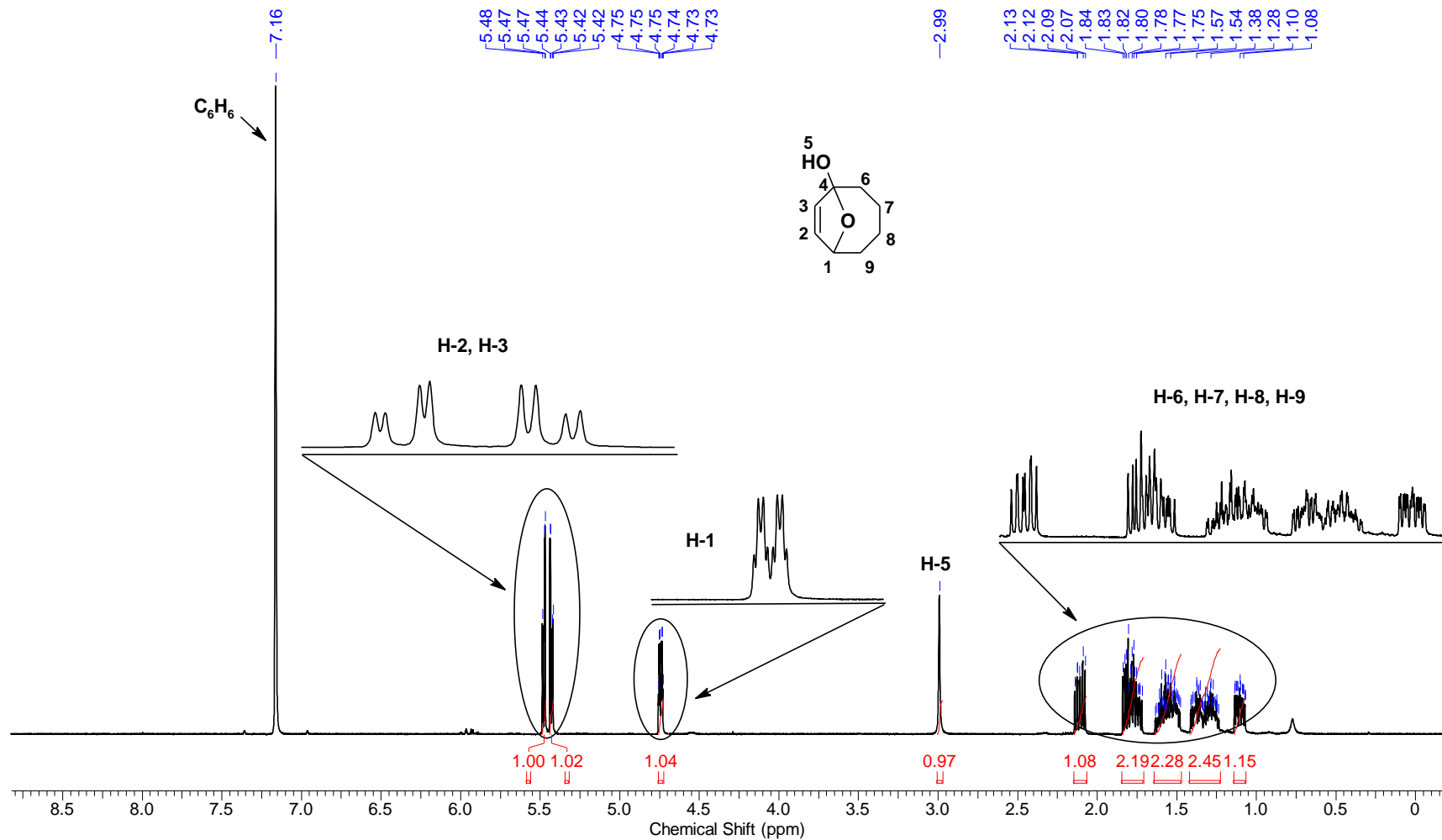
Frequency (MHz)	100.62	Nucleus	¹³ C	Number of Transients	1024	Origin	spect
Original Points Count	16384	Owner	root	Points Count	32768	Pulse Sequence	zgpg30
Receiver Gain	2050.00	SW(cyclical) (Hz)	24671.05	Solvent	CDCl ₃	Spectrum Offset (Hz)	10056.3408
Spectrum Type	STANDARD	Sweep Width (Hz)	24670.30	Temperature (degree C)	119.300	Acquisition Time (sec)	0.6641



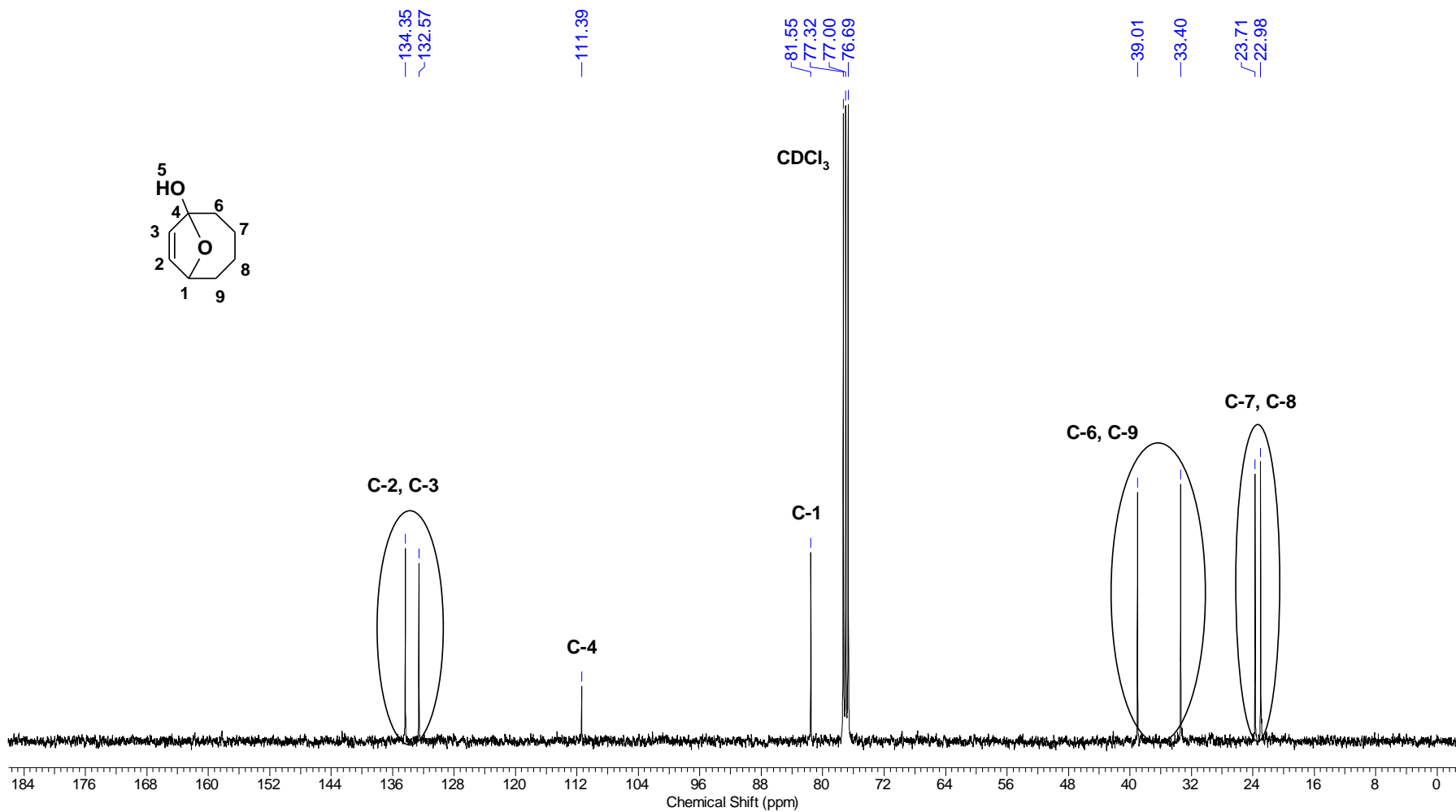
Frequency (MHz)	100.62	Nucleus	¹³ C	Number of Transients	1024	Origin	spect
Original Points Count	16384	Owner	root	Points Count	32768	Pulse Sequence	deptsp135
Receiver Gain	1620.00	SW(cyclical) (Hz)	20161.29	Solvent	CDCl ₃	Spectrum Offset (Hz)	8043.7173
Spectrum Type	DEPT135	Sweep Width (Hz)	20160.68	Temperature (degree C)	119.400	Acquisition Time (sec)	0.8126



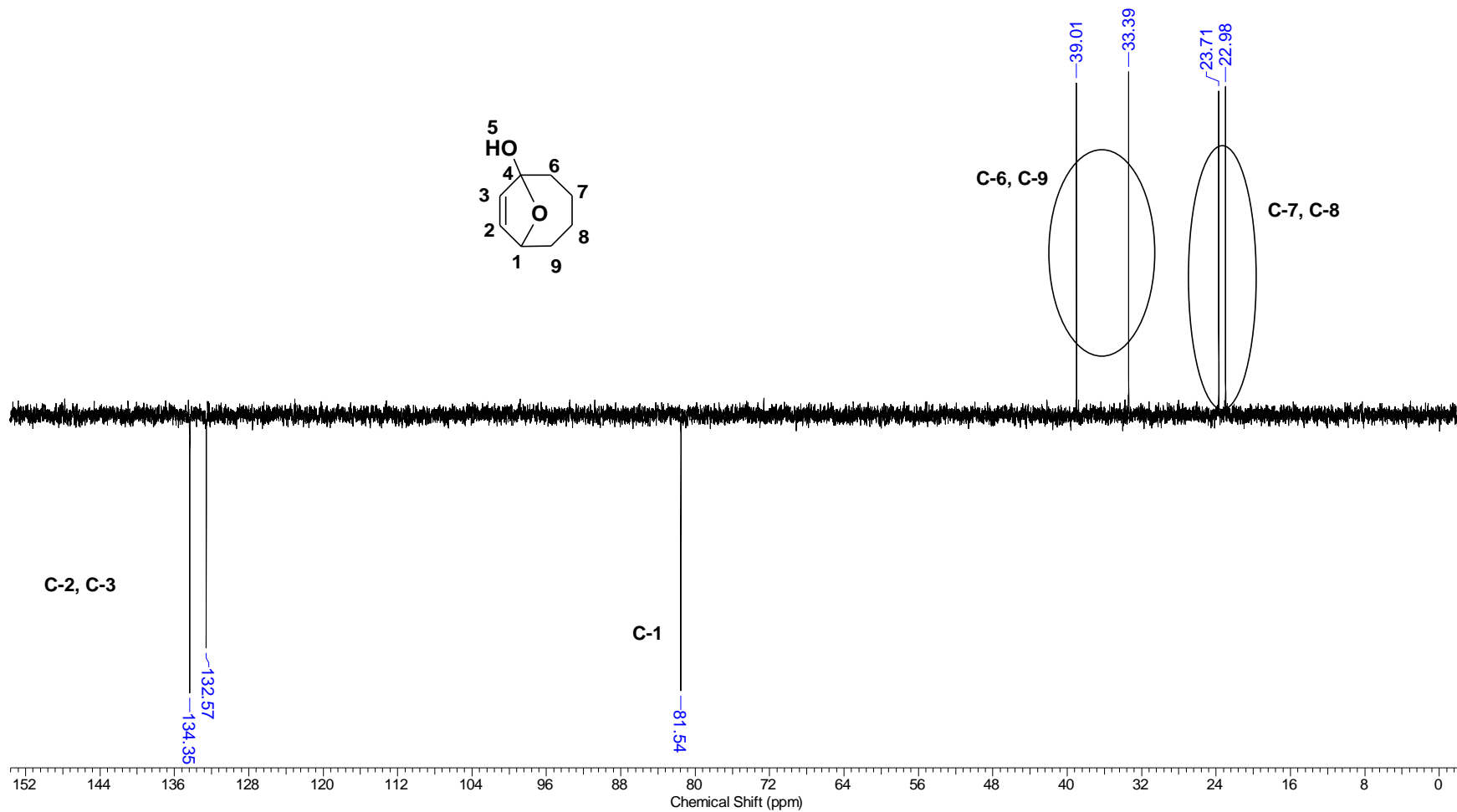
Frequency (MHz)	400.15	Nucleus	1H	Number of Transients	16	Origin	spect
Original Points Count	32768	Owner	root	Points Count	65536	Pulse Sequence	zg30
Receiver Gain	114.00	SW(cyclical) (Hz)	6818.18	Solvent	BENZENE-d6	Spectrum Offset (Hz)	3004.5359
Spectrum Type	STANDARD	Sweep Width (Hz)	6818.08	Temperature (degree C)	119.400	Acquisition Time (sec)	4.8060



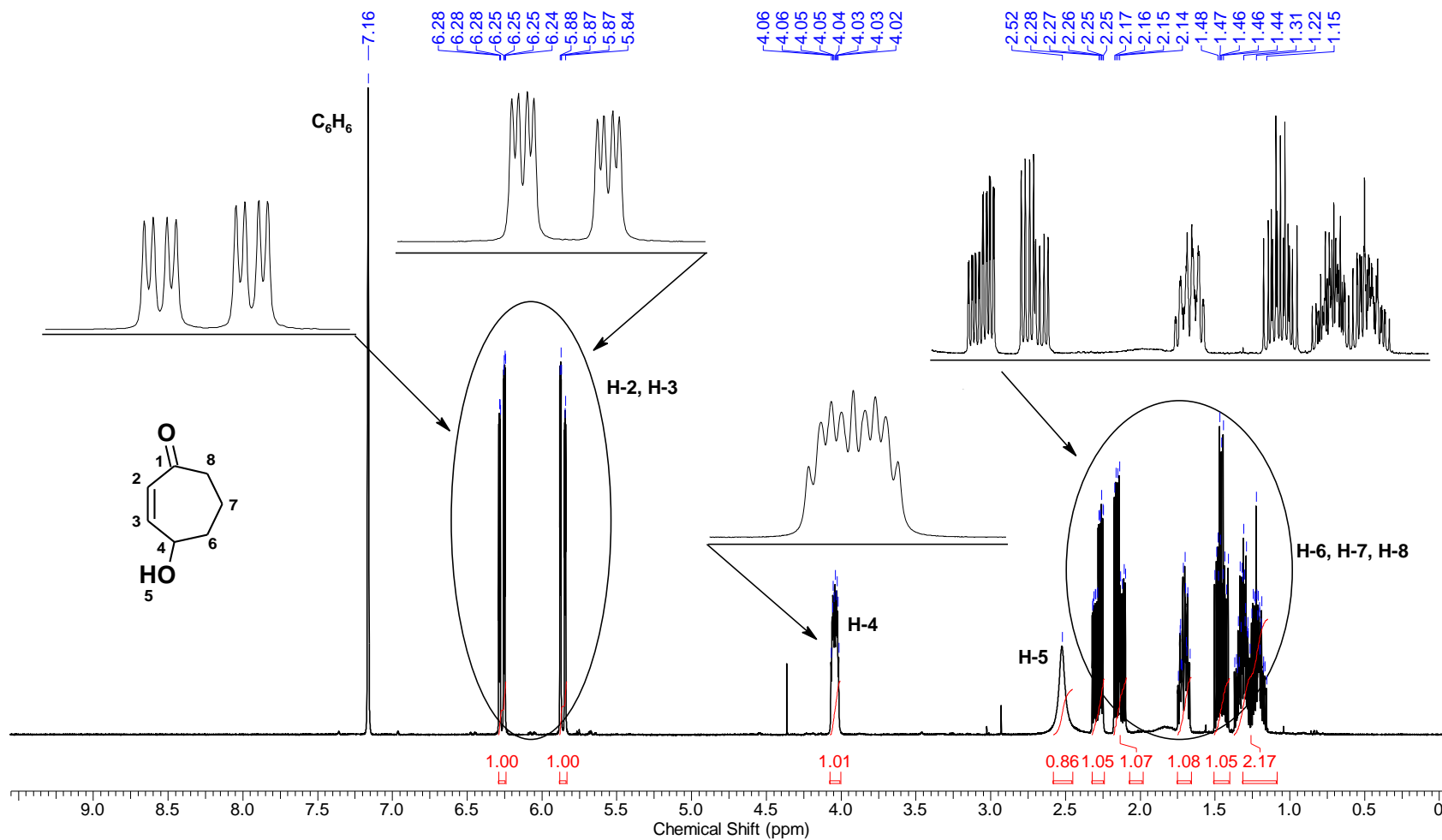
Frequency (MHz)	100.62	Nucleus	¹³ C	Number of Transients	1024	Origin	spect
Original Points Count	16384	Owner	root	Points Count	32768	Pulse Sequence	zpgpg30
Receiver Gain	2050.00	SW(cyclical) (Hz)	24671.05	Solvent	CDCl ₃	Spectrum Offset (Hz)	10058.5996
Spectrum Type	STANDARD	Sweep Width (Hz)	24670.30	Temperature (degree C)	119.000	Acquisition Time (sec)	0.6641



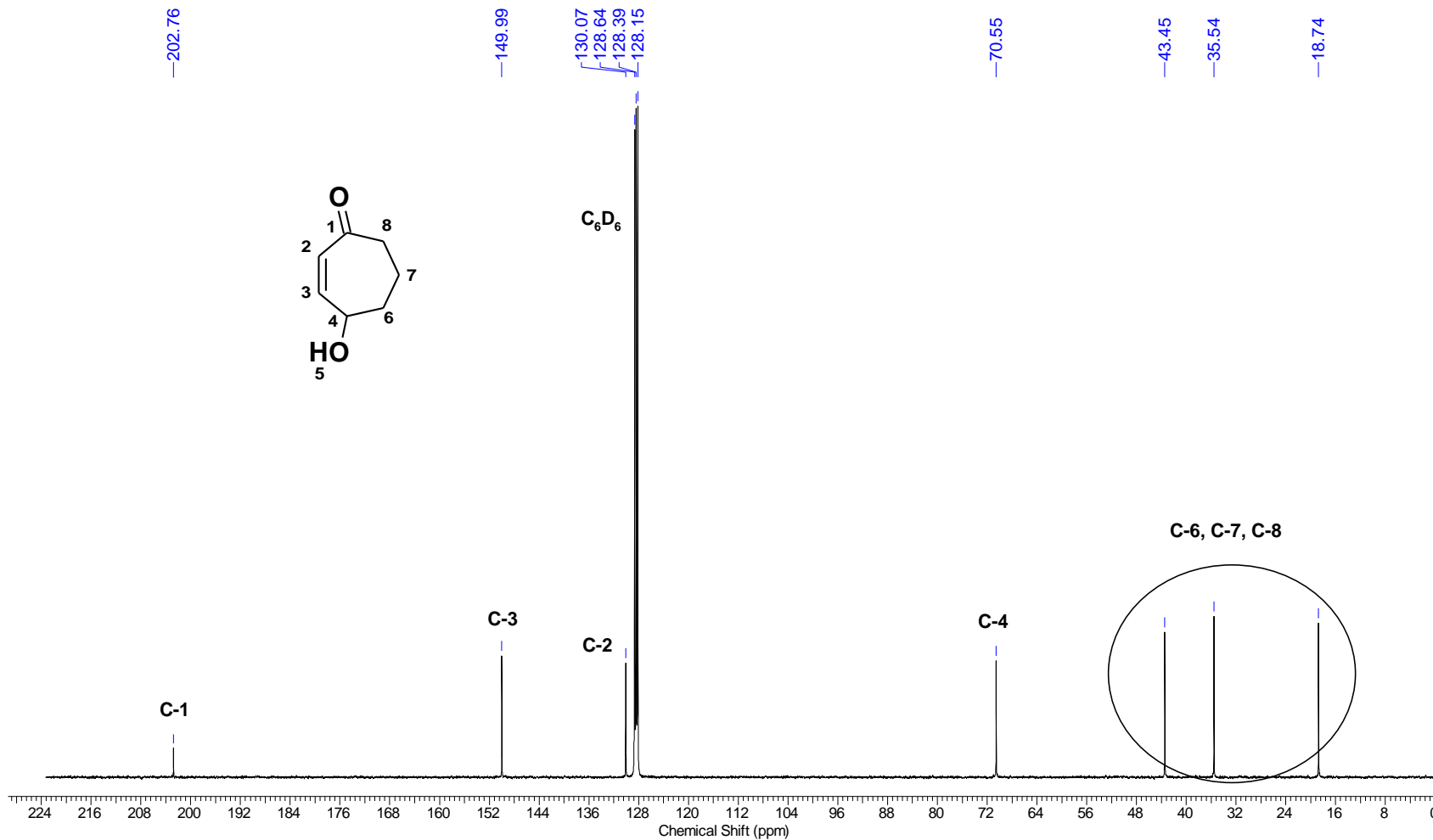
Frequency (MHz)	100.62	Nucleus	¹³ C	Number of Transients	1024	Origin	spect
Original Points Count	16384	Owner	root	Points Count	32768	Pulse Sequence	deptsp135
Receiver Gain	2050.00	SW(cyclical) (Hz)	20161.29	Solvent	CDCl ₃	Spectrum Offset (Hz)	8045.6255
Spectrum Type	DEPT135	Sweep Width (Hz)	20160.68	Temperature (degree C)	118.900	Acquisition Time (sec)	0.8126



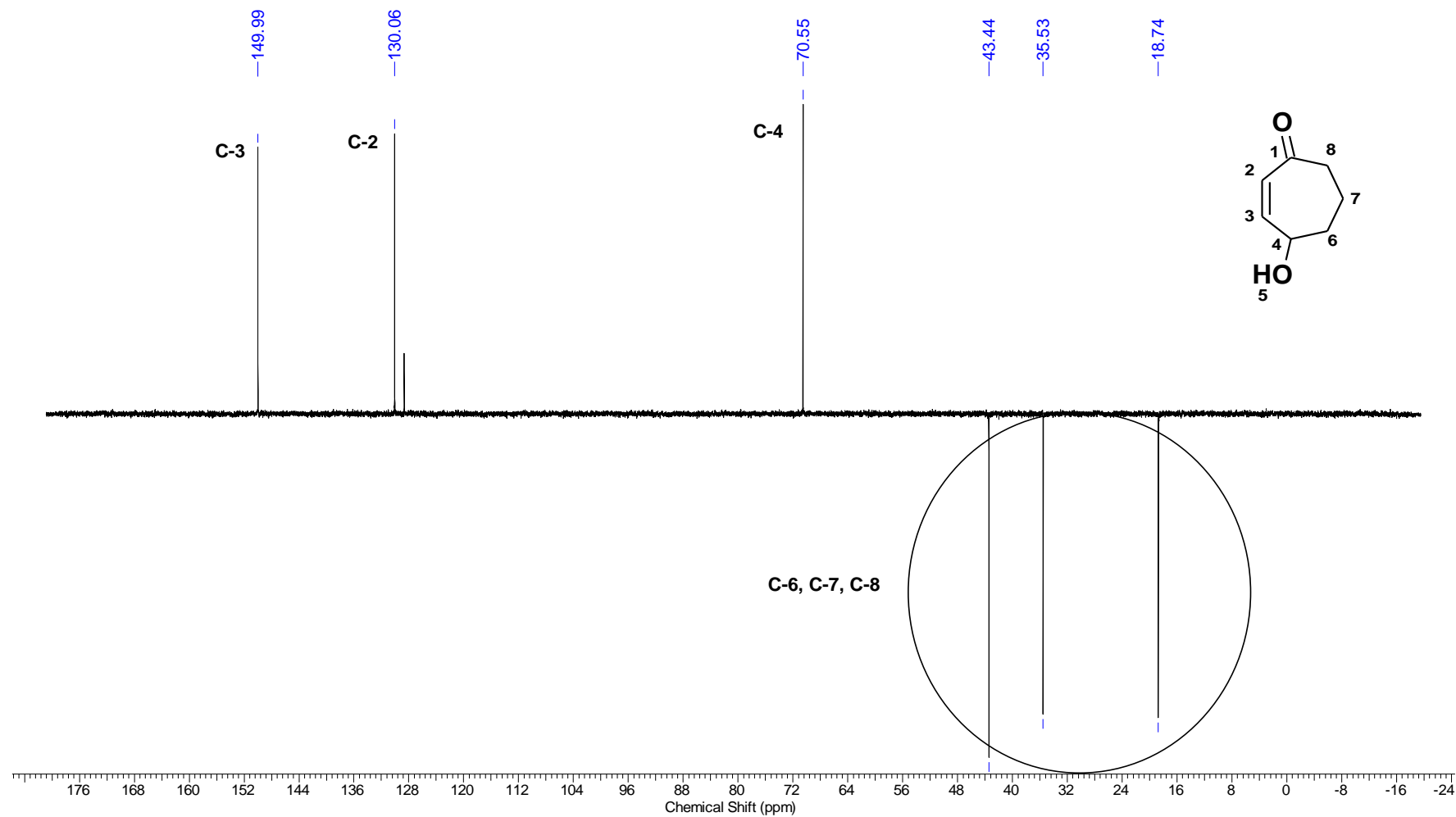
Frequency (MHz)	400.15	Nucleus	1H	Number of Transients	16	Origin	spect
Original Points Count	32768	Owner	nmrsu	Points Count	65536	Pulse Sequence	zg30
Receiver Gain	64.00	SW(cyclical) (Hz)	6818.18	Solvent	BENZENE-d6	Spectrum Offset (Hz)	3004.7437
Spectrum Type	STANDARD	Sweep Width (Hz)	6818.08	Temperature (degree C)	24.900	Acquisition Time (sec)	4.8060



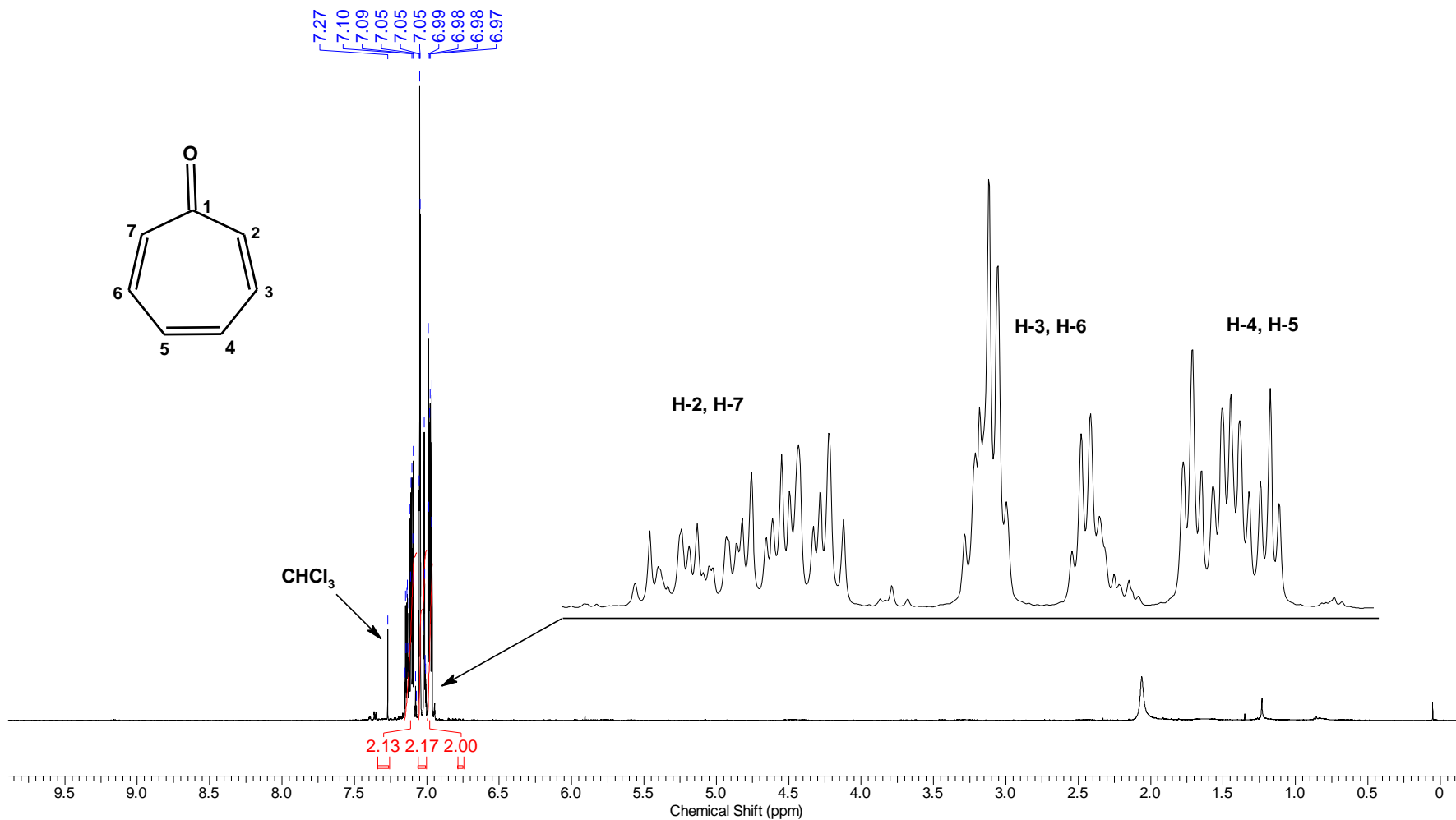
Frequency (MHz)	100.62	Nucleus	13C	Number of Transients	1024	Origin	spect
Original Points Count	16384	Owner	nmrslu	Points Count	32768	Pulse Sequence	zgpg30
Receiver Gain	2050.00	SW(cyclical) (Hz)	24671.05	Solvent	BENZENE-d6	Spectrum Offset (Hz)	10131.4541
Spectrum Type	STANDARD	Sweep Width (Hz)	24670.30	Temperature (degree C)	25.000	Acquisition Time (sec)	0.6641



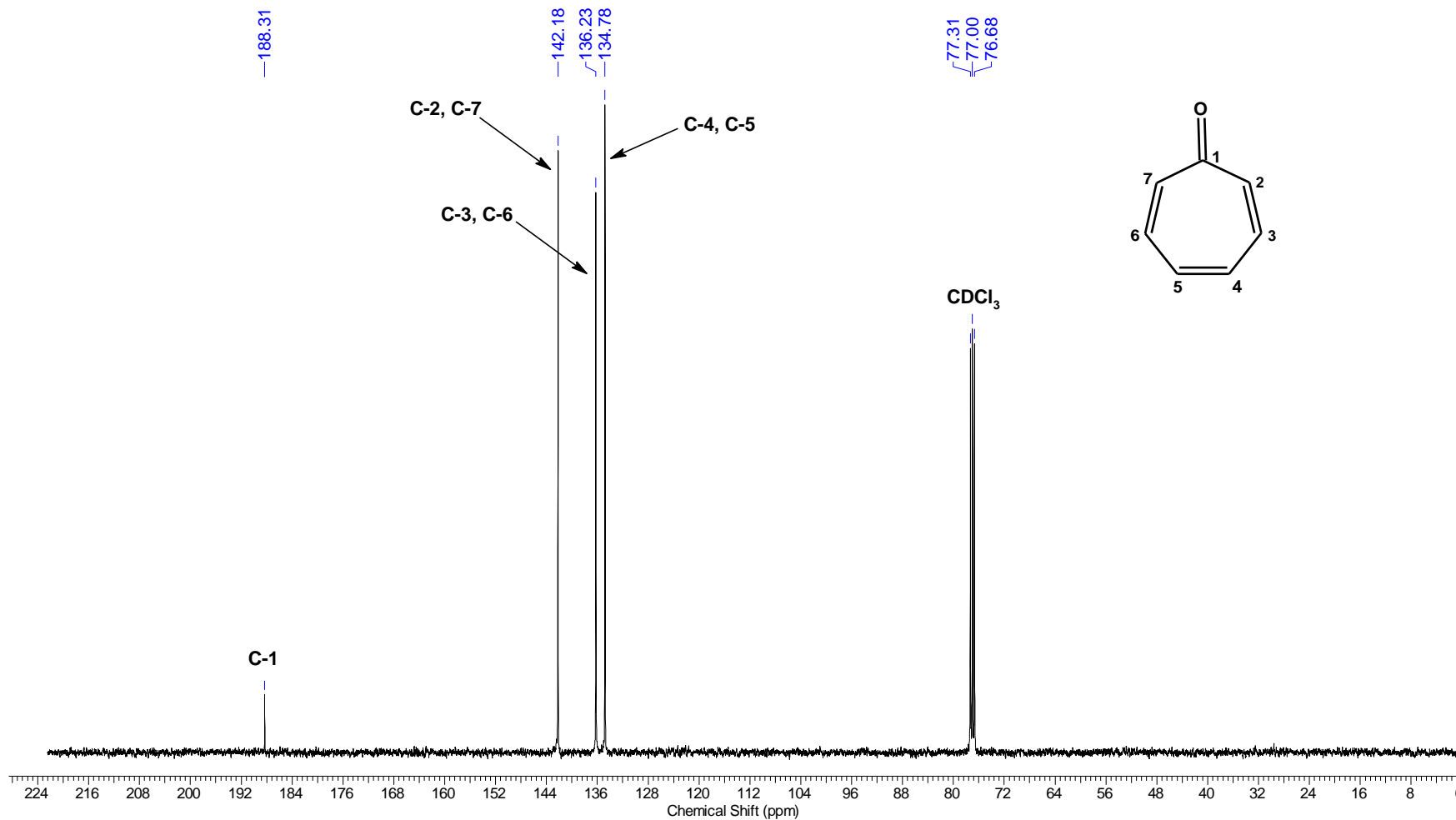
Frequency (MHz)	100.62	Nucleus	¹³ C	Number of Transients	1024	Origin	spect
Original Points Count	16384	Owner	nmsu	Points Count	32768	Pulse Sequence	deptsp135
Receiver Gain	2050.00	SW(cyclical) (Hz)	20161.29	Solvent	BENZENE-d6	Spectrum Offset (Hz)	8117.9927
Spectrum Type	DEPT135	Sweep Width (Hz)	20160.68	Temperature (degree C)	25.000	Acquisition Time (sec)	0.8126



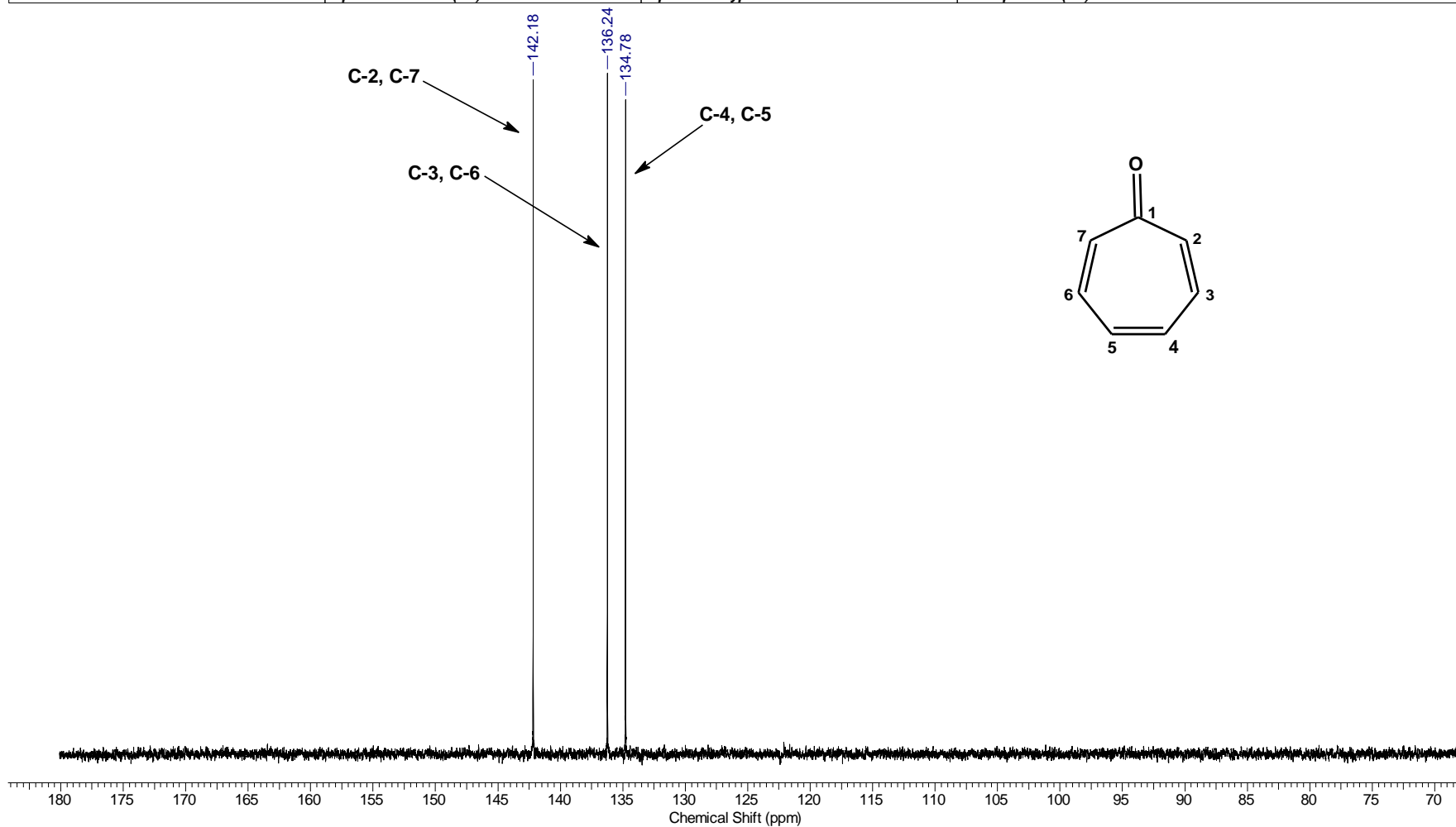
Acquisition Time (sec)	Temperature (degree C)	23.800	Frequency (MHz)	400.15	Nucleus	1H	
Number of Transients	16	Origin	spect	Original Points Count	32768	Owner	nmrsu
Points Count	65536	Pulse Sequence	zg30	Receiver Gain	114.00	SW(cyclical) (Hz)	6818.18
Solvent	CDCl3	Spectrum Offset (Hz)	2995.5974	Spectrum Type	STANDARD	Sweep Width (Hz)	6818.08



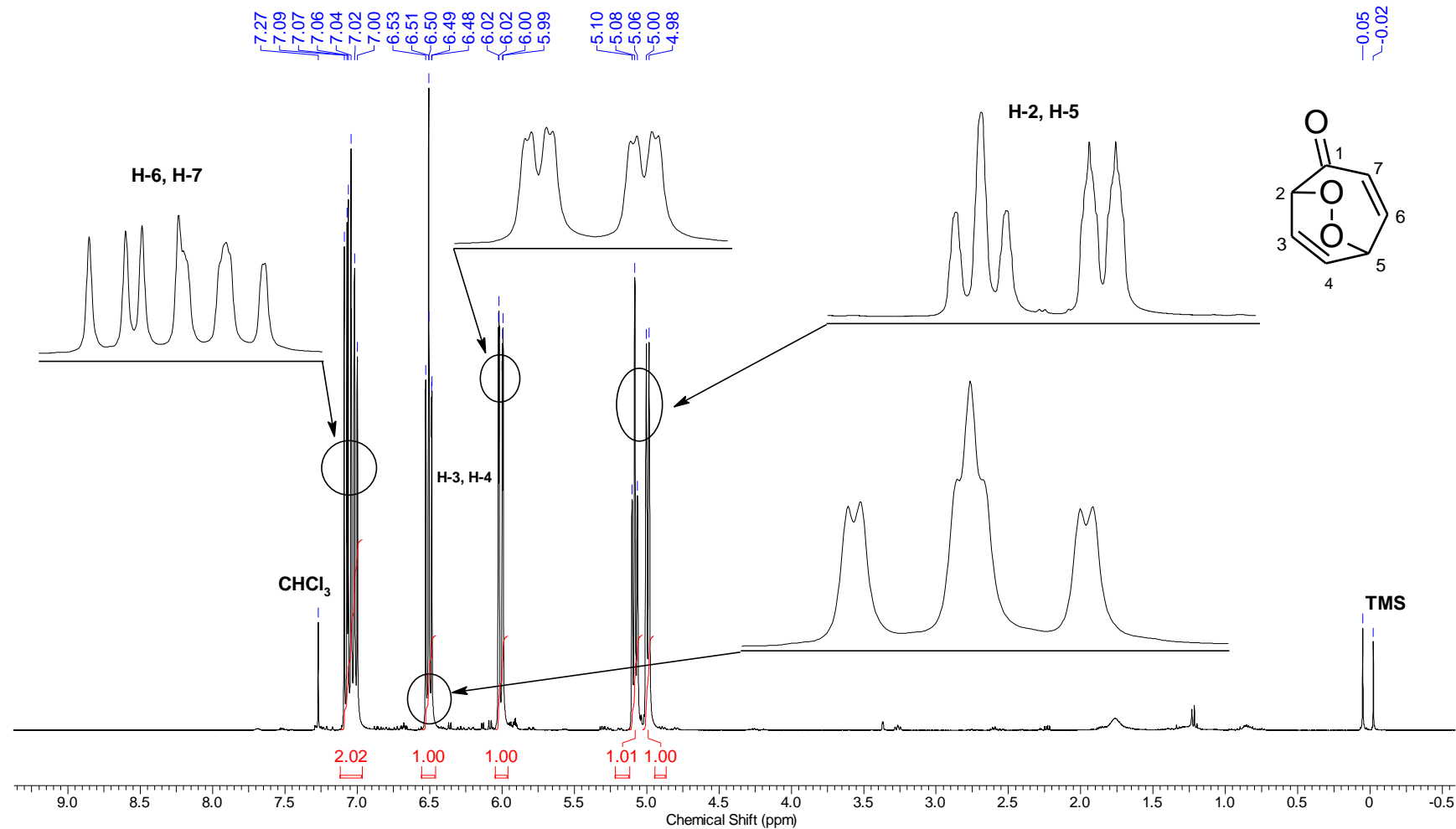
Acquisition Time (sec)	0.6641	Temperature (degree C)	24.400	Frequency (MHz)	100.62	Nucleus	¹³ C
Number of Transients	1024	Origin	spect	Original Points Count	16384	Owner	nmr-su
Points Count	32768	Pulse Sequence	zgpg30	Receiver Gain	2050.00	SW(cyclical) (Hz)	24671.05
Solvent	CDCl ₃	Spectrum Offset (Hz)	10053.3291	Spectrum Type	STANDARD	Sweep Width (Hz)	24670.30



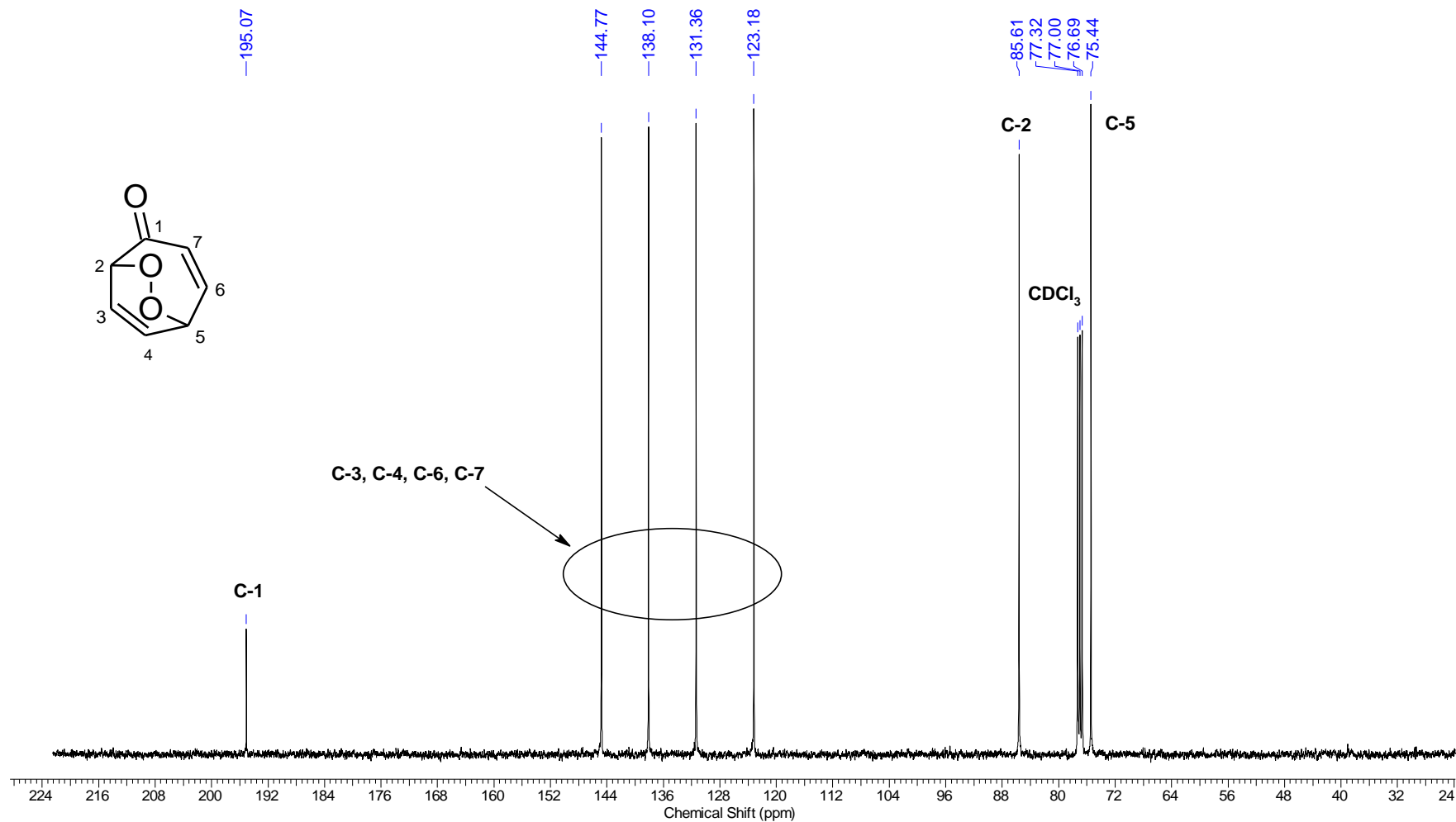
Acquisition Time (sec)	0.8126	Temperature (degree C)	24.100	Frequency (MHz)	100.62	Nucleus	¹³ C
Number of Transients	1024	Origin	spect	Original Points Count	16384	Owner	nmrsu
Points Count	32768	Pulse Sequence	depts135	Receiver Gain	2050.00	SW(cyclical) (Hz)	20161.29
Solvent	CDCl ₃	Spectrum Offset (Hz)	8040.1074	Spectrum Type	DEPT135	Sweep Width (Hz)	20160.68



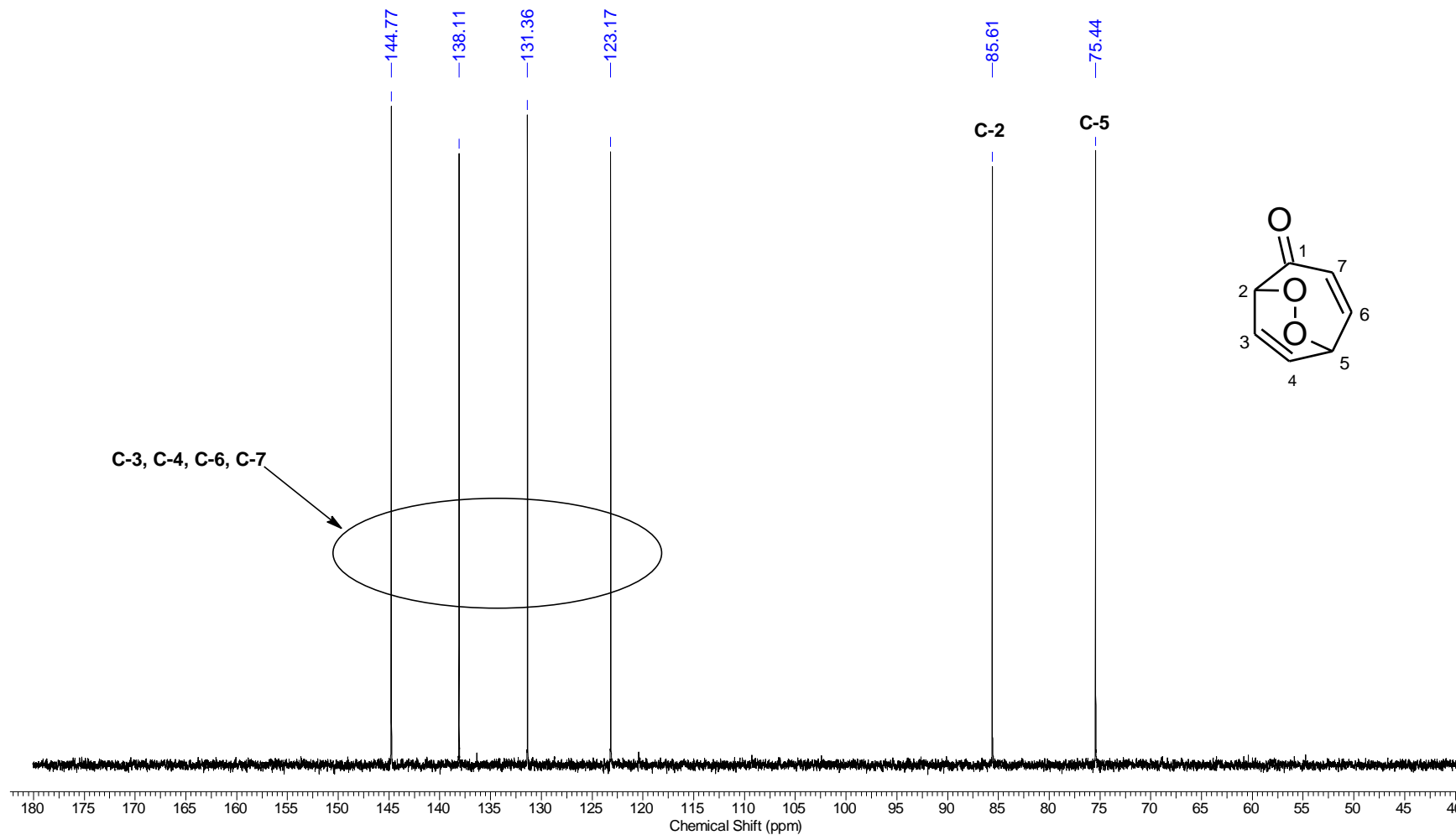
Frequency (MHz)	400.15	Nucleus	1H	Number of Transients	64	Origin	spect
Original Points Count	32768	Owner	root	Points Count	65536	Pulse Sequence	zg30
Receiver Gain	90.50	SW(cyclical) (Hz)	6818.18	Solvent	CDCl3	Spectrum Offset (Hz)	2995.4934
Spectrum Type	STANDARD	Sweep Width (Hz)	6818.08	Temperature (degree C)	119.800	Acquisition Time (sec)	4.8060



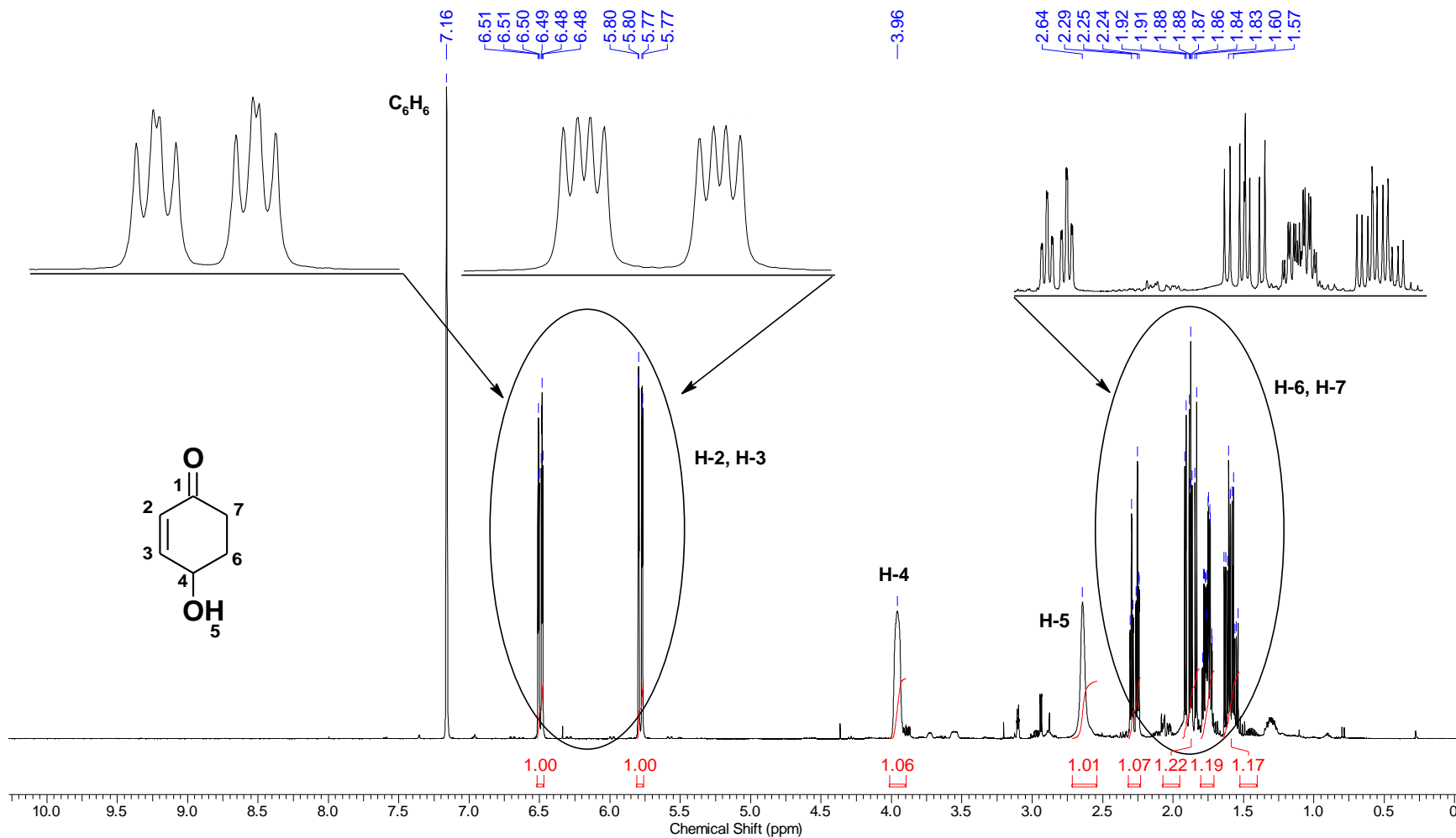
Frequency (MHz)	100.62	Nucleus	¹³ C	Number of Transients	1024	Origin	spect
Original Points Count	16384	Owner	root	Points Count	32768	Pulse Sequence	zgpg30
Receiver Gain	2050.00	SW(cyclical) (Hz)	24671.05	Solvent	CDCl ₃	Spectrum Offset (Hz)	10051.0703
Spectrum Type	STANDARD	Sweep Width (Hz)	24670.30	Temperature (degree C)	119.600	Acquisition Time (sec)	0.6641



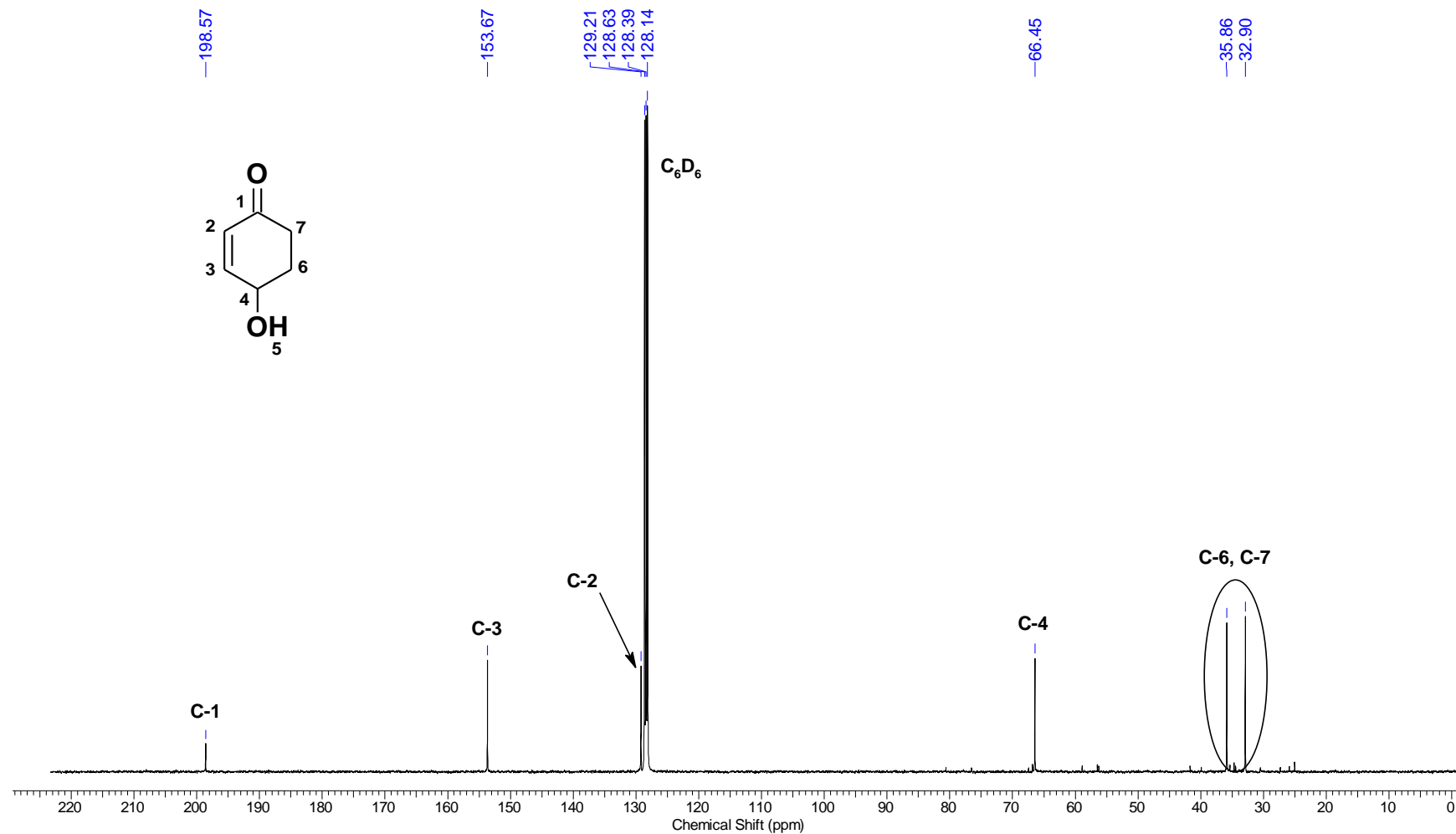
Frequency (MHz)	100.62	Nucleus	¹³ C	Number of Transients	1024	Origin	spect
Original Points Count	16384	Owner	root	Points Count	32768	Pulse Sequence	deptsp135
Receiver Gain	2050.00	SW(cyclical) (Hz)	20161.29	Solvent	CDCl ₃	Spectrum Offset (Hz)	8038.2192
Spectrum Type	DEPT135	Sweep Width (Hz)	20160.68	Temperature (degree C)	119.600	Acquisition Time (sec)	0.8126



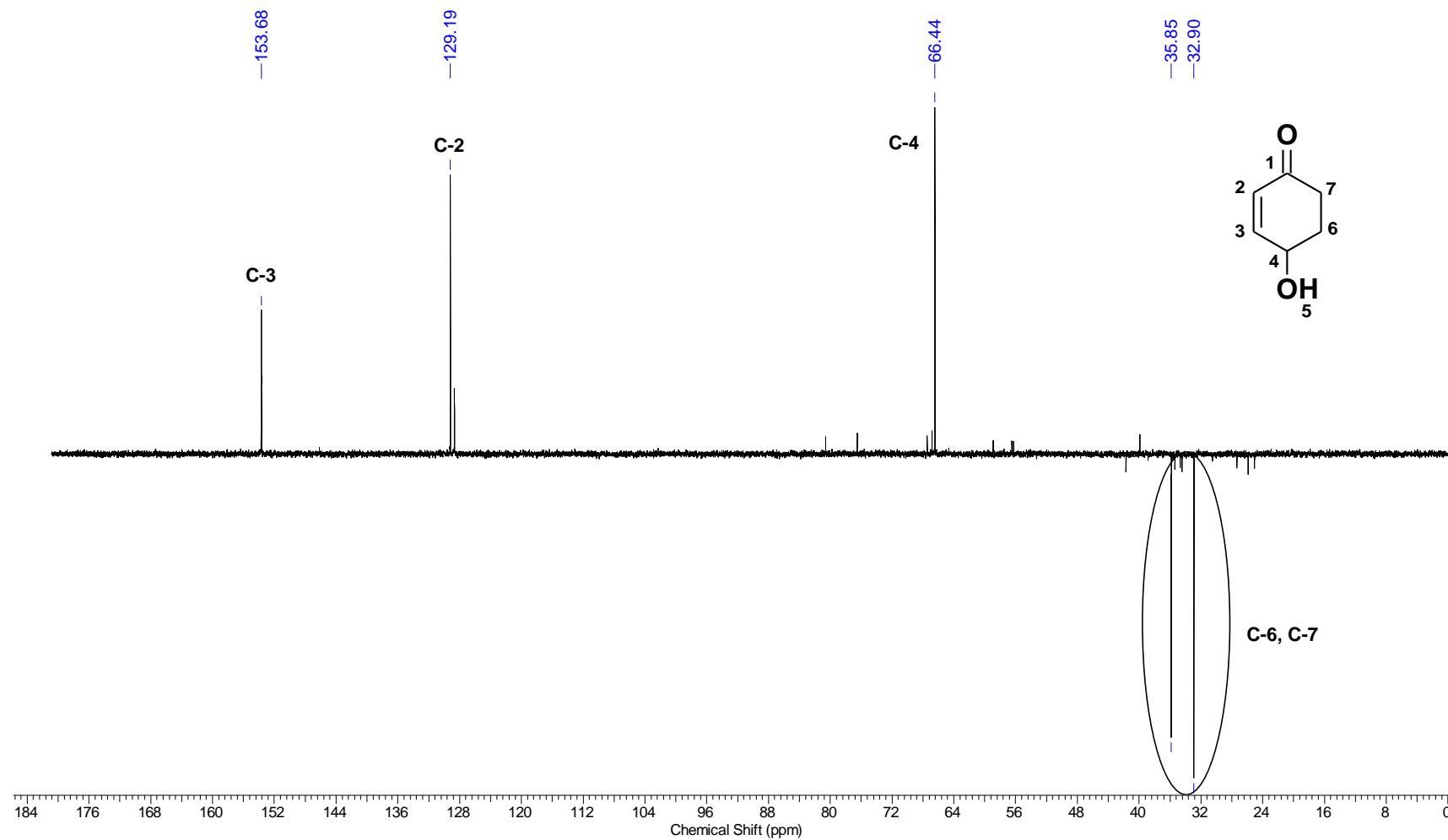
Frequency (MHz)	400.15	Nucleus	1H	Number of Transients	64	Origin	spect
Original Points Count	32768	Owner	nmrsu	Points Count	65536	Pulse Sequence	zg30
Receiver Gain	71.80	SW(cyclical) (Hz)	6818.18	Solvent	BENZENE-d6	Spectrum Offset (Hz)	3004.7437
Spectrum Type	STANDARD	Sweep Width (Hz)	6818.08	Temperature (degree C)	25.000	Acquisition Time (sec)	4.8060



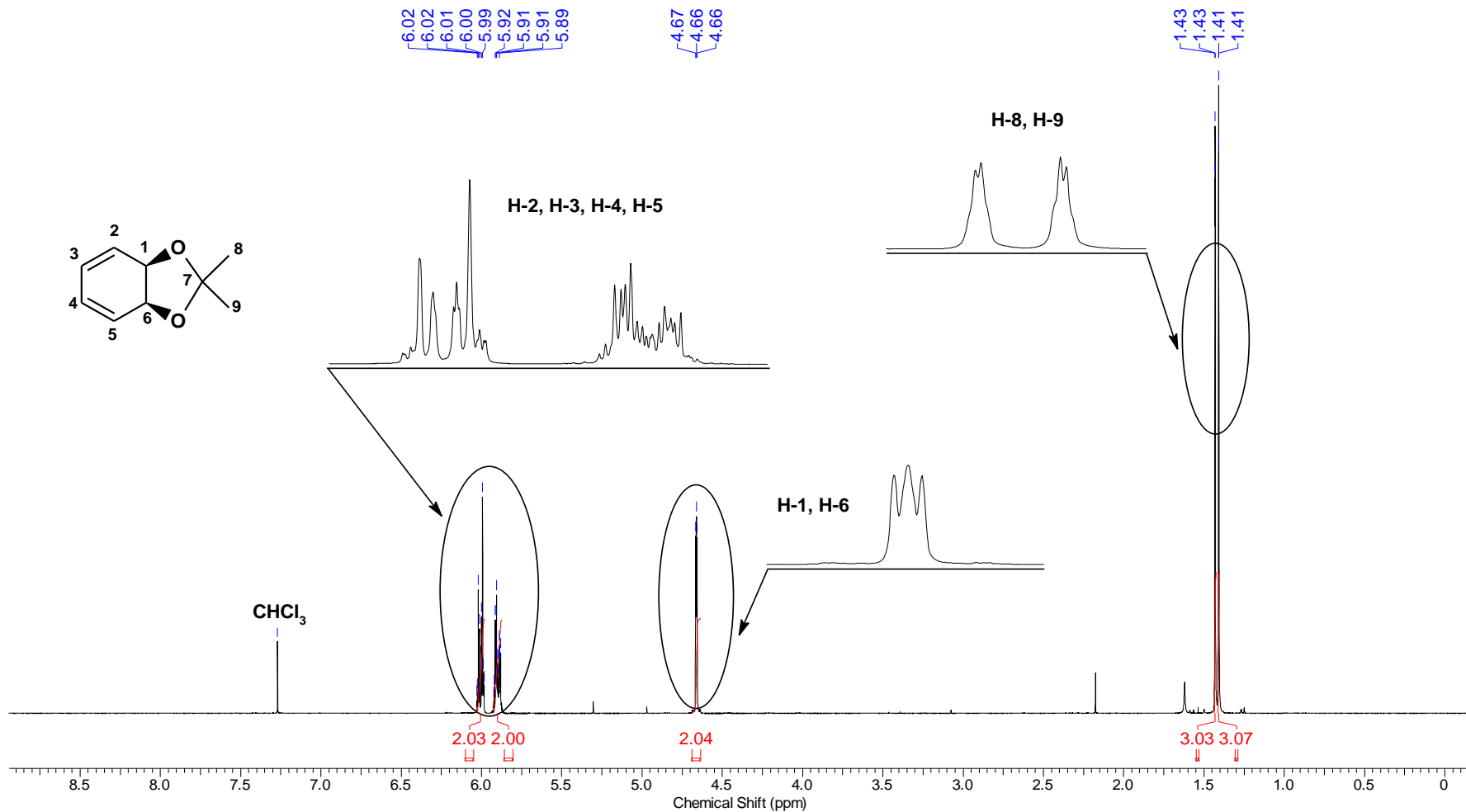
Frequency (MHz)	100.62	Nucleus	^{13}C	Number of Transients	1024	Origin	spect
Original Points Count	16384	Owner	nmsu	Points Count	32768	Pulse Sequence	zgpg30
Receiver Gain	2050.00	SW(cyclical) (Hz)	24671.05	Solvent	BENZENE-d6	Spectrum Offset (Hz)	10130.7002
Spectrum Type	STANDARD	Sweep Width (Hz)	24670.30	Temperature (degree C)	25.000	Acquisition Time (sec)	0.6641



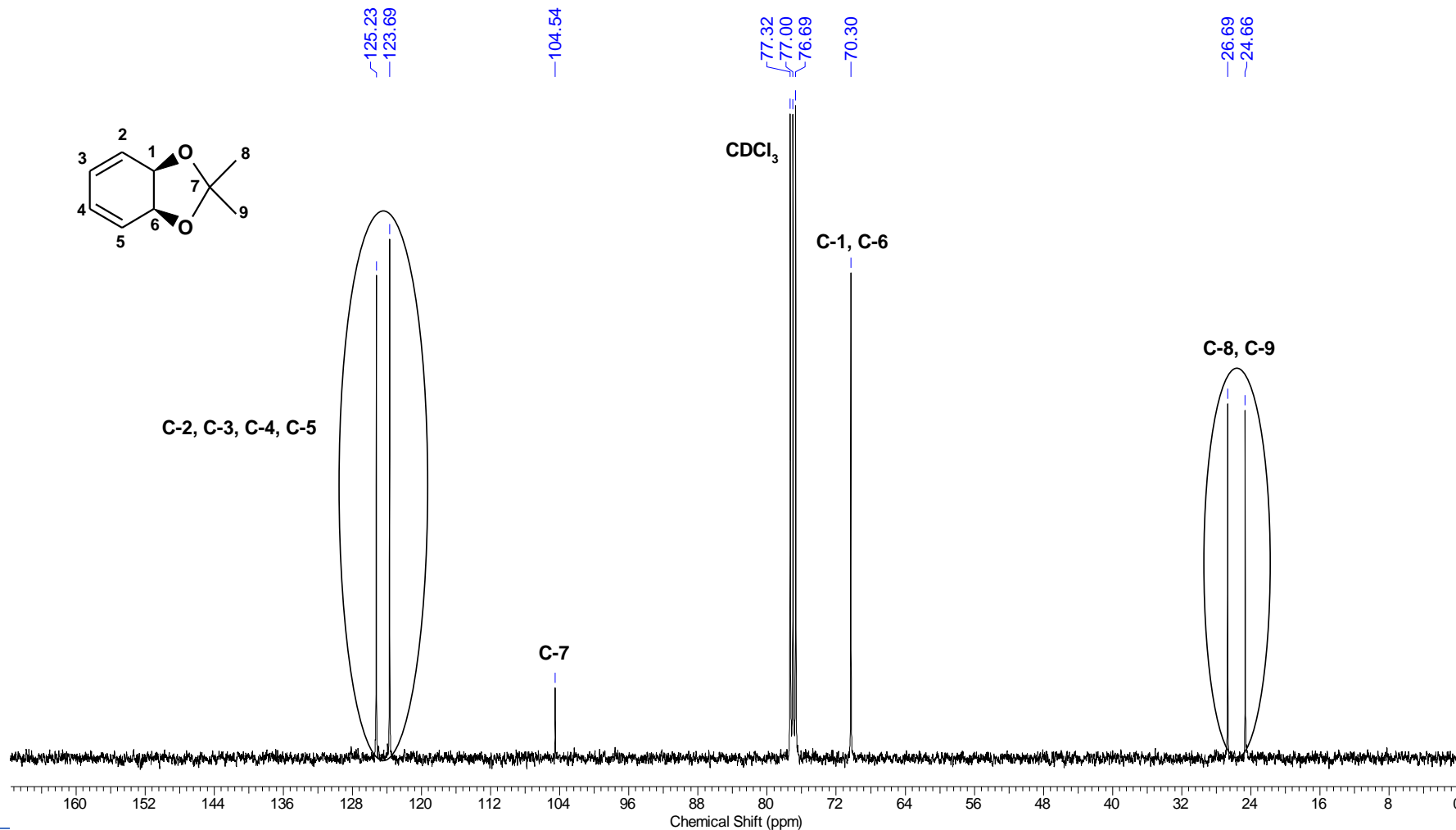
Frequency (MHz)	100.62	Nucleus	¹³ C	Number of Transients	1024	Origin	spect
Original Points Count	16384	Owner	nmsu	Points Count	32768	Pulse Sequence	depts135
Receiver Gain	2050.00	SW(cyclical) (Hz)	20161.29	Solvent	BENZENE-d6	Spectrum Offset (Hz)	8117.1514
Spectrum Type	DEPT135	Sweep Width (Hz)	20160.68	Temperature (degree C)	25.000	Acquisition Time (sec)	0.8126



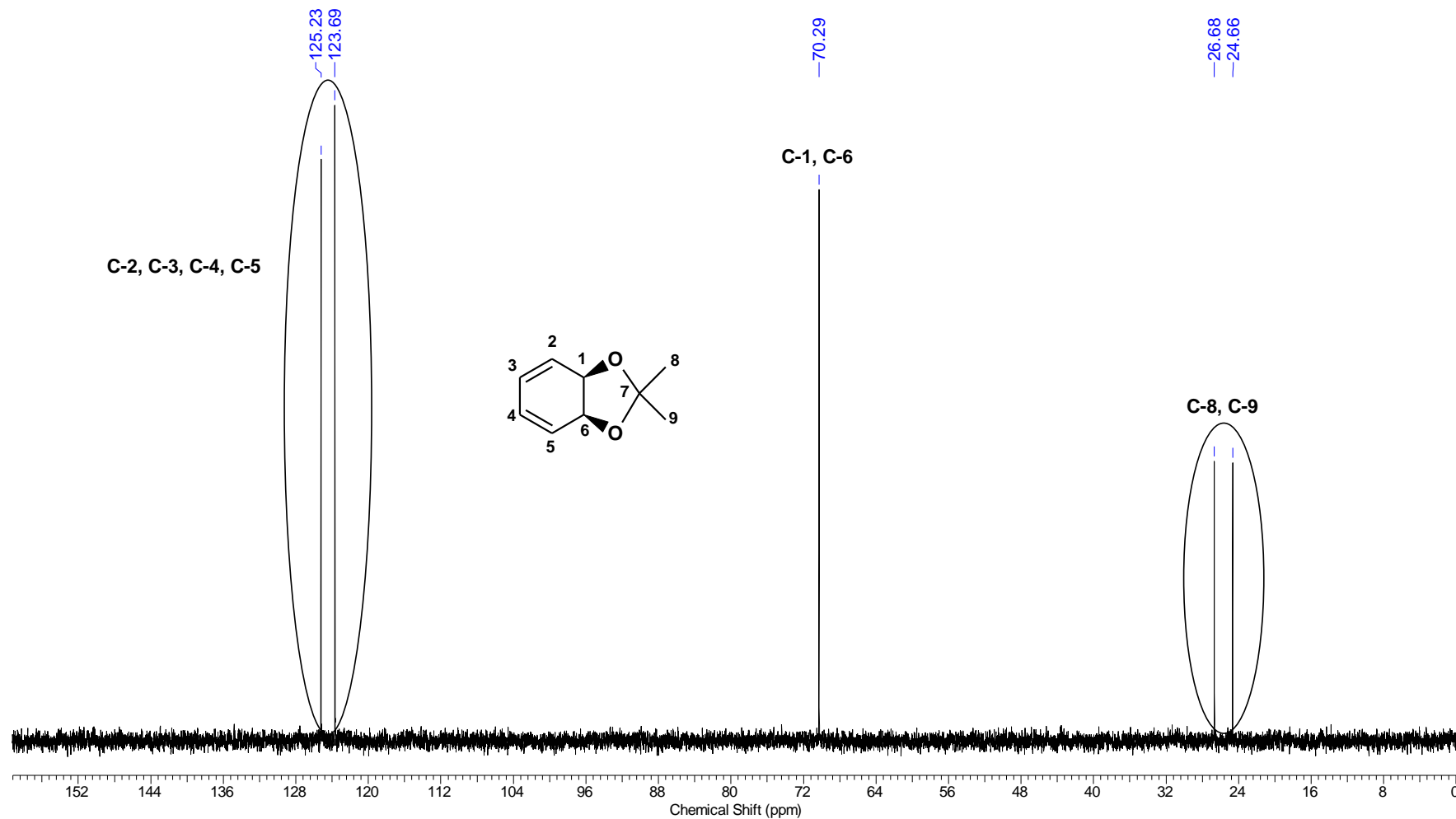
Acquisition Time (sec)	4.8060	Sweep Width (Hz)	6818.08	Temperature (degree C)	24.100	Frequency (MHz)	400.15
Nucleus	1H	Number of Transients	16	Origin	spect	Original Points Count	32768
Owner	nmrsu	Points Count	65536	Pulse Sequence	zg30	Receiver Gain	114.00
SW(cyclical) (Hz)	6818.18	Solvent	CDCl3	Spectrum Offset (Hz)	2995.5972	Spectrum Type	STANDARD



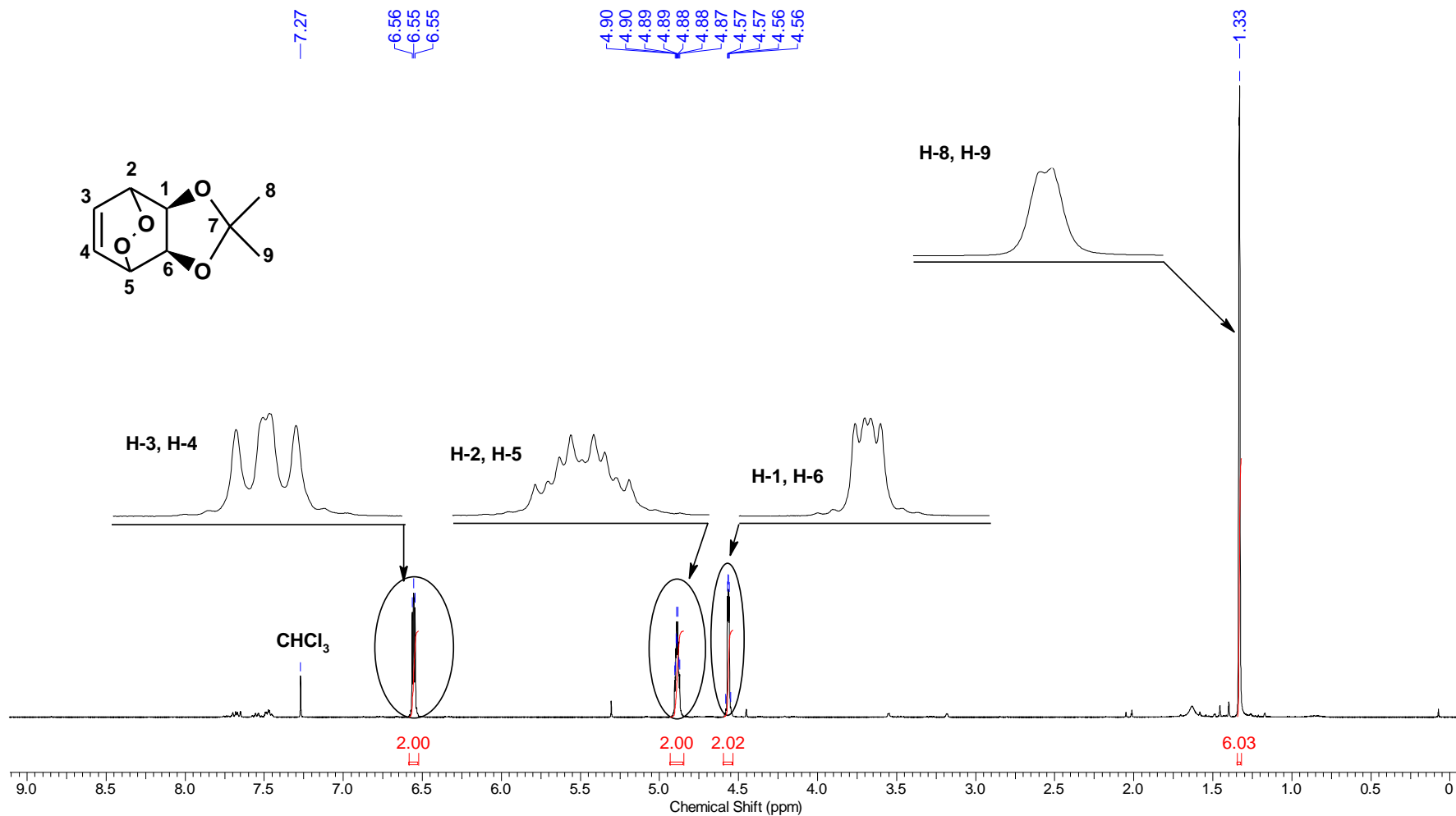
Acquisition Time (sec)	0.6641	Sweep Width (Hz)	24670.30	Temperature (degree C)	24.900	Frequency (MHz)	100.62
Nucleus	13C	Number of Transients	1024	Origin	spect	Original Points Count	16384
Owner	nmsu	Points Count	32768	Pulse Sequence	zgpg30	Receiver Gain	2050.00
SW(cyclical) (Hz)	24671.05	Solvent	CDCI3	Spectrum Offset (Hz)	10059.3525	Spectrum Type	STANDARD



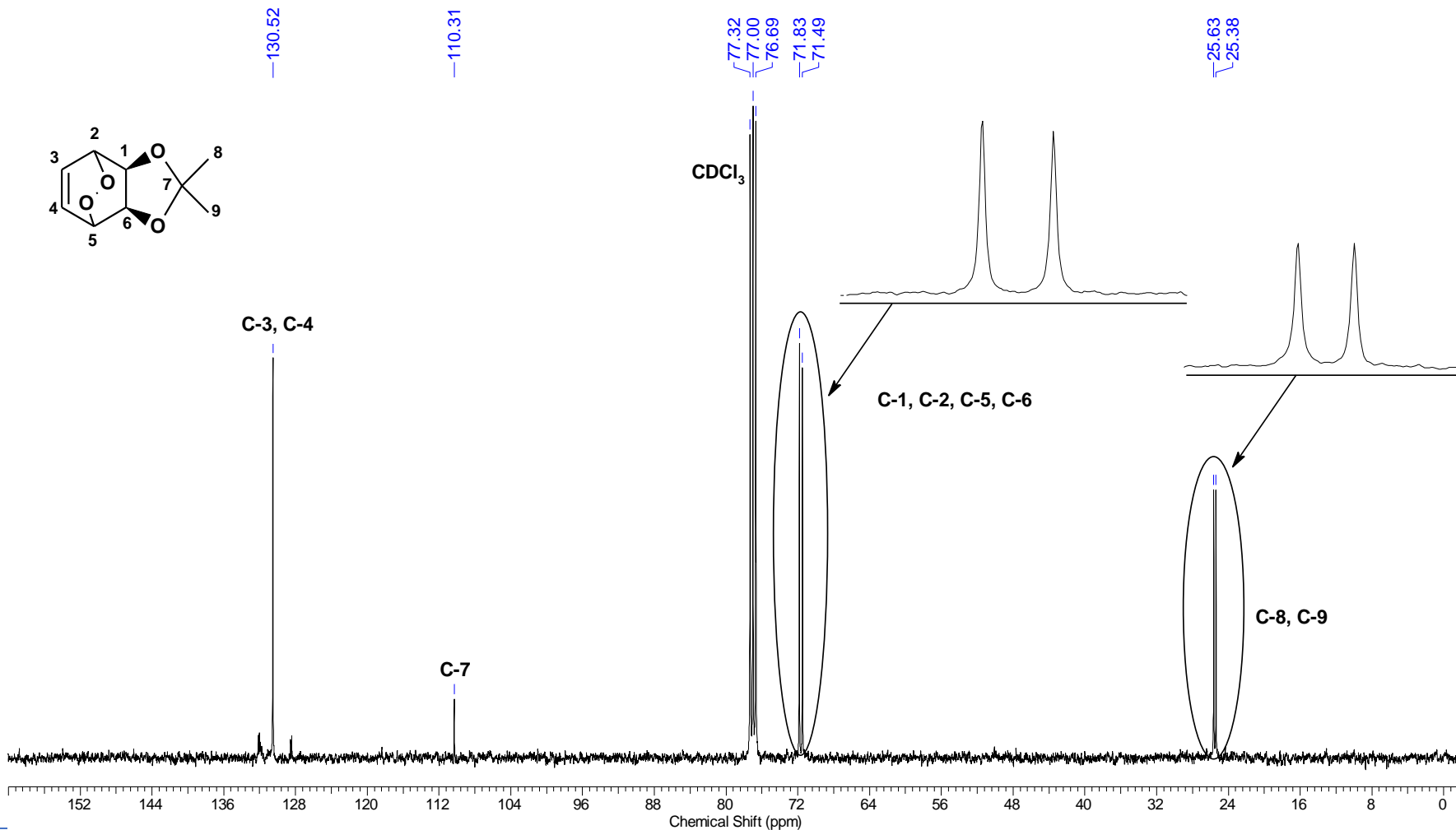
Acquisition Time (sec)	0.8126	Sweep Width (Hz)	20160.68	Temperature (degree C)	24.600	Frequency (MHz)	100.62
Nucleus	13C	Number of Transients	1024	Origin	spect	Original Points Count	16384
Owner	nmsu	Points Count	32768	Pulse Sequence	depts135	Receiver Gain	2050.00
SW(cyclical) (Hz)	20161.29	Solvent	CDCl3	Spectrum Offset (Hz)	8046.0786	Spectrum Type	DEPT135



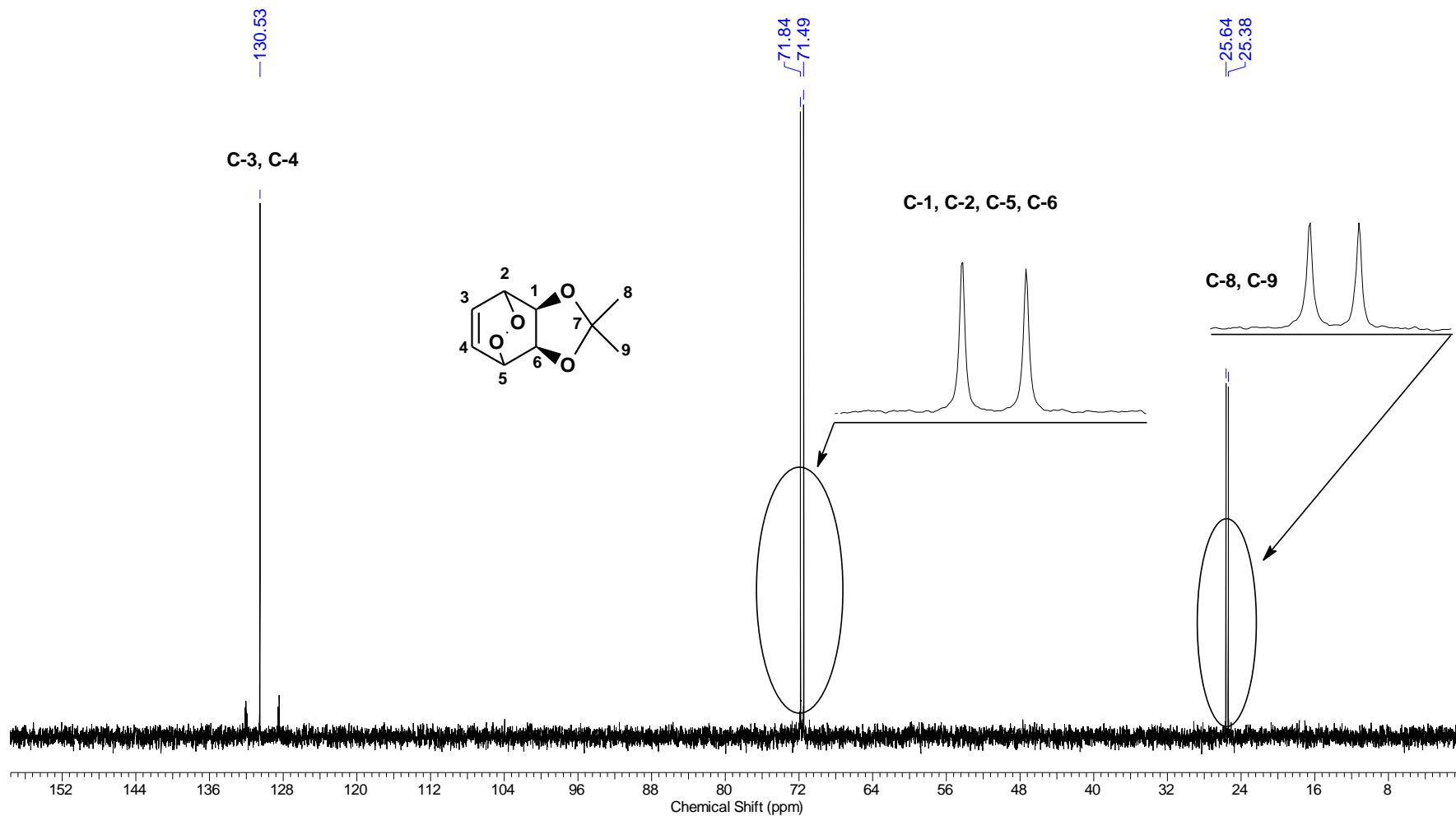
Acquisition Time (sec)	4.8060	Sweep Width (Hz)	6818.08	Temperature (degree C)	23.800	Frequency (MHz)	400.15
Nucleus	1H	Number of Transients	16	Origin	spect	Original Points Count	32768
Owner	nmrsu	Points Count	65536	Pulse Sequence	zg30	Receiver Gain	114.00
SW(cyclical) (Hz)	6818.18	Solvent	CDCI3	Spectrum Offset (Hz)	2995.1814	Spectrum Type	STANDARD



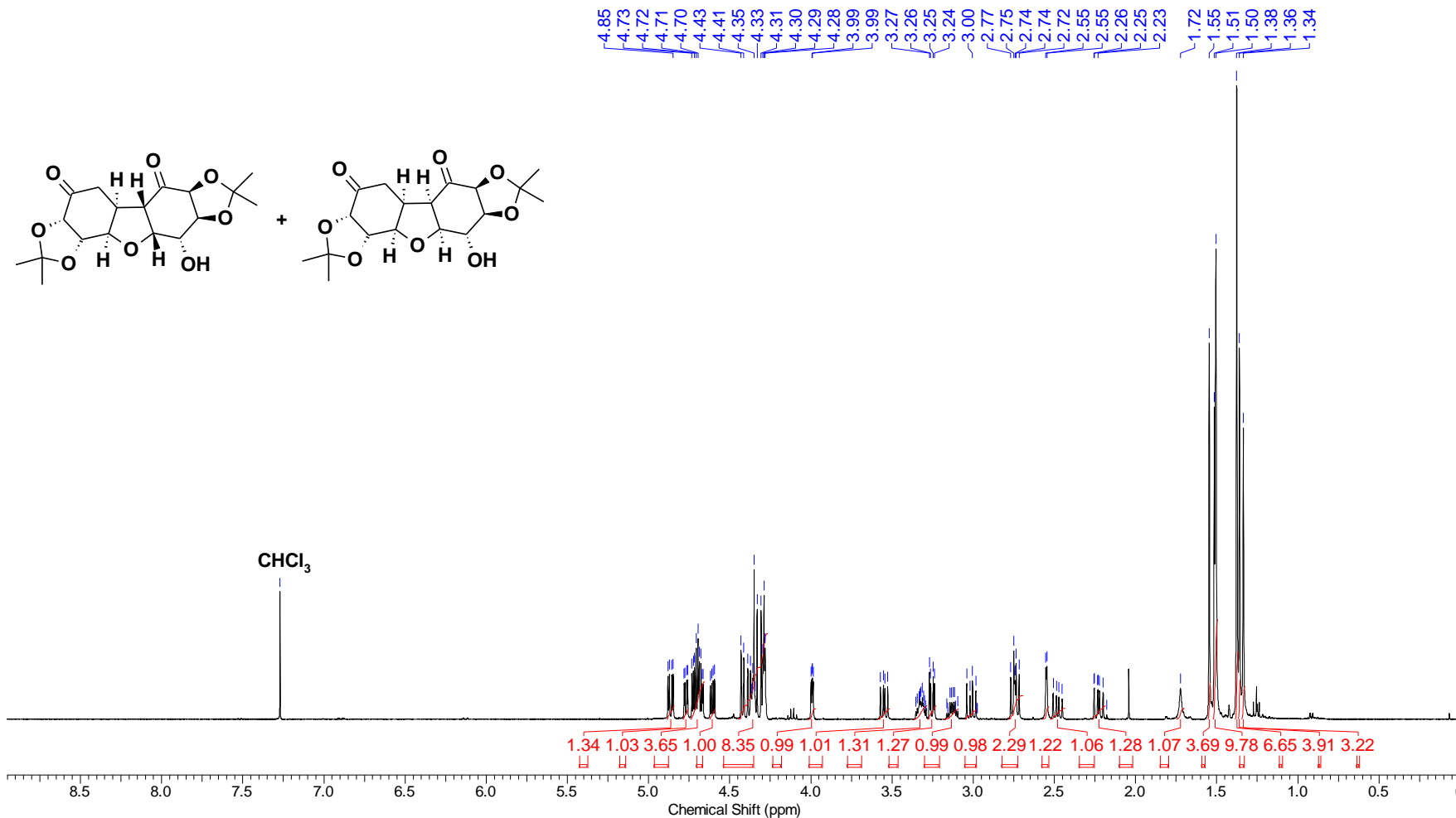
Acquisition Time (sec)	0.6641	Sweep Width (Hz)	24670.30	Temperature (degree C)	24.600	Frequency (MHz)	100.62
Nucleus	13C	Number of Transients	1024	Origin	spect	Original Points Count	16384
Owner	nmsu	Points Count	32768	Pulse Sequence	zgpg30	Receiver Gain	2050.00
SW(cyclical) (Hz)	24671.05	Solvent	CDCl3	Spectrum Offset (Hz)	10058.5996	Spectrum Type	STANDARD



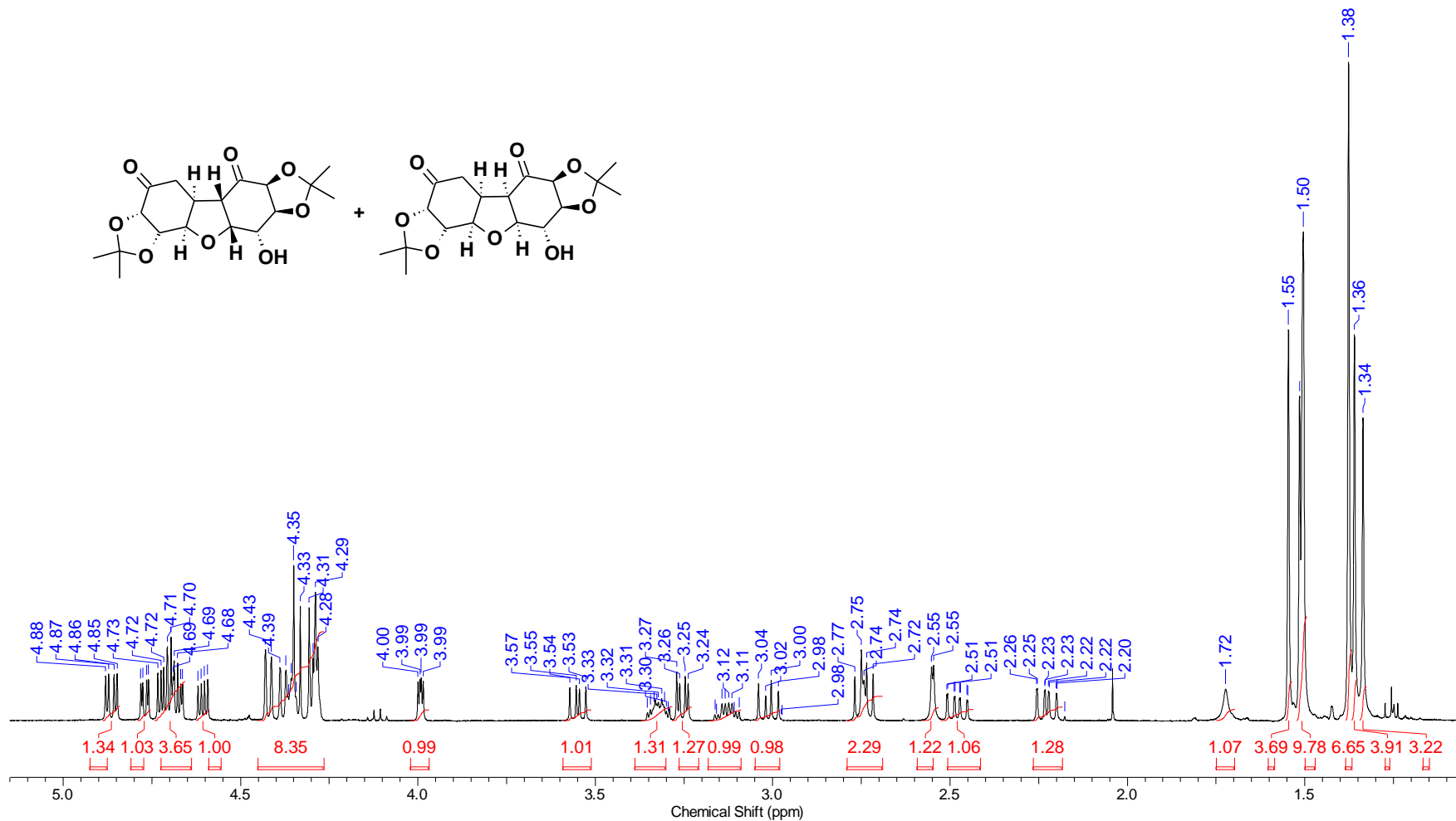
Acquisition Time (sec)	0.8126	Sweep Width (Hz)	20160.68	Temperature (degree C)	24.300	Frequency (MHz)	100.62
Nucleus	13C	Number of Transients	1024	Origin	spect	Original Points Count	16384
Owner	nmsu	Points Count	32768	Pulse Sequence	depts135	Receiver Gain	2050.00
SW(cyclical) (Hz)	20161.29	Solvent	CDCl3	Spectrum Offset (Hz)	8046.5361	Spectrum Type	DEPT135



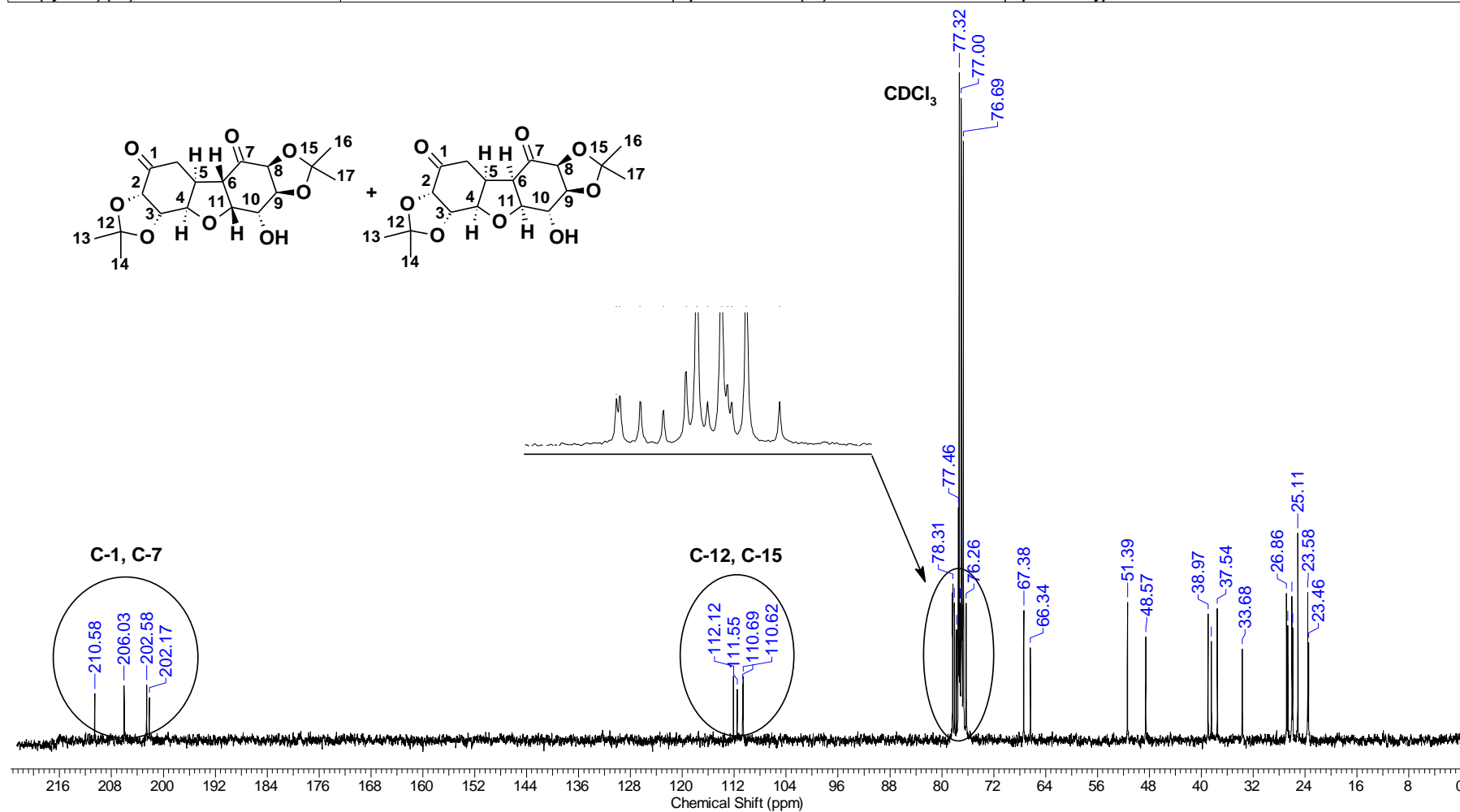
Acquisition Time (sec)	4.8060	Sweep Width (Hz)	6818.08	Temperature (degree C)	23.500	Frequency (MHz)	400.15
Nucleus	1H	Number of Transients	16	Origin	spect	Original Points Count	32768
Owner	nmsu	Points Count	65536	Pulse Sequence	zg30	Receiver Gain	114.00
SW(cyclical) (Hz)	6818.18	Solvent	CDCl3	Spectrum Offset (Hz)	2995.4934	Spectrum Type	STANDARD



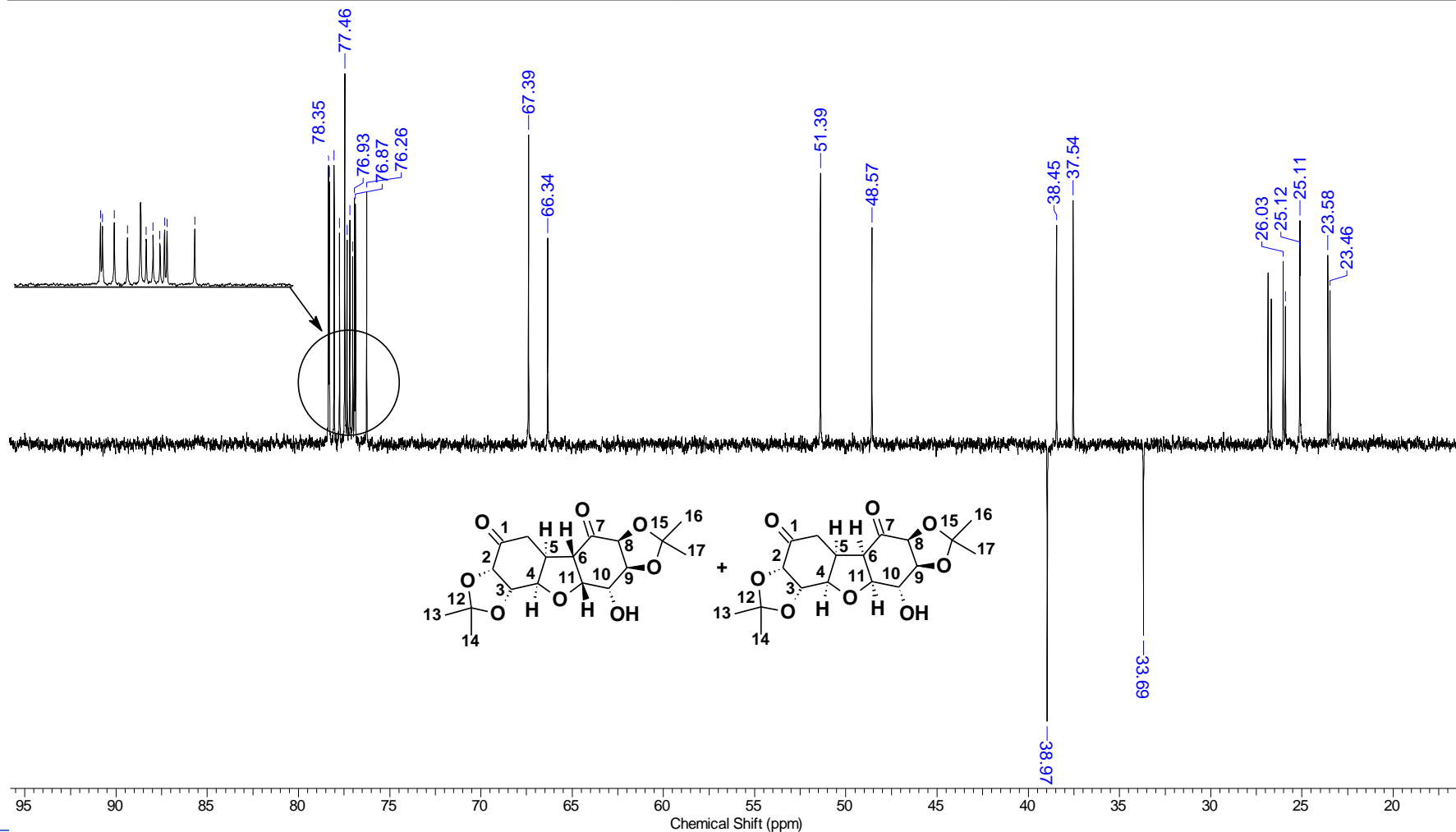
Acquisition Time (sec)	4.8060	Sweep Width (Hz)	6818.08	Temperature (degree C)	23.500	Frequency (MHz)	400.15
Nucleus	1H	Number of Transients	16	Origin	spect	Original Points Count	32768
Owner	nmrsu	Points Count	65536	Pulse Sequence	zg30	Receiver Gain	114.00
SW(cyclical) (Hz)	6818.18	Solvent	CDCl3	Spectrum Offset (Hz)	2995.4934	Spectrum Type	STANDARD



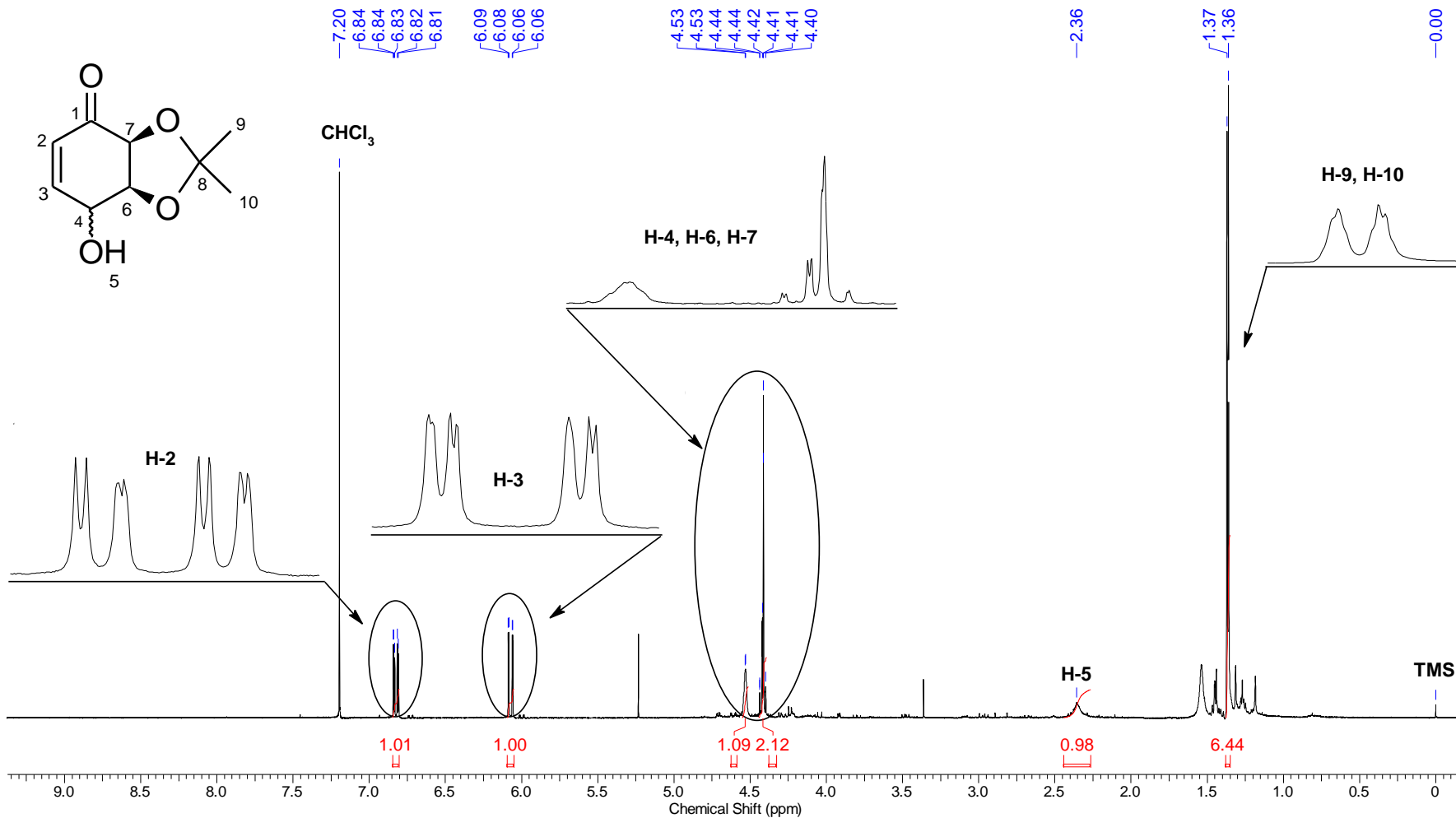
Acquisition Time (sec)	0.6641	Sweep Width (Hz)	24670.30	Temperature (degree C)	24.100	Frequency (MHz)	100.62
Nucleus	13C	Number of Transients	1024	Origin	spect	Original Points Count	16384
Owner	nmsu	Points Count	32768	Pulse Sequence	zgpg30	Receiver Gain	2050.00
SW(cyclical) (Hz)	24671.05	Solvent	CDCl3	Spectrum Offset (Hz)	10057.8467	Spectrum Type	STANDARD



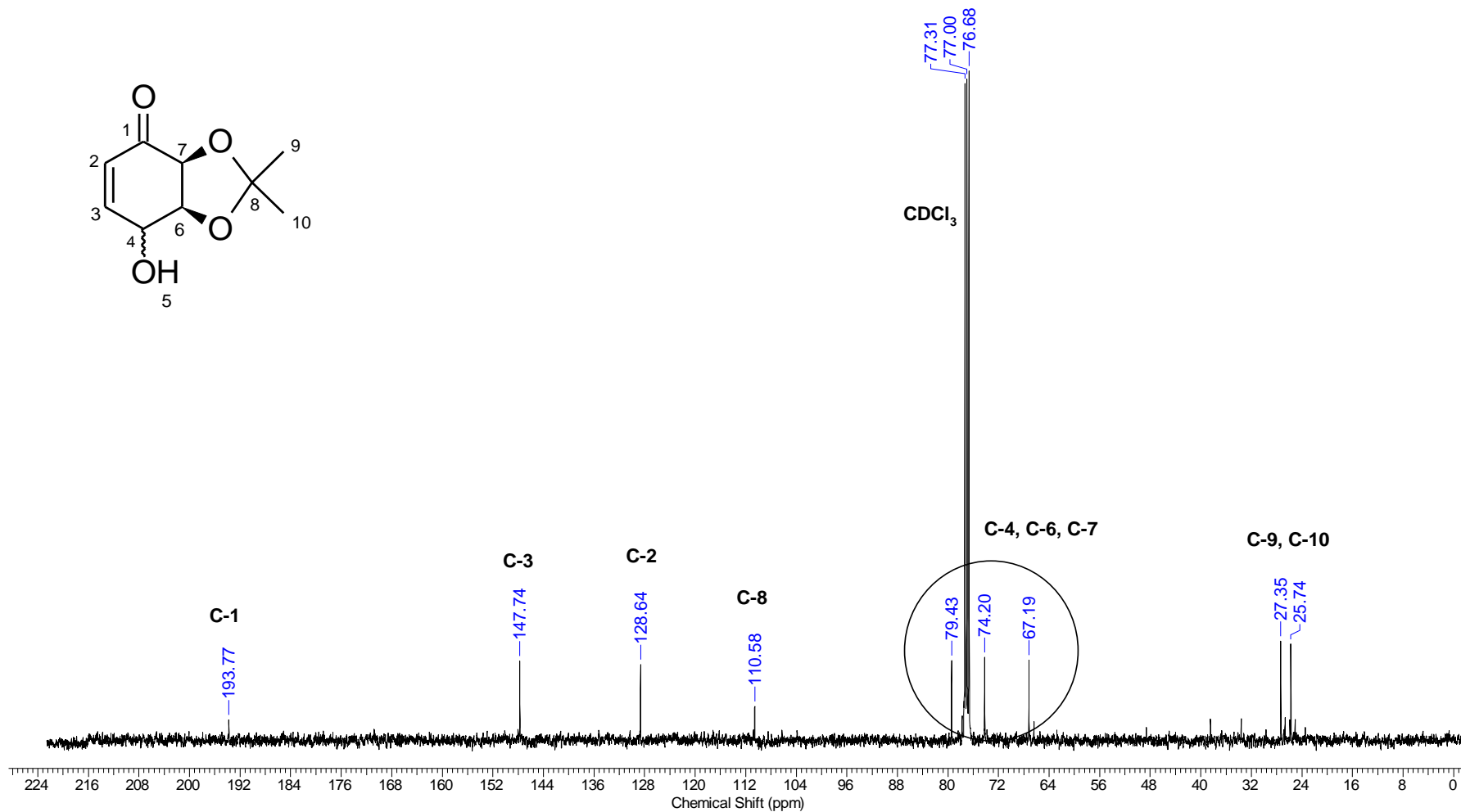
Acquisition Time (sec)	0.8126	Sweep Width (Hz)	20160.68	Temperature (degree C)	23.800	Frequency (MHz)	100.62
Nucleus	13C	Number of Transients	1024	Origin	spect	Original Points Count	16384
Owner	nmsu	Points Count	32768	Pulse Sequence	deptsp135	Receiver Gain	2050.00
SW(cyclical) (Hz)	20161.29	Solvent	CDCl3	Spectrum Offset (Hz)	8045.3154	Spectrum Type	DEPT135



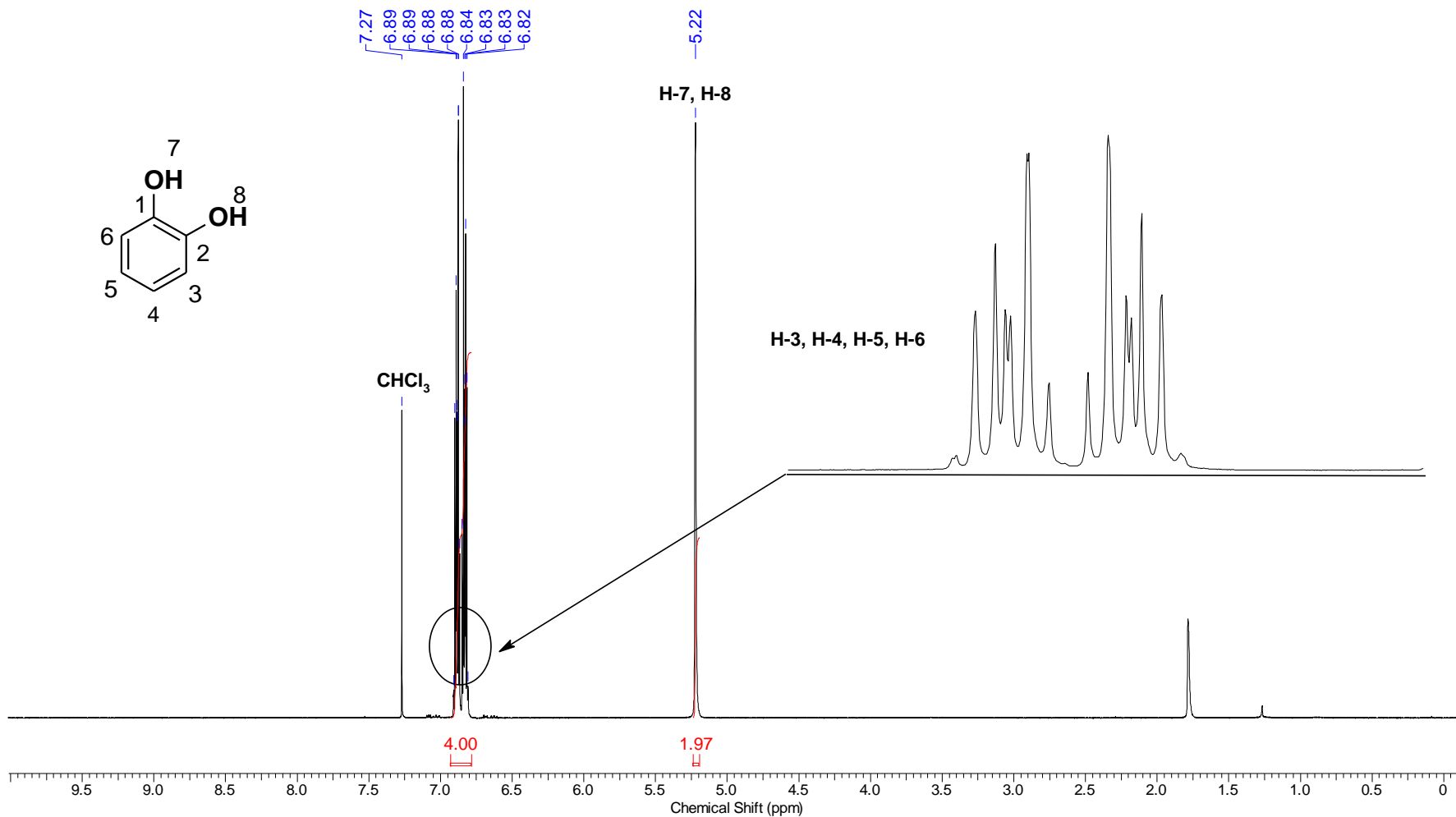
Nucleus	1H	Number of Transients	64	Origin	spect	Original Points Count	32768
Owner	nmsu	Points Count	65536	Pulse Sequence	zg30	Receiver Gain	114.00
SW(cyclical) (Hz)	8802.82	Solvent	CDCl3	Spectrum Offset (Hz)	3365.7317	Spectrum Type	STANDARD
Sweep Width (Hz)	8802.68	Temperature (degree C)	23.900	Acquisition Time (sec)	3.7224	Frequency (MHz)	400.15



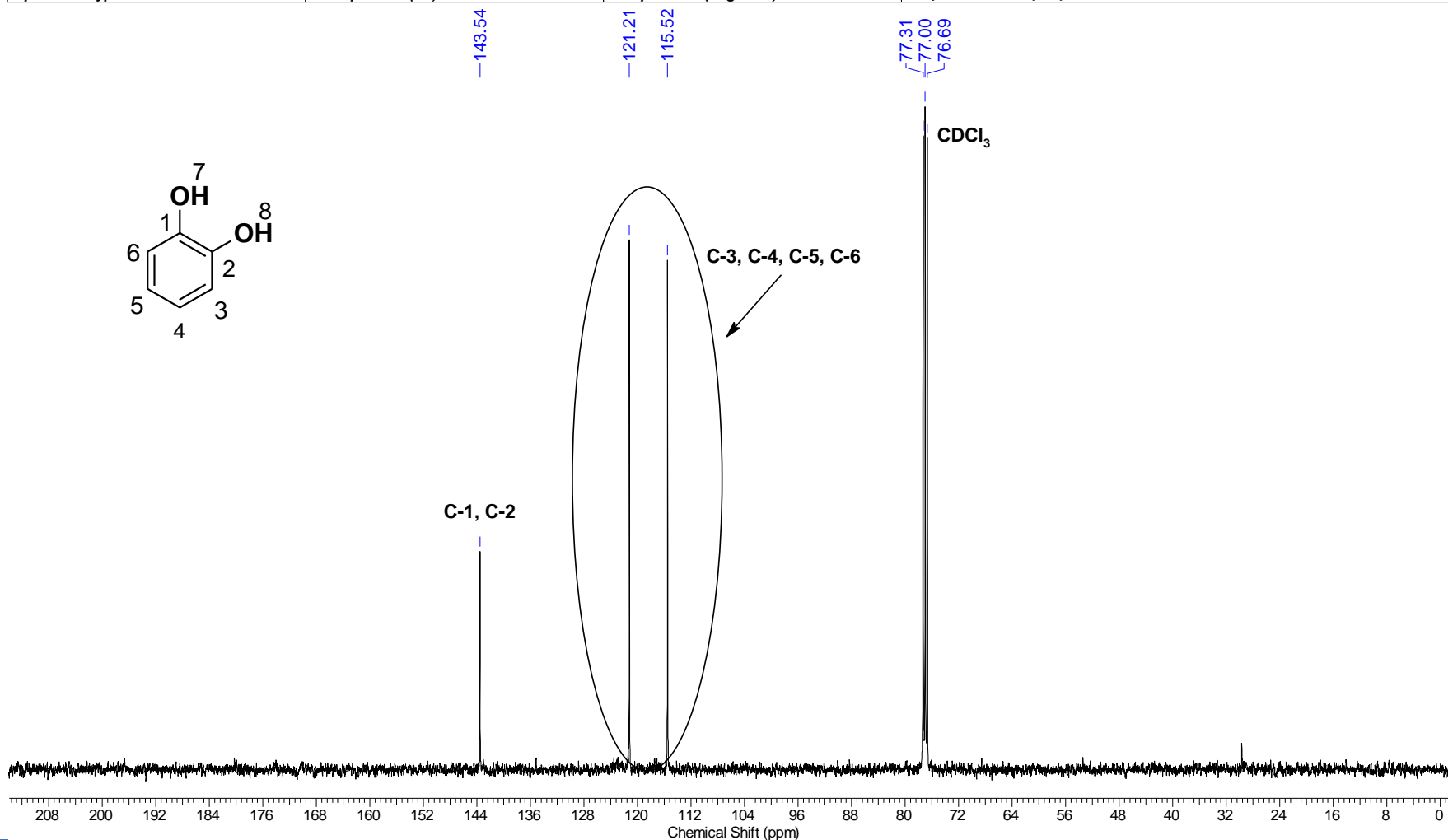
Nucleus	13C	Number of Transients	1024	Origin	spect	Original Points Count	16384
Owner	nmsu	Points Count	32768	Pulse Sequence	zgpg30	Receiver Gain	2050.00
SW(cyclical) (Hz)	24671.05	Solvent	CDCl3	Spectrum Offset (Hz)	10058.5996	Spectrum Type	STANDARD
Sweep Width (Hz)	24670.30	Temperature (degree C)	24.600	Acquisition Time (sec)	0.6641	Frequency (MHz)	100.62



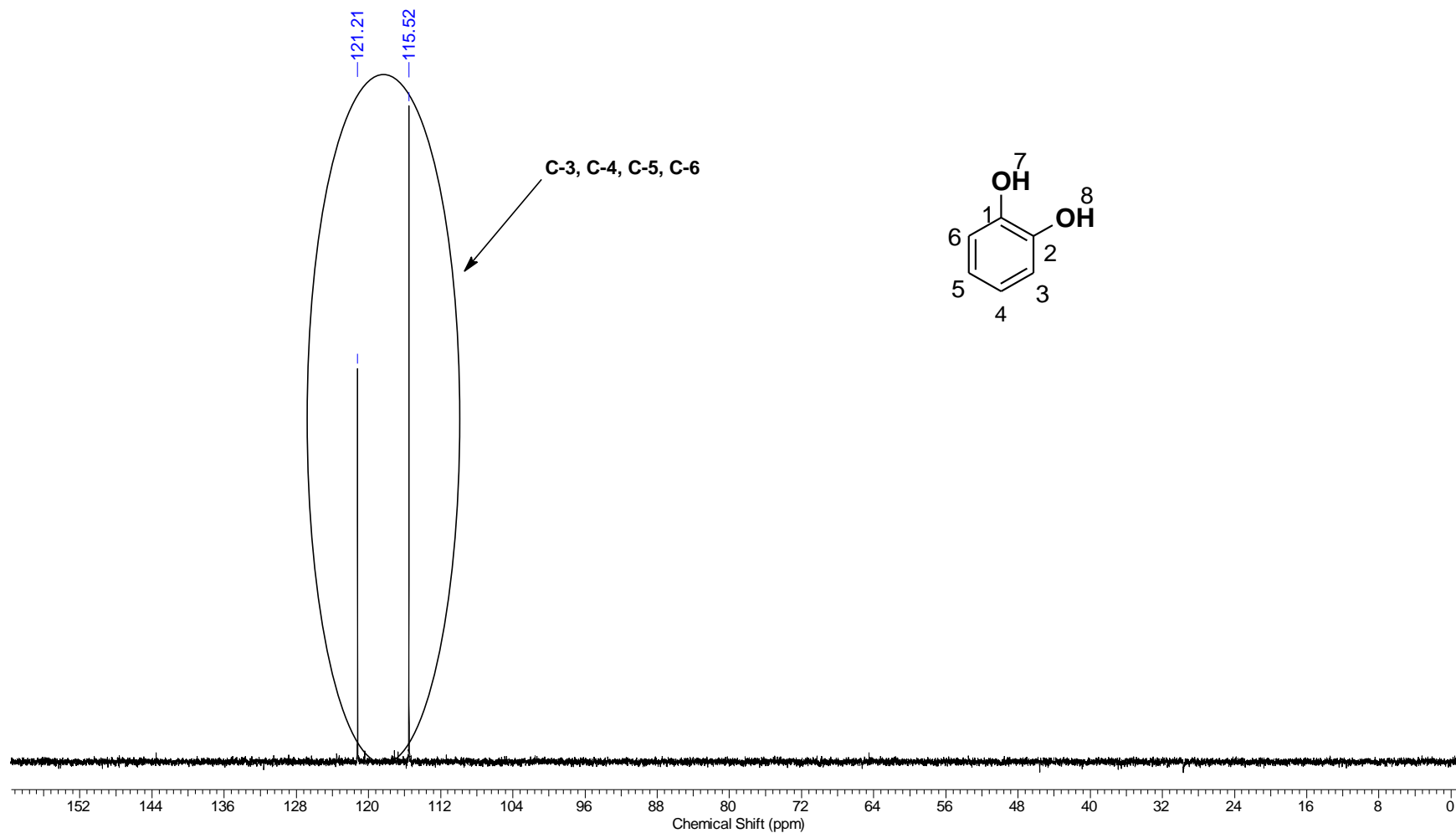
Acquisition Time (sec)	3.7224	Sweep Width (Hz)	8802.68	Temperature (degree C)	23.900	Frequency (MHz)	400.15
Nucleus	1H	Number of Transients	64	Origin	spect	Original Points Count	32768
Owner	nmrsu	Points Count	65536	Pulse Sequence	zg30	Receiver Gain	114.00
SW(cyclical) (Hz)	8802.82	Solvent	CDCl3	Spectrum Offset (Hz)	3395.6660	Spectrum Type	STANDARD



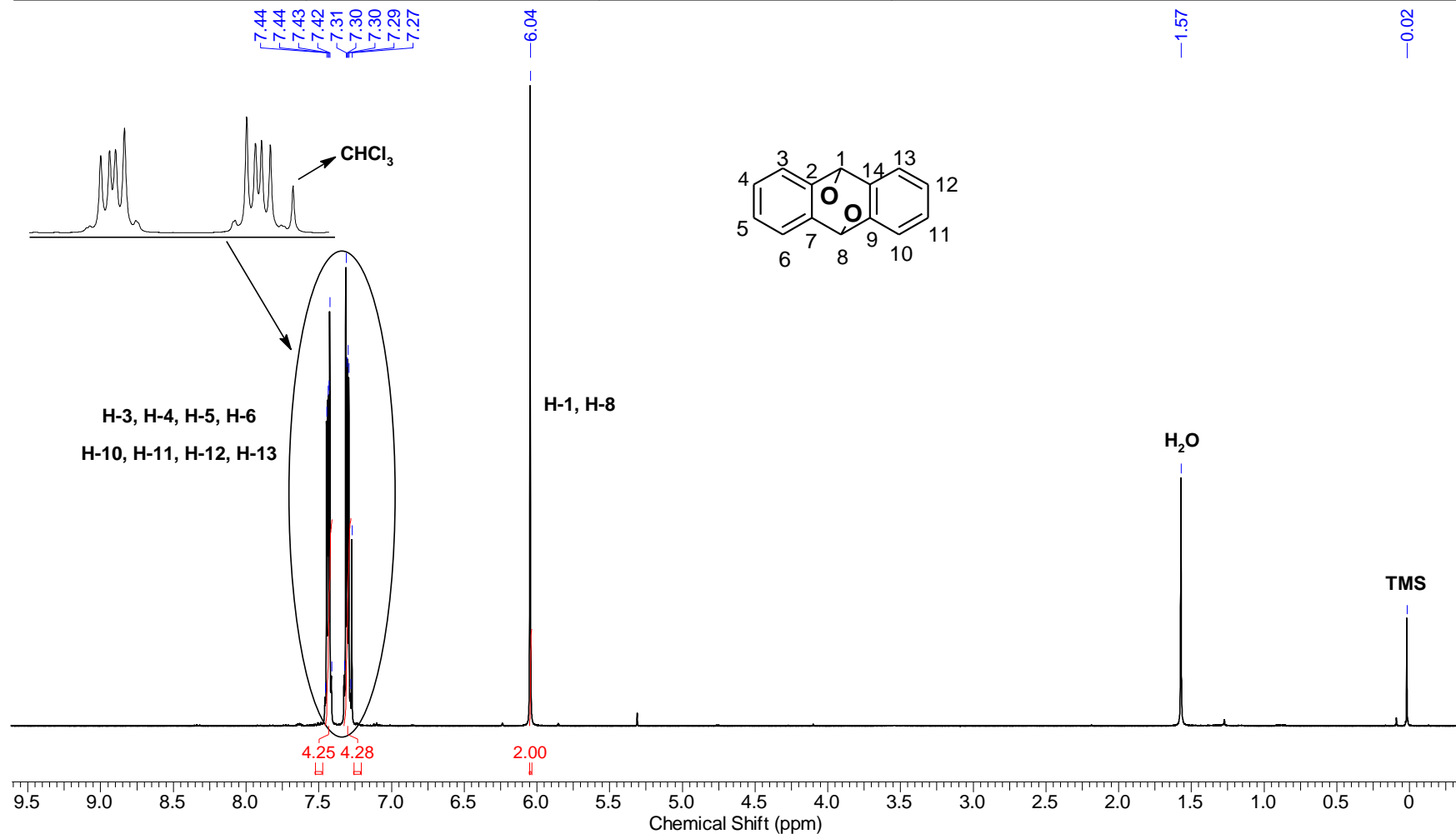
Frequency (MHz)	100.62	Nucleus	¹³ C	Number of Transients	1024	Origin	spect
Original Points Count	16384	Owner	nmsu	Points Count	32768	Pulse Sequence	zgpg30
Receiver Gain	2050.00	SW(cyclical) (Hz)	24671.05	Solvent	CDCl ₃	Spectrum Offset (Hz)	10057.8467
Spectrum Type	STANDARD	Sweep Width (Hz)	24670.30	Temperature (degree C)	25.000	Acquisition Time (sec)	0.6641



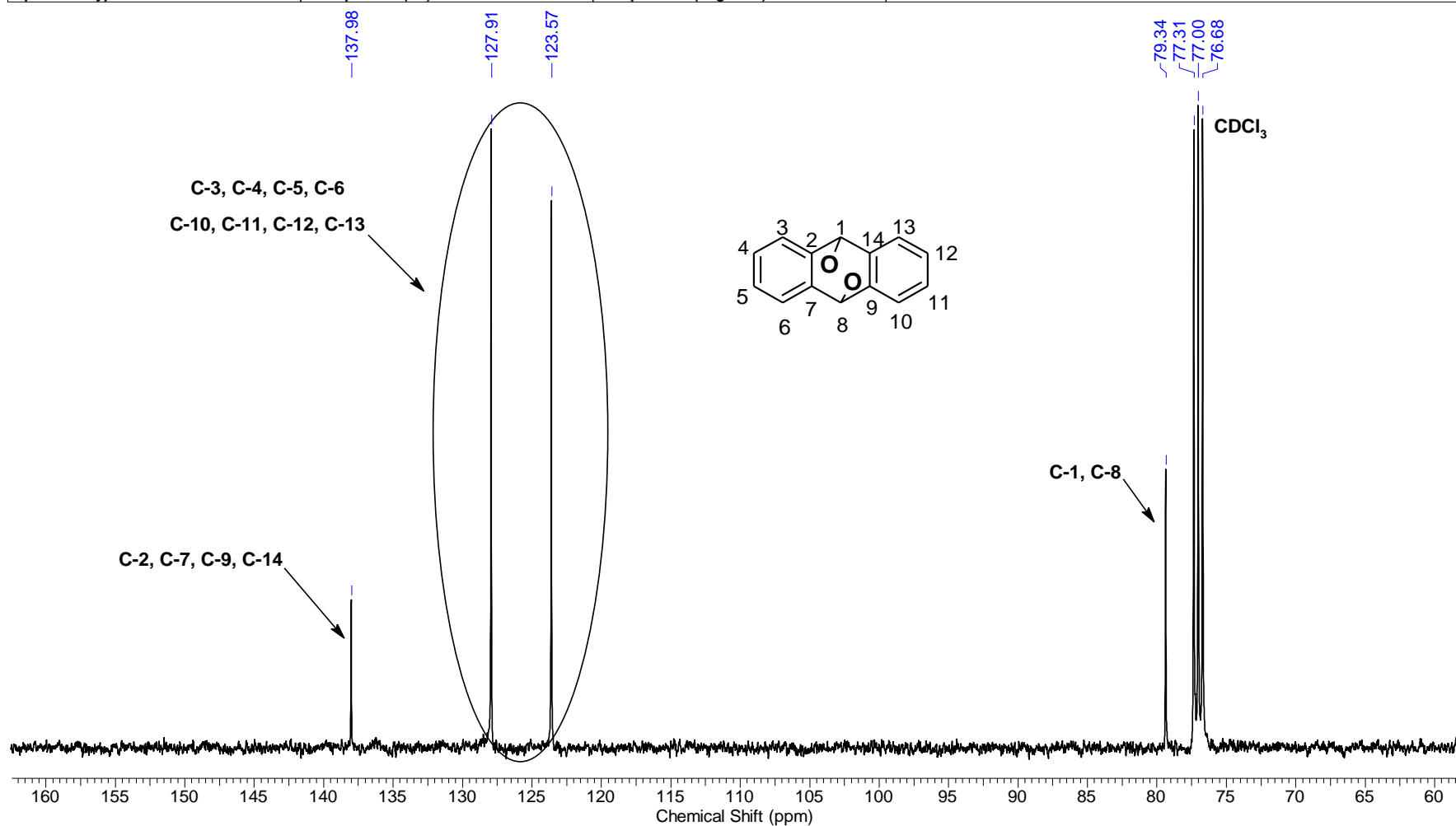
Frequency (MHz)	100.62	Nucleus	¹³ C	Number of Transients	1024	Origin	spect
Original Points Count	16384	Owner	nmrsu	Points Count	32768	Pulse Sequence	deptsp135
Receiver Gain	2050.00	SW(cyclical) (Hz)	20161.29	Solvent	CDCl ₃	Spectrum Offset (Hz)	8045.2432
Spectrum Type	DEPT135	Sweep Width (Hz)	20160.68	Temperature (degree C)	25.000	Acquisition Time (sec)	0.8126



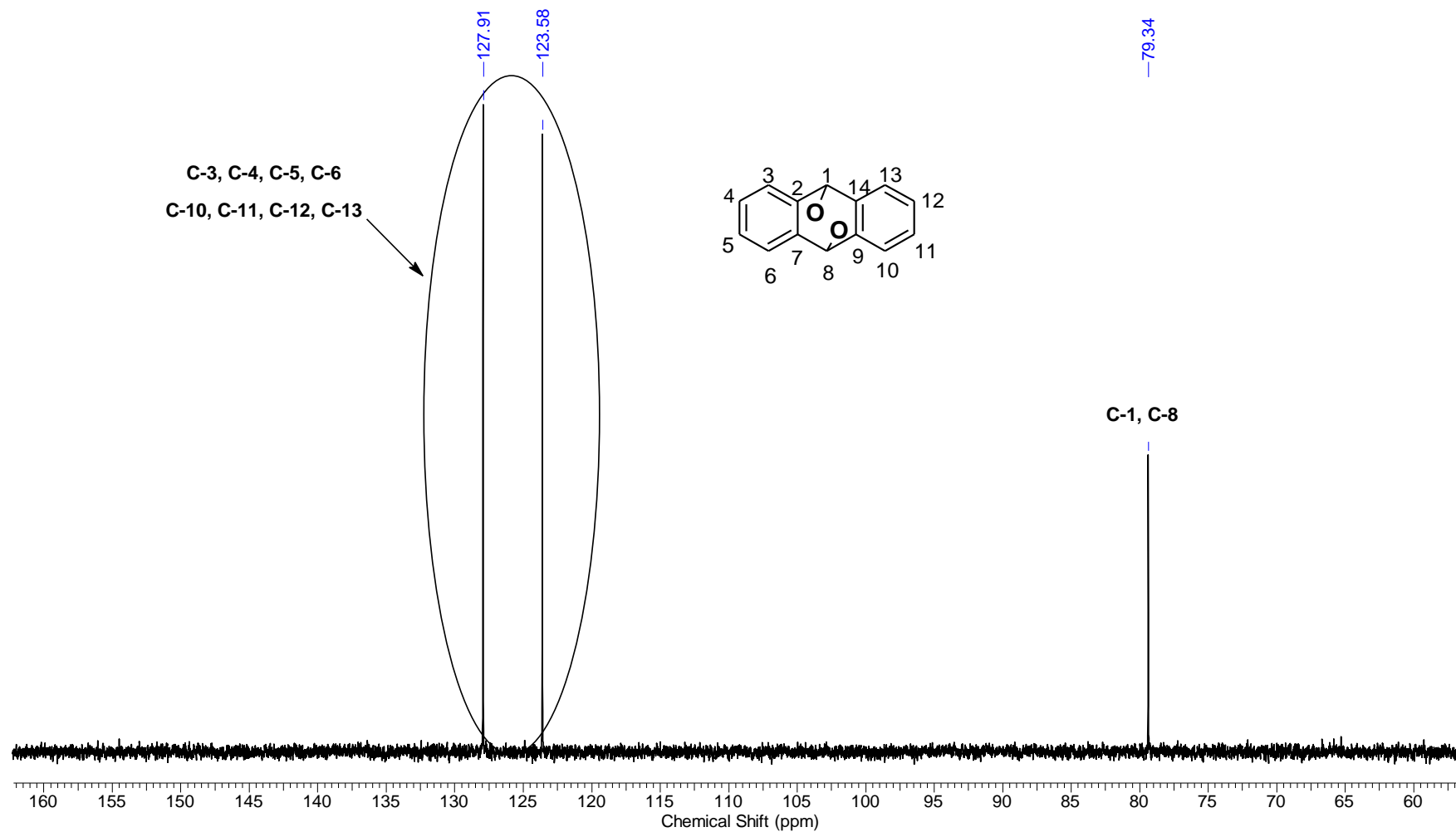
Frequency (MHz)	400.15	Nucleus	1H	Number of Transients	64	Origin	spect
Original Points Count	32768	Owner	root	Points Count	65536	Pulse Sequence	zg30
Receiver Gain	228.00	SW(cyclical) (Hz)	6818.18	Solvent	CDCl3	Spectrum Offset (Hz)	2995.3894
Spectrum Type	STANDARD	Sweep Width (Hz)	6818.08	Temperature (degree C)	119.800	Acquisition Time (sec)	4.8060



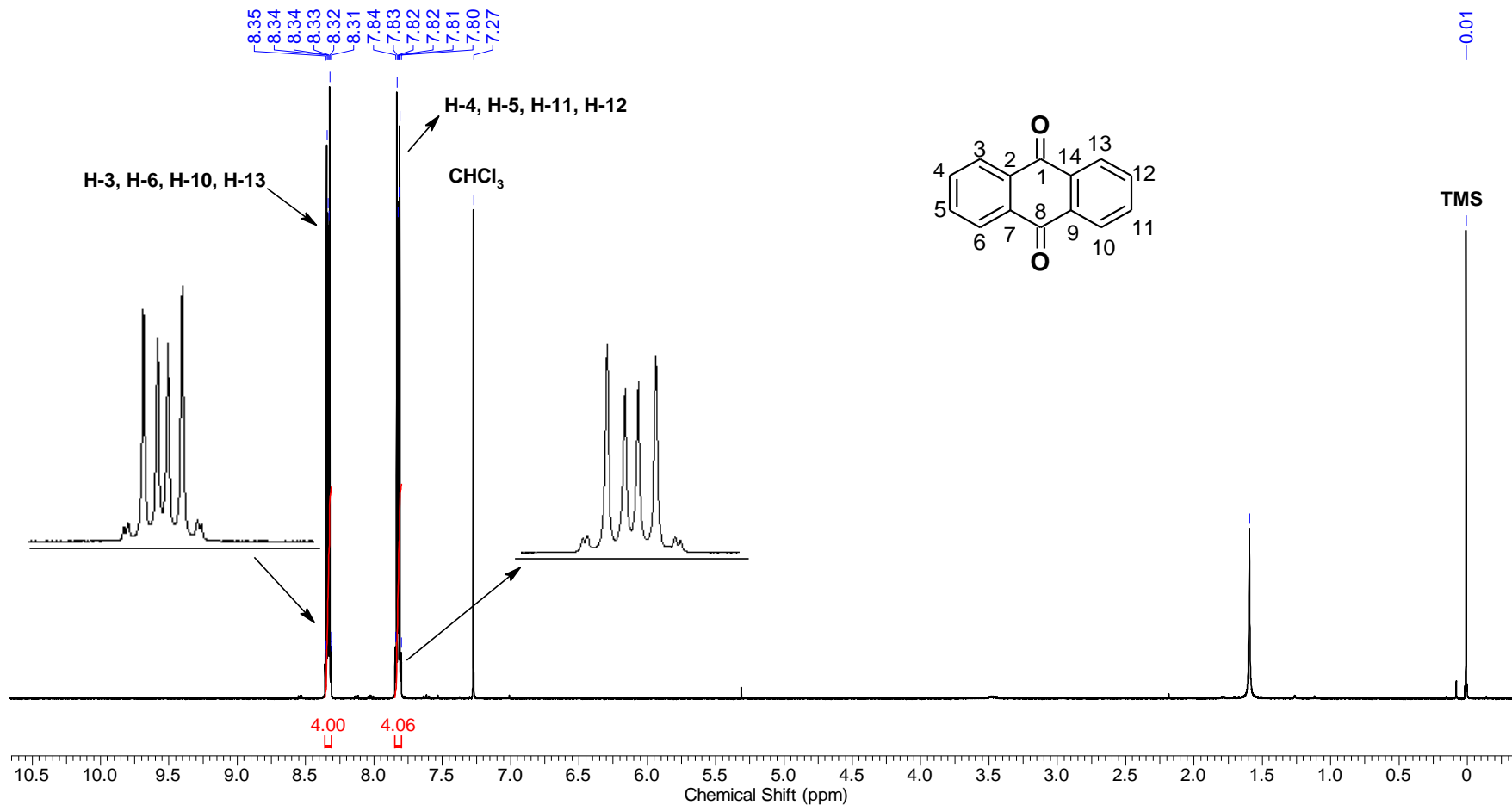
Frequency (MHz)	100.62	Nucleus	¹³ C	Number of Transients	1024	Origin	spect
Original Points Count	16384	Owner	root	Points Count	32768	Pulse Sequence	zgpg30
Receiver Gain	2050.00	SW(cyclical) (Hz)	24671.05	Solvent	CDCl ₃	Spectrum Offset (Hz)	10057.8467
Spectrum Type	STANDARD	Sweep Width (Hz)	24670.30	Temperature (degree C)	119.500	Acquisition Time (sec)	0.6641



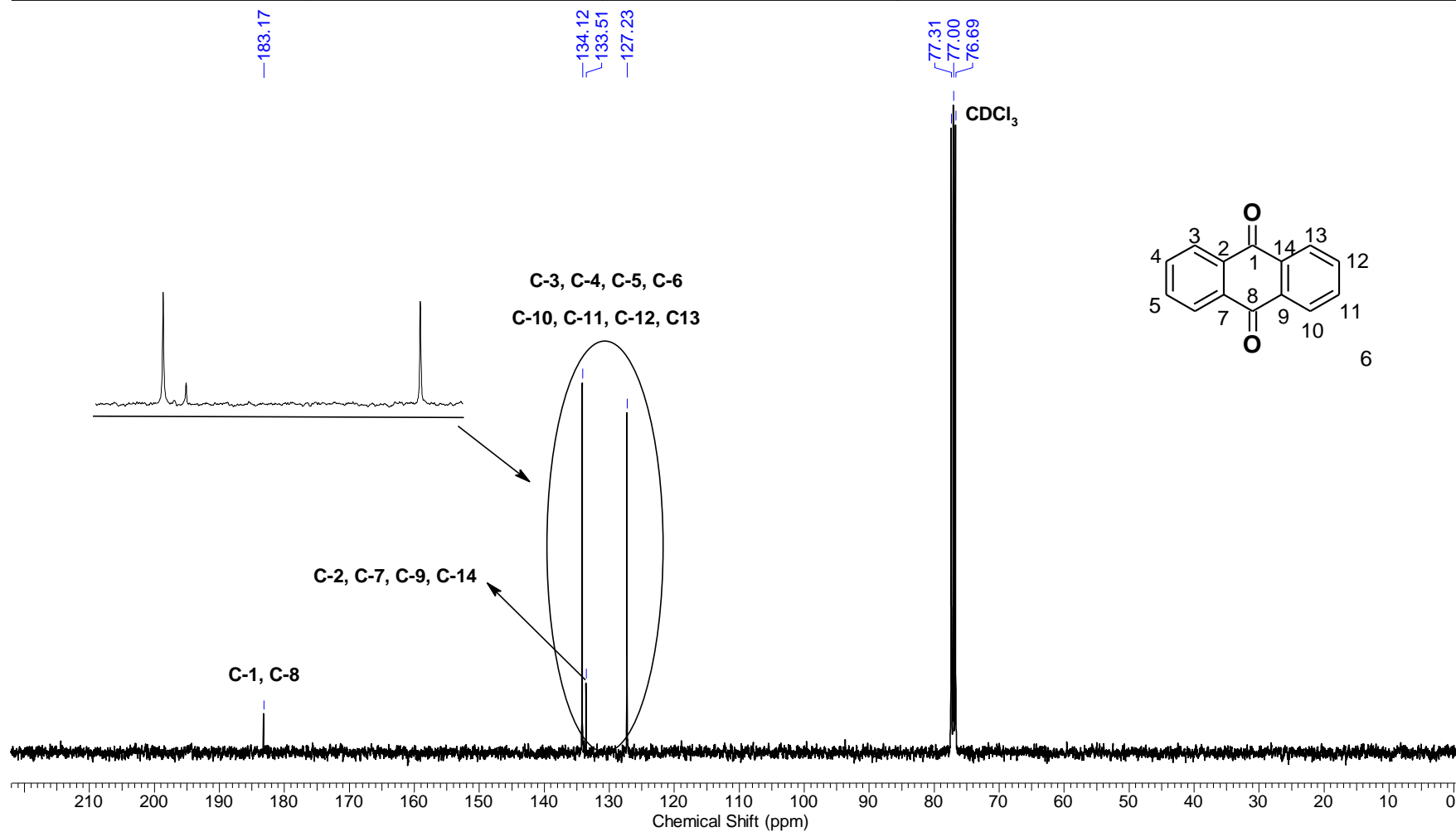
Frequency (MHz)	100.62	Nucleus	¹³ C	Number of Transients	1024	Origin	spect
Original Points Count	16384	Owner	root	Points Count	32768	Pulse Sequence	deptsp135
Receiver Gain	2050.00	SW(cyclical) (Hz)	20161.29	Solvent	CDCl ₃	Spectrum Offset (Hz)	8044.8511
Spectrum Type	DEPT135	Sweep Width (Hz)	20160.68	Temperature (degree C)	119.600	Acquisition Time (sec)	0.8126



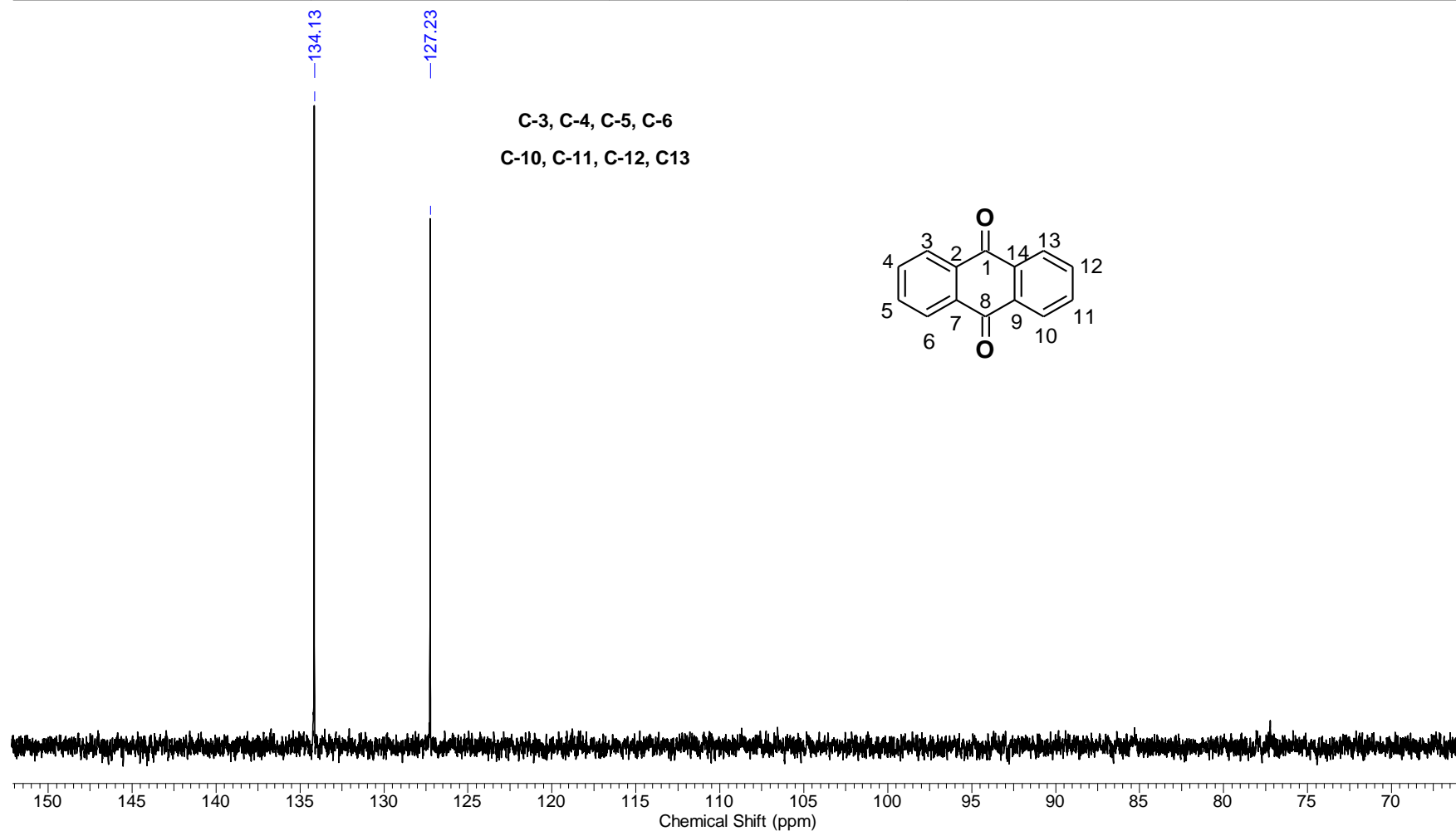
Frequency (MHz)	400.15	Nucleus	1H	Number of Transients	16	Origin	spect
Original Points Count	32768	Owner	root	Points Count	65536	Pulse Sequence	zg30
Receiver Gain	322.00	SW(cyclical) (Hz)	6818.18	Solvent	CDCl3	Spectrum Offset (Hz)	2995.5974
Spectrum Type	STANDARD	Sweep Width (Hz)	6818.08	Temperature (degree C)	119.300	Acquisition Time (sec)	4.8060



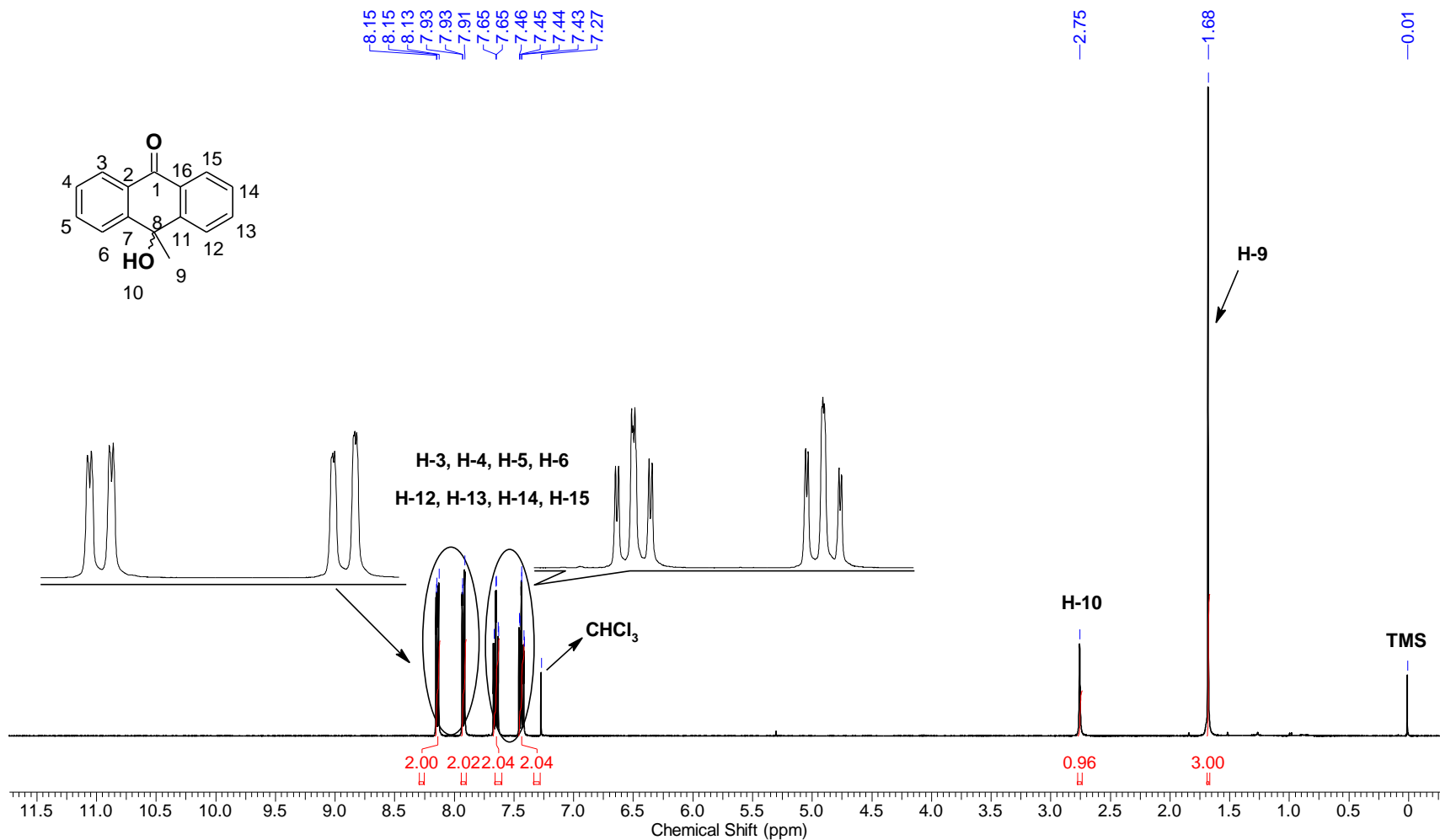
Frequency (MHz)	100.62	Nucleus	¹³ C	Number of Transients	1024	Origin	spect
Original Points Count	16384	Owner	root	Points Count	32768	Pulse Sequence	zpgg30
Receiver Gain	2050.00	SW(cyclical) (Hz)	24671.05	Solvent	CDCl ₃	Spectrum Offset (Hz)	10059.3525
Spectrum Type	STANDARD	Sweep Width (Hz)	24670.30	Temperature (degree C)	119.200	Acquisition Time (sec)	0.6641



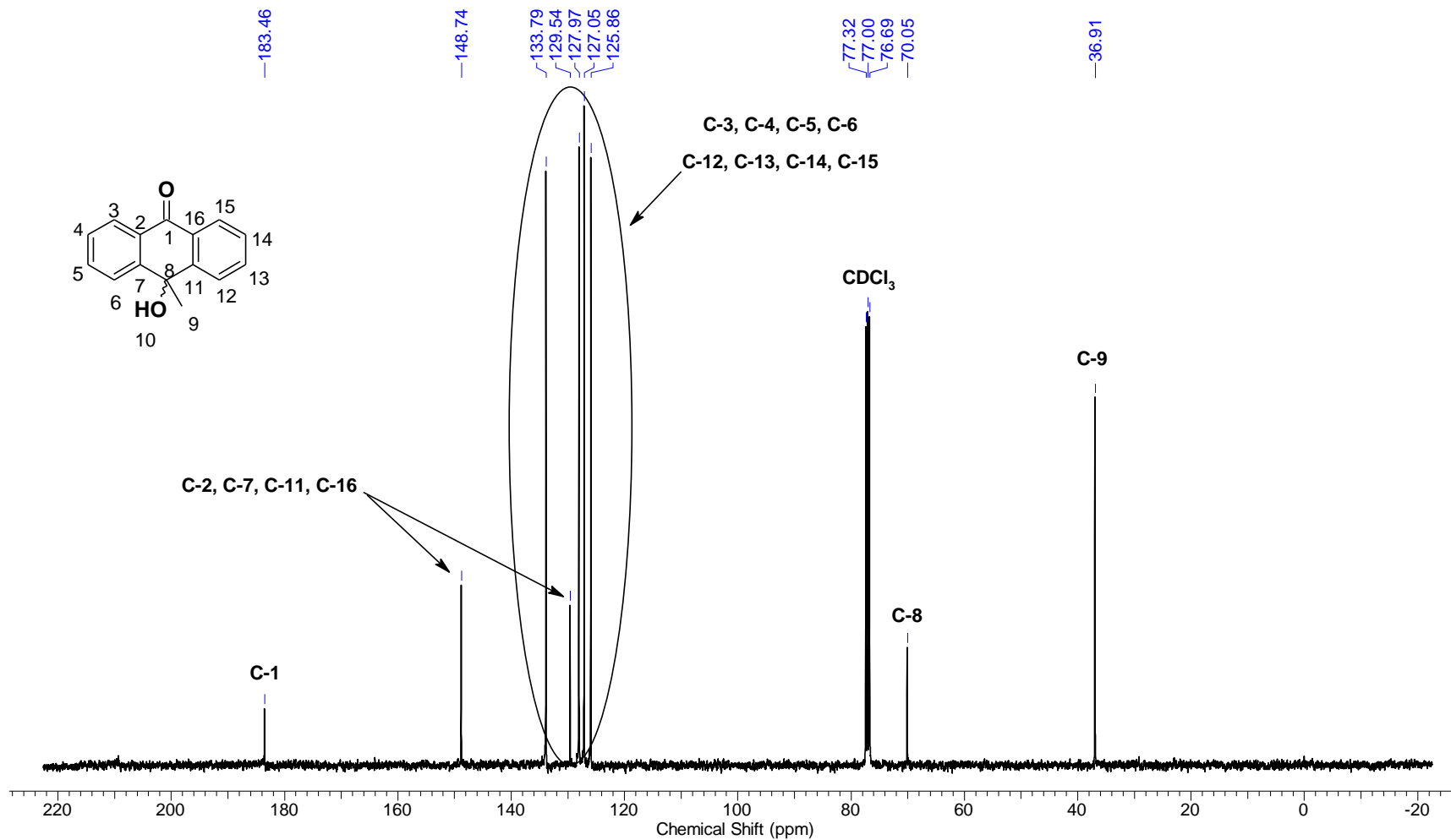
Frequency (MHz)	100.62	Nucleus	¹³ C	Number of Transients	1024	Origin	spect
Original Points Count	16384	Owner	root	Points Count	32768	Pulse Sequence	depts135
Receiver Gain	2050.00	SW(cyclical) (Hz)	20161.29	Solvent	CDCl ₃	Spectrum Offset (Hz)	8046.4600
Spectrum Type	DEPT135	Sweep Width (Hz)	20160.68	Temperature (degree C)	119.600	Acquisition Time (sec)	0.8126



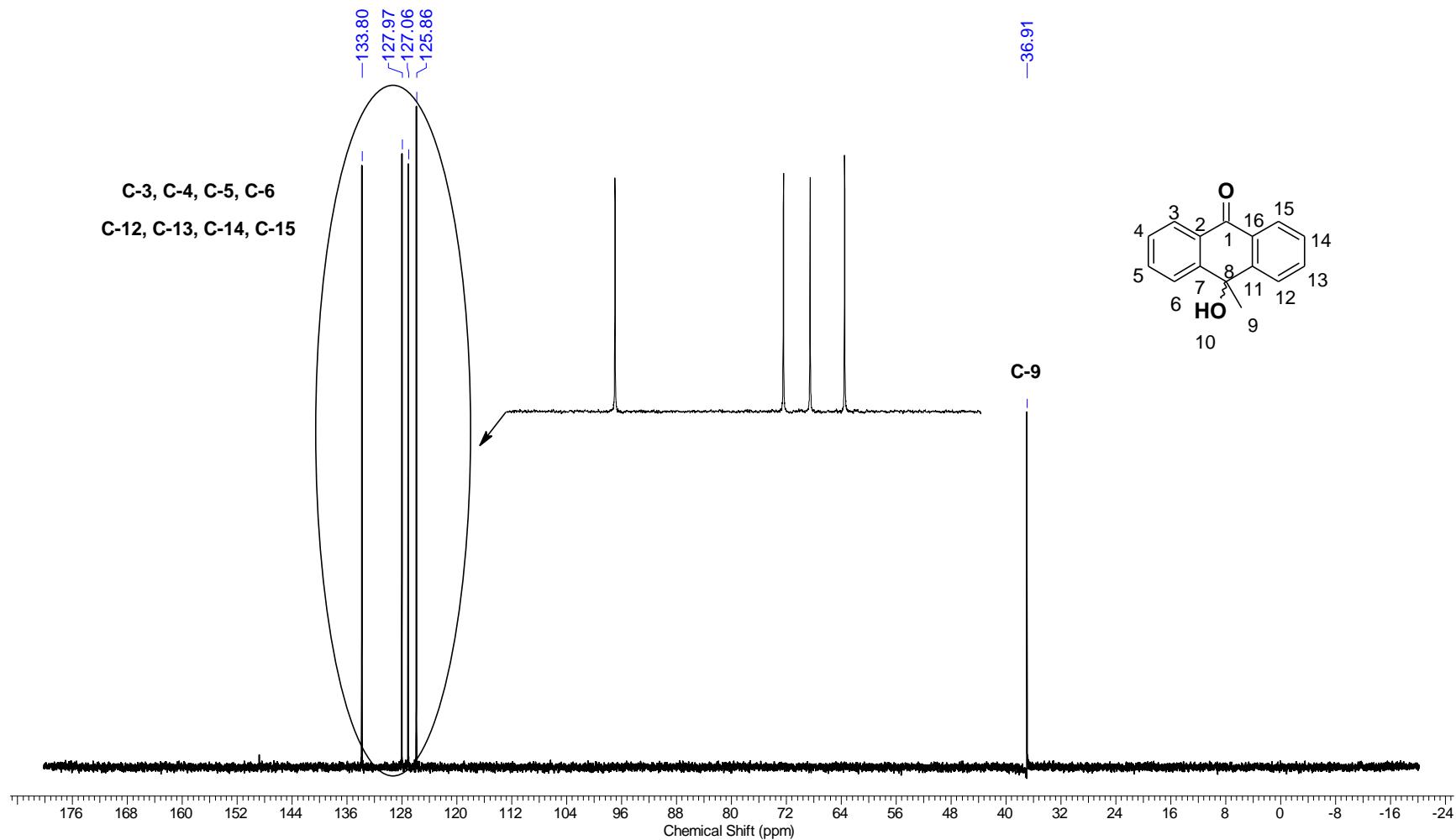
Frequency (MHz)	400.15	Nucleus	1H	Number of Transients	16	Origin	spect
Original Points Count	32768	Owner	root	Points Count	65536	Pulse Sequence	zg30
Receiver Gain	114.00	SW(cyclical) (Hz)	6818.18	Solvent	CDCl3	Spectrum Offset (Hz)	2995.7017
Spectrum Type	STANDARD	Sweep Width (Hz)	6818.08	Temperature (degree C)	119.500	Acquisition Time (sec)	4.8060



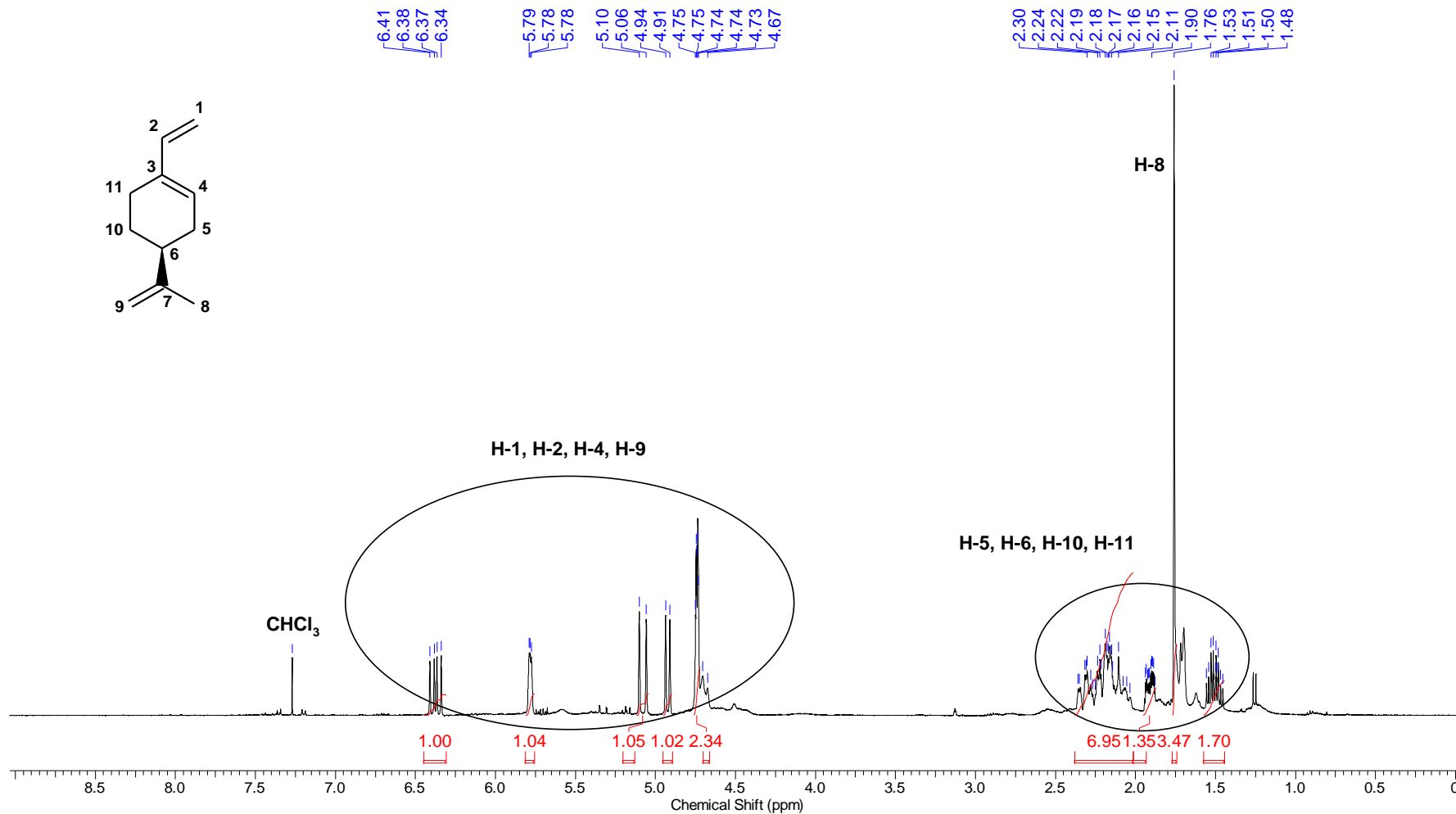
Frequency (MHz)	100.62	Nucleus	¹³ C	Number of Transients	1024	Origin	spect
Original Points Count	16384	Owner	root	Points Count	32768	Pulse Sequence	zgpg30
Receiver Gain	2050.00	SW(cyclical) (Hz)	24671.05	Solvent	CDCl ₃	Spectrum Offset (Hz)	10057.0938
Spectrum Type	STANDARD	Sweep Width (Hz)	24670.30	Temperature (degree C)	119.400	Acquisition Time (sec)	0.6641



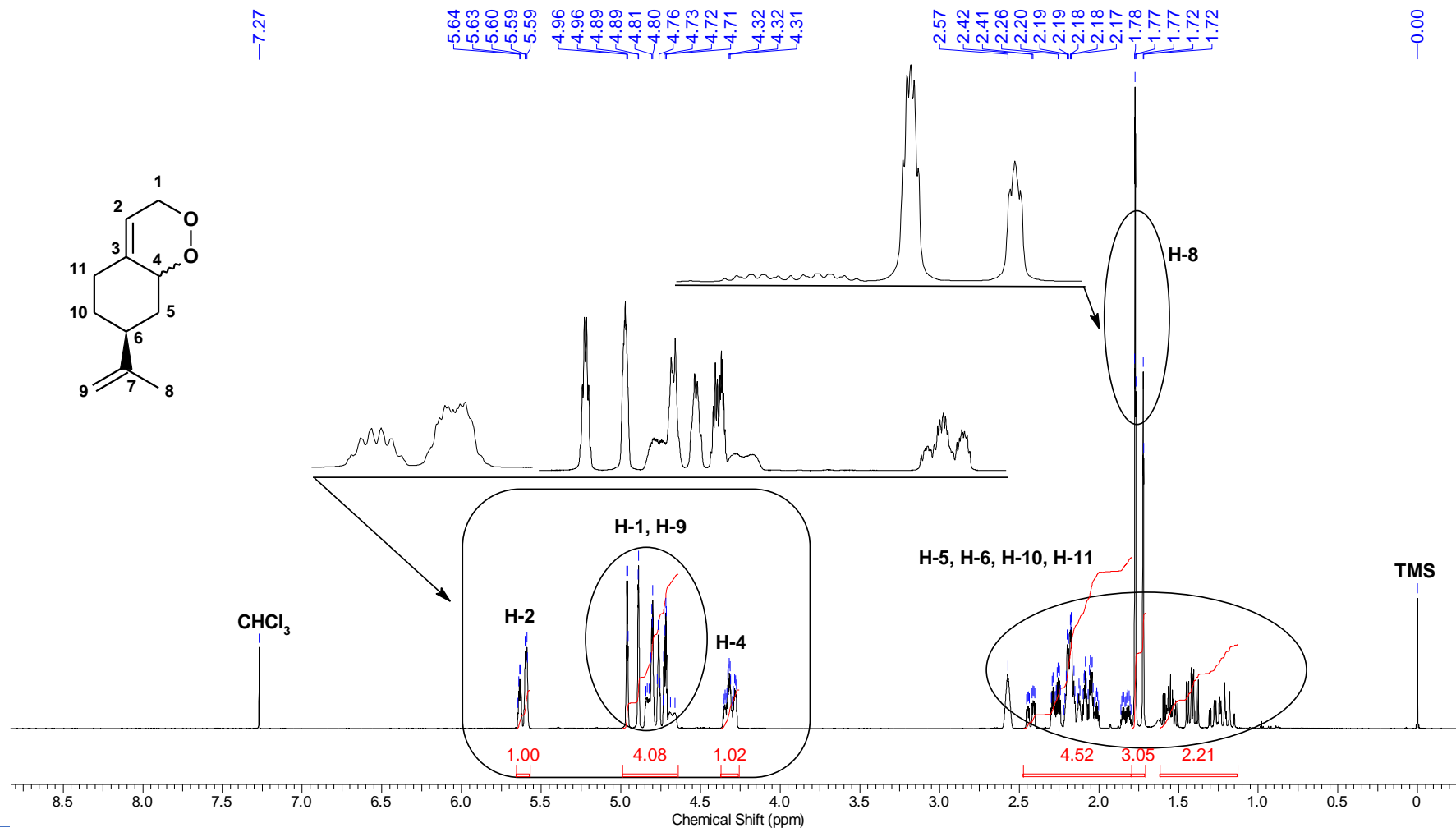
Frequency (MHz)	100.62	Nucleus	¹³ C	Number of Transients	1024	Origin	spect
Original Points Count	16384	Owner	root	Points Count	32768	Pulse Sequence	depts135
Receiver Gain	1030.00	SW(cyclical) (Hz)	20161.29	Solvent	CDCl ₃	Spectrum Offset (Hz)	8044.4077
Spectrum Type	DEPT135	Sweep Width (Hz)	20160.68	Temperature (degree C)	119.600	Acquisition Time (sec)	0.8126



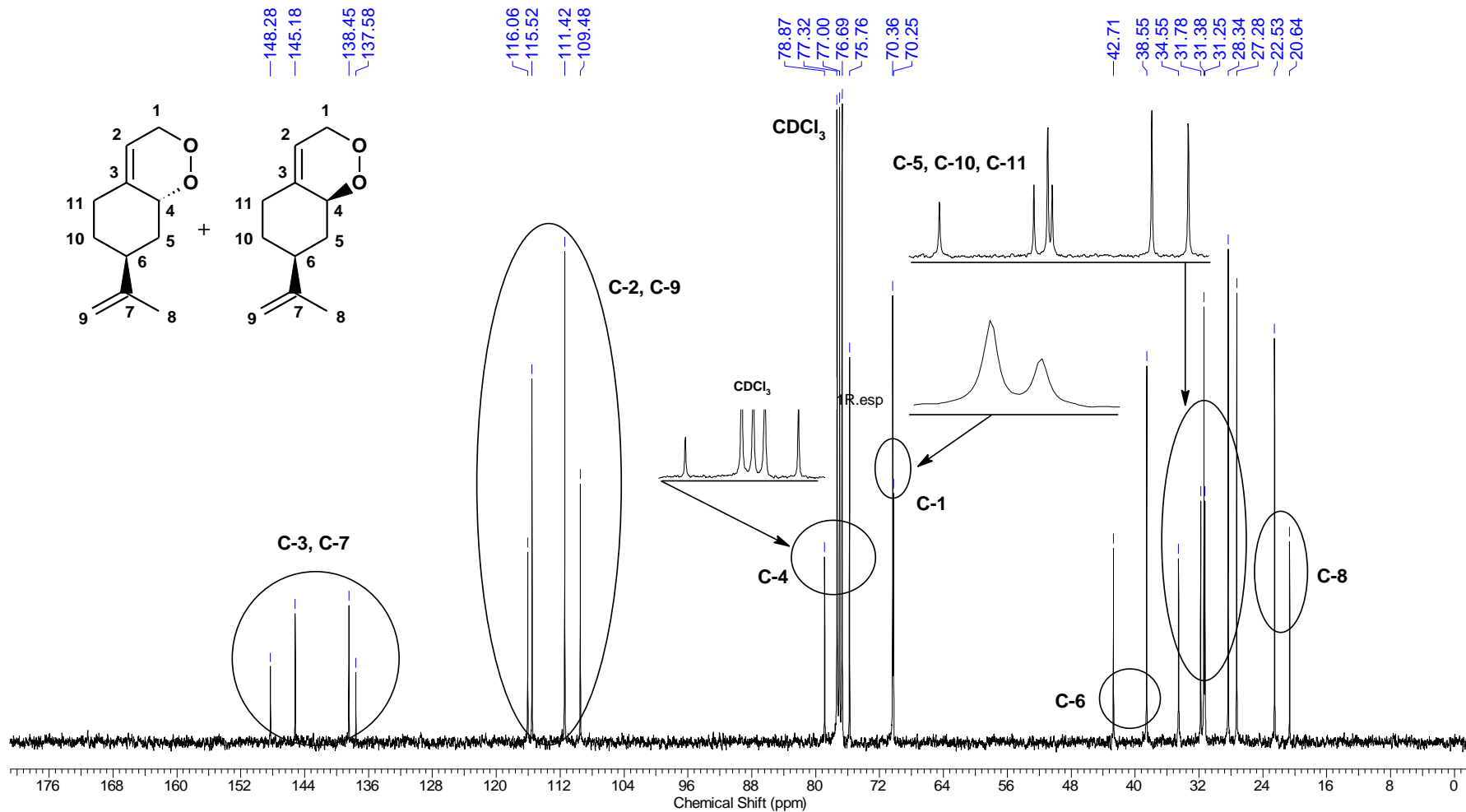
Acquisition Time (sec)	4.8060	Sweep Width (Hz)	6818.08	Temperature (degree C)	23.700	Frequency (MHz)	400.15
Nucleus	1H	Number of Transients	16	Origin	spect	Original Points Count	32768
Owner	nmrsu	Points Count	65536	Pulse Sequence	zg30	Receiver Gain	64.00
SW(cyclical) (Hz)	6818.18	Solvent	CDCl3	Spectrum Offset (Hz)	2995.4932	Spectrum Type	STANDARD



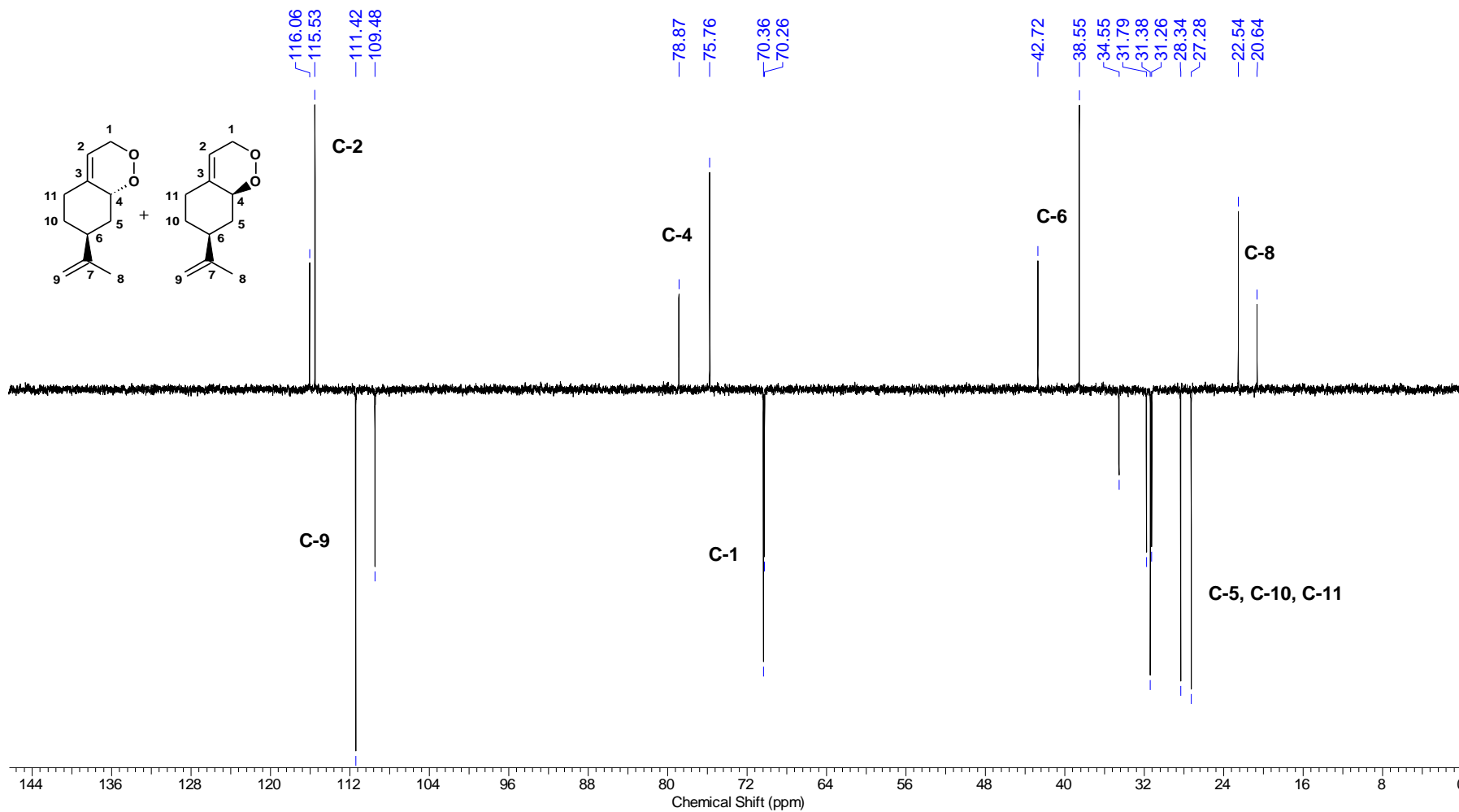
Acquisition Time (sec)	4.8060	Sweep Width (Hz)	6818.08	Temperature (degree C)	22.600	Frequency (MHz)	400.15
Nucleus	1H	Number of Transients	64	Origin	spect	Original Points Count	32768
Owner	nmrsu	Points Count	65536	Pulse Sequence	zg30	Receiver Gain	64.00
SW(cyclical) (Hz)	6818.18	Solvent	CDCl3	Spectrum Offset (Hz)	2995.6990	Spectrum Type	STANDARD



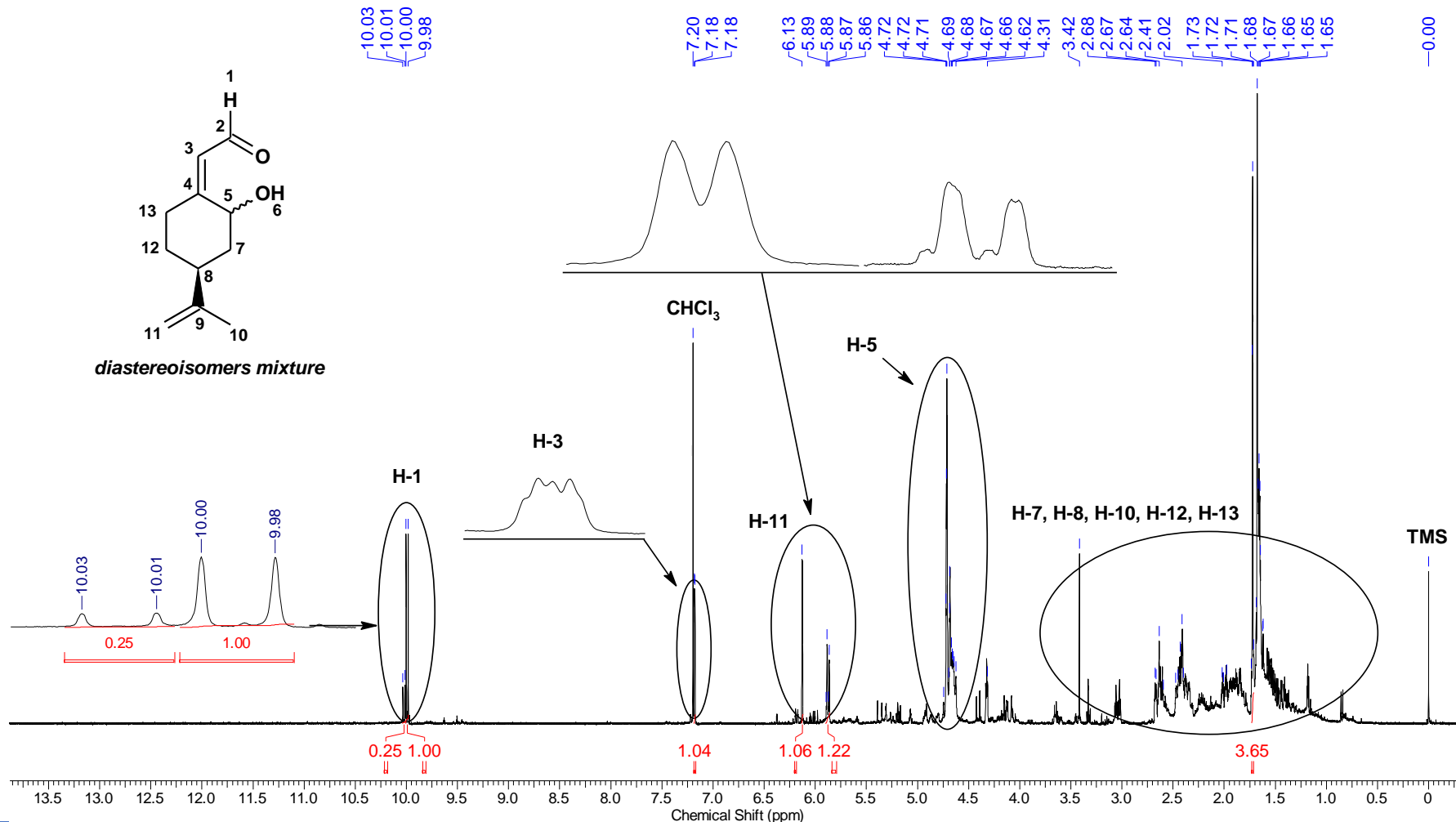
Acquisition Time (sec)	0.6641	Sweep Width (Hz)	24670.30	Temperature (degree C)	23.300	Frequency (MHz)	100.62
Nucleus	13C	Number of Transients	1024	Origin	spect	Original Points Count	16384
Owner	nmrsu	Points Count	32768	Pulse Sequence	zgpg30	Receiver Gain	2050.00
SW(cyclical) (Hz)	24671.05	Solvent	CDCl3	Spectrum Offset (Hz)	10057.0938	Spectrum Type	STANDARD



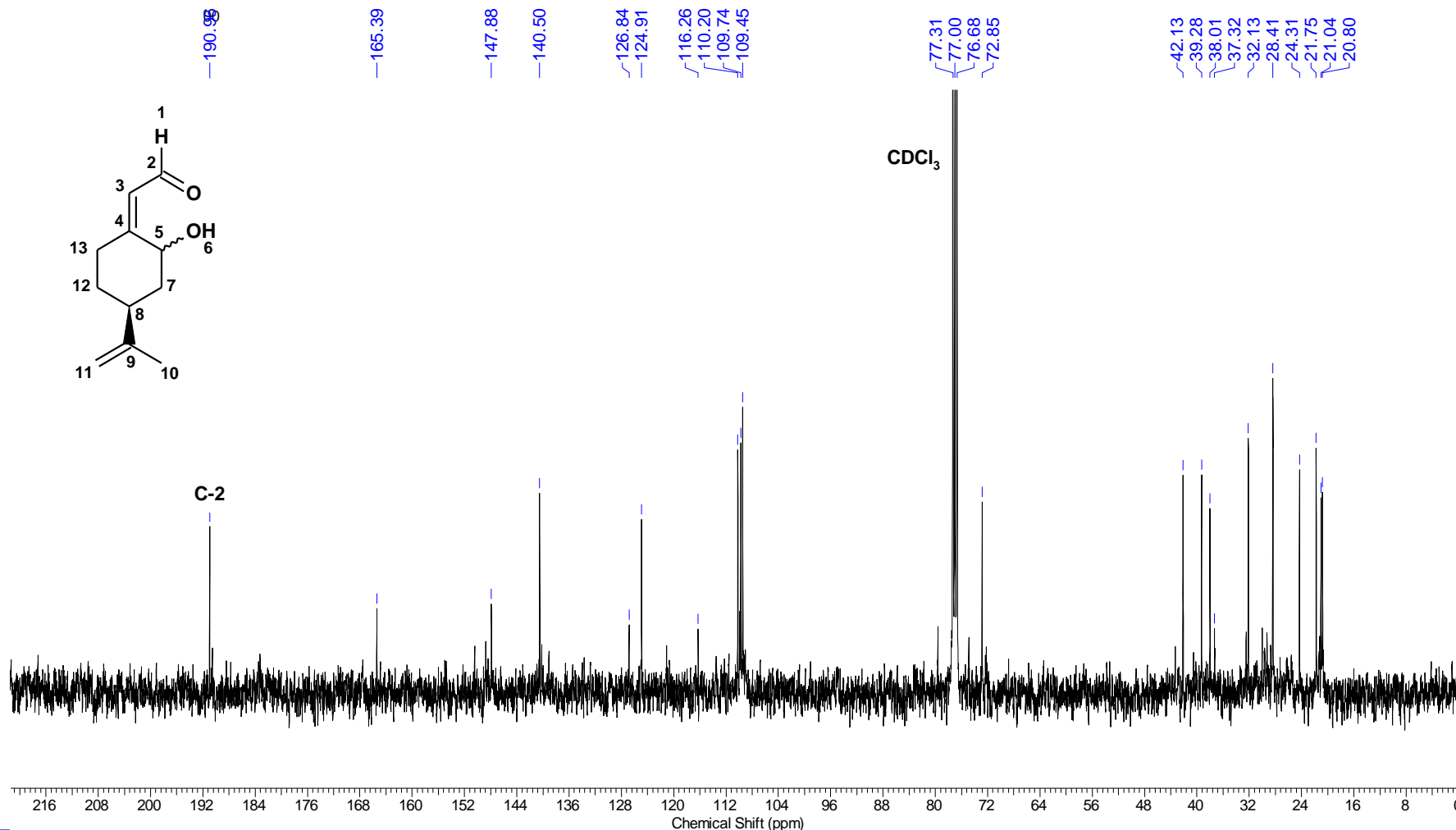
Acquisition Time (sec)	0.8126	Sweep Width (Hz)	20160.68	Temperature (degree C)	23.200	Frequency (MHz)	100.62
Nucleus	13C	Number of Transients	1024	Origin	spect	Original Points Count	16384
Owner	nmsu	Points Count	32768	Pulse Sequence	depts135	Receiver Gain	2050.00
SW(cyclical) (Hz)	20161.29	Solvent	CDC13	Spectrum Offset (Hz)	8044.5991	Spectrum Type	DEPT135



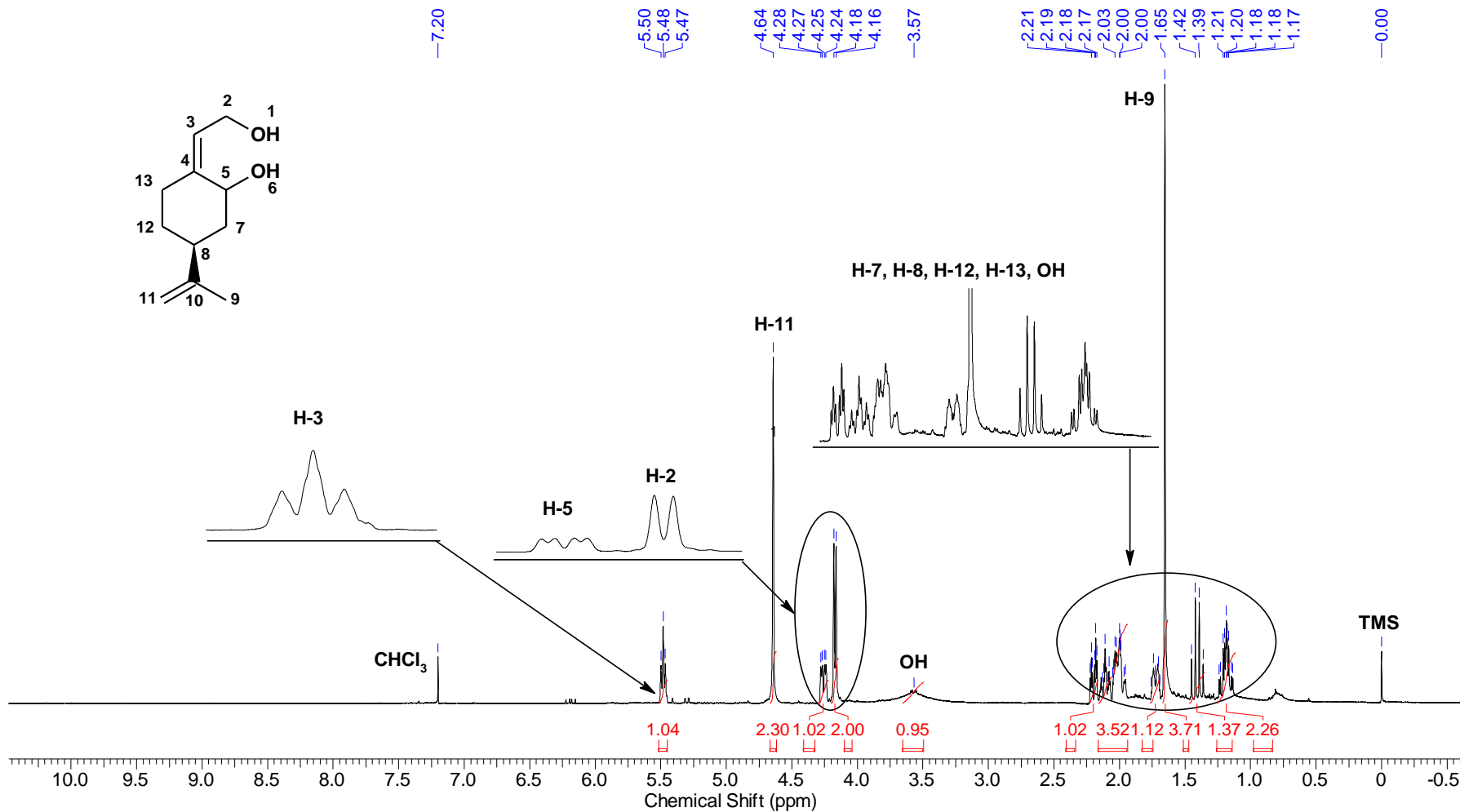
Acquisition Time (sec)	4.8060	Sweep Width (Hz)	6818.08	Temperature (degree C)	22.400	Frequency (MHz)	400.15
Nucleus	1H	Number of Transients	16	Origin	spect	Original Points Count	32768
Owner	nmsu	Points Count	65536	Pulse Sequence	zg30	Receiver Gain	114.00
SW(cyclical) (Hz)	6818.18	Solvent	CDCI3	Spectrum Offset (Hz)	2965.8403	Spectrum Type	STANDARD



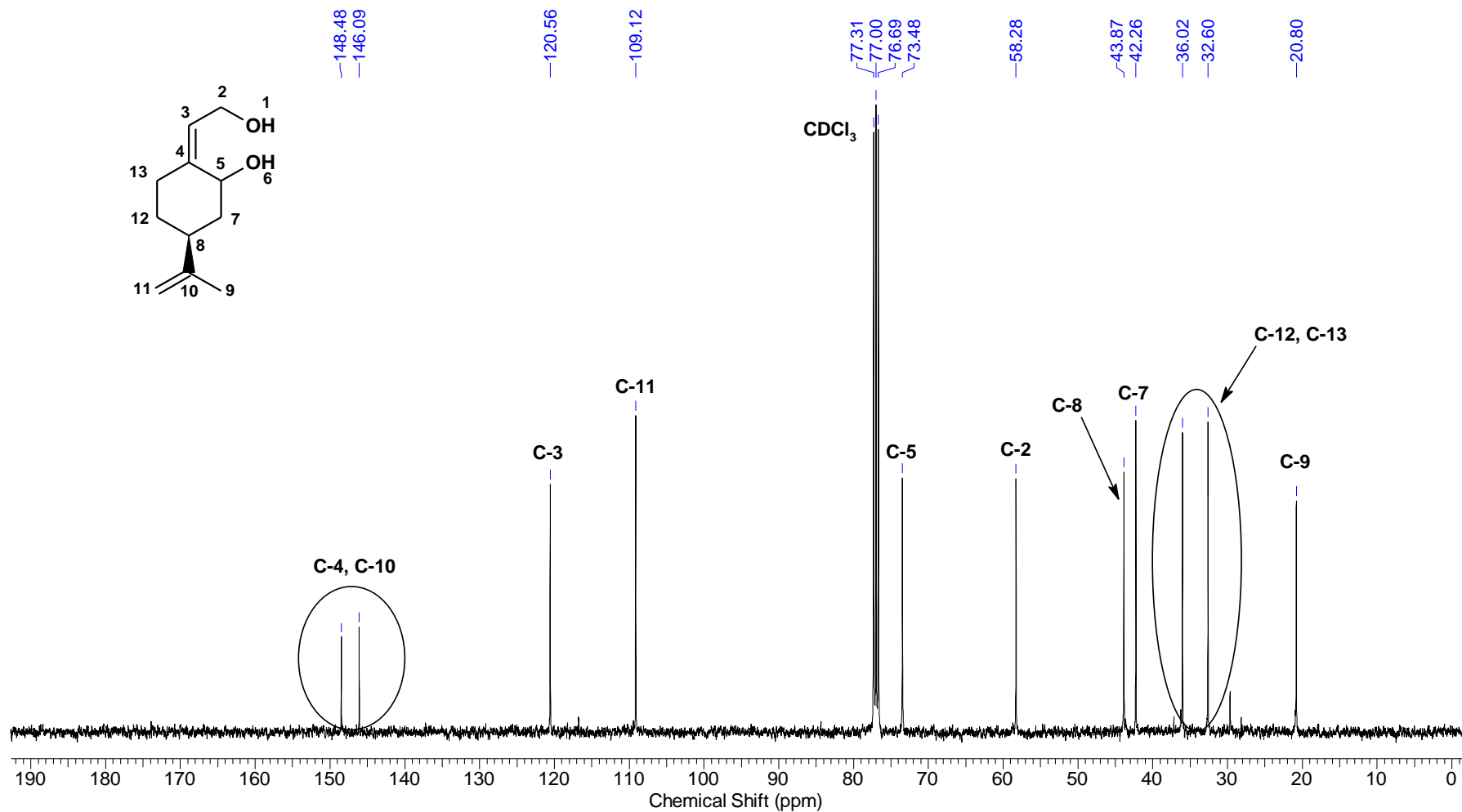
Acquisition Time (sec)	0.6641	Sweep Width (Hz)	24670.30	Temperature (degree C)	23.200	Frequency (MHz)	100.62
Nucleus	13C	Number of Transients	1024	Origin	spect	Original Points Count	16384
Owner	nmsu	Points Count	32768	Pulse Sequence	zgpg30	Receiver Gain	2050.00
SW(cyclical) (Hz)	24671.05	Solvent	CDCl3	Spectrum Offset (Hz)	10057.8467	Spectrum Type	STANDARD



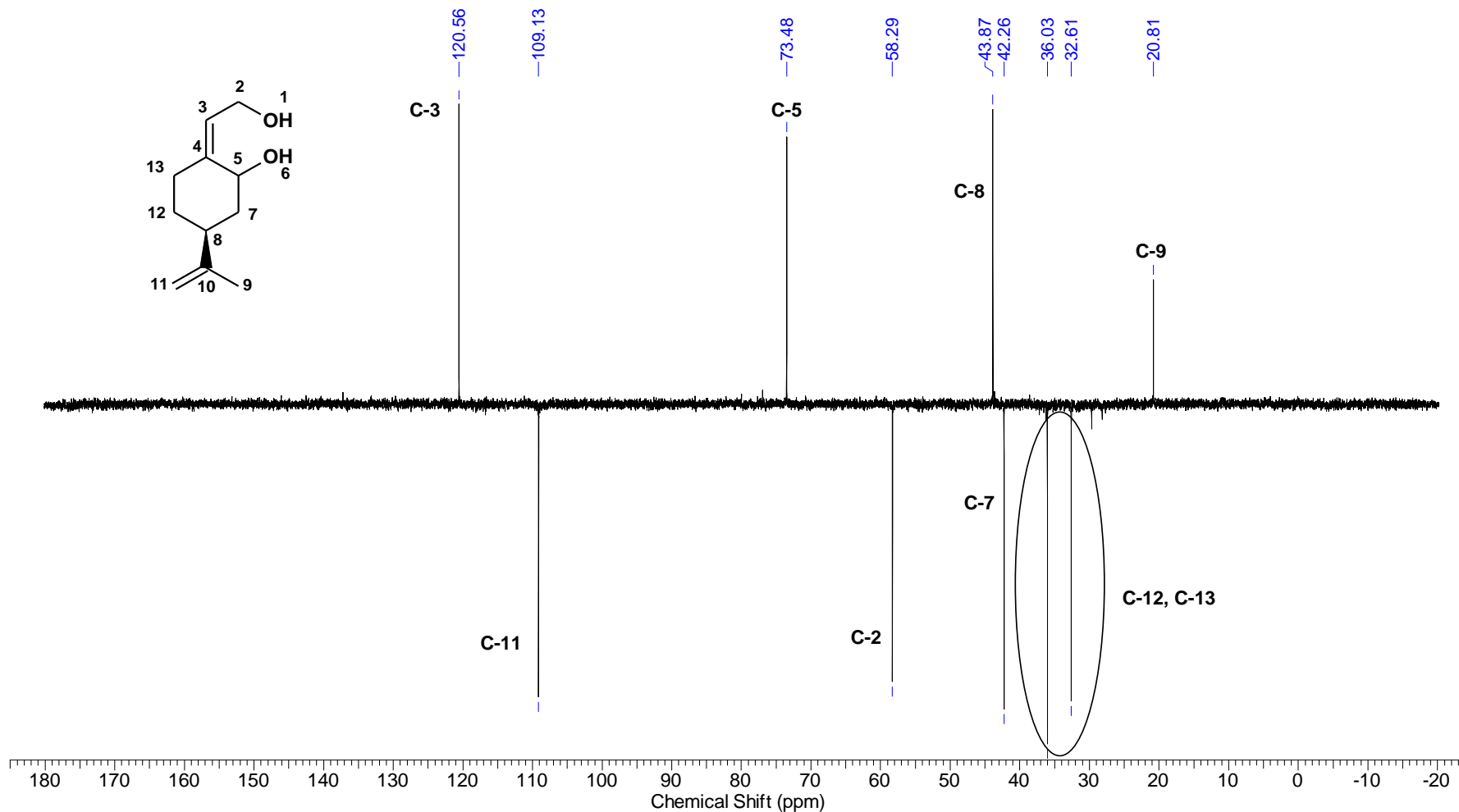
Acquisition Time (sec)	4.8060	Sweep Width (Hz)	6818.08	Temperature (degree C)	24.200	Frequency (MHz)	400.15
Nucleus	1H	Number of Transients	16	Origin	spect	Original Points Count	32768
Owner	nmsu	Points Count	65536	Pulse Sequence	zg30	Receiver Gain	114.00
SW(cyclical) (Hz)	6818.18	Solvent	CDCl3	Spectrum Offset (Hz)	2967.1929	Spectrum Type	STANDARD



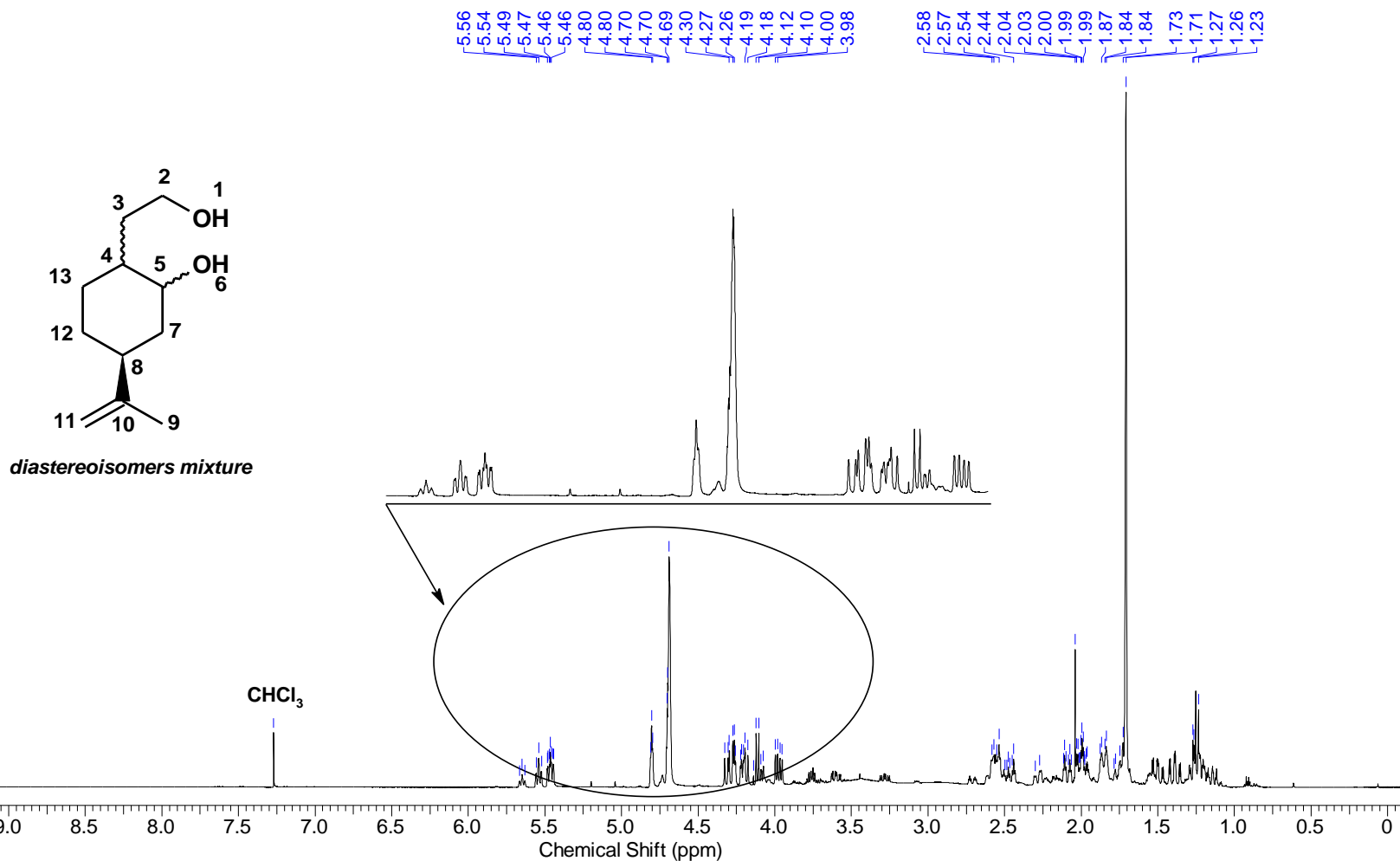
Acquisition Time (sec)	0.6641	Sweep Width (Hz)	24670.30	Temperature (degree C)	24.800	Frequency (MHz)	100.62
Nucleus	13C	Number of Transients	1024	Origin	spect	Original Points Count	16384
Owner	nmsu	Points Count	32768	Pulse Sequence	zgpg30	Receiver Gain	2050.00
SW(cyclical) (Hz)	24671.05	Solvent	CDCl3	Spectrum Offset (Hz)	10057.8467	Spectrum Type	STANDARD



Acquisition Time (sec)	0.8126	Sweep Width (Hz)	20160.68	Temperature (degree C)	24.600	Frequency (MHz)	100.62
Nucleus	13C	Number of Transients	1024	Origin	spect	Original Points Count	16384
Owner	nmsu	Points Count	32768	Pulse Sequence	deptsp135	Receiver Gain	2050.00
SW(cyclical) (Hz)	20161.29	Solvent	CDCl3	Spectrum Offset (Hz)	8045.9868	Spectrum Type	DEPT135

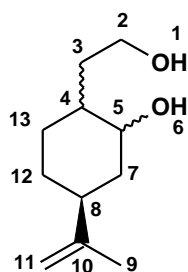


Acquisition Time (sec)	4.8060	Sweep Width (Hz)	6818.08	Temperature (degree C)	23.300	Frequency (MHz)	400.15
Nucleus	1H	Number of Transients	64	Origin	spect	Original Points Count	32768
Owner	nmsu	Points Count	65536	Pulse Sequence	zg30	Receiver Gain	50.80
SW(cyclical) (Hz)	6818.18	Solvent	CDCl3	Spectrum Offset (Hz)	2995.5974	Spectrum Type	STANDARD

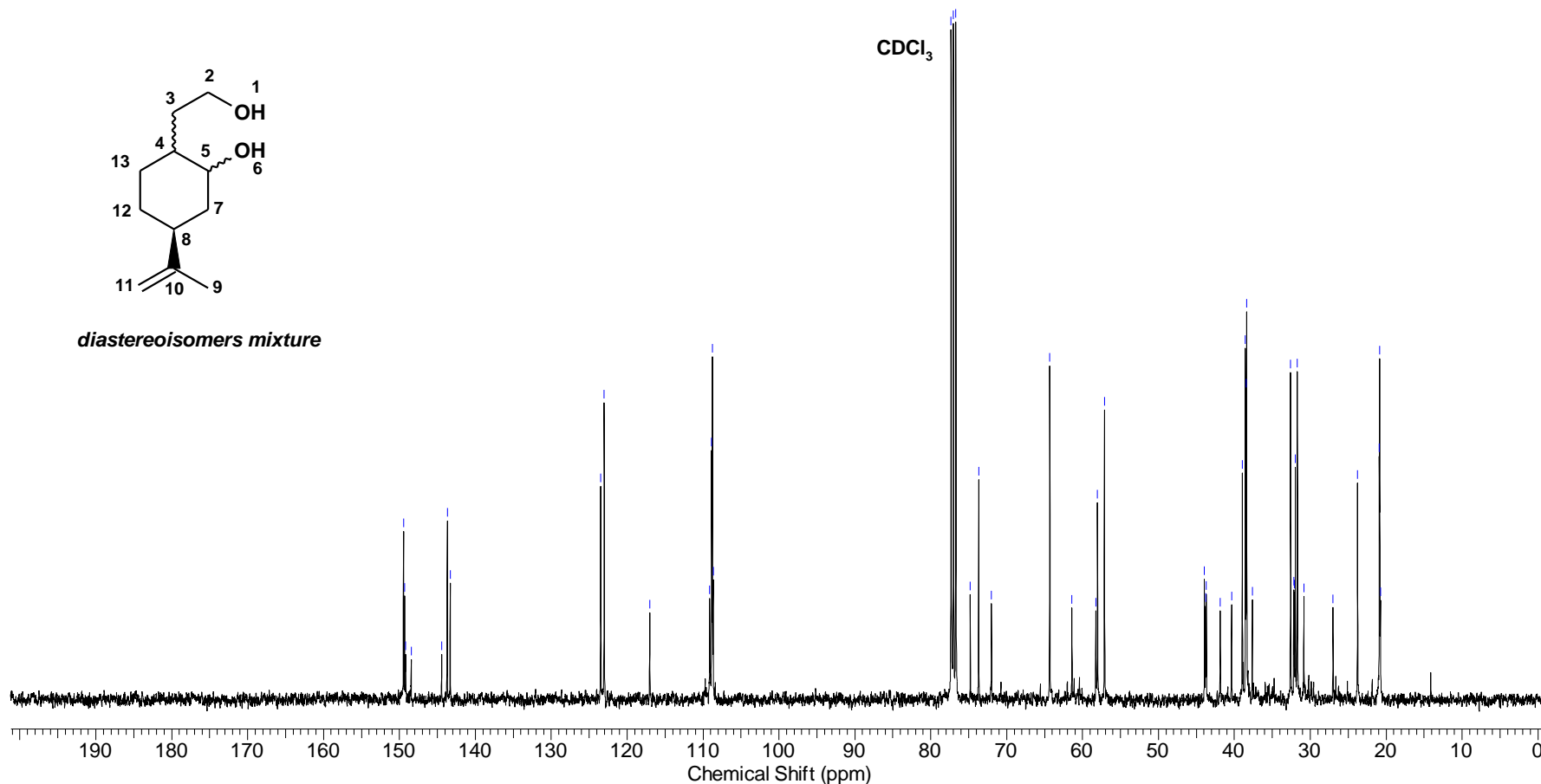


Acquisition Time (sec)	0.6641	Sweep Width (Hz)	24670.30	Temperature (degree C)	24.100	Frequency (MHz)	100.62
Nucleus	13C	Number of Transients	1024	Origin	spect	Original Points Count	16384
Owner	nmsu	Points Count	32768	Pulse Sequence	zgpg30	Receiver Gain	2050.00
SW(cyclical) (Hz)	24671.05	Solvent	CDCl3	Spectrum Offset (Hz)	10056.3408	Spectrum Type	STANDARD

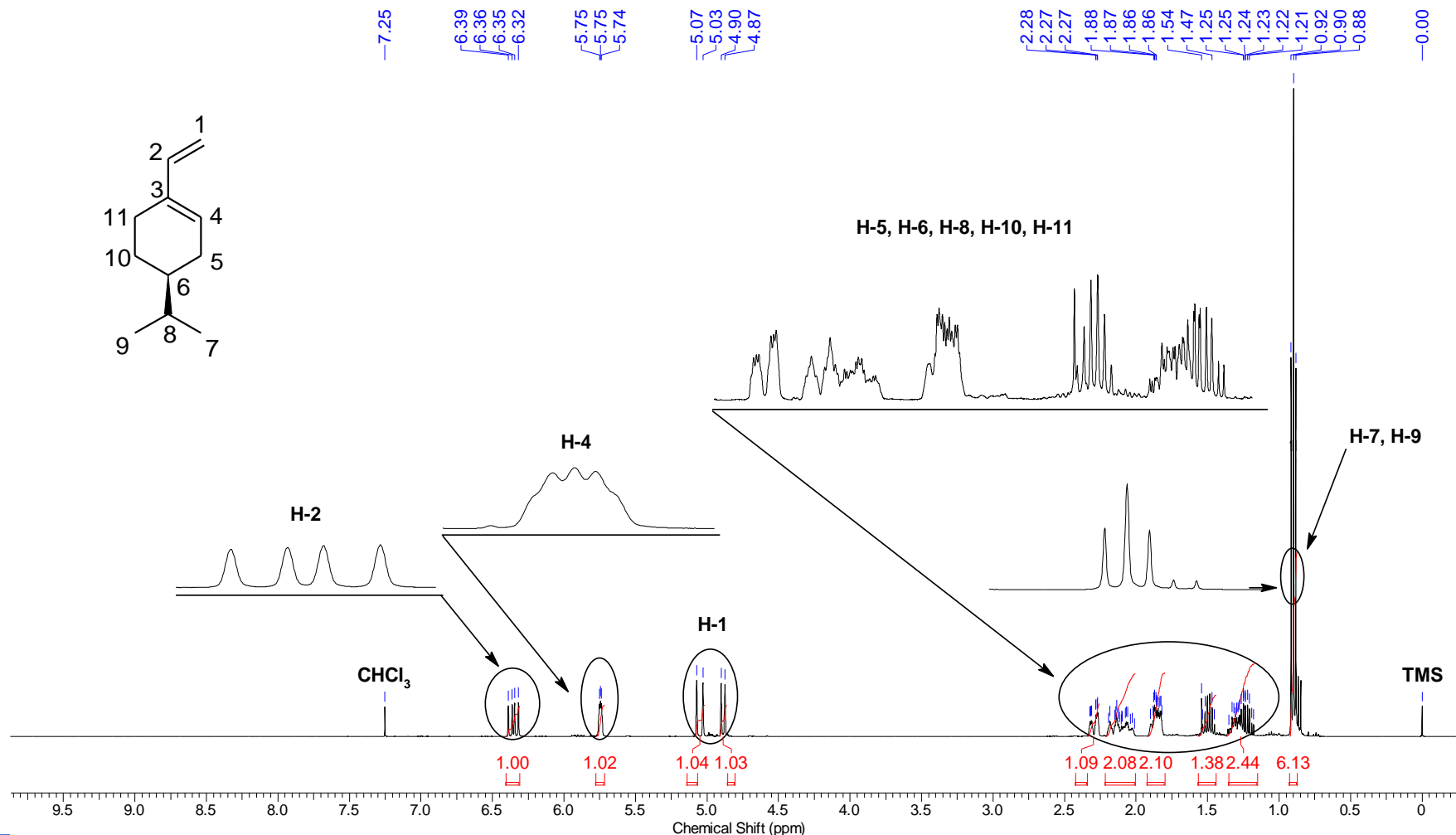
149.73, 149.63, 149.58, 148.45, 144.45, 143.70, 143.31, 123.48, 123.03, 117.02, 109.12, 108.87, 108.77, 108.66, 77.32, 77.00, 76.69, 74.79, 73.69, 72.00, 64.32, 61.41, 58.25, 58.03, 57.11, 43.93, 43.69, 38.95, 38.54, 38.43, 38.39, 37.64, 32.59, 32.18, 32.11, 31.97, 31.69, 30.84, 23.77, 20.90, 20.86, 20.75



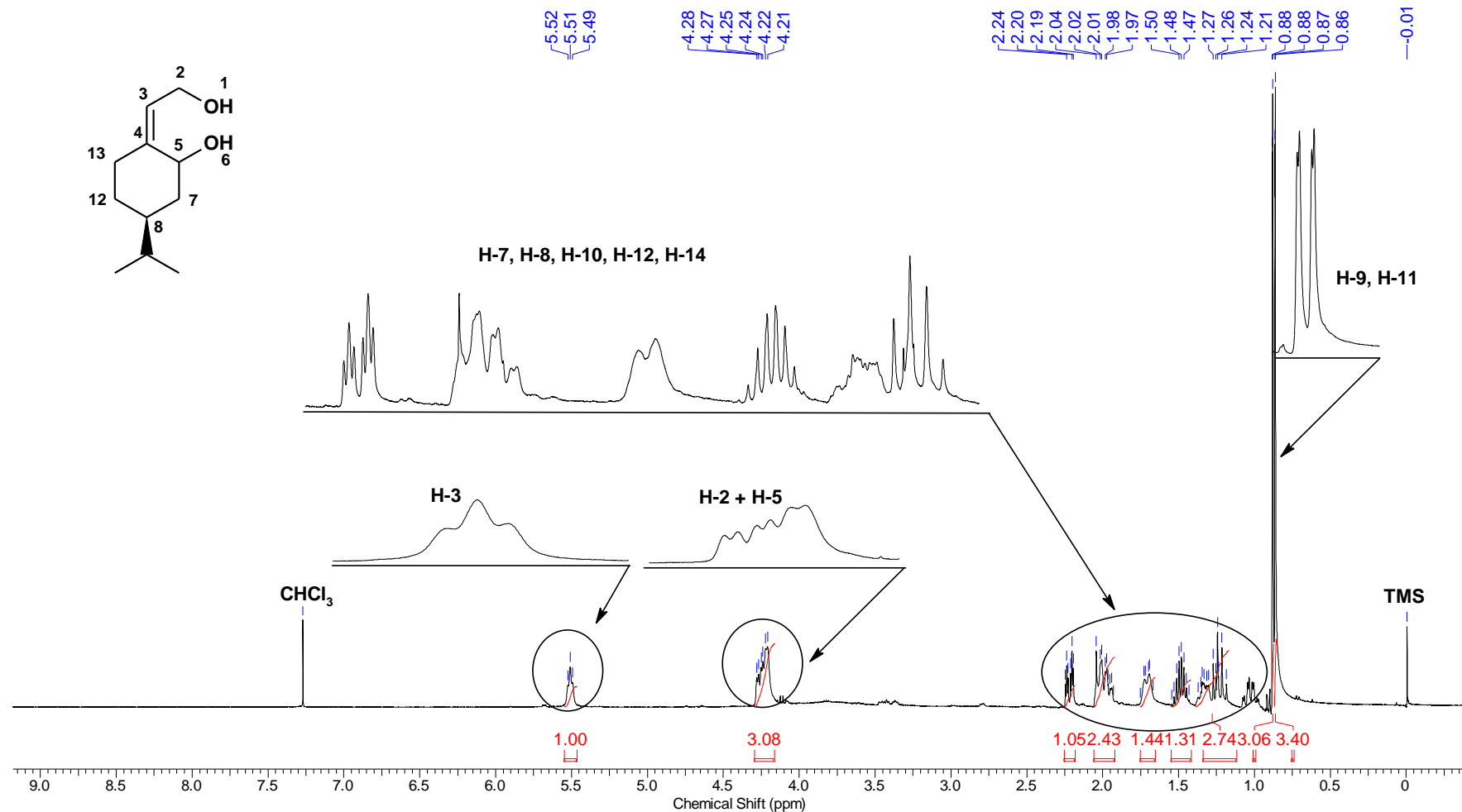
diastereoisomers mixture



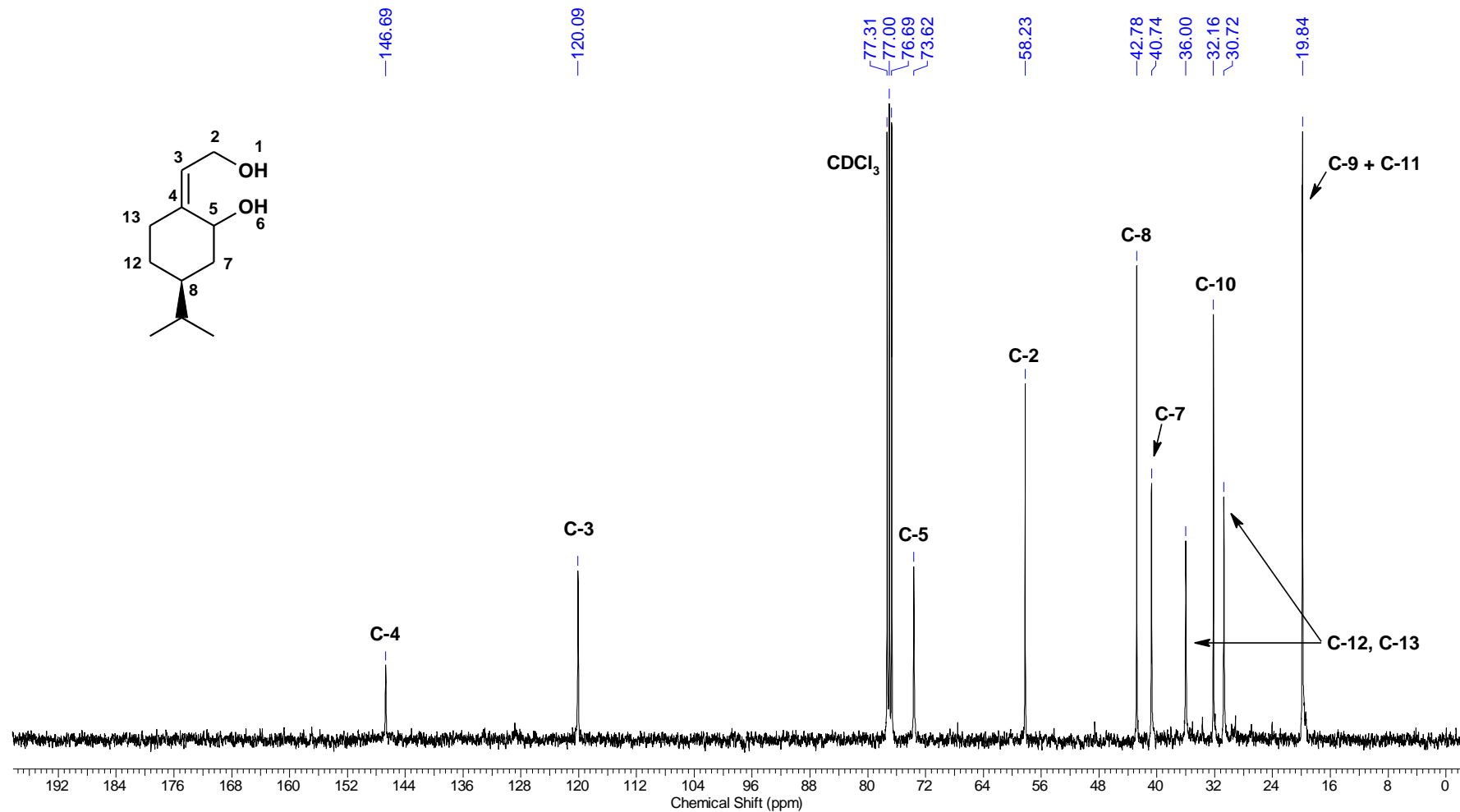
Nucleus	1H	Number of Transients	16	Origin	spect	Original Points Count	32768
Owner	nmsu	Points Count	65536	Pulse Sequence	zg30	Receiver Gain	45.20
SW(cyclical) (Hz)	6818.18	Solvent	CDCl3	Spectrum Offset (Hz)	2988.5205	Spectrum Type	STANDARD
Sweep Width (Hz)	6818.08	Temperature (degree C)	24.000	Acquisition Time (sec)	4.8060	Frequency (MHz)	400.15



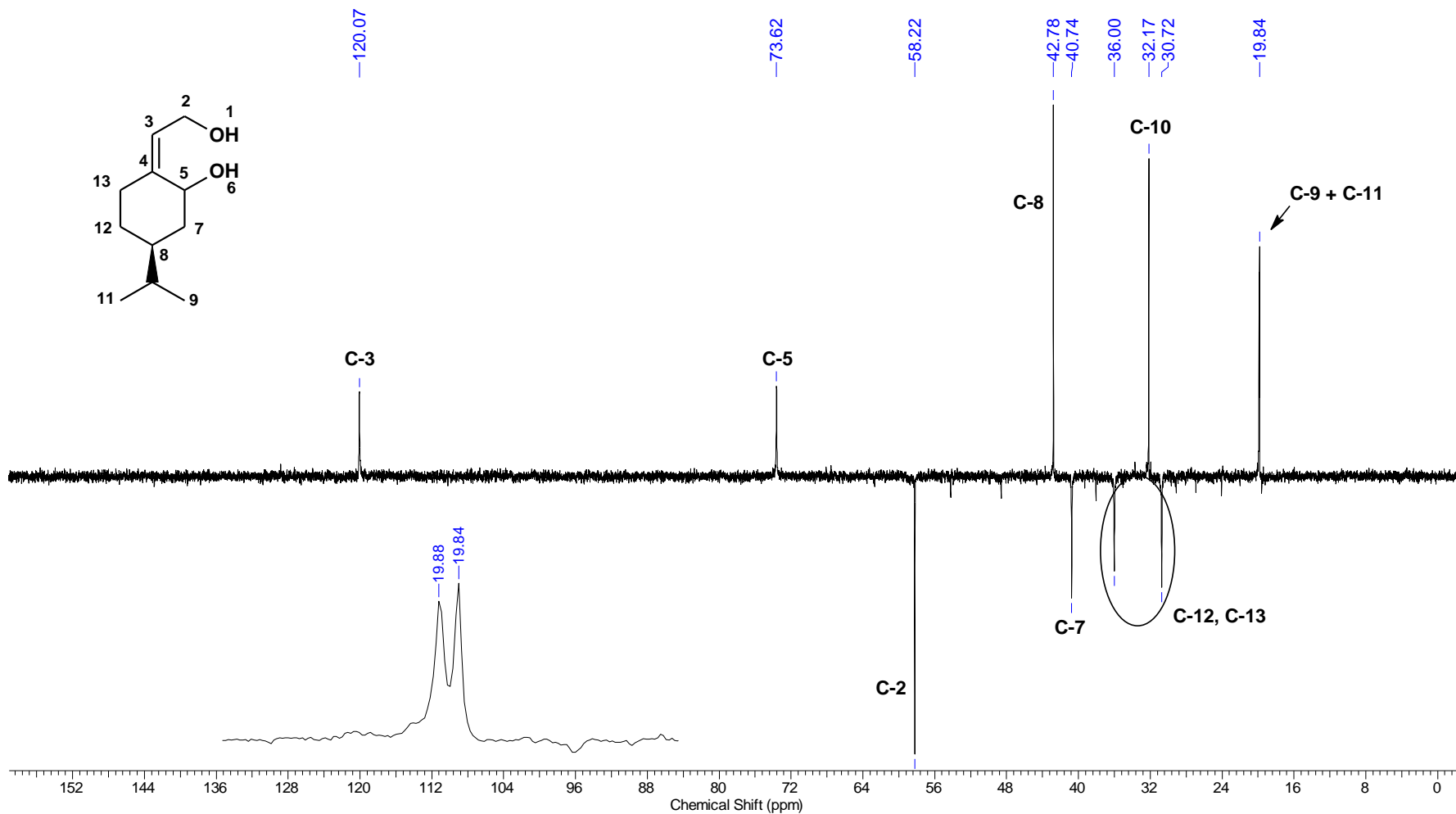
Nucleus	1H	Number of Transients	16	Origin	spect	Original Points Count	32768
Owner	nmsu	Points Count	65536	Pulse Sequence	zg30	Receiver Gain	22.60
SW(cyclical) (Hz)	6818.18	Solvent	CDCl3	Spectrum Offset (Hz)	2995.2854	Spectrum Type	STANDARD
Sweep Width (Hz)	6818.08	Temperature (degree C)	23.800	Acquisition Time (sec)	4.8060	Frequency (MHz)	400.15



Nucleus	13C	Number of Transients	1024	Origin	spect	Original Points Count	16384
Owner	nmrsu	Points Count	32768	Pulse Sequence	zgpg30	Receiver Gain	2050.00
SW(cyclical) (Hz)	24671.05	Solvent	CDCl3	Spectrum Offset (Hz)	10057.0938	Spectrum Type	STANDARD
Sweep Width (Hz)	24670.30	Temperature (degree C)	24.400	Acquisition Time (sec)	0.6641	Frequency (MHz)	100.62

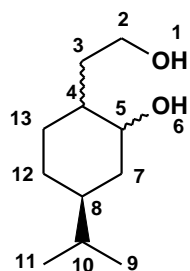


Nucleus	13C	Number of Transients	1024	Origin	spect	Original Points Count	16384
Owner	nmsu	Points Count	32768	Pulse Sequence	deptsp135	Receiver Gain	912.00
SW(cyclical) (Hz)	20161.29	Solvent	CDCl3	Spectrum Offset (Hz)	8044.0908	Spectrum Type	DEPT135
Sweep Width (Hz)	20160.68	Temperature (degree C)	24.100	Acquisition Time (sec)	0.8126	Frequency (MHz)	100.62

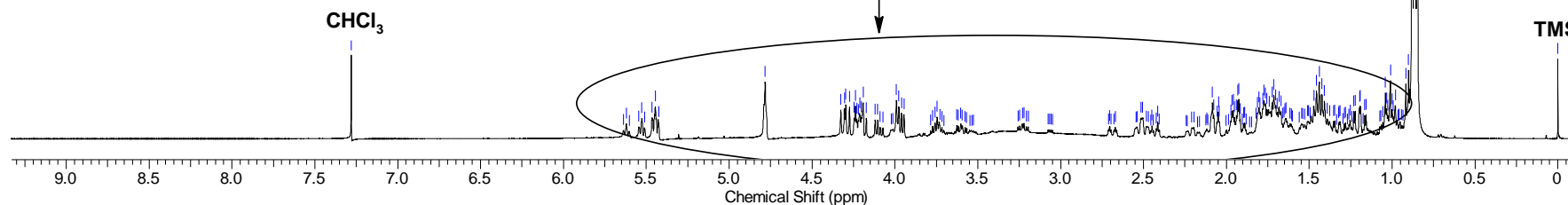
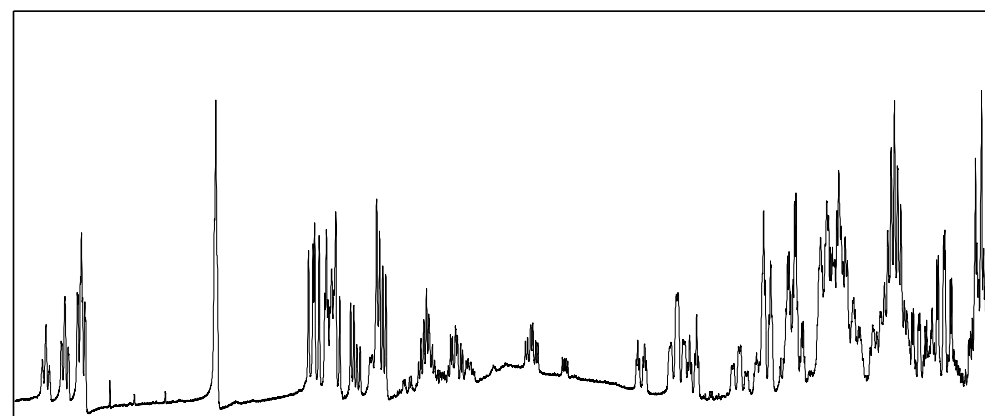


Acquisition Time (sec)	4.8060	Sweep Width (Hz)	6818.08	Temperature (degree C)	23.700	Frequency (MHz)	400.15
Nucleus	1H	Number of Transients	16	Origin	spect	Original Points Count	32768
Owner	nmsu	Points Count	65536	Pulse Sequence	zg30	Receiver Gain	20.20
SW(cyclical) (Hz)	6818.18	Solvent	CDCl3	Spectrum Offset (Hz)	2999.3403	Spectrum Type	STANDARD

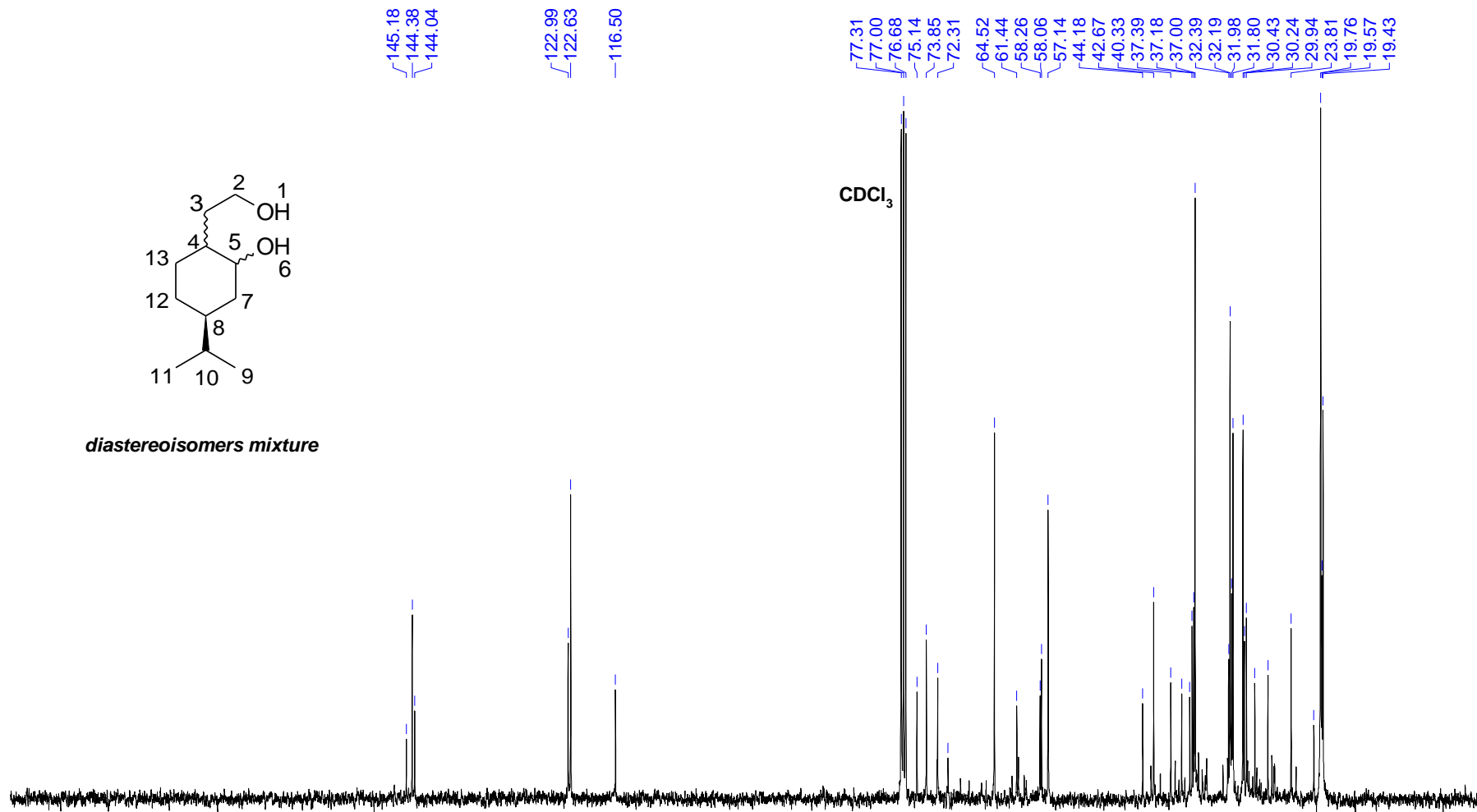
5.64 5.62 5.60 5.54 5.53 5.51 5.47 5.45 5.42 4.78 4.33 4.30 4.30 4.27 4.24 4.21 4.19 3.99 3.98 3.96 3.76 3.75 3.60 3.25 3.23 3.22 2.51 2.51 2.08 1.96 1.93 1.92 1.72 1.71 1.46 1.44 1.42 1.04 1.01 0.92 0.90 0.88 0.87 0.86 0.85 0.85 -0.00



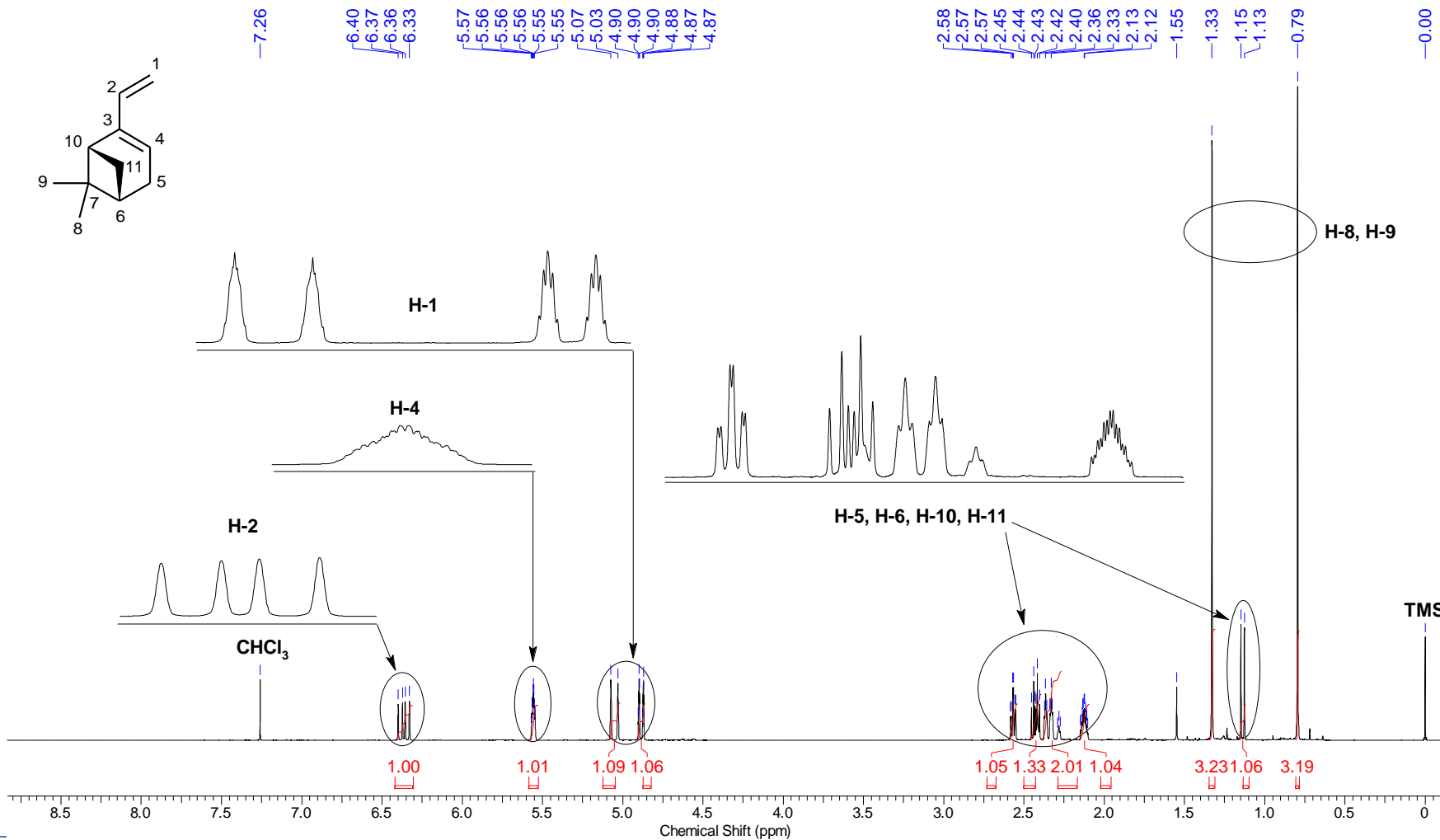
diastereomeric mixture



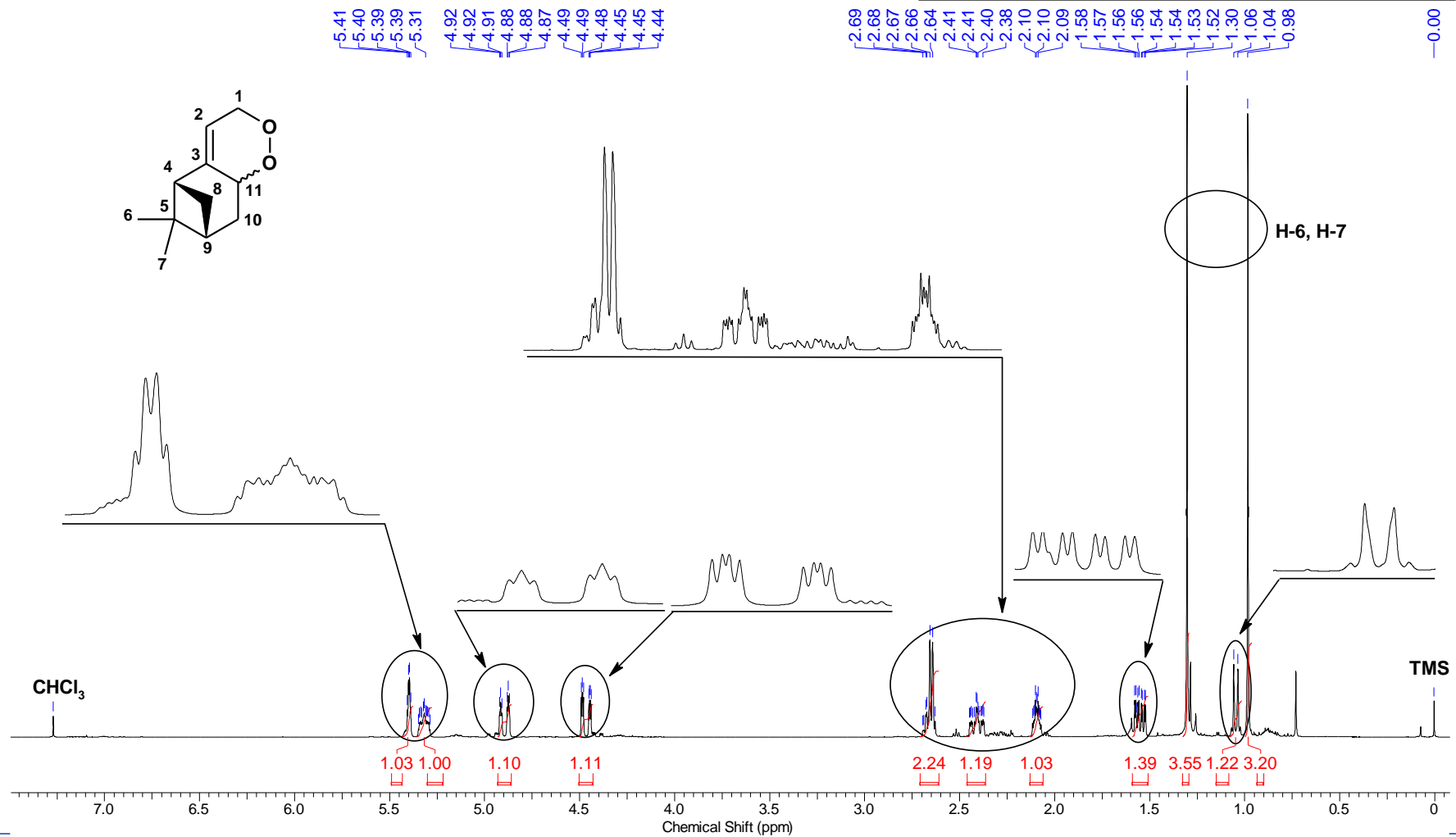
Nucleus	13C	Number of Transients	1024	Origin	spect	Original Points Count	16384
Owner	nmsu	Points Count	32768	Pulse Sequence	zgpg30	Receiver Gain	2050.00
SW(cyclical) (Hz)	24671.05	Solvent	CDCl ₃	Spectrum Offset (Hz)	10056.3408	Spectrum Type	STANDARD
Sweep Width (Hz)	24670.30	Temperature (degree C)	24.400	Acquisition Time (sec)	0.6641	Frequency (MHz)	100.62



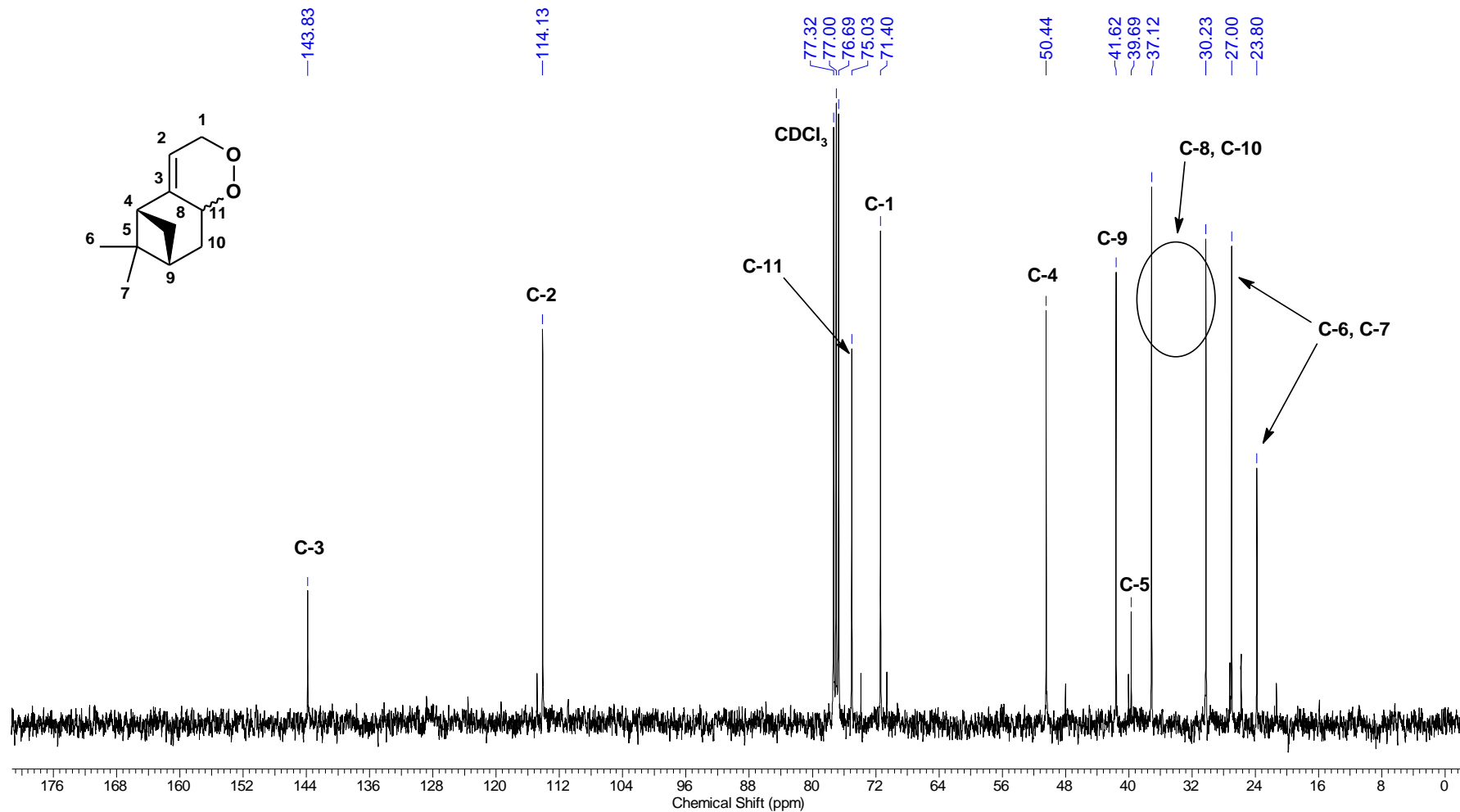
Frequency (MHz)	400.15	Nucleus	1H	Number of Transients	64	Origin	spect
Original Points Count	32768	Owner	nmrsu	Points Count	65536	Pulse Sequence	zg30
Receiver Gain	114.00	SW(cyclical) (Hz)	6818.18	Solvent	CHLOROFORM-d	Acquisition Time (sec)	4.8060
Spectrum Offset (Hz)	2991.1213	Spectrum Type	STANDARD	Sweep Width (Hz)	6818.08	Temperature (degree C)	22.600



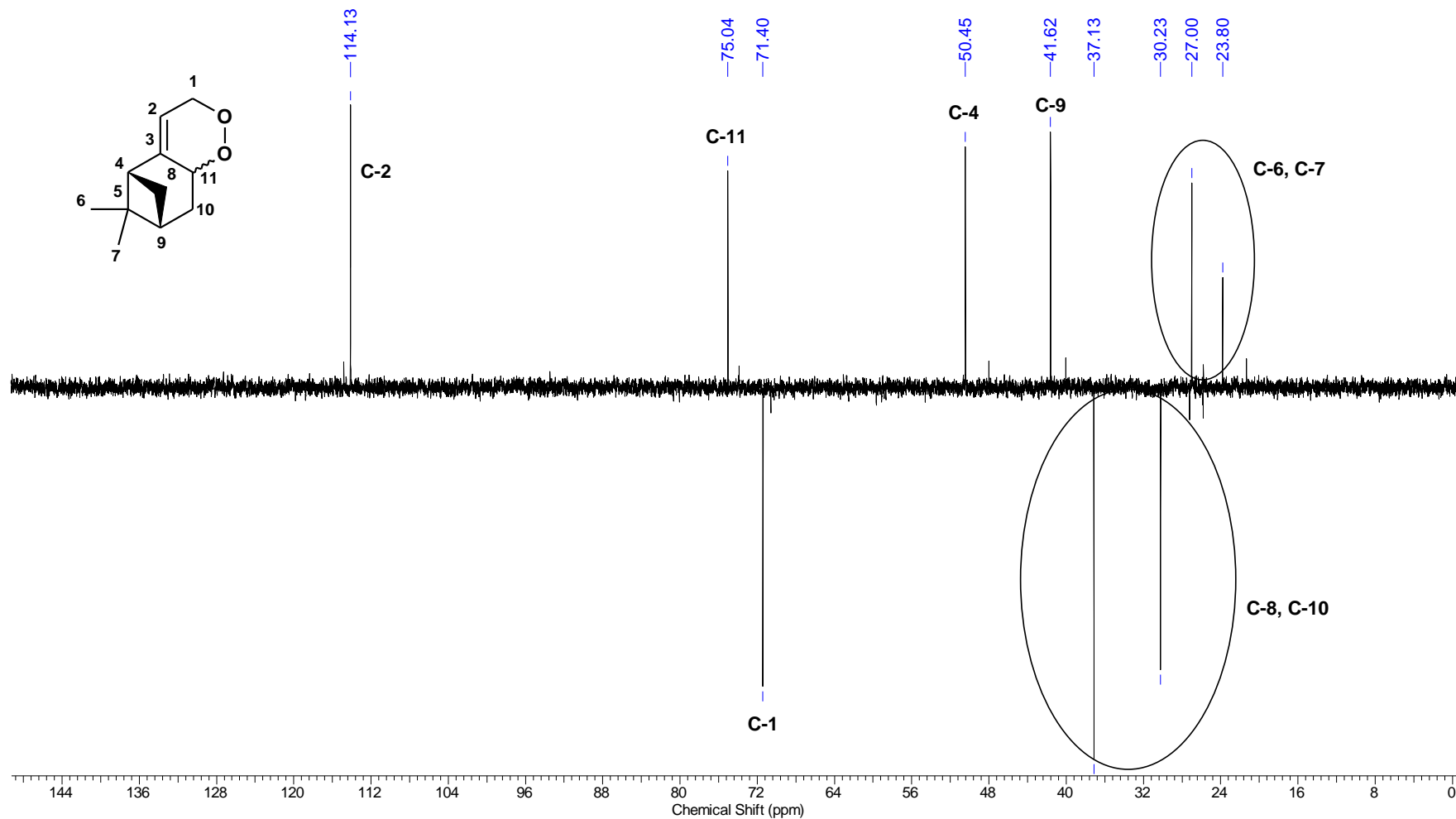
Frequency (MHz)	400.13	Nucleus	1H	Number of Transients	16	Origin	spect
Original Points Count	32768	Owner	root	Points Count	65536	Pulse Sequence	zg
Receiver Gain	28.50	SW(cyclical) (Hz)	4618.23	Solvent	CDCl3	Spectrum Offset (Hz)	2105.1455
Spectrum Type	STANDARD	Sweep Width (Hz)	4618.16	Temperature (degree C)	25.198	Acquisition Time (sec)	7.0954



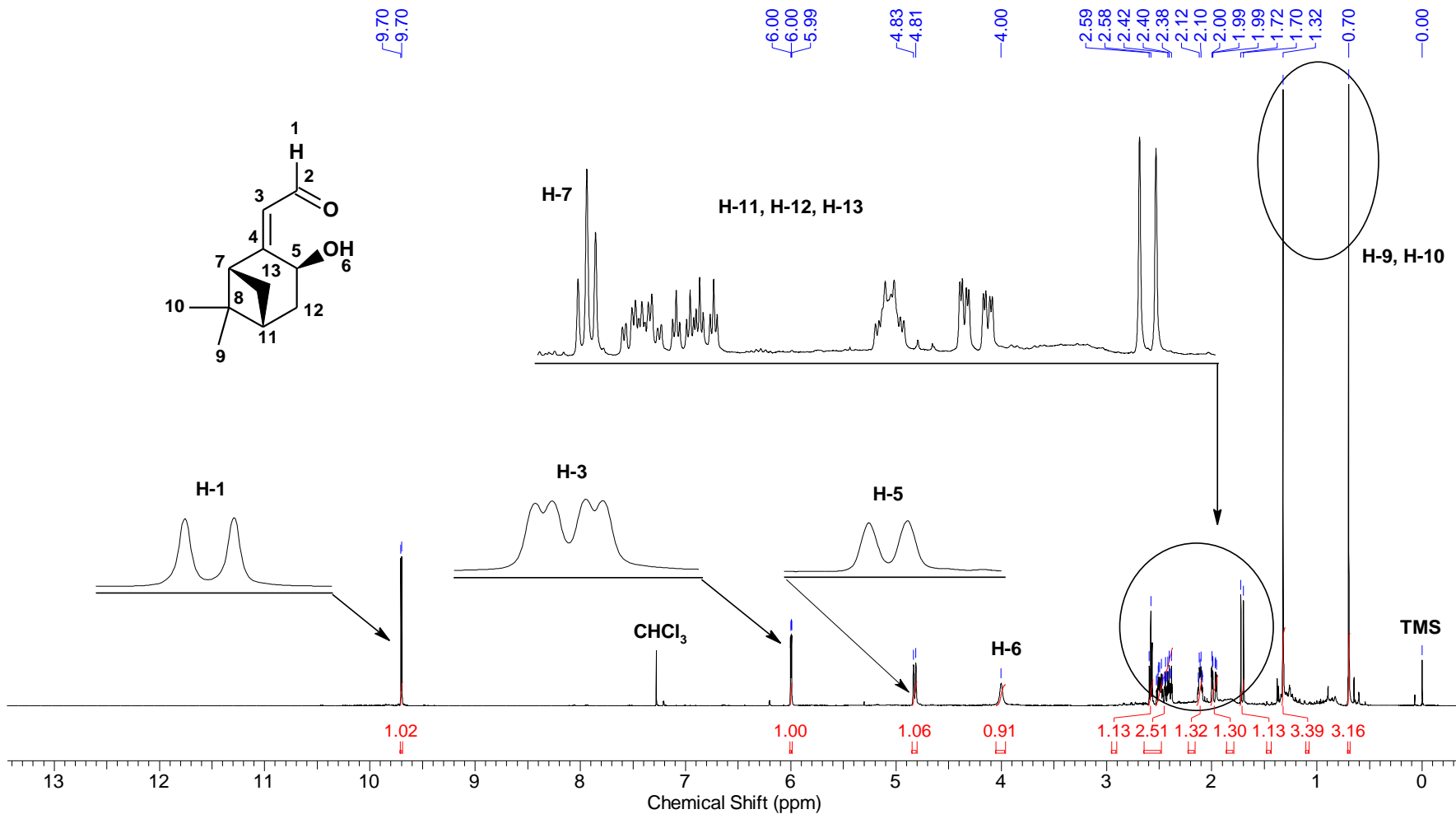
Frequency (MHz)	100.61	Nucleus	13C	Number of Transients	901	Origin	spect
Original Points Count	16384	Owner	root	Points Count	32768	Pulse Sequence	zgpg30
Receiver Gain	724.00	SW(cyclical) (Hz)	24038.46	Solvent	CDCl3	Spectrum Offset (Hz)	10058.3770
Spectrum Type	STANDARD	Sweep Width (Hz)	24037.73	Temperature (degree C)	25.234	Acquisition Time (sec)	0.6816



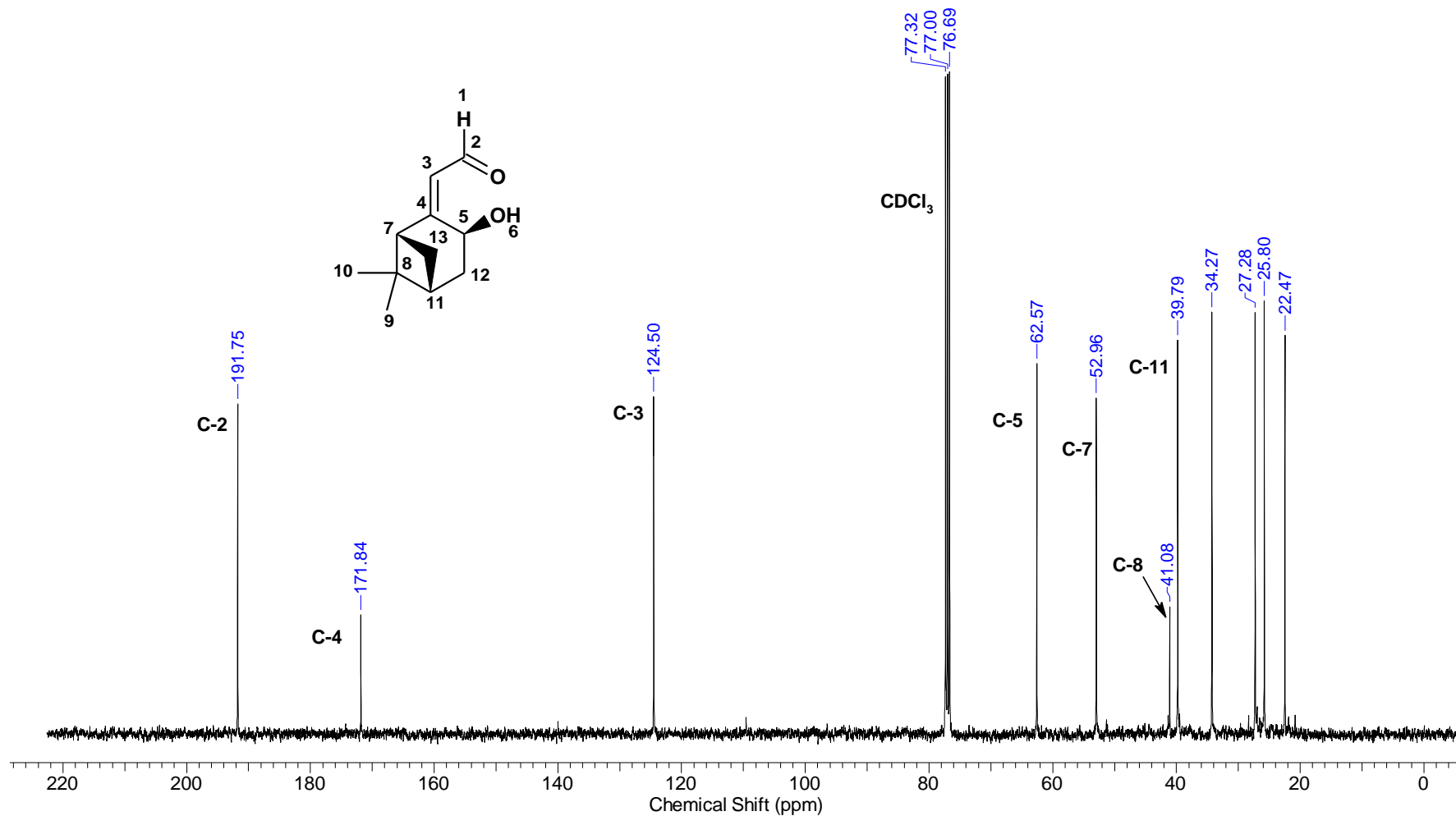
Frequency (MHz)	100.61	Nucleus	13C	Number of Transients	450	Origin	spect
Original Points Count	32768	Owner	root	Points Count	32768	Pulse Sequence	deptsp135
Receiver Gain	2050.00	SW(cyclical) (Hz)	21008.40	Solvent	CDCl3	Spectrum Offset (Hz)	9556.0313
Spectrum Type	DEPT135	Sweep Width (Hz)	21007.76	Temperature (degree C)	25.199	Acquisition Time (sec)	1.5598



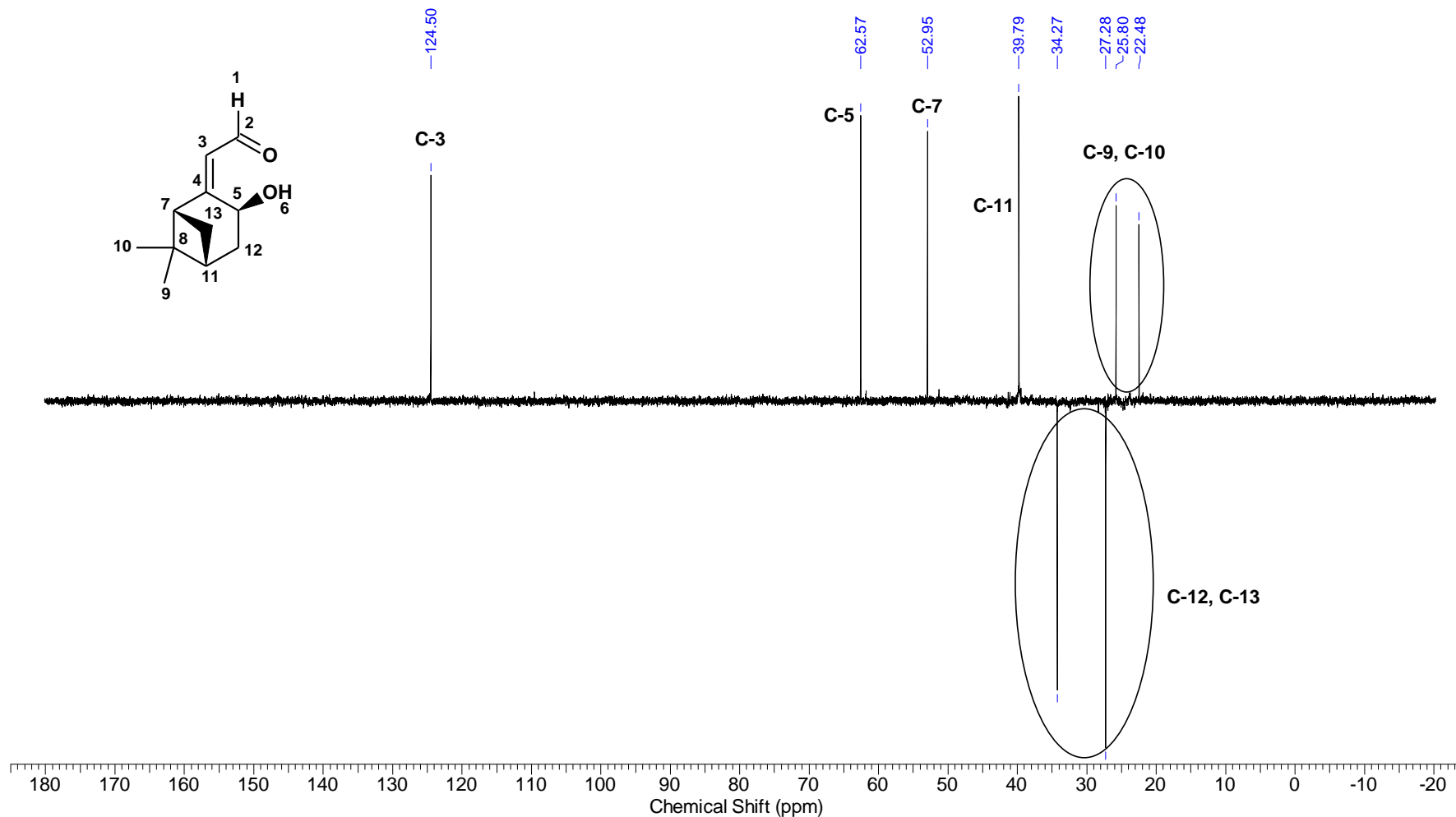
Acquisition Time (sec)	4.8060	Sweep Width (Hz)	6818.08	Temperature (degree C)	25.200	Frequency (MHz)	400.15
Nucleus	1H	Number of Transients	64	Origin	spect	Original Points Count	32768
Owner	nmsu	Points Count	65536	Pulse Sequence	zg30	Receiver Gain	64.00
SW(cyclical) (Hz)	6818.18	Solvent	CDCl3	Spectrum Offset (Hz)	2998.8201	Spectrum Type	STANDARD



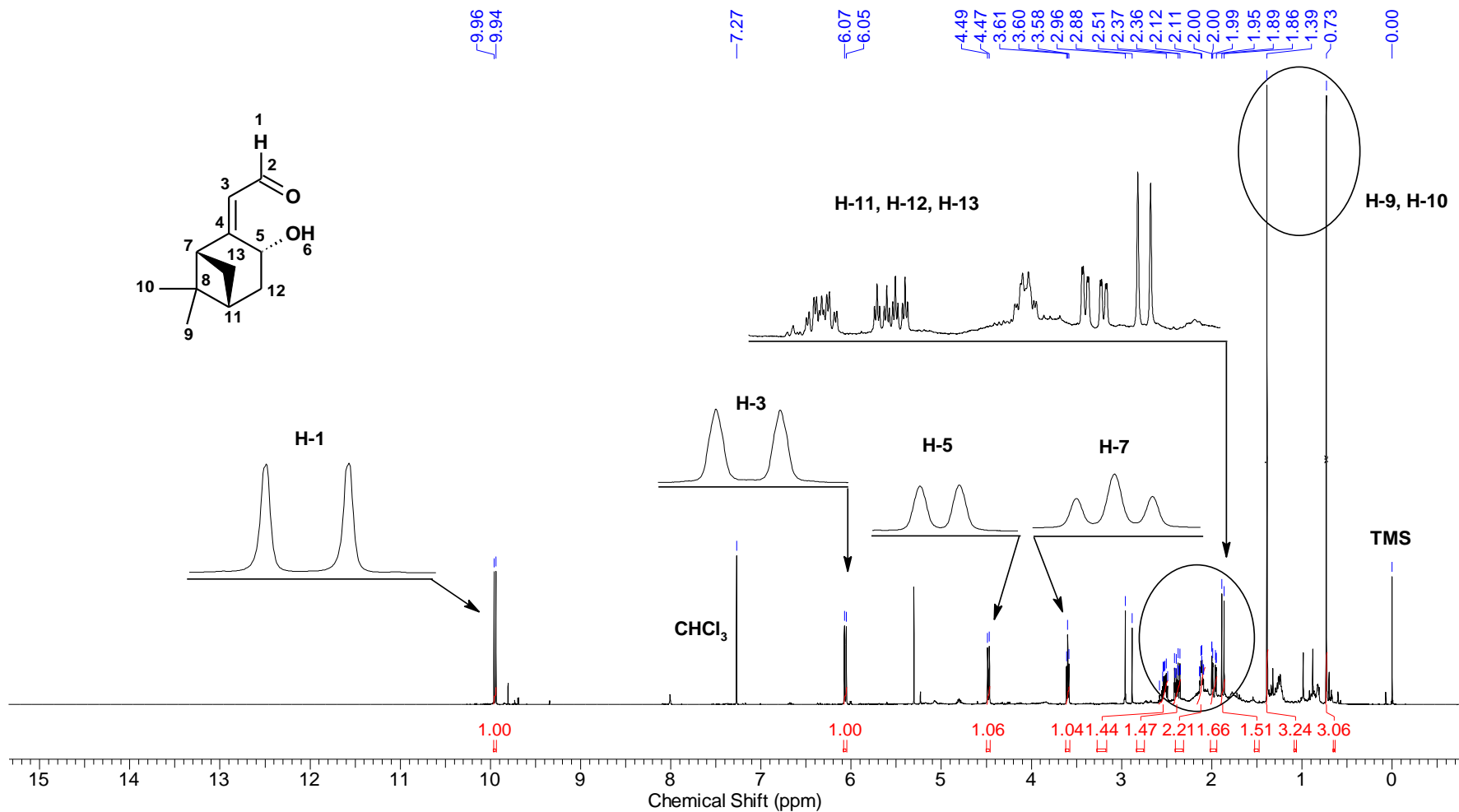
Acquisition Time (sec)	0.6641	Sweep Width (Hz)	24670.30	Temperature (degree C)	25.200	Frequency (MHz)	100.62
Nucleus	13C	Number of Transients	1024	Origin	spect	Original Points Count	16384
Owner	nmsu	Points Count	32768	Pulse Sequence	zgpg30	Receiver Gain	2050.00
SW(cyclical) (Hz)	24671.05	Solvent	CDCl3	Spectrum Offset (Hz)	10057.0938	Spectrum Type	STANDARD



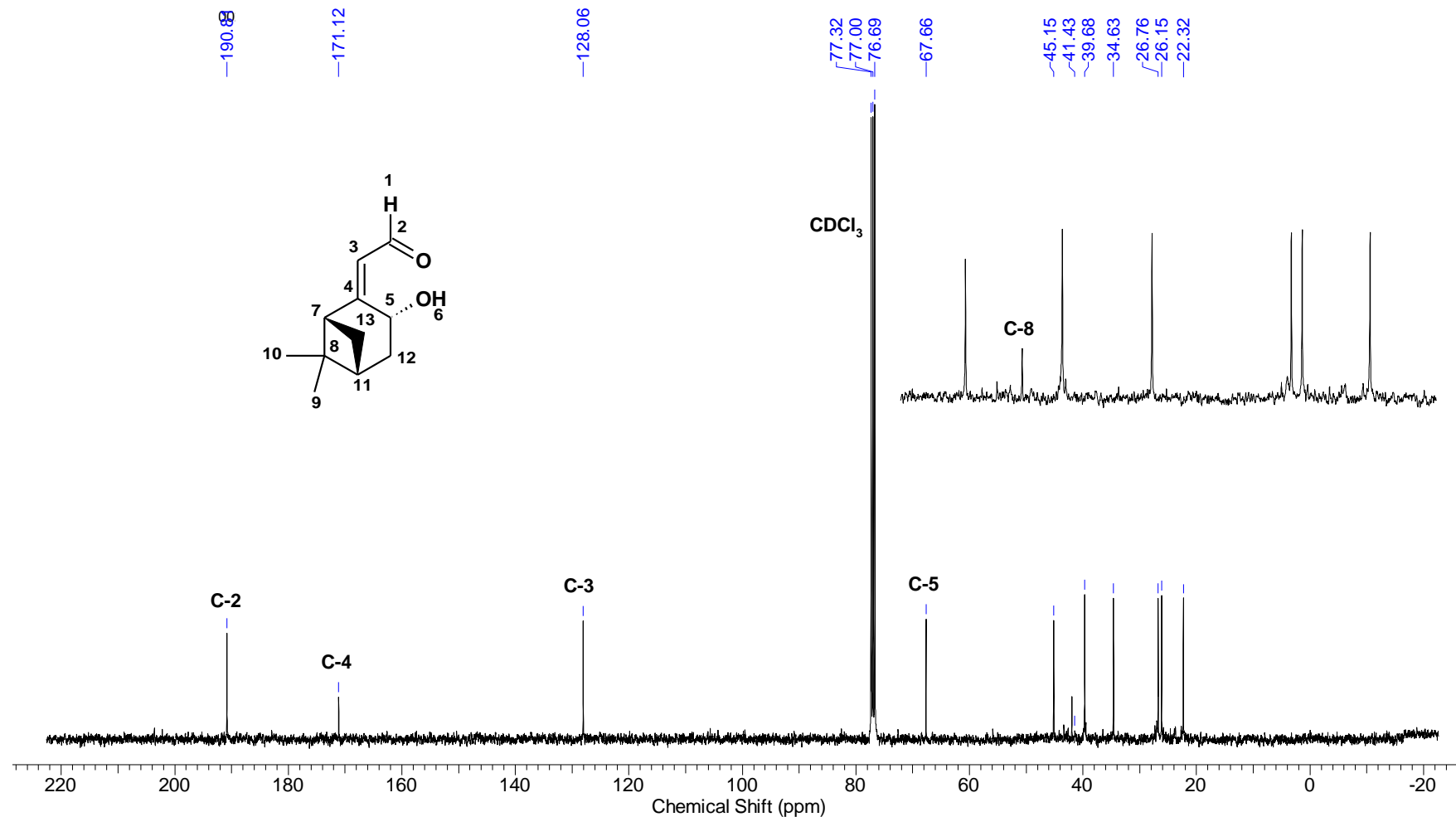
Acquisition Time (sec)	0.8126	Sweep Width (Hz)	20160.68	Temperature (degree C)	25.200	Frequency (MHz)	100.62
Nucleus	13C	Number of Transients	1024	Origin	spect	Original Points Count	16384
Owner	nmrsu	Points Count	32768	Pulse Sequence	deptsp135	Receiver Gain	2050.00
SW(cyclical) (Hz)	20161.29	Solvent	CDCl3	Spectrum Offset (Hz)	8044.3389	Spectrum Type	DEPT135



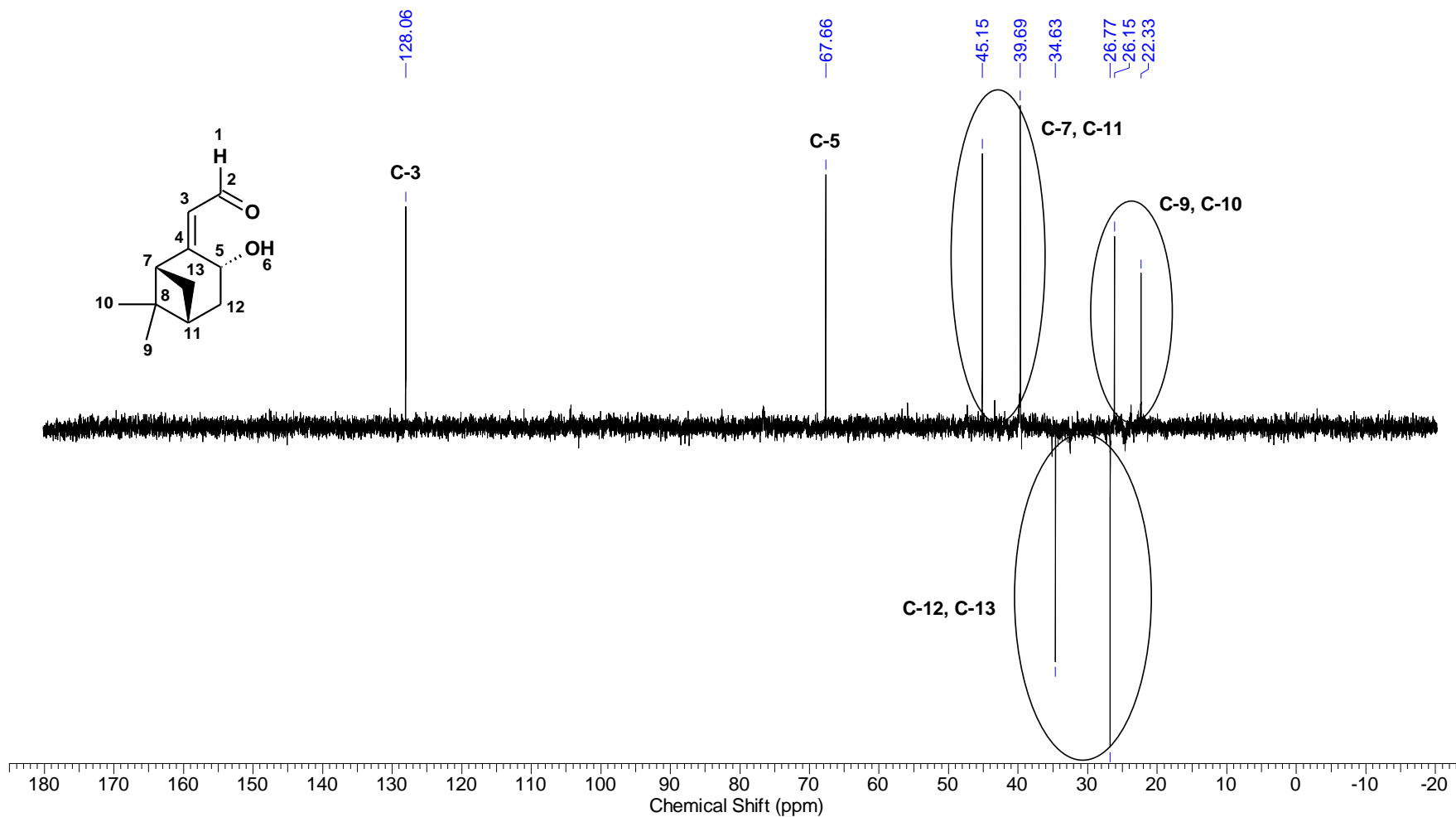
Nucleus	1H	Number of Transients	64	Origin	spect	Original Points Count	32768
Owner	nmrsu	Points Count	65536	Pulse Sequence	zg30	Receiver Gain	114.00
SW(cyclical) (Hz)	6818.18	Solvent	CDCl3	Spectrum Offset (Hz)	2995.6990	Spectrum Type	STANDARD



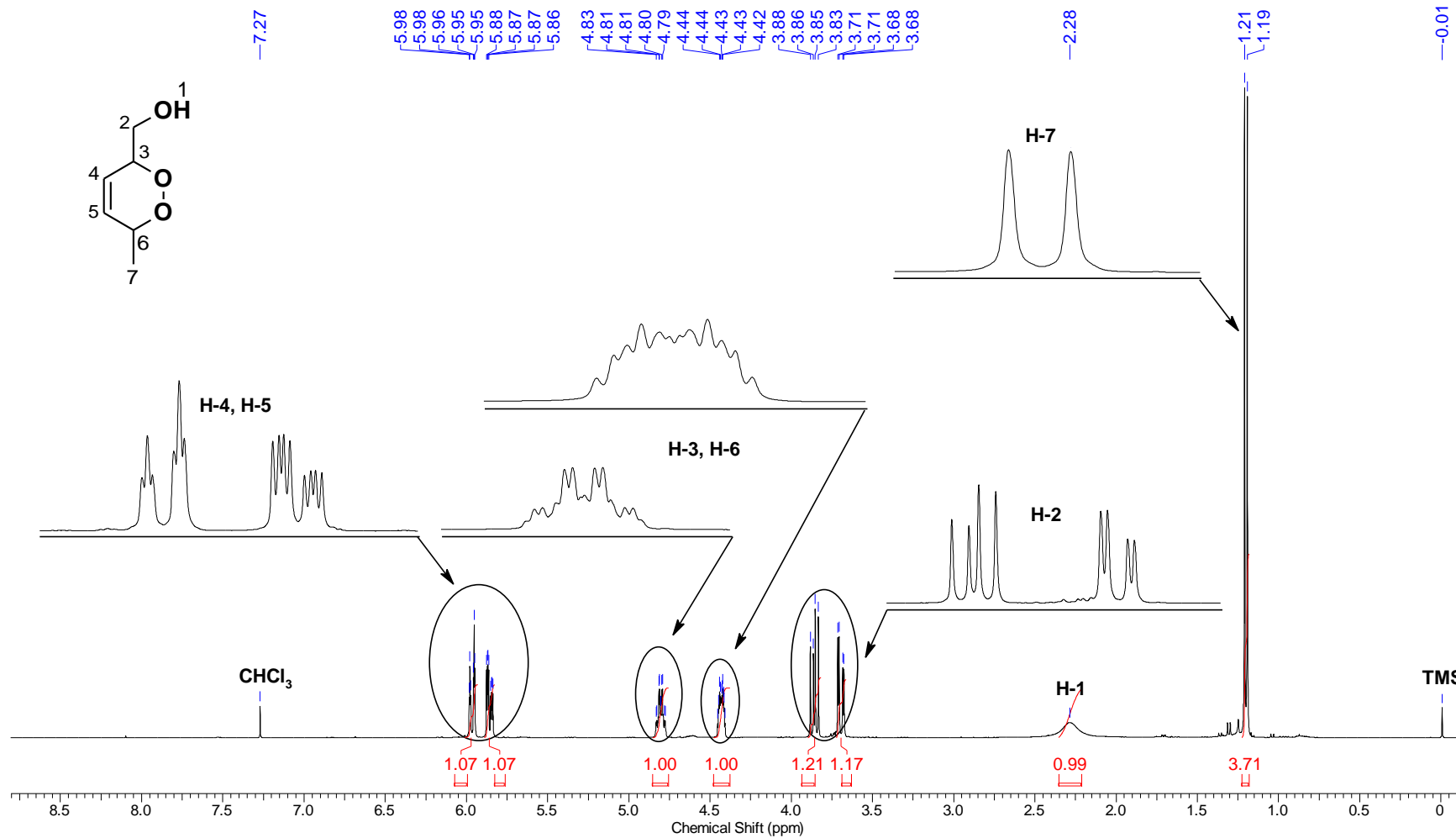
Acquisition Time (sec)	0.6641	Sweep Width (Hz)	24670.30	Temperature (degree C)	25.200	Frequency (MHz)	100.62
Nucleus	13C	Number of Transients	1024	Origin	spect	Original Points Count	16384
Owner	nmsu	Points Count	32768	Pulse Sequence	zgpg30	Receiver Gain	2050.00
SW(cyclical) (Hz)	24671.05	Solvent	CDCl3	Spectrum Offset (Hz)	10058.5996	Spectrum Type	STANDARD



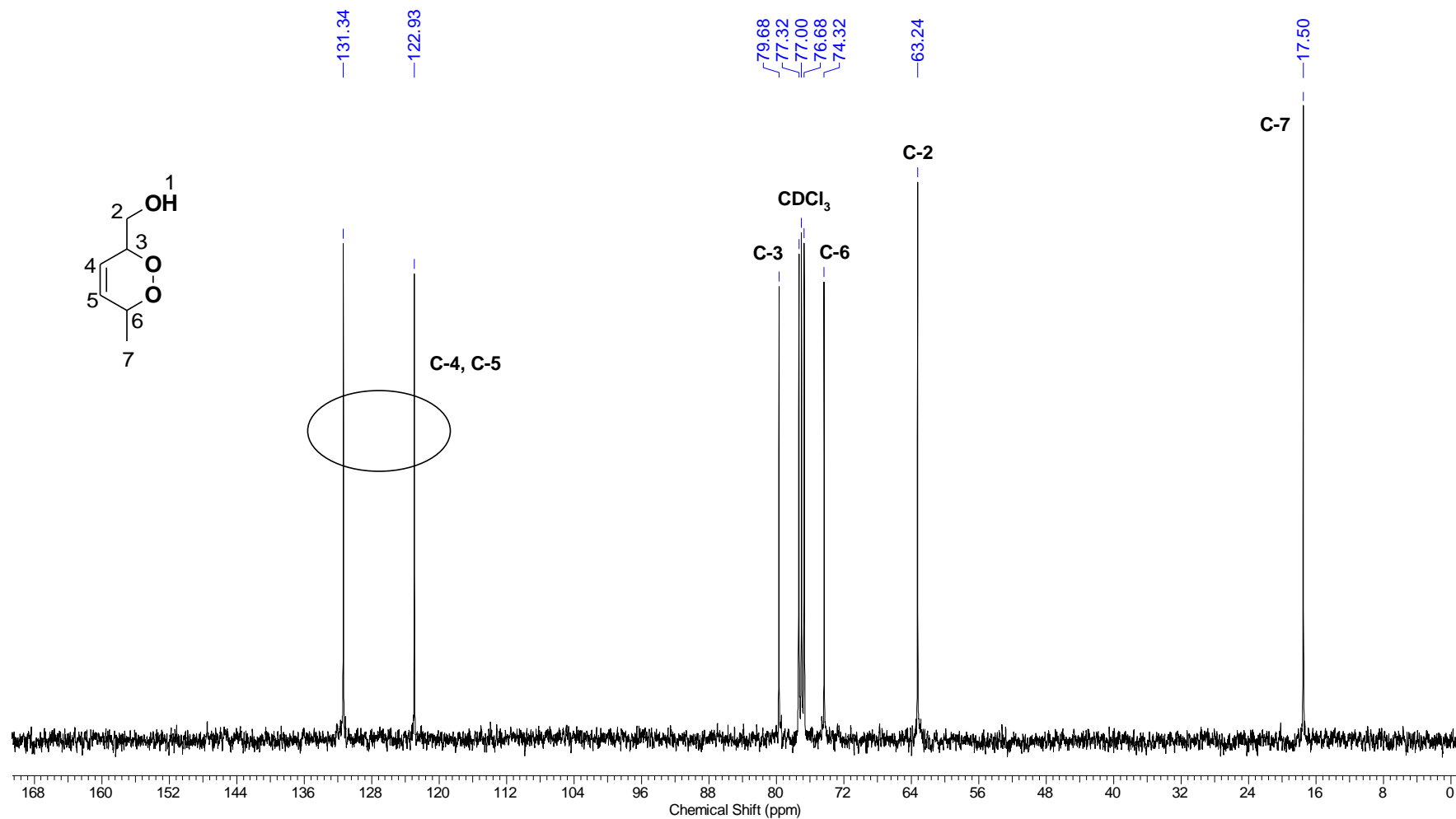
Acquisition Time (sec)	0.8126	Sweep Width (Hz)	20160.68	Temperature (degree C)	25.200	Frequency (MHz)	100.62
Nucleus	13C	Number of Transients	1024	Origin	spect	Original Points Count	16384
Owner	nmsu	Points Count	32768	Pulse Sequence	depts135	Receiver Gain	2050.00
SW(cyclical) (Hz)	20161.29	Solvent	CDCl3	Spectrum Offset (Hz)	8046.2949	Spectrum Type	DEPT135



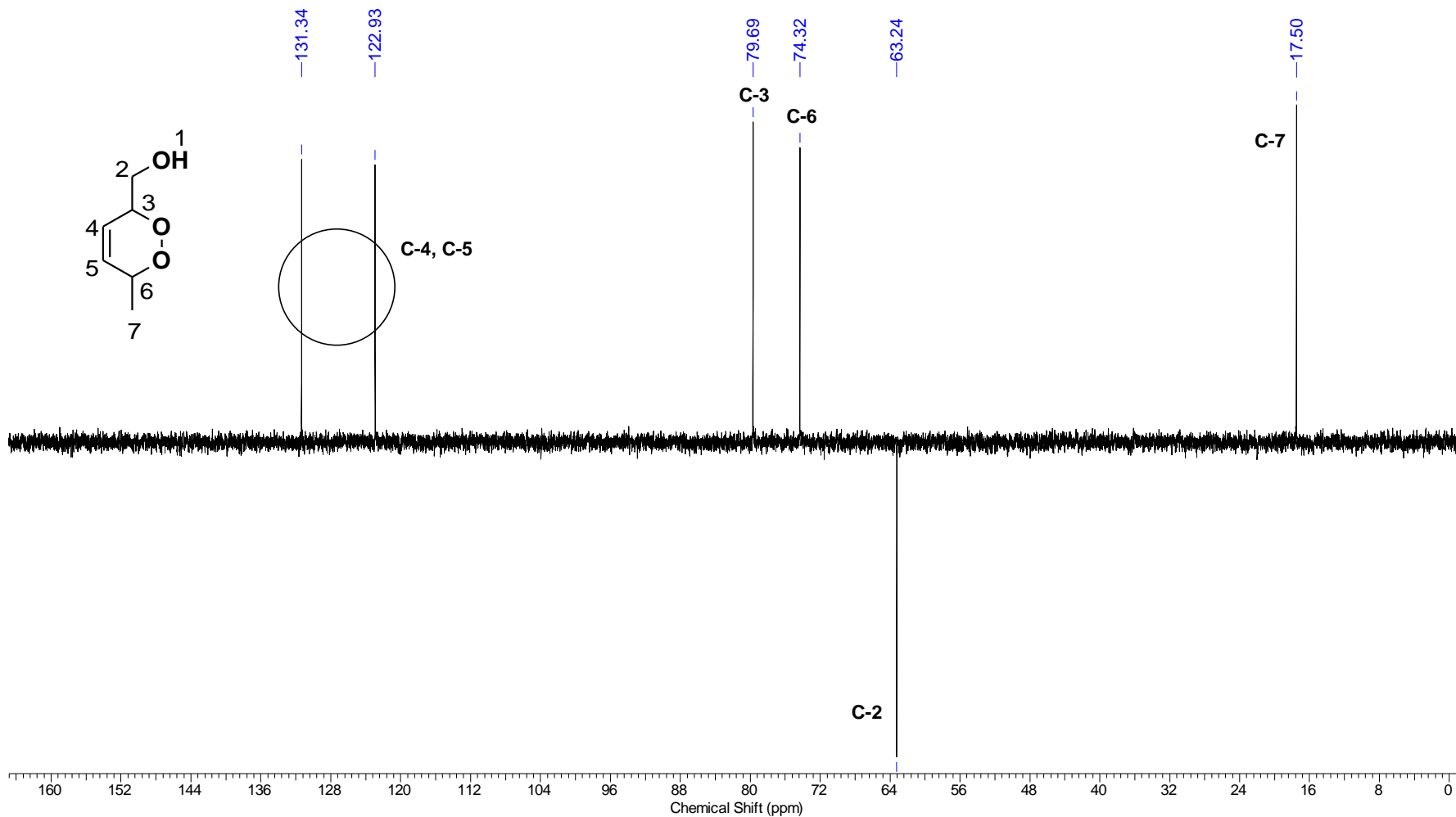
Frequency (MHz)	400.13	Nucleus	1H	Number of Transients	16	Origin	spect
Original Points Count	32768	Owner	root	Points Count	65536	Pulse Sequence	zg
Receiver Gain	28.50	SW(cyclical) (Hz)	4618.23	Solvent	CDCl3	Spectrum Offset (Hz)	2105.2163
Spectrum Type	STANDARD	Sweep Width (Hz)	4618.16	Temperature (degree C)	25.198	Acquisition Time (sec)	7.0954



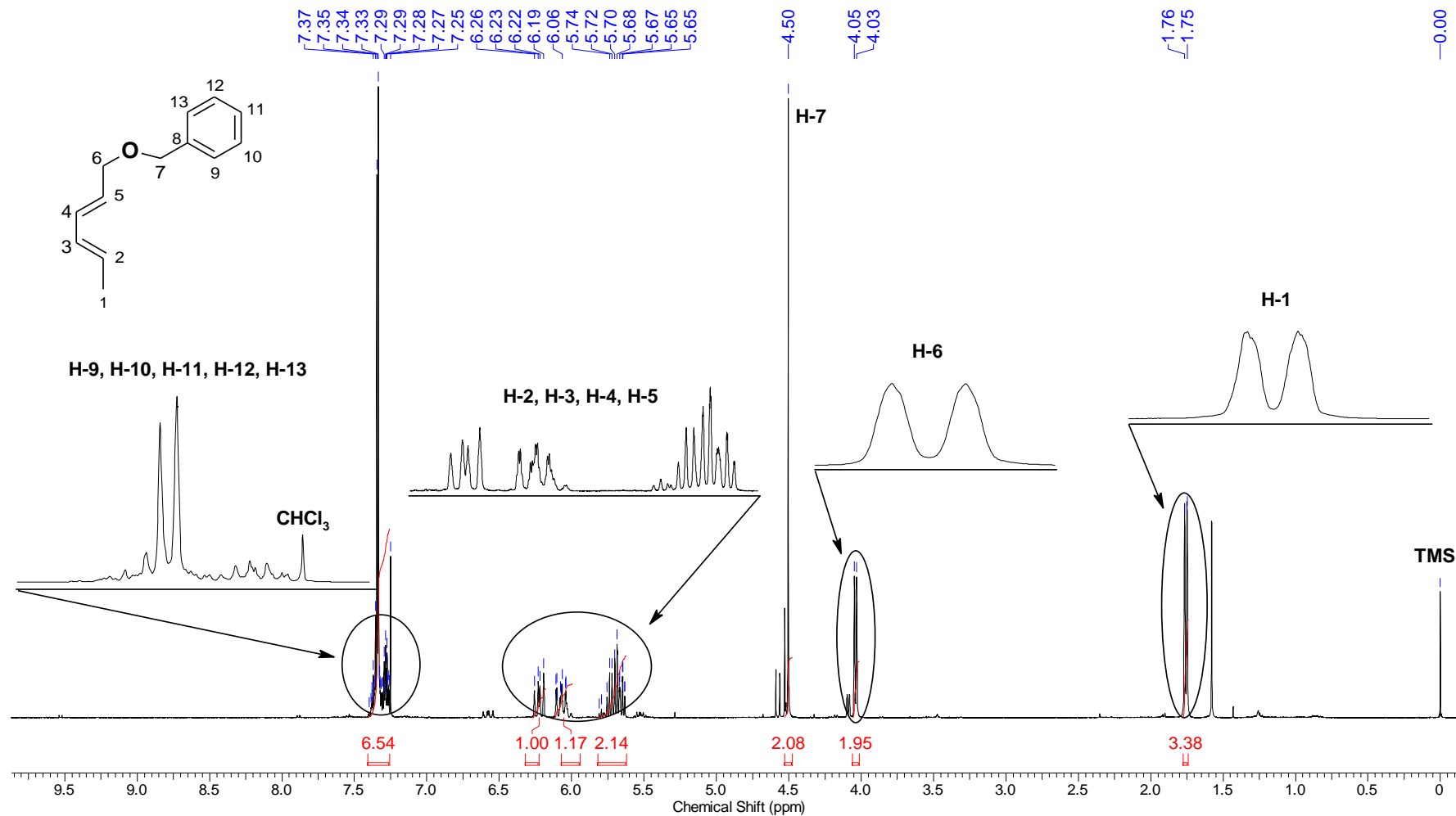
Frequency (MHz)	100.61	Nucleus	13C	Number of Transients	1024	Origin	spect
Original Points Count	16384	Owner	root	Points Count	32768	Pulse Sequence	zgpg30
Receiver Gain	2050.00	SW(cyclical) (Hz)	24038.46	Solvent	CDCl3	Spectrum Offset (Hz)	10056.1758
Spectrum Type	STANDARD	Sweep Width (Hz)	24037.73	Temperature (degree C)	25.201	Acquisition Time (sec)	0.6816



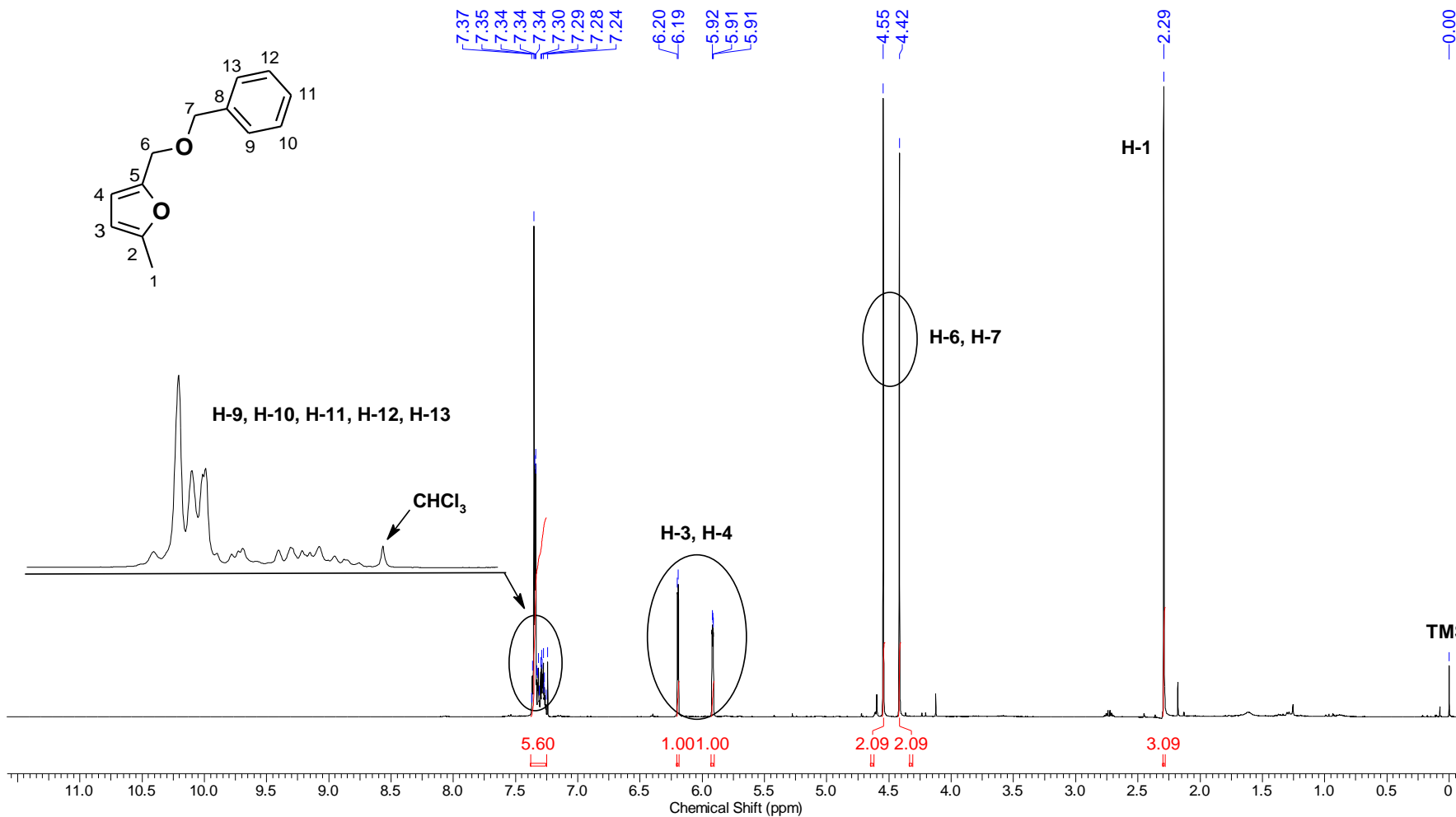
Frequency (MHz)	100.61	Nucleus	13C	Number of Transients	256	Origin	spect
Original Points Count	32768	Owner	root	Points Count	32768	Pulse Sequence	deptsp135
Receiver Gain	2050.00	SW(cyclical) (Hz)	21008.40	Solvent	CDCl3	Spectrum Offset (Hz)	9553.2852
Spectrum Type	DEPT135	Sweep Width (Hz)	21007.76	Temperature (degree C)	25.201	Acquisition Time (sec)	1.5598



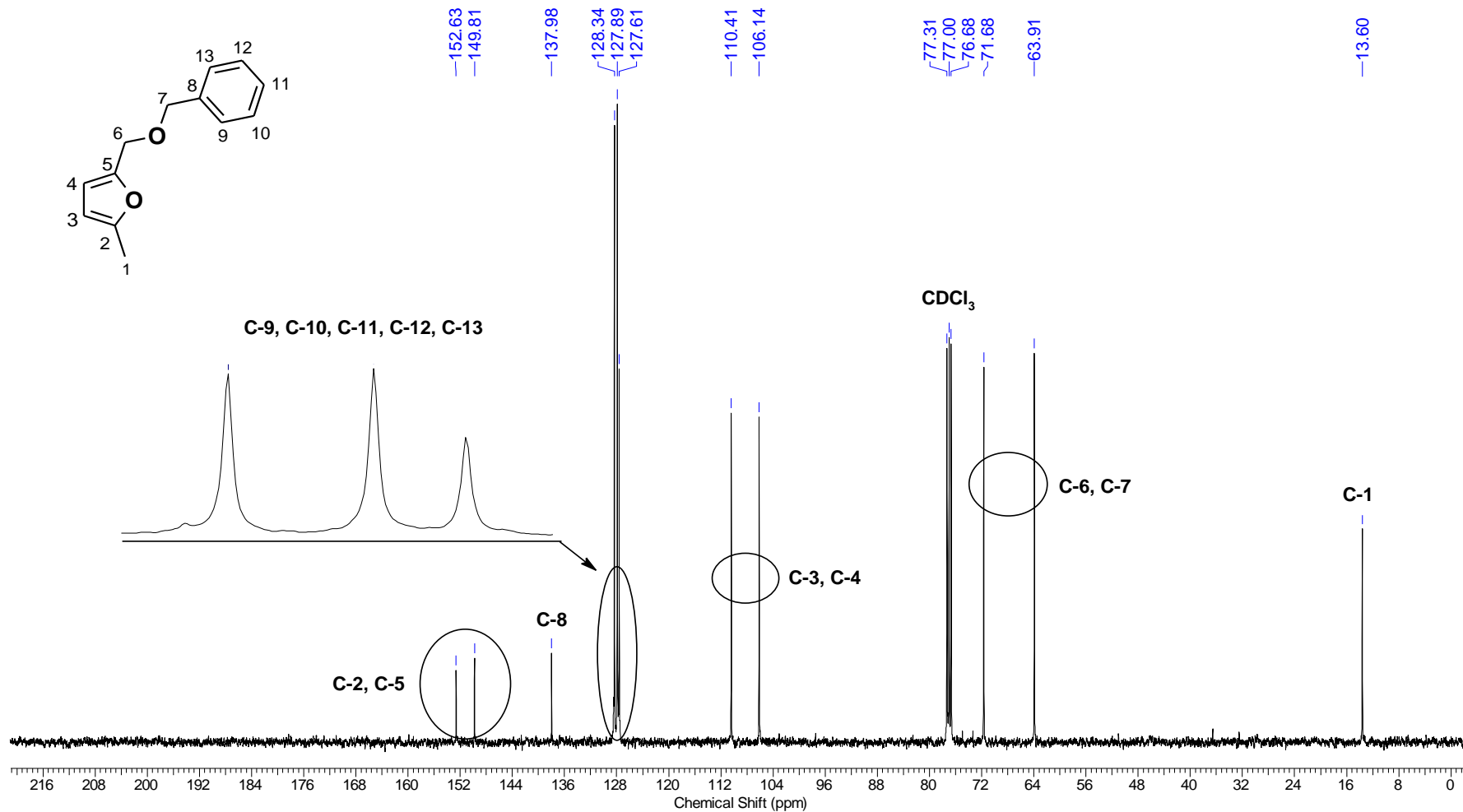
Nucleus	1H	Number of Transients	16	Origin	spect	Original Points Count	32768
Owner	nmsu	Points Count	65536	Pulse Sequence	zg30	Receiver Gain	114.00
SW(cyclical) (Hz)	6818.18	Solvent	CDCl3	Spectrum Offset (Hz)	2987.6882	Spectrum Type	STANDARD
Sweep Width (Hz)	6818.08	Temperature (degree C)	25.200	Acquisition Time (sec)	4.8060	Frequency (MHz)	400.15



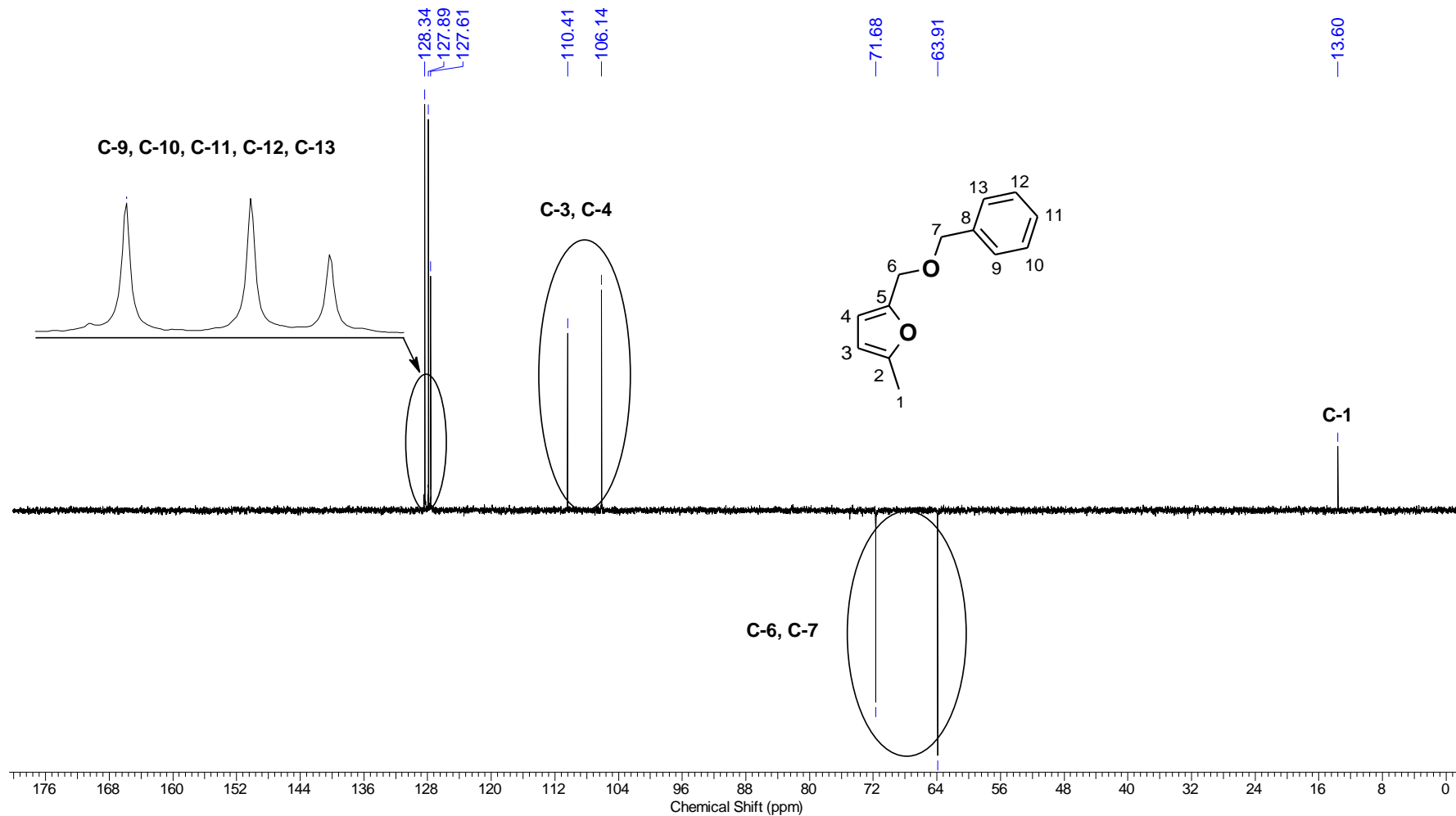
Nucleus	1H	Number of Transients	64	Origin	spect	Original Points Count	32768
Owner	nmrsu	Points Count	65536	Pulse Sequence	zg30	Receiver Gain	40.30
SW(cyclical) (Hz)	8802.82	Solvent	CDCI3	Spectrum Offset (Hz)	3384.4021	Spectrum Type	STANDARD
Sweep Width (Hz)	8802.68	Temperature (degree C)	24.100	Acquisition Time (sec)	3.7224	Frequency (MHz)	400.15



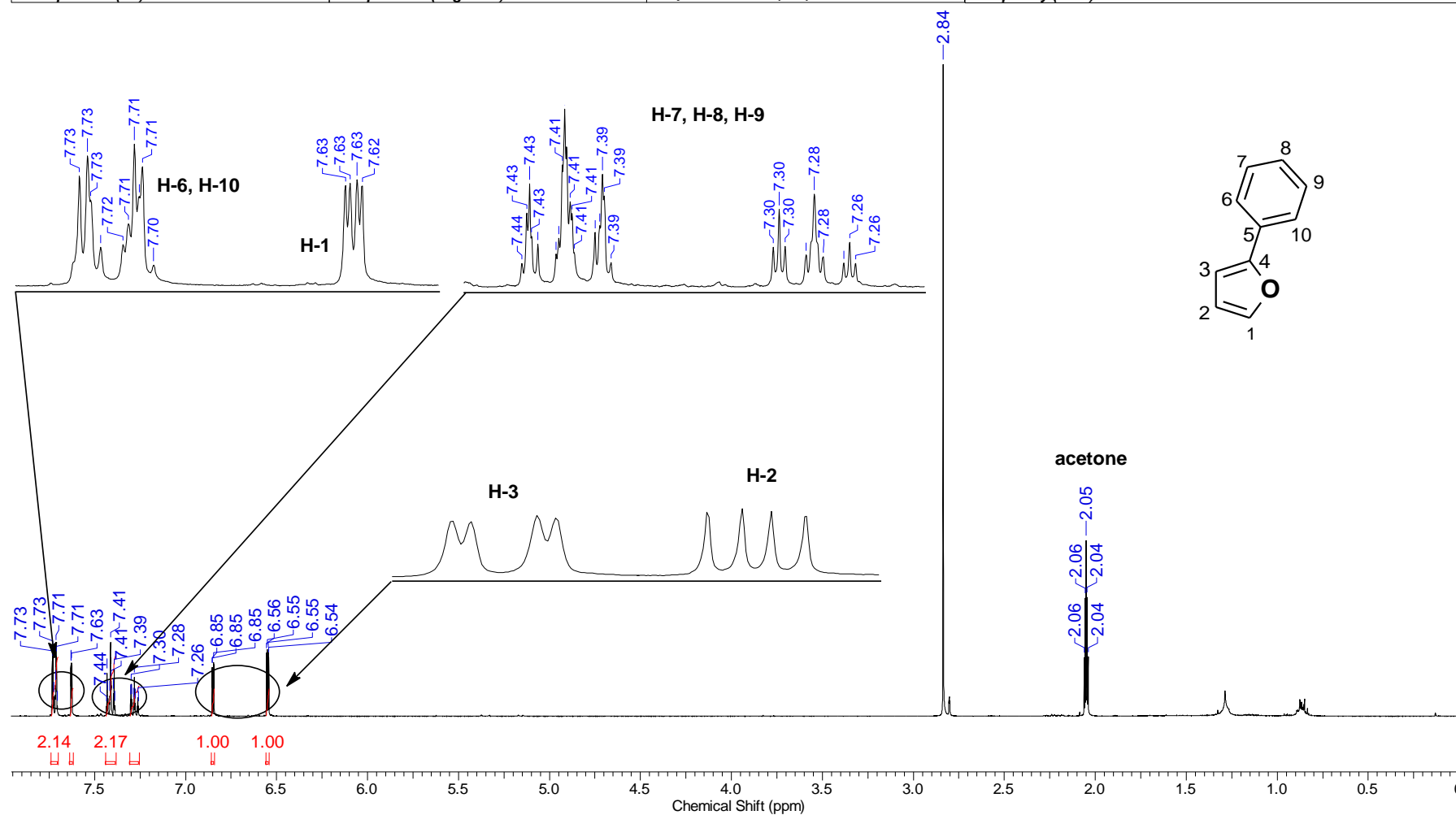
Nucleus	13C	Number of Transients	1024	Origin	spect	Original Points Count	16384
Owner	nmsu	Points Count	32768	Pulse Sequence	zgpg30	Receiver Gain	2050.00
SW(cyclical) (Hz)	24671.05	Solvent	CDCI3	Spectrum Offset (Hz)	10054.8350	Spectrum Type	STANDARD
Sweep Width (Hz)	24670.30	Temperature (degree C)	24.700	Acquisition Time (sec)	0.6641	Frequency (MHz)	100.62



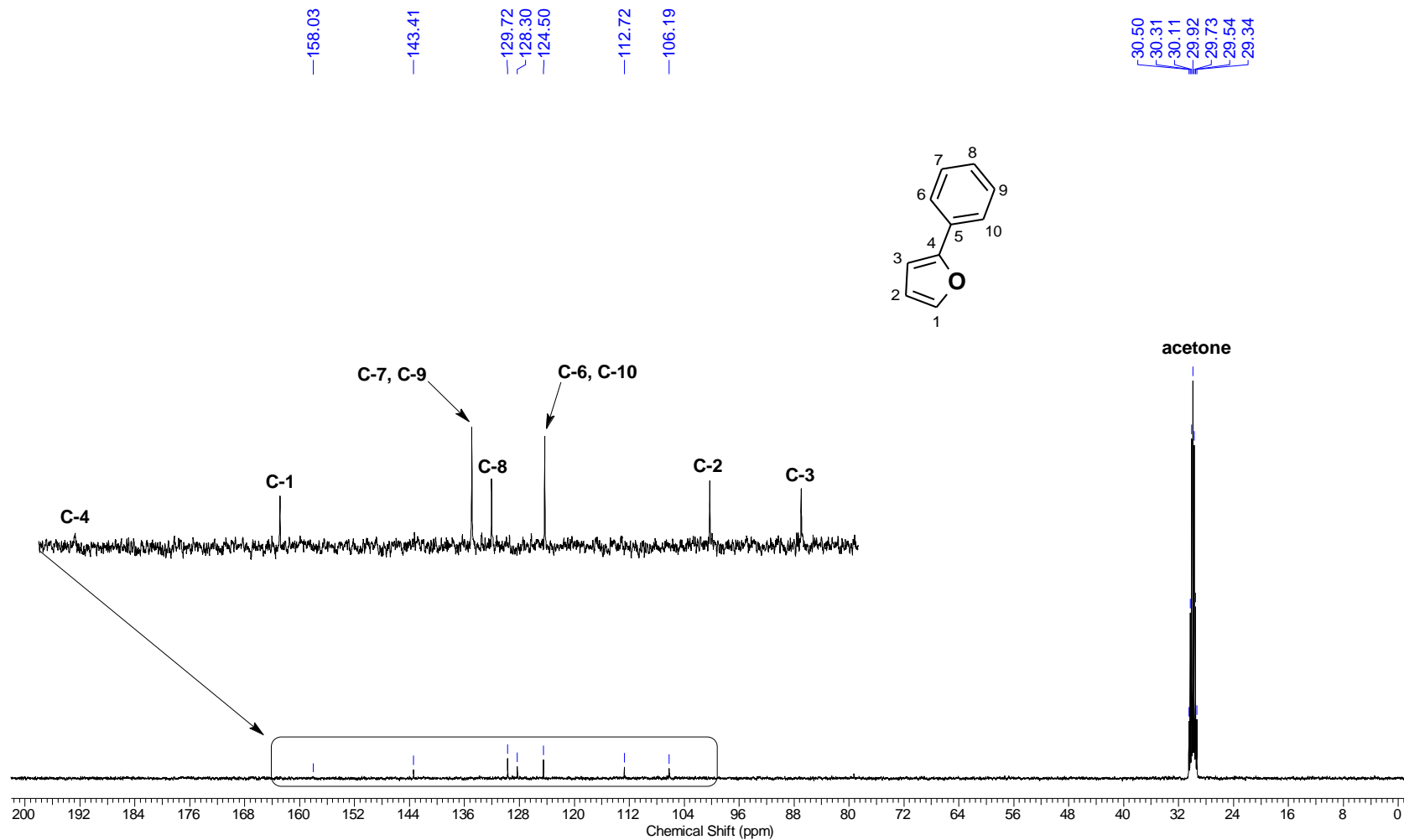
Nucleus	13C	Number of Transients	1024	Origin	spect	Original Points Count	16384
Owner	nmsu	Points Count	32768	Pulse Sequence	deptsp135	Receiver Gain	912.00
SW(cyclical) (Hz)	20161.29	Solvent	CDCl3	Spectrum Offset (Hz)	8041.9692	Spectrum Type	DEPT135
Sweep Width (Hz)	20160.68	Temperature (degree C)	24.700	Acquisition Time (sec)	0.8126	Frequency (MHz)	100.62



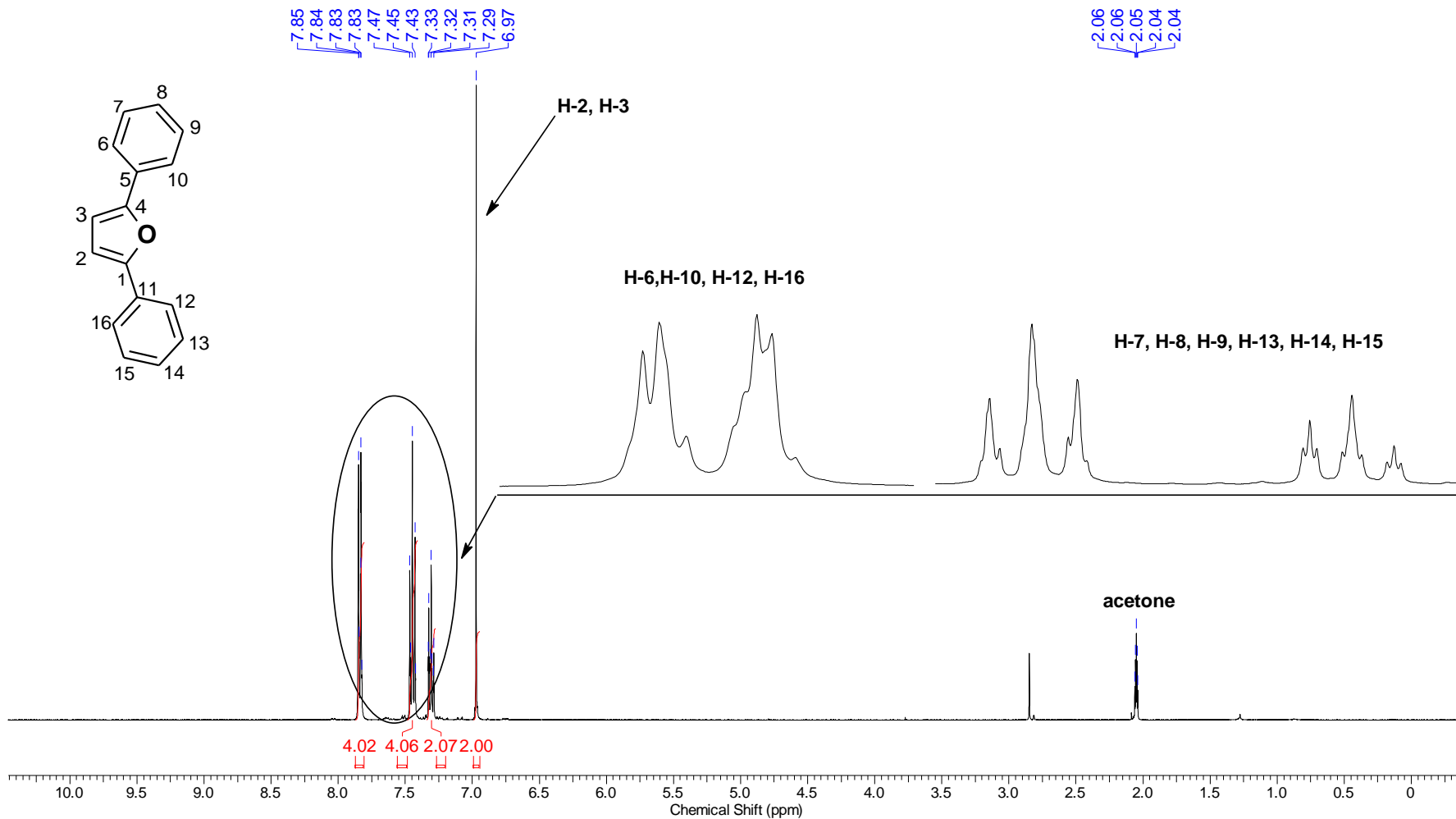
Nucleus	1H	Number of Transients	64	Origin	spect	Original Points Count	32768
Owner	nmsu	Points Count	65536	Pulse Sequence	zg30	Receiver Gain	114.00
SW(cyclical) (Hz)	6818.18	Solvent	Acetone	Spectrum Offset (Hz)	2994.8411	Spectrum Type	STANDARD
Sweep Width (Hz)	6818.08	Temperature (degree C)	23.000	Acquisition Time (sec)	4.8060	Frequency (MHz)	400.15



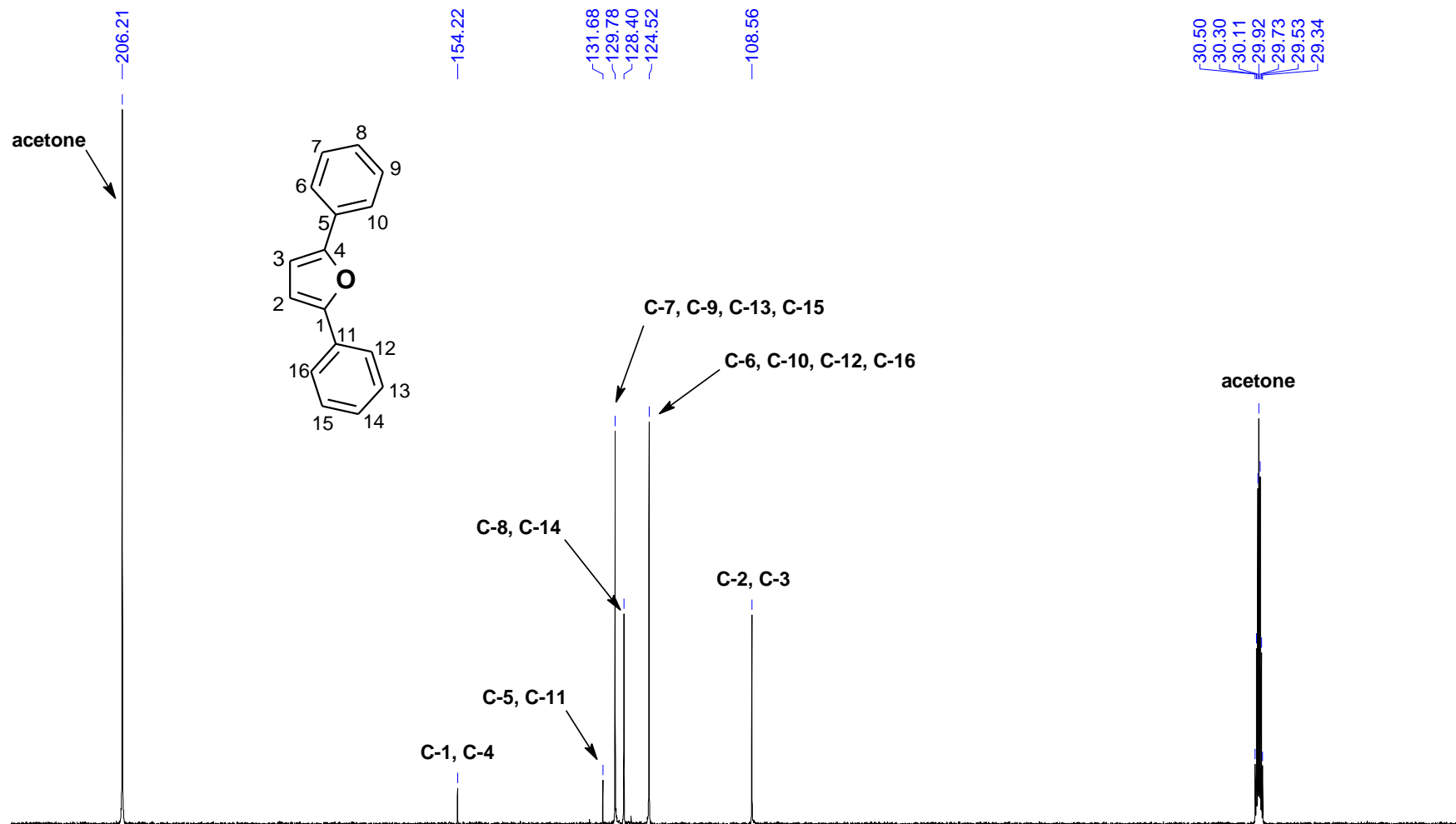
Nucleus	13C	Number of Transients	1024	Origin	spect	Original Points Count	16384
Owner	nmsu	Points Count	32768	Pulse Sequence	zgpg30	Receiver Gain	2050.00
SW(cyclical) (Hz)	24671.05	Solvent	Acetone	Spectrum Offset (Hz)	10159.6514	Spectrum Type	STANDARD
Sweep Width (Hz)	24670.30	Temperature (degree C)	23.800	Acquisition Time (sec)	0.6641	Frequency (MHz)	100.62



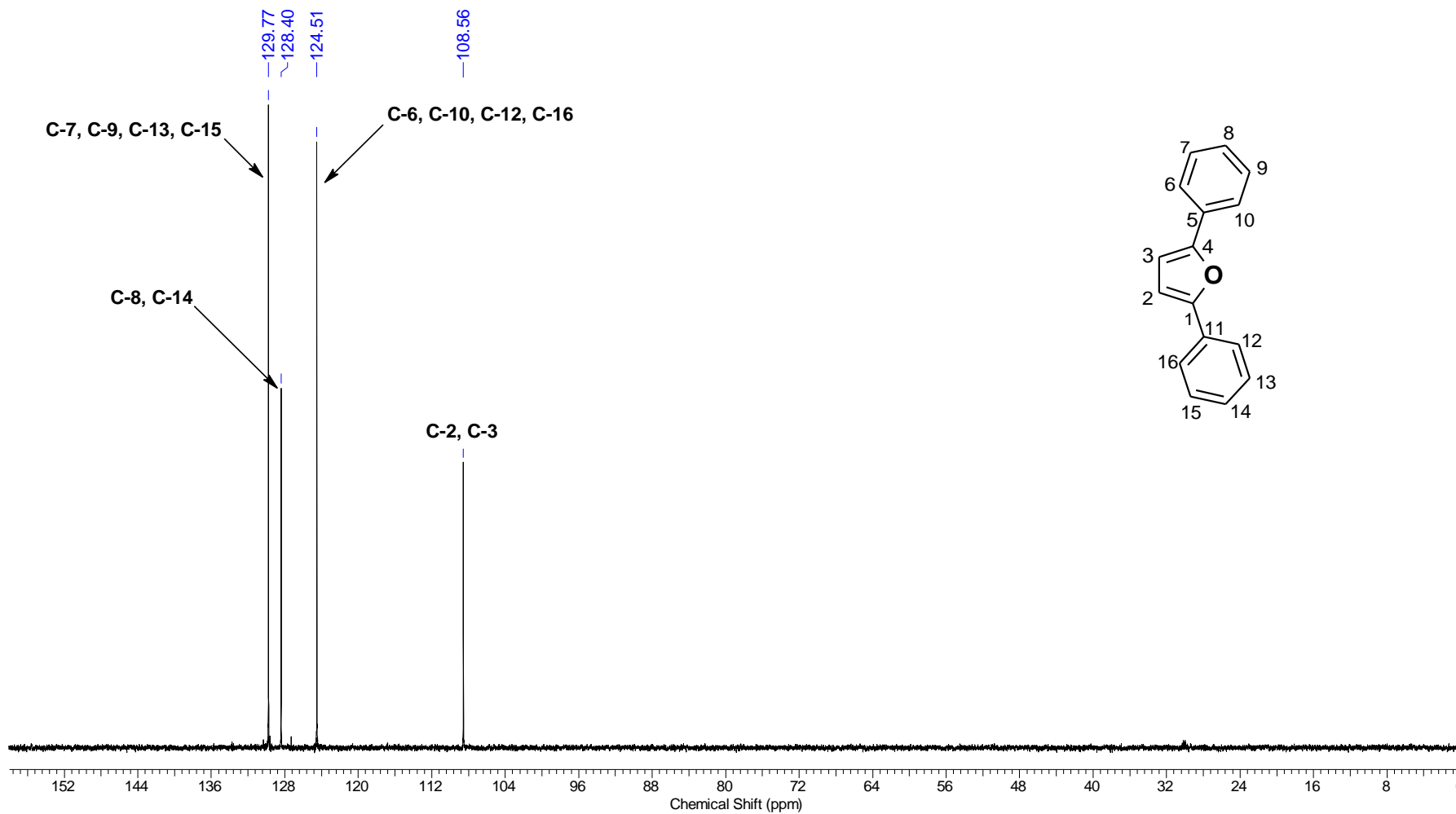
Nucleus	1H	Number of Transients	16	Origin	spect	Original Points Count	32768
Owner	nmsu	Points Count	65536	Pulse Sequence	zg30	Receiver Gain	114.00
SW(cyclical) (Hz)	6818.18	Solvent	Acetone	Spectrum Offset (Hz)	2994.7368	Spectrum Type	STANDARD
Sweep Width (Hz)	6818.08	Temperature (degree C)	23.500	Acquisition Time (sec)	4.8060	Frequency (MHz)	400.15



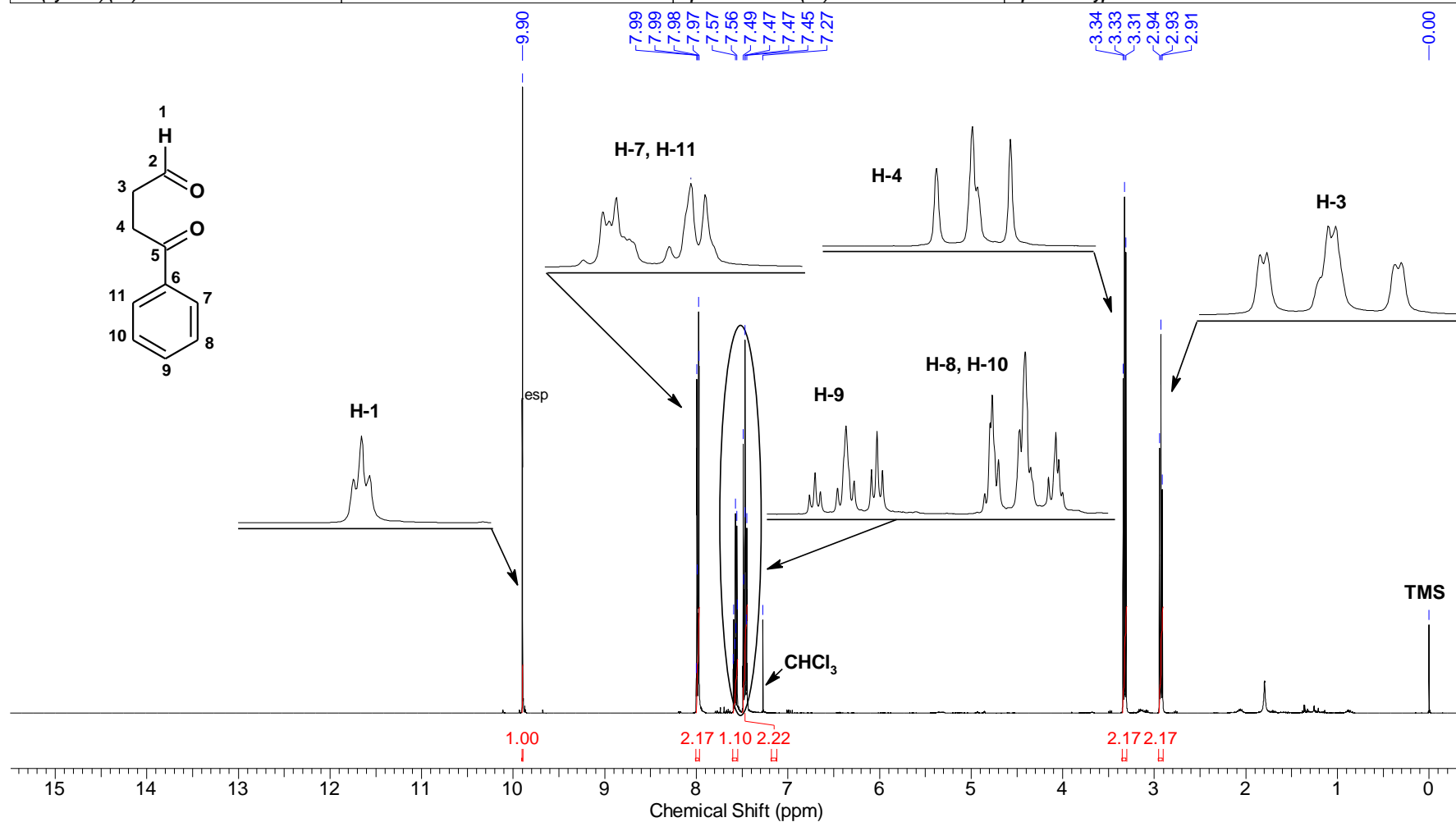
Acquisition Time (sec)	0.6641	Temperature (degree C)	24.300	Frequency (MHz)	100.62	Nucleus	13C
Number of Transients	1024	Origin	spect	Original Points Count	16384	Owner	nmrsu
Points Count	32768	Pulse Sequence	zgpg30	Receiver Gain	2050.00	SW(cyclical) (Hz)	24671.05
Solvent	Acetone	Spectrum Offset (Hz)	10157.3926	Spectrum Type	STANDARD	Sweep Width (Hz)	24670.30



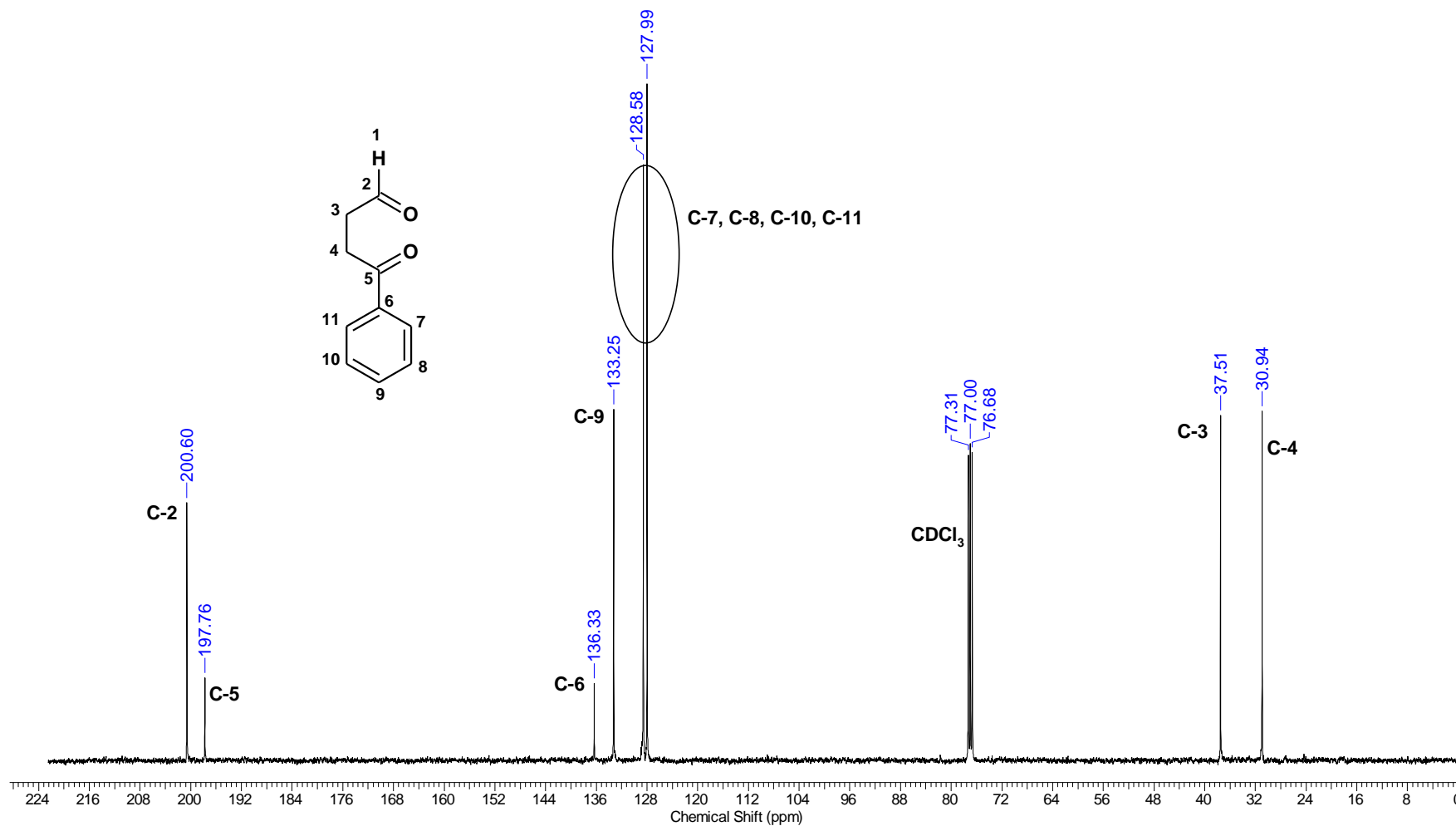
Acquisition Time (sec)	0.8126	Temperature (degree C)	24.200	Frequency (MHz)	100.62	Nucleus	¹³ C
Number of Transients	1024	Origin	spect	Original Points Count	16384	Owner	nmrsu
Points Count	32768	Pulse Sequence	deptsq135	Receiver Gain	912.00	SW(cyclical) (Hz)	20161.29
Solvent	Acetone	Spectrum Offset (Hz)	8144.1743	Spectrum Type	DEPT135	Sweep Width (Hz)	20160.68



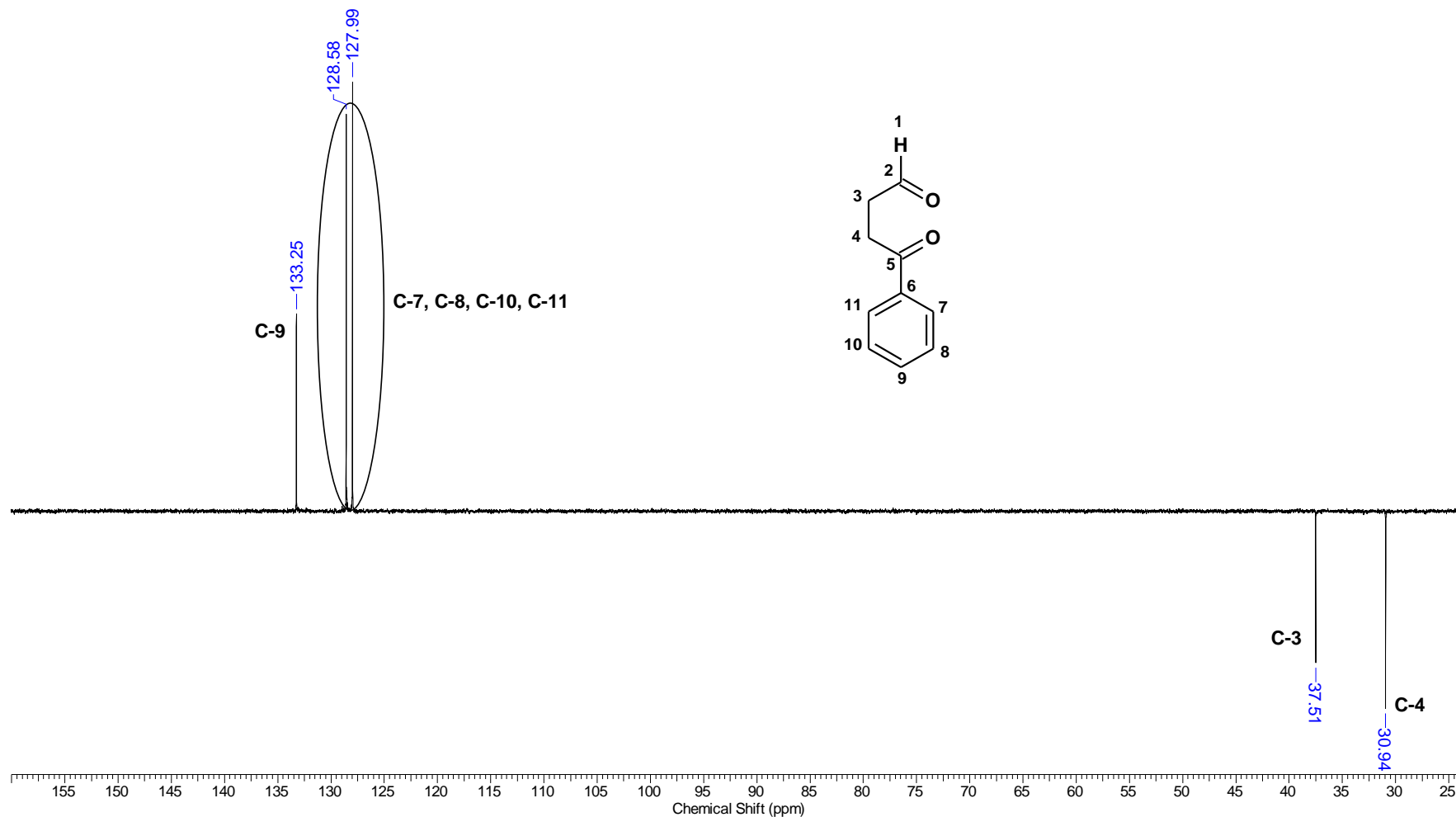
Acquisition Time (sec)	4.8060	Sweep Width (Hz)	6818.08	Temperature (degree C)	25.200	Frequency (MHz)	400.15
Nucleus	1H	Number of Transients	16	Origin	spect	Original Points Count	32768
Owner	nmrsu	Points Count	65536	Pulse Sequence	zg30	Receiver Gain	64.00
SW(cyclical) (Hz)	6818.18	Solvent	CDCl3	Spectrum Offset (Hz)	2996.7395	Spectrum Type	STANDARD



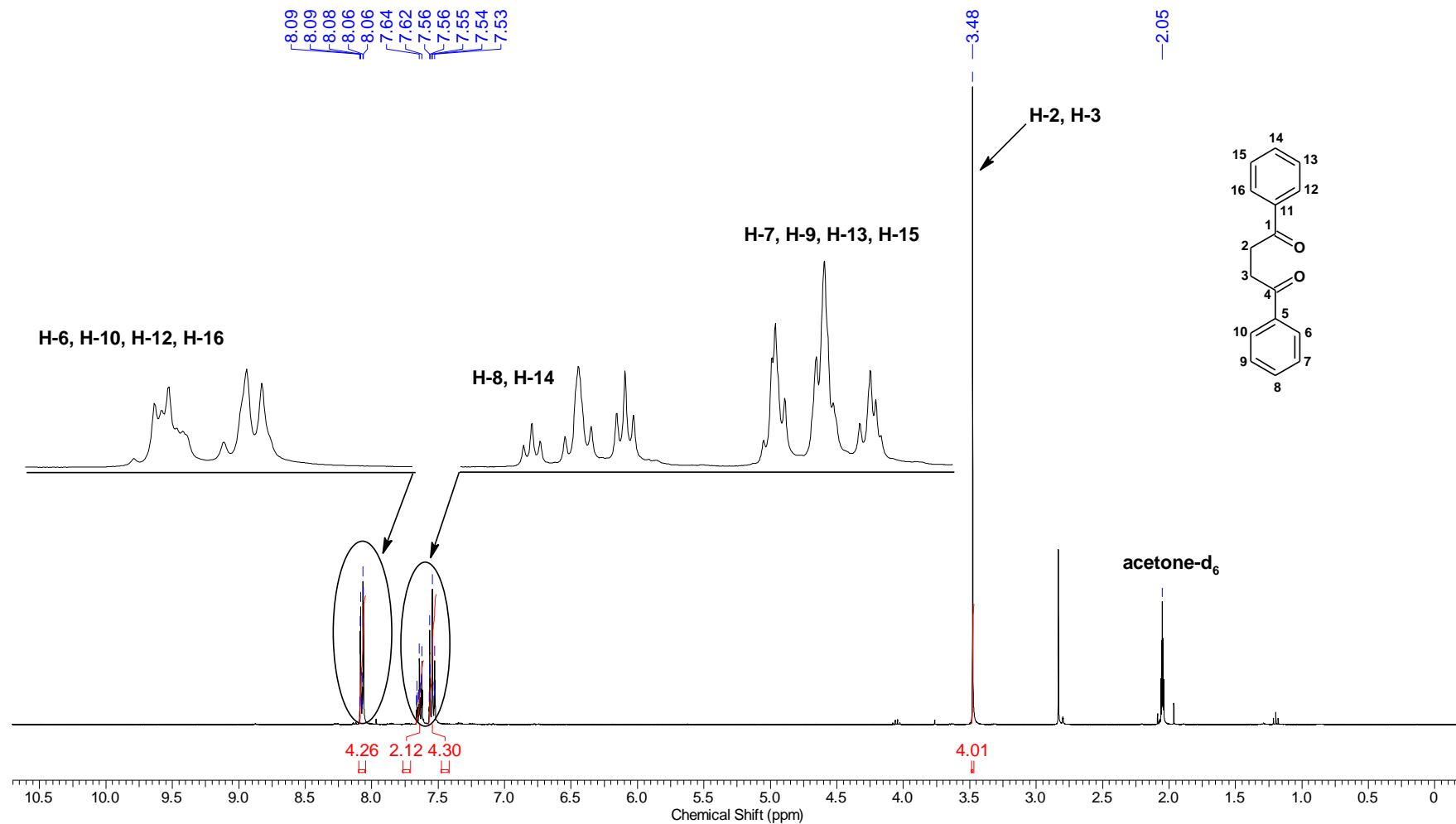
Acquisition Time (sec)	0.6641	Sweep Width (Hz)	24670.30	Temperature (degree C)	25.200	Frequency (MHz)	100.62
Nucleus	13C	Number of Transients	1024	Origin	spect	Original Points Count	16384
Owner	nmsu	Points Count	32768	Pulse Sequence	zgpg30	Receiver Gain	2050.00
SW(cyclical) (Hz)	24671.05	Solvent	CDCl3	Spectrum Offset (Hz)	10053.3291	Spectrum Type	STANDARD



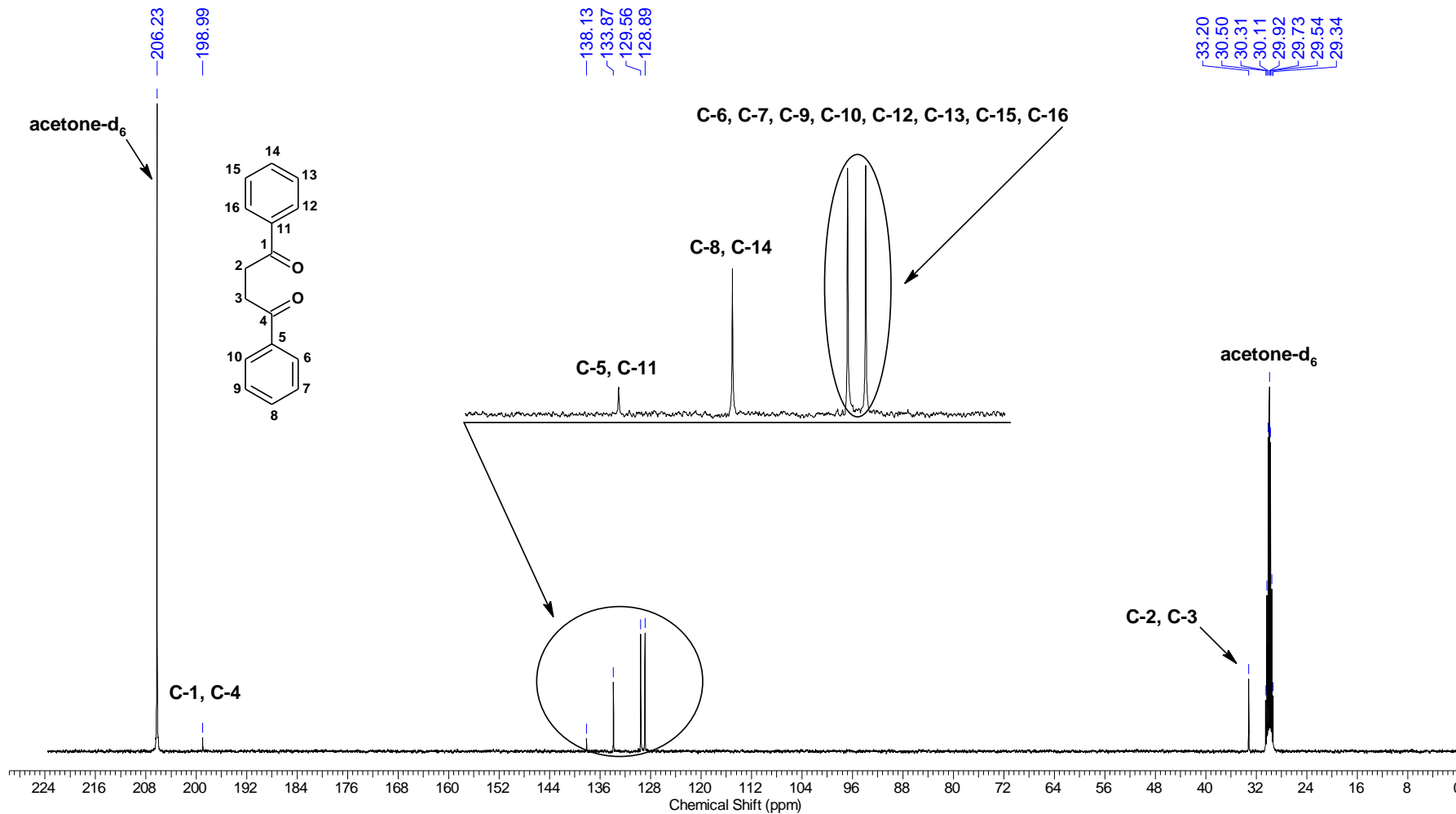
Acquisition Time (sec)	0.8126	Sweep Width (Hz)	20160.68	Temperature (degree C)	25.200	Frequency (MHz)	100.62
Nucleus	13C	Number of Transients	1024	Origin	spect	Original Points Count	16384
Owner	nmsu	Points Count	32768	Pulse Sequence	depts135	Receiver Gain	2050.00
SW(cyclical) (Hz)	20161.29	Solvent	CDCl3	Spectrum Offset (Hz)	8040.4814	Spectrum Type	DEPT135



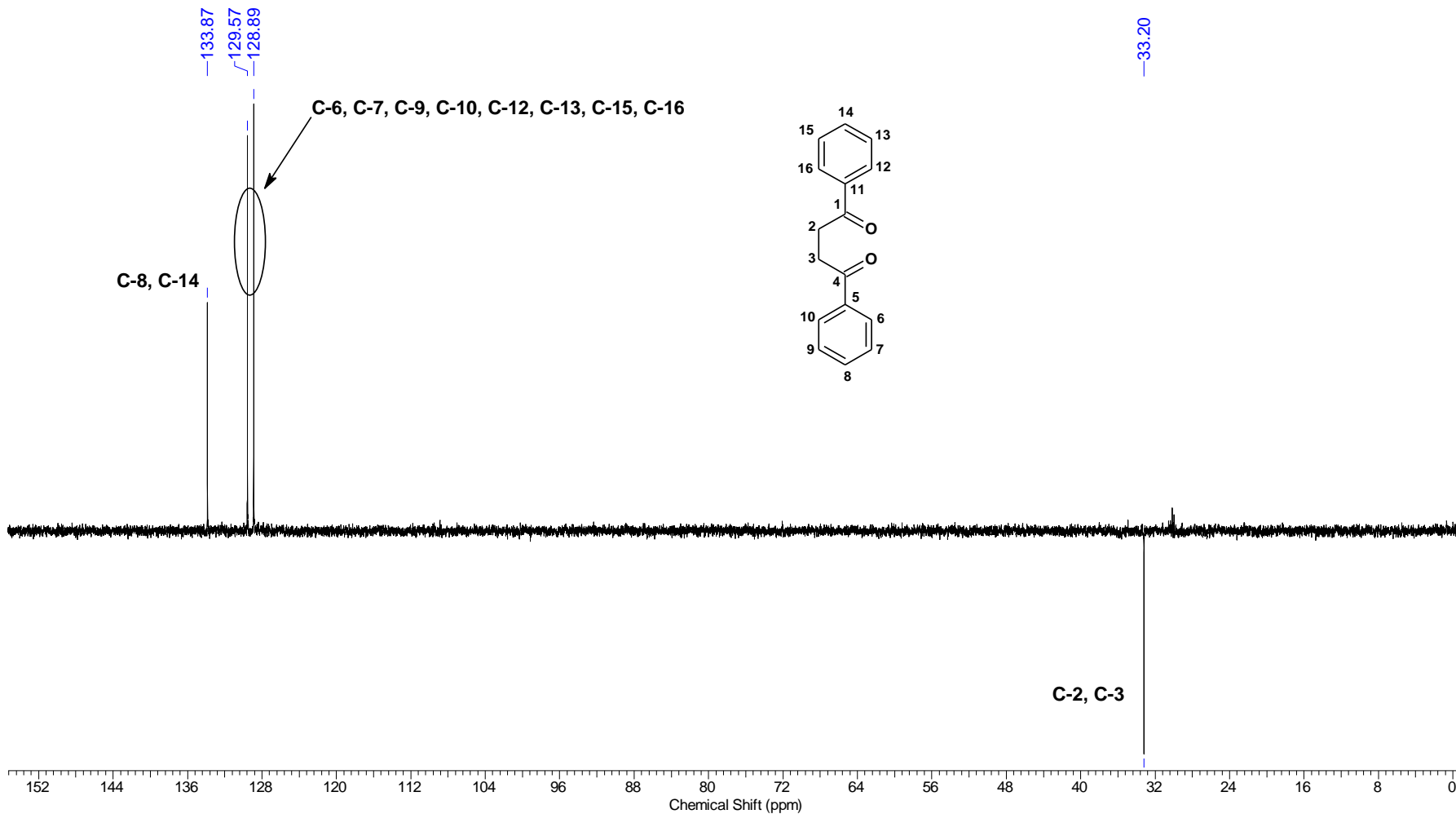
Acquisition Time (sec)	4.8060	Sweep Width (Hz)	6818.08	Temperature (degree C)	24.000	Frequency (MHz)	400.15
Nucleus	1H	Number of Transients	16	Origin	spect	Original Points Count	32768
Owner	nmsu	Points Count	65536	Pulse Sequence	zg30	Receiver Gain	114.00
SW(cyclical) (Hz)	6818.18	Solvent	Acetone	Spectrum Offset (Hz)	2994.8408	Spectrum Type	STANDARD



Acquisition Time (sec)	0.6641	Temperature (degree C)	24.600	Frequency (MHz)	100.62	Nucleus	13C
Number of Transients	1024	Origin	spect	Original Points Count	16384	Owner	nmrslu
Points Count	32768	Pulse Sequence	zgpg30	Receiver Gain	2050.00	SW(cyclical) (Hz)	24671.05
Solvent	Acetone	Spectrum Offset (Hz)	10159.6514	Spectrum Type	STANDARD	Sweep Width (Hz)	24670.30



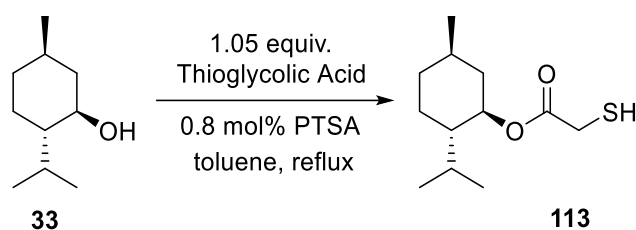
Acquisition Time (sec)	0.8126	Temperature (degree C)	24.400	Frequency (MHz)	100.62	Nucleus	¹³ C
Number of Transients	1024	Origin	spect	Original Points Count	16384	Owner	nmrsu
Points Count	32768	Pulse Sequence	deptsq135	Receiver Gain	912.00	SW(cyclical) (Hz)	20161.29
Solvent	Acetone	Spectrum Offset (Hz)	8146.7192	Spectrum Type	DEPT135	Sweep Width (Hz)	20160.68



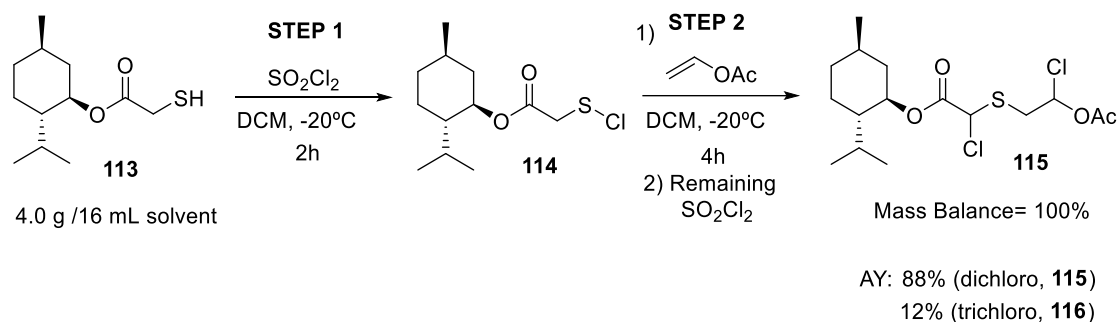
5.2. Continuous Synthesis of a New Intermediate for Lamivudine and Emtricitabine Production

5.2.1. Experimental Procedure – Batch Experiments

Synthesis of Thiol **113**



L-menthol (**33**) (100 g, 0.64 mol) was placed in a 500-mL round-bottom flask and then 100 mL of toluene was added. After solubilizing part of the L-menthol, 1.05 equiv. (46.0 mL, 61.7 g, 0.67 mol) of thioglycolic acid and 0.8 mol% (881.7 mg, 5.12 mmol) of PTSA was added at room temperature. The resulting mixture was refluxed over 2.5 h using a Dean-Stark apparatus to remove the water formed during the reaction. The mixture was cooled down and then extracted with NaOH 1M aqueous solution and toluene (3 x 100 mL). The organic phase was separated then concentrated under reduced pressure and dried with anhydrous Na₂SO₄. After removing the remaining toluene in the rotatory evaporator and vacuum pump for a few hours, compound **113** was obtained in 96% AY (141.5 g, 0.61 mol) with 87% purity. Thiol **113** was used in the next step without any further purification.

Synthesis Dichloro Acetate **115**

Batch: Thiol **113** (4.0 g; 17.4 mmol) was added to a round-bottom flask and then 16 mL of dry DCM. After solubilizing **113** in DCM, the resulting solution was transferred to the EasyMax reactor under nitrogen atmosphere. When the system reached -20°C , SO_2Cl_2 (3.2 mL; 38.2 mmol; 2.2 equiv.) was added to the solution (15 minutes addition). The reaction was kept under these conditions for 2 h. Vinyl acetate (3.2 mL; 34.8 mmol; 2.0 equiv.) was added (varying addition times). After 4 h, the reaction was quenched with a saturated NaHCO_3 aqueous solution. The organic phase was dried with anhydrous Na_2SO_4 and the solvent was removed under reduced pressure. ^1H NMR analysis was performed using the resulting crude mixture. Compound **115** was obtained in 88% AY and trichloro acetate **116** in 12% AY.

Figure 29 shows the EasyMax reactor from Mettler Toledo that was chosen not only for improved temperature control during reagent addition, but also to perform the HFCal runnings.



Figure 29. EasyMax 102 from Mettler Toledo used to carry out batch experiments.

5.2.2. Experimental procedure – Continuous Conditions Experiments

Flow (Chemyx syringe pumps): *Initial experiments to study sulfenyl chloride 114 formation*

Thiol **113** (4.0 g; 17.4 mmol) was weighted in a 10-mL volumetric flask, which was completed with DCM (Solution A). The same was performed separately to prepare SO_2Cl_2 (3.2 mL; 38.2 mmol; 2.2 equiv.) solution in DCM (Solution B). All tubing and reactor that constitute the system were previously filled with DCM and pressurized with a 75 psi BPR. A shut-off valve was placed right after the mixing point to allow the system to be closed and kept pressurized, in order to switch the solvent syringe, used to fill the tubing, by the ones containing the reagents. Solution A and B were transferred to a separate 8 mL Harvard syringe and pumped at the same flow rate ($0.336 \text{ mL}\cdot\text{min}^{-1}$ total) into the 10 mL PFA coil reactor (1/16" O.D. tubing, Vapourtec). Chemyx syringe pumps were utilized for doing so. After 2.5 mL of each solution was injected, the pumps with

reagent were stopped and solvent was pumped into the system ($0.336 \text{ mL}\cdot\text{min}^{-1}$) to keep moving the reaction mixture forward.

Flow (Chemyx syringe pumps):

Initial experiments to perform the end-to-end approach and synthesis of compound 115.

The setup for the previously described sulfenyl chloride **114** synthesis was linked to a second mixing point and a third Chemyx syringe pump with an 8 mL Harvard syringe containing vinyl acetate. The flow rate in the Chemyx syringe pump was adjusted to inject exactly 2 equiv. of vinyl acetate relative to the starting material **113**. A second reactor was inserted after the second mixing zone (15 mL PFA coil) and then the 75 psi BPR was moved to the end of the setup, ensuring both reactors were pressurized.

Flow (Vapourtec pumps):

Thiol **113** (8.0 g; 34.8 mmol) was weighted in a 20-mL volumetric flask, which was completed with toluene (Solution A). The same was performed separately to prepare the SO_2Cl_2 (6.24 mL; 76.4 mmol; 2.2 equiv.) solution in toluene (Solution B). Each solution was transferred to a 20-mL vial and kept under nitrogen atmosphere, then connected to the V-3 pumps (E-Series). Before starting the pumps with reagents, the system was completely filled with toluene and the reactor pressurized with a 40 psi BPR. A 50 mL Harvard syringe was filled with neat vinyl acetate and pumped constantly to the system utilizing a Chemyx syringe pump, ensuring vinyl acetate would be present in T-piece 2 when mixed Solution A and B reach the second mixing point. All reactions were executed at room temperature. The crude mixture was quenched in an aqueous solution of NaHCO_3 preceding ^1H NMR analysis.

The thiol **113** used in these reactions was not purified by chromatographic column with silica gel. The crude starting material was treated only with a basic wash to remove the PTSA. The final outcome was still the same as the obtained with the purified material. However, the presence of water traces can alter the needed amount of SO_2Cl_2 . After the

basic wash the material must be properly dried, otherwise the reaction conditions will need some adjustments.

5.2.3. Crystallization of the dichloro acetate **115**

After extraction with saturated solution of $\text{NaHCO}_3(\text{aq})$, compound **115** was obtained as an oil that becomes a white goop after some hours in the freezer. We tried crystallizing compound **115** several times to no avail. Nevertheless, drying of this material in vacuum pump resulted in a better aspect solid, which was solubilized in DCM to perform the crystallization with hexanes (Figure 30). High quality crystal was finally achieved for the X-ray analysis. Only one of the possible isomers (**115a**) crystallizes however, while the other three remain in the mother liquor (Figure 31). Thus, we determined it more practicable to use the crude mixture extracted with NaHCO_3 aqueous solution only. Consequently, the crude material would be free of remaining SO_2Cl_2 and no acid residue from this step would be present during the cyclization step towards oxathiolane formation.

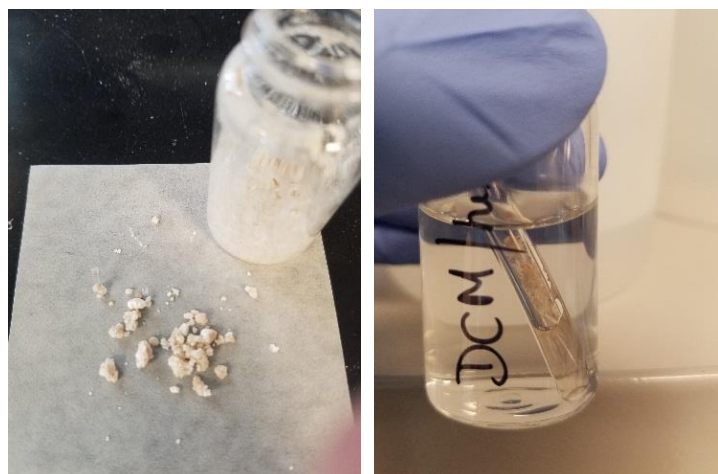
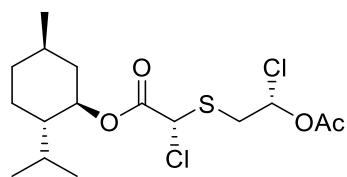
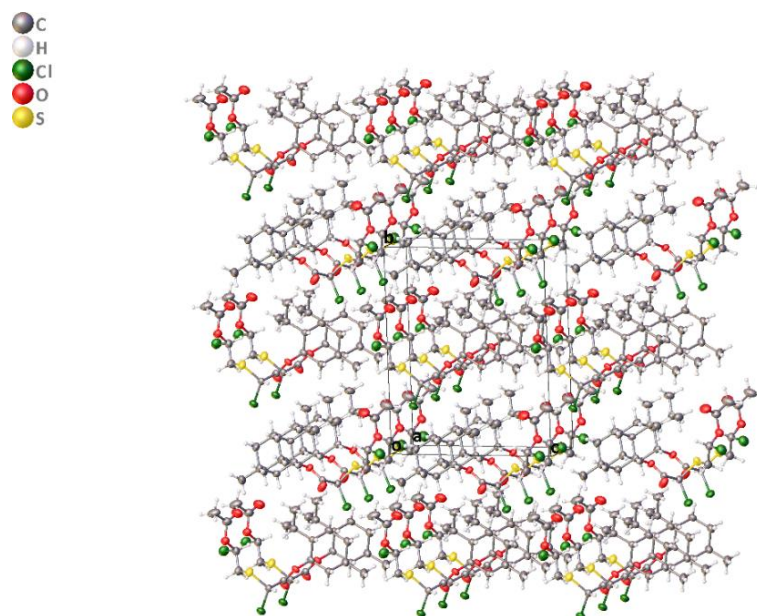
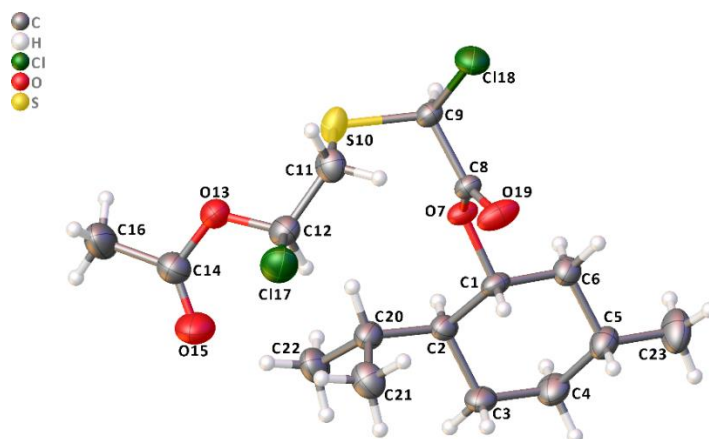


Figure 30. Dichloro-acetate **115** crystallization in DCM/hexanes.

**115a****Figure 31.** X-ray crystallography of the compound **115a**.

5.2.4. Reaction of Vinyl Acetate with SO_2Cl_2

The ^1H NMR of the crude reaction mixture after full consumption of the monochlorinated specie **114a** is shown in Figure 32C. The signals are integrated relative to mesitylene (3H, 6.8 ppm) and used as an internal standard in 1:1 ratio (compound **113**: mesitylene). Byproduct **119** is highlighted in red in Figure 32B and 32C. Its signals match perfectly with the previously unidentified byproducts in the crude mixture.

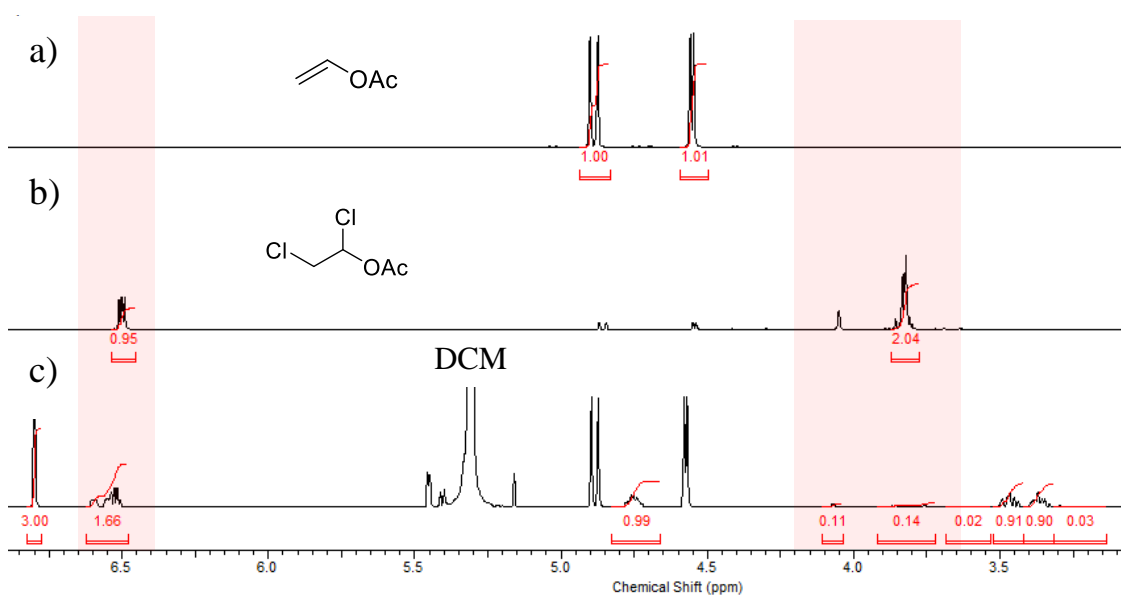


Figure 32. ^1H NMR of byproduct **119** in the crude reaction mixture: a) vinyl acetate; b) vinyl acetate after reaction with SO_2Cl_2 ; c) Crude reaction mixture in DCM.

5.2.5. 1,2,3-trichloropropane as the NMR Internal Standard

The ^1H NMR analysis of the crude mixture coming out of the reactor is displayed in Figure 40A. Dichloro acetate **115** was formed in 97% AY based on the new standard (Table 8, Entry 1). Saturated solution of NaHCO_3 was added to all samples collected from the steady state before NMR analysis to guarantee the full neutralization of remaining SO_2Cl_2 . To ensure 1,2,3-trichloropropane was truly inert to SO_2Cl_2 , one sample was kept overnight with no prior quenching. Figure 33B reveals the ^1H NMR of this sample, suggesting the remaining SO_2Cl_2 reacted with the residual vinyl acetate present in the

crude mixture. Furthermore, the increase of trichloro **116** from the reaction of **115** with SO_2Cl_2 is also observed. Even after an overnight period, 1,2,3-trichloropropane remains intact. The -CH- hydrogen signal (1H) in 4.23 ppm shows up in a very clean region of the spectrum, while the -CH₂- groups in 3.85 ppm (4H) overlap with some small impurities (Figure 33).

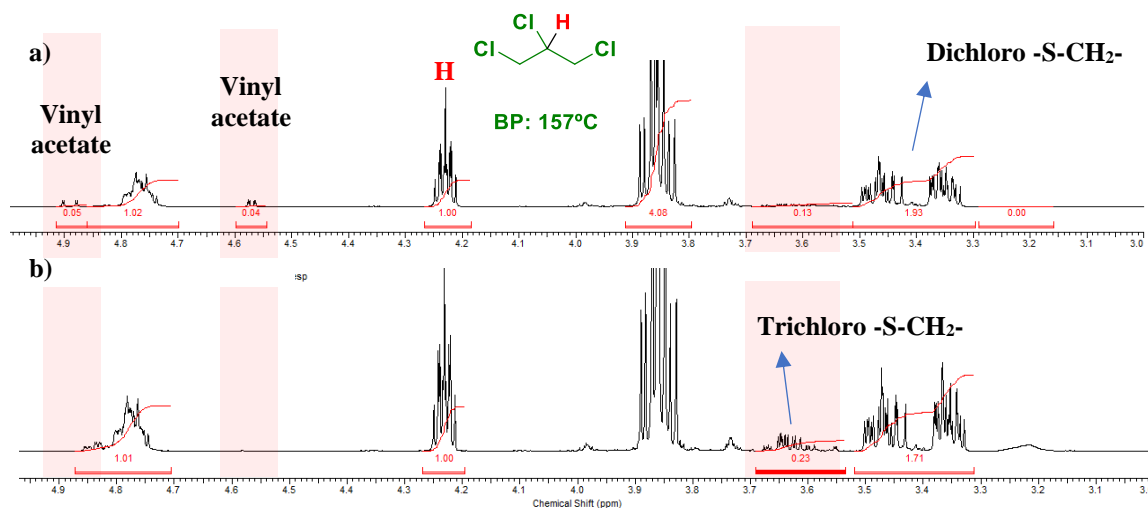
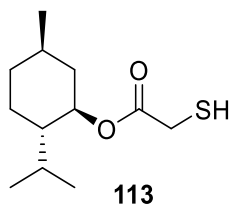
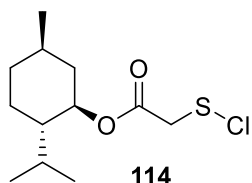


Figure 33. Use of 1,2,3-trichloropropane as NMR internal standard for the steady state studies. a) Crude mixture + 1,2,3-trichloropropane/ steady state (¹H NMR right after fraction was collected); b) Same sample with no extraction with NaHCO₃ (¹H NMR overnight).

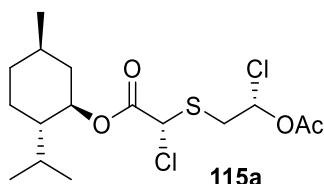
5.2.6. NMR – Product Characterization

**113***(1R,2S,5R)-2-isopropyl-5-methylcyclohexyl 2-mercaptoacetate (113).*

Compound **113** was obtained as a colorless oil in 96% AY (141.5 g, 0.61 mol) and 83–87% purity, starting from 0.64 mol (100 g) of L-menthol. ^1H NMR (600 MHz, CDCl_3): δ_{H} 4.64 (dt, $J_1=11.0$ Hz, $J_2=4.40$ Hz, 1H), 3.15 (d, $J=8.25$ Hz, 2H), 1.91–1.99 (m, 2H), 1.80–1.89 (m, 1H), 1.58–1.66 (m, 2H), 1.38–1.48 (m, 1H), 1.30–1.38 (m, 1H), 0.89–1.05 (m, 2H), 0.76–0.88 (m, 7H), 0.70 (d, $J=7.15$ Hz, 3H); ^{13}C NMR (150 MHz, CDCl_3): δ_{C} 170.1, 75.3, 46.8, 40.4, 34.0, 31.2, 26.6, 26.0, 23.2, 21.8, 20.6, 16.1.

**114***(1R,2S,5R)-2-isopropyl-5-methylcyclohexyl 2-(chlorothio)acetate (114).*

Not isolated. Crude mixture: ^1H NMR (600 MHz, CDCl_3): δ_{H} 4.77 (dt, $J_1=10.8$ Hz, $J_2=4.40$ Hz, 1H), 3.88 (s, 2H), 2.00–2.06 (m, 1H), 1.89–1.97 (m, 1H), 1.67–1.73 (m, 2H), 1.34–1.55 (m, 2H), 0.99–1.12 (m, 2H), 0.84–0.94 (m, 7H), 0.77 (d, $J=6.97$ Hz, 3H).

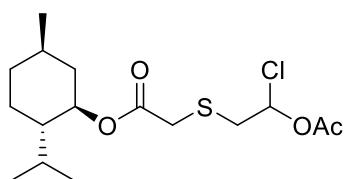
**115a***(1R,2S,5R)-2-isopropyl-5-methylcyclohexyl 2-((2-acetoxy-2-chloroethyl)thio)-2-chloroacetate (115).*

Compound **115** was obtained as a white goop after extraction with a saturated solution of $\text{NaHCO}_3(\text{aq})$. Overall assay yield starting from thiol **113** is 98% (0.67 mol; 258.2 g considering 158 g scale-up condition in flow): Crystal (**115a**) – ^1H NMR (600 MHz, CDCl_3): δ_{H} 6.56 (dd, $J_1=8.2$ Hz, $J_2=4.0$ Hz, 1H), 4.75 (dt, $J_1=11.0$ Hz, $J_2=4.4$ Hz, 1H), 5.43 (s, 1H), 3.48 (dd, $J_1=14.7$ Hz, $J_2=8.2$ Hz, 1H), 3.37

(dd, $J_1= 14.7$ Hz, $J_2= 4.0$ Hz, 1H), 2.17 (s, 3H), 2.02–2.07 (m, 1H), 1.87–1.97 (m, 1H), 1.43–1.56 (m, 2H), 1.01–1.12 (m, 2H), 0.92 (dd, $J_1= 14.0$ Hz, $J_2= 6.6$ Hz, 6H), 0.84–0.94 (m, 1H),* 0.77 (d, $J= 6.9$ Hz, 3H); ^{13}C NMR (150 MHz, CDCl_3): δ_{C} 168.1, 165.5, 81.6, 77.6, 61.5, 47.0, 40.3, 37.4, 34.0, 31.4, 26.1, 23.3, 22.0, 20.7, 20.6, 16.1.

*Hydrogen signals overlap with dd in 0.92 ppm.

Crude mixture containing four diastereoisomers presents more complex signals. Due to the similar chemical shifts of the isomers, many signals overlap.

**114a**

(1*R*,2*S*,5*R*)-2-isopropyl-5-methylcyclohexyl 2-((2-acetoxy-2-chloroethyl)thio)acetate (**114a**).

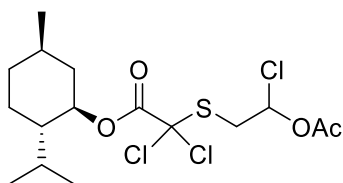
Intermediate isolated only to use as a reference to compare with the ^1H NMR of the crude reaction mixture. It was obtained as a colorless oil. ^1H NMR (600 MHz, CDCl_3): δ_{H} 6.48 (dd, $J_1= 8.0$ Hz, $J_2= 4.0$ Hz, 1H), 4.65–4.74 (m, 1H), 3.26–3.11 (m, 4H),* 2.11 (s, 3H), 1.94–2.01 (m, 1H), 1.81–1.89 (m, 1H), 1.62–1.68 (m, 2H), 1.33–1.51 (m, 2H), 0.93–1.07 (m, 2H), 0.79–0.90 (m, 7H), 0.73 and 0.72 (d, $J= 2.75$ Hz, 3H).**

*Overlap of $-\text{CH}_2-\text{S}-\text{CH}_2-$ hydrogens.

** Duplicate signal (diastereoisomers mixture).

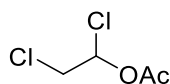
^{13}C NMR (150 MHz, CDCl_3): δ_{C} 169.2,* 168.1, 81.8,* 75.5 and 75.4,* 46.9 and 46.8,* 40.6 and 40.5,* 39.0 and 38.9,* 34.2 and 34.1,* 34.0, 31.2, 26.1 and 26.0,* 23.2, 21.8, 20.6,* 16.1.

**Duplicate signal (diastereoisomers mixture).

**116***(1R,2S,5R)-2-isopropyl-5-methylcyclohexyl 2-((2-acetoxy-2-*

chloroethyl)thio)-2,2-dichloroacetate (116). Intermediate isolated only for use as a reference to compare the ^1H NMR of the crude reaction mixture. It was obtained as a slightly yellow oil. ^1H NMR (600 MHz, CDCl_3): δ_{H} 6.65–6.76 (m, 1H), 4.74–4.81 (m, 1H), 3.55–3.68 (m, 2H), 1.89–2.18 (m, 5H), 1.66–1.74 (m, 2H), 1.44–1.58 (m, 2H), 1.02–1.16 (m, 2H), 0.85–0.95 (m, 7H), 0.76 (d, $J = 6.97$ Hz, 3H). ^{13}C NMR (150 MHz, CDCl_3): δ_{C} 167.8, 163.0, 87.3 and 87.2,* 80.7 and 80.6,* 79.8,* 46.8,* 40.2, 39.8 and 39.7,* 33.8, 31.3, 26.0, 23.1, 21.8, 20.6 and 20.5,* 16.0.

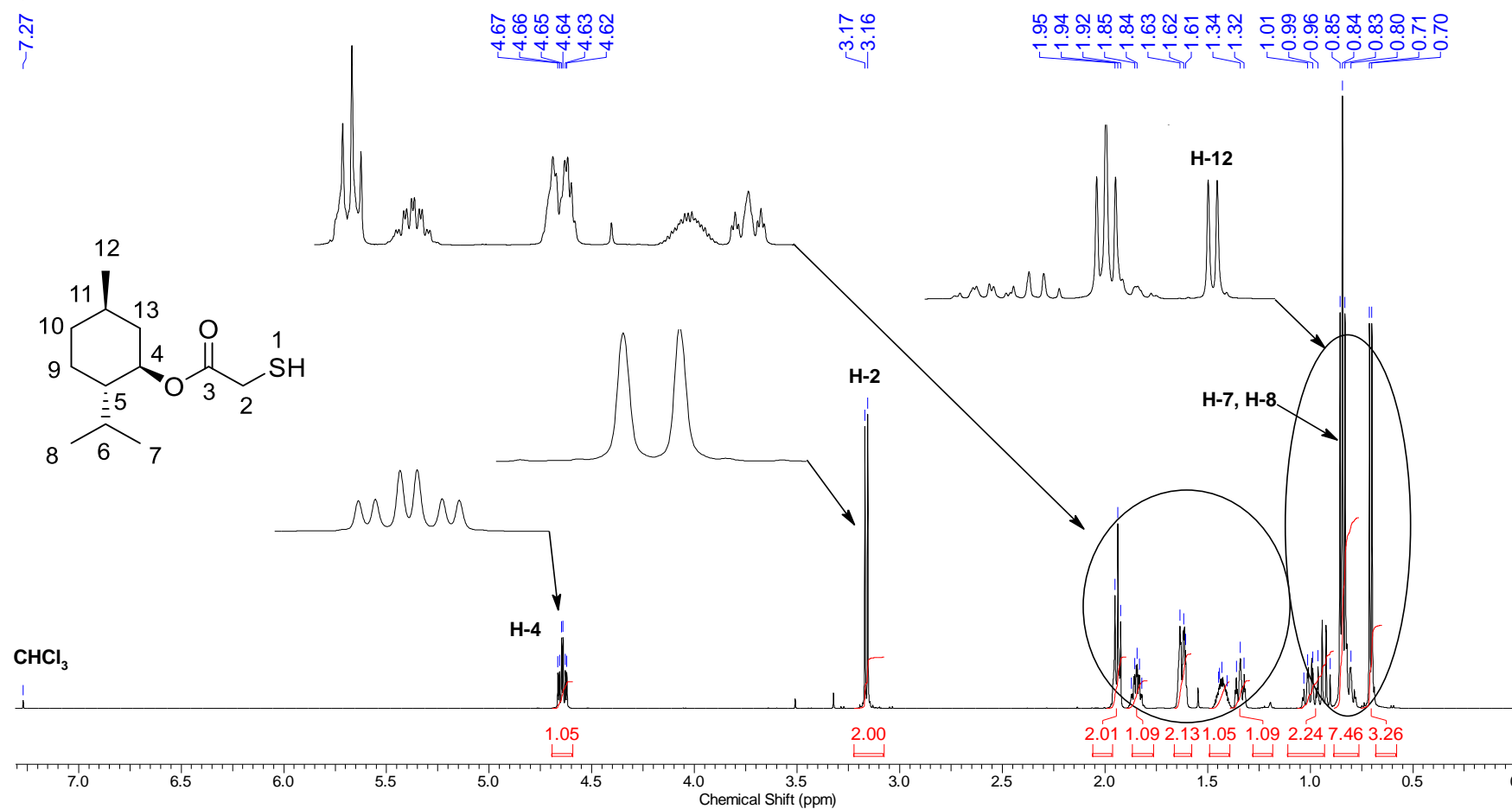
*Duplicate signal (diastereoisomers mixture).

**119***1,2-dichloroethyl acetate (119)*. Obtained from the reaction of vinyl acetate

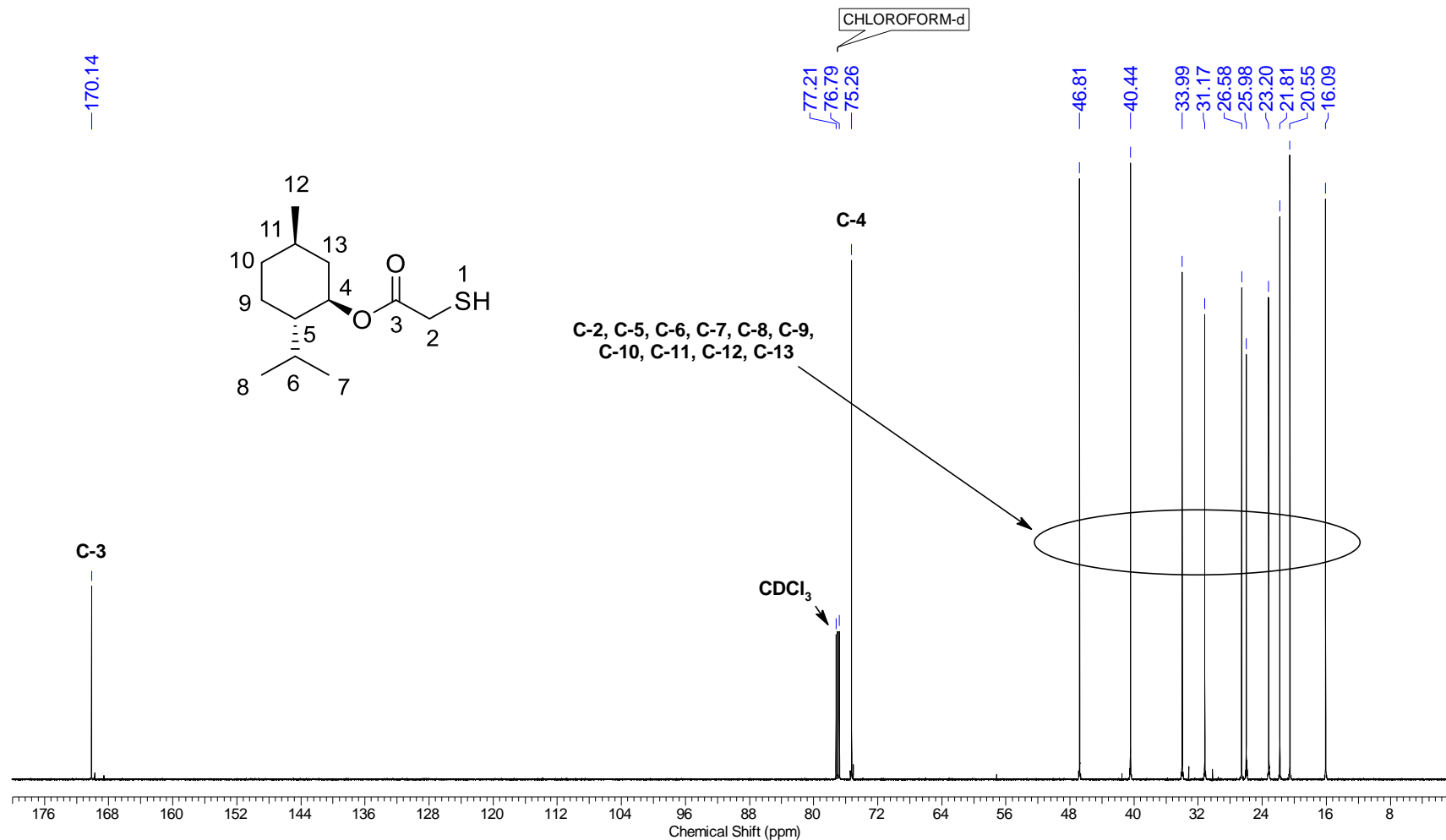
with SO_2Cl_2 . It was synthesized to be use as a reference to compare with the ^1H NMR of the crude reaction mixture. ^1H NMR (600 MHz, CDCl_3): δ_{H} 6.45 (dd, $J_1 = 7.1$ Hz, $J_2 = 4.4$ Hz, 1H), 3.77–3.85 (m, 2H), 2.13 (s, 3H).

5.2.7. NMR Spectra

Frequency (MHz)	600.01	Nucleus	¹ H	Number of Transients	16	Origin	spect
Original Points Count	32768	Owner	nmrslu	Points Count	65536	Pulse Sequence	zg30
Receiver Gain	9.97	SW(cyclical) (Hz)	12019.23	Acquisition Time (sec)	2.7263	Spectrum Offset (Hz)	3743.7068
Spectrum Type	STANDARD	Sweep Width (Hz)	12019.05	Temperature (degree C)	23.557		

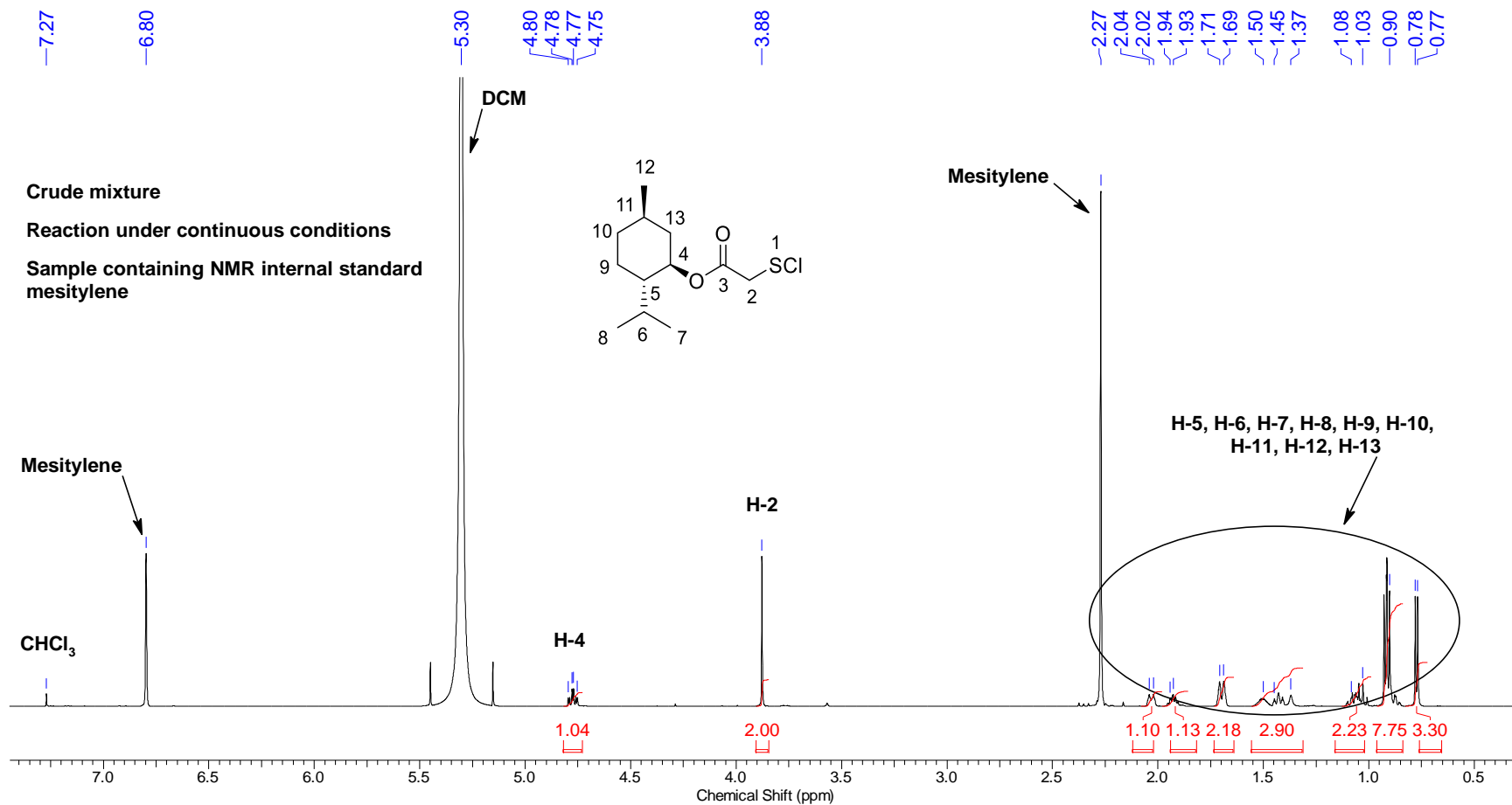


Frequency (MHz)	150.87	Nucleus	¹³ C	Number of Transients	300	Origin	spect
Original Points Count	32768	Owner	nmsu	Points Count	32768	Pulse Sequence	zgpg30
Receiver Gain	199.73	SW(cyclical) (Hz)	36231.88	Acquisition Time (sec)	0.9044	Spectrum Offset (Hz)	15075.2021
Spectrum Type	STANDARD	Sweep Width (Hz)	36230.78	Temperature (degree C)	25.319		

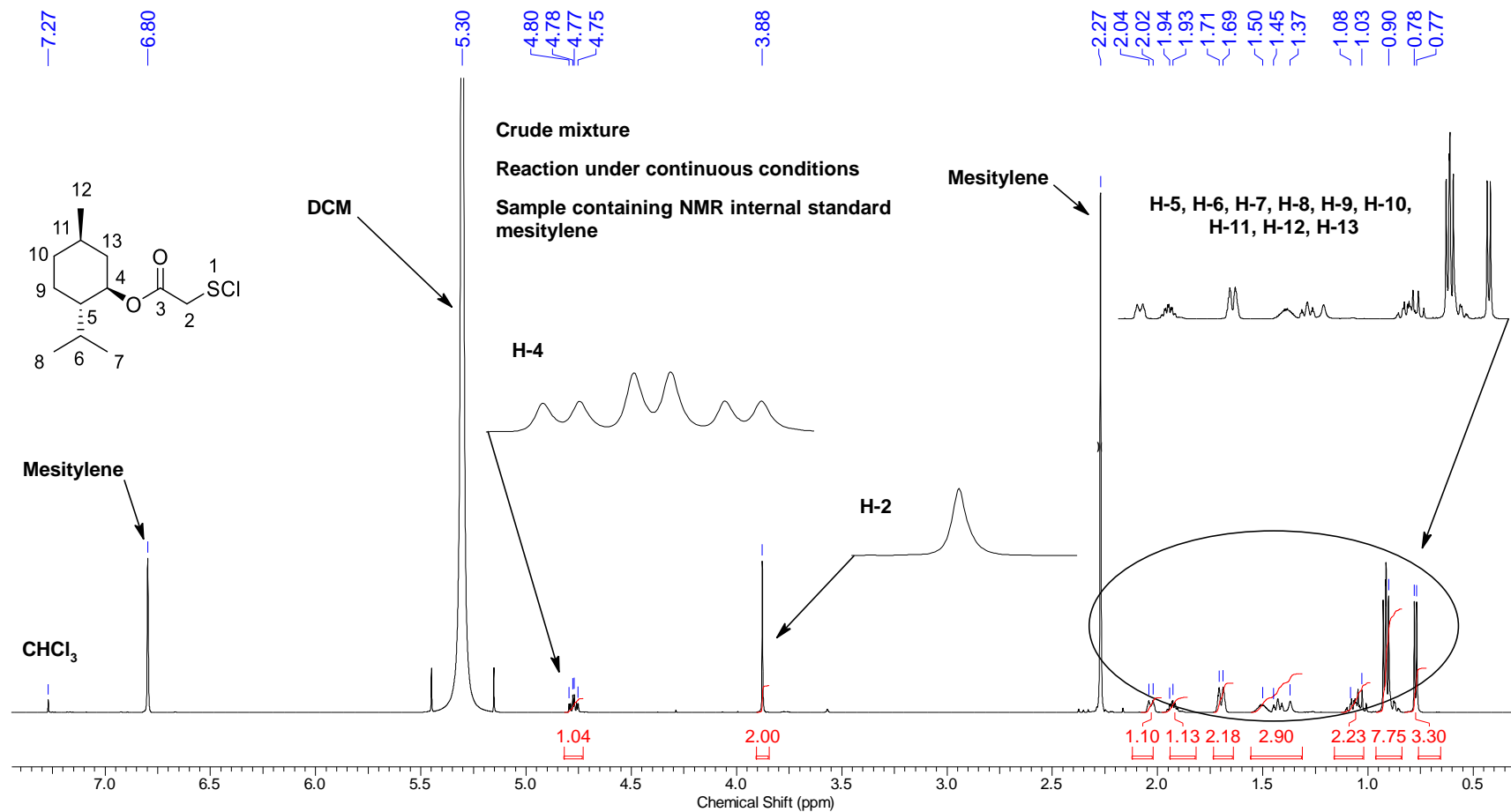


Flow Chemistry Applied to Hazardous Reactions, and Fluorophores Synthesis with Photophysics Studies

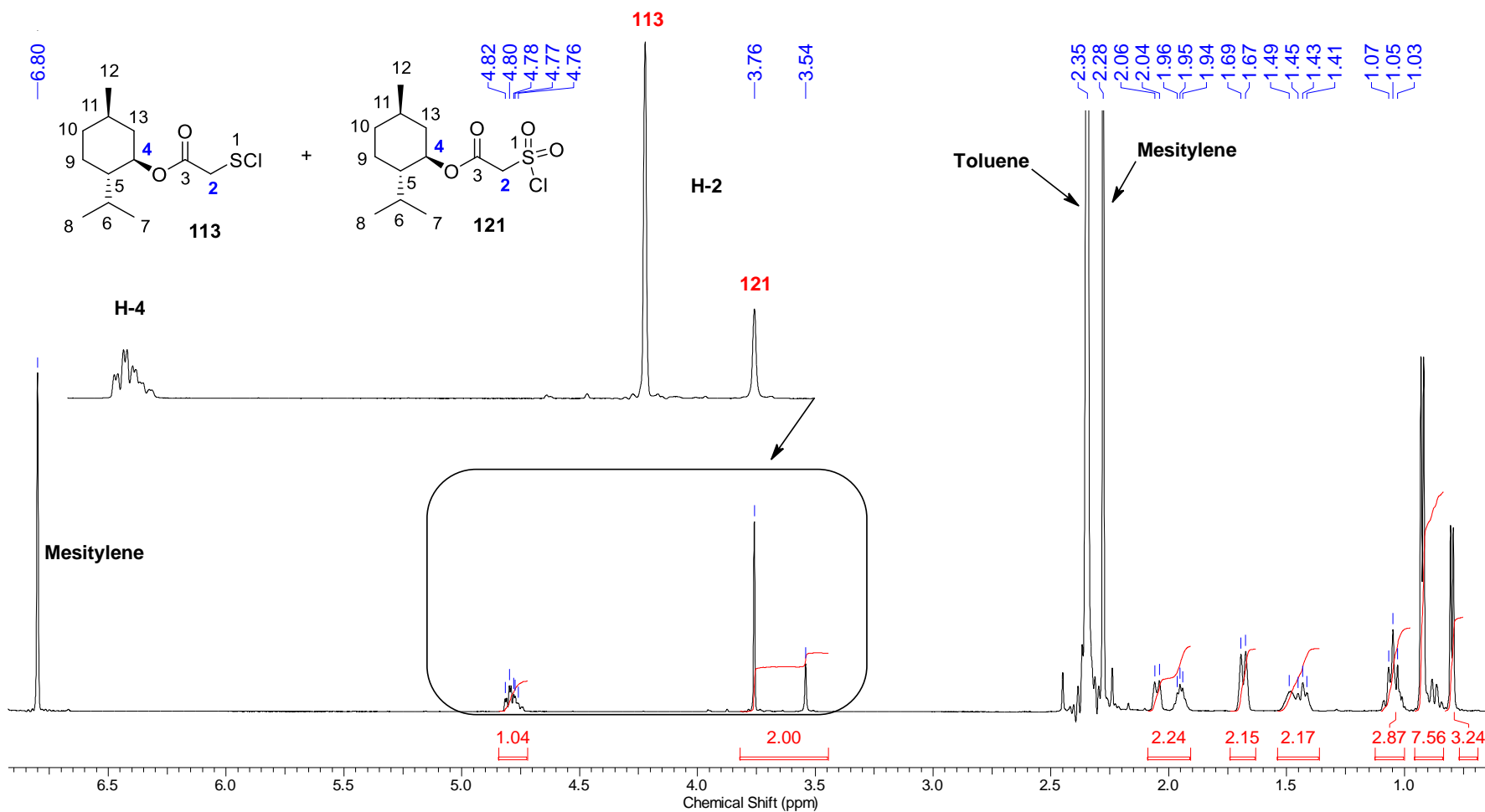
Frequency (MHz)	599.96	Nucleus	1H	Number of Transients	16	Origin	spect
Original Points Count	32768	Owner	nmsu	Points Count	65536	Pulse Sequence	zg30
Receiver Gain	9.05	SW(cyclical) (Hz)	12019.23	Solvent	CDCl3	Spectrum Offset (Hz)	3695.2930
Spectrum Type	STANDARD	Sweep Width (Hz)	12019.05	Temperature (degree C)	20.513	Acquisition Time (sec)	2.7263



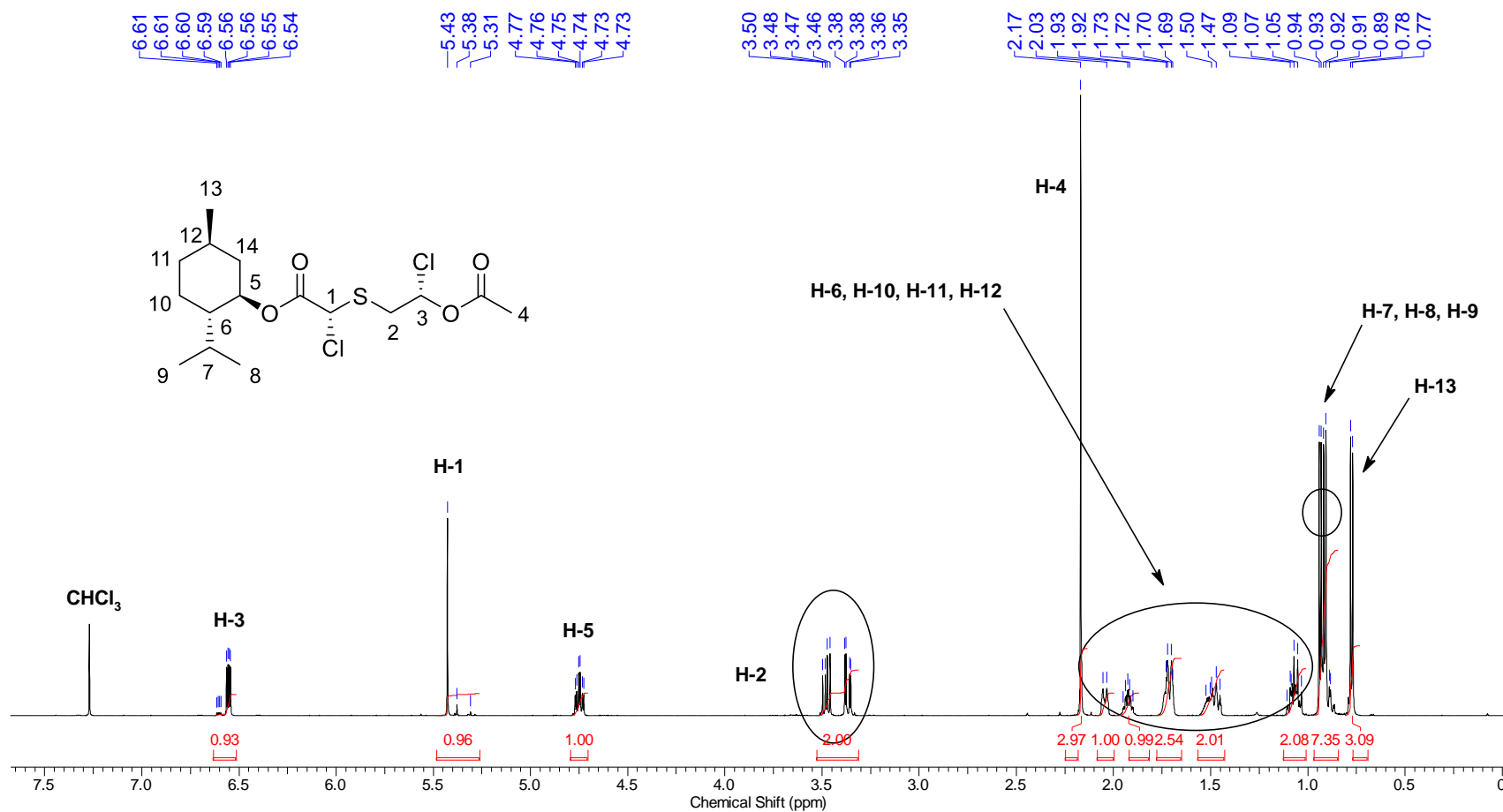
Frequency (MHz)	599.96	Nucleus	1H	Number of Transients	16	Origin	spect
Original Points Count	32768	Owner	nmrsu	Points Count	65536	Pulse Sequence	zg30
Receiver Gain	9.05	SW(cyclical) (Hz)	12019.23	Solvent	CDCl3	Spectrum Offset (Hz)	3695.2930
Spectrum Type	STANDARD	Sweep Width (Hz)	12019.05	Temperature (degree C)	20.513	Acquisition Time (sec)	2.7263



Nucleus	1H	Number of Transients	8	Origin	spect	Original Points Count	32768
Owner	nmrsu	Points Count	65536	Pulse Sequence	zg30	Receiver Gain	18.20
SW(cyclical) (Hz)	12019.23	Solvent	CDCl3	Spectrum Offset (Hz)	3581.0977	Spectrum Type	STANDARD
Sweep Width (Hz)	12019.05	Temperature (degree C)	23.314	Frequency (MHz)	600.01	Acquisition Time (sec)	2.7263

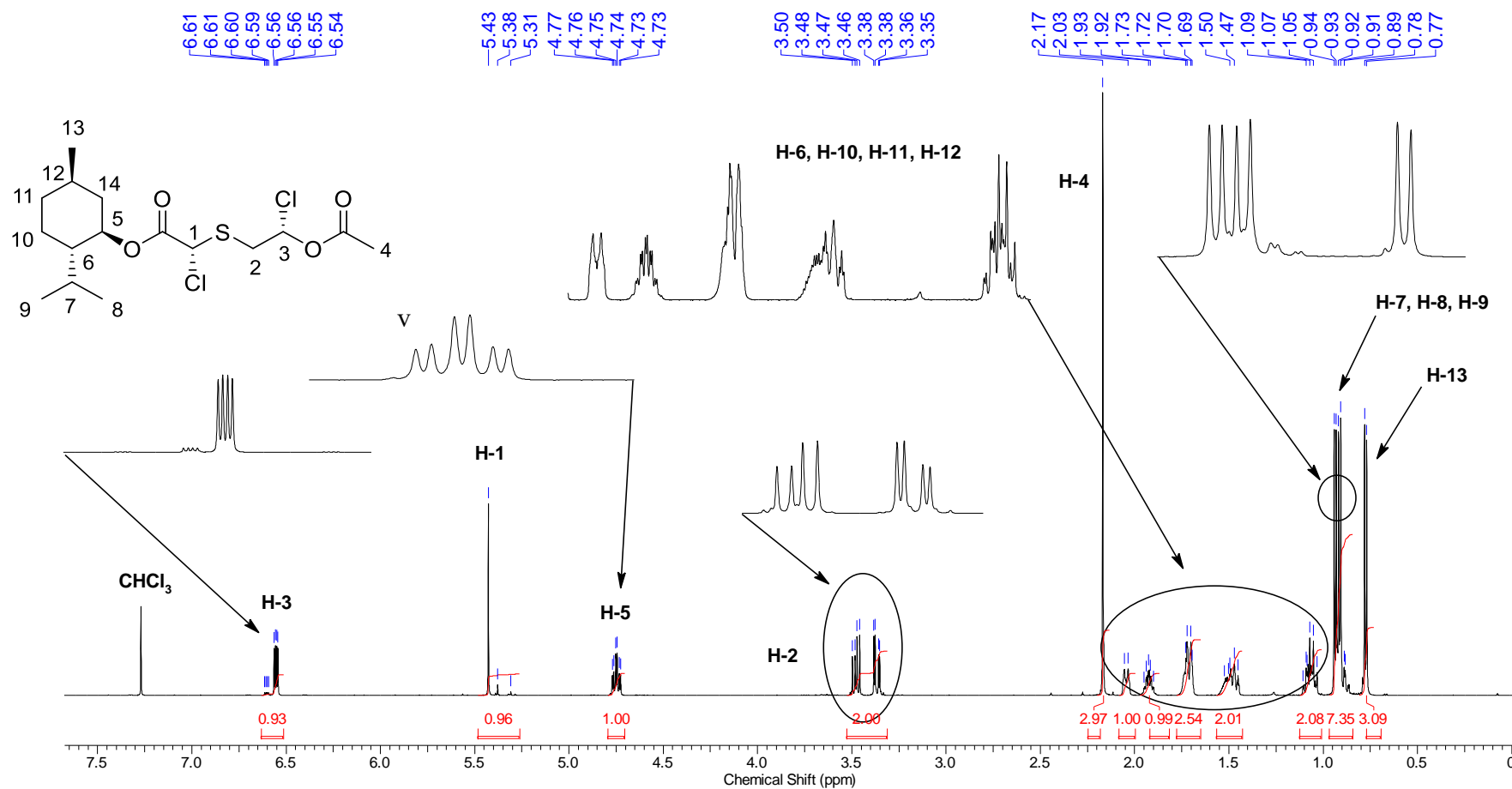


Frequency (MHz)	600.01	Nucleus	¹ H	Number of Transients	16	Origin	spect
Original Points Count	32768	Owner	nmsu	Points Count	65536	Pulse Sequence	zg30
Receiver Gain	176.24	SW(cyclical) (Hz)	12019.23	Acquisition Time (sec)	2.7263	Spectrum Offset (Hz)	3743.5234
Spectrum Type	STANDARD	Sweep Width (Hz)	12019.05	Temperature (degree C)	23.682		



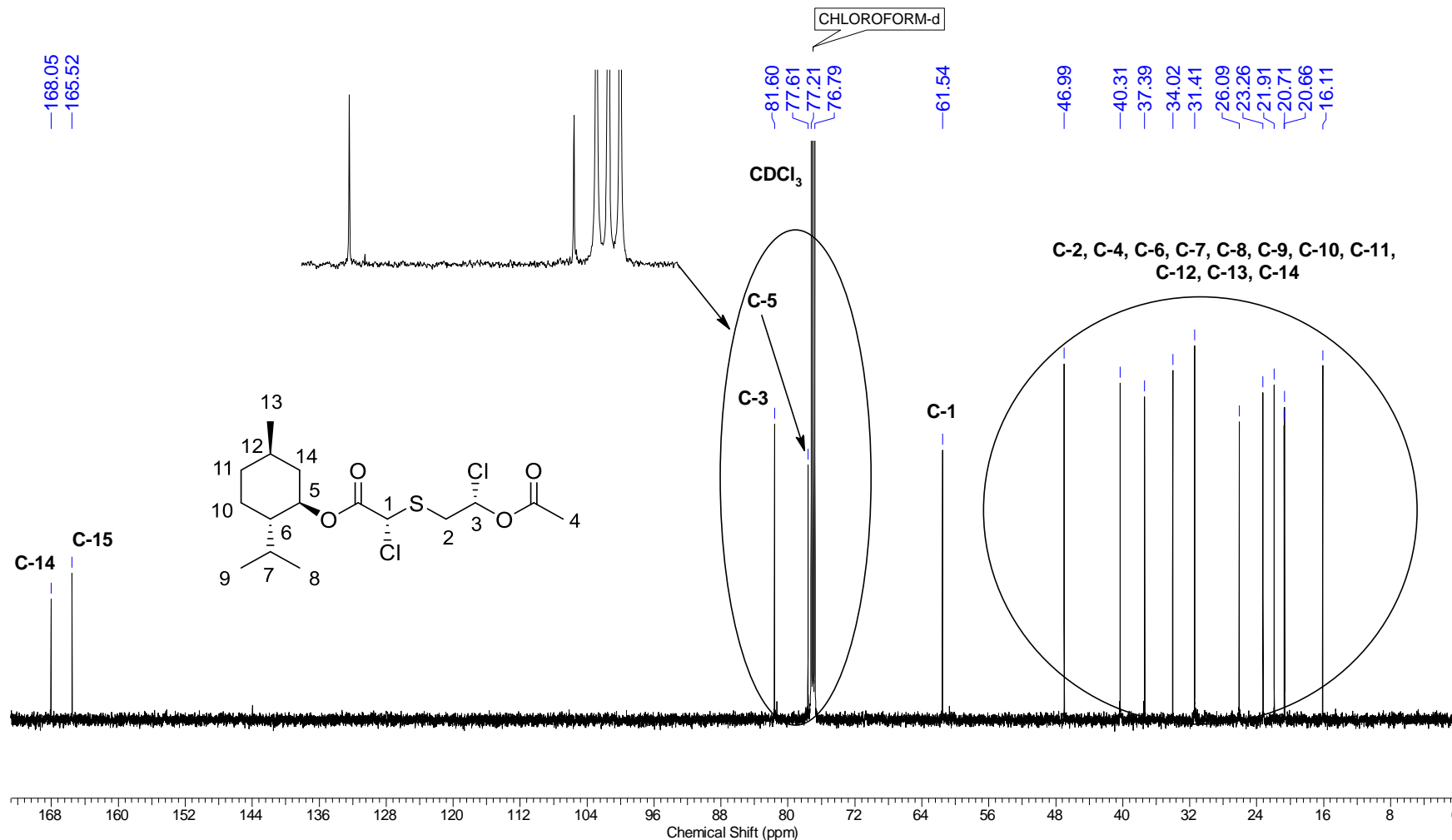
Flow Chemistry Applied to Hazardous Reactions, and Fluorophores Synthesis with Photophysics Studies

Frequency (MHz)	600.01	Nucleus	¹ H	Number of Transients	16	Origin	spect
Original Points Count	32768	Owner	nmsu	Points Count	65536	Pulse Sequence	zg30
Receiver Gain	176.24	SW(cyclical) (Hz)	12019.23	Acquisition Time (sec)	2.7263	Spectrum Offset (Hz)	3743.5234
Spectrum Type	STANDARD	Sweep Width (Hz)	12019.05	Temperature (degree C)	23.682		



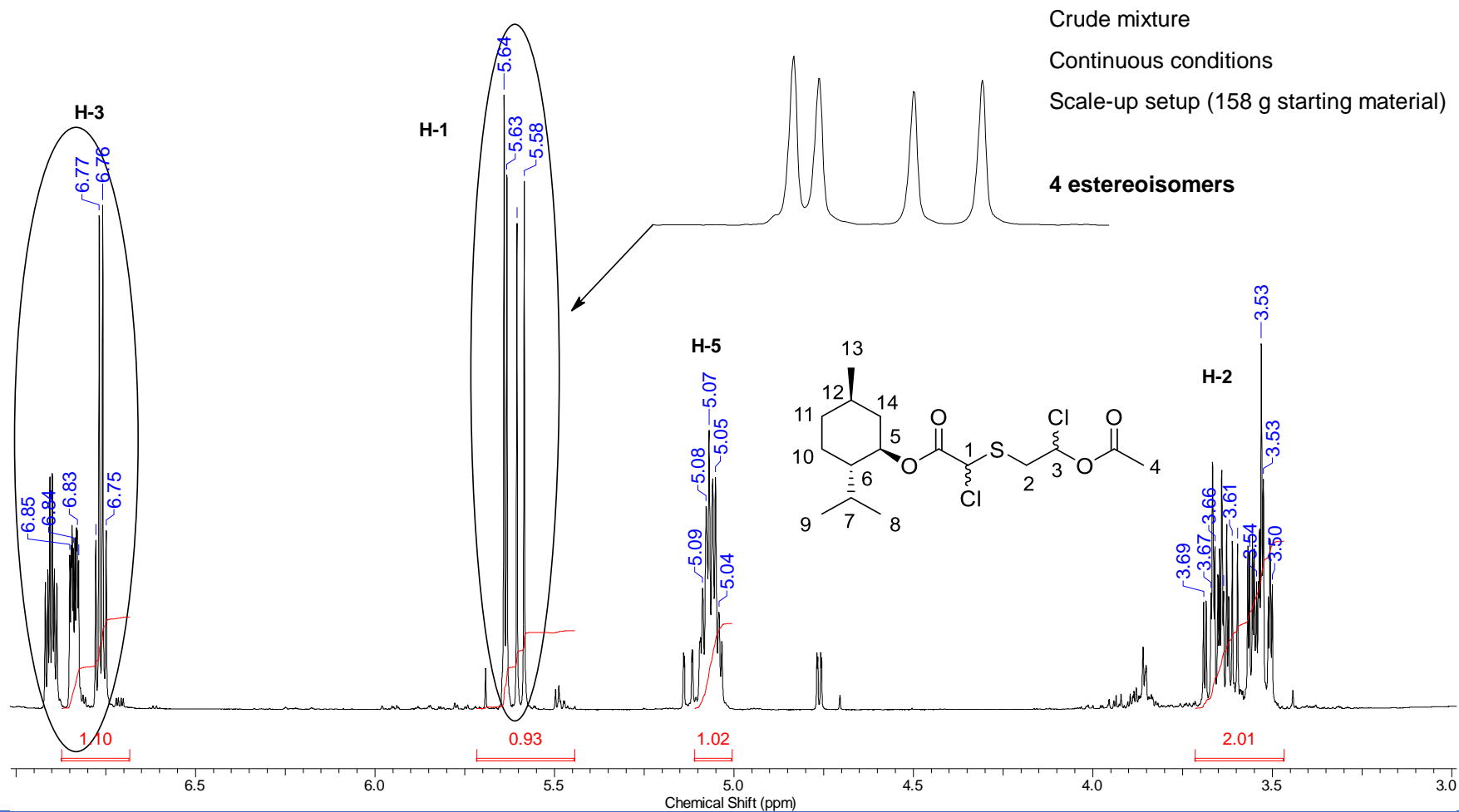
Flow Chemistry Applied to Hazardous Reactions, and Fluorophores Synthesis with Photophysics Studies

Frequency (MHz)	150.87	Nucleus	¹³ C	Number of Transients	1024	Origin	spect
Original Points Count	32768	Owner	nmrsu	Points Count	32768	Pulse Sequence	zgpg30
Receiver Gain	199.73	SW(cyclical) (Hz)	36231.88	Acquisition Time (sec)	0.9044	Spectrum Offset (Hz)	15096.2100
Spectrum Type	STANDARD	Sweep Width (Hz)	36230.78	Temperature (degree C)	25.272		



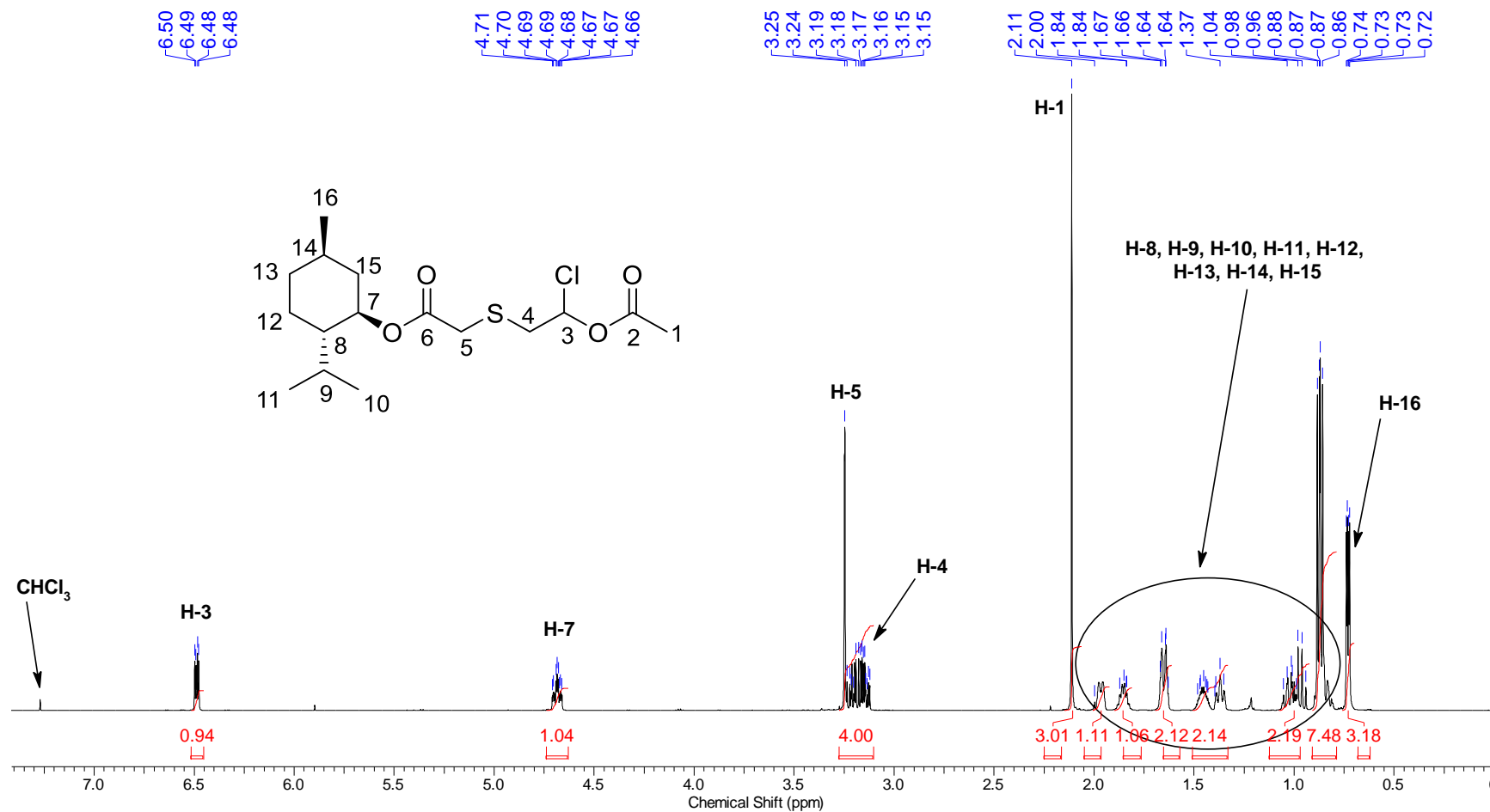
Flow Chemistry Applied to Hazardous Reactions, and Fluorophores Synthesis with Photophysics Studies

Frequency (MHz)	599.96	Nucleus	1H	Number of Transients	16	Origin	spect
Original Points Count	32768	Owner	nmrslu	Points Count	65536	Pulse Sequence	zg30
Receiver Gain	3.63	SW(cyclical) (Hz)	12019.23	Acquisition Time (sec)	2.7263	Spectrum Offset (Hz)	3704.7244
Spectrum Type	STANDARD	Sweep Width (Hz)	12019.05	Temperature (degree C)	23.303		



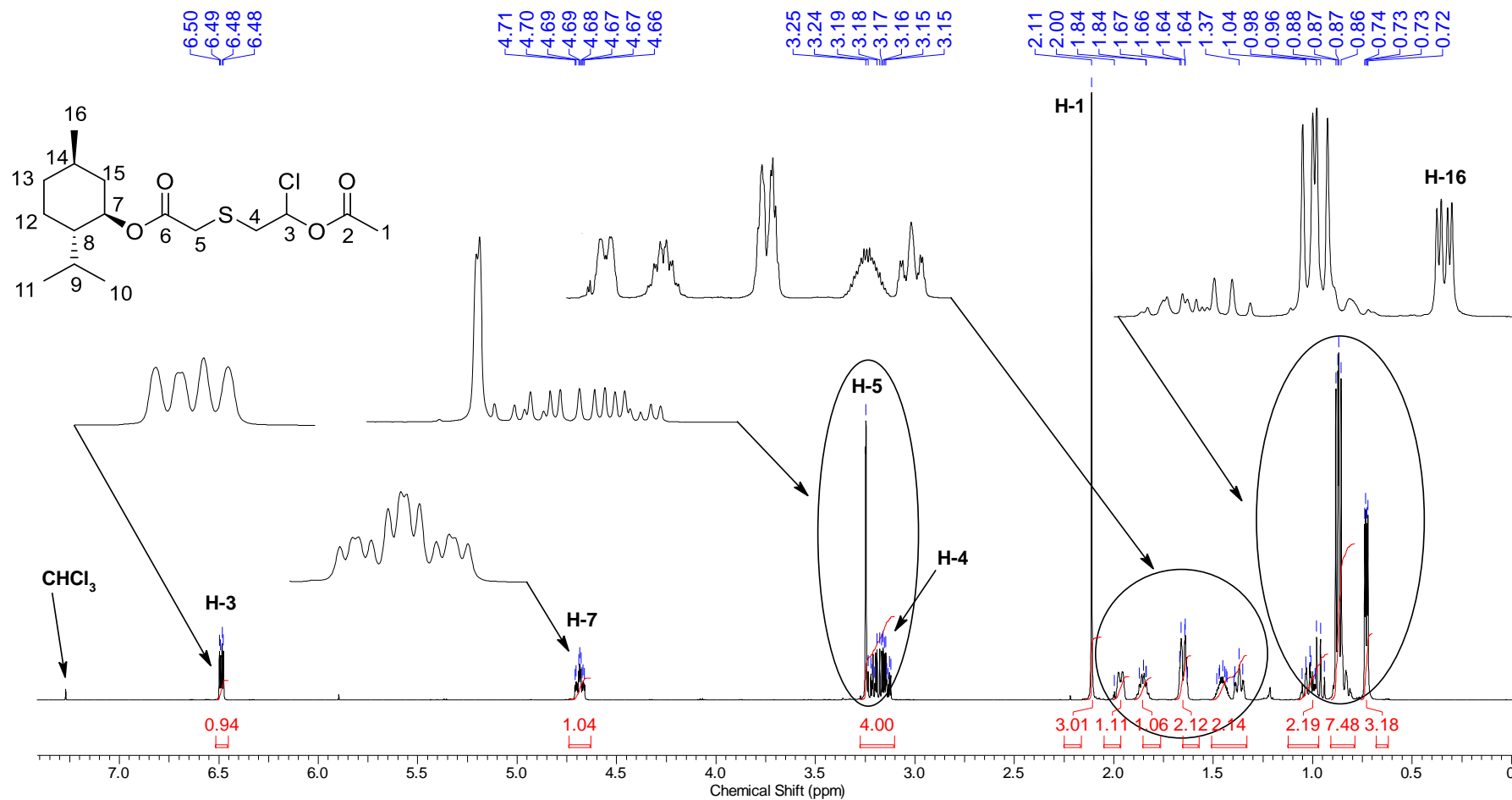
Flow Chemistry Applied to Hazardous Reactions, and Fluorophores Synthesis with Photophysics Studies

Frequency (MHz)	600.01	Nucleus	¹ H	Number of Transients	16	Origin	spect
Original Points Count	32768	Owner	nmsu	Points Count	65536	Pulse Sequence	zg30
Receiver Gain	15.88	SW(cyclical) (Hz)	12019.23	Acquisition Time (sec)	2.7263	Spectrum Offset (Hz)	3743.7068
Spectrum Type	STANDARD	Sweep Width (Hz)	12019.05	Temperature (degree C)	23.513		



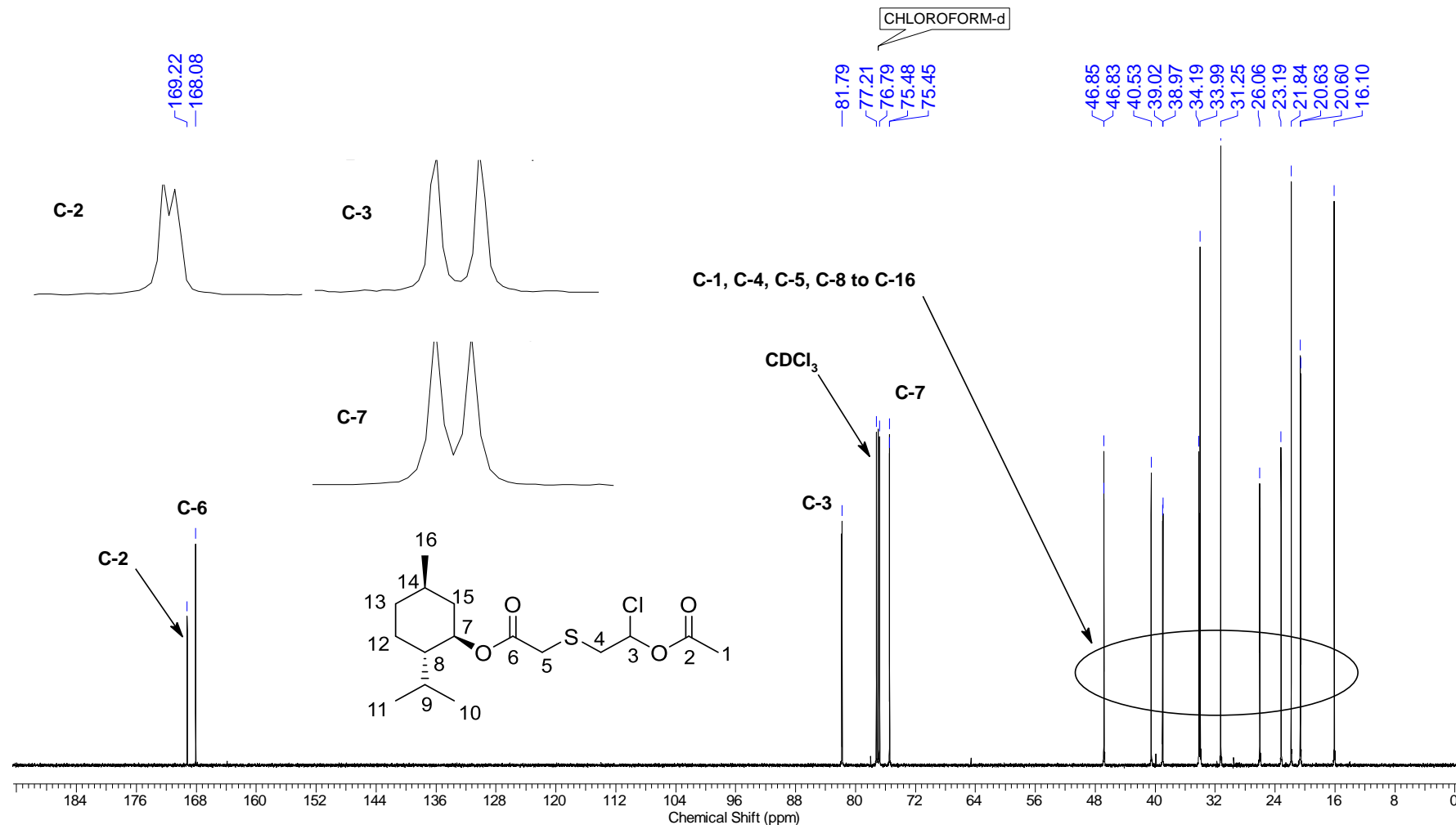
Flow Chemistry Applied to Hazardous Reactions, and Fluorophores Synthesis with Photophysics Studies

Frequency (MHz)	600.01	Nucleus	1H	Number of Transients	16	Origin	spect
Original Points Count	32768	Owner	nmrsu	Points Count	65536	Pulse Sequence	zg30
Receiver Gain	15.88	SW(cyclical) (Hz)	12019.23	Acquisition Time (sec)	2.7263	Spectrum Offset (Hz)	3743.7068
Spectrum Type	STANDARD	Sweep Width (Hz)	12019.05	Temperature (degree C)	23.513		



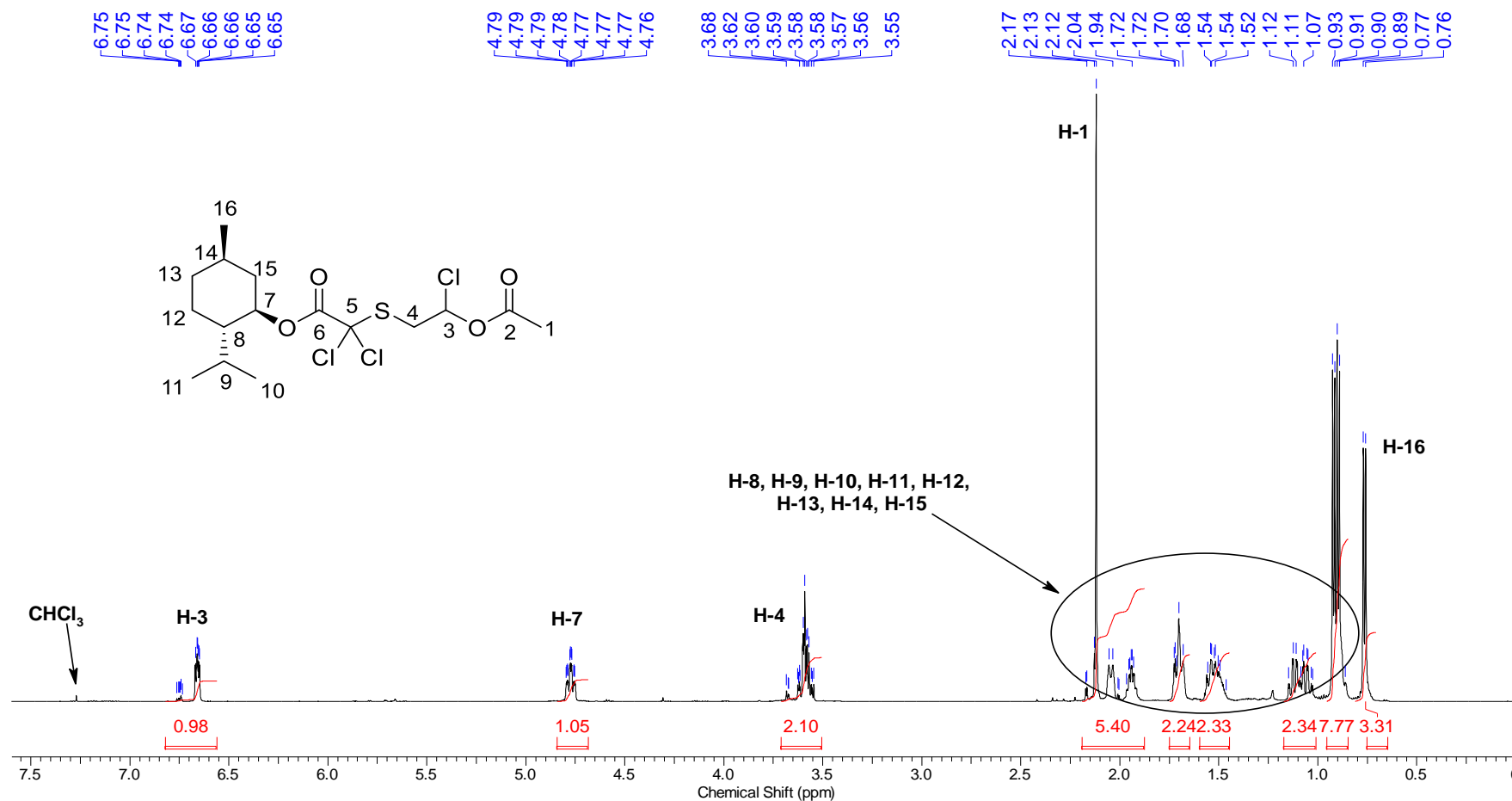
Flow Chemistry Applied to Hazardous Reactions, and Fluorophores Synthesis with Photophysics Studies

Frequency (MHz)	150.87	Nucleus	13C	Number of Transients	300	Origin	spect
Original Points Count	32768	Owner	nmsu	Points Count	32768	Pulse Sequence	zgpg30
Receiver Gain	199.73	SW(cyclical) (Hz)	36231.88	Acquisition Time (sec)	0.9044	Spectrum Offset (Hz)	15080.7305
Spectrum Type	STANDARD	Sweep Width (Hz)	36230.78	Temperature (degree C)	25.251		



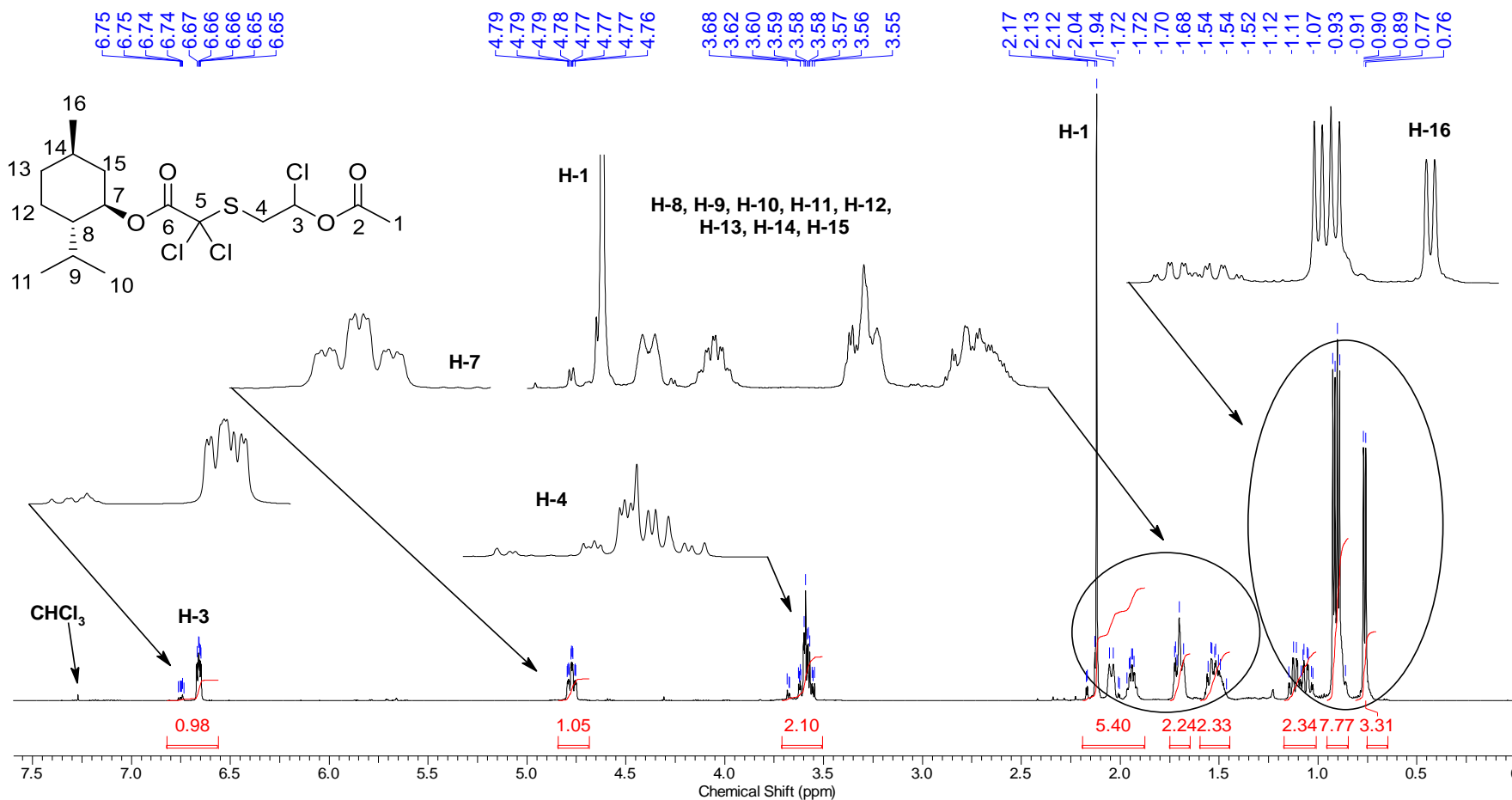
Flow Chemistry Applied to Hazardous Reactions, and Fluorophores Synthesis with Photophysics Studies

Frequency (MHz)	600.01	Nucleus	1H	Number of Transients	16	Origin	spect
Original Points Count	32768	Owner	nmrsu	Points Count	65536	Pulse Sequence	zg30
Receiver Gain	14.42	SW(cyclical) (Hz)	12019.23	Acquisition Time (sec)	2.7263	Spectrum Offset (Hz)	3743.7068
Spectrum Type	STANDARD	Sweep Width (Hz)	12019.05	Temperature (degree C)	23.567		



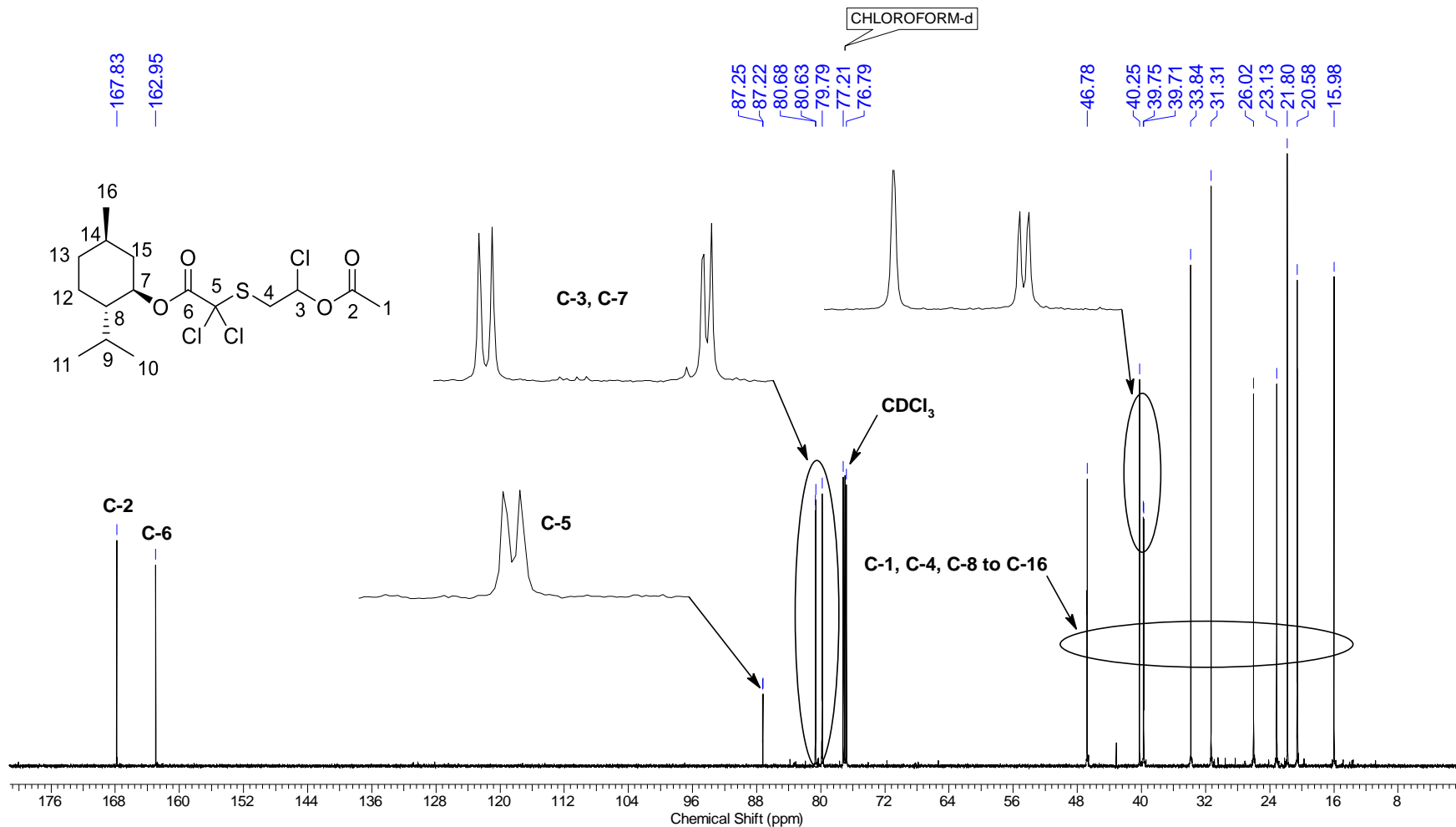
Flow Chemistry Applied to Hazardous Reactions, and Fluorophores Synthesis with Photophysics Studies

Frequency (MHz)	600.01	Nucleus	1H	Number of Transients	16	Origin	spect
Original Points Count	32768	Owner	nmrsu	Points Count	65536	Pulse Sequence	zg30
Receiver Gain	14.42	SW(cyclical) (Hz)	12019.23	Acquisition Time (sec)	2.7263	Spectrum Offset (Hz)	3743.7068
Spectrum Type	STANDARD	Sweep Width (Hz)	12019.05	Temperature (degree C)	23.567		

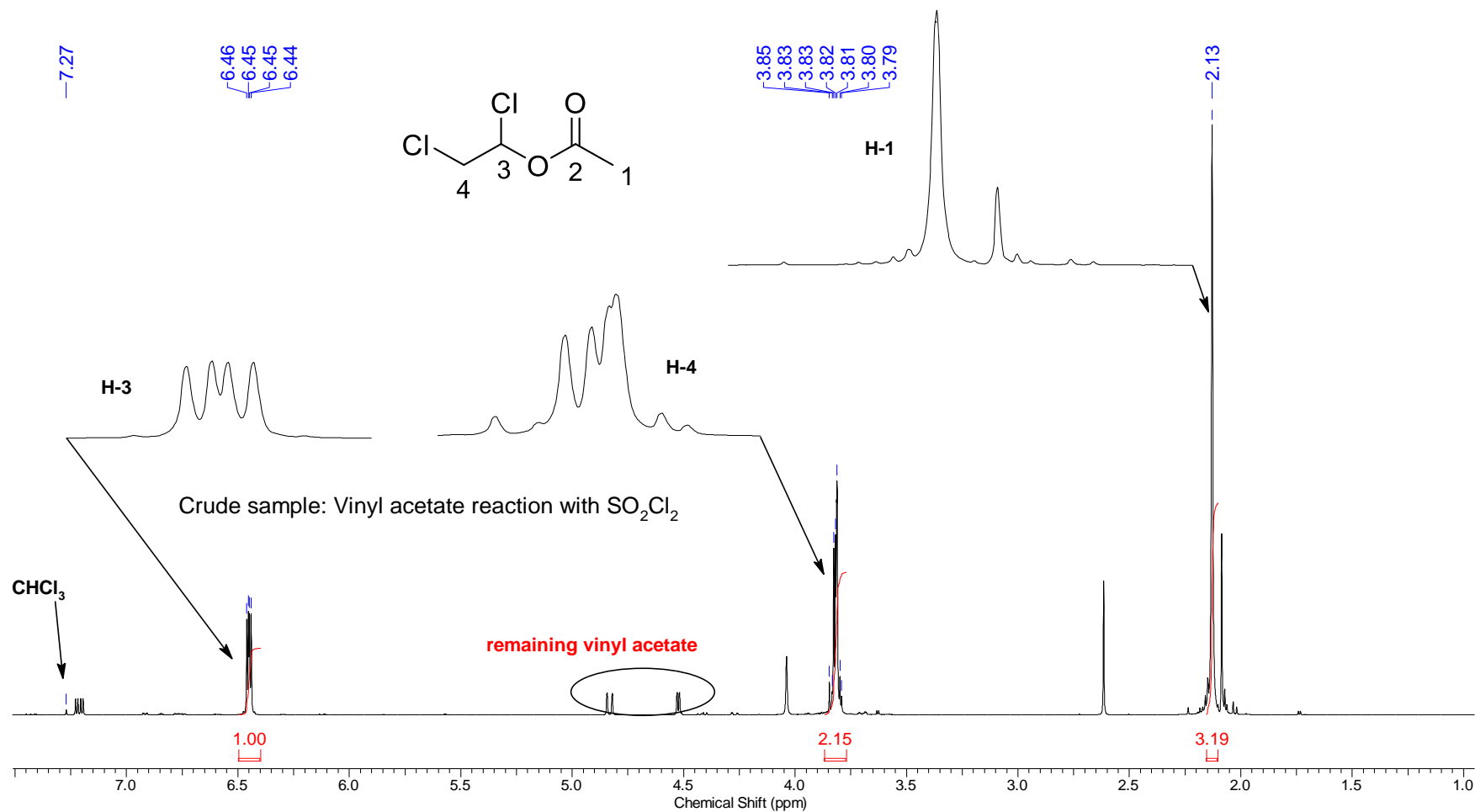


Flow Chemistry Applied to Hazardous Reactions, and Fluorophores Synthesis with Photophysics Studies

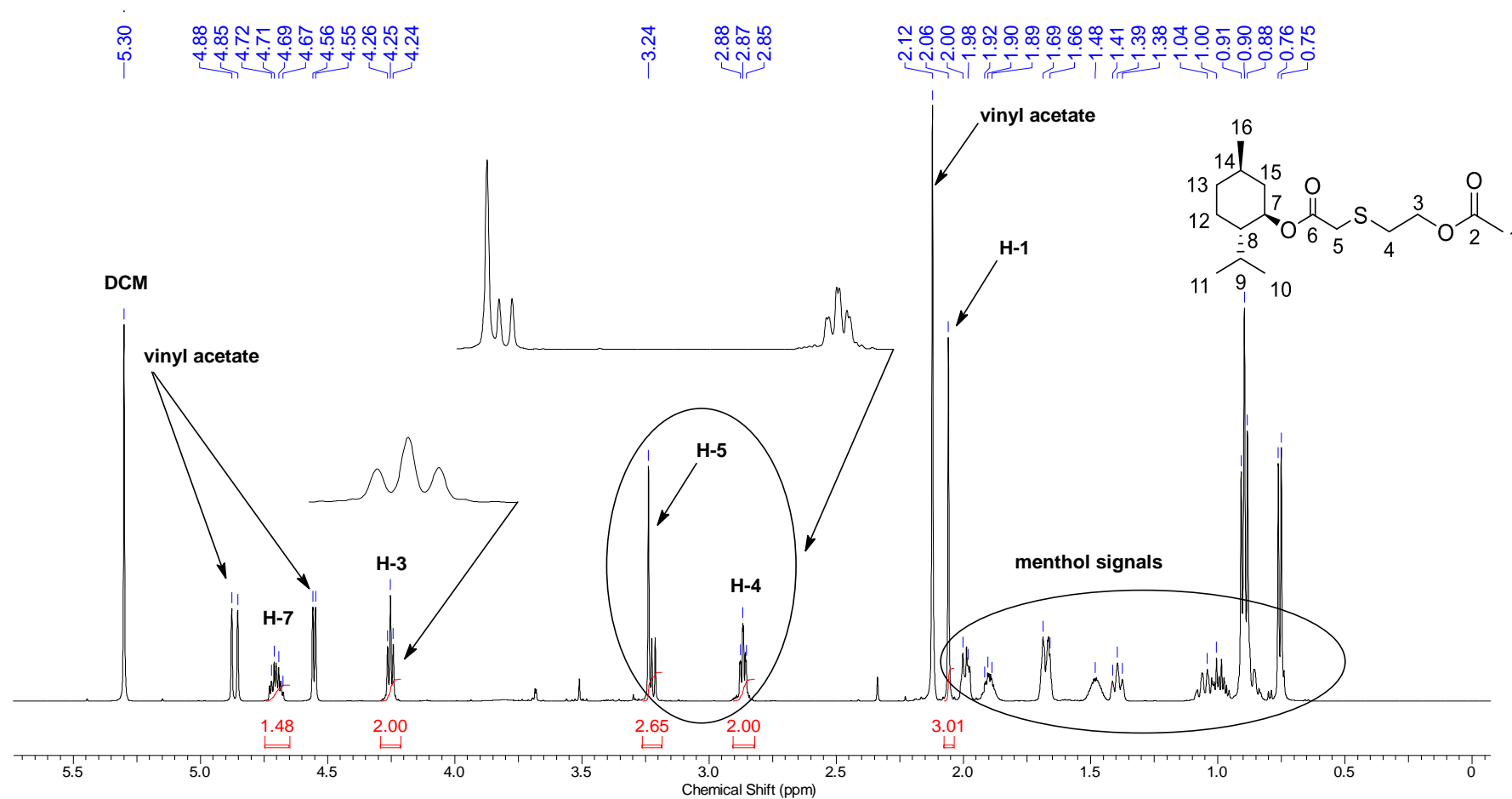
Frequency (MHz)	150.87	Nucleus	¹³ C	Number of Transients	300	Origin	spect
Original Points Count	32768	Owner	nmrsu	Points Count	32768	Pulse Sequence	zgpg30
Receiver Gain	199.73	SW(cyclical) (Hz)	36231.88	Acquisition Time (sec)	0.9044	Spectrum Offset (Hz)	15081.8369
Spectrum Type	STANDARD	Sweep Width (Hz)	36230.78	Temperature (degree C)	25.253		



Frequency (MHz)	599.96	Nucleus	¹ H	Number of Transients	16	Origin	spect
Original Points Count	32768	Owner	nmrslu	Points Count	65536	Pulse Sequence	zg30
Receiver Gain	20.16	SW(cyclical) (Hz)	12019.23	Acquisition Time (sec)	2.7263	Spectrum Offset (Hz)	3695.6599
Spectrum Type	STANDARD	Sweep Width (Hz)	12019.05	Temperature (degree C)	23.091		



Frequency (MHz)	599.96	Nucleus	1H	Number of Transients	16	Origin	spect
Original Points Count	32768	Owner	nmrsu	Points Count	65536	Pulse Sequence	zg30
Receiver Gain	9.89	SW(cyclical) (Hz)	12019.23	Acquisition Time (sec)	2.7263	Spectrum Offset (Hz)	3714.6445
Spectrum Type	STANDARD	Sweep Width (Hz)	12019.05	Temperature (degree C)	23.228		



PART 2

FLUOROPHORES SYNTHESIS WITH PHOTOPHYSICS STUDIES

Part of the “Introduction”, “Results and Discussion” and “Experimental Section” are reproduced with permission from **DE SOUZA, J. M.**; ABDIAJ, I.; CHEN, J.; HANSON, K.; DE OLIVEIRA, K. T.; MCQUADE, D. T. “Increasing Scope of Clickable Fluorophores: Electrophilic Substitution of Ylidenemalononitriles” *J. Org. Chem.* **2020**, 85, 18, 11822–11834. Copyright 2020 American Chemical Society.

and

Reproduced from **DE SOUZA, J. M.**; ABDIAJ, I.; CHEN, J.; DE OLIVEIRA, K. T.; HANSON, K.; MCQUADE, D. T. “Synthesis of multi-substituted pyridines from ylidenemalononitriles and their emission properties” *Org. Biomol. Chem.* **2021**, 19, 1991-1999, with permission from the Royal Society of Chemistry.

INTRODUCTION

1. Introduction

1.1. Fluorophores Synthesis with Photophysics Studies

1.1.1. Basic Concepts

Regarding molecular organic photochemistry, two general concepts must be mentioned: (i) Photophysics of organic compounds and (ii) its Photochemistry. The former corresponds to the interactions of light with organic molecules that result in physical changes. The latter results in chemical modifications, as discussed in the Part 1 for the photooxygenation reactions (Figure 1).¹²⁷

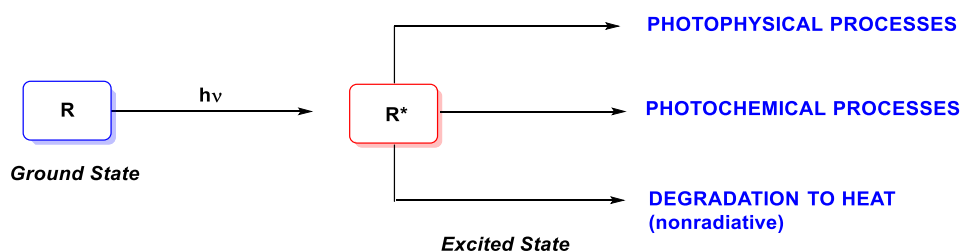


Figure 1. General concepts regarding molecular organic photochemistry.

Fluorophores are molecules capable of absorbing light energy in specific wavelengths and releasing this energy at longer wavelengths (Figure 2). Any parameters related to this process such as quantum yield, decay times and others depend on the fluorophore structure and its chemical environment. Excitation energies range from UV through the visible light, and emission energies can continue from visible light into the near infrared region.

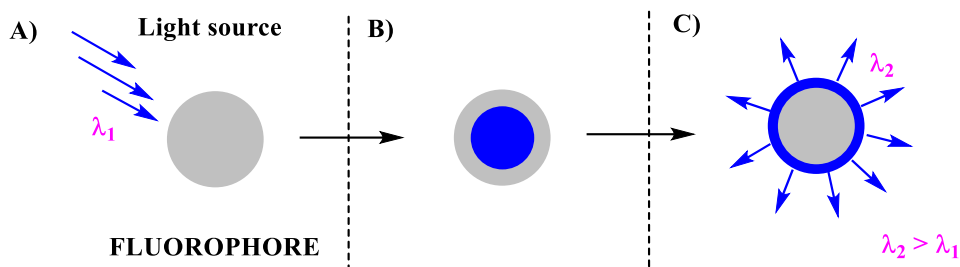


Figure 2. Absorption and emission of light by fluorophores.

To better understand photophysical processes, one must consider how the electrons from the molecules behave in the presence of suitable light sources. When the molecule in its singlet state (S) absorbs energy through electromagnetic radiation, one of its electrons moves to a higher energy level (${}^1A \rightarrow {}^1A^*$, Figure 3). In this case, an allowed transition occurs and the spin number is conserved. Energy is lost by vibrational relaxation and internal conversion while maintaining the same spin (non-radiative processes). There are two additional alternatives to release the absorbed energy: emission by fluorescence or by phosphorescence process.

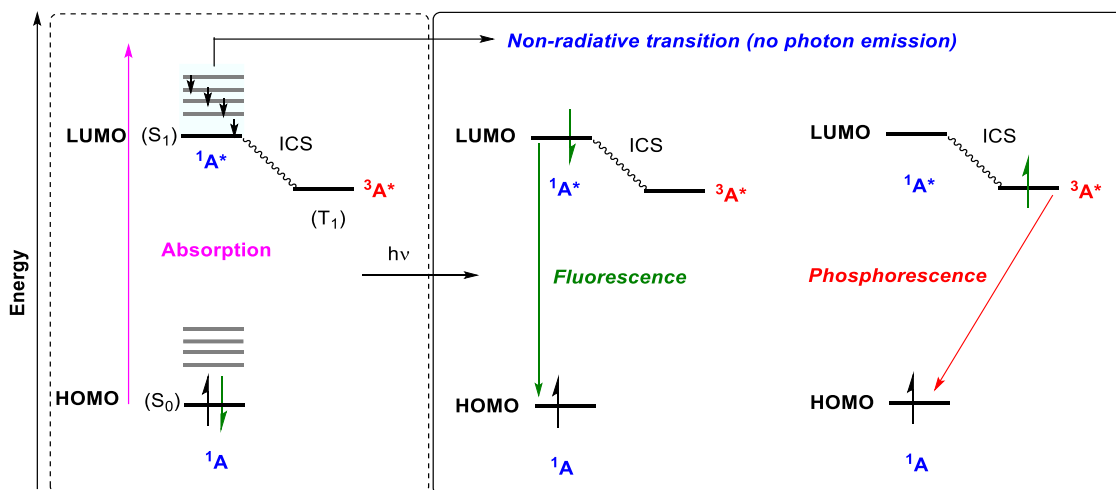


Figure 3. Jablonski Diagram – difference between fluorescence and phosphorescence.

Fluorescence is the light emitted when the excited specie (${}^1A^*$) relaxes to its ground electronic level (${}^1A^* \rightarrow {}^1A$, Figure 3). In this case, the excited state lasts mere nanoseconds. In the phosphorescence process, excitation happens in the same manner as

fluorescence. When the molecule reaches the S_1 singlet state, intersystem crossing (ISC) can occur since the T_1 triplet state is energetically more favorable than S_1 ($^1A^* \rightarrow ^3A^*$, Figure 3). Like the internal conversion, ISC also involves an electronic transition between two excited states. However, ISC is associated with a spin inversion from singlet to triplet. The ISC process is described as a "spin-forbidden" transition. This explains why phosphorescent molecules do not re-emit absorbed radiation immediately. Phosphorescence emission happens commonly around 10^{-8} sec and, in some cases, can be observed several hours after the original excitation.¹²⁸

1.1.2. A Brief History Regarding Fluorescence

Fluorescence was first reported in 1565 by Nicolás Monardes as the blue coloration of the infusion of a Mexican medicinal wood, known as *Lignum nephriticum* (from Latin, meaning "kidney wood").¹²⁹ It is obtained from the wood of two different tree species, *Eysenhardtia polystachya* and *Pterocarpus indicus*. Monardes' publication was based on a Franciscan missionary's accounts from 1560, Bernardino de Sahagun. The missionary described how the Aztecs prepared pain relievers by adding water to the wood. This mixture presented an intriguing bluish color when exposed to the sunlight. Several years hence, A. Ulises Acuna and co-workers demonstrated that the original blue color observed by the Aztecs corresponds to a product from flavonoids oxidation found in this wood. This fluorescent compound is known as Matlaline (**1**) (from Matlali, Aztec word meaning blue)¹³⁰ (Figure 4).

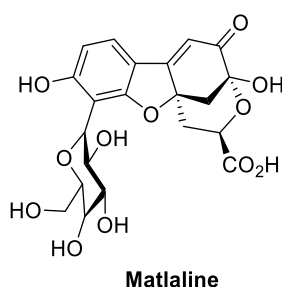


Figure 4. Matlaline, the fluorescent substance in the wood of the tree *Eysenhardtia polystachya*.

Indeed, Monardes' writings attracted the attention of many people. Popularity of fluorescence increased as observations of this kind were reported over the years.¹³¹ It was only in 1852 a name was given to this interesting phenomenon. Sir George Gabriel Stokes, a mathematics professor at the University of Cambridge, noticed the color-changing effects in fluorspar, the mineral form of CaF_2 . Prior to this, other fluoride minerals were reported to present this phenomenon under UV light irradiation. Today it is known to be caused due to certain impurities in the crystal such as traces of metals like divalent europium, yttrium, ytterbium, or even organic matter.¹³²

Stokes described the ability of fluorspar and uranium glass to change invisible ultraviolet light into visible blue light. Initially, Stokes called this phenomenon “dispersive reflection”, which implies the reflection to a different wavelength. As a footnote in his publication he wrote: “*I confess that I do not like this term. I am almost inclined to coin a word, and call the appearance **fluorescence**, from fluor-spar, as the analogous term opalescence is derived from the name of a mineral.*”¹³³

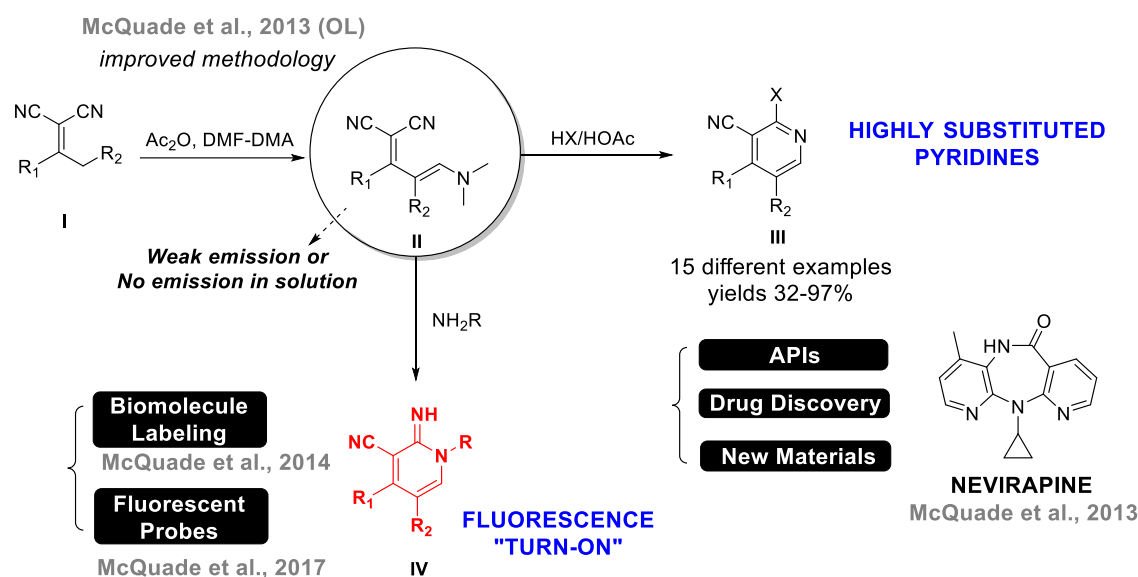
Nowadays, Stokes is considered the “Father of Fluorescence”. He contributed much more to the field than simply naming it. He was the first to propose that the phenomenon observed by many was not related to reflection or refraction of the light, but the absorption of light by the studied material followed by the emission of a different wavelength. He made use of a prism to disperse the solar light before irradiating the sample. He noticed fluorescence was not observed in all wavelengths, only in the ultraviolet region. Stokes also affirmed that the emission was of longer wavelength than the exciting light. That is why the displacement between the maximum absorption and emission bands is called Stokes shift; it was named in his honor.¹³⁴

1.1.3. Applications of Fluorescent Molecules

Fluorescence popularity has increased considerably in the last two decades. Developments of highly sophisticated probes have been directed toward chemical, physical and life science matters. Due to its extraordinary sensitivity, fluorescence has been used in many biochemical applications as a tool to image and label biological materials. This technique supports investigations into the structure and dynamics of nucleic acids, proteins, and other biological macromolecules.¹³⁵

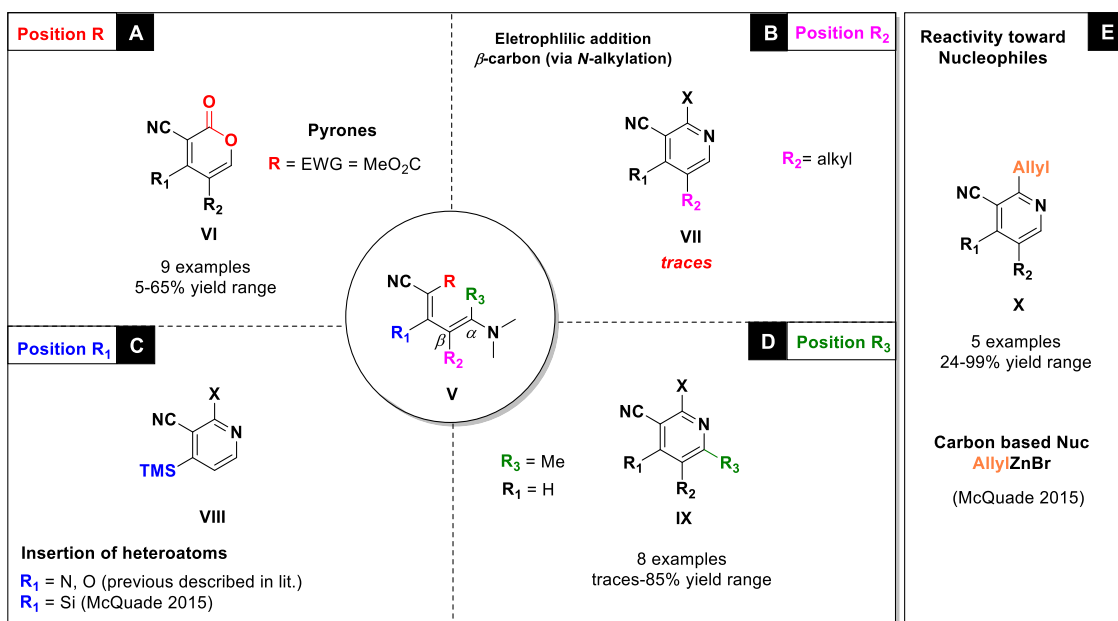
1.1.4. Synthesis of Ylidenemalononitriles (YMs)

Ylidenemalononitrile (YM, **II** Scheme 1) derivatives are versatile intermediates that facilitate the synthesis of multi-substituted heterocycles (pyridines and pyrones) and fluorescent amidine-based probes.^{136,137,138,139} Despite these promising features, YMs suffer a few limitations that hinder their use as universal pyridine/pyrone intermediates and prevent their broad use as reactive luminescent probes. While these two applications may seem unrelated, they are associated via access to multi-substituted YMs (Scheme 1).



Scheme 1. Previous reports overview.

Previously, McQuade's group described YM synthesis methods and applications that yielded unique fluorophores, located low-cost routes to Nevirapine¹³⁷ and provided access to a wide range of substituted pyridines and pyrones.¹⁴⁰ While these approaches produce a broad scope, their methods were still limited without efficient procedures for functionalizing the R₂-position (Scheme 2).



B, C and D: X = halogen; Bronsted-Lowry acids cyclization methodologies.

Scheme 2. Overview of different substitutions of YM and their position once cyclized.

In 2015 it was demonstrated that YMs and ester variants react with both electrophiles and nucleophiles to yield pyridines or pyrones.¹⁴⁰ YMs (**V**) where all the positions except **R**₂ (Scheme 2) were described. First, it was shown (Scheme 2A) that swapping one cyano group (**R** group) with an ester provided α -pyrones upon cyclization instead of a pyridine. Exploring this position in great detail is still necessary, the results illustrate that this position is modifiable and leads to useful products. McQuade and others have demonstrated that **R**₁ is readily varied with aryl, alkyl groups as well as heteroatoms such as *N*, *O* and *Si* (Scheme 2C). The aryl and alkyl variations are derived from non-symmetric methyl ketones and the silyl examples are obtained from acylsilanes. The *N*- and *O*- variations are accessed from more complex approaches to **V**.¹⁴¹ The **R**₃ position is also readily varied using DMF-DMA analogs such as those described by AstraZeneca (Scheme 2D).¹³⁸ Variations at the 2-position can also be achieved by cyclizing **V** via Pinner or nucleophilic additions (Scheme 2E). **R**₂ represents a challenge because the simplest approach to these YMs is substituting ketones that exhibit poor selectivity and low yields when condensed with malononitrile and DMF-DMA. If a new approach to

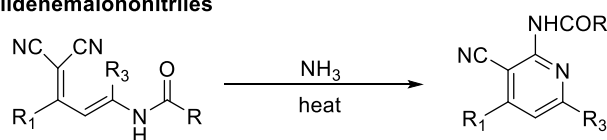
functionalizing R₂ was identified, a more universal approach to α -pyrones, pyridines and amidines might be achieved.

Treatment of YMs (R₂ = H) with allyl bromide yielded trace amounts of pyridines with an allyl group in the R₂ position (Scheme 2B).¹⁴⁰ McQuade et al. proposed an aza-Claisen rearrangement and concluded that electrophiles react with the nitrogen on the dimethylamine moiety. Oddly when the R-position (V) contained an ester, the treatment of this type of ylidene resulted in higher yields of α -pyrones (Scheme 2A). In this case, the ylidenes reacted as if they were enamines. This dichotomy did not make sense at the time and prompted us to reinvestigate electrophile/YM reactivity. In the work shown in Part 2, we elected to use stronger electrophiles than allyl bromide and *N*-chlorosuccinimide and Aryl/Alkyl-S-Cl species were selected.

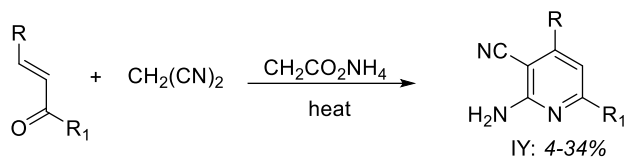
1.1.5. Synthesis of pyridines from ylidene malonitriles

Pyridine substructures are important features in many bioactive substances.¹⁴² Nicotinonitriles are common precursors in syntheses leading to pyridine-containing structures. In particular, amino-nicotinonitriles (aka 3-cyano-2-aminopyridines) are very common. Scheme 3 illustrates some of the most relevant methods used to prepare 3-cyano-2-aminopyridines. Two general approaches are used to produce 3-cyano-2-aminopyridines: (1) methods that modify 3-cyano-2-halopyridines¹⁴³ and (2) methods that build the pyridine from an acyclic precursor.^{144,145,146} Scheme 3 features a few examples where acyclic precursors were used to produce a variety of cyclic derivatives. Although numerous methodologies are available, few involve 2, 3, 4 or 2, 3, 4, 5 substituted pyridines that are prevalent in many pyridine-containing species (Scheme 4).

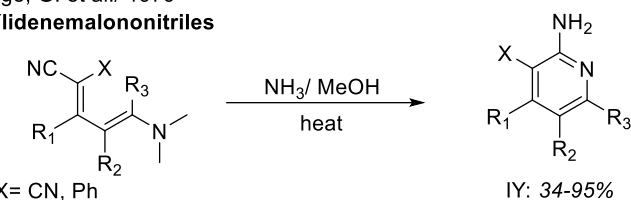
Schmidt, R. R. / 1965

Ylidenemalononitriles

Sakurai, A. and Midorikawa, H. / 1968

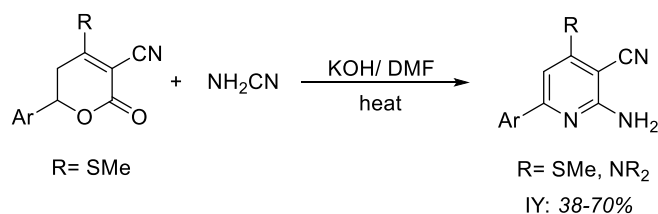
Condensation of malononitrile and ketones

Ege, G. et al. / 1979

Ylidenemalononitriles

X= CN, Ph

Ram, V. J. et al. / 2003

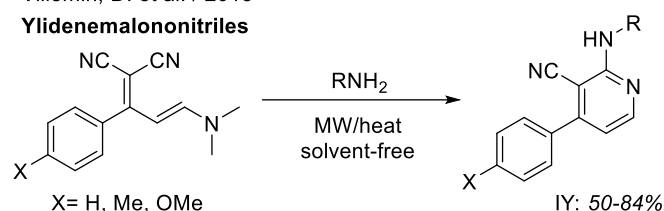
2H-pyran-2-ones

R= SMe

R= SMe, NR₂

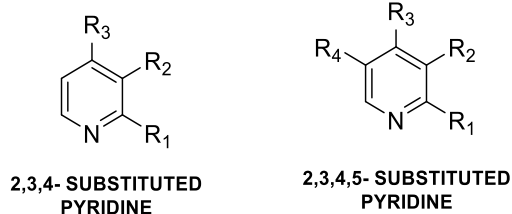
YI: 38-70%

Villemin, D. et al. / 2013

Ylidenemalononitriles

X= H, Me, OMe

YI: 50-84%

Scheme 3. Main methodologies described in the literature to produce 3-cyano-2-aminopyridines.**2,3,4- SUBSTITUTED
PYRIDINE****2,3,4,5- SUBSTITUTED
PYRIDINE****Scheme 4.** Substituted pyridines.

2. Objectives

The main objective was to develop an efficient methodology to achieve the functionalization of YMs at the R₂-position with chlorine (Cl) and sulfur-substituents (S-R). NCS and sulfenyl chloride (RSCl) were selected as the electrophilic species. The resulting R₂-substituted YMs can be used as starting blocks in an additional cyclization step that leads to pyridines or fluorescent amidines, depending on the reaction conditions. These transformations were studied to better understand the difference in the cyclization rate of each substrate toward amidine formation and furthermore, how the variation of the YMs substituents (R₁ and R₂) can provide tunability of their fluorescence colors (λ_{\max}).

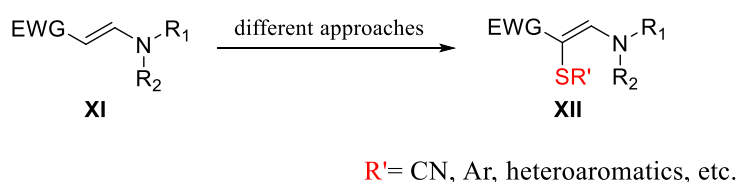
RESULTS AND DISCUSSION

3. Results and Discussion

3.1. Increasing Scope of Clickable Fluorophores: Electrophilic Substitution of Ylidenemalononitriles

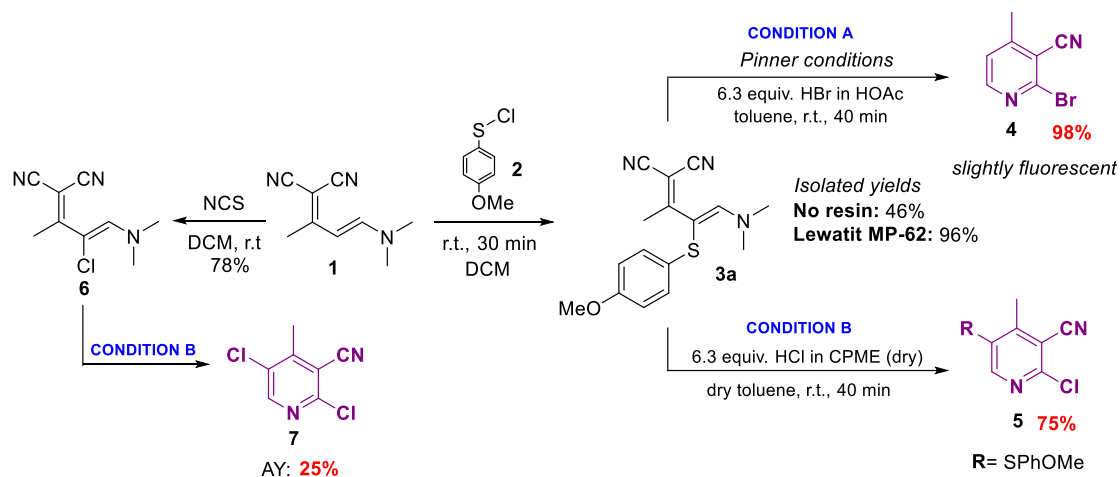
The addition of NCS and Aryl-S-Cl to enamines is known.^{139,147,148} A variety of sulfur-enamine derivatives are described in the literature and produced using different approaches, including electrophilic addition of sulfenyl chloride to enamines (Scheme 5).¹³⁸

Recent literature: **Sulfur Enaminones**



Scheme 5. Recent literature of addition of NCS and Aryl-S-Cl to enamines.

To characterize the reaction between these electrophiles and YMs, we used **1** as a test substrate (Scheme 6). Compound **1** was treated with NCS (1.1 equiv.) in DCM and the solution changed color from light-yellow to dark-yellow. A new compound was isolated in 78% yield and the subsequent ¹H, ¹³C NMR and LC/MS analyses were consistent with compound **6**. A loss of ¹H-couplings associated with enamine portion of the starting material indicated that the chemoselectivity was directed to the enamine portion, however, the regio/diastereoselectivity of the product remained unassigned.



Scheme 6. Exploratory experiments - Better understanding of new substrates behavior under conditions previously established by our group.

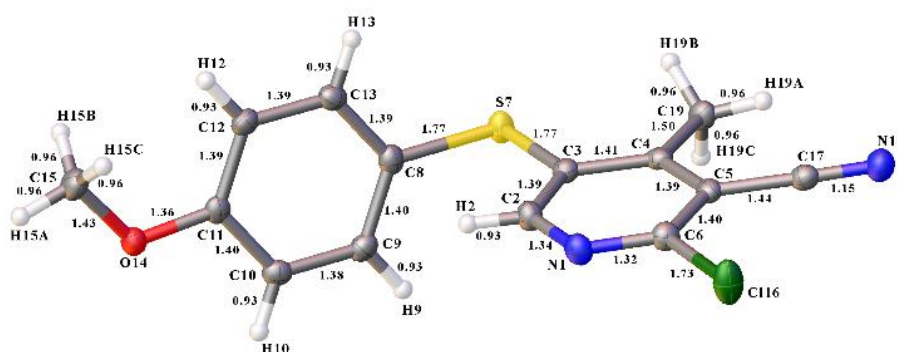


Figure 5. Compound **5** X-ray crystallography.

The identity of **6** was confirmed by X-ray crystallography (Figure 6). The compound crystallizes in an *s-trans* orientation with respect to the two double bonds and appears to be reinforced by a chlorine-H agostic interaction (Figure 5). Compound **6** cyclized to form the pyridine dichloride (**7**) at 25% AY under acid conditions (Scheme 6). Attempts to isolate **7** were met with failure. The important

conclusion from this experiment is that YMs react at the enamine position and undergo addition/elimination selectively.

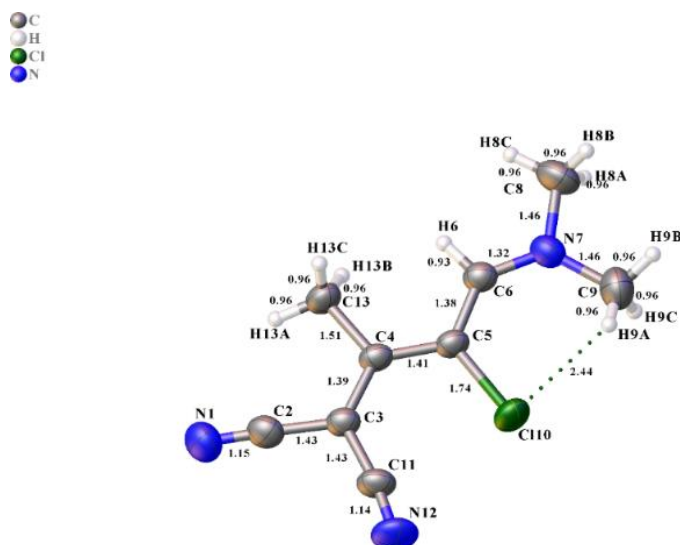


Figure 6. Compound **6** X-ray crystallography – obtained from reaction of **1** with NCS.

We continued testing this enamine-like reactivity model using sulfonyl chloride (R-S-Cl) electrophiles. We were curious if the reactivity pattern would change. Aryl and alkyl sulfonyl chlorides were prepared from the reaction of thiols with NCS or SO_2Cl_2 in DCM. We selected **2** because this material is simple to prepare from the corresponding thiol. The reaction of YM **1** and the sulfonyl chloride **2** yielded a new product which was isolated at 46% yield and characterized as **3a**. Crystallographic analysis confirmed the structure **3a** (Figure 7), demonstrating that YMs react with electrophiles via the enamine fragment and in this case, react at the sulfur position and not the chlorine. Using an acid scavenger (basic resin Lewatit[®] MP-62 free base) during the reaction, it was possible to improve yields of **3a** to 96% IY.

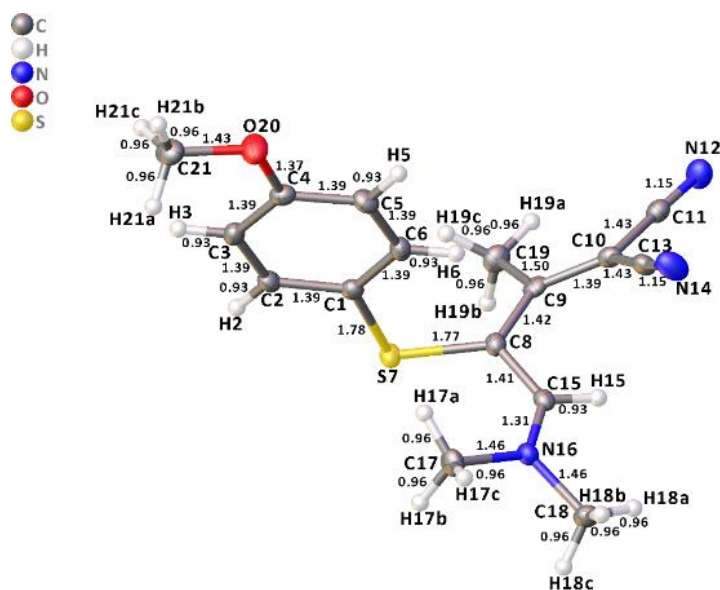


Figure 7. Compound **3a** X-ray crystallography.

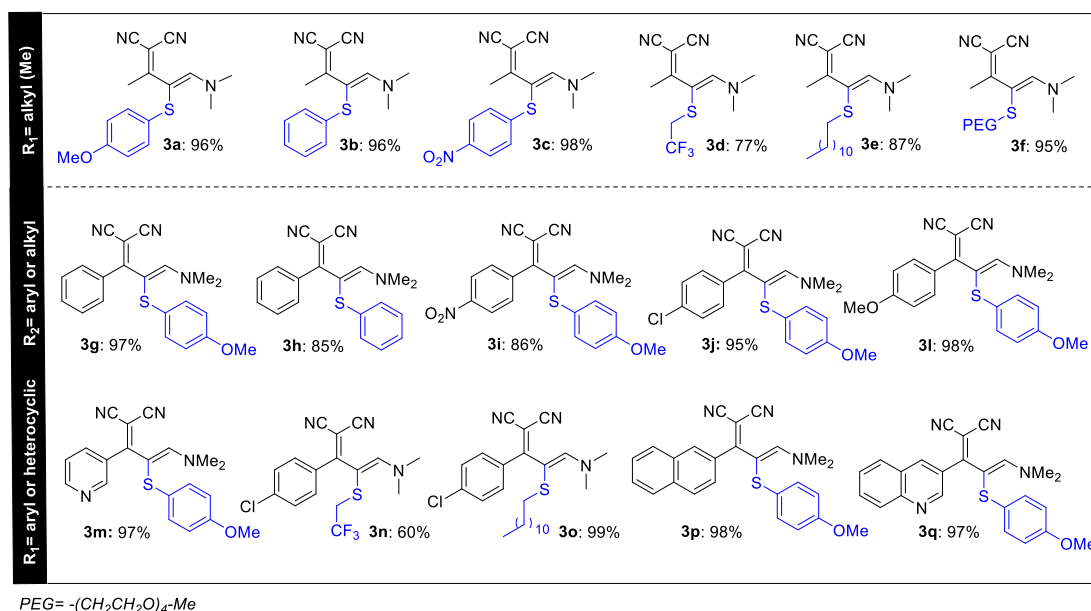
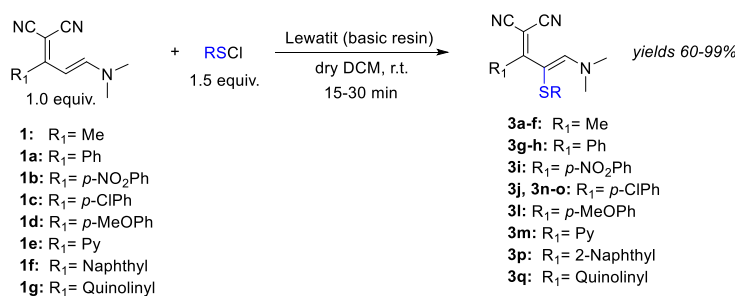
When **3a** was treated under Pinner conditions HBr/AcOH we observed elimination of the *S*-Aryl group giving compound **4** in 98% yield. We produced **4** by cyclizing **1** directly and using the same conditions. However, when HCl in CPME (anhydrous) was used, the desired *S*-substituted pyridine **5** was obtained in 75% yield. We confirmed the structure of **5** via crystallography (Scheme 6).

3.2. Demonstrating the Scope

The conditions to produce sulfur-YMs were applied to a series of different thiols and YMs containing varying R₁ groups (Scheme 7). The one-pot sulfenyl chloride generation is easily observed by the change of color of the reaction mixture from clear/colorless to yellow/orange depending on the thiol. The R-S-Cl was then added to a DCM solution containing the YM **1** at room temperature. Heat generation is observed during addition as well as changes in color. Performing the reaction at 0 °C resulted in decreased yields. We propose that the elevated temperature promotes the proton elimination step that restores the enamine double bond after sulfur addition. For all substrates shown in Scheme 7, fast reaction rates

were observed - between 15 to 30 min to full conversion of starting material to product. This methodology appears robust because all substrates employed had similar behavior under the same reaction conditions. All products shown in Scheme 7 were isolated as brightly colored solids. In some cases, the materials crystallized or solidified slowly (see Experimental Section – Part 2 for X-ray data).

GENERAL REACTION:



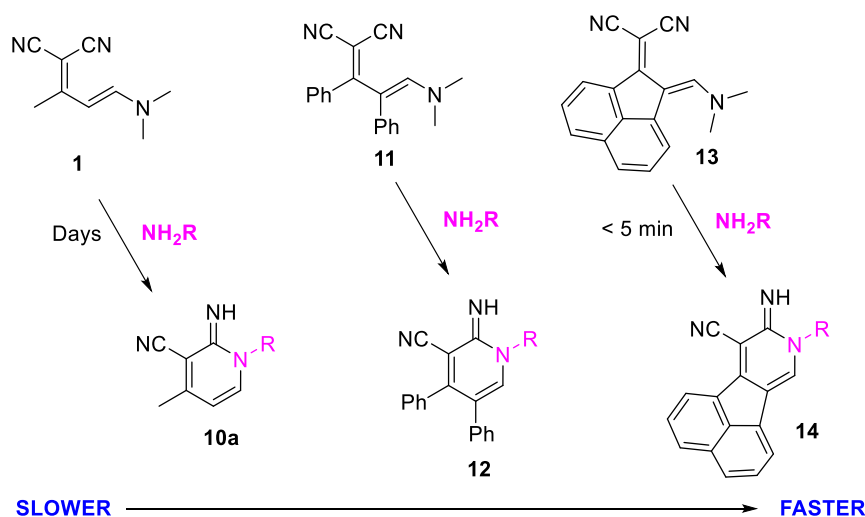
Scheme 7. General reaction and scope of sulfur-ylidenemalononitriles substrates.

For substrates where R₁ = Alkyl and R₂ = *S*-Aryl, **3a–c**, the electronic properties of the aryl group (EDG or EWG) had little impact on the yield. On the other hand, substrates containing R₁ = Alkyl and R₂ = *S*-Alkyl the presence of an EWG such as CF₃ resulted in lower yields (**3d**; 77%). Comparing **3d**, **3e** (85%) and **3f** (95%) suggests that employing more electron withdrawing R₂ substituents negatively affects yield. Similar to compound **3a** (Scheme 7), **3d** also can be

submitted to Pinner cyclization conditions to produce a pyridine product. Envisioning future applications, we prepared **3f** to increase the solubility in polar solvents. As designed, the polyethylene glycol chain increased water solubility (*ca.* 30 mM) of the final product compared to other compounds tested (See Experimental Section/Part 2) (Scheme 7).

After R-S-Cl addition, YMs with R₁=Aryl (**3g–q**) had redder colors than **3a–f**. In solution, products possessing R₁=Alkyl are yellow/orange while R₁=Aryl are red regardless of the sulfur substituent type (alkyl or aryl) in the R₂ position. We observed modest yield fluctuations depending on the R-S-Cl species and the R₁ group. The yield changes are so miniscule that rationalizing the origin of the effect is difficult to quantify. Electron-rich aromatic R-S-Cl species provide higher yields (**3g**, 97%) relative to electron-neutral R-S-Cl species (**3h**, 85%). When the R₁ group is a strongly electron-deficient aryl ring (**3i**) the yield decreases (86%) even when the R-S-Cl species is an electron rich R-S-Cl species (Scheme 7). Compound **3n** presented the lowest yield (60%), however, this only occurred when starting material remained at the end of the reaction (36% was recovered). We did not observe this behavior during **3d** formation. R₁= heteroaromatic (pyridine) and R₁= naphthyl were also tested, corresponding **3m** and **3p**, respectively. The presence of heteroatoms and bulkier aromatic substituents did not change reactivity relative to smaller aromatic groups.

In our previous work¹⁴⁹ we demonstrated that YMs can undergo click-like reactions with primary amines to yield fluorescent molecules (Scheme 8). The resulting cyclic amidines exhibit emission intensities as high as 900-fold greater relative to starting materials. In addition to this strong “turn-on” feature, the fluorescence λ_{max} can be tuned, yielding colors ranging from cyan to orange by varying the substituents. We also observed that structural variation of the YMs changed the cyclization rate (Scheme 8).



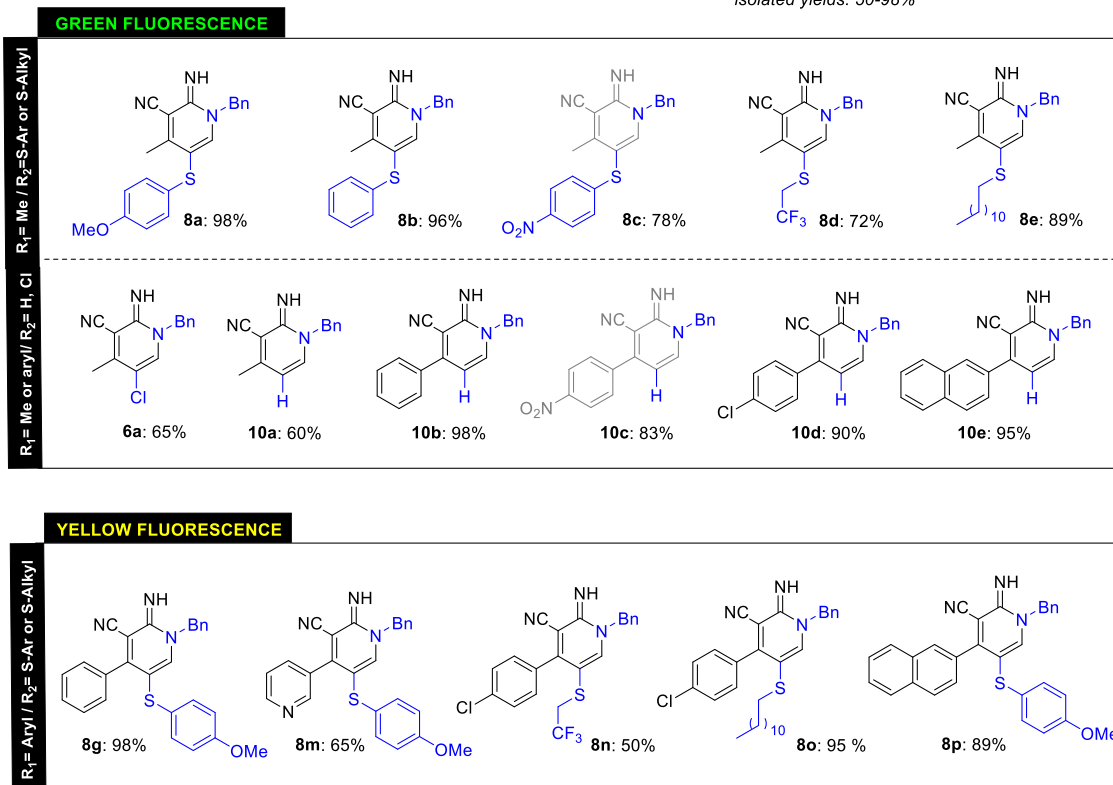
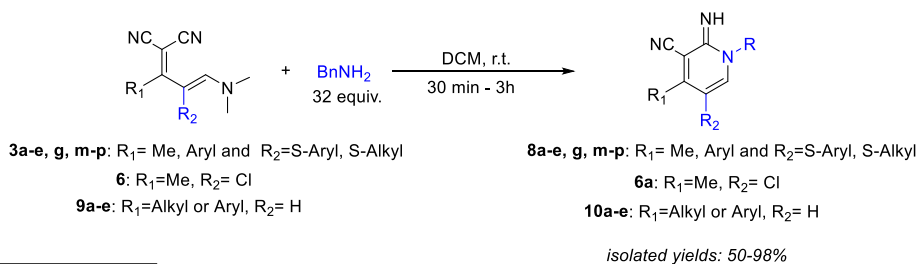
*Reaction concentration 0.1 mmol/0.8 mmol benzylamine (R=Bn) / 1.0 mL CDCl₃.

Scheme 8. “Turn-on” reaction of ylidenemalononitrile enamines **1**, **11** and **13** with primary amines to yield fluorescent molecules.

3.3. Cyclization to Amidine

We reacted the YMs shown in Scheme 7 with benzylamine to determine how well R₂-substituted YMs cyclize to the amidine. Scheme 9 displays the overall reaction and the isolated yields of each amidine. Overall, the amidine cyclization proceeded smoothly for each of the YMs tested. The yields ranged from 50–98%. YMs with electron deficient or small substituents provided lower yields compared to YMs with other patterns.

GENERAL REACTION:



Scheme 9. Green and yellow fluorescent molecules obtained from reaction of benzylamine with ylidene malononitriles (varying R₁ and R₂).

3.4. Photophysical Observations and Measurements

All photophysics measurements were performed by our partners, Jiaqi Chen and Professor Dr. Kenneth Hanson, from the Department of Chemistry & Biochemistry of the Florida State University in Tallahassee, FL, USA.

We observed that the majority of cyclic amidines presented in Scheme 9 are fluorescent where their starting YMs were not. This is consistent with our previous

observations. The interesting feature is that the combination of different R_1 and R_2 groups yielded different λ_{\max} . Figure 8 features a subset of the amidines solutions in NMR tubes being illuminated by 365 nm light. The emission colors range from cyan to yellow. The least substituted amidine (**10a**) has a cyan emission while amidines where either R_1 or R_2 has a smaller substituent are green. Cases where R_1 and R_2 are large have yellow fluorescence suggesting that large adjacent rings may cause distortions to the ring system raising the HOMO.

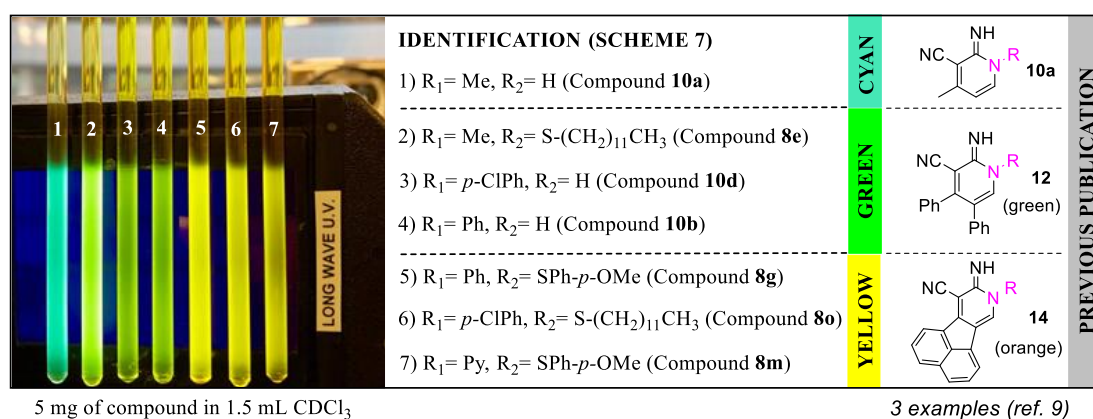


Figure 8. Change of emission color from cyan/green to yellow by R_1 and R_2 variation and comparison with previous work.

Compounds **8c** and **10c** do not follow the observed trends. The starting YMs **3c** and **3i** are unexpectedly not fluorescent. Compounds **8c** and **10c** do not turn-on when cyclized – the compounds show no emission on excitation. Although both structures were solids, we were only able to crystallize **8c**. X-ray crystallographic analysis of the grown crystals provided the structure shown in Figure 9. The cyclic amidine is similar than other amidines where the central amidine ring is flat and each bond length is similar. We attribute the loss of fluorescence to photoelectron transfer between the nitroaromatic group and the amidine ring.¹⁵⁰

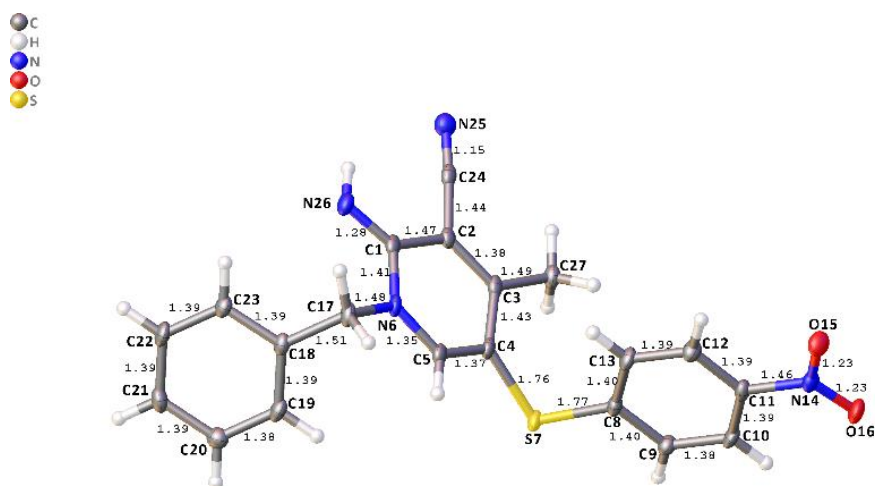


Figure 9. Compound **8c** X-ray crystallography.

We measured absorbance, emission, lifetime and quantum yield data for some of the materials presented in Scheme 9. These are presented in Table 1. The quantum yields range from 4% to 14%. The lowest quantum yields **8d**, **10d**, **8o** all have halides. The highest quantum yield (14%) is from **8e** and is same value as observed for **14** which is interesting because we originally assumed that **14**'s relatively higher yield was due to its rigid acenaphthene ring. The most remarkable feature of the photoluminescence data is the large stokes shifts average 132 nm. Large stokes shifts can be useful for cellular imaging probes because self-quenching tends to be much lower for structures with large stokes shifts.

Table 1. Photophysical properties of **8d-e**, **10d**, **8g** and **8o-p** in DCM in ambient conditions.

Compound	Absorbance λ (nm)	Emission at rt ^a			k_r ($\times 10^7$ s ⁻¹) ^b	k_{nr} ($\times 10^8$ s ⁻¹) ^c
		λ_{\max} (nm)	τ (ns)	Φ_{PL}		
8d	392	527	2.2	0.04	2.0	4.4
8e	397	534	5.7	0.14	2.4	1.5
10d	411	541	1.7	0.03	1.8	5.7
8g	417	548	5.7	0.11	1.9	1.5
8o	419	547	4.2	0.07	1.7	2.2
8p	420	550	4.8	0.09	1.9	1.9

(a) Emission data acquired using dilute solutions and lifetimes calculated from monoexponential fits. (b) $k_r = \Phi/\tau$. (c) $k_{nr} = (1-\Phi)/\tau$.

3.5. Cyclization rate with primary amines

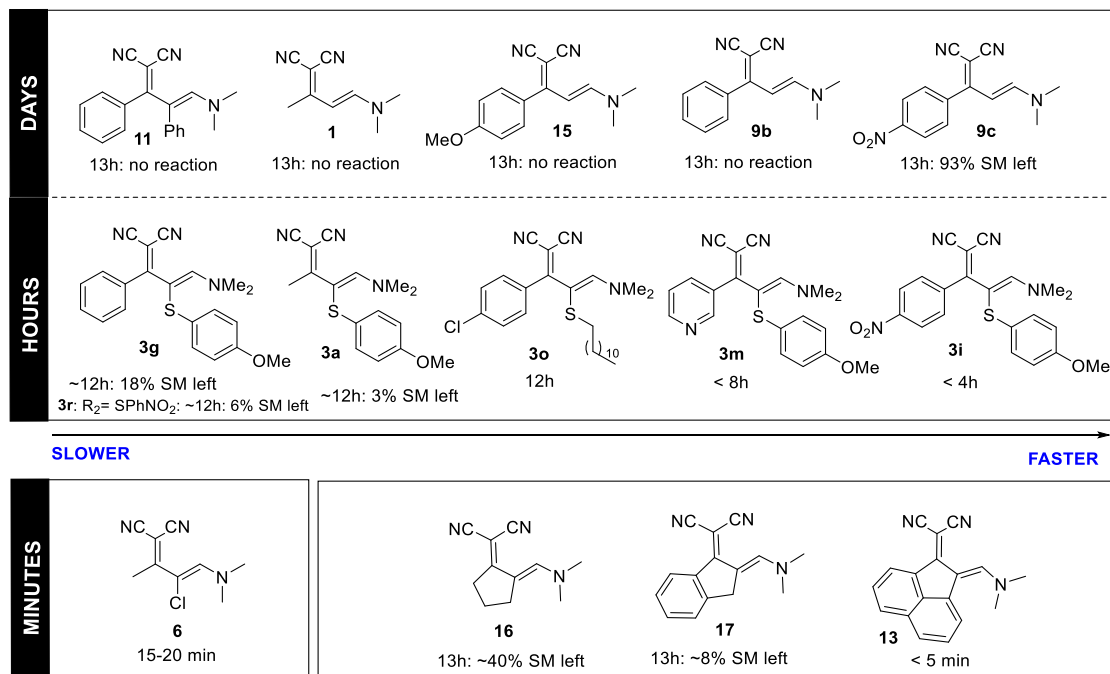
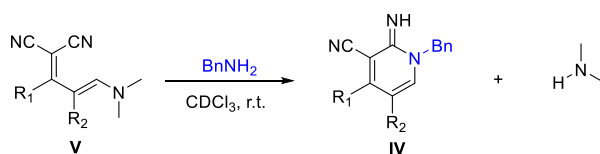
We observed different cyclization rates depending on the substrate (Scheme 8).⁹ The reaction of **13** generating **14** is >100-fold faster than observed with **1** and **11** (Scheme 8). Compound **13** is attractive due to its fast cyclization rate and chromic shift yet is unattractive because the species is not soluble in many solvents including water and polar aprotics. We require an alternative structure that is soluble in polar solvents and cyclizes quickly. While one can speculate that the preorganization of **13** is the key to the fast cyclization rate, we wanted to understand factors that control cyclization rate in more detail. Using the compounds in Scheme 10, we monitored cyclization rate (0.1 mmol YM/1.0 mL CDCl₃ and 8 equiv. of BnNH₂) to increase our understanding of factors that influence cyclization (Scheme 10). YMs with R₂= H (**1**, **11**, **15**, **9b-c**) cyclize over days. After 13 h, no cyclization was observed for **1**, **11**, **15** and **9b** (Scheme 10) and only 7% for **9c** – suggesting that the EWG (NO₂) had a minor accelerating effect.

When R₂=S-Aryl, the cyclization rate increases and full consumption of starting material can be accomplished in hours. Replacement of R₁= Ph (**3g**) by R₁= *p*-NO₂Ph (**3r**) has minimal effect in reaction rate. After 12 h, there is still starting material left, 18% and 6%, respectively.

Compound **3o**, where $R_1 = p\text{-ClPh}$, also provides faster rates compared to **3g** indicating that ring electronics impacts the system when $R_2 = \text{S-Aryl}$. R_1 position containing a pyridine group (**3m**) instead of phenyl (**3g**) results in increased cyclization rates of 8 h and >12 h, respectively. More electron-deficient groups in R_1 such as $p\text{-NO}_2\text{Ph}$ (**3i**) speeds the reaction by reducing the reaction time to less than 4 h. YM **6** possessing $R_2 = \text{halogen (Cl)}$ had the greatest impact in accelerating the reaction with BnNH_2 , reducing the time from days/hours to only minutes (15–20 min). The presence of a highly electronegative atom (Cl) in proximity to the C=C bond makes the carbon that receives the amine attack even more electrophilic, favoring the cyclization.

The X-ray analysis (see Experimental Section – Part 2) shows that YMs containing $R_1 = \text{Alkyl}/R_2 = \text{S-Aryl}$ or $R_1 = \text{Aryl}/R_2 = \text{S-Aryl}$ or S-Alkyl present *s-cis* preferred conformation over *s-trans*. The more stable conformation of YMs possessing $R_1 = \text{Alkyl}$ or Aryl and $R_2 = \text{H}$ or Aryl is *s-trans*. This explains why **3a**, **3g**, **3i**, **3m** and **3o** react faster than **1**, **11**, **15**, **9b** and **9c**.

GENERAL REACTION:



0.1 mmol enamine/ 0.8 mmol benzylamine/ 1.0 mL CDCl₃; SM: starting material

Scheme 10. YMs reaction with benzylamine – understanding how R₁ and R₂ affect the cyclization rates.

Comparing structure **11** and **3g** shows that the sulfur atom also has a role as a “spacer” minimizing repulsion between the R₁ and R₂ groups and thus favoring *s-cis* double-bond conformation. These consequently increase the cyclization rate. Compounds **16**, **17** and **13** (*s-cis*) were used as models to better comprehend other factors that can affect the reaction rate. Compound **16** presents a slower cyclization rate (13 h: *ca.* 40% SM left), while the insertion of a benzo unit fused to the five-member ring in **17** increases the reaction rate (13 h: *ca.* 8% SM left). Considerable differences are observed when two benzo units are fused with the five-member ring, such as in **13** (< 5 min to full SM conversion). Compounds **16** and **17** have no extra stabilization, and their cyclization rate is comparable to the *s-cis* YMs. On the other hand, **13** shows increased conjugation, which efficiently stabilizes

formation of the desired product. In Figure 10, one is able to observe the hypothesized planarity between the rings and the C=C bonds.

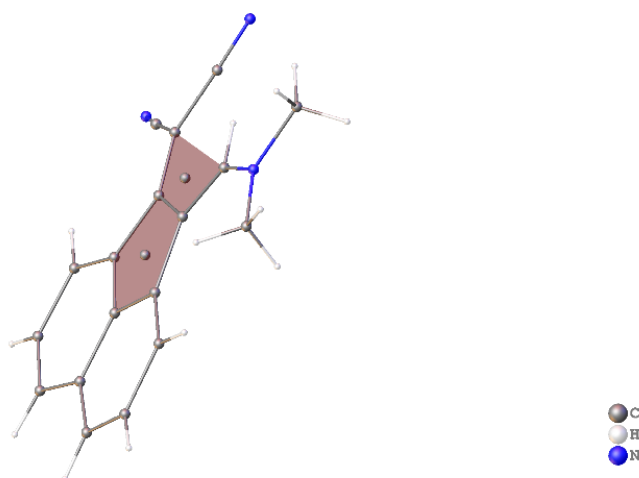


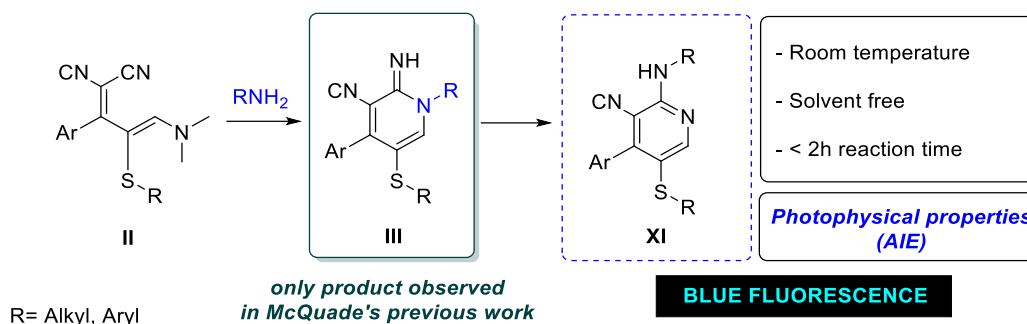
Figure 10. YM 13 planarity representation.

3.6. Pyridine synthesis from YMs

McQuade's group attempts to produce amino-nicotinonitriles using YMs substrates did not coincide with the observation of others.^{146c} When we treated the particular YMs we were studying with primary amines, only structures like **III** were formed (Scheme 11). When we contemplated this contradiction, we observed a number of reaction condition differences such as heat/MW conditions, long reaction times and/or substrate differences. We hypothesized that the fluorescent amidine structures we observed when the YMs reacted with primary amines might be intermediates on the reaction coordinate leading to amino-nicotinonitriles.

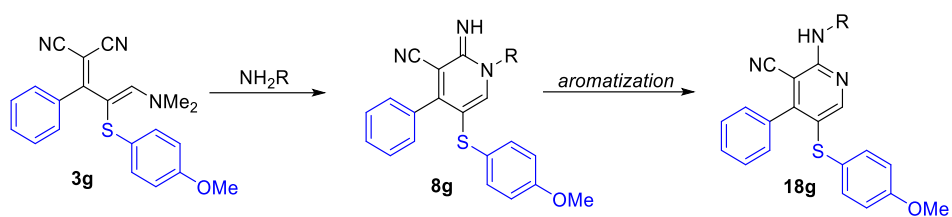
While performing the substrate scope study (Scheme 9), all synthesized YMs produced the expected amidine after reacting with the primary amine. Some of the amidines were unstable however and produced a single amino-pyridine product. Herein, we present these results in detail with a new method for producing multi-substituted pyridines. We provide an example where one of the products exhibits aggregation-

induced emission (AIE), a trait that can have optoelectronic and biological applications (Scheme 11).¹⁵¹



Scheme 11. Facile synthesis of highly substituted pyridines from YMs.

The aforementioned outcome was observed when **3g** reacted with excess primary amine (Scheme 12). We observed initial formation of a product that exhibited yellow fluorescence (**8g**) and the emission spectra transitioned to blue (visual inspection using 365 nm illumination). Monitoring the reaction by TLC revealed that the more polar **8g** transitioned to a single, much less polar specie. LC/MS analysis revealed that the new species had the same mass as the amidine. When we monitored the reaction using ¹H NMR the expected chemical shift for the ring C–H 7.48 ppm shifted downfield to 8.25 ppm. This shift is more consistent with a pyridine (Figure 11, see Experimental Section for detailed NMR analysis). The isolated compound is a solid and crystallization from CHCl₃/hexanes yields slightly yellow colored needle shaped crystals. X-ray crystallographic analysis of **18g** confirmed that the new blue fluorescent species was the amino-nicotinonitrile as suggested by the ¹H NMR shifts (Figure 12).



Scheme 12. Obtention of pyridine **18g** from sulfur-substituted YMs **3g**.

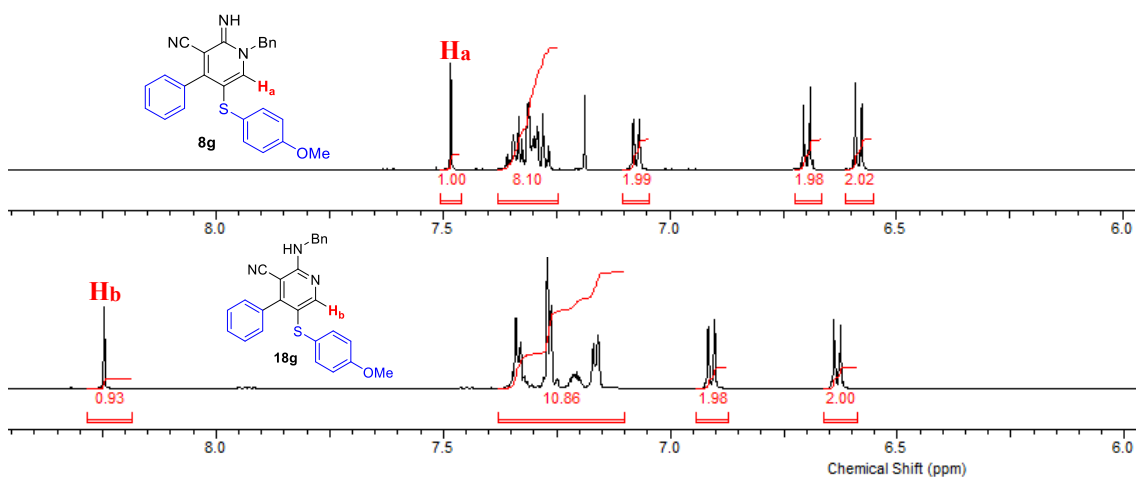


Figure 11. ^1H NMR of amidine **8g** and pyridine **18g** obtained after aromatization.

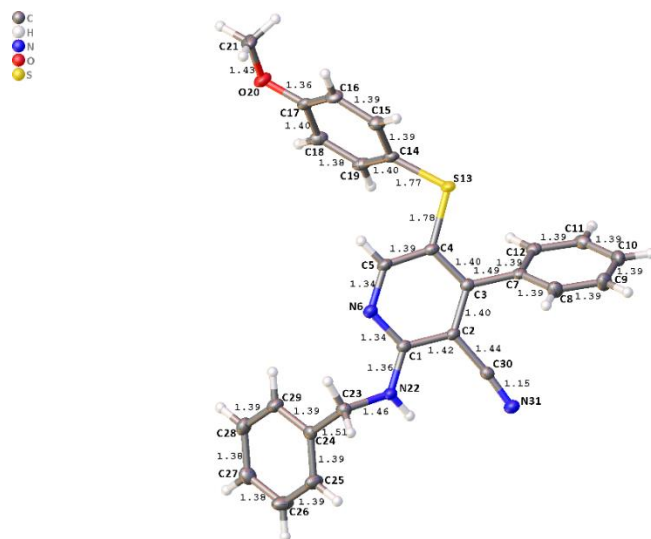
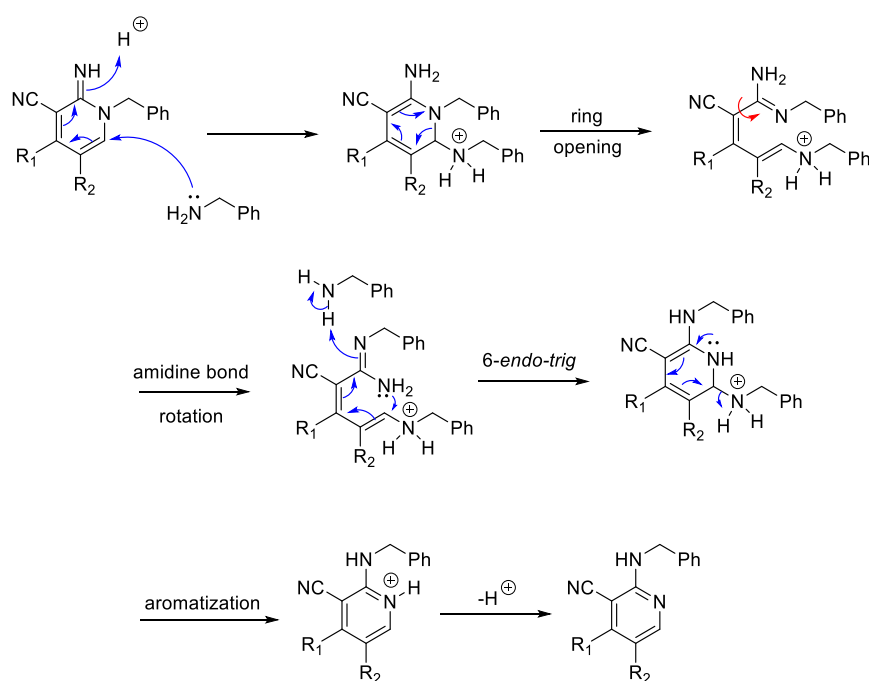


Figure 12. Pyridine **18g** X-ray crystallography.

We believe the aromatization of **8g** to the corresponding amino-pyridine occurs via a Dimroth rearrangement mechanism as described by Odom and co-workers for similar amidine intermediates.¹⁴⁴¹ Their group tested a one-pot synthesis of amino-pyridines under heat conditions (80 °C), starting with different building blocks than YMs. Based on their work, we propose our reaction consists of BnNH₂ attacking the amidine followed by a ring opening. A bond rotation rapidly occurs in order to minimize the repulsion between the two benzyl groups. Then, a 6-*endo-trig* cyclization step, favored by Baldwin's rules, takes place and a final aromatization step with benzylamine elimination produces the observed amino-pyridine (Scheme 13).

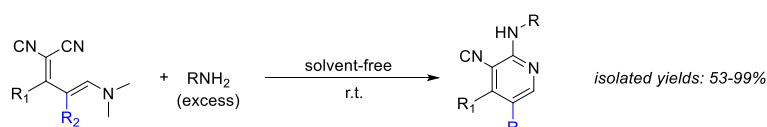
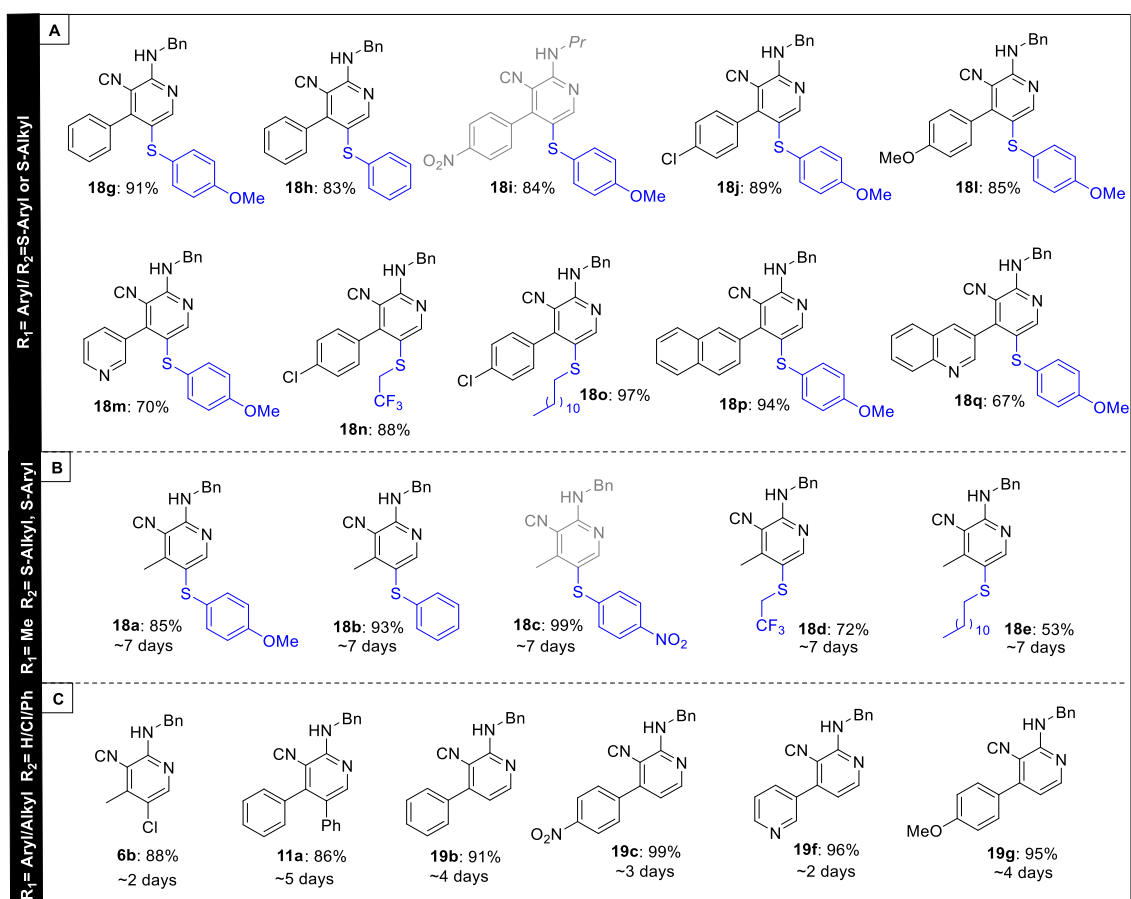


Scheme 13. Proposed mechanism to amino-pyridines formation – Dimroth rearrangement mechanism.

We attempted to reproduce Odom's group conditions with our substrates but no reaction was observed. Some of them did produce trace amounts of the expected amino-pyridines however. Since our substrates present bulky R_2 groups, the steric hinderance between R_2 and the base (in their case, DBU was used) likely retards the reaction. A primary amine does not present the same effect as DBU.

The scheme below reacts some of the YMs possessing R_1 =Aryl and R_2 = S-Aryl (Scheme 14A) and R_1 =Alkyl and R_2 = S-Aryl (Scheme 14B) with excess of benzylamine or propylamine (reagent and solvent) at room temperature. The same was performed on YMs with R_2 = H, Cl, Ph (Scheme 14C). Compounds from **3g–q** react in a matter of 1–2 h to produce the respective amino-pyridines (Scheme 14A). Nevertheless, starting materials shown in Scheme 14B and 14C show extremely slow cyclization/aromatization rate and days are necessary for the full conversion into the desired product.

GENERAL REACTION:

**3a-e:** R_1 = Alkyl, R_2 = S-Alkyl or S-Aryl**3g-q:** R_1 = Aryl, R_2 = S-Alkyl or S-Aryl**6:** R_1 = Me, R_2 = Cl**9b-c, f-g:** R_1 = Alkyl or Aryl, R_2 = H**11:** R_1 = Ph, R_2 = Ph**18a-e:** R_1 = Alkyl, R_2 = S-Alkyl or S-Aryl**18g-q:** R_1 = Aryl, R_2 = S-Alkyl or S-Aryl**6b:** R_1 = Me, R_2 = Cl**19b-c, f-g:** R_1 = Alkyl or Aryl, R_2 = H**11a:** R_1 = Ph, R_2 = Ph

Scheme 14. Amino-pyridines obtained from YMs with varying R_1 and R_2 groups.

During our first experiments not all of the amidines transitioned to the pyridine form. We realized that the extremely slow reaction rates of those specific substrates were the cause. Comparing the structures that remained amidines to those that produced pyridines revealed that those yielding pyridines always featured aryl rings at position R₁ and R₂= S-Aryl or S-Alkyl.

Regarding the electronic effects in Scheme 14A, the increase of the EWG potential from **18g** < **18j** < **18i** shows that electron withdrawing substituents at R₁ position tend to decrease the amino-pyridine yield (91%, 89% and 84%, respectively). The same holds true for substrates **18n** (88%) and **18o** (97%), where the CF₃ group in R₂ position results in lower product yield when compared to a S-Alkyl group. However, comparing **18g** (91%) and **18l** (85%), shows that the presence of an EDW at R₁ (**18l**) does not improve the outcome. Substrates possessing Py substituents at R₁ position **18m** and **18q** presented inferior yields of 70 and 67%, respectively. We believe the reason for this relies on the fact that some impurities from the YM synthesis contributes toward faster YM degradation. Such impurities are not easily removed during purification by column chromatography.

Compounds **18g** (91%) and **18h** (83%) show the presence of EDG at R₂ position ring at **18g**, increases the pyridine yield nearly 10%. Extending conjugation of phenyl group (**18g**) to naphthyl (**18p**, 94%) at R₁ position does not noticeably change the yield (Scheme 14A). In scheme 14B, the opposite effect is observed when R₁= Me instead of aryl. Amino-pyridine yield is positively correlated with increases in EWG potential at R₂ position from **18a** < **18b** < **18c**, 85%, 93% and 99%, respectively. The same behavior is also observed with **18d** (72%) and **18e** (53%), where the more electronegative CF₃ group at R₂ has the greatest effect in the yield over R₂= S-Alkyl.

In Scheme 14C, products **6b** (88%) possessing R₂=Cl present yields about 10% lower than **18c** (99%). This indicates that substituting an electronegative atom directly in the double bond at R₂ position is not advantageous in terms of pyridine yield. When R₂= H, the electronic effect changes when R₁ variation is insignificant. In all instances the amino-pyridines obtained yields are superior to 90%. It appears that EWG favors product formation however. Pyridines **19f** and **19c** for example are obtained in 96% and 99%, respectively.

We measured the photophysical properties for a cross-section of molecules in Scheme 14 and the data are presented in Table 2. In DCM, these compounds exhibit similar blue emission (460–487 nm), excited state lifetimes (2.6–3.1 ns), and quantum yields (0.07–0.16) indicating that the photophysics is primarily dominated by the pyridine core with minimal influence by the aryl substituents (i.e. Cl, OMe, H). The compounds also exhibit a large Stokes shift ($\sim 6,500 \text{ cm}^{-1}$) that is similar to the cyclic amidine analogs.

Table 2. Photophysical properties of **18g**, **18h**, **18j**, and **18m** in DCM in ambient conditions.

Compound	Absorbance λ (nm)	Emission at rt ^a			$k_r (\times 10^7 \text{ s}^{-1})^b$	$k_{nr} (\times 10^8 \text{ s}^{-1})^c$
		λ_{max} (nm)	τ (ns)	ϕ_{PL}		
18g	358	474	3.0	0.09	3.0	3.0
18h	354	460	3.1	0.16	5.2	2.7
18j	358	486	2.6	0.07	2.8	3.6
18m	360	487	3.0	0.08	2.5	3.1

(a) Emission data acquired using dilute solutions and lifetimes calculated from monoexponential fits. (b) $k_r = \phi/\tau$. (c) $k_{nr} = (1-\phi)/\tau$.

Despite having a similar structure to those in Table 2, compound **18i** (highlighted in grey, Scheme 6) was non-emissive in DCM. It is not unusual for nitroaromatics to quench emission via a photoinduced electron transfer (PET).¹⁵² Given that nitroaromatic containing compound **18c** was also non-emissive, a similar mechanism may be active here. Interestingly, in contrast to in solution, crystals of **18i** exhibit yellow-green emission (Figure 13). The lack of emission in dilute solution and strong fluorescence in the solid state is typically described as aggregation-induced emission (AIE).¹⁵³

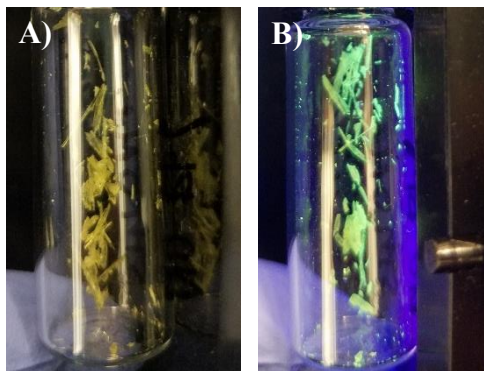
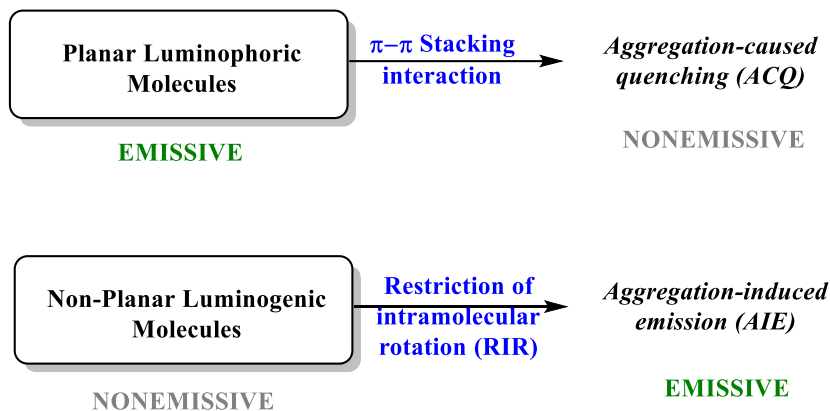


Figure 13. Crystalline samples of **18i** under A) ambient light and B) 365 nm excitation.

This concept of abnormal fluorescent behavior was introduced in 2001. Normally, highly conjugated and aromatic systems tend to lose their fluorescence in higher concentrations, mainly due to the π - π Stacking interaction – Aggregation-caused quenching (ACQ). However, the fluorescence in non-planar luminogenic molecules is only observed when there is restriction of intramolecular rotation (RIR) (Scheme 15).



Scheme 15. Aggregation of different types of molecules and its relation to fluorescence.

From the X-ray crystal structure of **18i** (Figure 14), the nitrobenzene group is nearly perpendicular (79°) to the pyridyl core. This orthogonality reduces electronic communication between the nitroaryl group and the fluorophoric core, which could slow PET, resulting in emission in the solid state. In solution, there is greater rotational freedom and more favorable electronic coupling resulting in PET

quenching. In contrast, for **18c** where the 4-nitrothiophenol substituent cannot be orthogonal to the pyridyl core, PET quenching could still be active in the solid state. Alternatively, the crystal of **18i** may inhibit non-radiative decay through the restriction of intramolecular rotation (RIR). However, if that is the case then it is not clear why RIR would not enhance emission of **18c** in the solid state, nor why **18i** is emissive in solution when a similar rotational deactivation mechanism would be active. Also, worth note from the crystal structure is hydrogen bond interactions between the amino group (NH) and nitrile (CN) between two **18i** molecules (Figure 14). It is unclear what role, if any, excited state proton transfer may play in the unusual phase dependent photophysics of **18i**.

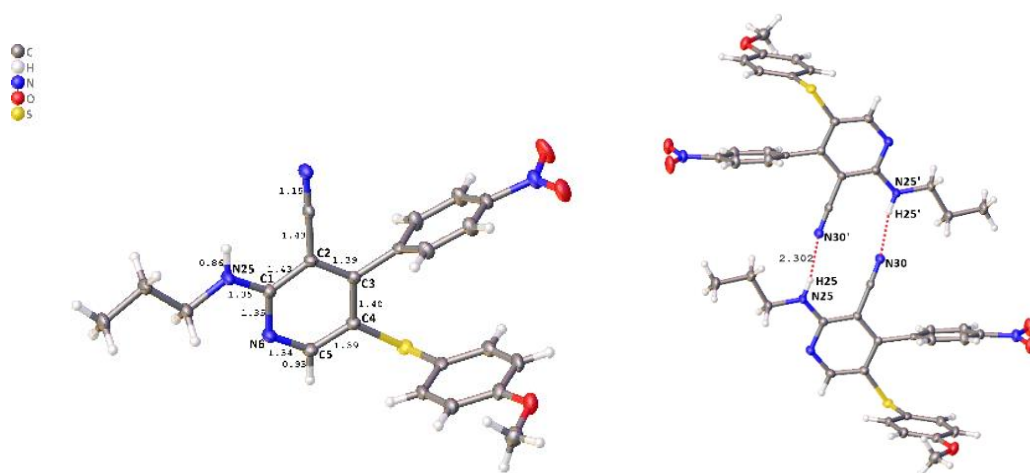


Figure 14. Pyridine **18i** X-ray crystallography – hydrogen bond interaction between amino group (NH) and nitrile (CN).

To gain further insights into the intriguing photophysics of **18i**, we performed solvent dependent emission measurements and the results are shown in Figure 15. Compound **18i** is non-emissive in polar solvents (EtOH, EtOAc, MeCN, DCM) but exhibited yellow-green emission in non-polar solvents (mesitylene, toluene, pentane and hexanes). Worth note is that while the concentrations were similar, the solubility of **18i** decreases from polar to non-polar solvents with obvious particulate formation in pentane and hexanes. The addition of EtOAc to the non-polar solutions resulted in the disappearance of insoluble particles and a complete

loss of fluorescence (Figure 15D). The decreased solubility and increased emission in non-polar solvents further supports an AIE mechanism.

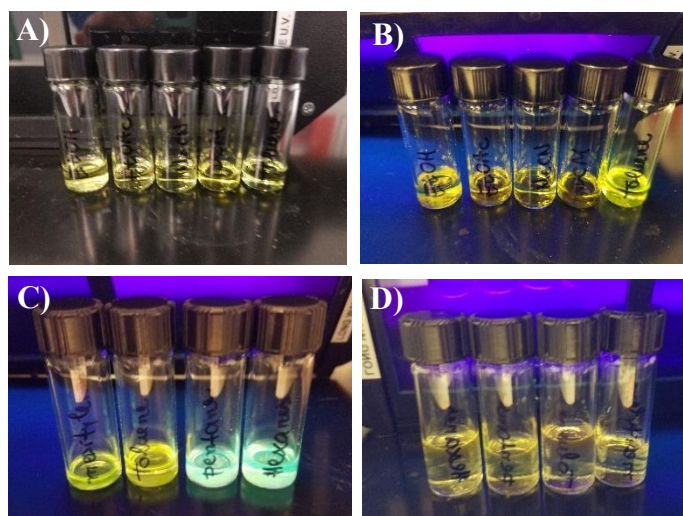


Figure 15. Pyridine **18i** fluorescence in different solvents – A and B) EtOH, EtOAc, MeCN, DCM, toluene (left to right); C) Mesitylene, toluene, pentane and hexanes; D) Same as in C, after addition of EtOAc.

For more quantitative insights into the solvent dependent photophysics, we measured emission spectra for **18i** in ratios of toluene:DCM ranging from 100:0 (100%) to 70:30 (70%) and the results are shown in Figure 16. With solution of < 70% toluene, minimal emission was observed, and the data was omitted. In contrast, from 70% to 90% toluene, there was a subtle blue shift in emission from 610 to 605 nm and a linear increase in emission intensity (see Experimental Section). At > 90% toluene, there was a more pronounced increase in intensity and a further blueshift to 570 nm. These results are consistent with the above observations (i.e. increased aggregation and enhanced emission in non-polar solvents) further supporting an AIE mechanism. In this case the AIE is likely accompanied by polarity dependent solvatochromism.

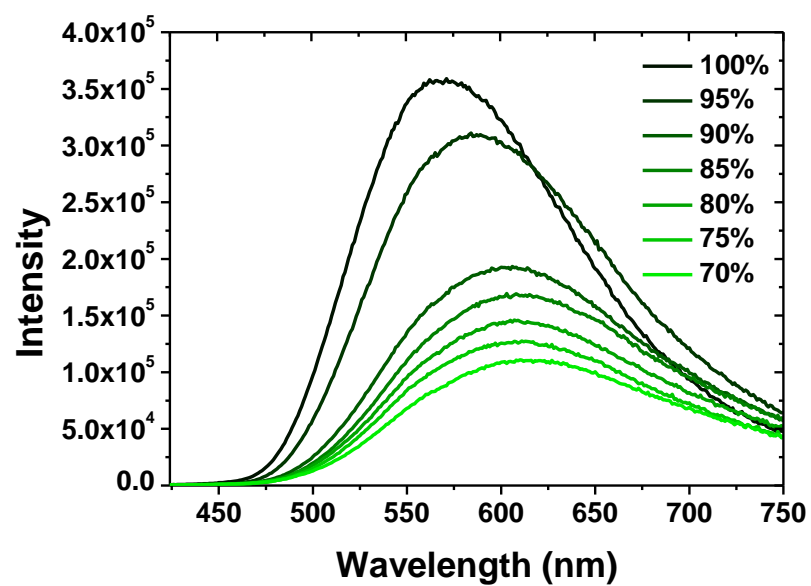


Figure 16. Emission spectra of **18i** in a solution of toluene (from 100% to 70%) and DCM (from 0% to 30%).

4. Conclusions

We developed an efficient and robust methodology for R₂-position functionalization of YMs. Sulfenyl chloride (RSCl) was applied as the electrophilic species in the reaction with the enamine substrates to yield sulfur-substituted YMs. Chlorination at the R₂ position was achieved through the reaction of YM with NCS.

We conducted further cyclization studies with the synthesized substrates to produce fluorescent amidines. During the scope development, we began to understand how different substituents could affect the cyclization rate of YMs with primary amines. We demonstrated that the new fluorescent cyclic amidines emission wavelength can be tuned simply by varying groups R₁ and R₂.

The sulfur-YMs enabled the development of a facile and solvent-free methodology to obtain amino-pyridines in high yields, considerably reduced reaction time with milder conditions than described in the literature. The “locked” *s-cis* conformation of YMs possessing R₁= Aryl and R₂= S-Aryl or S-Alkyl facilitates the rearrangement and aromatization toward amino-pyridines. These results motivate us to continually pursue this chemistry. We intend to obtain fluorescent amidines with a broader wavelength variation as well as the obtention and application of new fluorescent materials.

EXPERIMENTAL SECTION

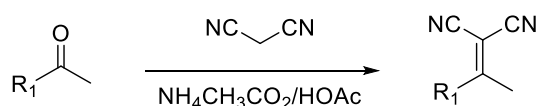
- *PART 2* -

5. Experimental Section

5.1. General Information

All commercially available reagents were purchased from Acros Organics, Sigma Aldrich, TCI or Alfa Aesar and used as received. Thin layered chromatography (TLC) was performed using silica gel 60 F254 plates. Hydrogen and carbon nuclear magnetic resonance (^1H and ^{13}C NMR) spectra were recorded on a Bruker-600 MHz. Chemical shifts are reported in parts per million (ppm) downfield from tetramethylsilane or referenced to residual solvent. Data is represented as follows: chemical shift, multiplicity (br = broad, s = singlet, d = doublet, t = triplet, q = quartet, m = multiplet), coupling constant in Hertz (Hz), integration. HPLC chromatographs were acquired with an Agilent 1260 Infinity system using an Agilent Poroshell 120 EC-C18 column (2.7 μm , 4.6 mm x 50 mm) applying a gradient of 5% MeCN in H_2O to 95% MeCN in H_2O from 0.5 min to 6.5 min at a flow rate of 1.5 mL/min. High resolution mass spectra were obtained through the Virginia Commonwealth University Chemical and Proteomic Mass Spectrometry Core Facility using a Orbitrap Velos mass spectrometer from Thermo Electron Corporation.

5.2. General Procedure for Alkylidene Malononitrile Preparation

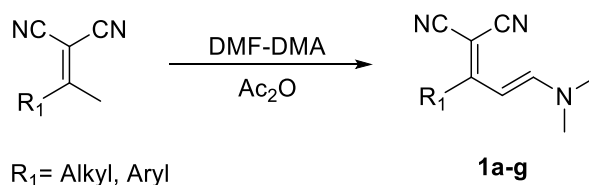


$\text{R}_1 = \text{Alkyl, Aryl}$

It was prepared according to our group's previously reported procedure.¹⁵⁴ Malononitrile (3.17 g, 48 mmol, 1 equiv.), ammonium acetate (0.74 g, 9.60 mmol, 0.2 equiv.), the corresponding ketone (48 mmol, 1 equiv.), acetic acid (3.0 mL, 52.8 mmol, 1.1 equiv), and toluene (30 mL) were added to a 100-mL round-bottom flask. The flask was attached to a Dean-Stark apparatus and heated to reflux for 1–2 h until > 0.8 mL of water was observed in the apparatus. The reaction was removed from heat, cooled to room temperature, and then washed with 3 x 50 mL of saturated NaHCO_3 solution followed by

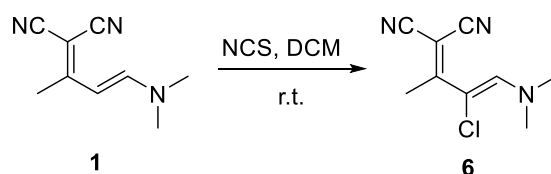
50 mL of water. The organic layer was dried with MgSO_4 and concentrated in vacuo. The resulting solid was recrystallized in EtOH.

5.3. General Procedure for Enamine Preparation



It was prepared according to our group's previously reported procedure.¹⁵⁵ A 50 mL solution of the corresponding alkylidene malononitrile (0.1 M, 1 equiv.) and Ac_2O (0.2 M, 0.095 mL, 0.2 equiv) in anhydrous DCM was prepared. The solution was transferred to a round-bottom flask equipped with a stir bar. DMF-DMA (0.80 mL, 6 mmol, 1.2 equiv.) was added to the reaction while stirring vigorously. After 24 h, the solvent was removed under vacuo. The solvent was evaporated and the product was purified by column chromatography in Hexanes/EtOAc.

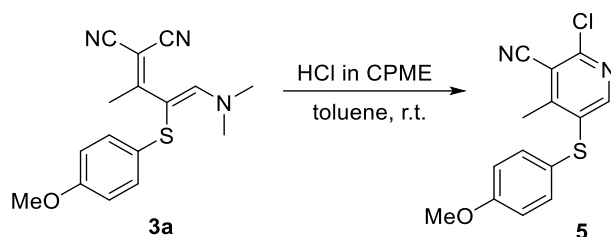
5.4. Procedure for Enamine 1 Reaction with NCS



Enamine **1** (1 mmol, 161.2 mg) and dry DCM (4 mL) was transferred to a 20-mL flask equipped with a stir bar. NCS (146.6 mg, 1.1 mmol, 1.1 equiv.) was added slowly and reaction mixture was kept at room temperature and N_2 atmosphere.* After 30 min, all starting material was consumed and the crude material immediately purified by chromatographic column over silica gel (Hexanes/EtOAc (7:3)). Compound **6** was obtained as a yellow solid in 78% yield (152.6 mg, 0.78 mmol).

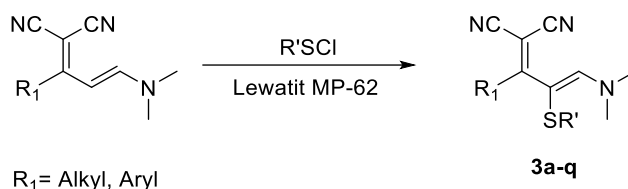
*The solution acquires a darker yellow color immediately after addition. If left under reaction conditions for longer time, it becomes brown due the compound **6** degradation.

5.5. Pinner Conditions for Cyclization of Compound 3a



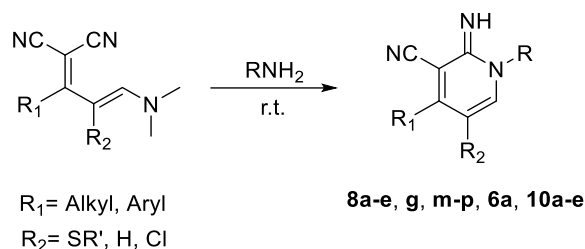
Sulfur-enamine **3a** (1 mmol, 299.4 mg) and 4 mL of dry toluene was transferred to a 20-mL flask equipped with a stir bar under nitrogen atmosphere. After complete solubilization of **3a**, a solution of HCl in CPME 3 M (6.3 equiv.) from a sure-sealed bottle was added dropwise. After 40 min at room temperature, **3a** was completely consumed and pyridine **5** was obtained as a white solid in 75% yield (218.1 mg, 0.75 mmol) after purification by chromatographic column over silica gel (Hexanes/EtOAc).

5.6. General Procedure for Enamine Reaction with R-S-Cl



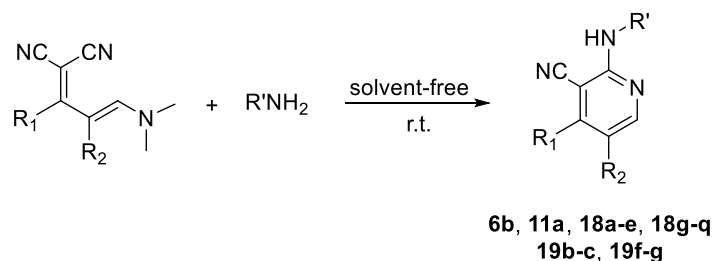
Thiol R'SH (1.5 mmol) was added slowly to a solution of NCS (230 mg, 1.7 mmol, 1.1 equiv.) in dry DCM (2 mL) (Solution A) at room temperature and stirred for 1.5 h. Afterwards, Solution A was added dropwise to a solution of enamine (1 mmol) in dry DCM (2 mL) containing Lewatit[®] MP-62 free base (*ca.* 1.0 g) (Solution B). The mixture was stirred for 30–40 min until no more starting material was observed by TLC. The solvent was evaporated under vacuum and the product was purified by column chromatography using Hexanes/EtOAc as eluent.

5.7. General Procedure for Cyclization with Primary Amines



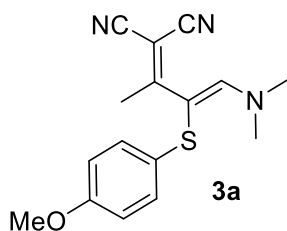
A solution of enamine (1 mmol) in DCM (2 mL) was transferred to a 20-mL flask. The primary amine (benzylamine or propylamine, 32 equiv.) was added to this solution at room temperature and the reaction was stirred vigorously until the enamine was consumed entirely. The reaction was monitored by TLC. The solvent was evaporated under vacuum and the amidine was purified by column chromatography using Hexanes/EtOAc as eluent.

5.8. General Procedure for Pyridines Synthesis from YMs



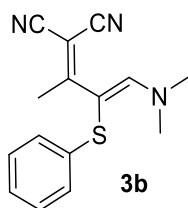
Enamine (1 mmol) was dissolved in 3 mL of benzylamine (or propylamine). The reaction mixture was stirred at room temperature and the starting material consumption was monitored by TLC. After the enamine was consumed entirely, part of the remaining amine was removed under vacuum and the crude mixture containing the amino-pyridine was purified by chromatographic column over silica gel (gradient Hexanes/EtOAc).

5.9. NMR – Product Characterization



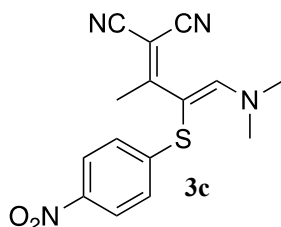
(Z)-2-(4-(dimethylamino)-3-((4-methoxyphenyl)thio)but-3-en-

2-ylidene)malononitrile (3a): It was prepared in accordance to the *General procedure for enamine reaction with R-S-Cl*. Purification by column chromatography in Hexanes/EtOAc starting from 0% to 20% EtOAc provided the desired product in 96% yield (0.57 g, 1.92 mmol). ^1H NMR (600 MHz, Acetone- d_6) δ 7.91 (s, 1H), 7.22–7.04 (m, 2H), 7.01–6.83 (m, 2H), 3.79 (s, 3H), 3.35 (s, 6H), 2.34 (s, 3H); ^{13}C NMR (150 MHz, Acetone- d_6) δ 175.1, 158.2, 156.8, 129.5, 127.1, 116.4, 116.0, 115.0, 93.6, 54.7, 21.6.



(Z)-2-(4-(dimethylamino)-3-(phenylthio)but-3-en-2-

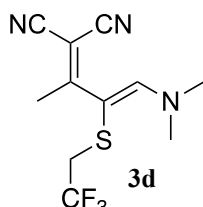
ylidene)malononitrile (3b): It was prepared in accordance to the *General procedure for enamine reaction with R-S-Cl*. Purification by column chromatography in Hexanes/EtOAc starting from 0% to 20% EtOAc provided the desired product in 96% yield (0.52 g, 1.92 mmol). ^1H NMR (600 MHz, CDCl_3) δ 7.69 (s, 1H), 7.34–7.29 (m, 2H), 7.20–7.14 (m, 1H), 7.13–7.08 (m, 2H), 3.28 (s, 6H), 2.35 (s, 3H); ^{13}C NMR (150 MHz, CDCl_3) δ 156.0, 138.6, 129.5, 129.4, 125.5, 125.0, 116.8, 115.7, 93.0, 69.7, 60.4, 22.4.



(Z)-2-(4-(dimethylamino)-3-((4-nitrophenyl)thio)but-3-en-2-

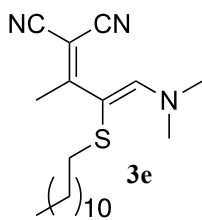
ylidene)malononitrile (3c): It was prepared in accordance to the *General procedure for enamine reaction with R-S-Cl*. Purification by column chromatography in

Hexanes/EtOAc starting from 0% to 20% EtOAc provided the desired product in 98% yield (0.62 g, 1.96 mmol). ^1H NMR (600 MHz, CDCl_3) δ 8.34–8.09 (m, 2H), 7.73 (s, 1H), 7.27–7.05 (m, 2H), 3.29 (s, 6H), 2.34 (s, 3H); ^{13}C NMR (150 MHz, CDCl_3) δ 175.8, 156.4, 148.5, 145.6, 126.4, 124.8, 124.6, 124.5, 124.4, 116.3, 115.2, 90.1, 71.2, 29.6, 22.4.



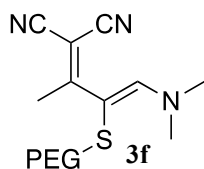
(Z)-2-(4-(dimethylamino)-3-((2,2,2-trifluoroethyl)thio)but-3-en-2-

ylidene)malononitrile (3d): It was prepared in accordance to the *General procedure for enamine reaction with R-S-Cl*. Purification by column chromatography in Hexanes/EtOAc starting from 0% to 20% EtOAc provided the desired product in 77% yield (0.42 g, 1.54 mmol). ^1H NMR (600 MHz, CDCl_3) δ 7.37 (s, 1H), 3.16 (s, 6H), 2.92 (q, $J = 9.9$ Hz, 2H), 2.40 (s, 3H); ^{19}F NMR (565 MHz, CDCl_3) δ -65.36; ^{13}C NMR (150 MHz, CDCl_3) δ 174.8, 155.7, 127.9, 126.1, 124.2, 122.4, 115.5, 115.3, 93.7, 43.9, 39.7, 39.5, 39.3, 39.1, 29.6, 22.6.



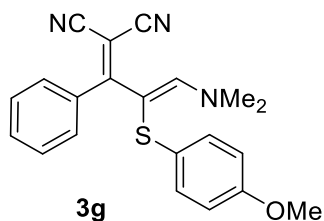
(Z)-2-(4-(dimethylamino)-3-(dodecylthio)but-3-en-2-

ylidene)malononitrile (3e): It was prepared in accordance to the *General procedure for enamine reaction with R-S-Cl*. Purification by column chromatography in Hexanes/EtOAc starting from 0% to 20% EtOAc provided the desired product in 87% yield (0.61 g, 1.74 mmol). ^1H NMR (600 MHz, CDCl_3) δ 7.32 (s, 1H), 3.18 (s, 6H), 2.40 (s, 3H), 2.39–2.28 (m, 2H), 1.46 (d, $J = 7.3$ Hz, 2H), 1.35–1.13 (m, 22H), 0.82 (t, $J = 7.0$ Hz, 3H); ^{13}C NMR (150 MHz, CDCl_3) δ 176.1, 154.3, 116.4, 115.8, 97.4, 69.5, 68.0, 43.7, 37.3, 35.3, 32.6, 31.8, 31.8, 29.5, 29.5, 29.5, 29.5, 29.4, 29.3, 29.3, 29.2, 29.2, 29.1, 29.1, 28.9, 28.8, 28.8, 28.7, 28.6, 28.5, 26.3, 22.7, 22.6, 22.4, 14.0.



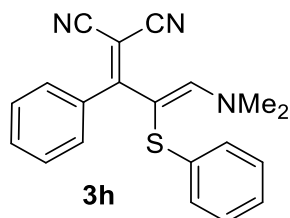
(Z)-2-(15-((dimethylamino)methylene)-2,5,8,11-tetraoxa-14-

thiaheptadecan-16-ylidene)malononitrile (3f): It was prepared in accordance to the *General procedure for enamine reaction with R-S-Cl*. Purification by column chromatography in DCM/MeOH starting from 0% to 10% MeOH provided the desired product in 95% yield (0.73 g, 1.9 mmol). ^1H NMR (600 MHz, CDCl_3) δ 7.34 (s, 1H), 3.65–3.56 (m, 9H), 3.55–3.47 (m, 7H), 3.31 (s, 3H), 3.19 (s, 7H), 2.56 (t, $J = 6.4$ Hz, 2H), 2.41 (s, 3H), 1.56 (s, 3H); ^{13}C NMR (150 MHz, CDCl_3) δ 176.9, 176.2, 154.8, 116.3, 115.8, 96.0, 74.8, 71.8, 71.1, 70.7, 70.6, 70.5, 70.5, 70.5, 70.5, 70.5, 70.4, 70.4, 70.4, 70.2, 69.5, 68.9, 66.9, 64.5, 63.2, 58.9, 36.3, 29.5, 22.6.



(Z)-2-(3-(dimethylamino)-2-((4-methoxyphenyl)thio)-1-

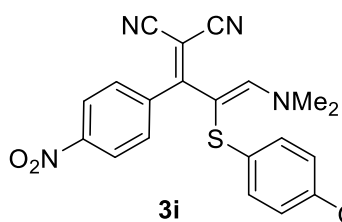
phenylallylidene)malononitrile (3g): It was prepared in accordance to the *General procedure for enamine reaction with R-S-Cl*. Purification by column chromatography in Hexanes/EtOAc starting from 0% to 20% EtOAc provided the desired product in 97% yield (0.70 g, 1.94 mmol). ^1H NMR (600 MHz, Acetone- d_6) δ 7.53 (s, 1H), 7.42–7.32 (m, 1H), 7.27 (s, 1H), 7.24–7.11 (m, 2H), 7.03–6.85 (m, 2H), 6.83–6.67 (m, 2H), 3.65 (s, 3H), 3.22 (s, 6H). ^{13}C NMR (150 MHz, Acetone- d_6) δ 205.2, 205.1, 158.5, 158.3, 137.4, 132.9, 130.5, 129.6, 129.6, 128.8, 128.5, 128.2, 127.8, 116.5, 116.4, 114.7, 114.6, 94.6, 54.7, 54.7, 45.1, 37.1.



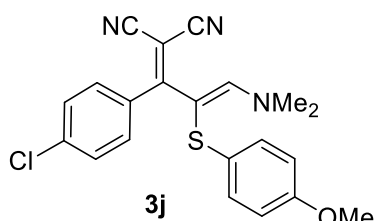
(Z)-2-(3-(dimethylamino)-1-phenyl-2-

(phenylthio)allylidene)malononitrile (3h): It was prepared in accordance to the *General procedure for enamine reaction with R-S-Cl*. Purification by column chromatography in

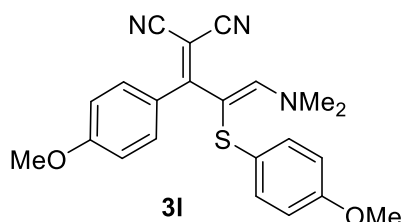
Hexanes/EtOAc starting from 0% to 20% EtOAc provided the desired product in 85% yield (0.56 g, 1.7 mmol). ^1H NMR (600 MHz, CDCl_3) δ 7.41–7.34 (m, 2H), 7.29 (t, $J = 7.6$ Hz, 2H), 7.21 (dd, $J = 8.4, 7.1$ Hz, 2H), 7.19–7.15 (m, 2H), 7.12–7.06 (m, 1H), 7.02–6.97 (m, 2H), 3.19 (s, 6H); ^{13}C NMR (150 MHz, CDCl_3) δ 176.3, 157.5, 138.6, 136.5, 132.0, 130.8, 129.8, 129.4, 129.3, 129.1, 128.3, 125.8, 125.5, 116.5, 116.2, 94.1, 69.5, 28.5.



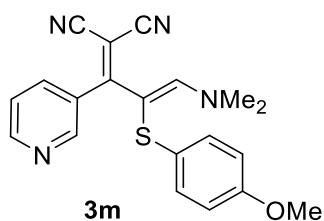
(Z)-2-(3-(dimethylamino)-2-((4-methoxyphenyl)thio)-1-(4-nitrophenyl)allylidene)malononitrile (3i): It was prepared in accordance to the *General procedure for enamine reaction with R-S-Cl*. Purification by column chromatography in Hexanes/EtOAc starting from 0% to 20% EtOAc provided the desired product in 86% yield (0.69 g, 1.72 mmol). ^1H NMR (600 MHz, CDCl_3) δ 8.14–8.04 (m, 2H), 7.31–7.22 (m, 2H), 6.85–6.77 (m, 2H), 6.77–6.71 (m, 2H), 3.73 (s, 3H), 3.28 (s, 6H); ^{13}C NMR (150 MHz, C_6D_6) δ 176.4, 158.3, 156.5, 148.9, 142.6, 137.3, 130.5, 128.2, 128.0, 123.3, 115.0, 114.9, 114.6, 58.4, 55.3, 55.3, 28.4, 18.3.



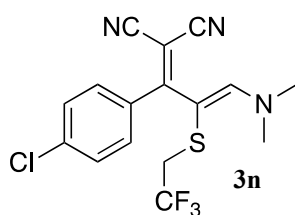
(Z)-2-(1-(4-chlorophenyl)-3-(dimethylamino)-2-((4-methoxyphenyl)thio)allylidene)malononitrile (3j): It was prepared in accordance to the *General procedure for enamine reaction with R-S-Cl*. Purification by column chromatography in Hexanes/EtOAc starting from 0% to 20% EtOAc provided the desired product in 95% yield (0.75 g, 1.9 mmol) of. ^1H NMR (600 MHz, CDCl_3) δ 7.40 (s, 1H), 7.30–7.21 (m, 2H), 7.11–7.03 (m, 2H), 6.88–6.80 (m, 2H), 6.79–6.69 (m, 2H), 3.72 (s, 3H), 3.22 (s, 6H); ^{13}C NMR (150 MHz, CDCl_3) δ 158.2, 156.5, 137.1, 134.6, 131.0, 128.6, 115.8, 114.7, 95.6, 55.3, 43.6.



3l (*(Z)*-2-(3-(dimethylamino)-1-(4-methoxyphenyl)-2-((4-methoxyphenyl)thio)allylidene)malononitrile (**3l**): It was prepared in accordance to the *General procedure for enamine reaction with R-S-Cl*. Purification by column chromatography in Hexanes/EtOAc starting from 0% to 20% EtOAc provided the desired product in 98% yield (0.77 g, 1.96 mmol). ^1H NMR (600 MHz, CDCl_3) δ 7.27–7.21 (m, 2H), 6.97 (d, $J = 8.3$ Hz, 2H), 6.87 (dd, $J = 8.8, 3.2$ Hz, 2H), 6.84–6.77 (m, 2H), 3.83 (s, 3H), 3.79 (s, 3H), 3.26 (s, 6H); ^{13}C NMR (150 MHz, CDCl_3) δ 176.5, 162.1, 161.7, 158.2, 156.4, 137.2, 131.9, 128.4, 124.5, 114.7, 114.7, 113.7, 55.4, 55.4, 55.3, 43.9, 28.5.

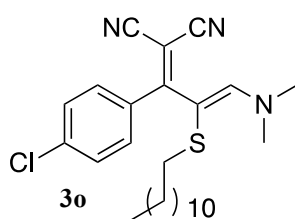


3m (*(Z)*-2-(3-(dimethylamino)-2-((4-methoxyphenyl)thio)-1-(pyridin-3-yl)allylidene)malononitrile (**3m**): It was prepared in accordance to the *General procedure for enamine reaction with R-S-Cl*. Purification by column chromatography in DCM/MeOH starting from 0% to 10% MeOH provided the desired product in 97% yield (0.71 g, 1.94 mmol). ^1H NMR (600 MHz, CDCl_3) δ 8.56 (dd, $J = 4.9, 1.6$ Hz, 1H), 8.36 (d, $J = 2.3$ Hz, 1H), 7.51 (s, 1H), 7.42 (dt, $J = 7.9, 2.0$ Hz, 1H), 7.20–7.15 (m, 1H), 6.84–6.77 (m, 2H), 6.75–6.69 (m, 2H), 3.71 (s, 3H), 3.25 (s, 6H); ^{13}C NMR (150 MHz, CDCl_3) δ 158.3, 156.6, 151.4, 149.9, 137.1, 132.3, 128.5, 128.0, 122.8, 116.2, 115.5, 114.8, 95.7, 55.3, 44.2, 29.5.



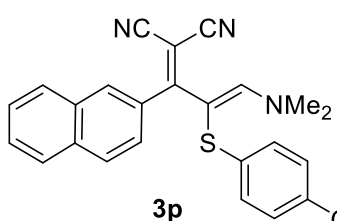
3n (*(Z)*-2-(1-(4-chlorophenyl)-3-(dimethylamino)-2-((2,2,2-trifluoroethyl)thio)allylidene)malononitrile (**3n**): It was prepared in accordance to the

General procedure for enamine reaction with R-S-Cl. Purification by column chromatography in Hexanes/EtOAc starting from 0% to 20% EtOAc provided the desired product in 60% yield (0.45 g, 1.2 mmol). ^1H NMR (600 MHz, CDCl_3) δ 7.50–7.42 (m, 2H), 7.33 (d, $J = 8.1$ Hz, 2H), 7.16 (s, 1H), 3.26 (s, 6H), 3.03–2.86 (m, 2H); ^{19}F NMR (565 MHz, CDCl_3) δ -64.9; ^{13}C NMR (150 MHz, CDCl_3) δ 172.9, 158.2, 137.5, 135.1, 135.0, 131.2, 131.0, 130.1, 130.0, 128.1, 126.3, 124.4, 122.6, 116.3, 115.7, 94.4, 86.6 (q, $J = 36.4$ Hz), 69.2, 60.4, 39.0, 38.7 (q, $J = 30.8$ Hz).



(Z)-2-(1-(4-chlorophenyl)-3-(dimethylamino)-2-

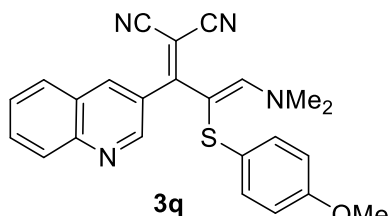
(dodecylthio)allylidene)malononitrile (3o): It was prepared in accordance to the *General procedure for enamine reaction with R-S-Cl*. Purification by column chromatography in Hexanes/EtOAc starting from 0% to 20% EtOAc provided the desired product in 99% yield (0.88 g, 1.98 mmol). ^1H NMR (600 MHz, CDCl_3) δ 7.38–7.33 (m, 2H), 7.30 (d, $J = 8.2$ Hz, 2H), 3.44–3.02 (m, 6H), 2.25 (t, $J = 7.6$ Hz, 2H), 1.37 (dt, $J = 12.7, 6.1$ Hz, 2H), 1.25–1.10 (m, 22H), 0.81 (t, $J = 7.0$ Hz, 3H); ^{13}C NMR (150 MHz, CDCl_3) δ 158.7, 155.1, 148.0, 135.8, 134.8, 133.3, 129.9, 129.0, 128.5, 128.4, 128.3, 115.5, 106.5, 103.5, 53.8, 36.2, 31.8, 29.5, 29.5, 29.4, 29.2, 29.0, 28.5, 28.1, 22.6, 14.0.



(Z)-2-(3-(dimethylamino)-2-((4-methoxyphenyl)thio)-1-

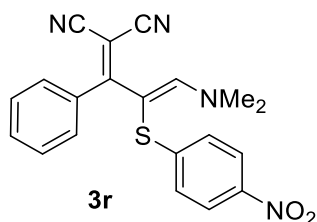
(naphthalen-2-yl)allylidene)malononitrile (3p): I was prepared in accordance to the *General procedure for enamine reaction with R-S-Cl*. Purification by column chromatography in Hexanes/EtOAc starting from 0% to 20% EtOAc provided the desired product in 98% yield (0.81 g, 1.96 mmol). ^1H NMR (600 MHz, CDCl_3) δ 7.77 (dd, $J = 8.4, 4.5$ Hz, 2H), 7.73 (d, $J = 8.1$ Hz, 1H), 7.69–7.65 (m, 1H), 7.45 (dddd, $J = 26.0, 8.1, 6.9, 1.3$ Hz, 2H), 7.35 (s, 1H), 7.27 (dd, $J = 8.5, 1.8$ Hz, 1H), 6.92 (d, $J = 8.3$ Hz, 2H),

6.75 (d, $J = 8.5$ Hz, 2H), 3.70 (s, 3H), 3.12 (s, 6H); ^{13}C NMR (150 MHz, CDCl_3) δ 176.5, 158.2, 157.0, 137.0, 134.2, 134.1, 132.5, 130.1, 128.9, 128.7, 128.5, 128.0, 127.8, 127.7, 127.6, 126.6, 126.4, 116.7, 116.5, 114.8, 114.7, 96.1, 60.3, 55.4, 55.3, 43.9.



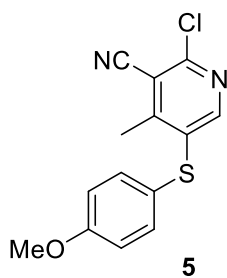
(Z)-2-(3-(dimethylamino)-1-(isoquinolin-3-yl)-2-((4-

methoxyphenyl)thio)allylidene)malononitrile (3q): It was prepared in accordance to the *General procedure for enamine reaction with R-S-Cl*. Purification by column chromatography in Hexanes/EtOAc starting from 0% to 20% EtOAc provided the desired product in 97% yield (0.80 g, 1.94 mmol). ^1H NMR (600 MHz, CDCl_3) δ 8.67 (d, $J = 2.3$ Hz, 1H), 8.07 (dd, $J = 8.3, 1.2$ Hz, 1H), 7.95–7.86 (m, 1H), 7.77–7.65 (m, 2H), 7.60 (s, 1H), 7.49 (ddd, $J = 8.1, 6.9, 1.2$ Hz, 1H), 6.74 (d, $J = 8.4$ Hz, 2H), 6.70–6.62 (m, 2H), 3.70 (s, 3H), 3.28 (s, 6H); ^{13}C NMR (150 MHz, CDCl_3) δ 177.8, 158.2, 156.6, 150.0, 148.3, 138.0, 131.2, 129.3, 128.9, 128.5, 127.9, 127.2, 126.7, 115.7, 114.8, 55.3, 29.5.



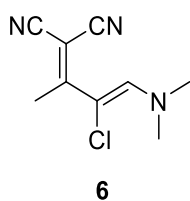
(Z)-2-(3-(dimethylamino)-2-((4-nitrophenyl)thio)-1-

phenylallylidene)malononitrile (3r): It was prepared in accordance to the *General procedure for cyclization with primary amines*. Purification by column chromatography in Hexanes/EtOAc starting from 0% to 20% EtOAc provided the desired product in 90% yield (0.68 g, 1.8 mmol). ^1H NMR (600 MHz, Acetone- d_6) δ 8.18 (d, 2H, $J = 8.99$ Hz), 7.82 (br. s, 1H), 7.50–7.47 (m, 1H), 7.43–7.38 (m, 6H), 3.37 (br. s, 6H); ^{13}C NMR (150 MHz, CDCl_3) δ 176.3, 157.5, 138.6, 136.5, 132.0, 130.8, 129.4, 129.1, 128.3, 125.5, 116.2, 94.1, 28.5.



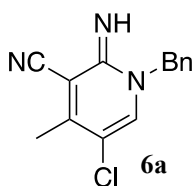
5 *2-chloro-5-((4-methoxyphenyl)thio)-4-methylnicotinonitrile (5):* ^1H

NMR (600 MHz, CDCl_3) δ 7.86 (s, 1H), 7.43–7.29 (m, 2H), 6.99–6.83 (m, 2H), 3.79 (s, 3H), 2.55 (s, 3H); ^{13}C NMR (150 MHz, CDCl_3) δ 160.9, 151.4, 149.8, 149.7, 135.9, 135.7, 132.5, 119.5, 115.7, 114.5, 113.9, 111.1, 55.4, 19.0.



6 *(Z)-2-(3-chloro-4-(dimethylamino)but-3-en-2-ylidene)malononitrile*

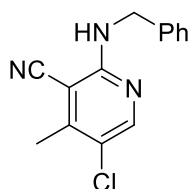
(**6**): ^1H NMR (600 MHz, CDCl_3) δ 7.42 (s, 1H), 3.25 (s, 6H), 2.27 (s, 3H); ^{13}C NMR (150 MHz, CDCl_3) δ 168.4, 147.5, 117.0, 116.3, 97.8, 66.6, 44.3, 22.2.



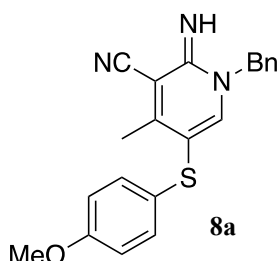
6a

1-benzyl-5-chloro-2-imino-4-methyl-1,2-dihydropyridine-3-

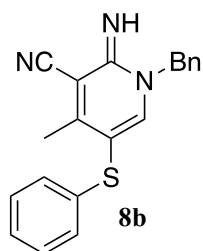
carbonitrile (6a): It was prepared in accordance to the *General procedure for cyclization with primary amines*. Purification by column chromatography in Hexanes/EtOAc starting from 0% to 20% EtOAc provided the desired product in 79% yield (0.20 g, 0.79 mmol). ^1H NMR (600 MHz, C_6D_6) δ 7.34–7.20 (m, 5H), 7.12 (s, 1H), 5.02 (s, 2H), 2.29 (s, 3H); ^{13}C NMR (150 MHz, C_6D_6) δ 154.6, 153.6, 139.0, 134.7, 129.0, 128.4, 128., 115.3, 109.4, 103.5, 53.6, 19.6; HRMS (ESI-FTMS): Theo. Mass $[\text{M}+\text{H}]^+$ 258.0798, Exp. Mass: 258.0798.

**6b**

2-(benzylamino)-5-chloro-4-methylnicotinonitrile (6b): It was prepared in accordance to the *General Procedure for Pyridines Synthesis from YMs*. Purification by flash chromatography EtOAc/Hexanes from 0:100 to 20:80 afforded the desired product as a white solid in 88% yield. ^1H NMR (600 MHz, CDCl_3) δ 8.20 (s, 1H), 7.54–7.29 (m, 5H), 5.51 (t, $J = 5.81$ Hz, 1H), 4.71 (d, $J = 5.81$ Hz, 2H), 2.51 (s, 3H); ^{13}C NMR (150 MHz, CDCl_3) δ 157.3, 150.9, 149.8, 138.2, 128.8, 127.7, 127.6, 120.2, 115.5, 93.3, 45.5, 18.8.

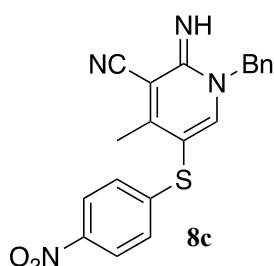
**8a**

1-benzyl-2-imino-5-((4-methoxyphenyl)thio)-4-methyl-1,2-dihydropyridine-3-carbonitrile (8a): It was prepared in accordance to the *General procedure for cyclization with primary amines*. Purification by column chromatography in Hexanes/EtOAc starting from 0% to 20% EtOAc provided the desired product in 98% yield (0.34 g, 0.98 mmol). ^1H NMR (600 MHz, CDCl_3) δ 7.53 (s, 1H), 7.45–7.31 (m, 4H), 7.15–7.02 (m, 2H), 6.96–6.75 (m, 2H), 5.17 (s, 2H), 3.81 (s, 3H), 2.35 (s, 3H). ^{13}C NMR (150 MHz, CDCl_3) δ 158.7, 158.4, 155.1, 147.4, 134.9, 129.2, 129.0, 128.3, 128.1, 126.7, 115.6, 114.9, 107.2, 103.7, 55.3, 53.5, 20.0; HRMS (ESI-FTMS): Theo. Mass $[\text{M}+\text{H}]^+$ 362.1327, Exp. Mass: 362.1326.

**8b**

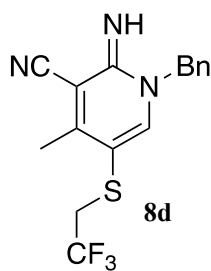
1-benzyl-2-imino-4-methyl-5-(phenylthio)-1,2-dihydropyridine-3-carbonitrile (8b): It was prepared in accordance to the *General procedure for cyclization*

with primary amines. Purification by column chromatography in Hexanes/EtOAc starting from 0% to 20% EtOAc provided the desired product in 96% yield (0.32 g, 0.96 mmol). ^1H NMR (600 MHz, CDCl_3) δ 7.47 (s, 1H), 7.35–7.29 (m, 2H), 7.29–7.24 (m, 3H), 7.22–7.15 (m, 3H), 7.13–7.07 (m, 1H), 7.02–6.94 (m, 2H), 5.09 (s, 2H), 2.24 (s, 3H); ^{13}C NMR (150 MHz, CDCl_3) δ 158.7, 155.1, 148.4, 136.9, 134.8, 129.2, 129.0, 129.0, 128.4, 128.1, 128.1, 126.0, 125.9, 115.5, 105.1, 103.8, 53.6, 20.0; HRMS (ESI-FTMS): Theo. Mass $[\text{M}+\text{H}]^+$ 332.1221, Exp. Mass: 332.1221.



1-benzyl-2-imino-4-methyl-5-((4-nitrophenyl)thio)-1,2-

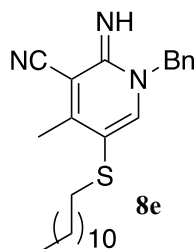
dihydropyridine-3-carbonitrile (8c): It was prepared in accordance to the *General procedure for cyclization with primary amines*. Purification by column chromatography in Hexanes/EtOAc starting from 0% to 20% EtOAc provided the desired product in 78% yield (0.29 g, 0.78 mmol). ^1H NMR (600 MHz, CDCl_3) δ 8.11–8.01 (m, 2H), 7.47 (s, 1H), 7.37–7.23 (m, 5H), 7.05 (d, $J = 8.9$ Hz, 1H), 5.10 (s, 2H), 2.23 (s, 3H); ^{13}C NMR (150 MHz, CDCl_3) δ 157.7, 154.7, 149.2, 147.1, 145.7, 129.1, 128.6, 128.2, 124.8, 124.4, 115.1, 104.4, 102.1, 53.8, 19.8; HRMS (ESI-FTMS): Theo. Mass $[\text{M}+\text{H}]^+$ 377.1072, Exp. Mass: 377.1075.



1-benzyl-2-imino-4-methyl-5-((2,2,2-trifluoroethyl)thio)-1,2-

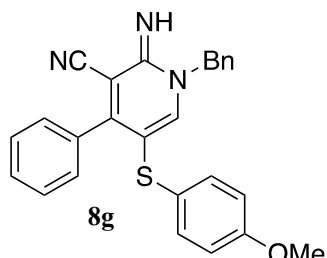
dihydropyridine-3-carbonitrile (8d): It was prepared in accordance to the *General procedure for cyclization with primary amines*. Purification by column chromatography in Hexanes/EtOAc starting from 0% to 20% EtOAc provided the desired product in 72% yield (0.24 g, 0.72 mmol). ^1H NMR (600 MHz, CDCl_3) δ 7.47 (s, 1H), 7.35–7.24 (m, 3H), 7.24–7.20 (m, 2H), 5.02 (s, 2H), 2.96 (q, $J = 9.6$ Hz, 2H), 2.40 (s, 3H). ^{19}F NMR (565

MHz, CDCl₃) δ -65.6; ¹³C NMR (150 MHz, CDCl₃) δ 157.8, 154.9, 149.5, 134.6, 129.6, 129.1, 128.5, 128.3, 128.2, 126.1, 124.3, 115.5, 104.9, 103.4, 53.8, 38.8 (q, J = 31.4 Hz), 29.7, 29.6, 29.6, 20.0; HRMS (ESI-FTMS): Theo. Mass [M+H]⁺ 338.0939, Exp. Mass: 338.0935.



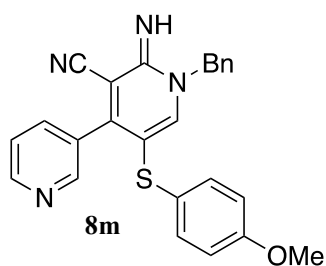
1-benzyl-2-imino-4-methyl-5-(dodecylthio)-1,2-dihydropyridine-3-

carbonitrile (8e): It was prepared in accordance to the *General procedure for cyclization with primary amines*. Purification by column chromatography in Hexanes/EtOAc starting from 0% to 20% EtOAc provided the desired product in 89% yield (0.36 g, 0.89 mmol). ¹H NMR (600 MHz, CDCl₃) δ 7.33 (s, 1H), 7.32–7.28 (m, 2H), 7.27–7.22 (m, 3H), 7.19 (s, 1H), 5.05 (s, 2H), 2.40 (d, J = 3.4 Hz, 5H), 1.41–1.30 (m, 2H), 1.27–1.09 (m, 22H), 0.81 (t, J = 7.0 Hz, 3H). ¹³C NMR (150 MHz, CDCl₃) δ 158.7, 155.3, 147.6, 135.1, 129.0, 128.3, 128.1, 115.9, 107.7, 103.2, 53.5, 36.7, 31.9, 29.6, 29.5, 29.5, 29.3, 29.2, 29.0, 28.5, 22.7, 20.1, 14.1.

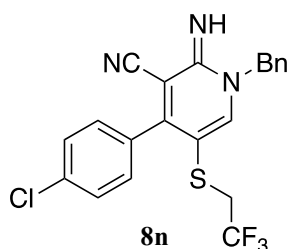


1-benzyl-2-imino-5-((4-methoxyphenyl)thio)-4-phenyl-1,2-

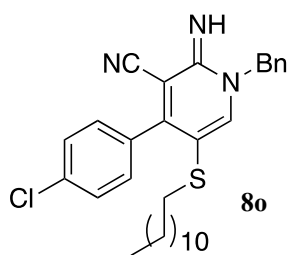
dihydropyridine-3-carbonitrile (8g): It was prepared in accordance to the *General procedure for cyclization with primary amines*. Purification by column chromatography in Hexanes/EtOAc starting from 0% to 20% EtOAc provided the desired product in 98% yield (0.41 g, 0.98 mmol). ¹H NMR (600 MHz, CDCl₃) δ 7.48 (s, 1H), 7.40–7.26 (m, 8H), 7.17–6.97 (m, 2H), 6.78–6.67 (m, 2H), 6.65–6.54 (m, 2H), 5.12 (s, 2H), 3.68 (s, 3H); ¹³C NMR (150 MHz, CDCl₃) δ 159.6, 159.2, 154.8, 146.0, 134.4, 134.2, 132.0, 129.7, 129.1, 129.1, 128.1, 128.1, 114.7, 103.4, 67.2, 66.0, 55.3, 55.2, 54.6, 29.6, 29.5; HRMS (ESI-FTMS): Theo. Mass [M+H]⁺ 422.1483, Exp. Mass: 422.1483.



1'-benzyl-2'-imino-5'-((4-methoxyphenyl)thio)-1,2'-dihydro-[3,4'-bipyridine]-3'-carbonitrile (8m): It was prepared in accordance to the *General procedure for cyclization with primary amines*. Purification by column chromatography in Hexanes/EtOAc starting from 0% to 40% EtOAc provided the desired product in 65% yield (0.27 g, 0.65 mmol). ^1H NMR (600 MHz, CDCl_3) δ 8.57 (dt, $J = 5.0, 1.3$ Hz, 1H), 8.44–8.27 (m, 1H), 7.54 (s, 1H), 7.44–7.29 (m, 6H), 7.22 (dd, $J = 7.8, 4.9$ Hz, 1H), 6.75–6.64 (m, 2H), 6.63–6.54 (m, 2H), 5.16 (s, 2H), 3.68 (d, $J = 0.8$ Hz, 3H); ^{13}C NMR (150 MHz, CDCl_3) δ 159.3, 156.3, 150.6, 148.5, 135.8, 129.2, 128.8, 128.7, 122.8, 114.9, 55.3, 29.7; HRMS (ESI-FTMS): Theo. Mass $[\text{M}+\text{H}]^+$ 425.1436, Exp. Mass: 425.1436.

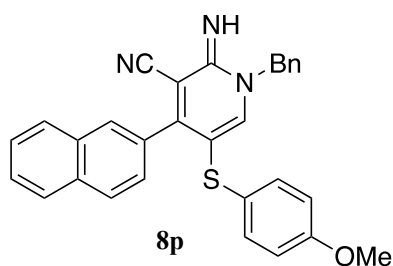


1-benzyl-4-(4-chlorophenyl)-2-imino-5-((2,2,2-trifluoroethyl)thio)-1,2-dihydropyridine-3-carbonitrile (8n): It was prepared in accordance to the *General procedure for cyclization with primary amines*. Purification by column chromatography in Hexanes/EtOAc starting from 0% to 20% EtOAc provided the desired product in 50% yield (0.22 g, 0.5 mmol). ^1H NMR (600 MHz, CDCl_3) δ 7.58 (s, 1H), 7.44–7.39 (m, 2H), 7.38–7.28 (m, 5H), 7.28–7.24 (m, 2H), 7.19 (s, 1H), 5.09 (s, 2H), 2.51 (q, $J = 9.5$ Hz, 2H); ^{19}F NMR (565 MHz, CDCl_3) δ -65.2; ^{13}C NMR (150 MHz, CDCl_3) δ 158.0, 154.6, 149.8, 136.2, 134.2, 132.7, 129.7, 129.6, 129.1, 128.9, 128.6, 128.4, 128.4, 128.2, 127.8, 125.9, 124.1, 115.1, 103.9, 103.2, 60.3, 54.1, 37.7 (q, $J = 31.4$ Hz); HRMS (ESI-FTMS): Theo. Mass $[\text{M}+\text{H}]^+$ 434.0706, Exp. Mass: 434.0706.



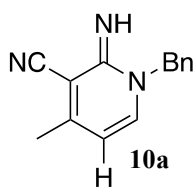
1-benzyl-4-(4-chlorophenyl)-2-imino-5-(dodecylthio)-1,2-

dihydropyridine-3-carbonitrile (8o): It was prepared in accordance to the *General procedure for cyclization with primary amines*. Purification by column chromatography in Hexanes/EtOAc starting from 0% to 20% EtOAc provided the desired product in 95% yield (0.48 g, 0.95 mmol). ^1H NMR (600 MHz, CDCl_3) δ 7.47 (s, 1H), 7.42–7.38 (m, 2H), 7.38–7.31 (m, 5H), 7.30–7.26 (m, 2H), 5.12 (s, 2H), 2.03 (t, $J = 7.3$ Hz, 2H), 1.42–0.98 (m, 18H), 0.83 (t, $J = 7.0$ Hz, 3H); ^{13}C NMR (150 MHz, CDCl_3) δ 158.7, 155.1, 148.0, 135.8, 134.8, 133.3, 129.9, 129.0, 128.5, 128.4, 128.3, 115.5, 106.5, 103.5, 53.8, 36.2, 31.8, 29.5, 29.5, 29.4, 29.2, 29.0, 28.5, 28.1, 22.6, 14.0.



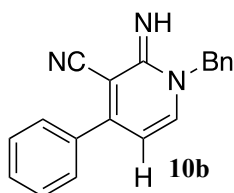
1-benzyl-2-imino-5-((4-methoxyphenyl)thio)-4-

(naphthalen-2-yl)-1,2-dihydropyridine-3-carbonitrile (8p): It was prepared in accordance to the *General procedure for cyclization with primary amines*. Purification by column chromatography in Hexanes/EtOAc starting from 0% to 20% EtOAc provided the desired product in 89% yield (0.42 g, 0.89 mmol). ^1H NMR (600 MHz, CDCl_3) δ 7.77 (t, $J = 8.9$ Hz, 2H), 7.66 (dd, $J = 8.0, 1.4$ Hz, 1H), 7.52 (s, 1H), 7.51–7.47 (m, 1H), 7.44 (dddd, $J = 25.4, 8.1, 6.8, 1.3$ Hz, 2H), 7.37–7.29 (m, 5H), 7.21–7.18 (m, 1H), 6.68–6.60 (m, 2H), 6.52–6.44 (m, 2H), 5.14 (s, 2H), 3.62 (s, 3H); ^{13}C NMR (150 MHz, CDCl_3) δ 159.7, 159.0, 155.3, 147.3, 134.9, 133.4, 132.5, 132.3, 131.5, 129.1, 128.5, 128.5, 128.4, 128.2, 127.8, 127.7, 127.1, 126.5, 126.4, 125.3, 115.6, 114.5, 108.5, 104.2, 55.3, 53.9; HRMS (ESI-FTMS): Theo. Mass $[\text{M}+\text{H}]^+$ 474.1640, Exp. Mass: 474.1638.



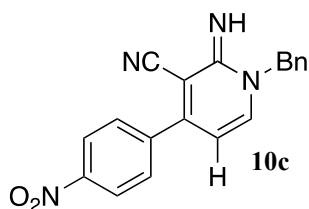
1-benzyl-2-imino-4-methyl-1,2-dihydropyridine-3-carbonitrile (10a): It

was prepared in accordance to the *General procedure for cyclization with primary amines*. Purification by column chromatography in Hexanes/EtOAc starting from 0% to 20% EtOAc provided the desired product in 60% yield (0.13 g, 0.6 mmol). ^1H NMR (600 MHz, CDCl_3) δ 7.38 (dd, $J = 8.1, 6.4$ Hz, 2H), 7.36–7.28 (m, 3H), 7.07 (d, $J = 7.0$ Hz, 1H), 5.66 (d, $J = 7.0$ Hz, 1H), 5.12 (s, 2H), 2.30 (s, 3H). ^{13}C NMR (150 MHz, CDCl_3) δ 156.1, 155.7, 140.9, 135.4, 129.0, 128.1, 128.1, 115.9, 104.5, 102.4, 77.3, 77.0, 76.8, 53.4, 21.1; HRMS (ESI-FTMS): Theo. Mass $[\text{M}+\text{H}]^+$ 224.1188; Exp. Mass: 224.1185.



1-benzyl-2-imino-4-phenyl-1,2-dihydropyridine-3-carbonitrile

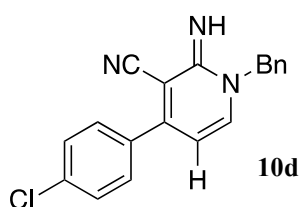
(10b): It was prepared in accordance to the *General procedure for cyclization with primary amines*. Purification by column chromatography in Hexanes/EtOAc starting from 0% to 20% EtOAc provided the desired product in 98% yield (0.28 g, 0.98 mmol). ^1H NMR (600 MHz, CDCl_3) δ 7.54–7.46 (m, 2H), 7.44–7.39 (m, 3H), 7.36–7.26 (m, 6H), 7.12 (d, $J = 7.1$ Hz, 1H), 5.76 (d, $J = 7.1$ Hz, 1H), 5.11 (s, 2H). ^{13}C NMR (150 MHz, CDCl_3) δ 156.3, 156.3, 141.2, 136.1, 135.2, 130.3, 129.0, 128.8, 128.2, 128.2, 127.6, 116.5, 103.5, 100.4, 53.6; HRMS (ESI-FTMS): Theo. Mass $[\text{M}+\text{H}]^+$ 286.1344, Exp. Mass: 286.1344.



1-benzyl-2-imino-4-(4-nitrophenyl)-1,2-dihydropyridine-3-

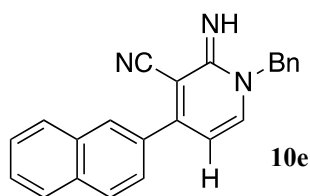
carbonitrile (10c): It was prepared in accordance to the *General procedure for cyclization with primary amines*. Purification by column chromatography in Hexanes/EtOAc starting from 0% to 20% EtOAc provided the desired product in 83% yield (0.27 g, 0.83 mmol).

^1H NMR (600 MHz, CDCl_3) δ 8.40–8.19 (m, 2H), 7.77–7.59 (m, 2H), 7.40–7.26 (m, 5H), 7.21 (d, $J = 7.1$ Hz, 1H), 5.74 (d, $J = 7.0$ Hz, 1H), 5.11 (s, 2H); ^{13}C NMR (150 MHz, CDCl_3) δ 155.7, 154.0, 148.8, 142.3, 142.2, 134.8, 129.1, 129.0, 128.9, 128.7, 128.5, 128.4, 124.1, 124.0, 115.8, 102.8, 101.1, 54.0, 29.7; HRMS (ESI-FTMS): Theo. Mass $[\text{M}+\text{H}]^+$ 331.1194, Exp. Mass: 331.1192.



1-benzyl-4-(4-chlorophenyl)-2-imino-1,2-dihydropyridine-3-

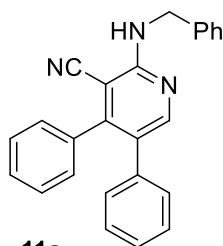
carbonitrile (10d): It was prepared in accordance to the *General procedure for cyclization with primary amines*. Purification by column chromatography in Hexanes/EtOAc starting from 0% to 20% EtOAc provided the desired product in 90% yield (0.29 g, 0.9 mmol). ^1H NMR (600 MHz, CDCl_3) δ 7.46–7.40 (m, 2H), 7.40–7.35 (m, 2H), 7.35–7.30 (m, 2H), 7.30–7.26 (m, 3H), 7.12 (d, $J = 7.1$ Hz, 1H), 5.71 (d, $J = 7.1$ Hz, 1H), 5.09 (s, 2H); ^{13}C NMR (150 MHz, CDCl_3) δ 156.1, 155.0, 141.6, 136.6, 135.0, 134.4, 129.1, 129.1, 129.0, 129.0, 128.3, 128.2, 116.4, 103.1, 100.4, 77.1, 76.9, 76.7, 53.7; HRMS (ESI-FTMS): Theo. Mass $[\text{M}+\text{H}]^+$ 320.0954, Exp. Mass: 320.0952.



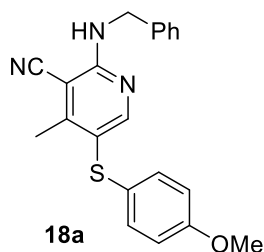
1-benzyl-2-imino-4-(naphthalen-2-yl)-1,2-dihydropyridine-3-

carbonitrile (10e): It was prepared in accordance to the *General procedure for cyclization with primary amines*. Purification by column chromatography in Hexanes/EtOAc starting from 0% to 20% EtOAc provided the desired product in 95% yield (0.32 g, 0.95 mmol). ^1H NMR (600 MHz, CD_3CN) δ 8.16 (dt, $J = 1.9, 0.7$ Hz, 1H), 8.07–8.02 (m, 1H), 7.99 (dddd, $J = 10.2, 7.3, 1.4, 0.7$ Hz, 2H), 7.69 (dd, $J = 8.5, 1.9$ Hz, 1H), 7.66–7.60 (m, 2H), 7.56 (d, $J = 7.0$ Hz, 1H), 7.43–7.41 (m, 4H), 7.37–7.33 (m, 2H), 6.05 (d, $J = 7.0$ Hz, 1H), 5.21 (s, 2H); ^{13}C NMR (150 MHz, CD_3CN) δ 157.2, 156.4, 143.7, 137.2, 134.5, 134.3, 133.3, 129.2, 129.0, 128.9, 128.8, 128.3, 128.3, 128.3, 128.2, 128.1, 127.6, 127.5, 126.8,

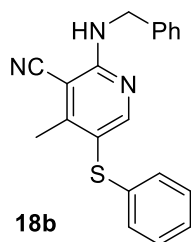
125.4, 103.9, 53.9, 46.5; HRMS (ESI-FTMS): Theo. Mass $[M+H]^+$ 336.1501, Exp. Mass: 336.1498.



2-(benzylamino)-4,5-diphenylnicotinonitrile (11a): It was prepared in accordance to the *General Procedure for Pyridines Synthesis from YMs*. Purification by flash chromatography EtOAc/Hexanes from 0:100 to 20:80 afforded the desired product as a white solid in 86% yield. ^1H NMR (600 MHz, CDCl_3): δ_{H} 8.41 (s, 1H), 7.49 – 7.45 (m, 2H), 7.44 – 7.40 (m, 2H), 7.39 – 7.32 (m, 4H), 7.26 – 7.21 (m, 5H), 7.07 – 7.02 (m, 2H), 5.79 (t, $J = 5.5$ Hz, 1H), 4.85 (d, $J = 5.5$ Hz, 2H). $^{13}\text{C}\{^1\text{H}\}$ NMR (150 MHz, CDCl_3): δ_{C} 158.0, 153.0, 152.8, 138.4, 136.6, 135.7, 129.5, 129.3, 128.8, 128.7, 128.4, 128.3, 128.1, 127.7, 127.5, 126.8, 126.1, 116.6, 91.9, 45.4. HRMS (ESI-FTMS) m/z : $[M+H]^+$ Calcd for $\text{C}_{25}\text{H}_{20}\text{N}_3$ 362.1657; Found 362.1656.

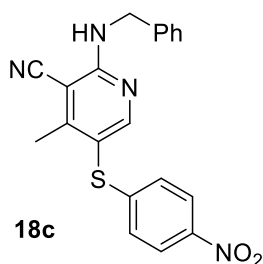


2-(benzylamino)-5-((4-methoxyphenyl)thio)-4-methylnicotinonitrile (18a): It was prepared following the general procedure. Purification by flash chromatography EtOAc/Hexanes from 0:100 to 20:80 afforded the desired product as a white solid in 85% yield. ^1H NMR (600 MHz, CDCl_3): δ_{H} 8.35 (s, 1H), 7.39 – 7.29 (m, 5H), 7.17 – 7.13 (m, 2H), 6.85 – 6.81 (m, 2H), 5.56 (t, $J = 5.5$ Hz, 1H), 4.73 (d, $J = 5.5$ Hz, 2H), 3.79 (s, 3H), 2.50 (s, 3H). $^{13}\text{C}\{^1\text{H}\}$ NMR (150 MHz, CDCl_3): δ_{C} 158.8, 158.4, 157.3, 155.8, 138.1, 130.8, 128.8, 127.7, 127.6, 126.5, 118.9, 115.9, 114.9, 93.4, 55.4, 45.4, 19.5. HRMS (ESI-FTMS) m/z : $[M+H]^+$ Calcd for $\text{C}_{21}\text{H}_{20}\text{N}_3\text{OS}$ 362.1327; Found 362.1326.



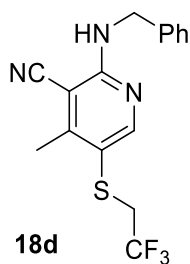
2-(benzylamino)-4-methyl-5-(phenylthio)nicotinonitrile (18b):

It was prepared in accordance to the *General Procedure for Pyridines Synthesis from YMs*. Purification by flash chromatography EtOAc/Hexanes from 0:100 to 20:80 afforded the desired product as a white solid in 93% yield. ^1H NMR (600 MHz, CDCl_3): δ_{H} 8.33 (s, 1H), 7.30 – 7.26 (m, 4H), 7.25 – 7.20 (m, 1H), 7.19 – 7.14 (m, 2H), 7.09 – 7.05 (m, 1H), 7.00 – 6.96 (m, 2H), 5.56 (t, $J = 5.5$ Hz, 1H), 4.66 (d, $J = 5.5$ Hz, 2H), 2.40 (s, 3H). $^{13}\text{C}\{^1\text{H}\}$ NMR (150 MHz, CDCl_3): δ_{C} 158.7, 158.6, 157.0, 138.0, 136.9, 129.1, 128.7, 127.6, 127.7, 127.6, 126.9, 125.9, 116.5, 115.8, 93.5, 45.4, 19.5. HRMS (ESI-FTMS) m/z : $[\text{M}+\text{H}]^+$ Calcd for $\text{C}_{20}\text{H}_{18}\text{N}_3\text{S}$ 332.1221; Found 332.1218.



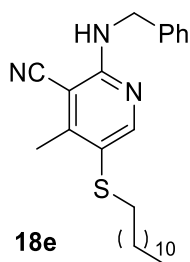
2-(benzylamino)-4-methyl-5-((4-nitrophenyl)thio)nicotinonitrile (18c):

It was prepared in accordance to the *General Procedure for Pyridines Synthesis from YMs*. Purification by flash chromatography EtOAc/Hexanes from 0:100 to 20:80 afforded the desired product as a white solid in 99% yield. ^1H NMR (600 MHz, CDCl_3): δ_{H} 8.42 (s, 1H), 8.11 (d, $J = 8.8$ Hz, 2H), 7.42 – 7.32 (m, 5H), 7.09 (d, $J = 8.8$ Hz, 2H), 5.78 (t, $J = 5.5$ Hz, 1H), 4.78 (d, $J = 5.5$ Hz, 2H), 2.49 (s, 3H). $^{13}\text{C}\{^1\text{H}\}$ NMR (150 MHz, CDCl_3): δ_{C} 159.4, 159.2, 157.3, 147.3, 145.5, 137.7, 128.9, 128.8, 127.7, 125.3, 124.3, 115.3, 113.3, 93.9, 45.5, 19.4. HRMS (ESI-FTMS) m/z : $[\text{M}+\text{H}]^+$ Calcd for $\text{C}_{20}\text{H}_{17}\text{N}_4\text{O}_2\text{S}$ 377.1072; Found 377.1069.



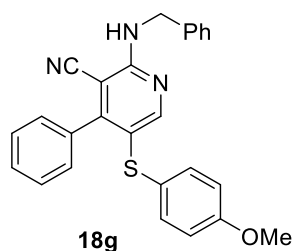
2-(benzylamino)-4-methyl-5-((2,2,2-

trifluoroethyl)thio)nicotinonitrile (18d): It was prepared in accordance to the *General Procedure for Pyridines Synthesis from YMs*. Purification by flash chromatography EtOAc/Hexanes from 0:100 to 20:80 afforded the desired product as a white solid in 72% yield. ^1H NMR (600 MHz, CDCl_3): δ_{H} 8.45 (s, 1H), 7.39 – 7.29 (m, 5H), 5.67 (t, $J = 5.5$ Hz, 1H), 4.73 (d, $J = 5.5$ Hz, 2H), 3.19 (q, $J = 9.7$ Hz, 2H), 2.63 (s, 3H). $^{19}\text{F}\{^1\text{H}\}$ NMR (565 MHz, CDCl_3): δ_{F} -66.1. $^{13}\text{C}\{^1\text{H}\}$ NMR (150 MHz, CDCl_3): δ_{C} 159.0, 158.7, 156.7, 137.9, 128.7, 127.7, 127.6, 126.1, 124.3, 116.5, 115.6, 93.0, 45.3, 39.0 (q, $J = 32.1$ Hz), 19.4. HRMS (ESI-FTMS) m/z : $[\text{M}+\text{H}]^+$ Calcd for $\text{C}_{16}\text{H}_{15}\text{F}_3\text{N}_3\text{S}$ 338.0939; Found 338.0939.

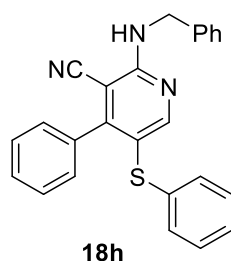


2-(benzylamino)-5-(decylthio)-4-methylnicotinonitrile (18e): It was

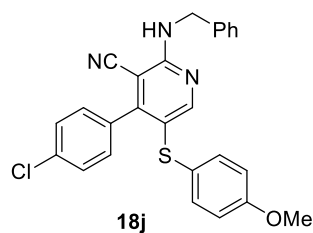
prepared in accordance to the *General Procedure for Pyridines Synthesis from YMs*. Purification by flash chromatography EtOAc/Hexanes from 0:100 to 20:80 afforded the desired product as a white solid in 53% yield. ^1H NMR (600 MHz, CDCl_3): δ_{H} 8.35 (s, 1H), 7.38 – 7.28 (m, 5H), 5.52 (t, $J = 5.5$ Hz, 1H), 4.72 (d, $J = 5.5$ Hz, 2H), 2.66 (t, $J = 7.3$ Hz, 2H), 2.60 (s, 3H), 1.53 (quint, $J = 7.7$ Hz, 2H), 1.42 – 1.24 (m, 18H), 0.90 (t, $J = 7.1$ Hz, 3H). $^{13}\text{C}\{^1\text{H}\}$ NMR (150 MHz, CDCl_3): δ_{C} 158.1, 157.3, 155.6, 138.2, 128.7, 127.6, 127.5, 119.3, 116.0, 93.0, 45.2, 36.3, 31.9, 29.6, 29.5, 29.4, 29.3, 29.2, 29.1, 28.6, 22.6, 19.5, 14.1. HRMS (ESI-FTMS) m/z : $[\text{M}+\text{H}]^+$ Calcd for $\text{C}_{26}\text{H}_{38}\text{N}_3\text{S}$ 424.2788; Found 424.2788.

**2-(benzylamino)-5-((4-methoxyphenyl)thio)-4-**

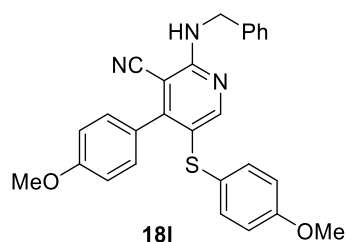
phenylnicotinonitrile (18g): It was prepared in accordance to the *General Procedure for Pyridines Synthesis from YMs*. Purification by flash chromatography EtOAc/Hexanes from 0:100 to 20:80 afforded the desired product as a light-yellow solid in 91% yield. ^1H NMR (600 MHz, CDCl_3): δ_{H} 8.27 (s, 1H), 7.38 – 7.34 (m, 3H), 7.32 – 7.28 (m, 4H), 7.27 – 7.21 (m, 1H), 7.20 – 7.17 (m, 2H), 6.93 (d, $J = 8.6$ Hz, 2H), 6.65 (d, $J = 8.6$ Hz, 2H), 5.56 (t, $J = 5.5$ Hz, 1H), 4.65 (d, $J = 5.5$ Hz, 2H), 3.68 (s, 3H). $^{13}\text{C}\{^1\text{H}\}$ NMR (150 MHz, CDCl_3): δ_{C} 159.2, 158.0, 156.7, 156.6, 138.1, 135.4, 132.9, 129.3, 128.8, 128.6, 128.3, 127.8, 127.7, 126.1, 119.9, 115.9, 114.7, 92.9, 55.3, 45.5. HRMS (ESI-FTMS) m/z : $[\text{M}+\text{H}]^+$ Calcd for $\text{C}_{26}\text{H}_{22}\text{N}_3\text{OS}$ 424.1483; Found 424.1481.

**2-(benzylamino)-4-phenyl-5-(phenylthio)nicotinonitrile (18h):** It

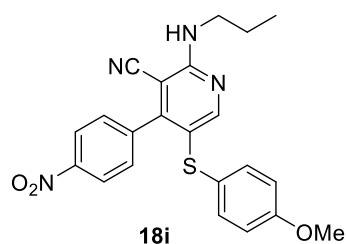
was prepared in accordance to the *General Procedure for Pyridines Synthesis from YMs*. Purification by flash chromatography EtOAc/Hexanes from 0:100 to 20:80 afforded the desired product as a light-yellow solid in 83% yield. ^1H NMR (600 MHz, CDCl_3): δ_{H} 8.49 (s, 1H), 7.44 – 7.38 (m, 7H), 7.35 – 7.31 (m, 1H), 7.26 – 7.23 (m, 2H), 7.20 – 7.16 (m, 2H), 7.16 – 7.11 (m, 1H), 7.00 (d, $J = 7.52$ Hz, 2H), 5.73 (t, $J = 5.5$ Hz, 1H), 4.77 (d, $J = 5.5$ Hz, 2H). $^{13}\text{C}\{^1\text{H}\}$ NMR (150 MHz, CDCl_3): δ_{C} 158.6, 158.5, 158.3, 137.9, 137.1, 135.4, 129.3, 128.9, 128.8, 128.8, 128.7, 128.5, 128.2, 127.8, 127.7, 126.3, 117.2, 115.8, 93.1, 45.6. HRMS (ESI-FTMS) m/z : $[\text{M}+\text{H}]^+$ Calcd for $\text{C}_{25}\text{H}_{20}\text{N}_3\text{S}$ 394.1378; Found 394.1379.



2-(benzylamino)-4-(4-chlorophenyl)-5-((4-methoxyphenyl)thio)nicotinonitrile (18j): It was prepared in accordance to the *General Procedure for Pyridines Synthesis from YMs*. Purification by flash chromatography EtOAc/Hexanes from 0:100 to 20:80 afforded the desired product as a light-yellow solid in 89% yield. ^1H NMR (600 MHz, CDCl_3): δ_{H} 8.39 (s, 1H), 7.43 – 7.39 (m, 2H), 7.39 – 7.35 (m, 4H), 7.35 – 7.30 (m, 1H), 7.22 – 7.19 (m, 2H), 7.02 – 6.99 (m, 2H), 6.77 – 6.73 (m, 2H), 5.68 (t, $J = 5.5$ Hz, 1H), 4.75 (d, $J = 5.5$ Hz, 2H), 3.78 (s, 3H). $^{13}\text{C}\{^1\text{H}\}$ NMR (150 MHz, CDCl_3): δ_{C} 159.2, 158.0, 156.9, 155.6, 138.0, 135.5, 133.8, 132.7, 130.1, 129.7, 128.9, 128.8, 128.7, 128.6, 128.3, 127.8, 127.7, 125.9, 119.6, 115.7, 114.8, 92.7, 55.4, 45.5. HRMS (ESI-FTMS) m/z : $[\text{M}+\text{H}]^+$ Calcd for $\text{C}_{26}\text{H}_{21}\text{ClN}_3\text{OS}$ 458.1094; Found 458.1090.

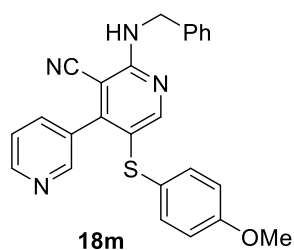


2-(benzylamino)-4-(4-methoxyphenyl)-5-((4-methoxyphenyl)thio)nicotinonitrile (18l): It was prepared in accordance to the *General Procedure for Pyridines Synthesis from YMs*. Purification by flash chromatography EtOAc/Hexanes from 0:100 to 20:80 afforded the desired product as a light-yellow solid in 85% yield. ^1H NMR (600 MHz, CDCl_3): δ_{H} 8.23 (s, 1H), 7.31 – 7.15 (m, 7H), 6.97 (d, $J = 8.8$ Hz, 2H), 6.89 (d, $J = 8.6$ Hz, 2H), 6.68 (d, $J = 8.8$ Hz, 2H), 5.54 (t, $J = 5.5$ Hz, 1H), 4.65 (d, $J = 5.5$ Hz, 2H), 3.78 (s, 3H), 3.69 (s, 3H). $^{13}\text{C}\{^1\text{H}\}$ NMR (150 MHz, CDCl_3): δ_{C} 162.0, 160.4, 159.2, 158.1, 156.5, 156.3, 138.1, 132.8, 130.3, 128.8, 127.8, 127.6, 127.6, 126.2, 120.0, 116.3, 114.7, 113.7, 92.9, 55.3, 45.5. HRMS (ESI-FTMS) m/z : $[\text{M}+\text{H}]^+$ Calcd for $\text{C}_{27}\text{H}_{24}\text{N}_3\text{O}_2\text{S}$ 454.1589; Found 454.1591.



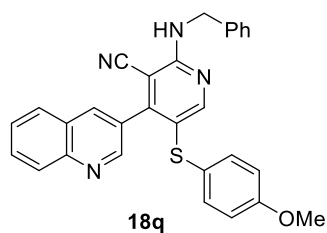
5-((4-methoxyphenyl)thio)-4-(4-nitrophenyl)-2-

(propylamino)nicotinonitrile (18i): It was prepared in accordance to the *General Procedure for Pyridines Synthesis from YMs*. Purification by flash chromatography EtOAc/Hexanes from 0:100 to 20:80 afforded the desired product as a light-yellow solid in 84% yield. ^1H NMR (600 MHz, CDCl_3): δ_{H} 8.45 (s, 1H), 8.27 (d, $J = 7.7$ Hz, 2H), 7.39 (d, $J = 7.7$ Hz, 2H), 6.92 (d, $J = 7.9$ Hz, 2H), 6.72 (d, $J = 7.9$ Hz, 2H), 5.43 (t, $J = 4.8$ Hz, 1H), 3.76 (s, 3H), 3.53 (q, $J = 6.6$ Hz, 2H), 1.70 (sext, $J = 7.3$ Hz, 2H), 1.02 (t, $J = 7.3$ Hz, 3H). $^{13}\text{C}\{^1\text{H}\}$ NMR (150 MHz, CDCl_3): δ_{C} 159.2, 158.4, 157.8, 154.8, 148.1, 141.9, 132.1, 129.8, 126.0, 123.5, 118.0, 115.4, 114.8, 92.0, 55.4, 43.5, 22.6, 11.3. HRMS (ESI-FTMS) m/z : $[\text{M}+\text{H}]^+$ Calcd for $\text{C}_{22}\text{H}_{21}\text{N}_4\text{O}_3\text{S}$ 421.1334; Found 421.1336.



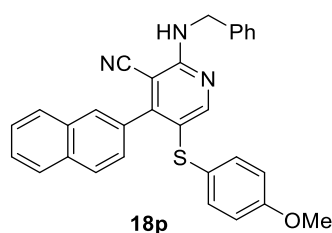
2'-(benzylamino)-5'-((4-methoxyphenyl)thio)-[3,4'-

bipyridine]-3'-carbonitrile (18m): It was prepared in accordance to the *General Procedure for Pyridines Synthesis from YMs*. Purification by flash chromatography EtOAc/Hexanes from 0:100 to 20:80 afforded the desired product as a white solid in 70% yield. ^1H NMR (600 MHz, CDCl_3): δ_{H} 8.68 (dd, $J = 4.9, 1.7$ Hz, 1H), 8.53 (d, $J = 2.0$ Hz, 1H), 8.47 (s, 1H), 7.58 (dt, $J = 7.9, 2.0$ Hz, 1H), 7.40 – 7.29 (m, 6H), 6.95 (d, $J = 8.8$ Hz, 2H), 6.72 (d, $J = 8.8$ Hz, 2H), 5.80 (t, $J = 5.5$ Hz, 1H), 4.76 (d, $J = 5.5$ Hz, 2H), 3.75 (s, 3H). $^{13}\text{C}\{^1\text{H}\}$ NMR (150 MHz, CDCl_3): δ_{C} 159.2, 158.2, 157.5, 153.5, 150.2, 149.1, 137.9, 137.9, 136.2, 132.4, 131.6, 128.8, 127.8, 127.7, 125.9, 122.9, 119.5, 119.5, 115.5, 114.8, 92.9, 55.3, 45.5. HRMS (ESI-FTMS) m/z : $[\text{M}+\text{H}]^+$ Calcd for $\text{C}_{25}\text{H}_{21}\text{N}_4\text{OS}$ 425.1436; Found 425.1437.



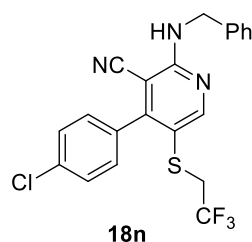
2-(benzylamino)-5-((4-methoxyphenyl)thio)-4-

(quinolin-3-yl)nicotinonitrile (18q): It was prepared in accordance to the *General Procedure for Pyridines Synthesis from YMs*. Purification by flash chromatography EtOAc/Hexanes from 0:100 to 20:80 afforded the desired product as a white solid in 67% yield. ^1H NMR (600 MHz, CDCl_3): δ_{H} 8.73 (s, 1H), 8.37 (s, 1H), 8.04 (d, $J = 8.6$ Hz, 1H), 7.85 (d, $J = 1.8$ Hz, 1H), 7.65 – 7.60 (m, 2H), 7.45 – 7.40 (m, 1H), 7.24 – 7.17 (m, 4H), 7.16 – 7.11 (m, 1H), 6.76 (d, $J = 8.6$ Hz, 2H), 6.46 (d, $J = 8.6$ Hz, 2H), 5.84 – 5.75 (m, 1H), 4.61 (d, $J = 5.5$ Hz, 2H), 3.51 (d, $J = 2.6$ Hz, 3H). $^{13}\text{C}\{^1\text{H}\}$ NMR (150 MHz, CDCl_3): δ_{C} 158.9, 158.1, 157.3, 153.4, 149.1, 147.6, 137.8, 136.1, 132.2, 130.3, 129.1, 128.6, 128.5, 128.5, 128.0, 127.6, 127.4, 127.4, 126.9, 126.7, 125.7, 119.5, 119.7, 115.4, 114.5, 92.8, 55.0, 45.2. HRMS (ESI-FTMS) m/z : $[\text{M}+\text{H}]^+$ Calcd for $\text{C}_{29}\text{H}_{23}\text{N}_4\text{OS}$ 475.1592; Found 475.1594.



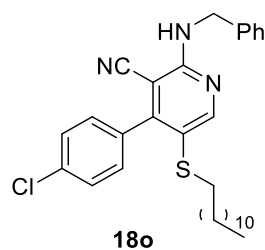
2-(benzylamino)-5-((4-methoxyphenyl)thio)-4-

(naphthalen-2-yl)nicotinonitrile (18p): It was prepared in accordance to the *General Procedure for Pyridines Synthesis from YMs*. Purification by flash chromatography EtOAc/Hexanes from 0:100 to 20:80 afforded the desired product as a white solid in 94% yield. ^1H NMR (600 MHz, CDCl_3): δ_{H} 8.25 (s, 1H), 7.77 – 7.72 (m, 2H), 7.67 (d, $J = 7.9$ Hz, 1H), 7.55 (s, 1H), 7.42 – 7.35 (m, 2H), 7.25 – 7.05 (m, 6H), 6.83 (d, $J = 8.6$ Hz, 2H), 6.52 (d, $J = 8.6$ Hz, 2H), 5.59 (t, $J = 5.5$ Hz, 1H), 4.61 (d, $J = 5.5$ Hz, 2H), 3.57 (s, 3H). $^{13}\text{C}\{^1\text{H}\}$ NMR (150 MHz, CDCl_3): δ_{C} 159.2, 158.1, 156.6, 143.3, 138.1, 133.4, 132.9, 132.8, 128.8, 128.7, 128.5, 128.4, 128.2, 128.0, 127.8, 127.7, 127.6, 127.0, 126.9, 126.7, 126.4, 126.1, 125.9, 120.1, 116.0, 114.7, 93.1, 55.3, 45.5. HRMS (ESI-FTMS) m/z : $[\text{M}+\text{H}]^+$ Calcd for $\text{C}_{30}\text{H}_{24}\text{N}_3\text{OS}$ 474.1640; Found 474.1603.



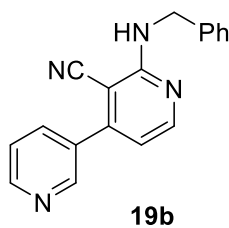
2-(benzylamino)-4-(4-chlorophenyl)-5-((2,2,2-

trifluoroethyl)thio)nicotinonitrile (18n): It was prepared in accordance to the *General Procedure for Pyridines Synthesis from YMs*. Purification by flash chromatography EtOAc/Hexanes from 0:100 to 20:80 afforded the desired product as a yellow solid in 88% yield. ^1H NMR (600 MHz, CDCl_3): δ_{H} 8.58 (s, 1H), 7.51 (d, $J = 8.4$ Hz, 2H), 7.41 – 7.36 (m, 4H), 7.36 – 7.30 (m, 3H), 5.77 (t, $J = 5.5$ Hz, 1H), 4.78 (d, $J = 5.5$ Hz, 2H), 2.86 (q, $J = 9.5$ Hz, 2H). $^{19}\text{F}\{^1\text{H}\}$ NMR (565 MHz, CDCl_3): δ_{F} -65.71. $^{13}\text{C}\{^1\text{H}\}$ NMR (150 MHz, CDCl_3): δ_{C} 159.1, 158.7, 157.2, 139.3, 137.7, 136.0, 133.4, 130.2, 128.9, 128.8, 127.8, 127.8, 127.8, 125.9, 124.1, 115.4, 115.1, 114.1, 92.8, 45.6, 38.2 (q, $J = 32.1$ Hz), 33.8, 31.9, 31.6, 29.7, 29.7, 29.6, 29.6, 29.5, 29.3, 29.1, 28.9, 22.7. HRMS (ESI-FTMS) m/z : $[\text{M}+\text{H}]^+$ Calcd for $\text{C}_{21}\text{H}_{16}\text{ClF}_3\text{N}_3\text{S}$ 434.0706; Found 434.0681.

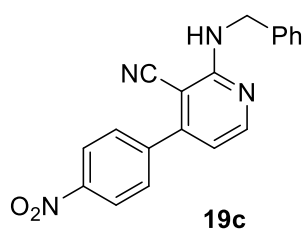


2-(benzylamino)-4-(4-chlorophenyl)-5-(decylthio)nicotinonitrile

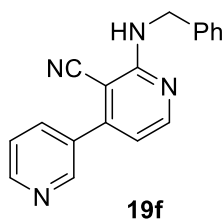
(18o): It was prepared in accordance to the *General Procedure for Pyridines Synthesis from YMs*. Purification by flash chromatography EtOAc/Hexanes from 0:100 to 20:80 afforded the desired product as a white solid in 97% yield. ^1H NMR (600 MHz, CDCl_3): δ_{H} 8.47 (s, 1H), 7.50 – 7.47 (m, 2H), 7.40 – 7.36 (m, 4H), 7.36 – 7.30 (m, 3H), 5.65 (t, $J = 5.5$ Hz, 1H), 4.76 (d, $J = 5.5$ Hz, 2H), 2.43 (t, $J = 7.1$ Hz, 2H), 1.39 – 1.12 (m, 20H), 0.90 (t, $J = 7.1$ Hz, 3H). $^{13}\text{C}\{^1\text{H}\}$ NMR (150 MHz, CDCl_3): δ_{C} 158.0, 157.2, 156.1, 138.0, 135.6, 134.0, 130.3, 128.8, 128.7, 127.8, 127.7, 118.4, 115.9, 92.5, 45.5, 36.1, 31.9, 29.6, 29.5, 29.4, 29.3, 29.0, 28.9, 28.4, 22.7, 14.1. HRMS (ESI-FTMS) m/z : $[\text{M}+\text{H}]^+$ Calcd for $\text{C}_{31}\text{H}_{39}\text{ClN}_3\text{S}$ 520.2555; Found 520.2556.



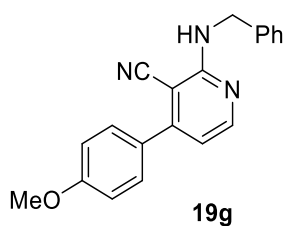
2-(benzylamino)-4-phenylnicotinonitrile (19b): It was prepared in accordance to the *General Procedure for Pyridines Synthesis from YMs*. Purification by flash chromatography EtOAc/Hexanes from 0:100 to 20:80 afforded the desired product as a white solid in 91% yield. ^1H NMR (600 MHz, CDCl_3): δ_{H} 8.80 (d, $J = 2.2$ Hz, 1H), 8.73 (d, $J = 5.0$ Hz, 1H), 8.36 (d, $J = 5.1$ Hz, 1H), 7.94 (dt, $J = 8.0, 2.1$ Hz, 1H), 7.44 (dd, $J = 7.9, 4.8$ Hz, 1H), 7.40 – 7.34 (m, 4H), 7.32 – 7.28 (m, 1H), 6.69 (d, $J = 5.1$ Hz, 1H), 5.81 (t, $J = 5.1$ Hz, 1H), 4.78 (d, $J = 5.7$ Hz, 2H). $^{13}\text{C}\{^1\text{H}\}$ NMR (150 MHz, CDCl_3): δ_{C} 159.2, 152.4, 150.8, 150.7, 149.7, 138.2, 135.4, 132.6, 128.7, 127.6, 127.5, 123.4, 116.3, 112.7, 90.0, 45.4. HRMS (ESI-FTMS) m/z : $[\text{M}+\text{H}]^+$ Calcd for $\text{C}_{18}\text{H}_{15}\text{N}_4$ 287.1296; Found 287.1292.



2-(benzylamino)-4-(4-nitrophenyl)nicotinonitrile (19c): It was prepared in accordance to the *General Procedure for Pyridines Synthesis from YMs*. Purification by flash chromatography EtOAc/Hexanes from 0:100 to 20:80 afforded the desired product as a white solid in 99% yield. ^1H NMR (600 MHz, CDCl_3): δ_{H} 8.42 – 8.35 (m, 3H), 7.75 (d, $J = 8.6$ Hz, 2H), 7.42 – 7.30 (m, 5H), 6.71 (d, $J = 5.1$ Hz, 1H), 5.73 (t, $J = 5.0$ Hz, 1H), 4.79 (d, $J = 5.5$ Hz, 2H). $^{13}\text{C}\{^1\text{H}\}$ NMR (150 MHz, CDCl_3): δ_{C} 159.1, 152.7, 151.9, 148.5, 142.9, 138.1, 129.3, 128.8, 127.8, 127.7, 124.1, 116.1, 112.6, 89.8, 45.6. HRMS (ESI-FTMS) m/z : $[\text{M}+\text{H}]^+$ Calcd for $\text{C}_{19}\text{H}_{15}\text{N}_4\text{O}_2$ 331.1197; Found 331.1198.



2'-(benzylamino)-[3,4'-bipyridine]-3'-carbonitrile (19f): It was prepared in accordance to the *General Procedure for Pyridines Synthesis from YMs*. Purification by flash chromatography EtOAc/Hexanes from 0:100 to 20:80 afforded the desired product as a white solid in 96% yield. ^1H NMR (600 MHz, CDCl_3): δ_{H} 8.80 (d, $J = 2.2$ Hz, 1H), 8.73 (d, $J = 5.0$ Hz, 1H), 8.36 (d, $J = 5.1$ Hz, 1H), 7.94 (dt, $J = 8.0, 2.1$ Hz, 1H), 7.44 (dd, $J = 7.9, 4.8$ Hz, 1H), 7.40 – 7.34 (m, 4H), 7.32 – 7.28 (m, 1H), 6.69 (d, $J = 5.1$ Hz, 1H), 5.81 (t, $J = 5.1$ Hz, 1H), 4.78 (d, $J = 5.7$ Hz, 2H). $^{13}\text{C}\{^1\text{H}\}$ NMR (150 MHz, CDCl_3): δ_{C} 159.2, 152.4, 150.8, 150.7, 149.7, 138.2, 135.4, 132.6, 128.7, 127.6, 127.5, 123.4, 116.3, 112.7, 90.0, 45.4. HRMS (ESI-FTMS) m/z : $[\text{M}+\text{H}]^+$ Calcd for $\text{C}_{18}\text{H}_{15}\text{N}_4$ 287.1296; Found 287.1292.



2-(benzylamino)-4-(4-methoxyphenyl)nicotinonitrile (19g): It was prepared in accordance to the *General Procedure for Pyridines Synthesis from YMs*. Purification by flash chromatography EtOAc/Hexanes from 0:100 to 20:80 afforded the desired product as a white solid in 95% yield. ^1H NMR (600 MHz, CDCl_3): δ_{H} 8.29 (d, $J = 5.3$ Hz, 1H), 7.59 – 7.55 (m, 2H), 7.42 – 7.35 (m, 4H), 7.34 – 7.30 (m, 1H), 7.05 – 7.01 (m, 2H), 6.69 (d, $J = 5.3$ Hz, 1H), 5.67 (t, $J = 5.3$ Hz, 1H), 4.78 (d, $J = 5.5$ Hz, 2H), 3.88 (s, 3H). $^{13}\text{C}\{^1\text{H}\}$ NMR (150 MHz, CDCl_3): δ_{C} 160.9, 159.3, 154.0, 151.8, 138.5, 129.6, 128.9, 128.7, 127.7, 127.5, 117.2, 114.3, 112.8, 89.7, 55.3, 45.5. HRMS (ESI-FTMS) m/z : $[\text{M}+\text{H}]^+$ Calcd for $\text{C}_{20}\text{H}_{18}\text{N}_3\text{O}$ 316.1450; Found 316.1446.

5.10. Enamine **3f** Increased Solubility in H₂O

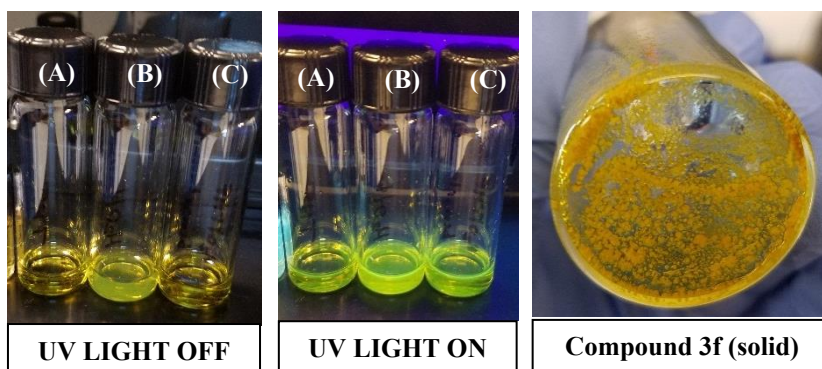


Figure 17. YM containing PEG (R₂ position) increased solubility in water; A) **3f** in THF/BnNH₂ (1:1); B) **3f** in H₂O/BnNH₂ (1:1); C) **3f** in THF/H₂O/BnNH₂ (1:1:1).

All solutions were prepared using 10 mg of compound **3f** in 1 mL mixture solvent/BnNH₂ (ca. 30mM). Enamine **3f** is completely soluble in mixtures A, B and C. However, mixture B (H₂O/BnNH₂ (1:1)) presents slightly stronger fluorescence compared to A and C. When the same concentration of enamine **6** was tested in H₂O/BnNH₂ (1:1) not all material was solubilized.

5.11. Photophysical Studies

Absorption data was recorded on an Agilent 8453 UV–visible photo diode array spectrophotometer using a 1 × 1 cm quartz cuvette.

Steady-State and Time-Resolved Emission data were collected at room temperature using an Edinburgh FLS980 spectrometer. Samples were excited using light output from a housed 450 W Xe lamp passed through a single grating (1800 l/mm, 250 nm blaze) Czerny-Turner monochromator. Emission from the sample was first passed through a 420 nm long-pass color filter, then a single grating (1800 l/mm, 500 nm blaze) Czerny-Turner monochromator and finally detected by a peltier-cooled Hamamatsu R928 photomultiplier tube.

The dynamics of emission decay were monitored using the FLS980's time-correlated single-photon counting capability (1024 channels; 100 ns window) with data

collection for 10,000 counts. Excitation for TCSPC was provided by an Edinburgh EPL-405 ps pulsed light emitting diode (405 ± 10 nm, pulse width 57.6 ps) operated at 10 MHz. Emission was passed through a 420 nm long-pass filter and then a single grating (1800 l/mm, 500 nm blaze) Czerny–Turner monochromator and finally detected by a Peltier-cooled Hamamatsu R928 photomultiplier tube. Time-resolved emission data were fit using a mono-exponential function (equation 1) using Edinburgh software package.

$$y = A_1 e^{-k_1 x} + y_0 \quad (\text{eq S1})$$

Quantum Yield data was collected at room temperature using a Hamamatsu Quantaury-QY Spectrometer. Samples and the solvent-only reference were placed in a 13 cm \times 1 cm round bottom quartz tube containing *ca.* 1 mL of solvent. Samples were excited using a 405 nm output from a 150 W Xenon arc lamp and detected by a back-illuminated cooled 1024 channel CCD detector. Quantum yields were calculated using the Quantaury software package.

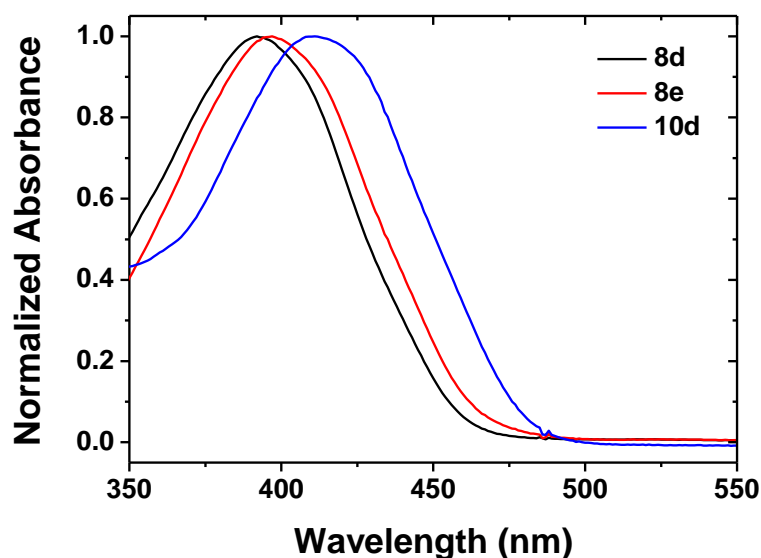


Figure 18. Normalized absorption spectra of **8d**, **8e** and **10d** in DCM.

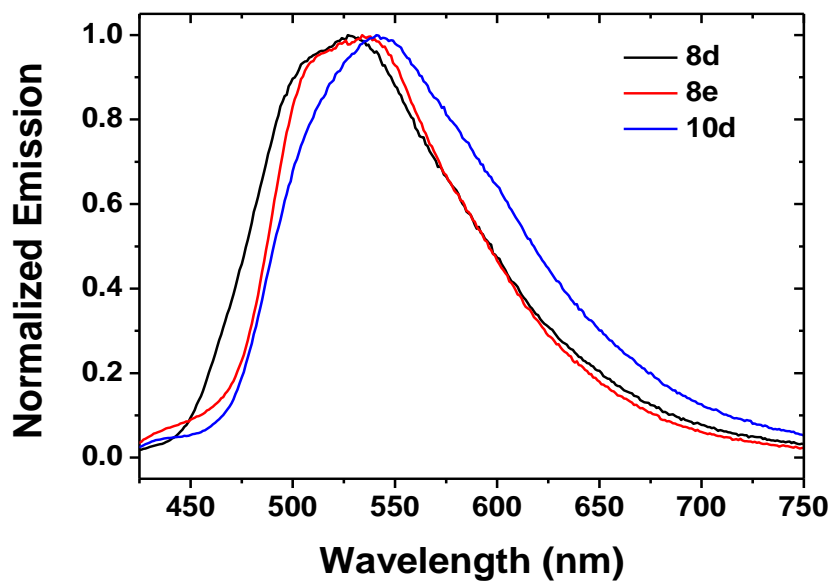


Figure 19. Normalized emission spectra of **8d**, **8e** and **10d** in DCM ($\lambda_{\text{ex}} = 405 \text{ nm}$).

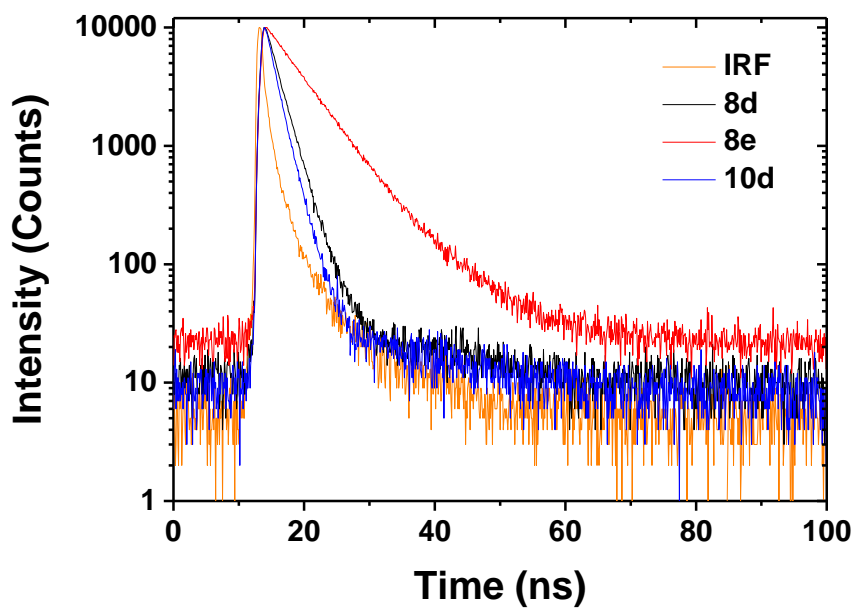


Figure 20. Emission decays for **8d**, **8e** and **10d** in DCM ($\lambda_{\text{ex}} = 405 \text{ nm}$, $\lambda_{\text{em}} = \text{emission maximum}$).

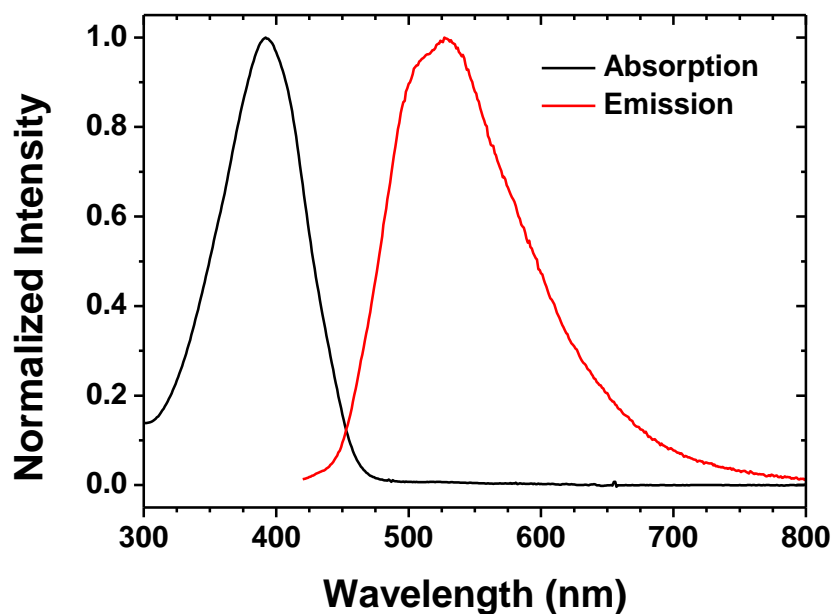


Figure 21. Normalized absorption and emission spectra of **8d** in DCM ($\lambda_{\text{ex}} = 405$ nm).

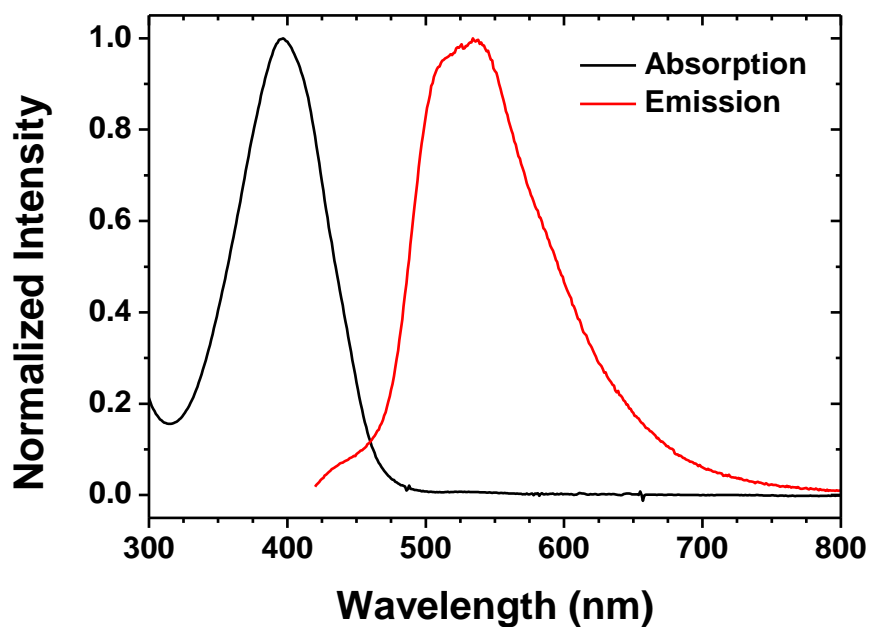


Figure 22. Normalized absorption and emission spectra of **8e** in DCM ($\lambda_{\text{ex}} = 405$ nm).

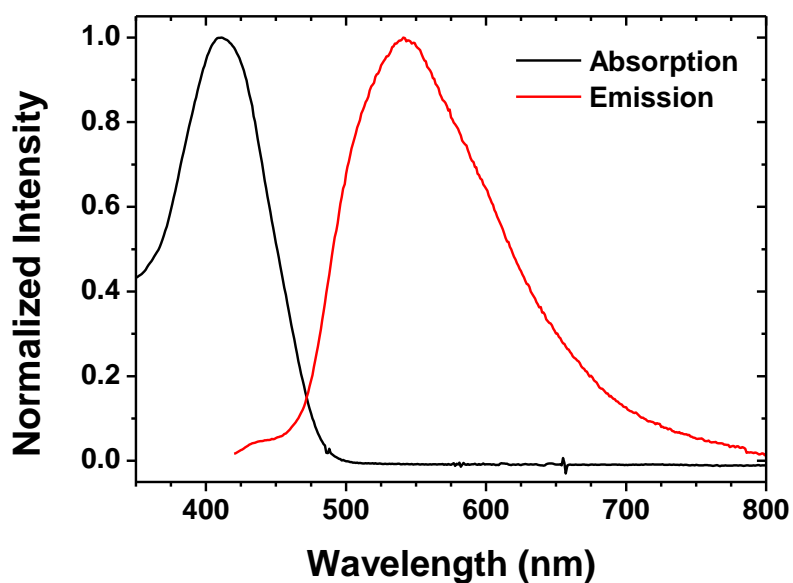


Figure 23. Normalized absorption and emission spectra of **10d** in DCM ($\lambda_{\text{ex}} = 405$ nm).

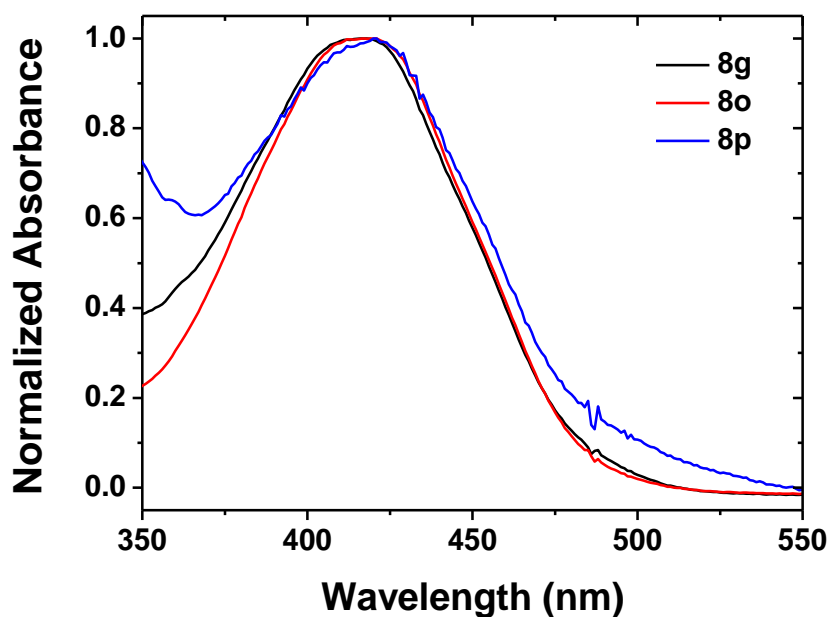


Figure 24. Normalized absorption spectra of **8g**, **8o** and **8p** in DCM.

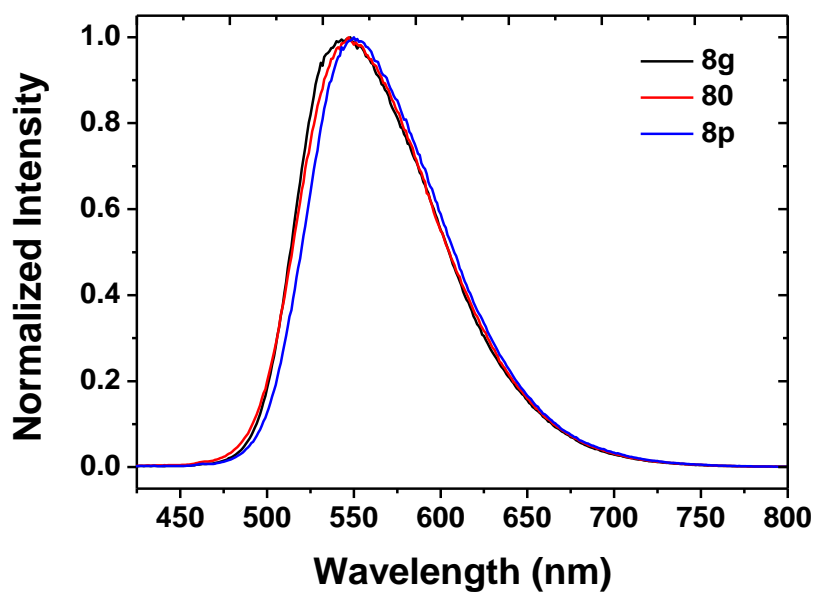


Figure 25. Normalized emission spectra of **8g**, **8o** and **8p** in DCM ($\lambda_{\text{ex}} = 405$ nm).

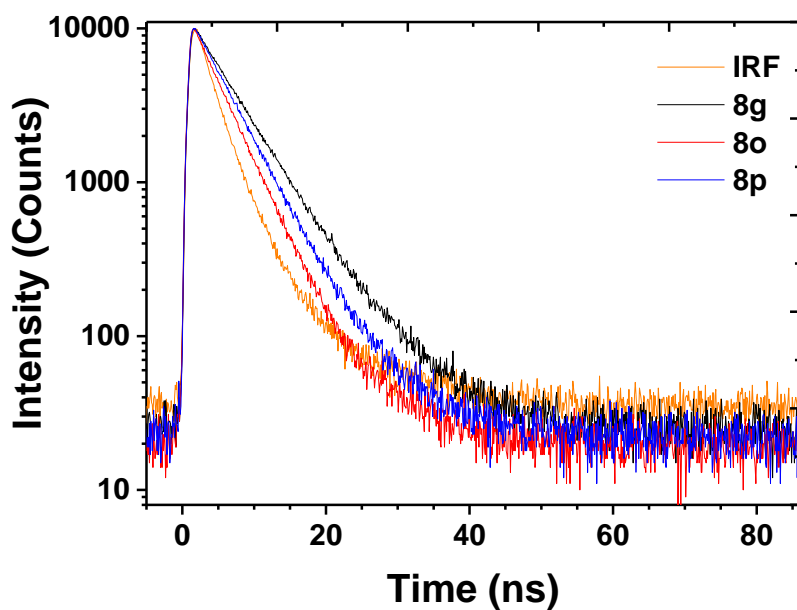


Figure 26. Emission decays for **8g**, **8o** and **8p** in DCM ($\lambda_{\text{ex}} = 405$ nm, $\lambda_{\text{em}} =$ emission maximum).

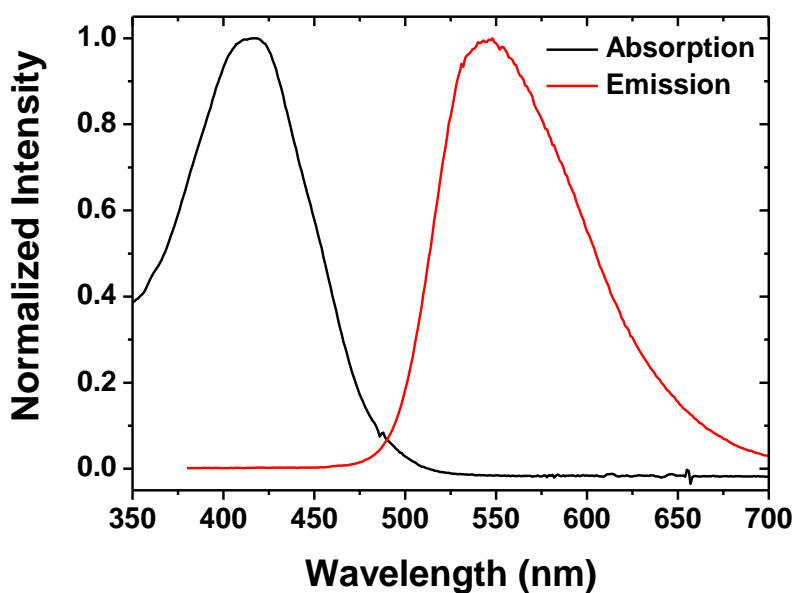


Figure 27. Normalized absorption and emission spectra of **8g** in DCM ($\lambda_{\text{ex}} = 405$ nm).

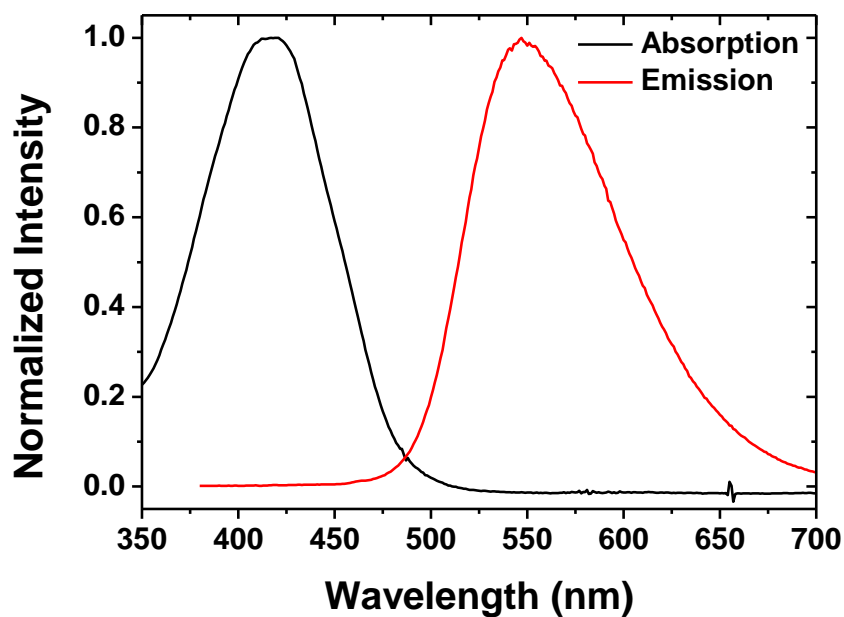


Figure 28. Normalized absorption and emission spectra of **8o** in DCM ($\lambda_{\text{ex}} = 405$ nm).

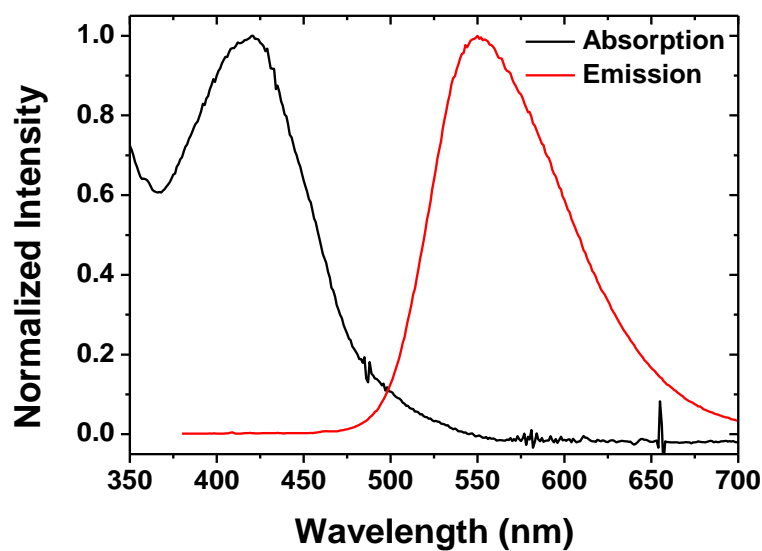


Figure 29. Normalized absorption and emission spectra of **8p** in DCM ($\lambda_{\text{ex}} = 405$ nm).

Pyridines from YMs Substrates - Blue Fluorescence:

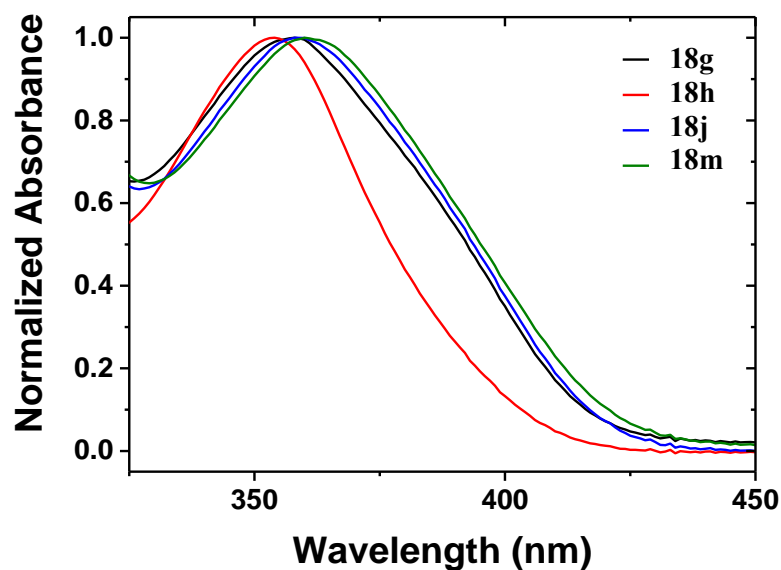


Figure 30. Normalized absorption spectra of **18g**, **18h**, **18j**, and **18m** in DCM.

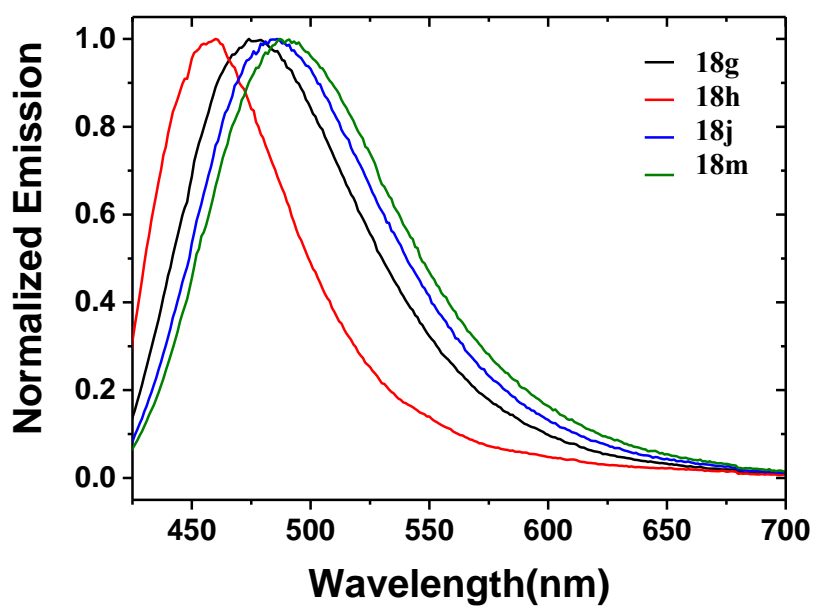


Figure 31. Normalized emission spectra of **18g**, **18h**, **18j**, and **18m** in DCM ($\lambda_{\text{ex}} = 405$ nm).

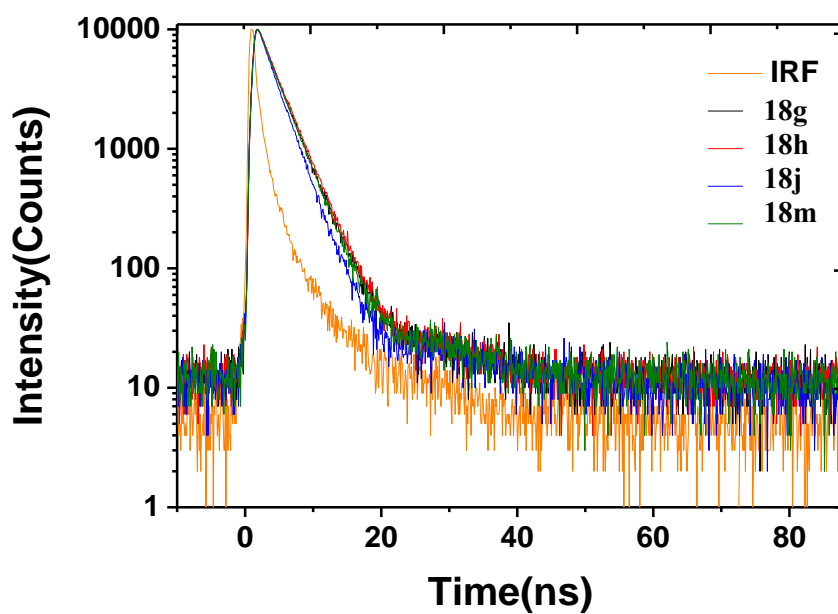


Figure 32. Emission decays for **18g**, **18h**, **18j**, and **18m** in DCM ($\lambda_{\text{ex}} = 405$ nm, $\lambda_{\text{em}} =$ emission maximum).

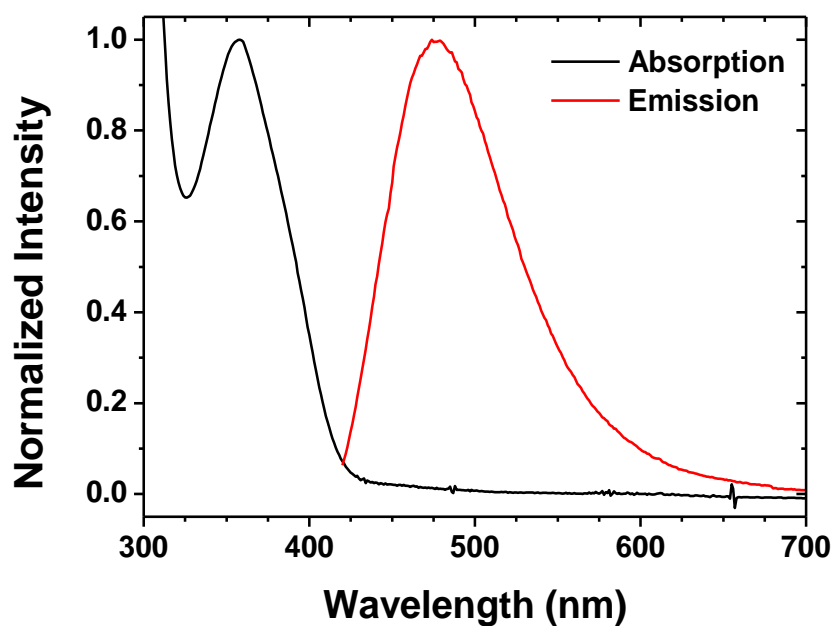


Figure 33. Normalized absorption and emission spectra of **18g** in DCM ($\lambda_{\text{ex}} = 405$ nm).

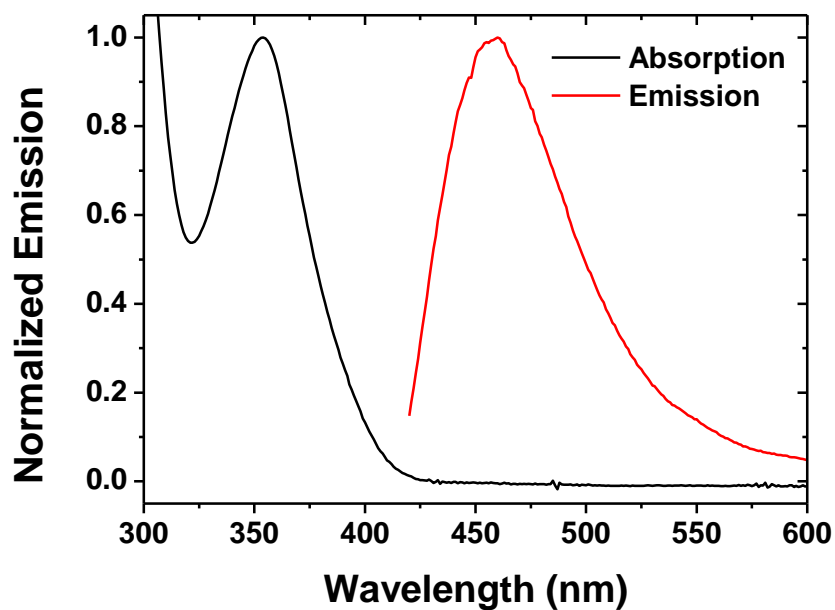


Figure 34. Normalized absorption and emission spectra of **18h** in DCM ($\lambda_{\text{ex}} = 405$ nm).

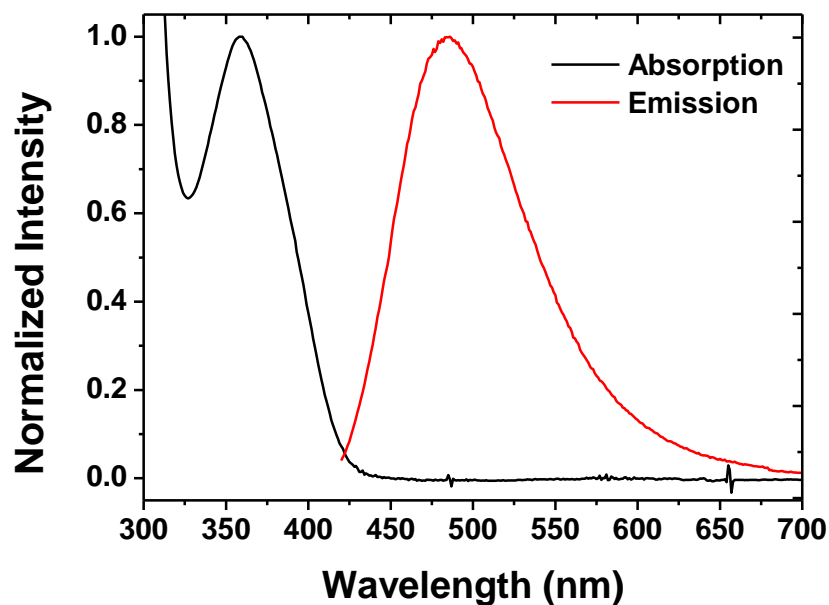


Figure 35. Normalized absorption and emission spectra of **18j** in DCM ($\lambda_{\text{ex}} = 405$ nm).

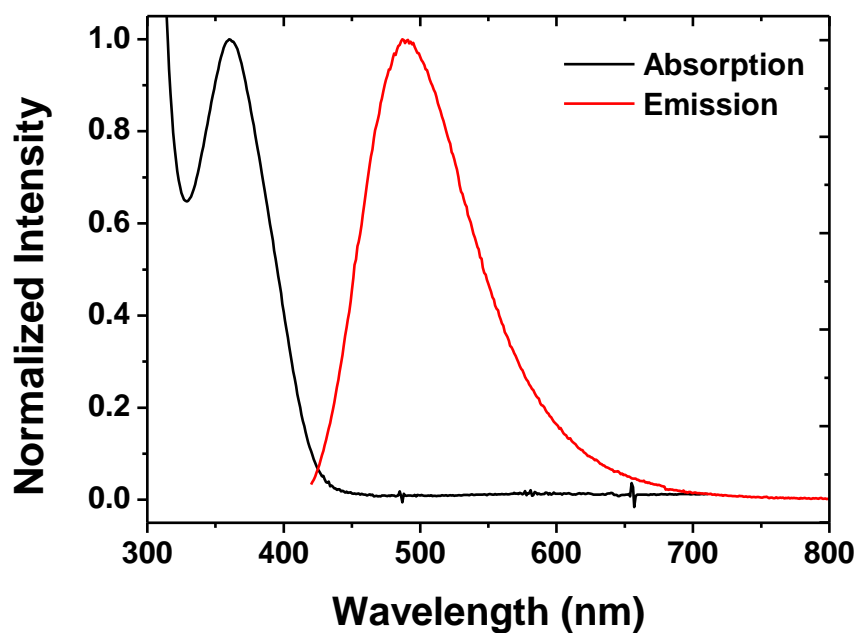


Figure 36. Normalized absorption and emission spectra of **18m** in DCM ($\lambda_{\text{ex}} = 405$ nm)

Aggregation-Induced Emission of Pyridine 18i

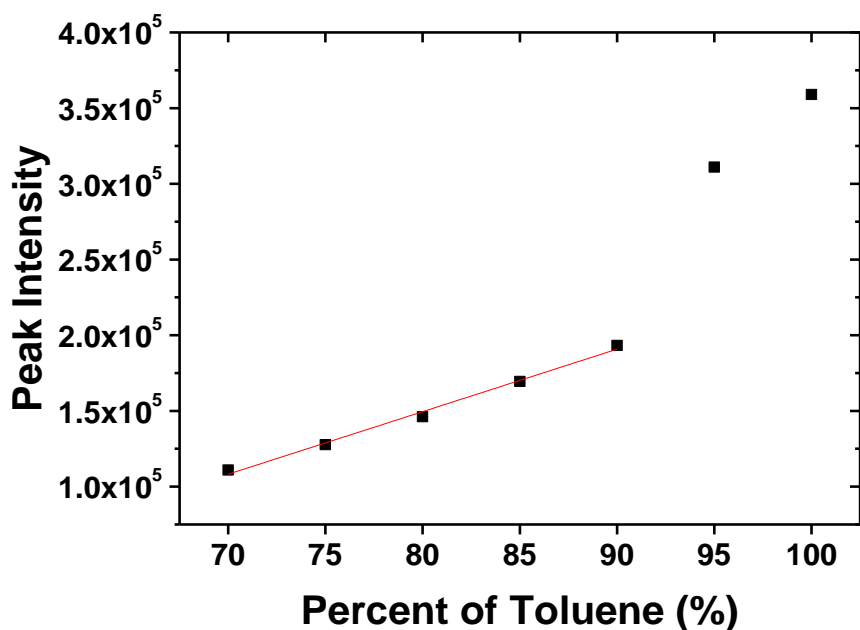


Figure 37. Relationship between emission peak intensity and the percentage of toluene.

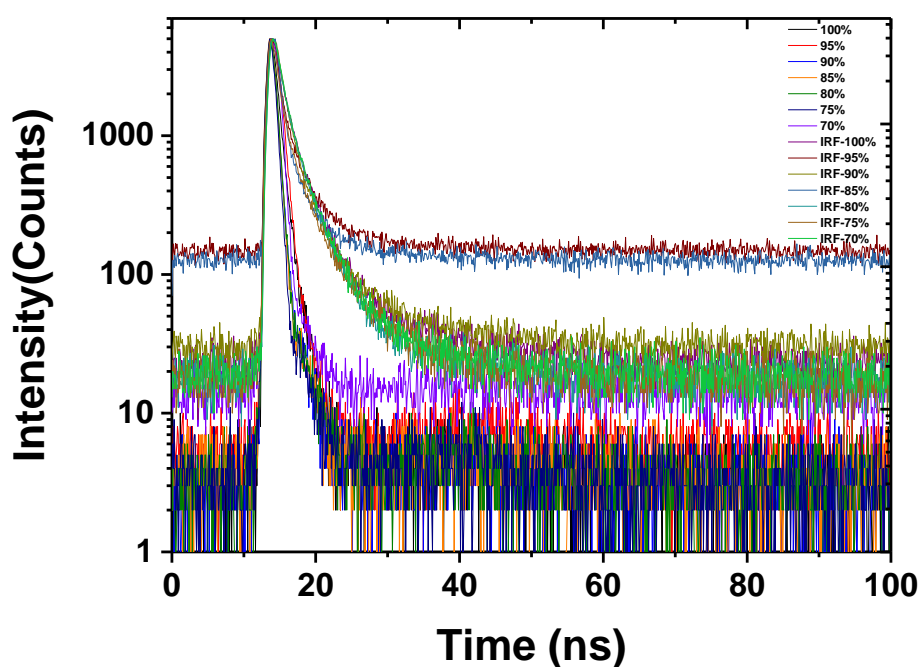


Figure 38. Emission decays for **18i** in a solution of toluene (from 100% to 70%) and DCM (from 0% to 30%). ($\lambda_{\text{ex}} = 405 \text{ nm}$, $\lambda_{\text{em}} = \text{emission maximum}$).

5.12. X-ray crystallography

All products submitted to X-ray crystallography were recrystallized in CHCl₃/Hexanes (1:20).

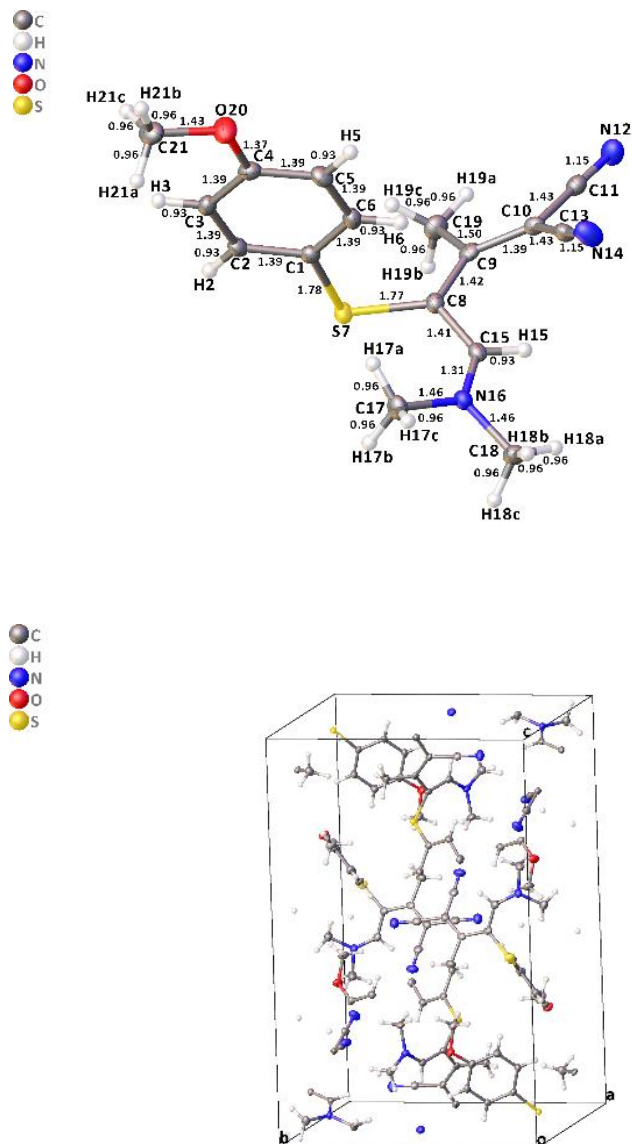
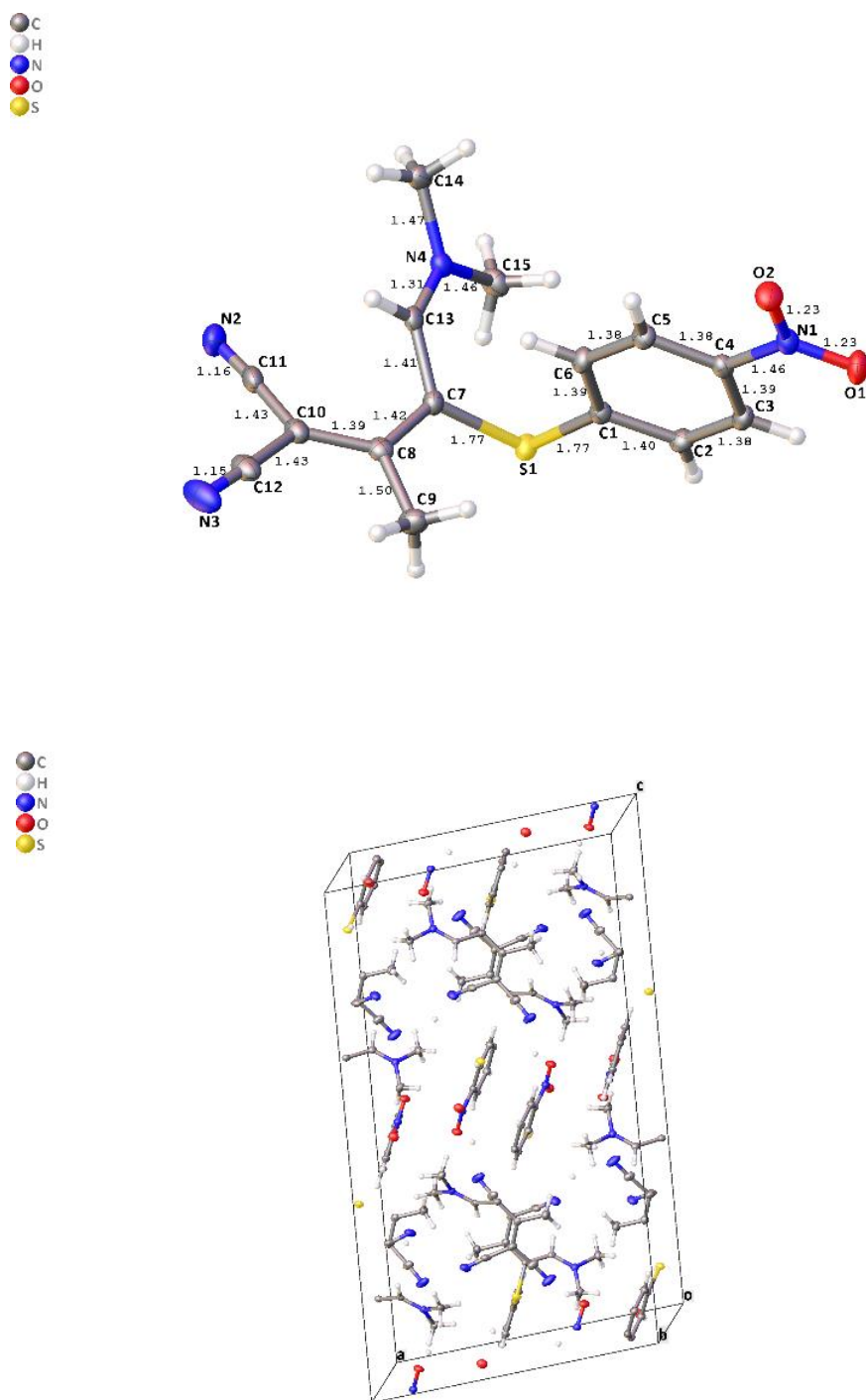
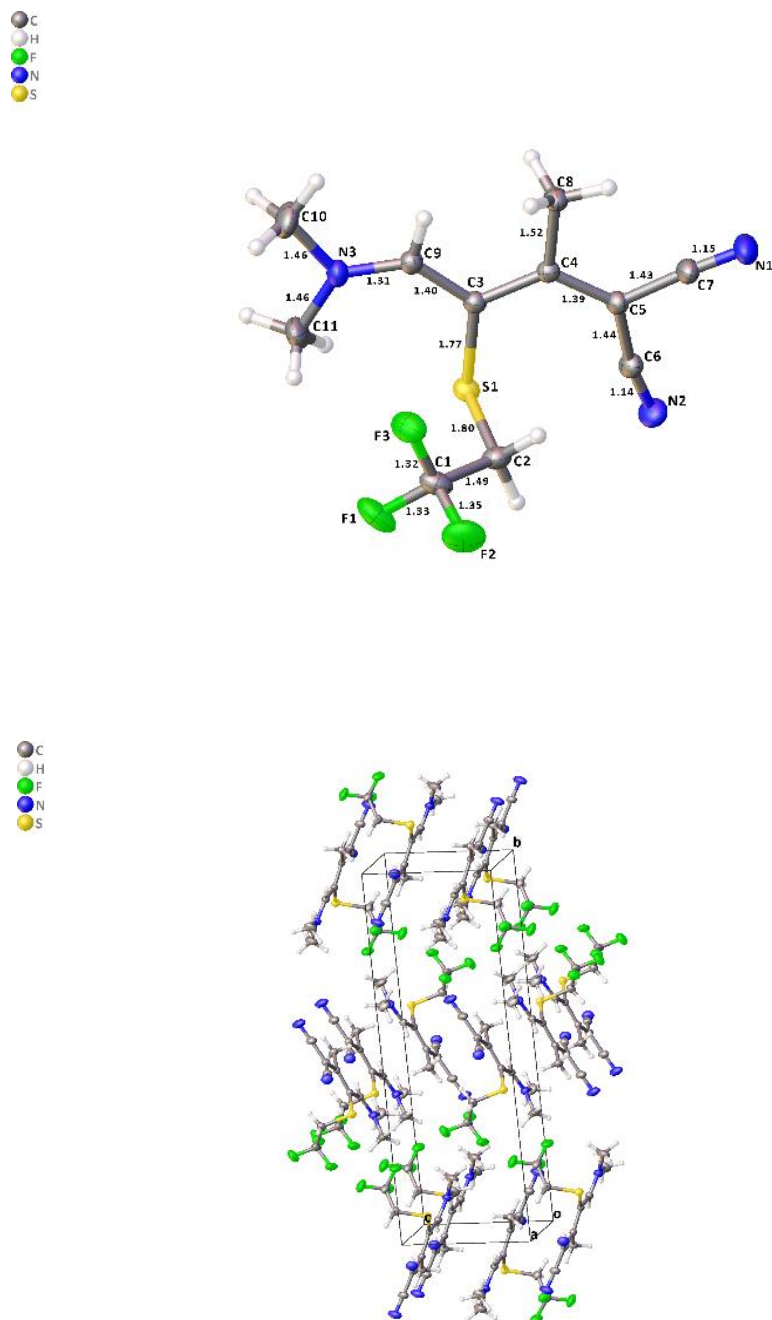


Figure 39. Compound 3a X-ray crystallography.





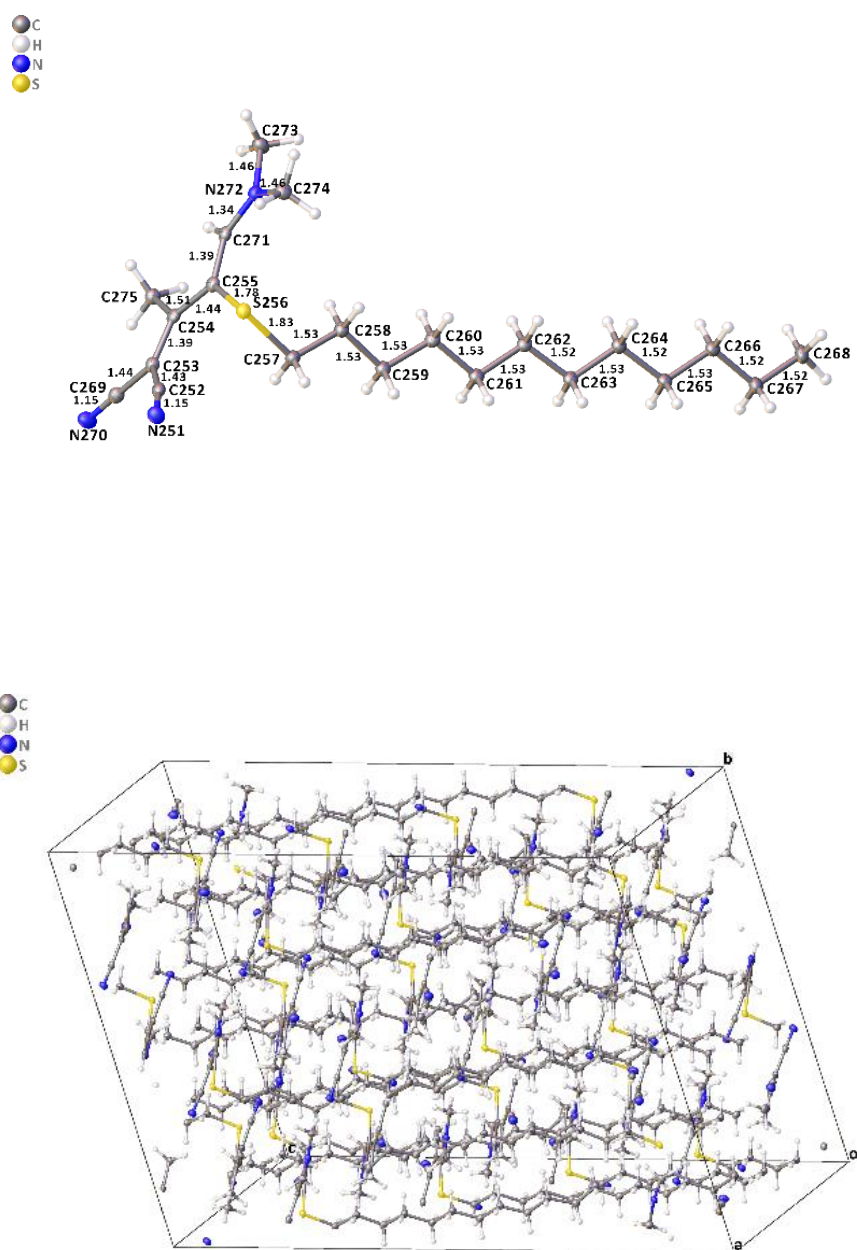


Figure 42. Compound 3e X-ray crystallography.

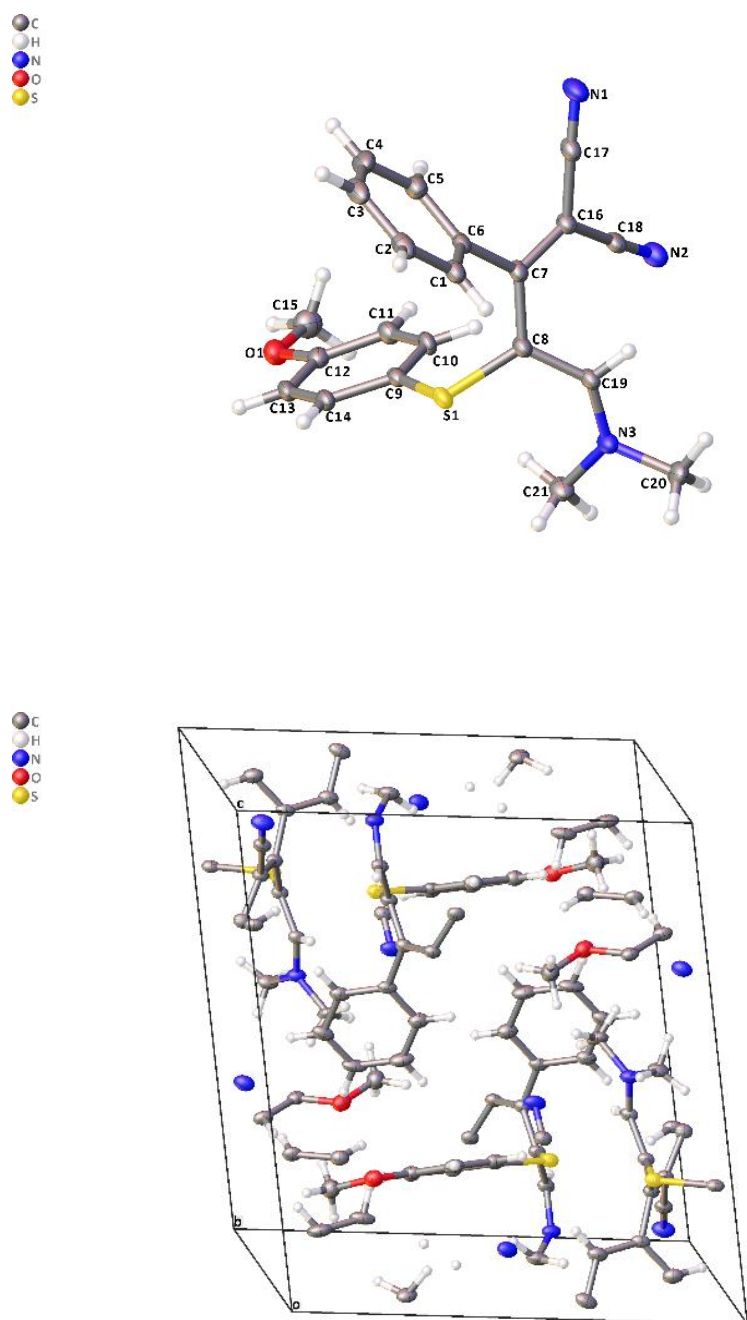


Figure 43. Compound 3g X-ray crystallography.

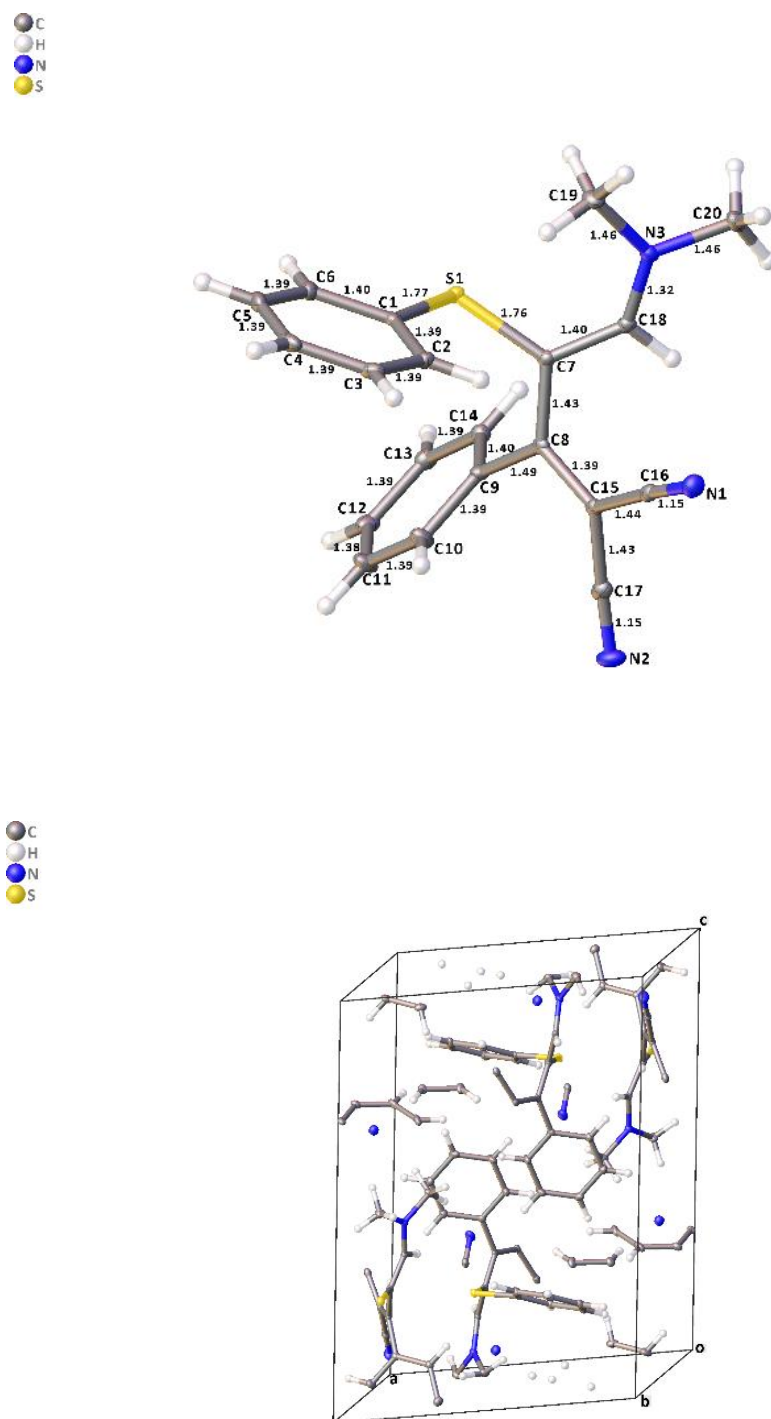


Figure 44. Compound 3h X-ray crystallography.

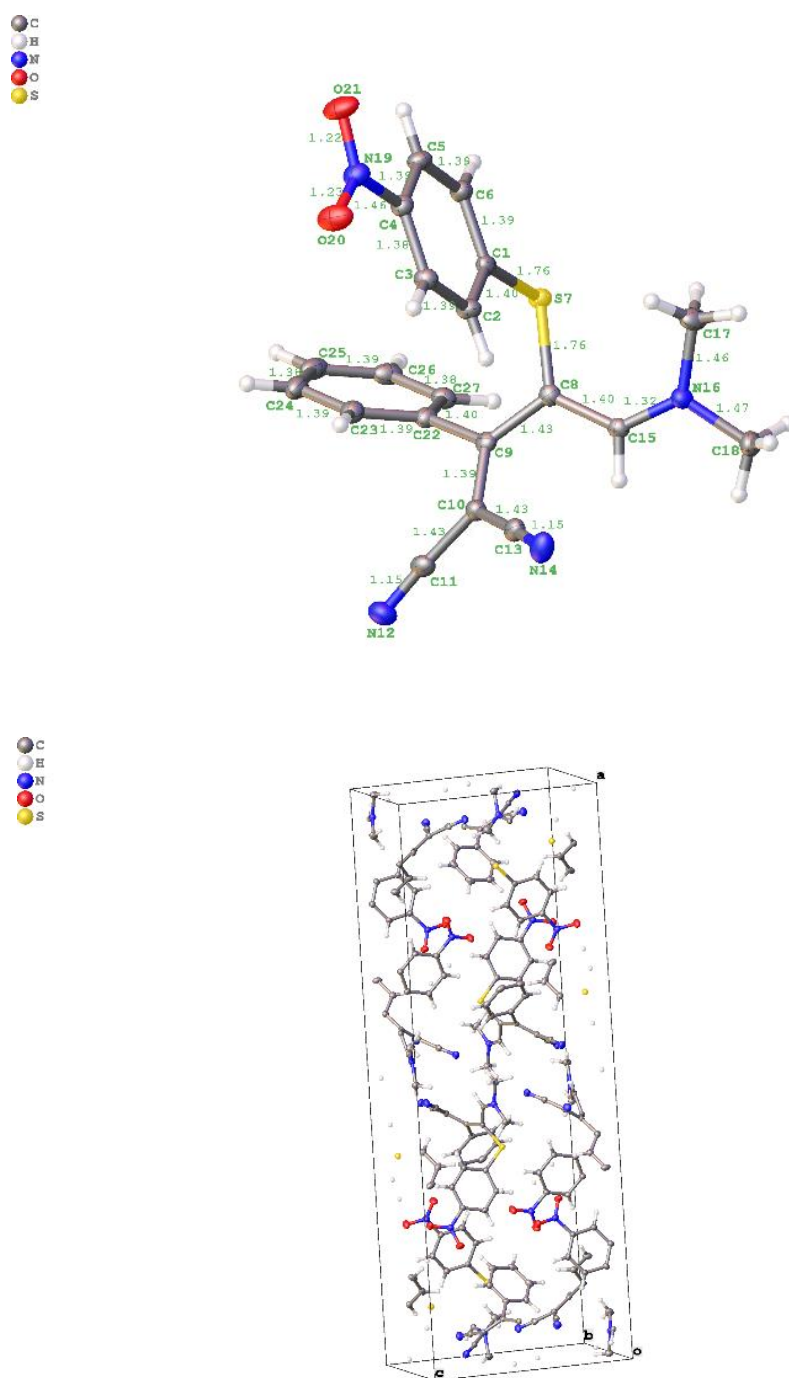


Figure 45. Compound 3r X-ray crystallography.

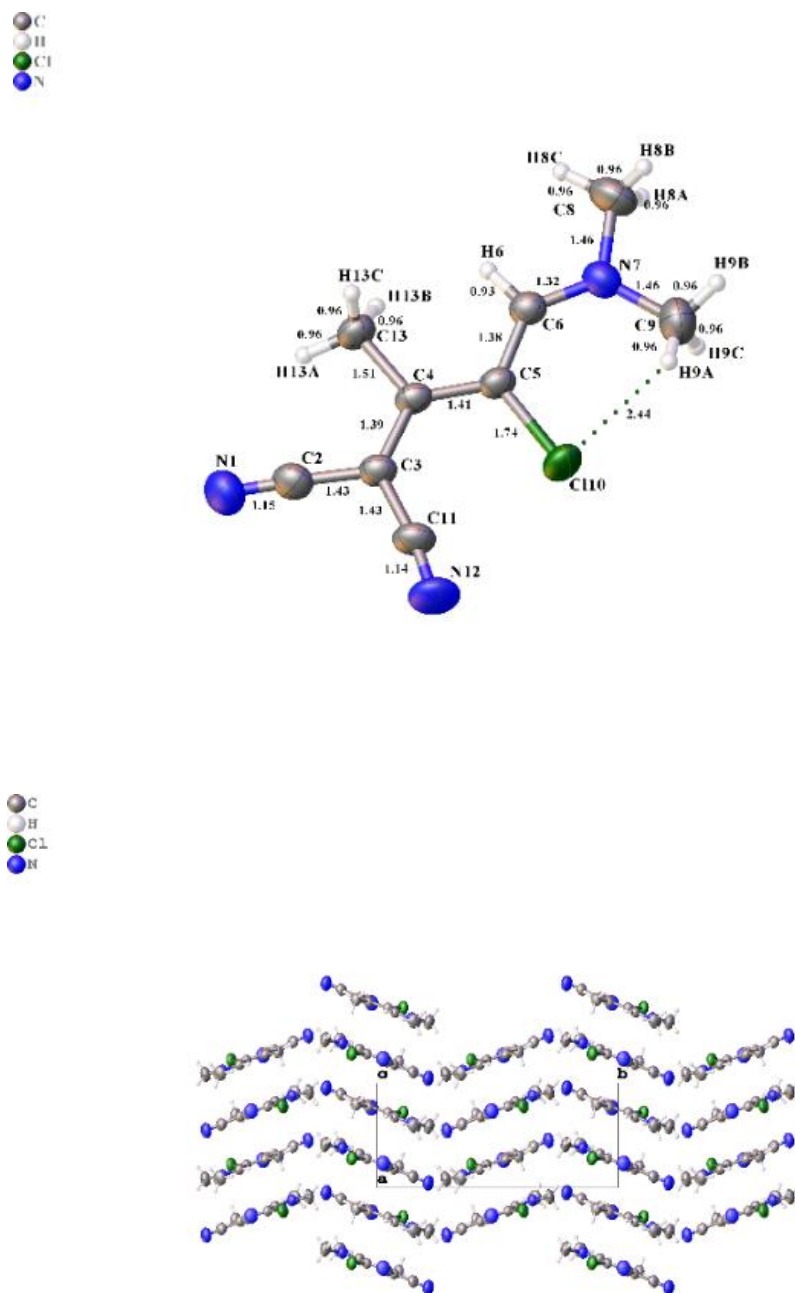


Figure 47. Compound 6 X-ray crystallography.

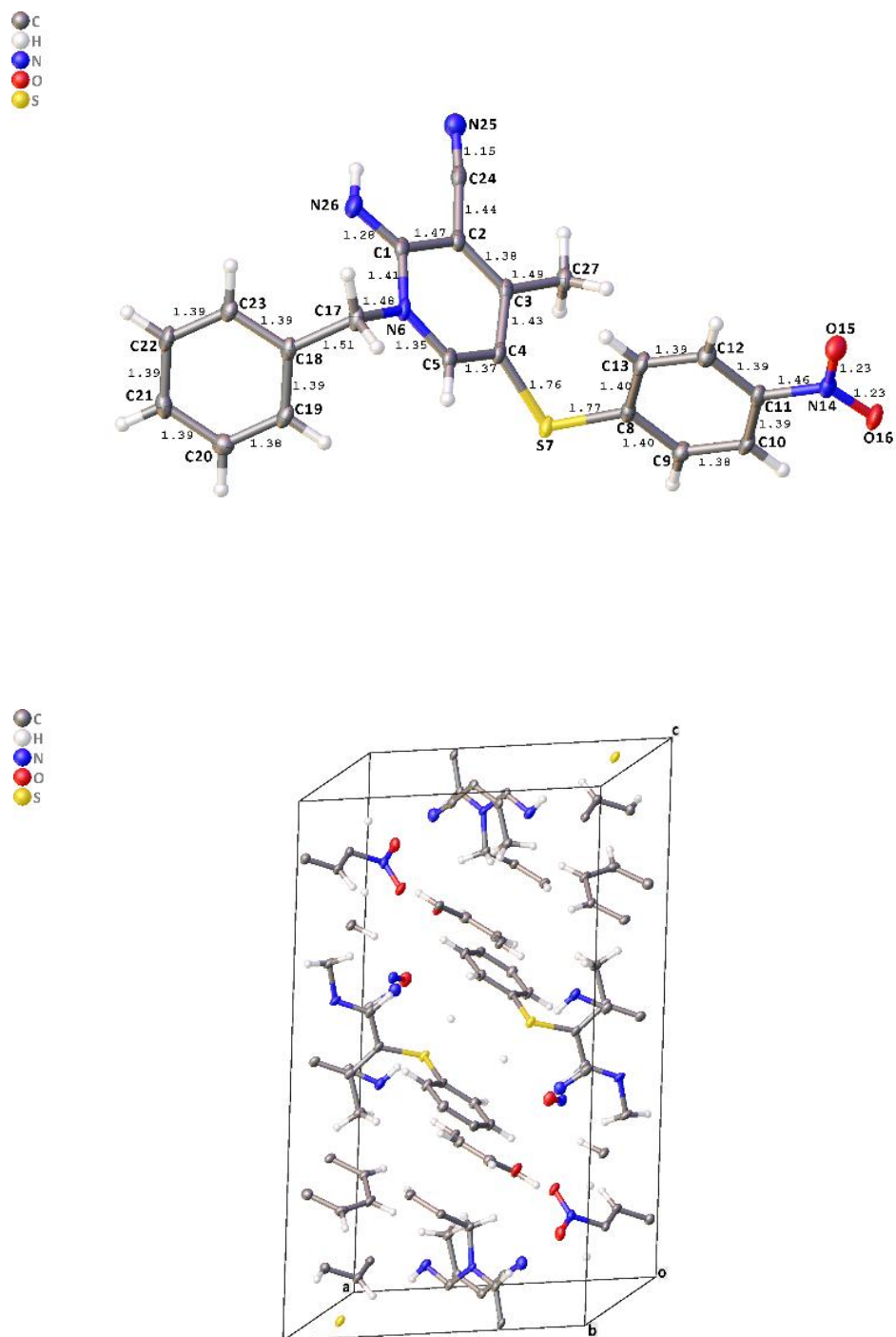


Figure 48. Compound 8c X-ray crystallography.

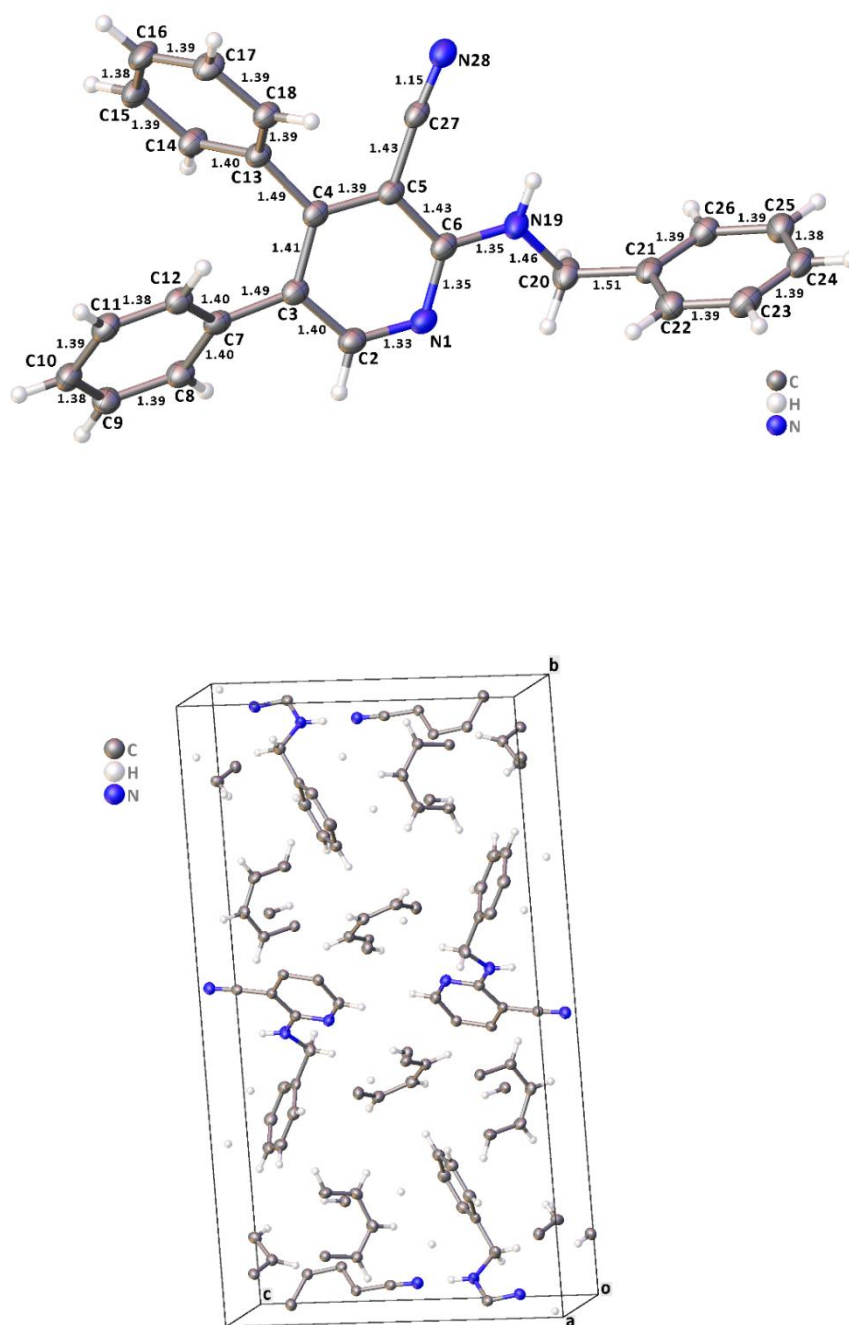


Figure 50. Pyridine 11a X-ray crystallography – R₂= Ph.

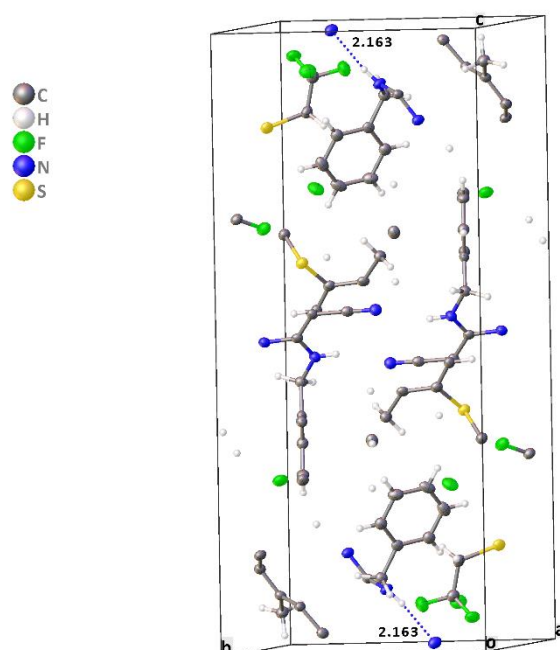
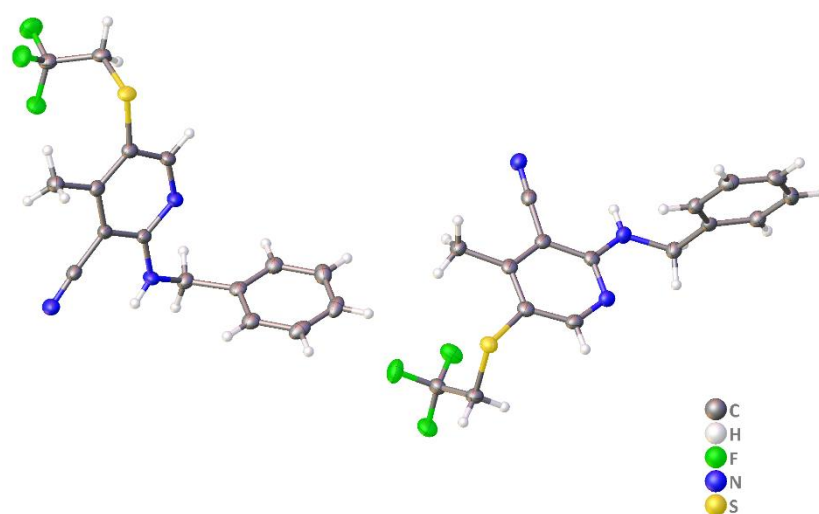
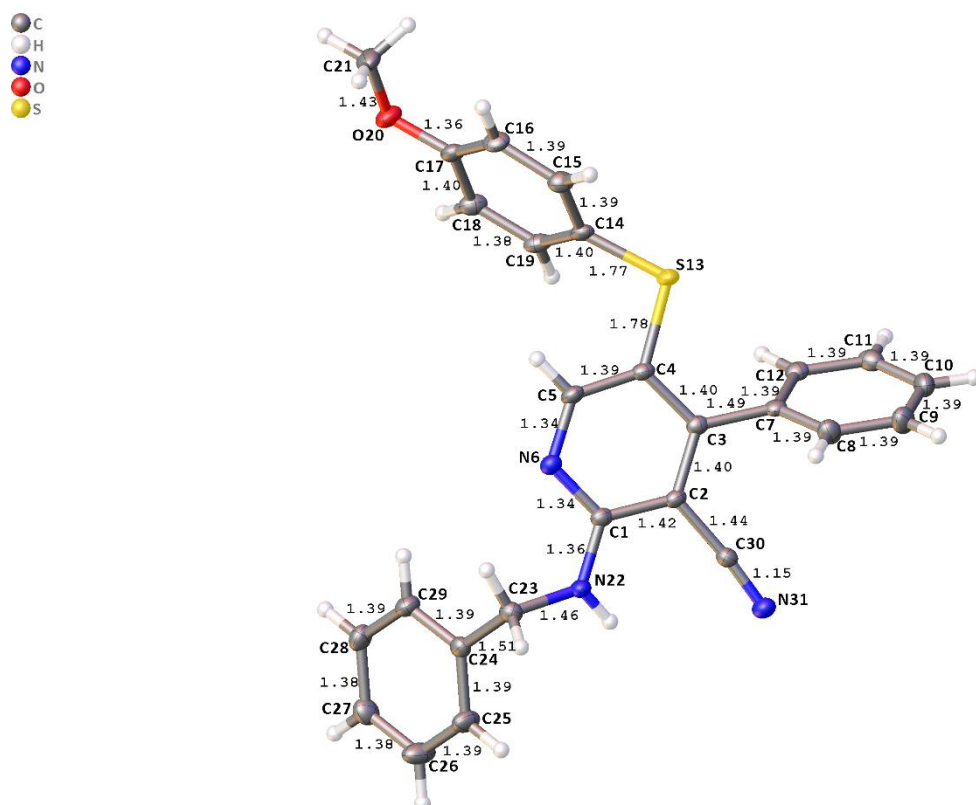


Figure 51. Pyridine **18d** X-ray crystallography – R₂= S-Alkyl.



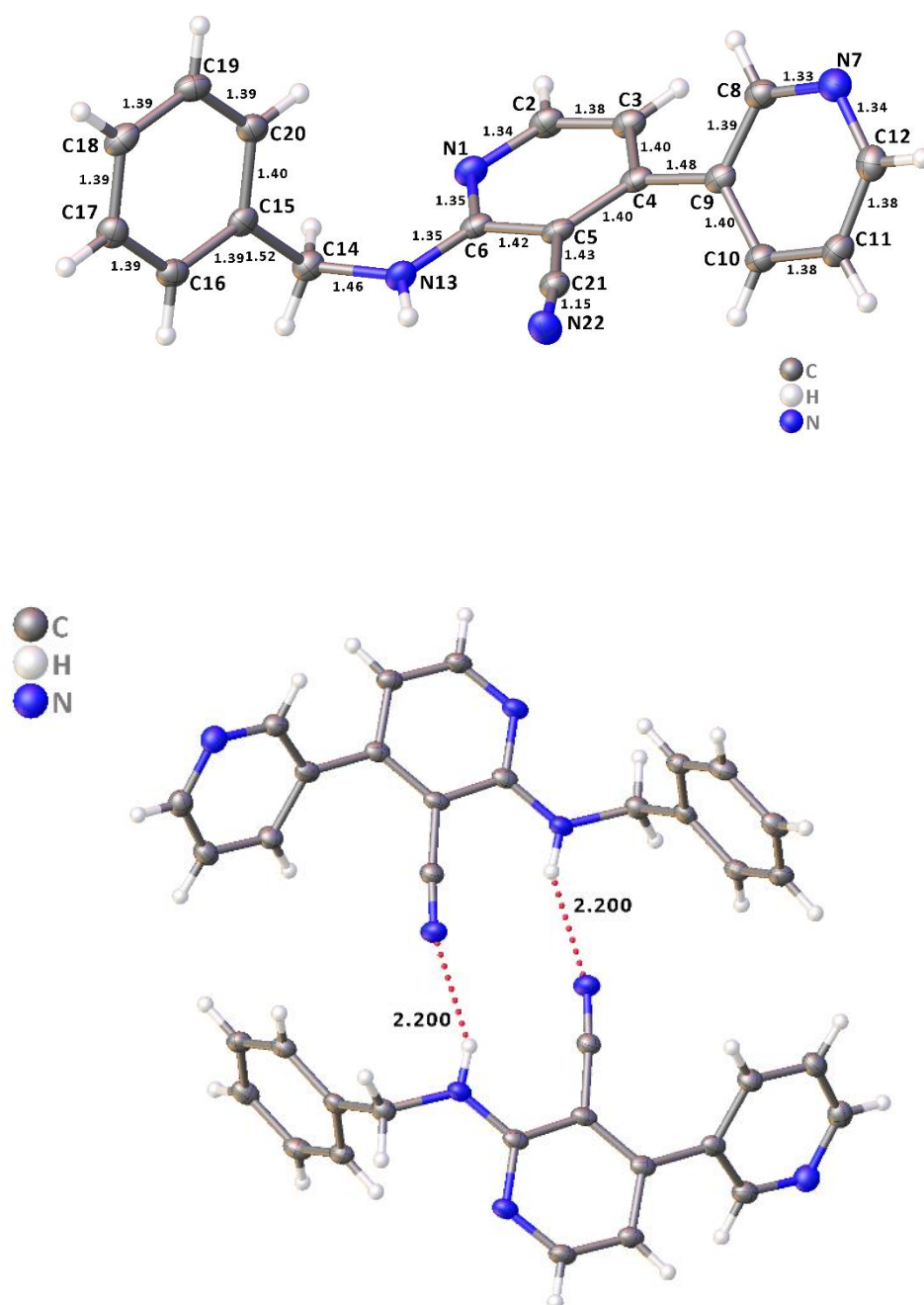
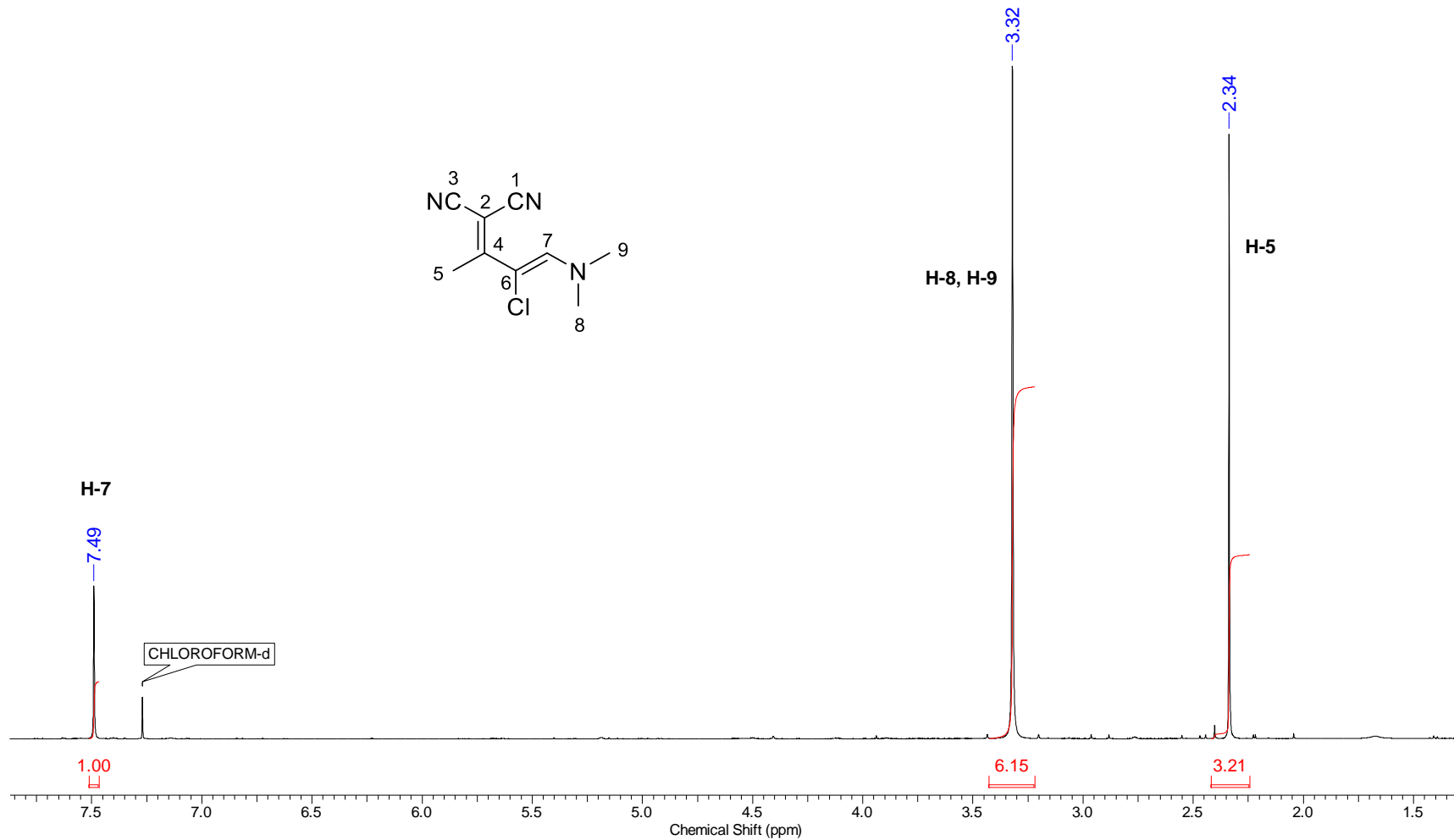


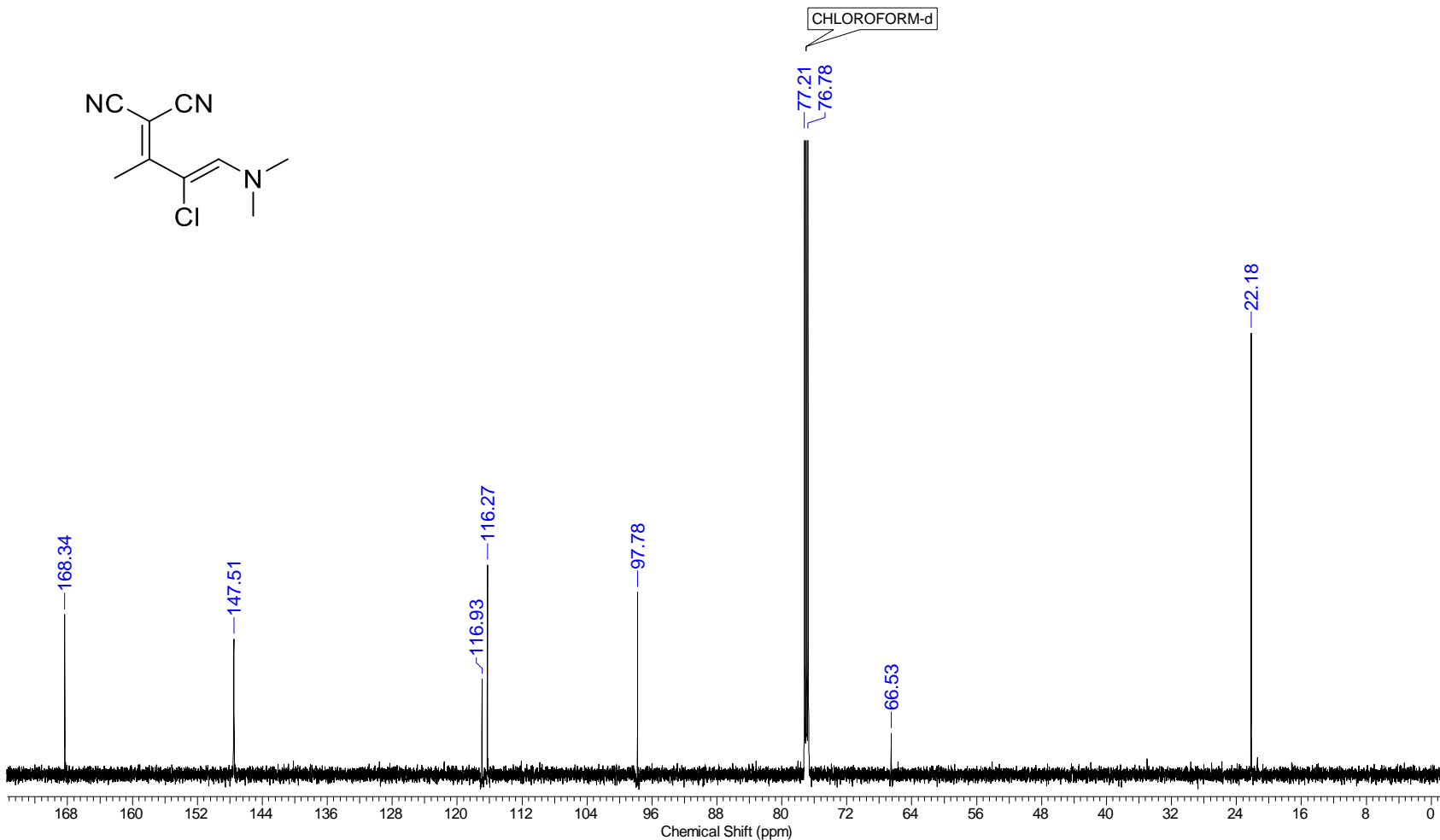
Figure 53. Pyridine 19f X-ray crystallography – R₂= H.

5.13. NMR spectra

Frequency (MHz)	600.01	Nucleus	1H	Number of Transients	16	Origin	spect
Original Points Count	32768	Owner	nmrsu	Points Count	65536	Pulse Sequence	zg30
Receiver Gain	106.90	SW(cyclical) (Hz)	12019.23	Solvent	CDCl3	Spectrum Offset (Hz)	3695.2900
Spectrum Type	STANDARD	Sweep Width (Hz)	12019.05	Temperature (degree C)	20.936	Acquisition Time (sec)	2.7263

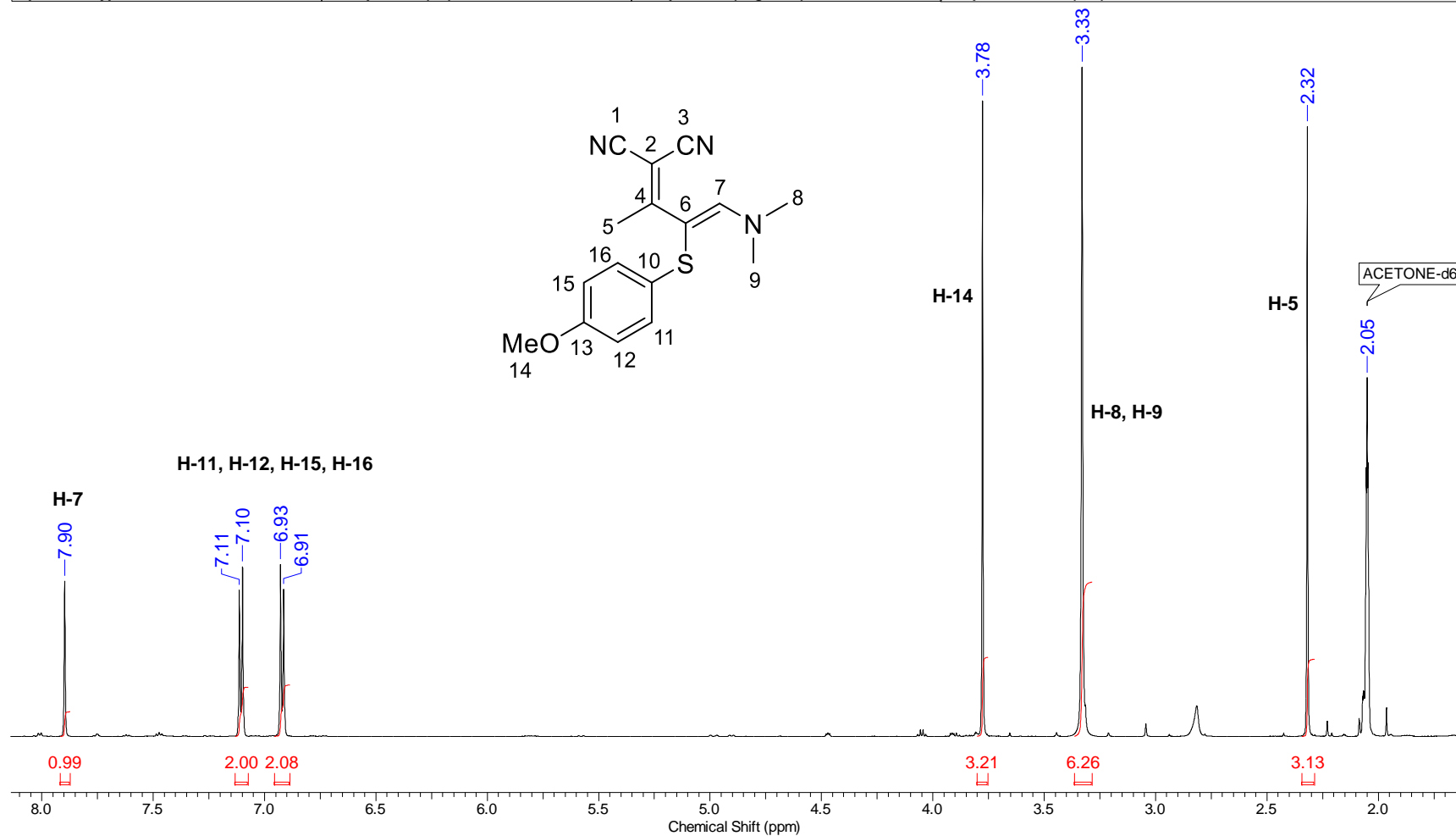


Frequency (MHz)	150.87	Nucleus	¹³ C	Number of Transients	1024	Origin	spect
Original Points Count	32768	Owner	nmsu	Points Count	32768	Pulse Sequence	zgpg30
Receiver Gain	199.73	SW(cyclical) (Hz)	36057.69	Solvent	CDCl ₃	Spectrum Offset (Hz)	15075.0830
Spectrum Type	STANDARD	Sweep Width (Hz)	36056.59	Temperature (degree C)	21.483	Acquisition Time (sec)	0.9088

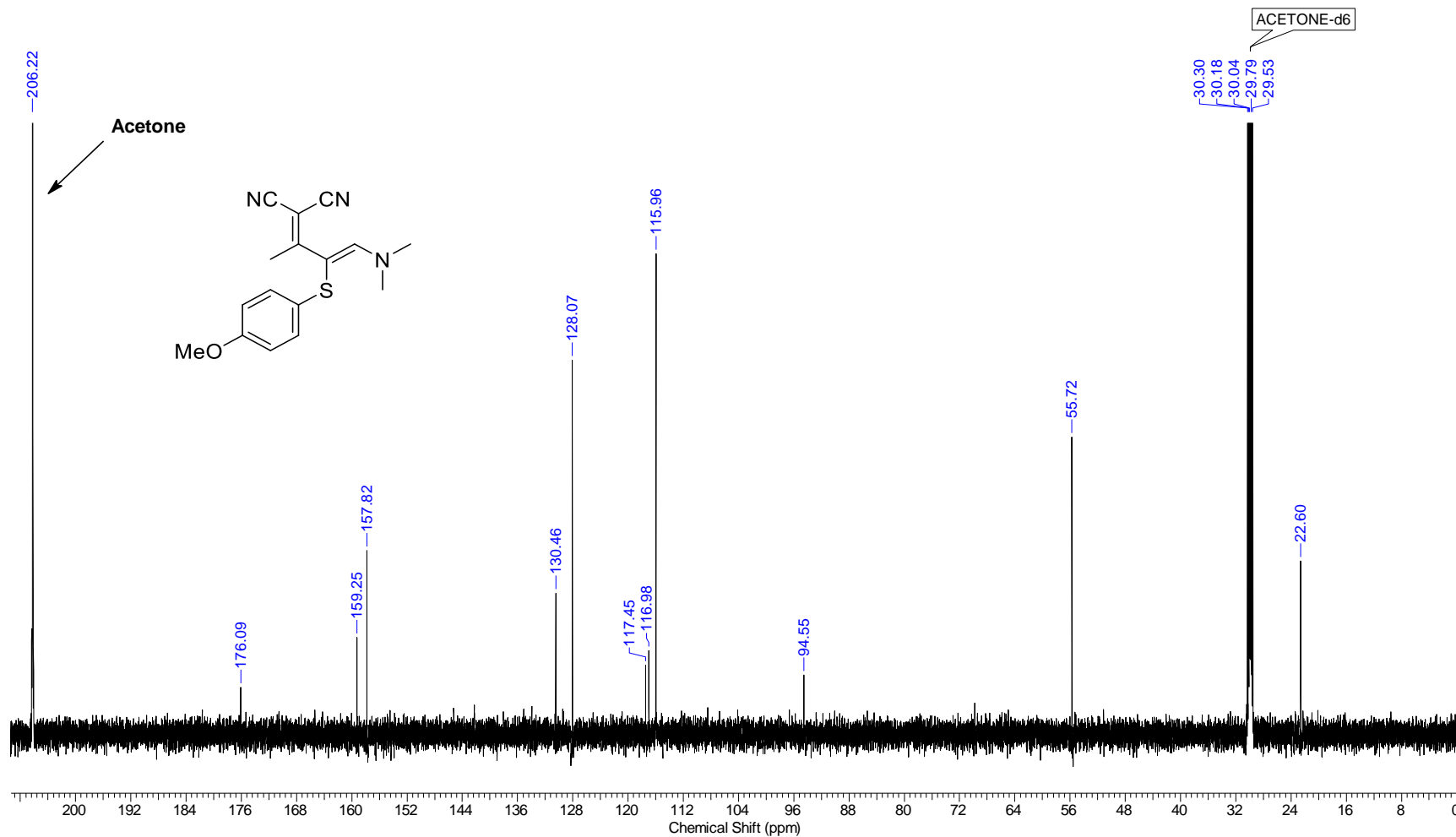


Continuous Conditions Applied to Hazardous Reactions and Fluorophores Synthesis with Photophysics Studies

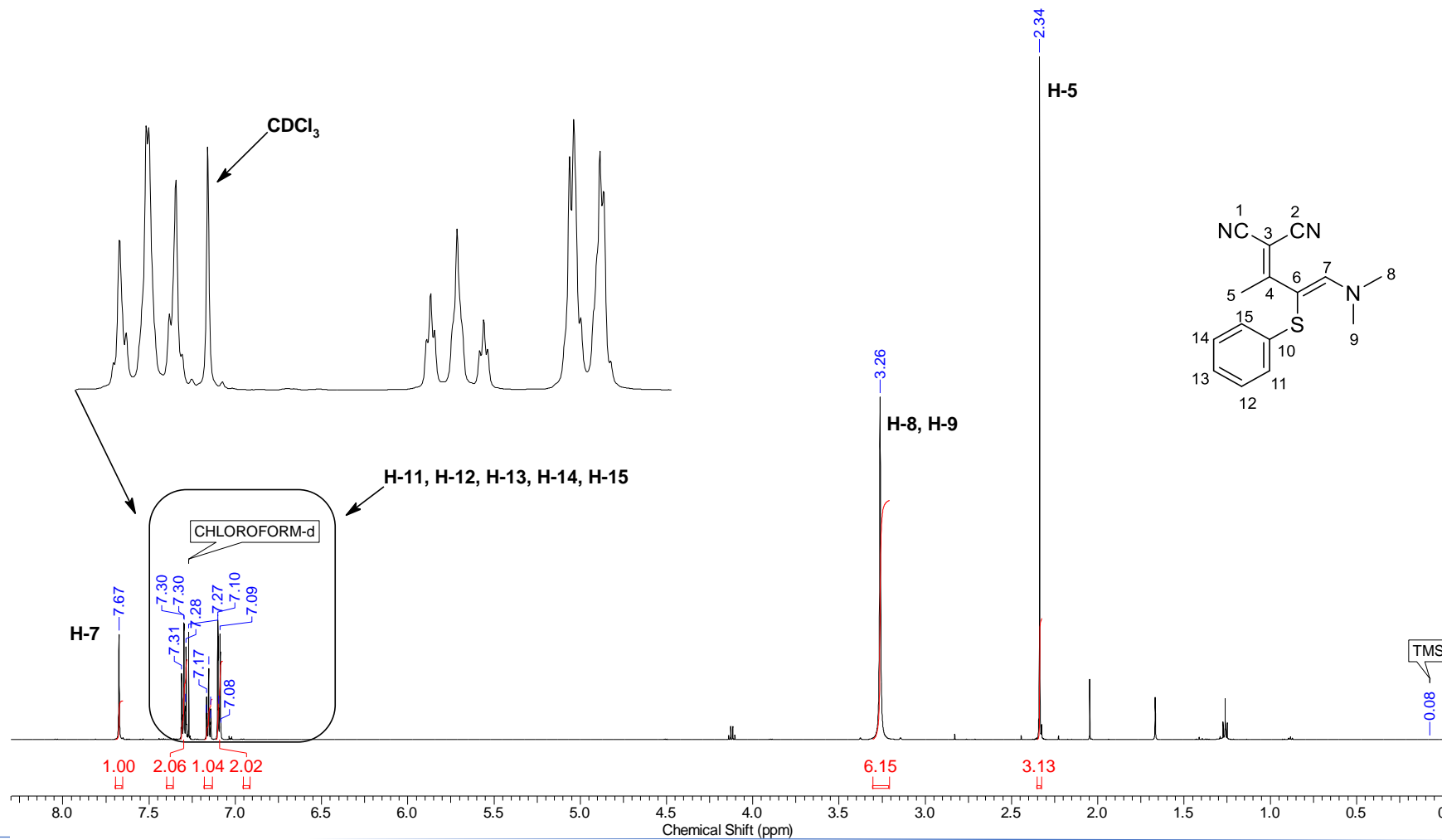
Frequency (MHz)	599.96	Nucleus	1H	Number of Transients	16	Origin	spect
Original Points Count	32768	Owner	nmrsu	Points Count	65536	Pulse Sequence	zg30
Receiver Gain	89.24	SW(cyclical) (Hz)	12019.23	Solvent	Acetone-d6	Spectrum Offset (Hz)	3695.2473
Spectrum Type	STANDARD	Sweep Width (Hz)	12019.05	Temperature (degree C)	22.284	Acquisition Time (sec)	2.7263



Frequency (MHz)	150.86	Nucleus	13C	Number of Transients	256	Origin	spect
Original Points Count	32768	Owner	nmrsu	Points Count	32768	Pulse Sequence	zgpg30
Receiver Gain	194.75	SW(cyclical) (Hz)	36057.69	Solvent	Acetone-d6	Spectrum Offset (Hz)	15229.8770
Spectrum Type	STANDARD	Sweep Width (Hz)	36056.59	Temperature (degree C)	23.103	Acquisition Time (sec)	0.9088

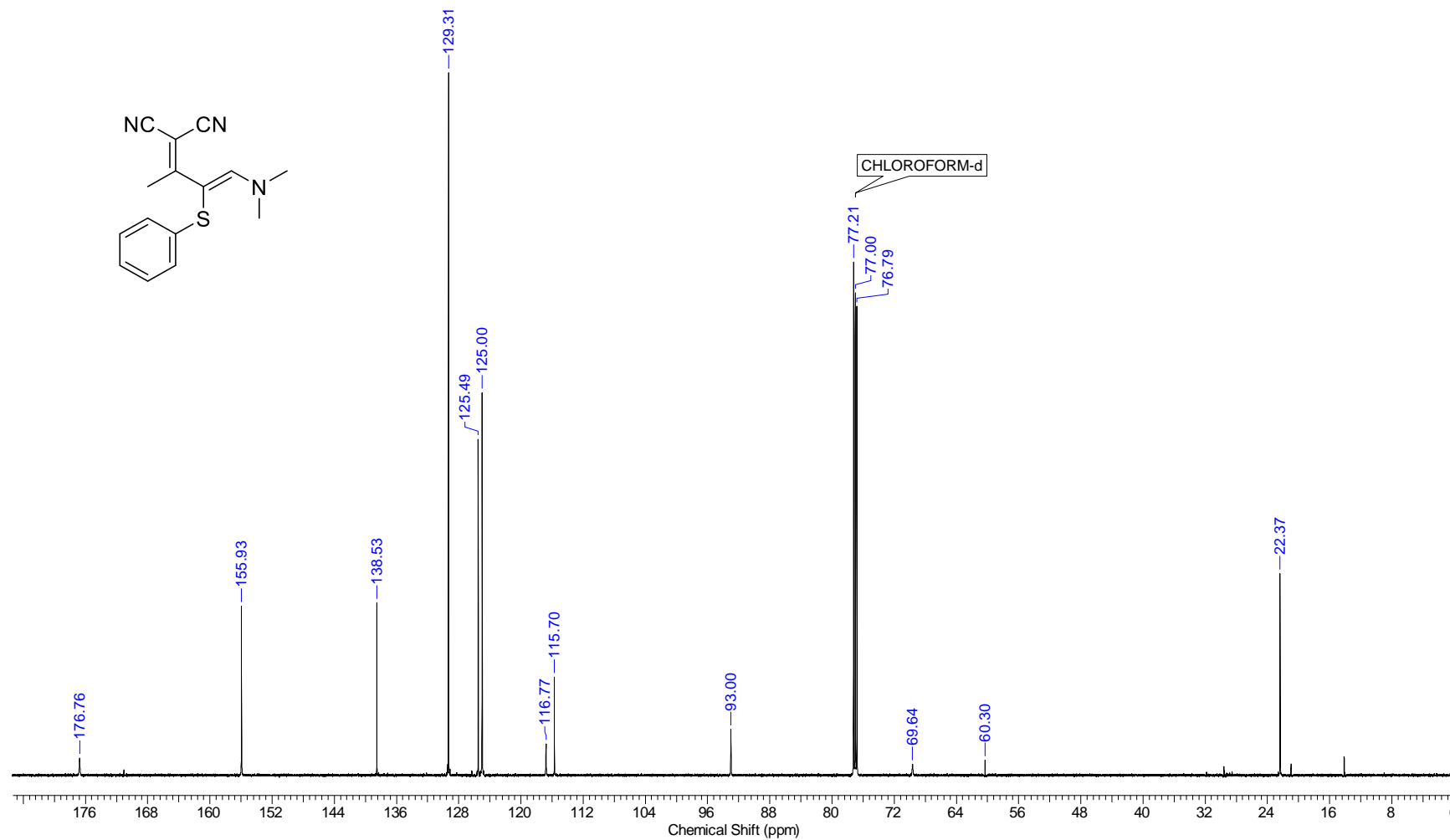


Frequency (MHz)	600.01	Nucleus	¹ H	Number of Transients	16	Origin	spect
Original Points Count	32768	Owner	nmr	Points Count	65536	Pulse Sequence	zg30
Receiver Gain	78.64	SW(cyclical) (Hz)	12019.23	Solvent	CDCl ₃	Spectrum Offset (Hz)	3695.4727
Spectrum Type	STANDARD	Sweep Width (Hz)	12019.05	Temperature (degree C)	23.195	Acquisition Time (sec)	2.7263



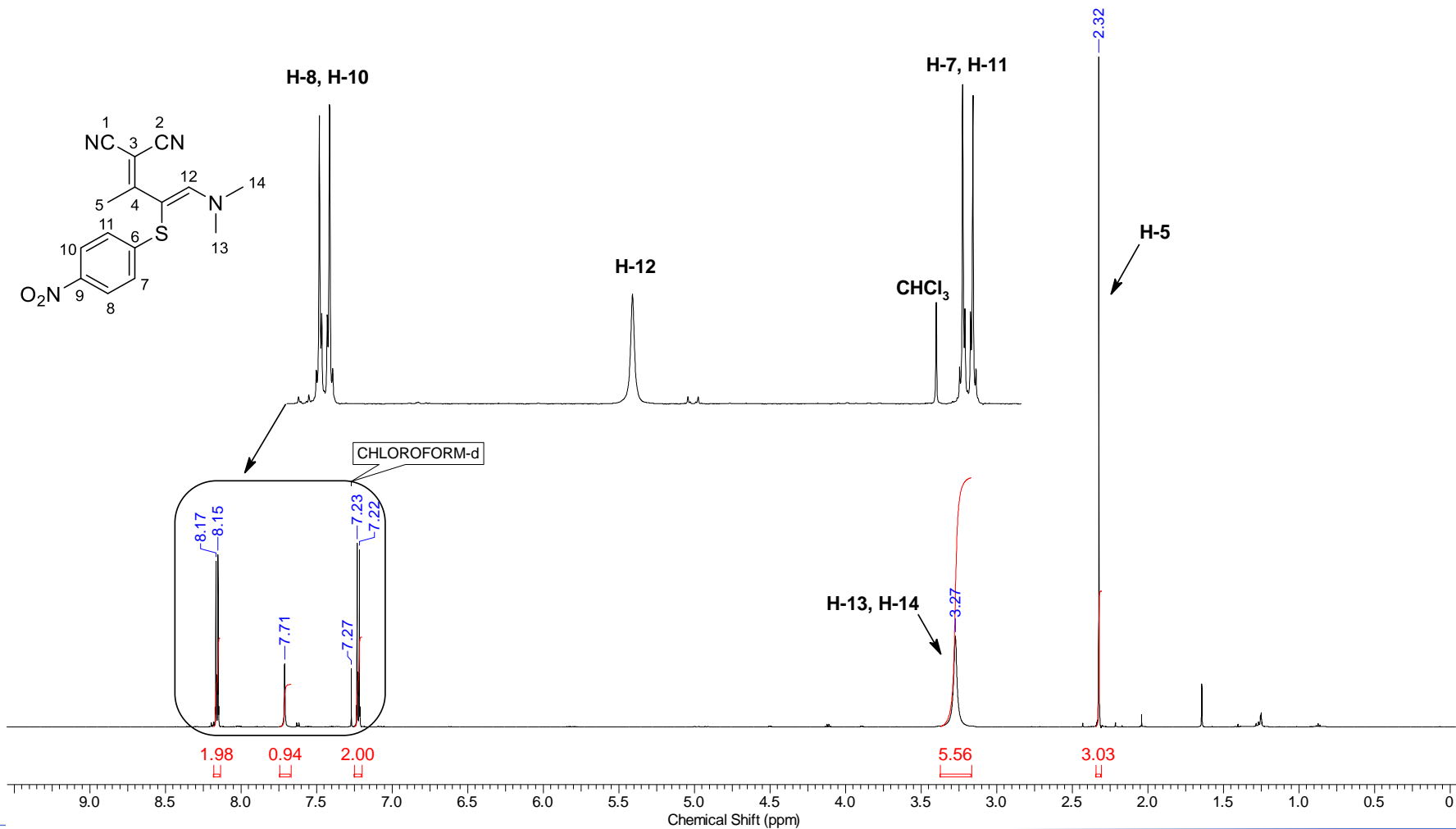
Continuous Conditions Applied to Hazardous Reactions and Fluorophores Synthesis with Photophysics Studies

Frequency (MHz)	150.87	Nucleus	¹³ C	Number of Transients	2500	Origin	spect
Original Points Count	32768	Owner	nmr	Points Count	32768	Pulse Sequence	zgpg30
Receiver Gain	199.73	SW(cyclical) (Hz)	36231.88	Solvent	CDCl ₃	Spectrum Offset (Hz)	15072.9912
Spectrum Type	STANDARD	Sweep Width (Hz)	36230.78	Temperature (degree C)	25.353	Acquisition Time (sec)	0.9044



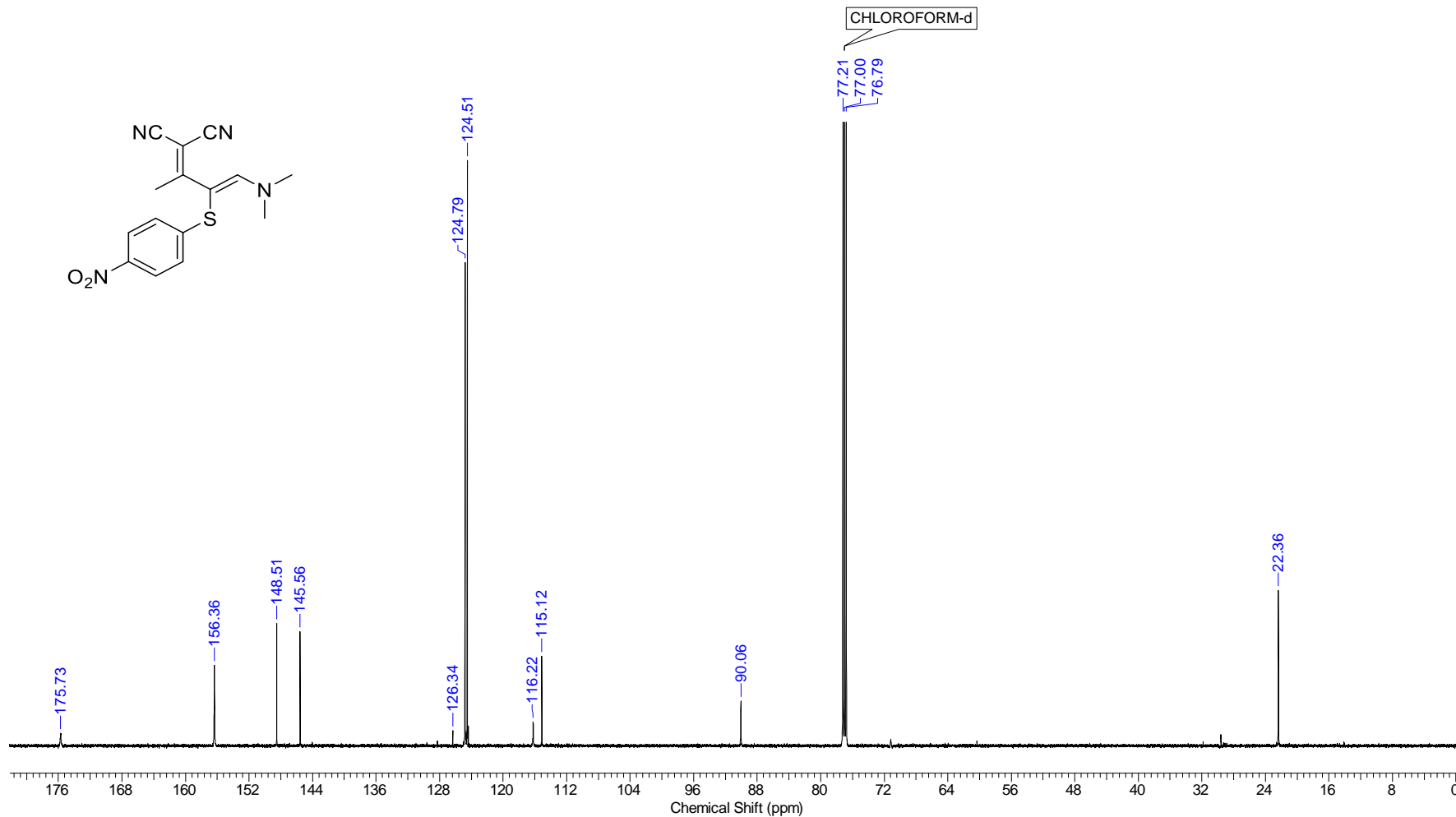
Continuous Conditions Applied to Hazardous Reactions and Fluorophores Synthesis with Photophysics Studies

Frequency (MHz)	600.01	Nucleus	¹ H	Number of Transients	16	Origin	spect
Original Points Count	32768	Owner	nmr	Points Count	65536	Pulse Sequence	zg30
Receiver Gain	106.90	SW(cyclical) (Hz)	12019.23	Solvent	CDCl ₃	Spectrum Offset (Hz)	3695.4729
Spectrum Type	STANDARD	Sweep Width (Hz)	12019.05	Temperature (degree C)	23.185	Acquisition Time (sec)	2.7263

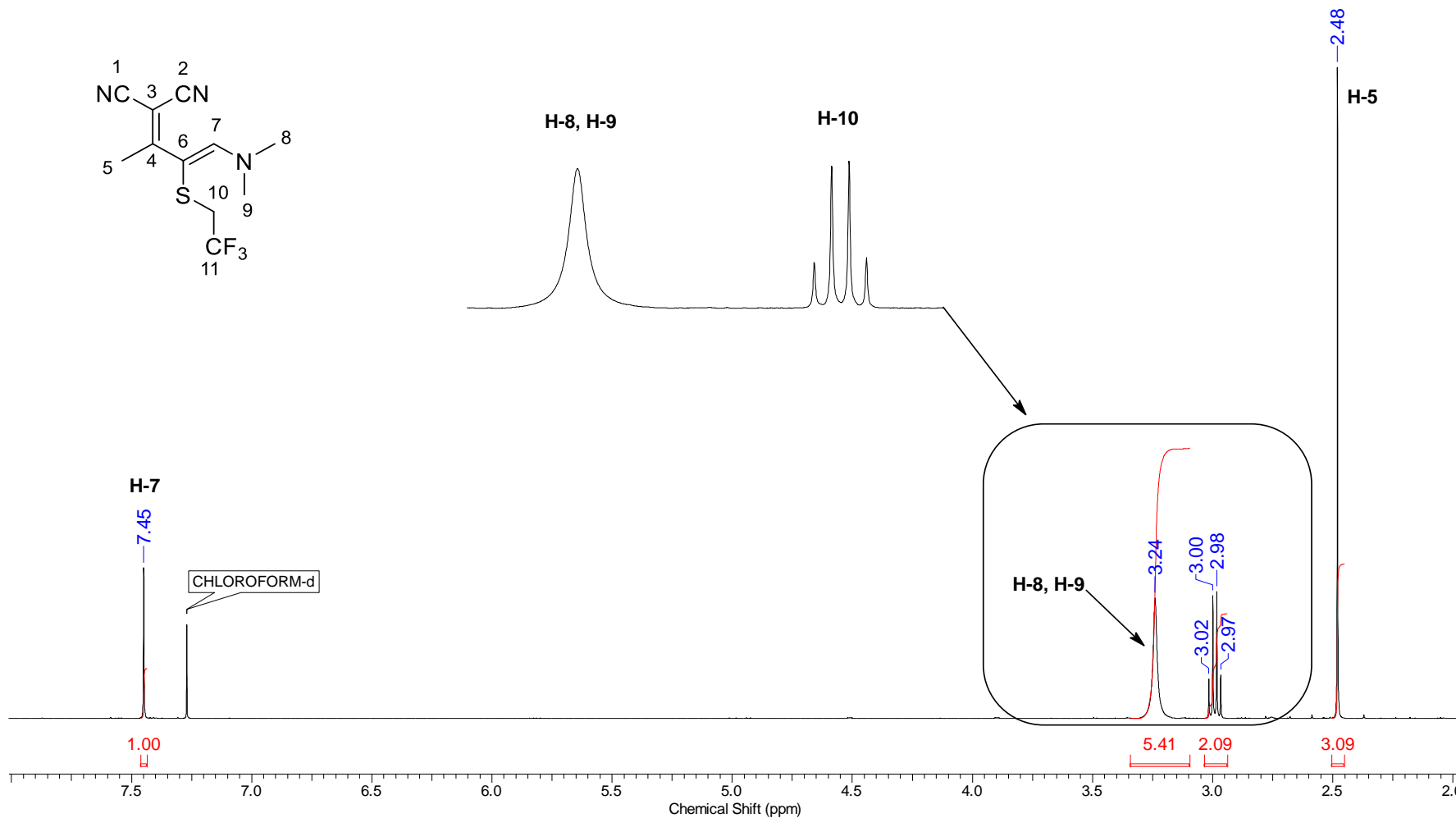


Continuous Conditions Applied to Hazardous Reactions and Fluorophores Synthesis with Photophysics Studies

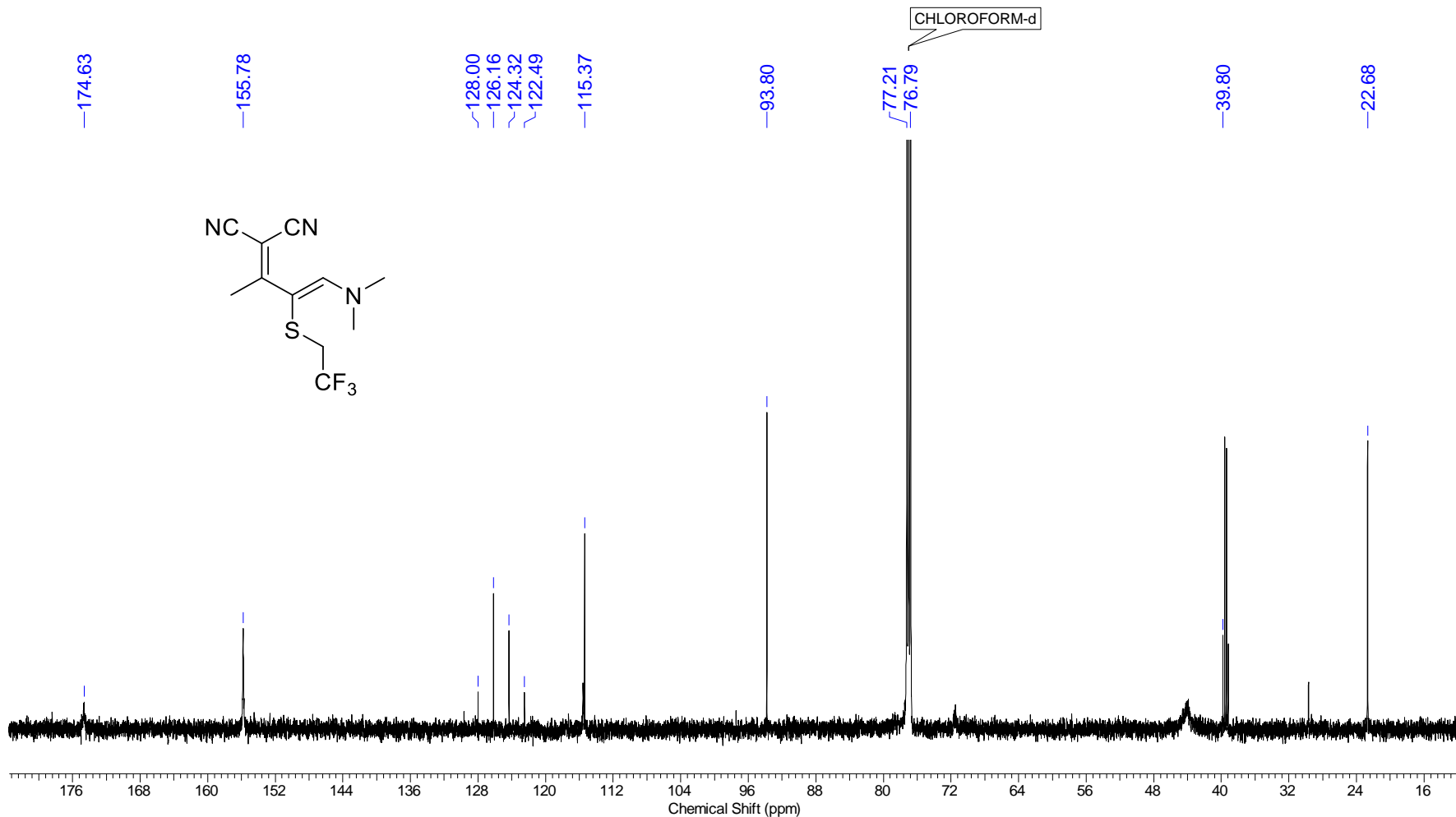
Frequency (MHz)	150.87	Nucleus	¹³ C	Number of Transients	2500	Origin	spect
Original Points Count	32768	Owner	nmr	Points Count	32768	Pulse Sequence	zgpg30
Receiver Gain	199.73	SW(cyclical) (Hz)	36231.88	Solvent	CDCl ₃	Spectrum Offset (Hz)	15075.2021
Spectrum Type	STANDARD	Sweep Width (Hz)	36230.78	Temperature (degree C)	25.259	Acquisition Time (sec)	0.9044



Nucleus	1H	Number of Transients	16	Origin	spect	Original Points Count	32768
Owner	nmr	Points Count	65536	Pulse Sequence	zg30	Receiver Gain	199.73
SW(cyclical) (Hz)	12019.23	Solvent	CDCI3	Spectrum Offset (Hz)	3695.4736	Spectrum Type	STANDARD
Sweep Width (Hz)	12019.05	Temperature (degree C)	24.997	Acquisition Time (sec)	2.7263	Frequency (MHz)	600.01

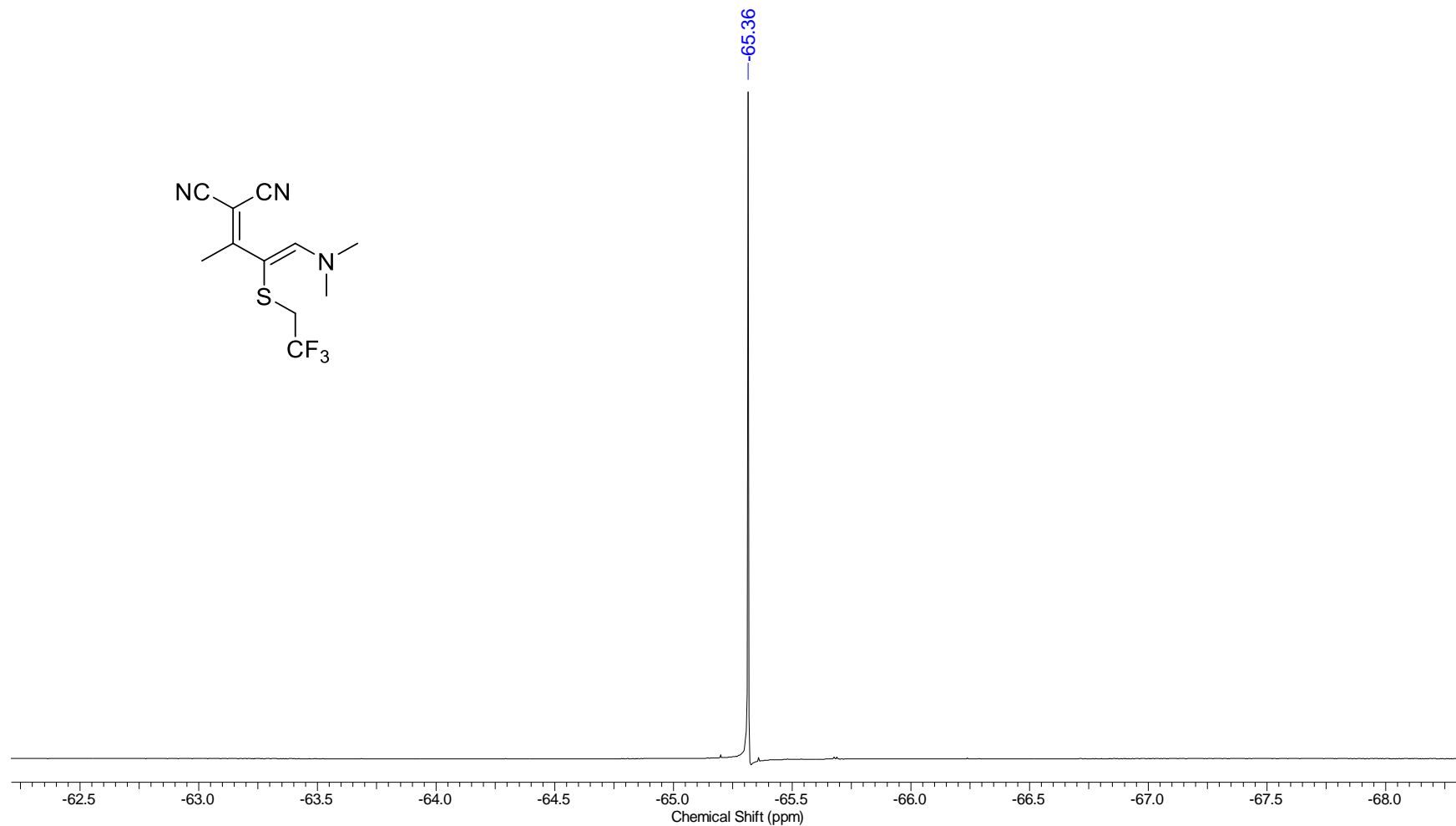


Nucleus	13C	Number of Transients	3600	Origin	spect	Original Points Count	32768
Owner	nmr	Points Count	32768	Pulse Sequence	zgpg30	Receiver Gain	199.73
SW(cyclical) (Hz)	36231.88	Solvent	CDCl3	Spectrum Offset (Hz)	15095.1055	Spectrum Type	STANDARD
Sweep Width (Hz)	36230.78	Temperature (degree C)	25.545	Acquisition Time (sec)	0.9044	Frequency (MHz)	150.87



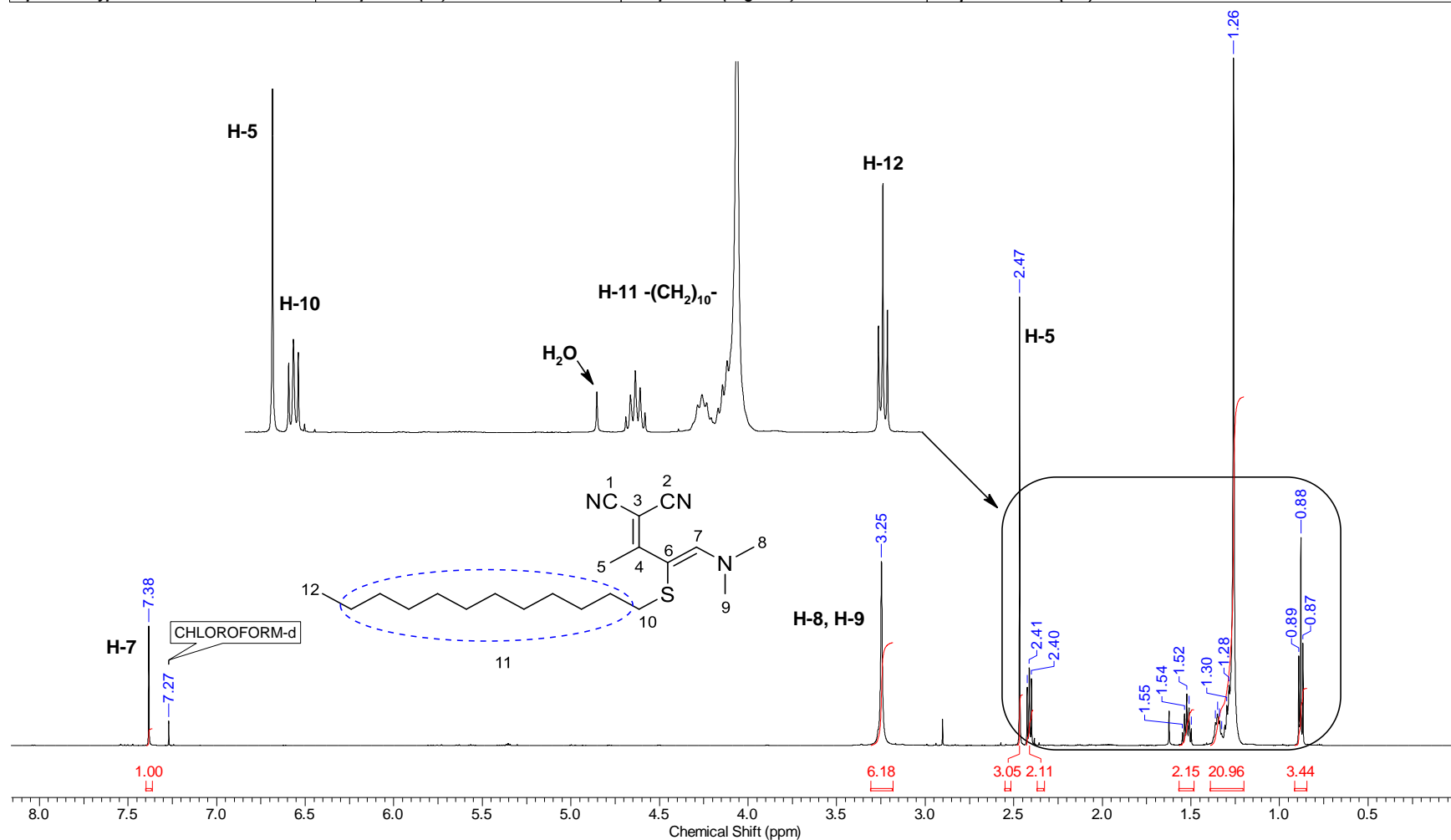
Continuous Conditions Applied to Hazardous Reactions and Fluorophores Synthesis with Photophysics Studies

Nucleus	19F	Number of Transients	16	Origin	spect	Original Points Count	65536
Owner	nmr	Points Count	65536	Pulse Sequence	zgfhigqn.2	Receiver Gain	199.73
SW(cyclical) (Hz)	133928.58	Solvent	CDCl3	Spectrum Offset (Hz)	-56456.8867	Spectrum Type	STANDARD
Sweep Width (Hz)	133926.53	Temperature (degree C)	25.182	Acquisition Time (sec)	0.4893	Frequency (MHz)	564.57

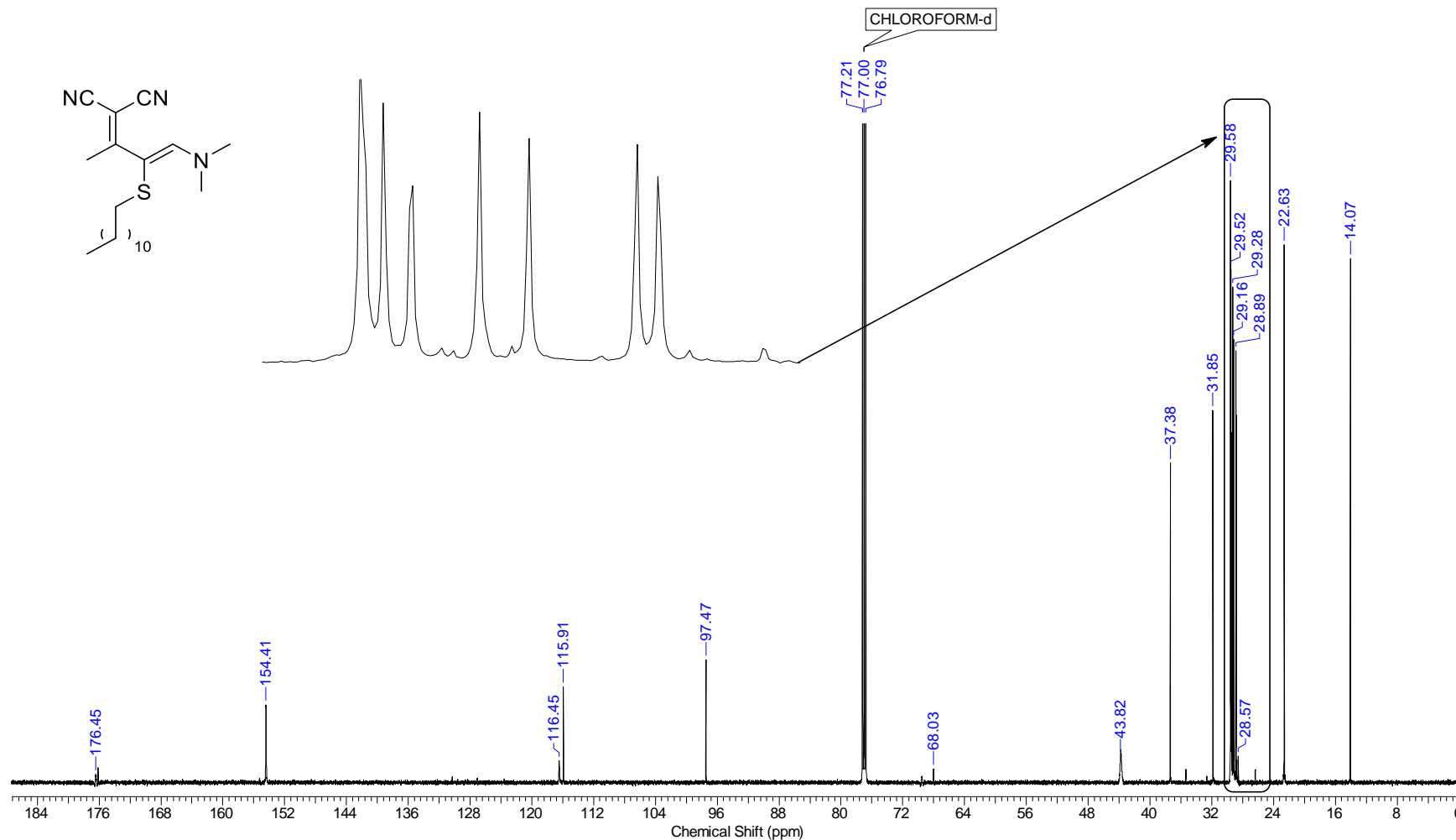


Continuous Conditions Applied to Hazardous Reactions and Fluorophores Synthesis with Photophysics Studies

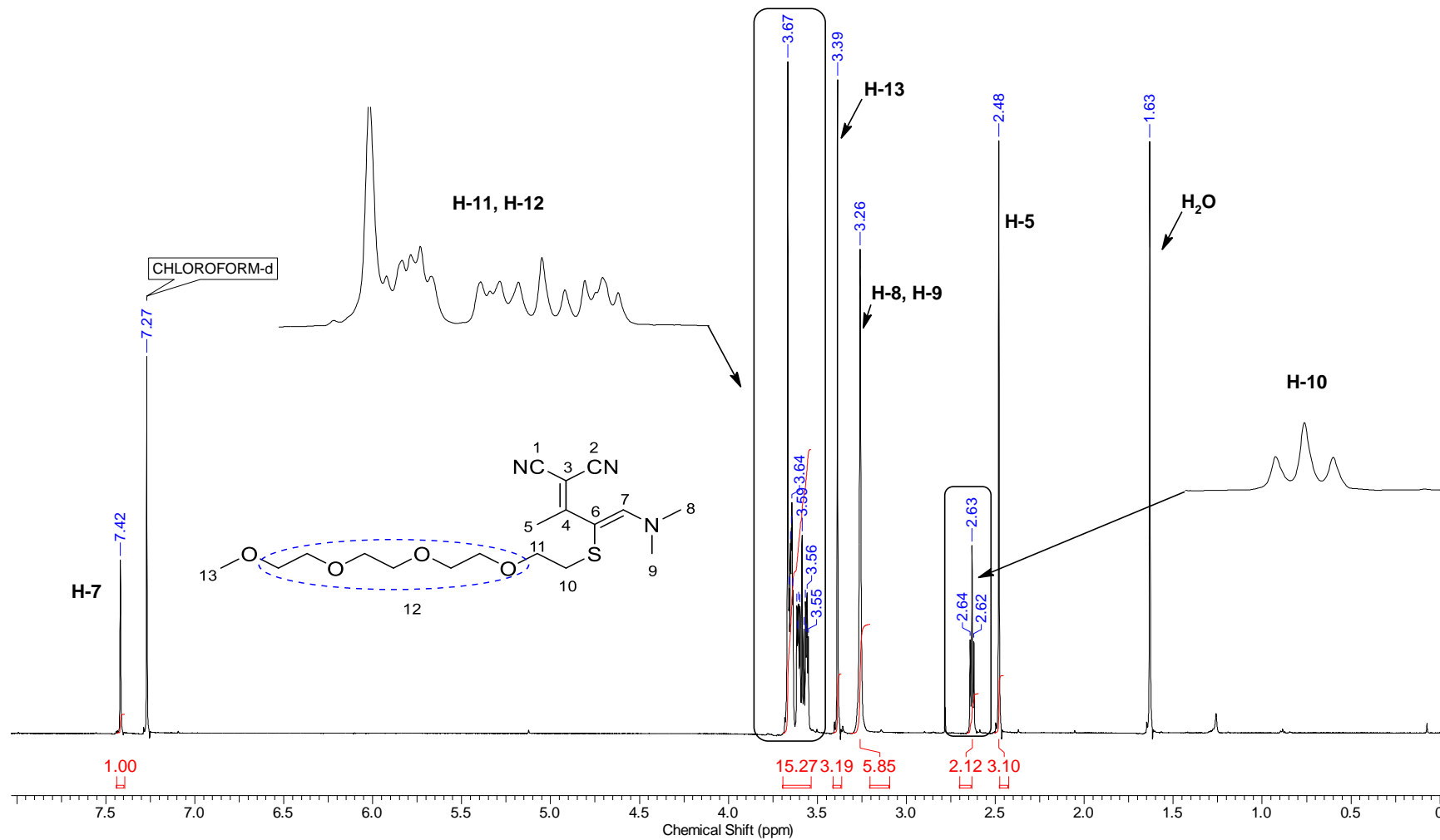
Frequency (MHz)	600.01	Nucleus	¹ H	Number of Transients	16	Origin	spect
Original Points Count	32768	Owner	nmsu	Points Count	65536	Pulse Sequence	zg30
Receiver Gain	61.00	SW(cyclical) (Hz)	12019.23	Solvent	CDCl ₃	Spectrum Offset (Hz)	3743.5237
Spectrum Type	STANDARD	Sweep Width (Hz)	12019.05	Temperature (degree C)	23.155	Acquisition Time (sec)	2.7263



Frequency (MHz)	150.87	Nucleus	¹³ C	Number of Transients	2500	Origin	spect
Original Points Count	32768	Owner	nmsu	Points Count	32768	Pulse Sequence	zpgg30
Receiver Gain	199.73	SW(cyclical) (Hz)	36231.88	Solvent	CDCl ₃	Spectrum Offset (Hz)	15090.6826
Spectrum Type	STANDARD	Sweep Width (Hz)	36230.78	Temperature (degree C)	25.249	Acquisition Time (sec)	0.9044

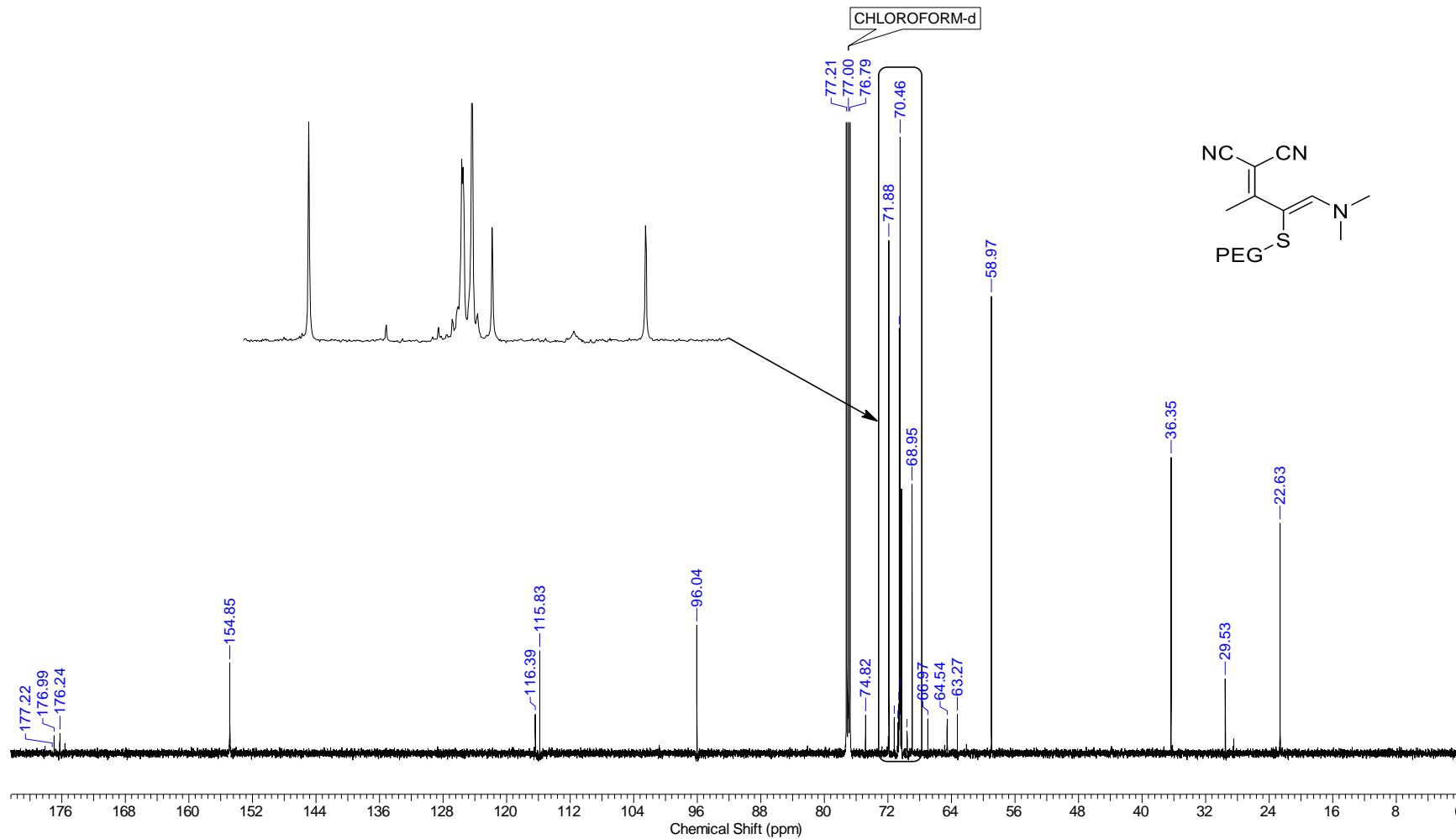


Frequency (MHz)	599.96	Nucleus	1H	Number of Transients	16	Origin	spect
Original Points Count	32768	Owner	nmsu	Points Count	65536	Pulse Sequence	zg30
Receiver Gain	172.91	SW(cyclical) (Hz)	12019.23	Solvent	CDCl3	Spectrum Offset (Hz)	3694.7437
Spectrum Type	STANDARD	Sweep Width (Hz)	12019.05	Temperature (degree C)	20.649	Acquisition Time (sec)	2.7263



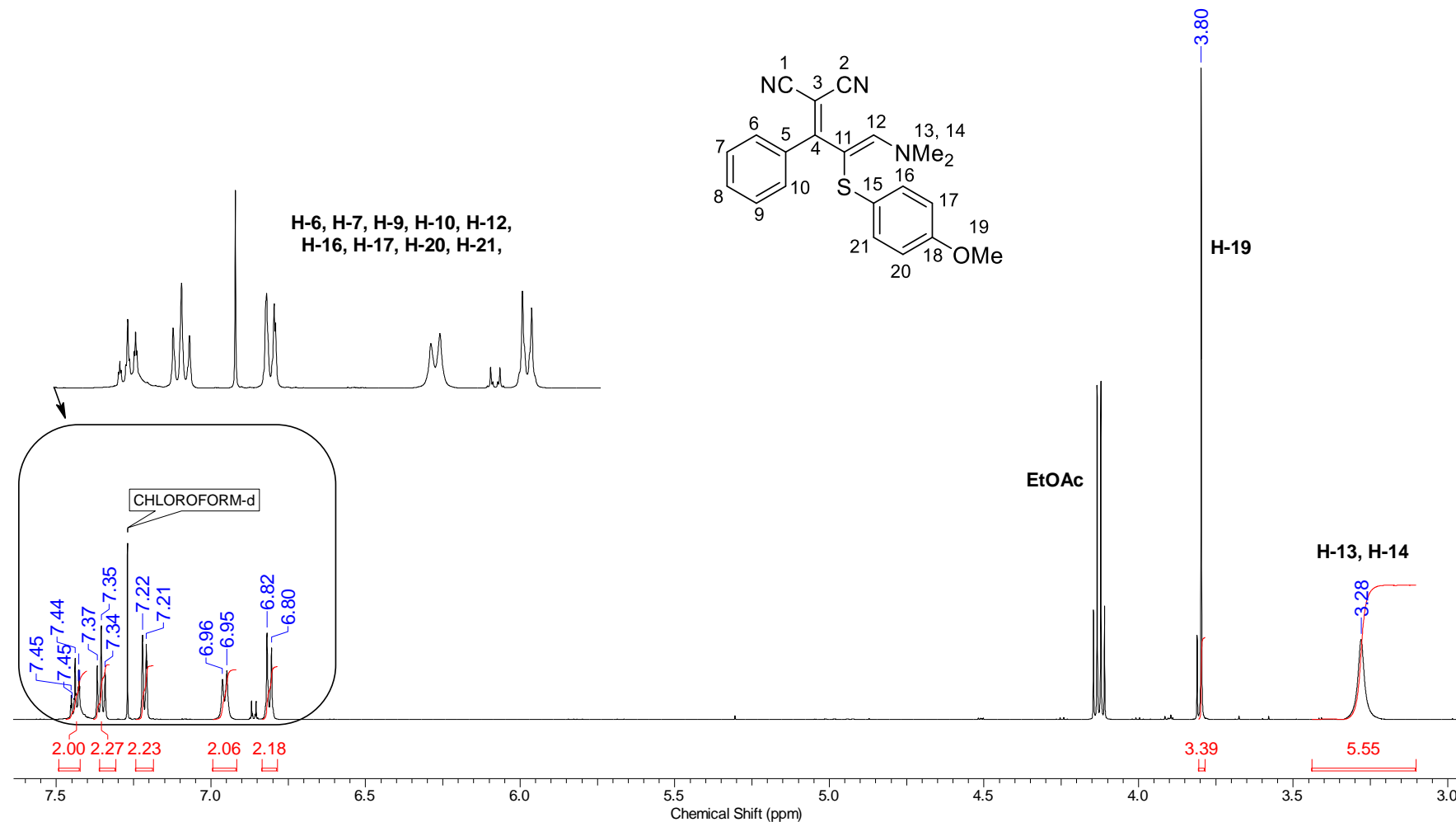
Continuous Conditions Applied to Hazardous Reactions and Fluorophores Synthesis with Photophysics Studies

Frequency (MHz)	150.87	Nucleus	¹³ C	Number of Transients	1160	Origin	spect
Original Points Count	32768	Owner	nmrsu	Points Count	32768	Pulse Sequence	zpgpg30
Receiver Gain	199.73	SW(cyclical) (Hz)	36231.88	Solvent	CDCl ₃	Spectrum Offset (Hz)	15089.5771
Spectrum Type	STANDARD	Sweep Width (Hz)	36230.78	Temperature (degree C)	25.208	Acquisition Time (sec)	0.9044

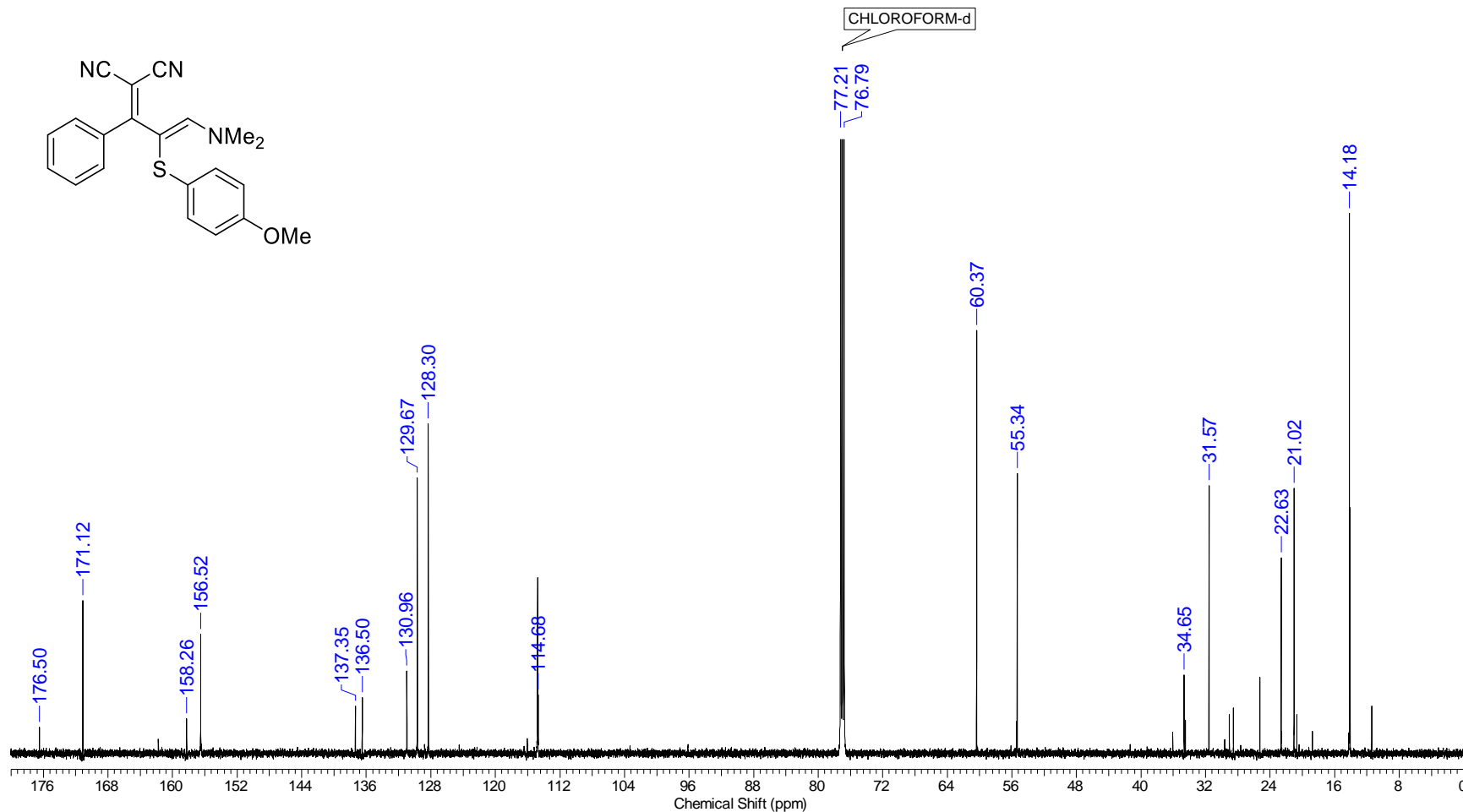


Continuous Conditions Applied to Hazardous Reactions and Fluorophores Synthesis with Photophysics Studies

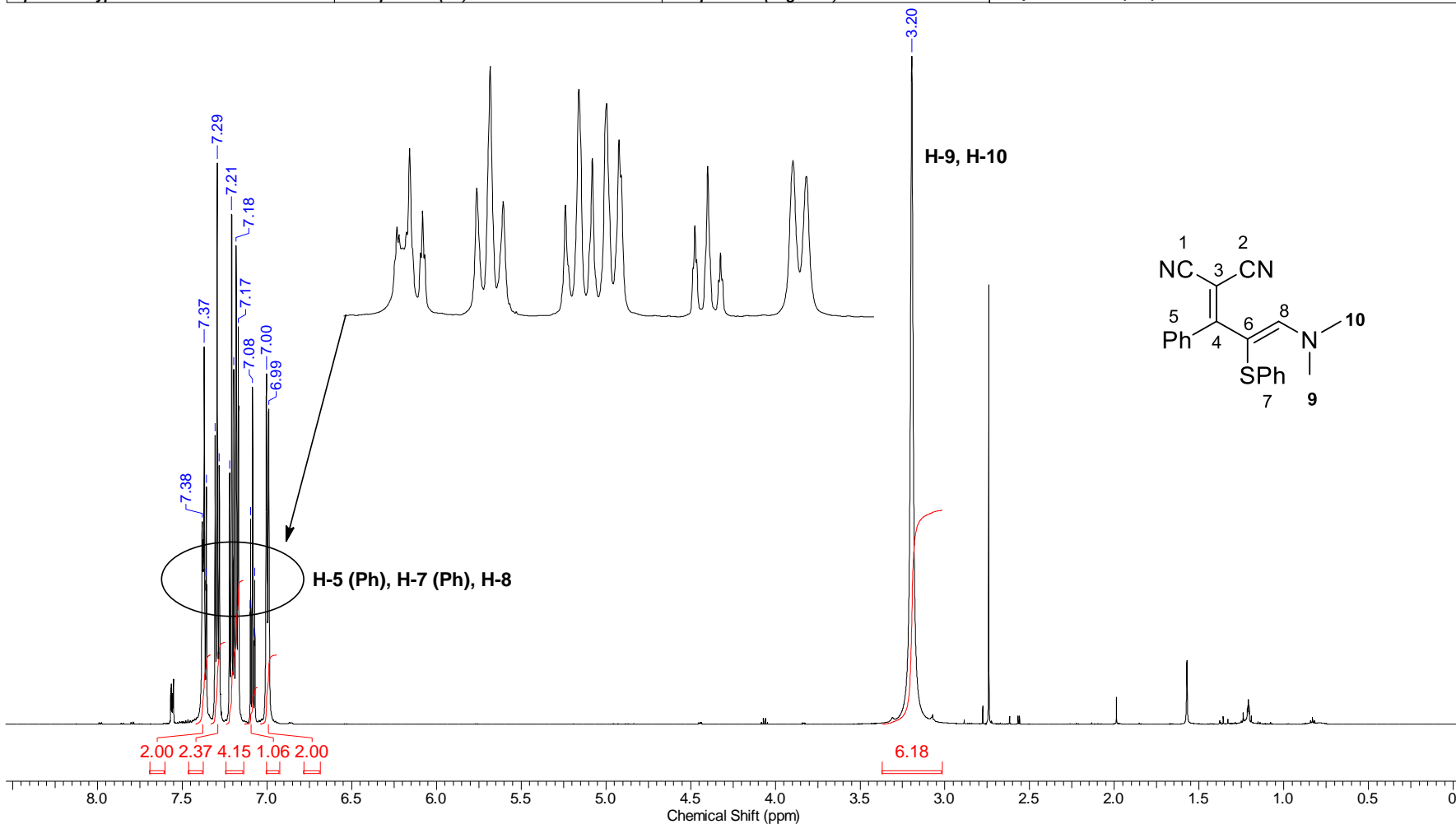
Frequency (MHz)	600.01	Nucleus	¹ H	Number of Transients	16	Origin	spect
Original Points Count	32768	Owner	nmr	Points Count	65536	Pulse Sequence	zg30
Receiver Gain	157.38	SW(cyclical) (Hz)	12019.23	Solvent	CDCl ₃	Spectrum Offset (Hz)	3743.7068
Spectrum Type	STANDARD	Sweep Width (Hz)	12019.05	Temperature (degree C)	24.996	Acquisition Time (sec)	2.7263



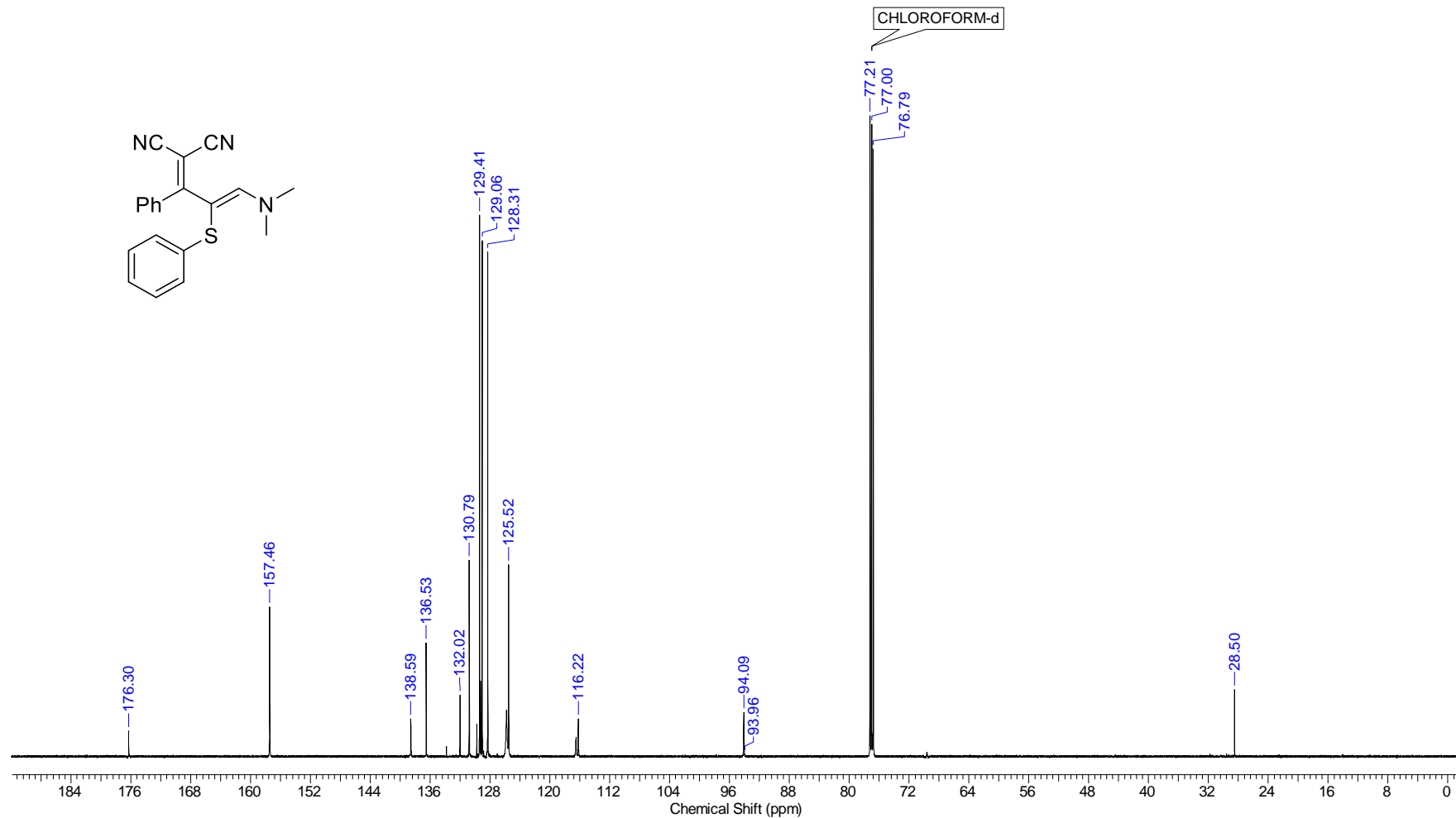
Frequency (MHz)	150.87	Nucleus	¹³ C	Number of Transients	3600	Origin	spect
Original Points Count	32768	Owner	nmr	Points Count	32768	Pulse Sequence	zgpg30
Receiver Gain	199.73	SW(cyclical) (Hz)	36231.88	Solvent	CDCl ₃	Spectrum Offset (Hz)	15095.1055
Spectrum Type	STANDARD	Sweep Width (Hz)	36230.78	Temperature (degree C)	25.397	Acquisition Time (sec)	0.9044



Frequency (MHz)	600.01	Nucleus	1H	Number of Transients	16	Origin	spect
Original Points Count	32768	Owner	nmrsu	Points Count	65536	Pulse Sequence	zq30
Receiver Gain	68.55	SW(cyclical) (Hz)	12019.23	Solvent	CDCl3	Spectrum Offset (Hz)	3705.0303
Spectrum Type	STANDARD	Sweep Width (Hz)	12019.05	Temperature (degree C)	23.245	Acquisition Time (sec)	2.7263

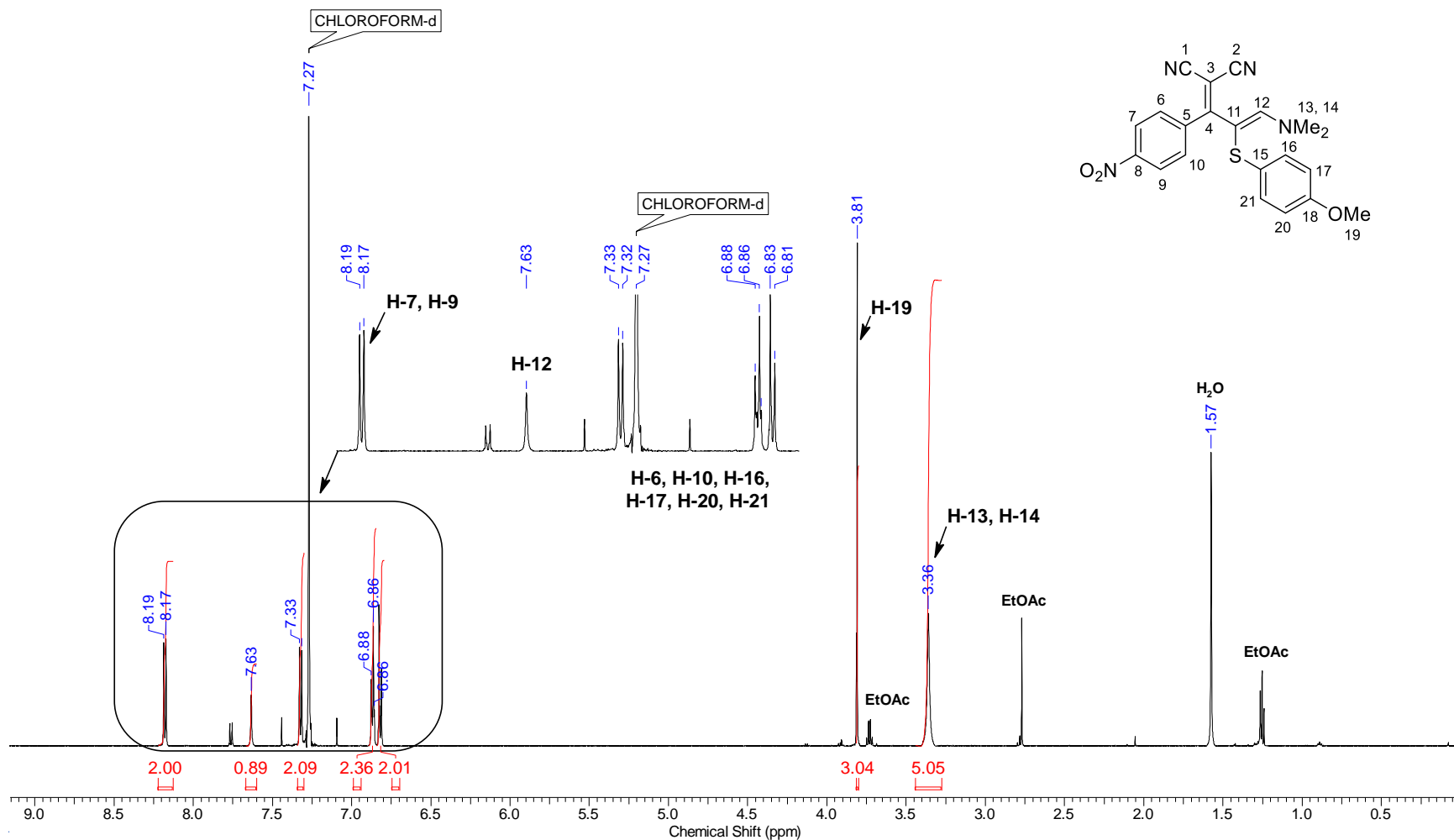


Frequency (MHz)	150.87	Nucleus	¹³ C	Number of Transients	2500	Origin	spect
Original Points Count	32768	Owner	nmrslu	Points Count	32768	Pulse Sequence	zgpg30
Receiver Gain	199.73	SW(cyclical) (Hz)	36231.88	Solvent	CDCl ₃	Spectrum Offset (Hz)	15078.5195
Spectrum Type	STANDARD	Sweep Width (Hz)	36230.78	Temperature (degree C)	25.230	Acquisition Time (sec)	0.9044



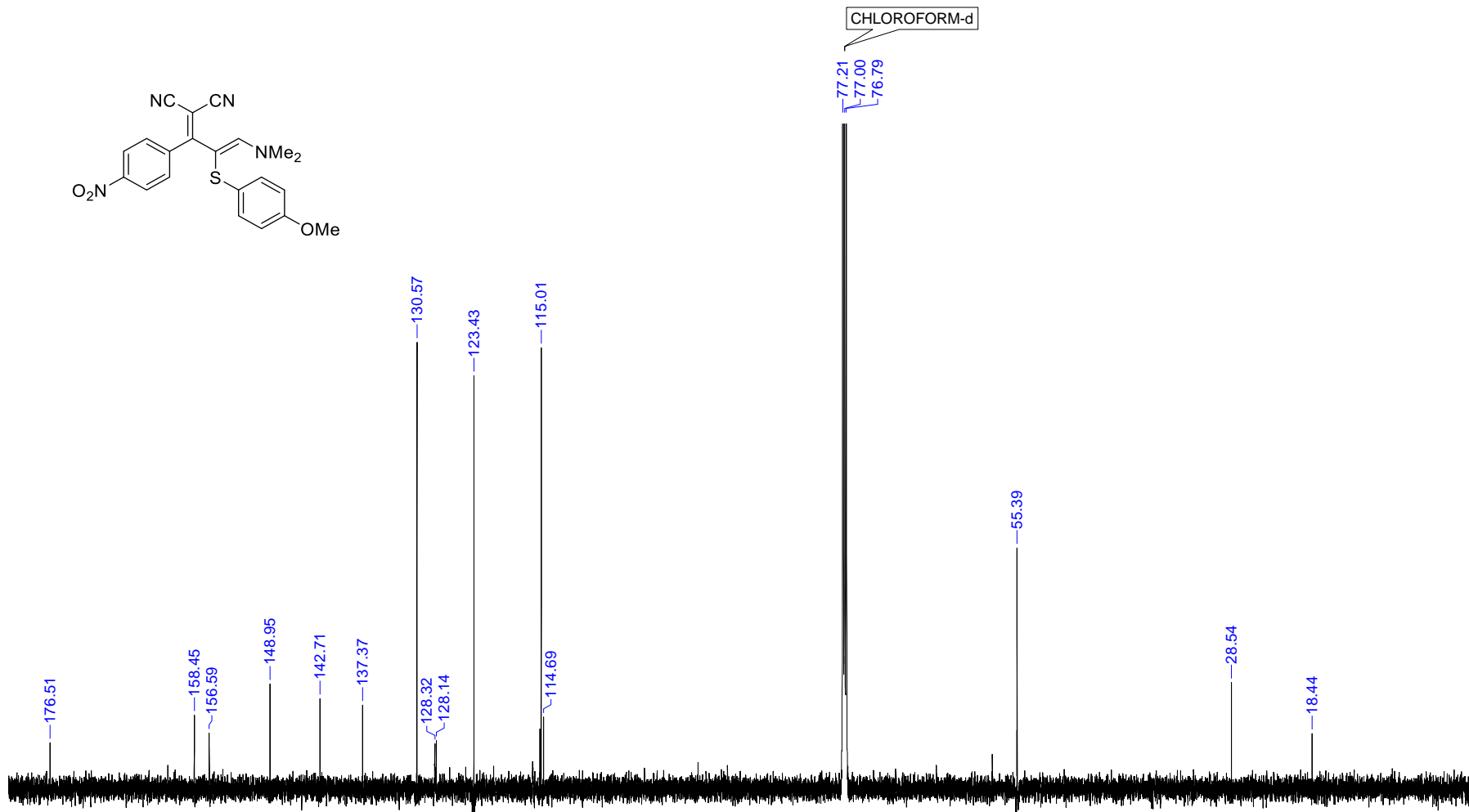
Continuous Conditions Applied to Hazardous Reactions and Fluorophores Synthesis with Photophysics Studies

Frequency (MHz)	600.01	Nucleus	¹ H	Number of Transients	16	Origin	spect
Original Points Count	32768	Owner	nmrslu	Points Count	65536	Pulse Sequence	zg30
Receiver Gain	199.73	SW(cyclical) (Hz)	12019.23	Solvent	CDCl ₃	Spectrum Offset (Hz)	3743.5234
Spectrum Type	STANDARD	Sweep Width (Hz)	12019.05	Temperature (degree C)	23.372	Acquisition Time (sec)	2.7263



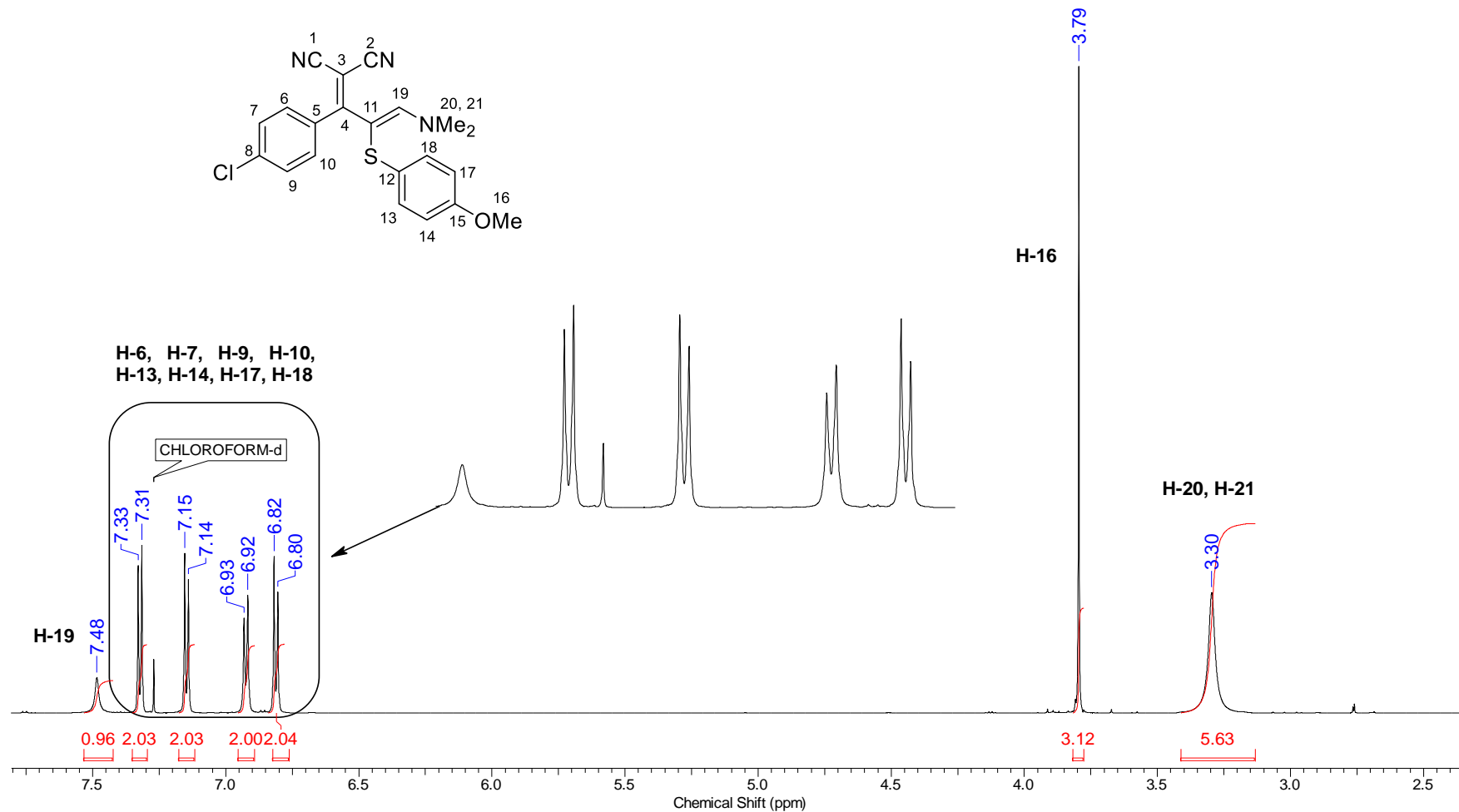
Continuous Conditions Applied to Hazardous Reactions and Fluorophores Synthesis with Photophysics Studies

Frequency (MHz)	150.87	Nucleus	¹³ C	Number of Transients	2500	Origin	spect
Original Points Count	32768	Owner	nmrsu	Points Count	32768	Pulse Sequence	zpgg30
Receiver Gain	199.73	SW(cyclical) (Hz)	36231.88	Solvent	CDCl ₃	Spectrum Offset (Hz)	15096.2100
Spectrum Type	STANDARD	Sweep Width (Hz)	36230.78	Temperature (degree C)	25.320	Acquisition Time (sec)	0.9044

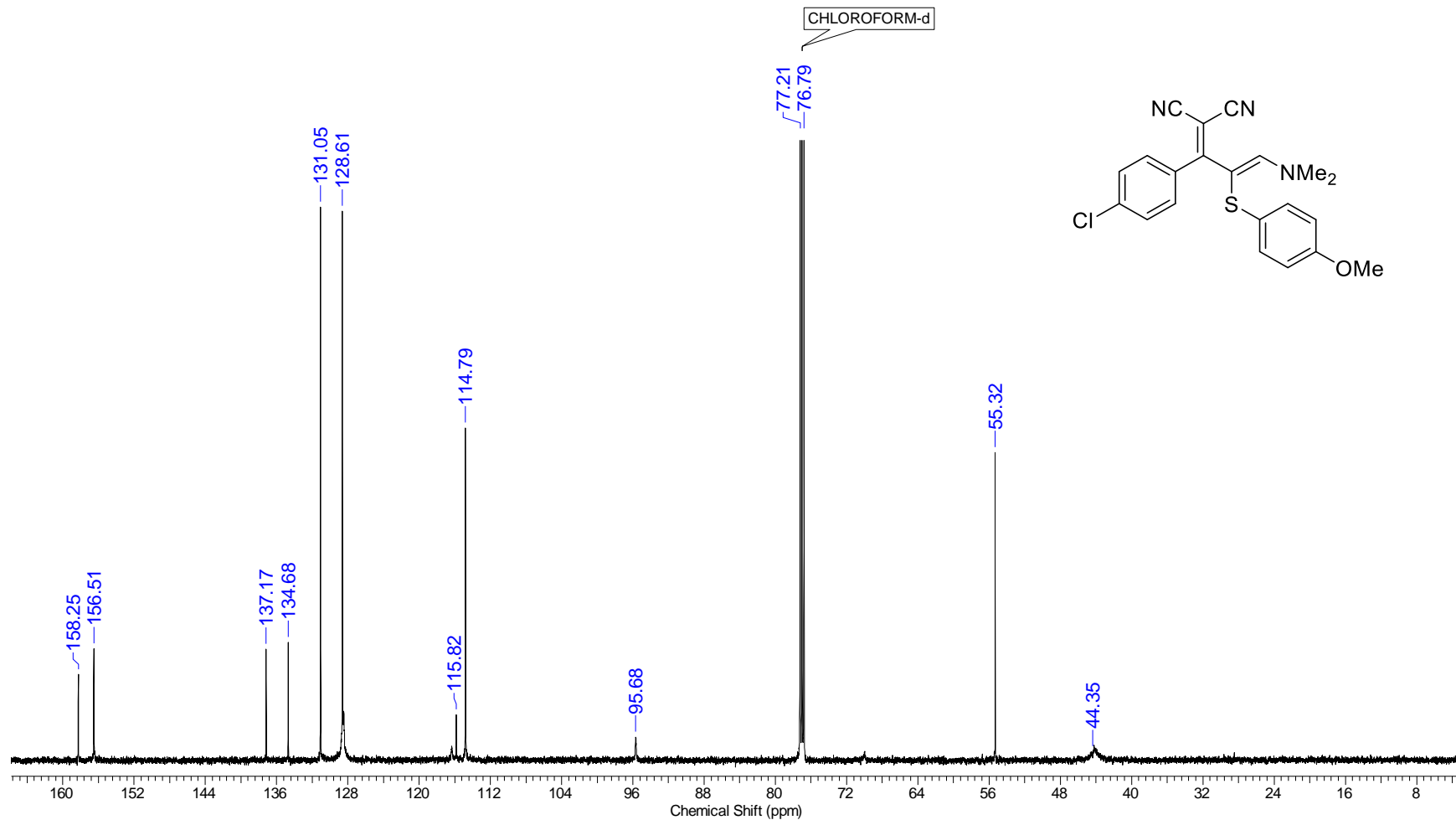


Continuous Conditions Applied to Hazardous Reactions and Fluorophores Synthesis with Photophysics Studies

Nucleus	1H	Number of Transients	16	Origin	spect	Original Points Count	32768
Owner	nmsu	Points Count	65536	Pulse Sequence	zg30	Receiver Gain	78.28
SW(cyclical) (Hz)	12019.23	Solvent	CDCl3	Spectrum Offset (Hz)	3743.3435	Spectrum Type	STANDARD
Sweep Width (Hz)	12019.05	Temperature (degree C)	23.058	Acquisition Time (sec)	2.7263	Frequency (MHz)	599.96

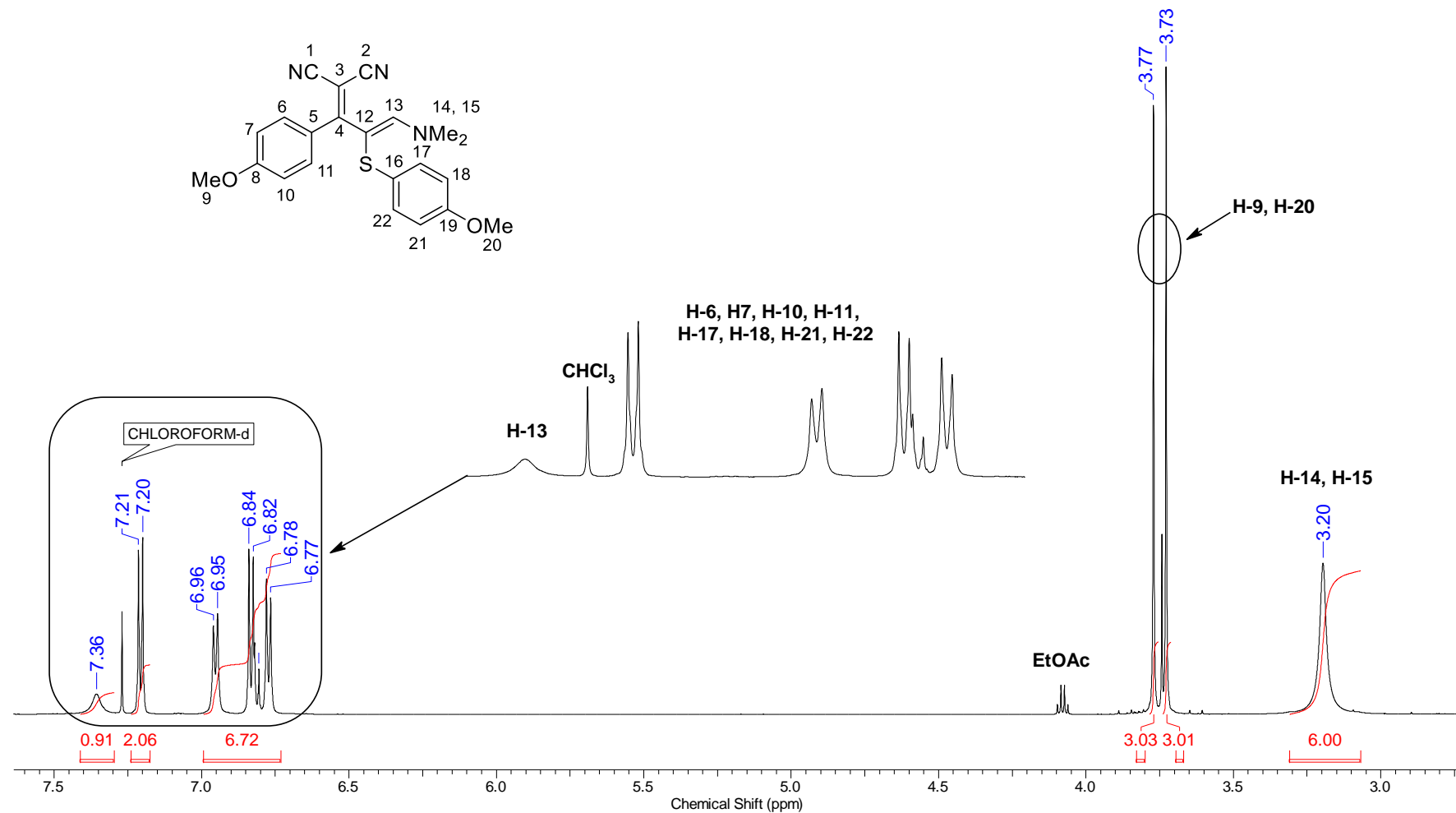


Nucleus	13C	Number of Transients	2500	Origin	spect	Original Points Count	32768
Owner	nmrsu	Points Count	32768	Pulse Sequence	zgpg30	Receiver Gain	194.75
SW(cyclical) (Hz)	36231.88	Solvent	CDCI3	Spectrum Offset (Hz)	15086.3965	Spectrum Type	STANDARD
Sweep Width (Hz)	36230.78	Temperature (degree C)	23.526	Acquisition Time (sec)	0.9044	Frequency (MHz)	150.86

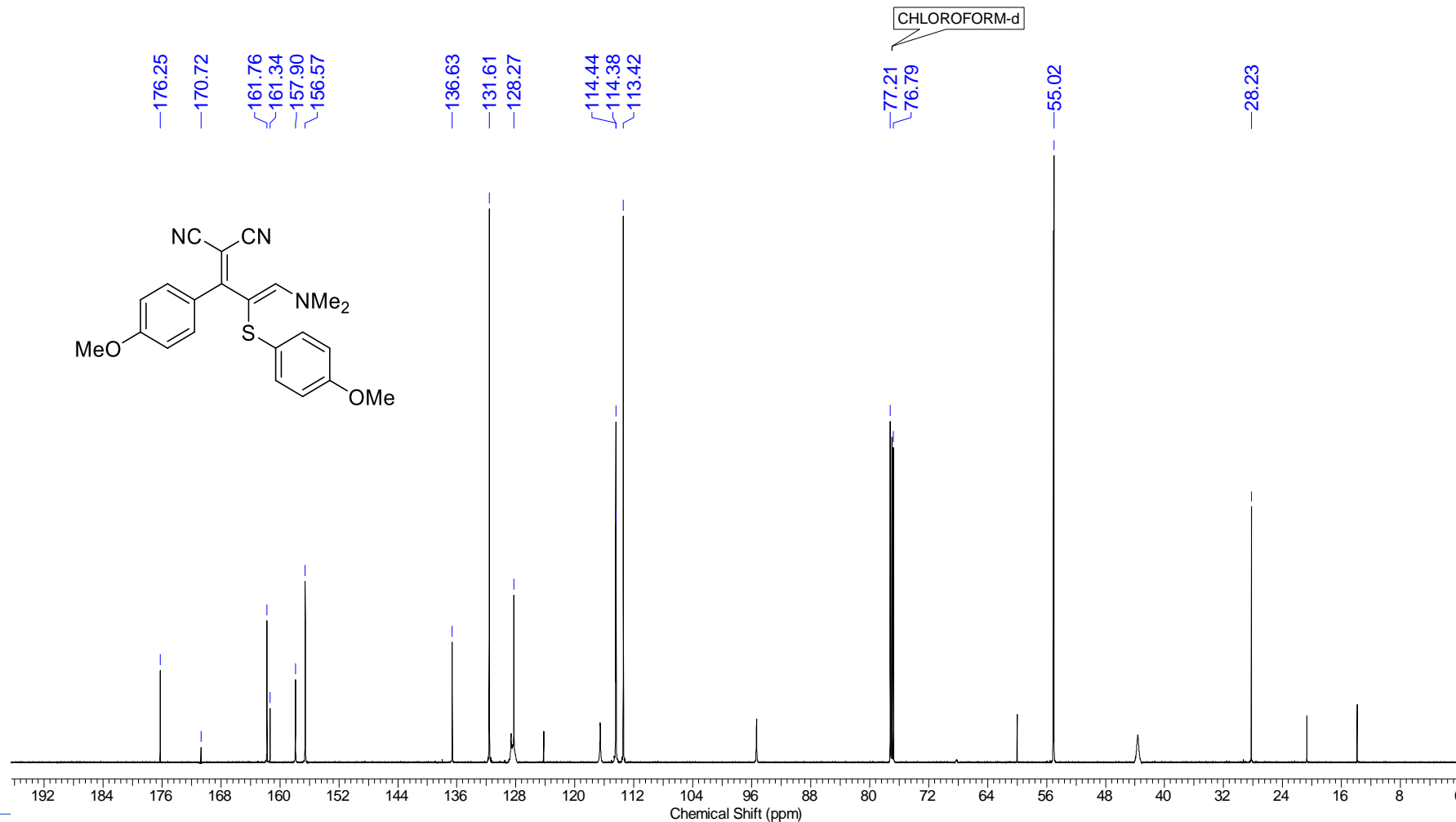


Continuous Conditions Applied to Hazardous Reactions and Fluorophores Synthesis with Photophysics Studies

Frequency (MHz)	600.01	Nucleus	¹ H	Number of Transients	16	Origin	spect
Original Points Count	32768	Owner	nmr	Points Count	65536	Pulse Sequence	zg30
Receiver Gain	19.61	SW(cyclical) (Hz)	12019.23	Solvent	CDCl ₃	Spectrum Offset (Hz)	3743.7068
Spectrum Type	STANDARD	Sweep Width (Hz)	12019.05	Temperature (degree C)	25.000	Acquisition Time (sec)	2.7263

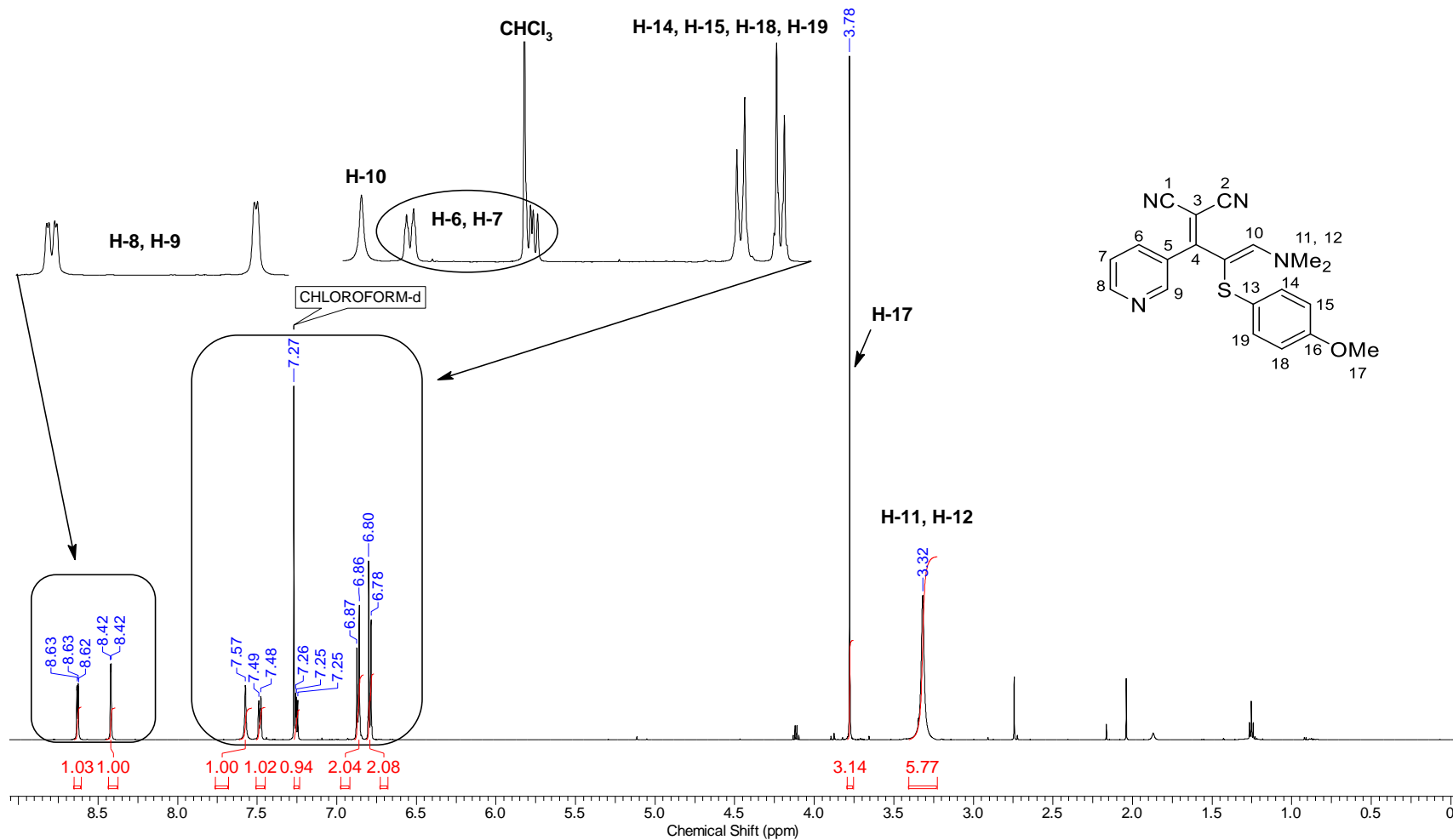


Nucleus	13C	Number of Transients	2500	Origin	spect	Original Points Count	32768
Owner	nmr	Points Count	32768	Pulse Sequence	zgpg30	Receiver Gain	199.73
SW(cyclical) (Hz)	36231.88	Solvent	CDCl3	Spectrum Offset (Hz)	15047.5596	Spectrum Type	STANDARD
Sweep Width (Hz)	36230.78	Temperature (degree C)	26.888	Acquisition Time (sec)	0.9044	Frequency (MHz)	150.87

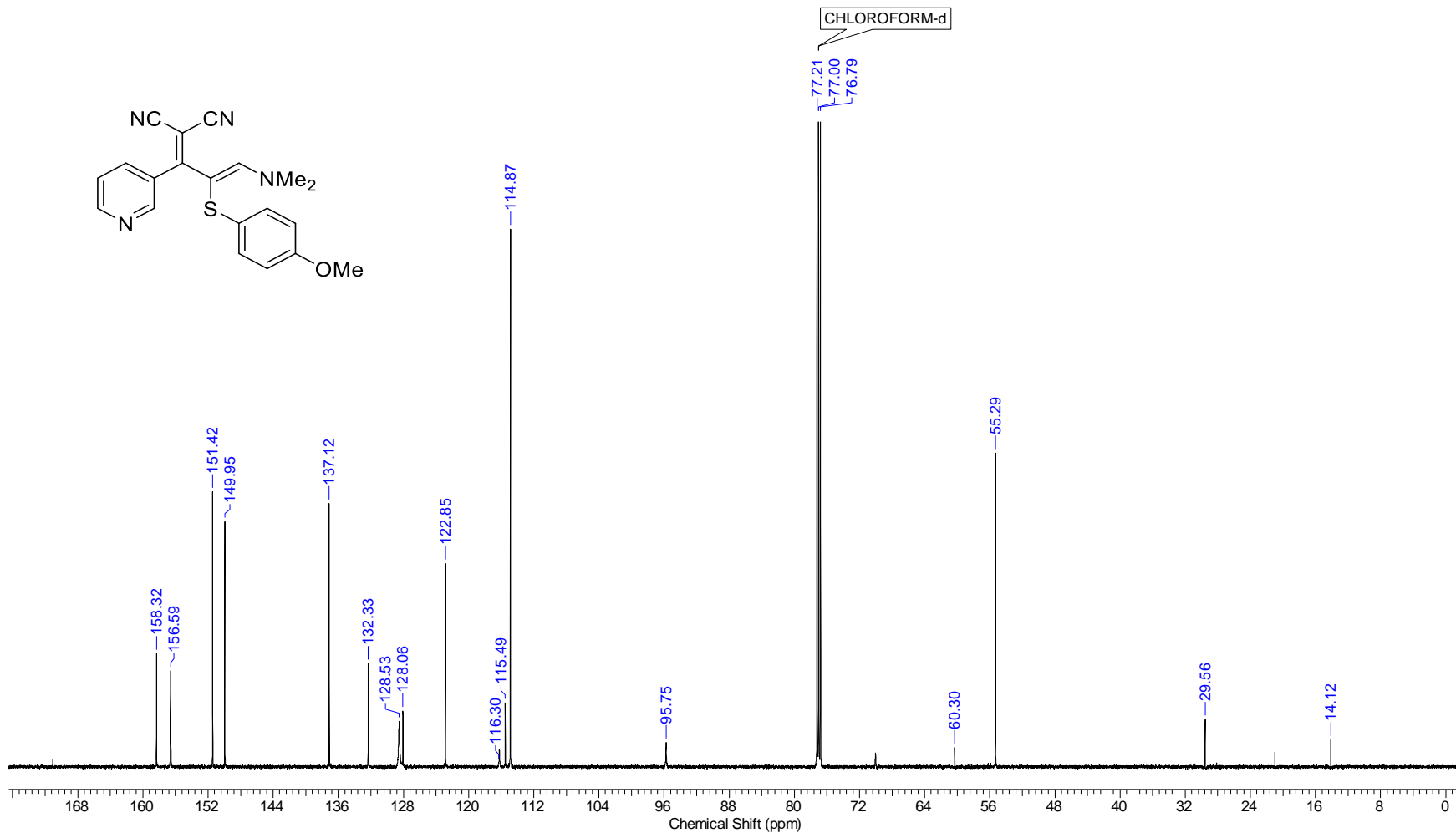


Continuous Conditions Applied to Hazardous Reactions and Fluorophores Synthesis with Photophysics Studies

Frequency (MHz)	600.01	Nucleus	1H	Number of Transients	16	Origin	spect
Original Points Count	32768	Owner	nmrsu	Points Count	65536	Pulse Sequence	zg30
Receiver Gain	99.50	SW(cyclical) (Hz)	12019.23	Solvent	CDCl3	Spectrum Offset (Hz)	3743.5237
Spectrum Type	STANDARD	Sweep Width (Hz)	12019.05	Temperature (degree C)	23.381	Acquisition Time (sec)	2.7263

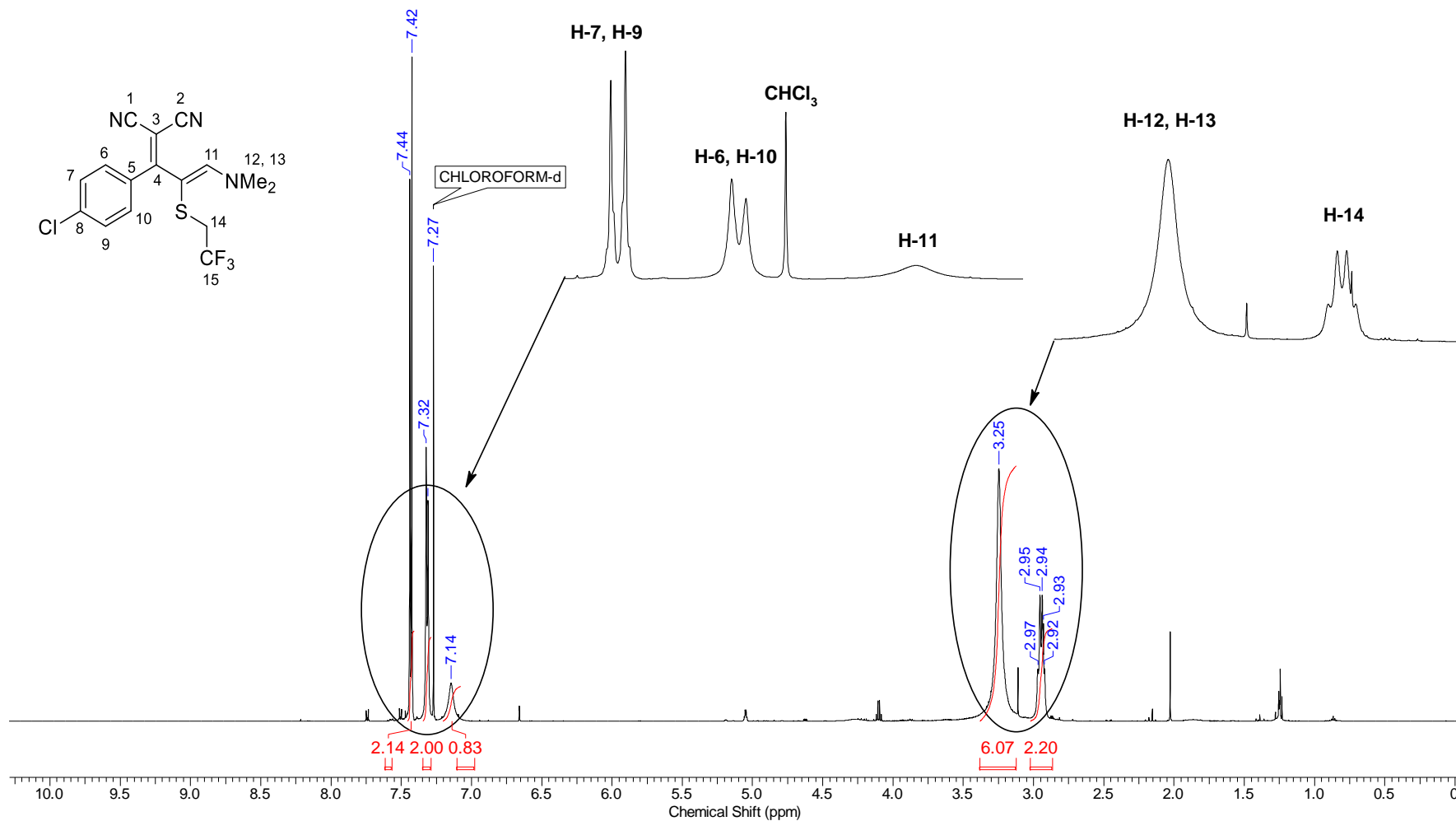


Frequency (MHz)	150.87	Nucleus	¹³ C	Number of Transients	2500	Origin	spect
Original Points Count	32768	Owner	nmsu	Points Count	32768	Pulse Sequence	zgpg30
Receiver Gain	199.73	SW(cyclical) (Hz)	36231.88	Solvent	CDCl ₃	Spectrum Offset (Hz)	15086.2598
Spectrum Type	STANDARD	Sweep Width (Hz)	36230.78	Temperature (degree C)	25.348	Acquisition Time (sec)	0.9044

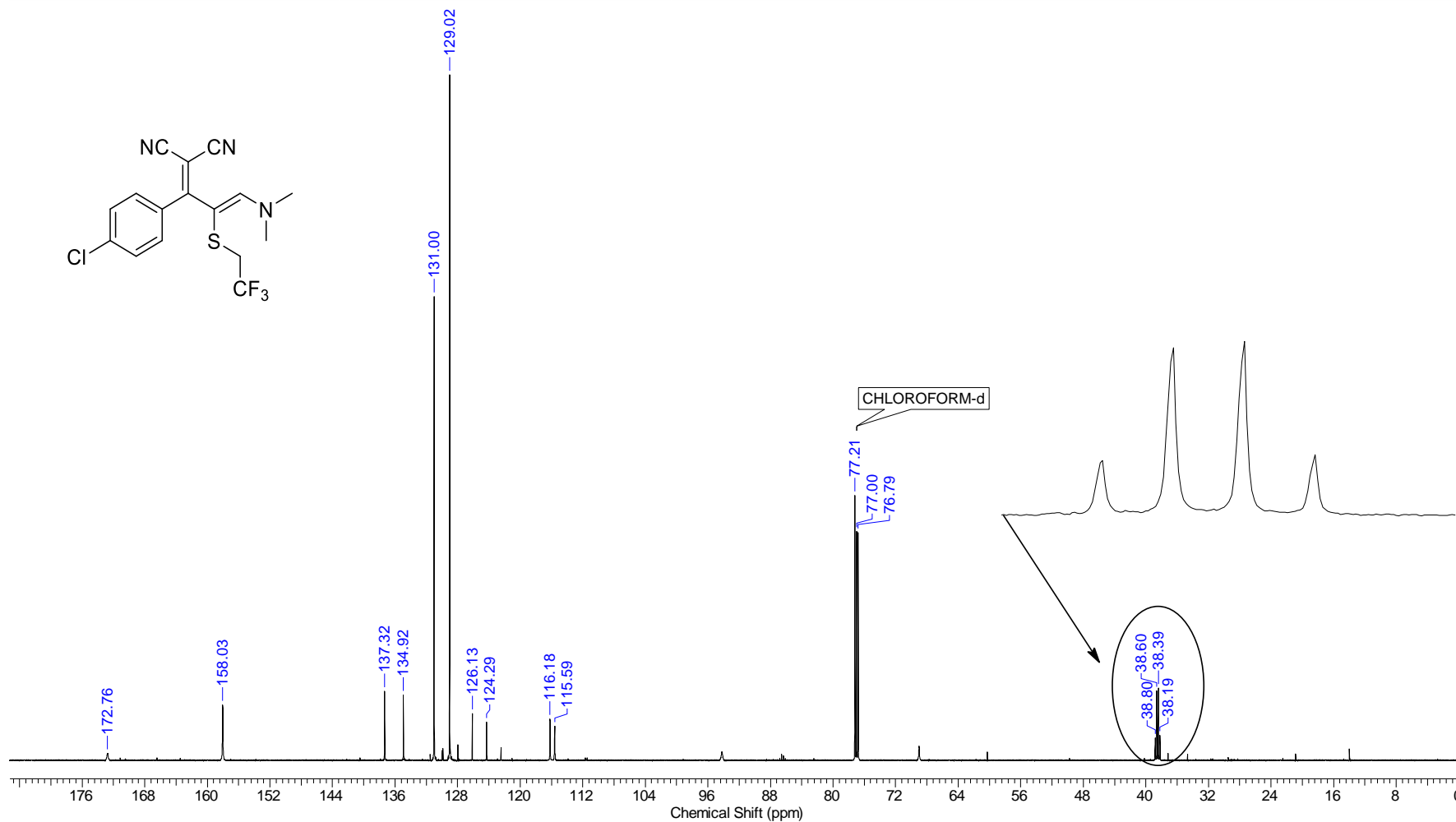


Continuous Conditions Applied to Hazardous Reactions and Fluorophores Synthesis with Photophysics Studies

Frequency (MHz)	600.01	Nucleus	¹ H	Number of Transients	16	Origin	spect
Original Points Count	32768	Owner	nmr	Points Count	65536	Pulse Sequence	zg30
Receiver Gain	31.31	SW(cyclical) (Hz)	12019.23	Solvent	CDCl ₃	Spectrum Offset (Hz)	3695.4729
Spectrum Type	STANDARD	Sweep Width (Hz)	12019.05	Temperature (degree C)	23.129	Acquisition Time (sec)	2.7263

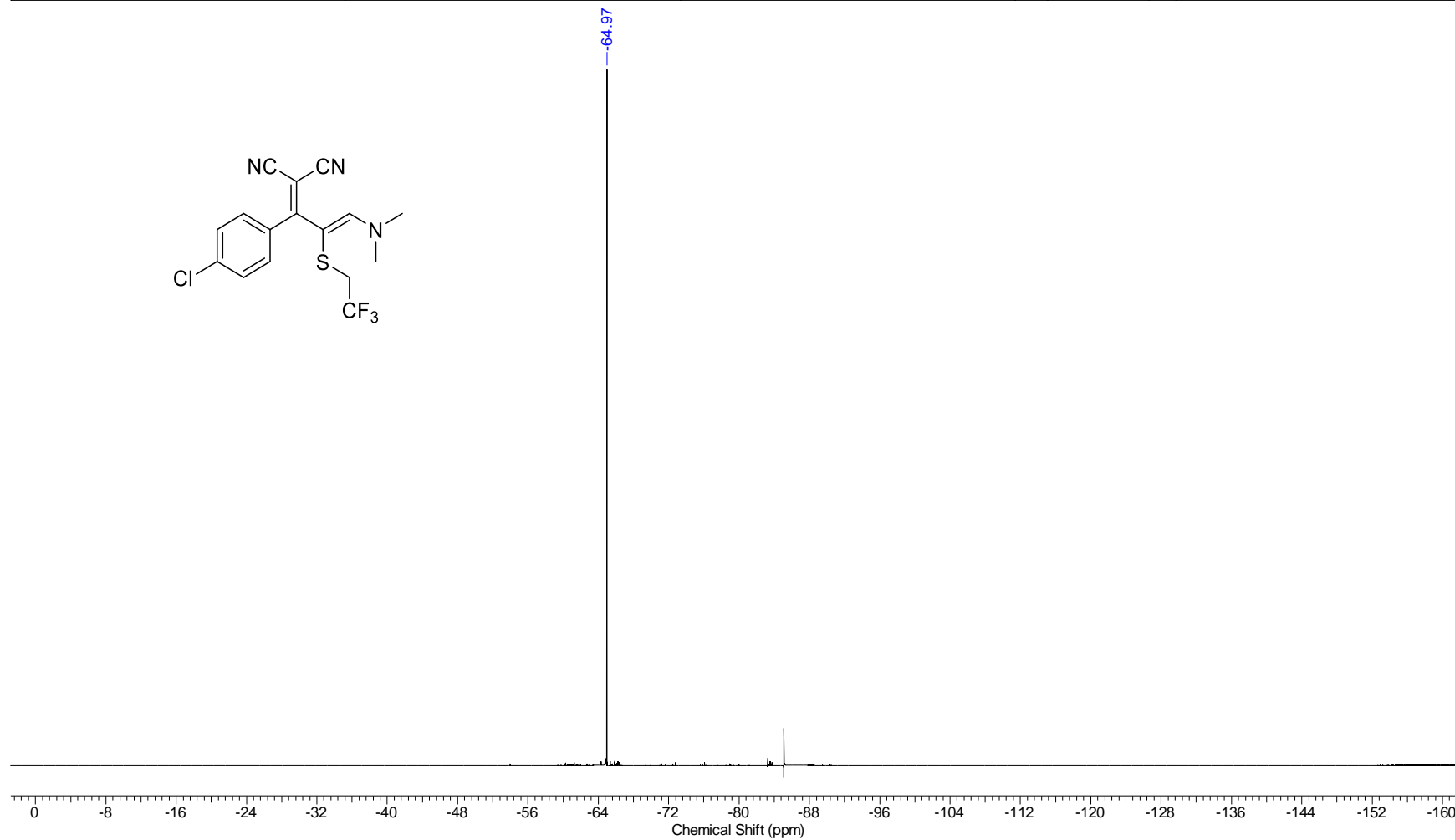


Frequency (MHz)	150.87	Nucleus	¹³ C	Number of Transients	2500	Origin	spect
Original Points Count	32768	Owner	nmr	Points Count	32768	Pulse Sequence	zgpg30
Receiver Gain	199.73	SW(cyclical) (Hz)	36231.88	Solvent	CDCl ₃	Spectrum Offset (Hz)	15057.5117
Spectrum Type	STANDARD	Sweep Width (Hz)	36230.78	Temperature (degree C)	25.295	Acquisition Time (sec)	0.9044



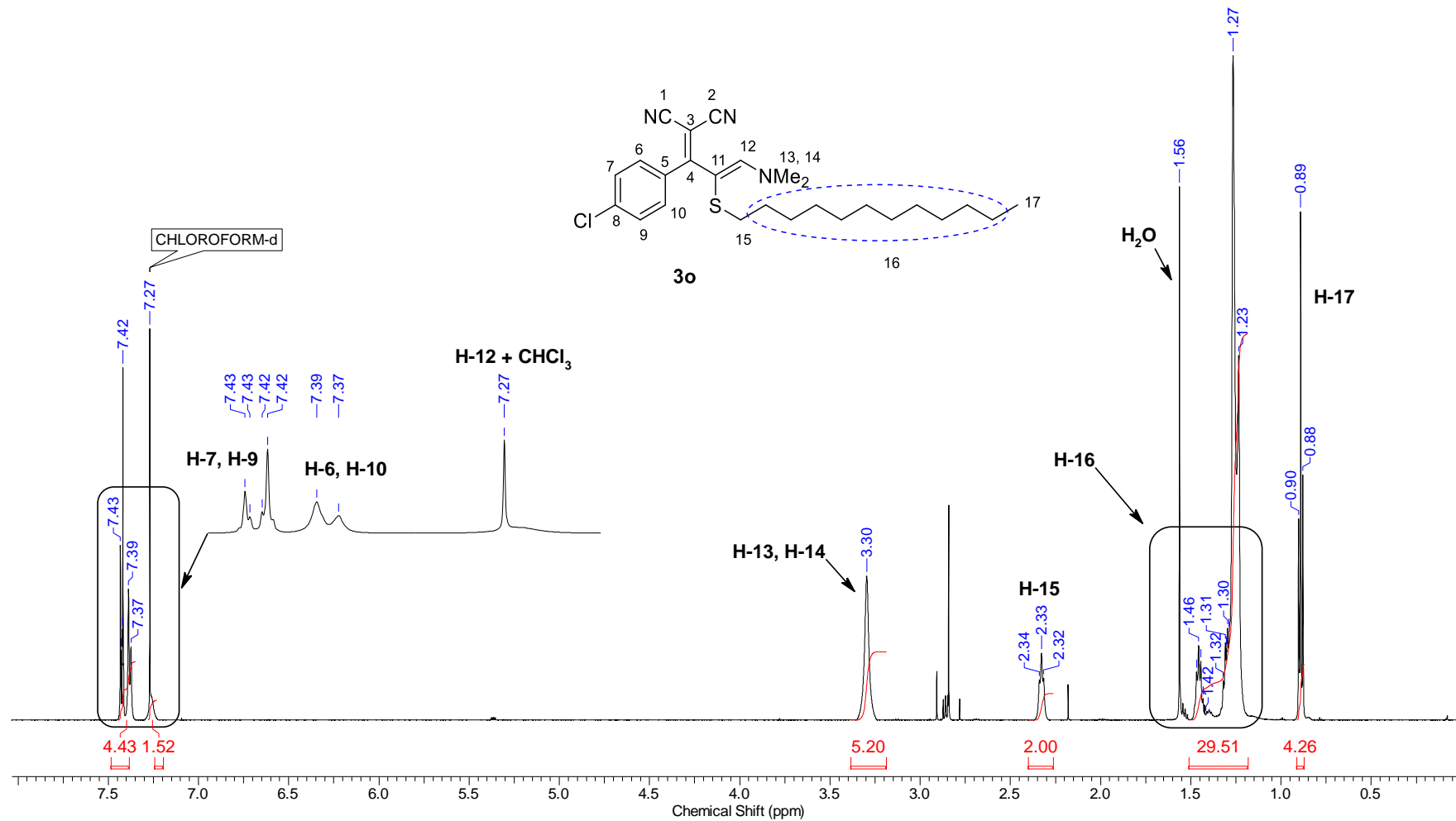
Continuous Conditions Applied to Hazardous Reactions and Fluorophores Synthesis with Photophysics Studies

Frequency (MHz)	564.57	Nucleus	¹⁹ F	Number of Transients	30	Origin	spect
Original Points Count	65536	Owner	nmr	Points Count	65536	Pulse Sequence	zgfthgqn.2
Receiver Gain	199.73	SW(cyclical) (Hz)	133928.58	Solvent	CDCl ₃	Spectrum Offset (Hz)	-56456.8867
Spectrum Type	STANDARD	Sweep Width (Hz)	133926.53	Temperature (degree C)	23.586	Acquisition Time (sec)	0.4893

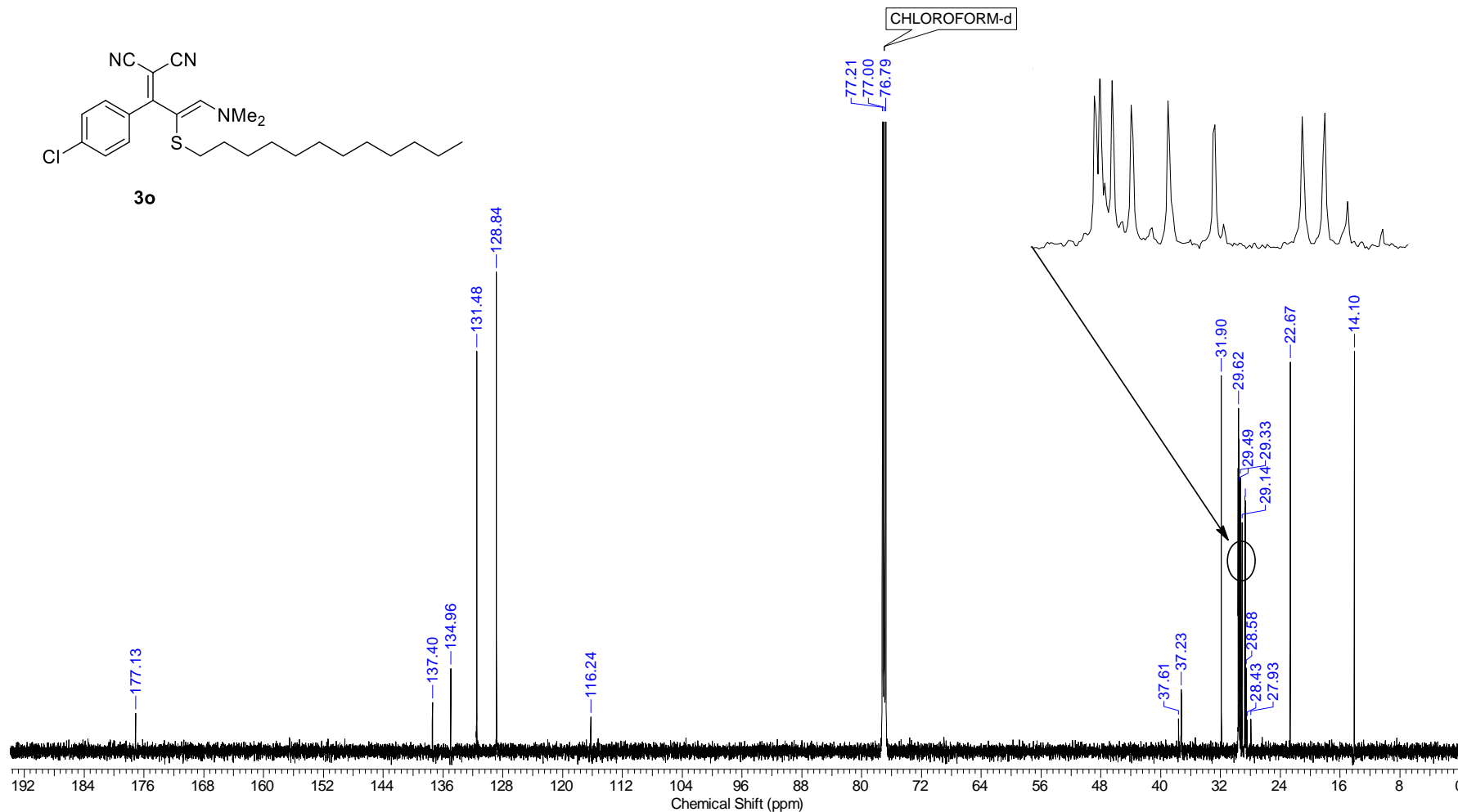


Continuous Conditions Applied to Hazardous Reactions and Fluorophores Synthesis with Photophysics Studies

Frequency (MHz)	600.01	Nucleus	¹ H	Number of Transients	16	Origin	spect
Original Points Count	32768	Owner	nmr	Points Count	65536	Pulse Sequence	zg30
Receiver Gain	199.73	SW(cyclical) (Hz)	12019.23	Solvent	CDCl ₃	Spectrum Offset (Hz)	3695.4734
Spectrum Type	STANDARD	Sweep Width (Hz)	12019.05	Temperature (degree C)	24.998	Acquisition Time (sec)	2.7263

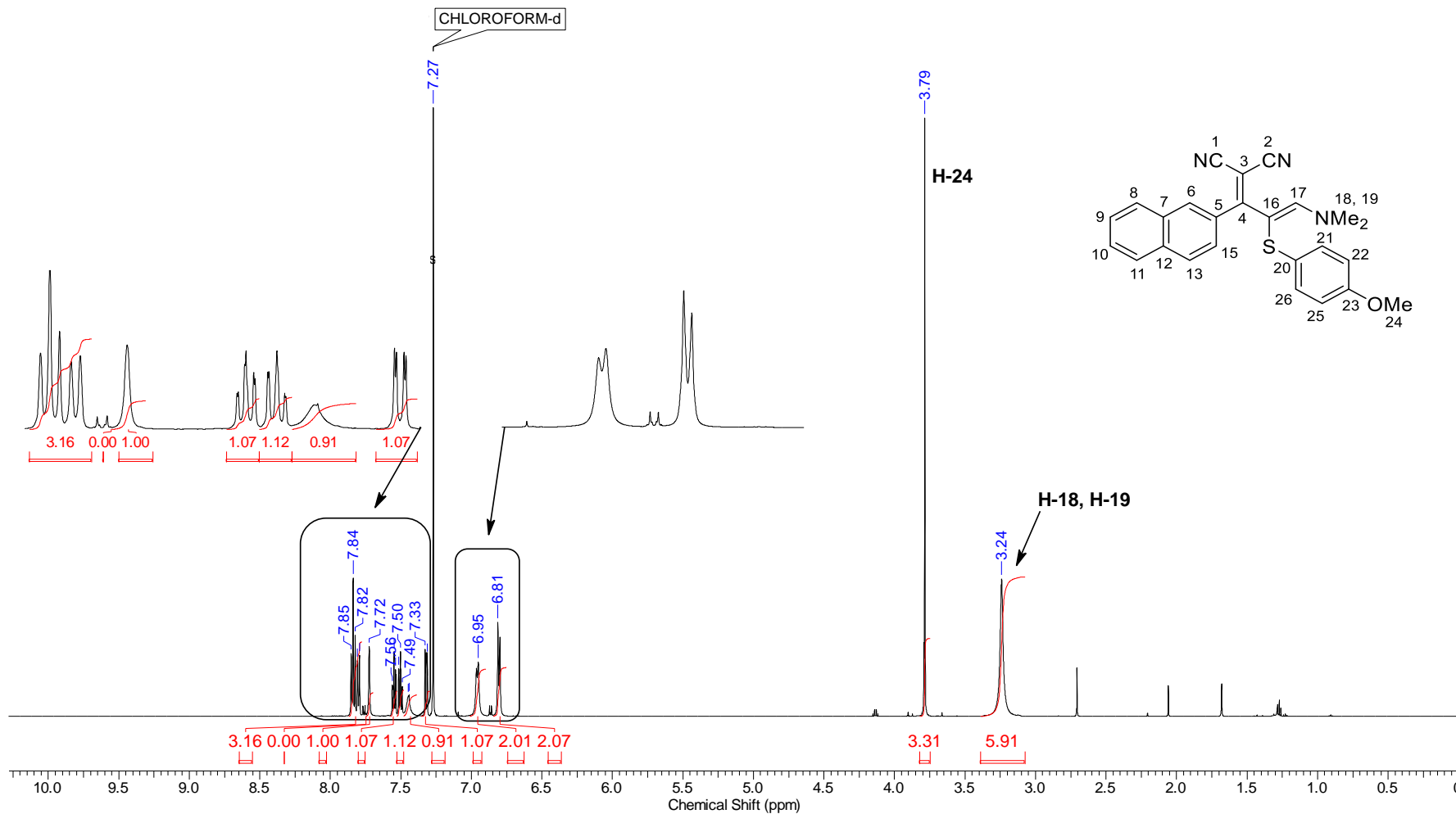


Frequency (MHz)	150.87	Nucleus	¹³ C	Number of Transients	2500	Origin	spect
Original Points Count	32768	Owner	nmr	Points Count	32768	Pulse Sequence	zgpg30
Receiver Gain	199.73	SW(cyclical) (Hz)	36231.88	Solvent	CDCl ₃	Spectrum Offset (Hz)	15095.1055
Spectrum Type	STANDARD	Sweep Width (Hz)	36230.78	Temperature (degree C)	25.310	Acquisition Time (sec)	0.9044



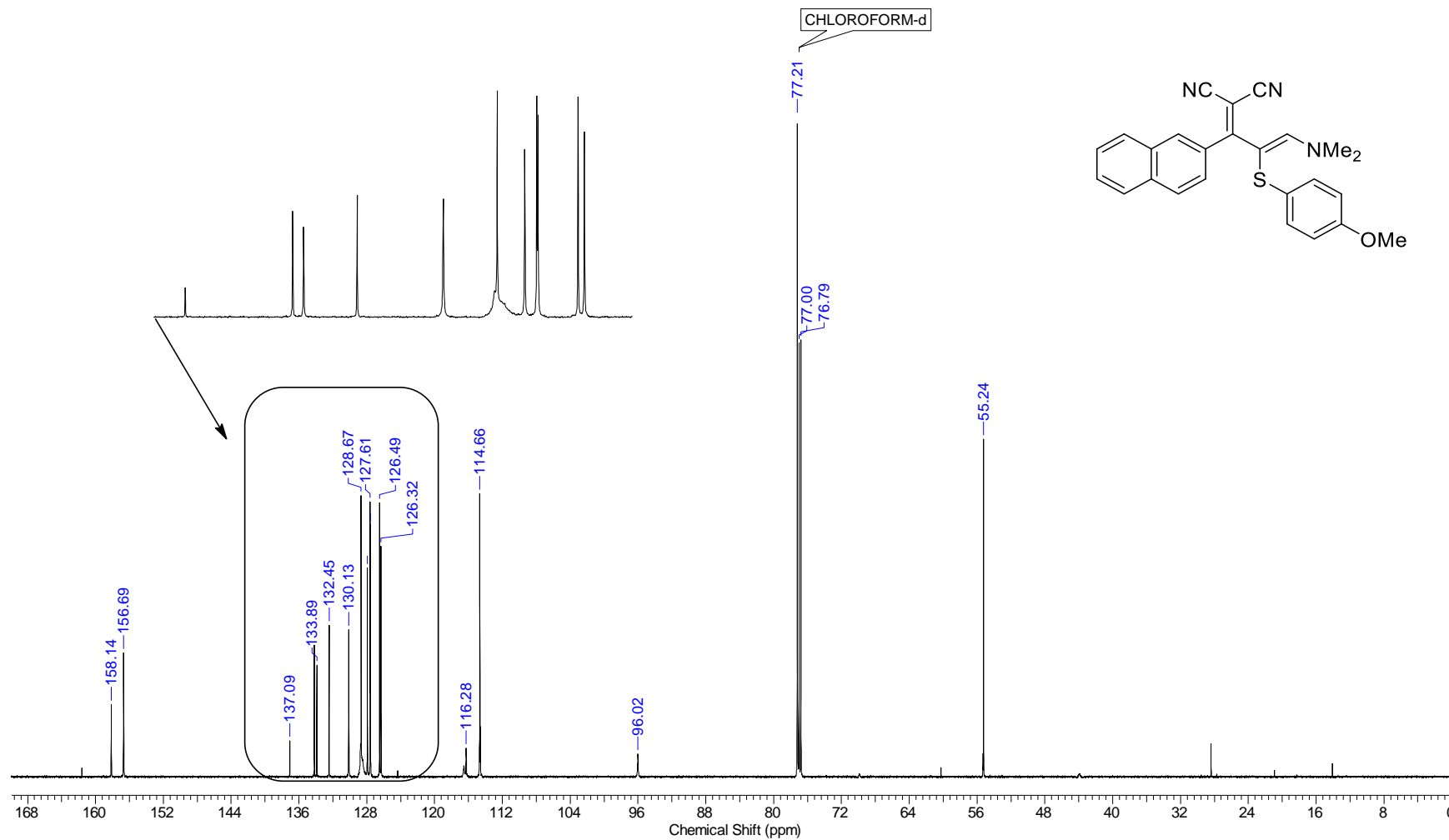
Continuous Conditions Applied to Hazardous Reactions and Fluorophores Synthesis with Photophysics Studies

Nucleus	1H	Number of Transients	16	Origin	spect	Original Points Count	32768
Owner	nmrsu	Points Count	65536	Pulse Sequence	zg30	Receiver Gain	30.85
SW(cyclical) (Hz)	12019.23	Solvent	CDCl3	Spectrum Offset (Hz)	3695.2930	Spectrum Type	STANDARD
Sweep Width (Hz)	12019.05	Temperature (degree C)	23.259	Acquisition Time (sec)	2.7263	Frequency (MHz)	599.96



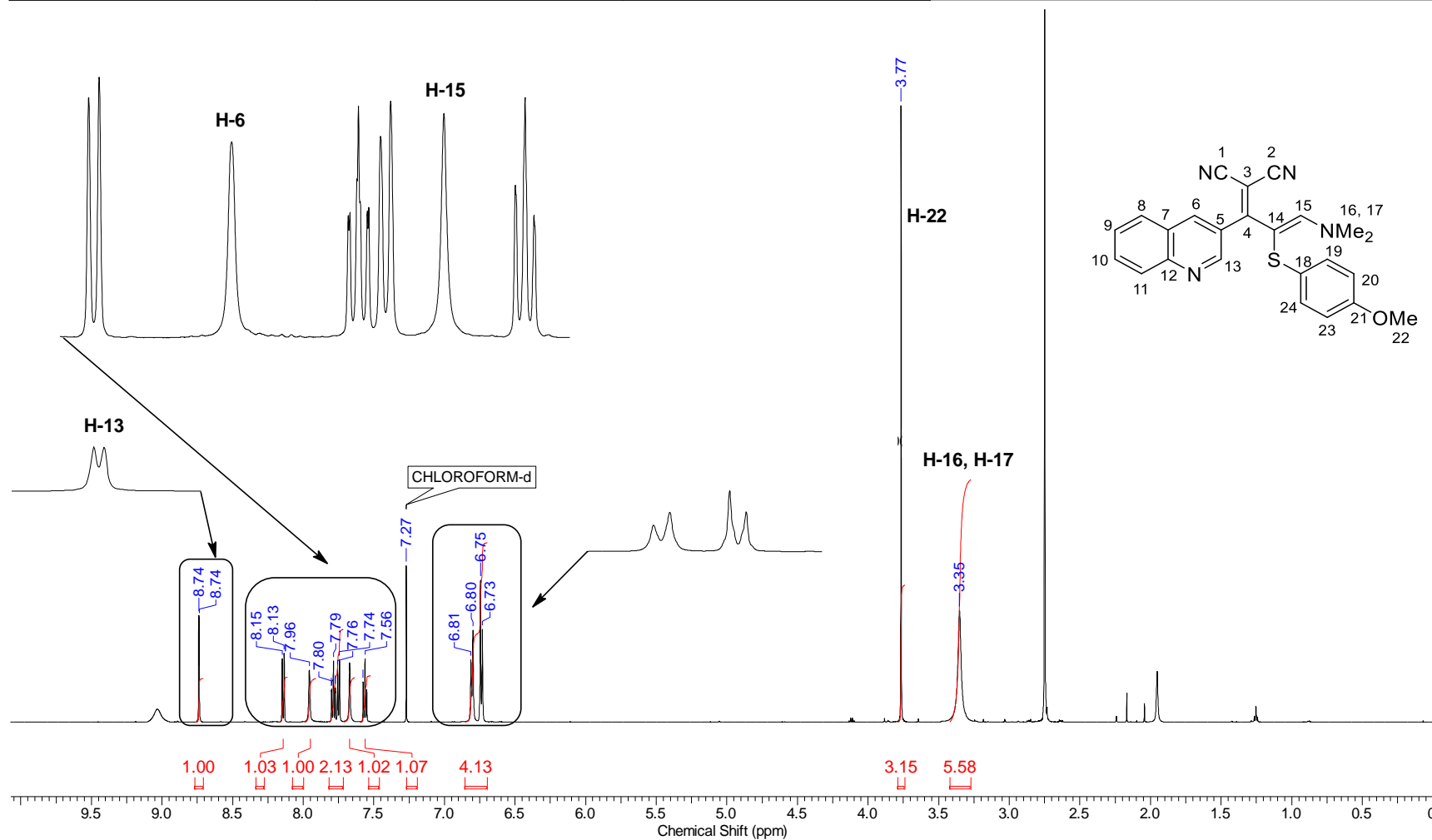
Continuous Conditions Applied to Hazardous Reactions and Fluorophores Synthesis with Photophysics Studies

Frequency (MHz)	150.87	Nucleus	¹³ C	Number of Transients	2500	Origin	spect
Original Points Count	32768	Owner	nmr	Points Count	32768	Pulse Sequence	zgpg30
Receiver Gain	199.73	SW(cyclical) (Hz)	36231.88	Solvent	CDCl ₃	Spectrum Offset (Hz)	15060.8281
Spectrum Type	STANDARD	Sweep Width (Hz)	36230.78	Temperature (degree C)	25.323	Acquisition Time (sec)	0.9044



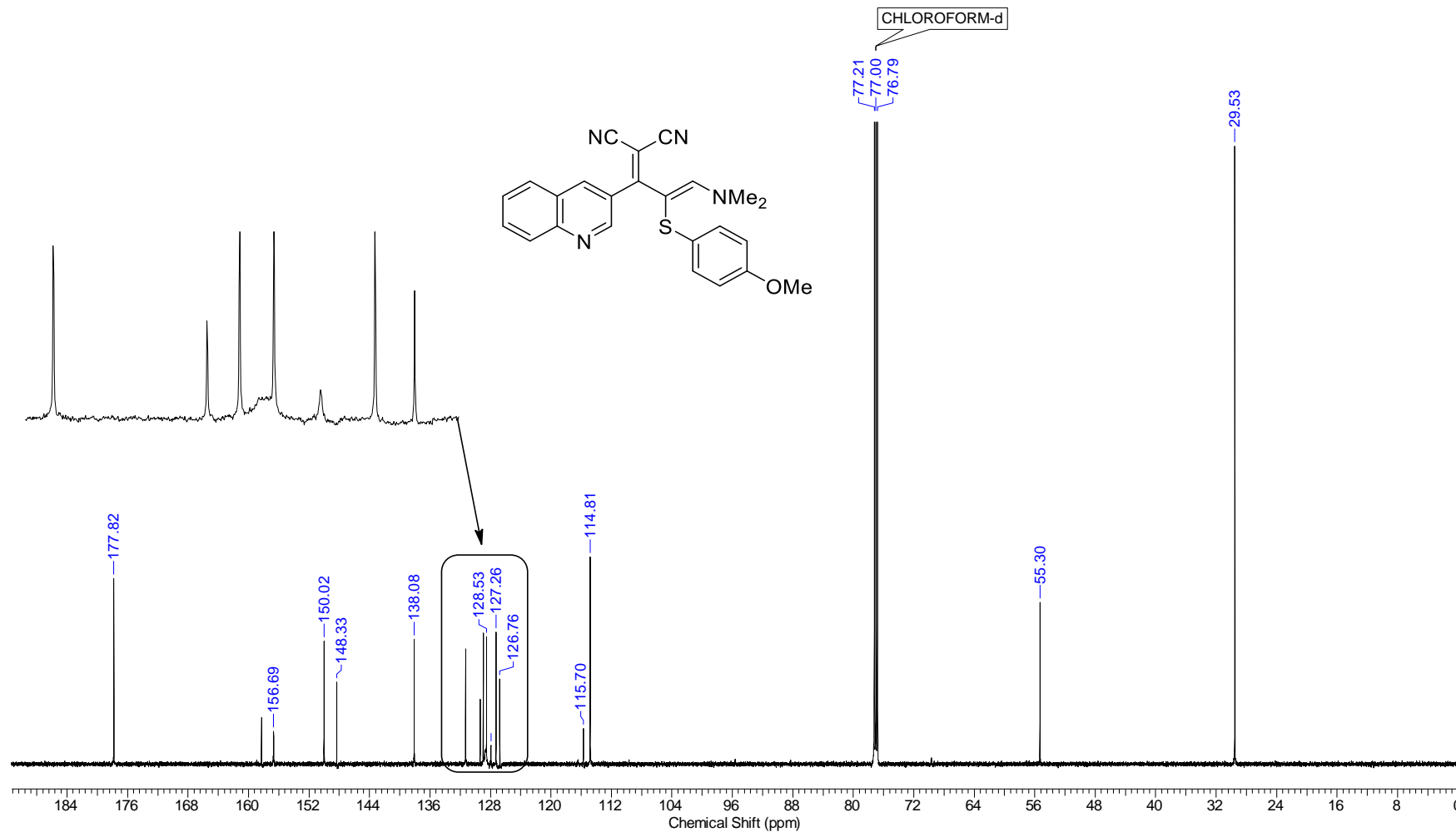
Continuous Conditions Applied to Hazardous Reactions and Fluorophores Synthesis with Photophysics Studies

Frequency (MHz)	599.96	Nucleus	1H	Number of Transients	16	Origin	spect
Original Points Count	32768	Owner	nrmrsu	Points Count	65536	Pulse Sequence	zg30
Receiver Gain	78.28	SW(cyclical) (Hz)	12019.23	Solvent	CDCl3	Spectrum Offset (Hz)	3743.3433
Spectrum Type	STANDARD	Sweep Width (Hz)	12019.05	Temperature (degree C)	23.046	Acquisition Time (sec)	2.7263



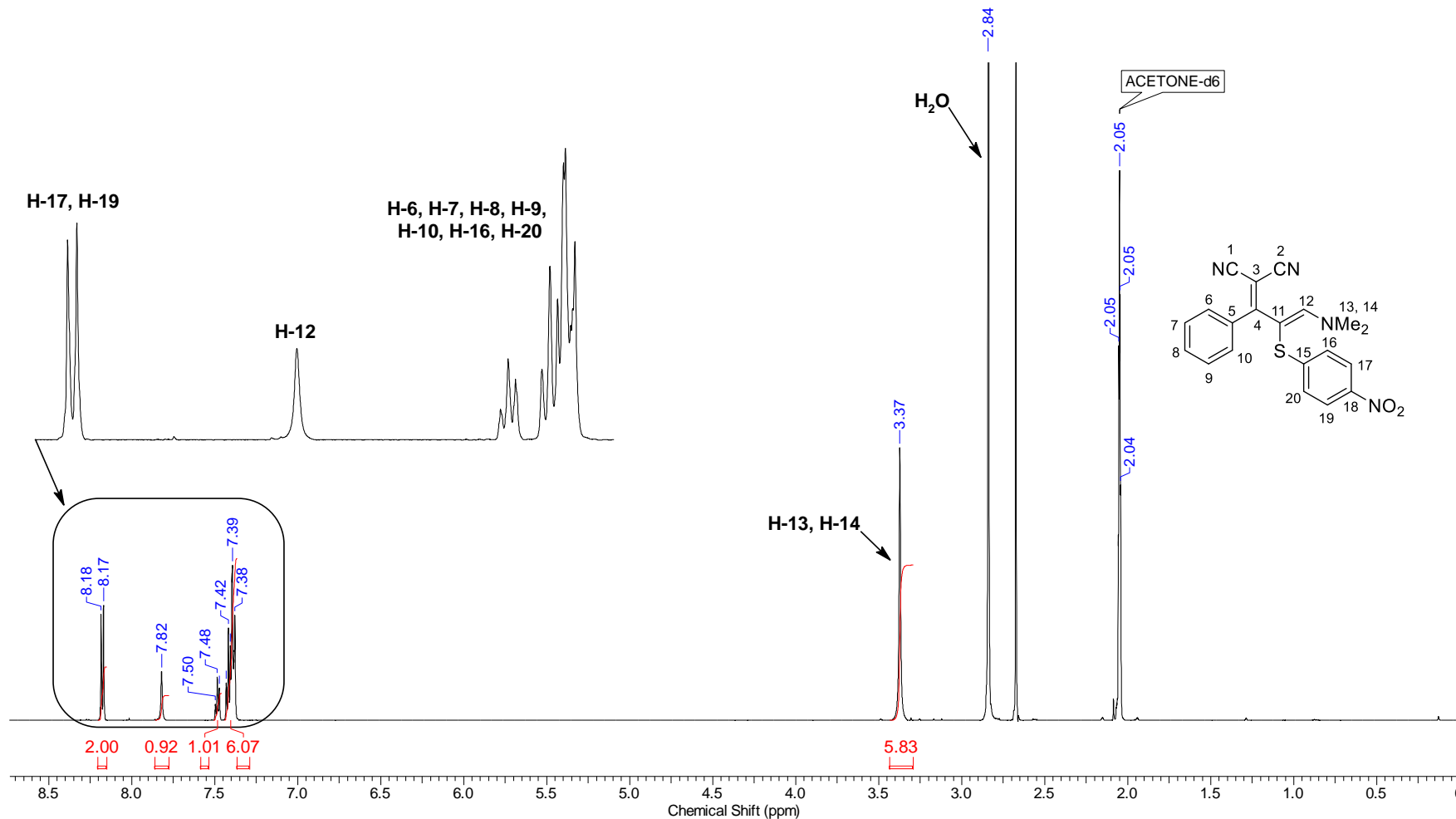
Continuous Conditions Applied to Hazardous Reactions and Fluorophores Synthesis with Photophysics Studies

Frequency (MHz)	150.86	Nucleus	¹³ C	Number of Transients	3600	Origin	spect
Original Points Count	32768	Owner	nmsu	Points Count	32768	Pulse Sequence	zgpg30
Receiver Gain	194.75	SW(cyclical) (Hz)	36231.88	Solvent	CDCl ₃	Spectrum Offset (Hz)	15085.2920
Spectrum Type	STANDARD	Sweep Width (Hz)	36230.78	Temperature (degree C)	23.495	Acquisition Time (sec)	0.9044

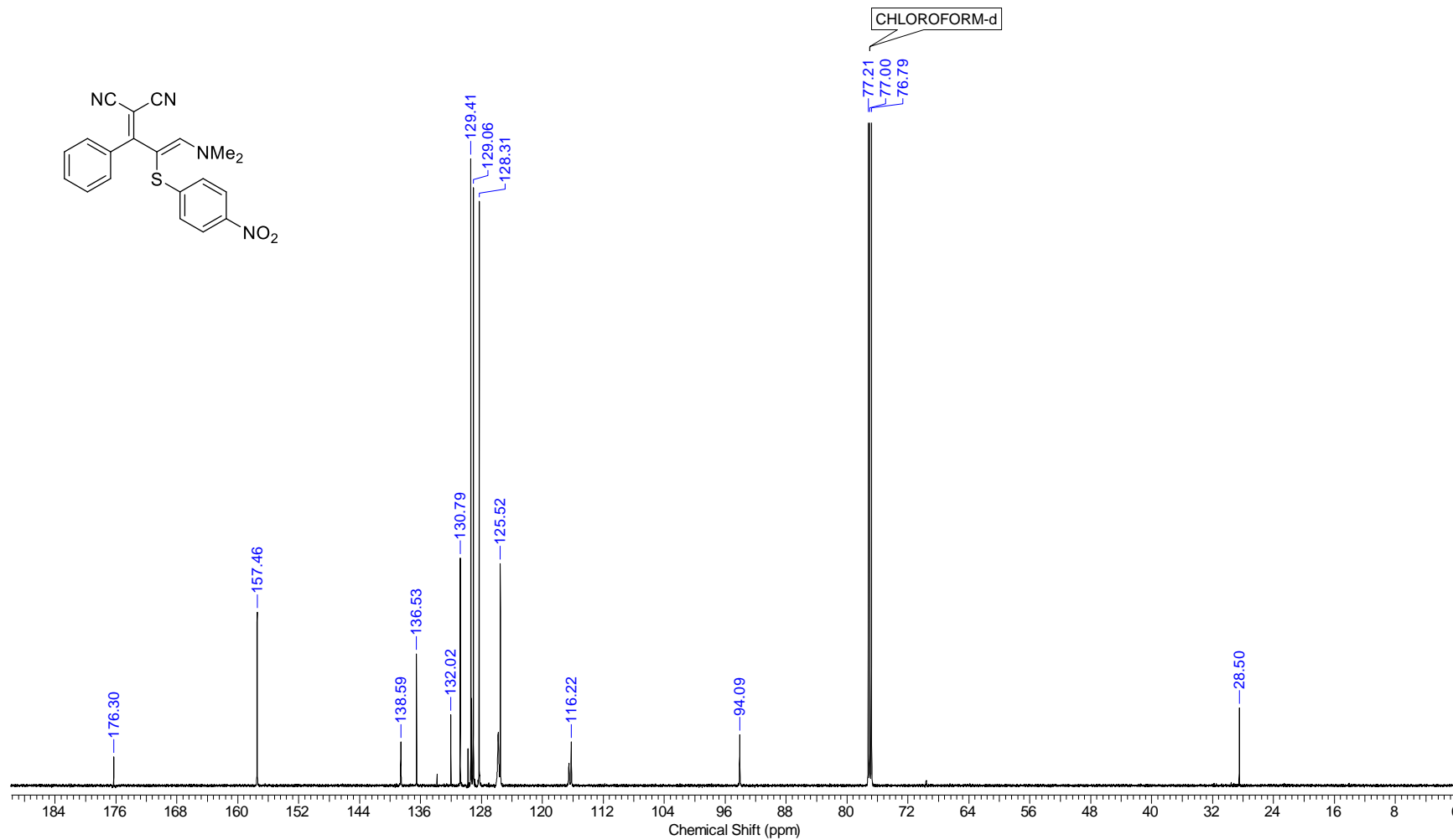


Continuous Conditions Applied to Hazardous Reactions and Fluorophores Synthesis with Photophysics Studies

Frequency (MHz)	599.96	Nucleus	1H	Number of Transients	16	Origin	spect
Original Points Count	32768	Owner	nmsu	Points Count	65536	Pulse Sequence	zg30
Receiver Gain	194.75	SW(cyclical) (Hz)	12019.23	Solvent	Acetone-d6	Spectrum Offset (Hz)	3693.4136
Spectrum Type	STANDARD	Sweep Width (Hz)	12019.05	Temperature (degree C)	23.085	Acquisition Time (sec)	2.7263

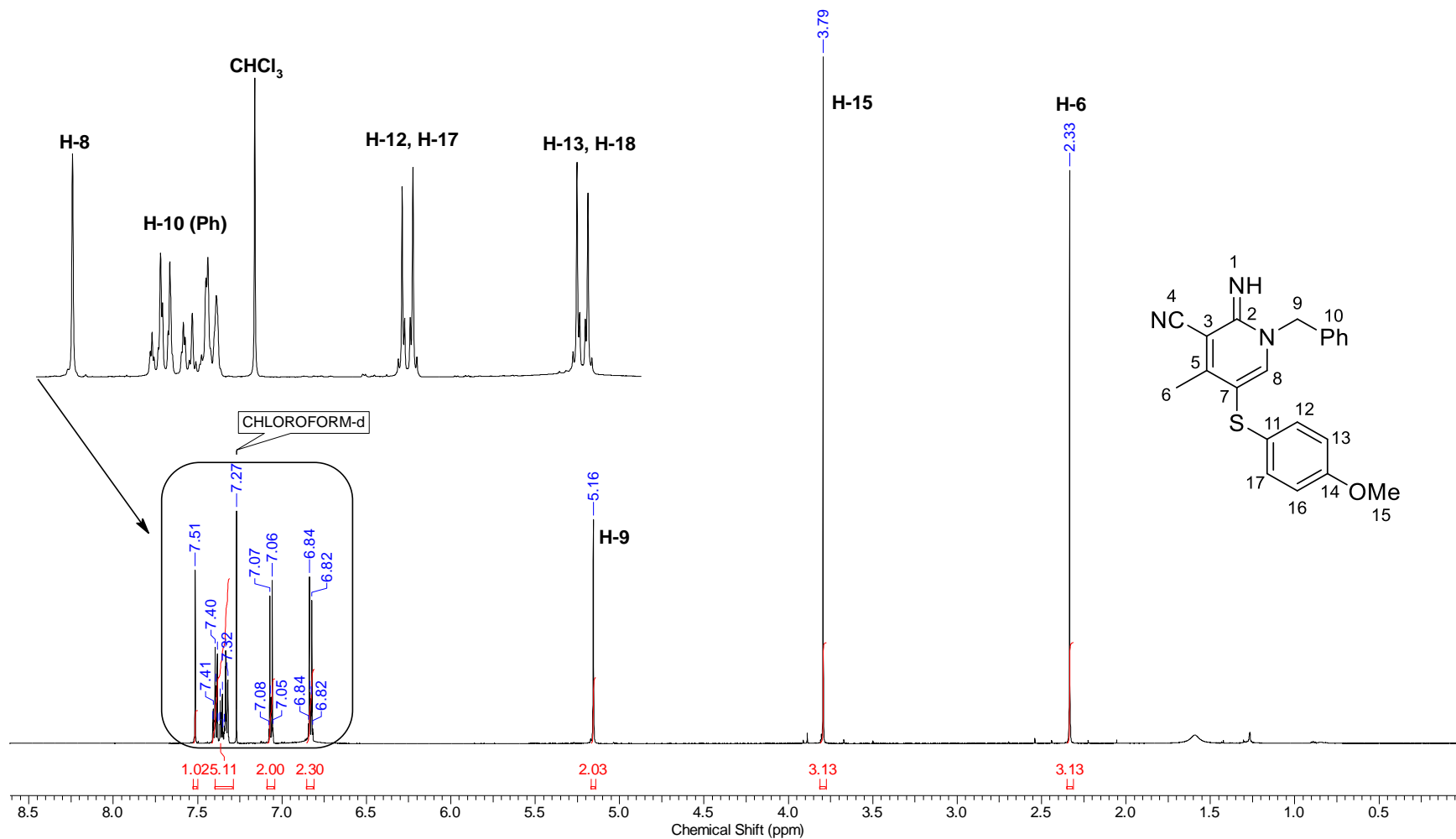


Frequency (MHz)	150.87	Nucleus	¹³ C	Number of Transients	2500	Origin	spect
Original Points Count	32768	Owner	nmrsu	Points Count	32768	Pulse Sequence	zgpg30
Receiver Gain	199.73	SW(cyclical) (Hz)	36231.88	Solvent	CDCl ₃	Spectrum Offset (Hz)	15078.5195
Spectrum Type	STANDARD	Sweep Width (Hz)	36230.78	Temperature (degree C)	25.230	Acquisition Time (sec)	0.9044



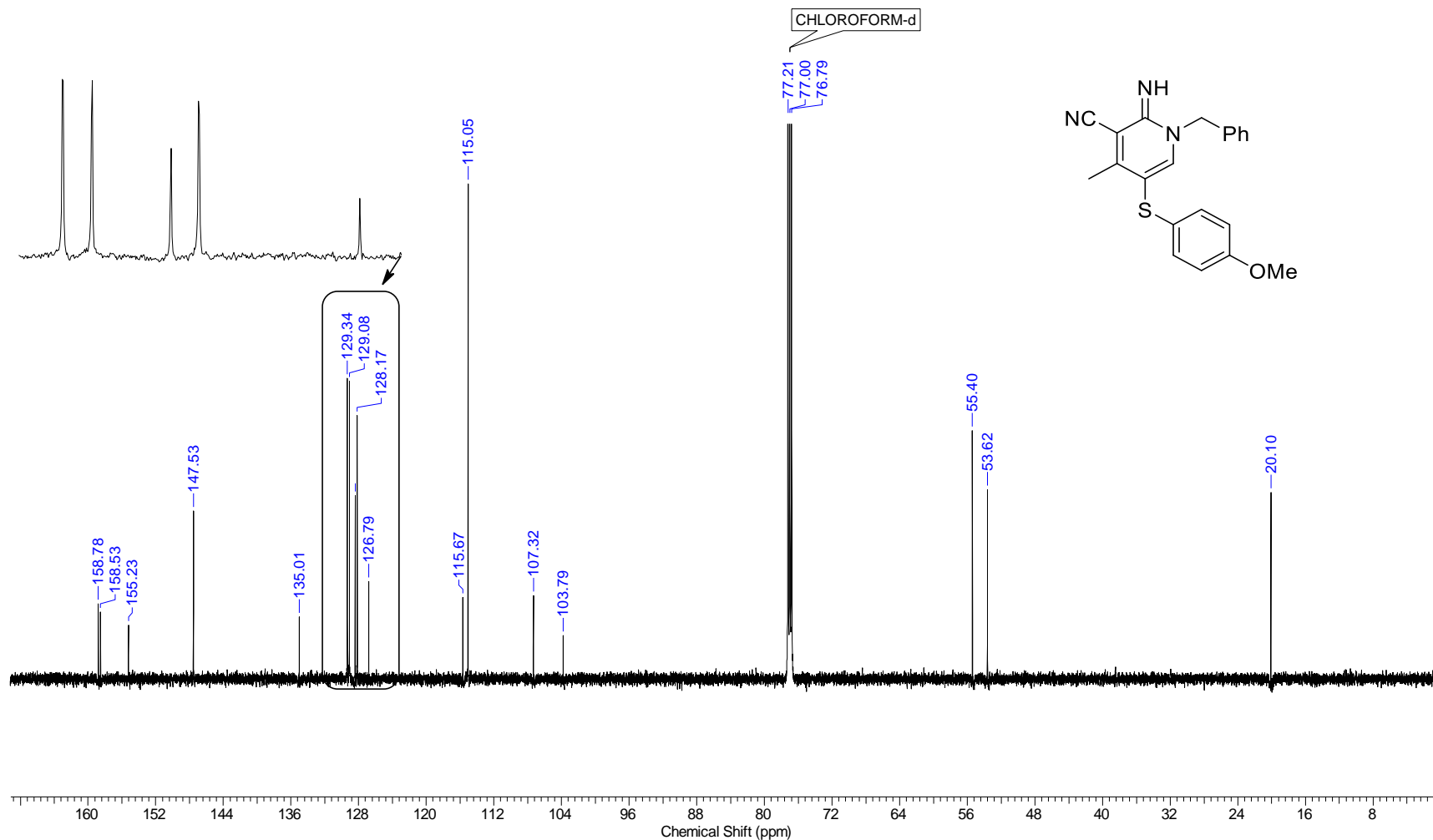
Continuous Conditions Applied to Hazardous Reactions and Fluorophores Synthesis with Photophysics Studies

Frequency (MHz)	600.01	Nucleus	1H	Number of Transients	16	Origin	spect
Original Points Count	32768	Owner	nmr	Points Count	65536	Pulse Sequence	zg30
Receiver Gain	199.73	SW(cyclical) (Hz)	12019.23	Solvent	CDCl3	Spectrum Offset (Hz)	3695.4729
Spectrum Type	STANDARD	Sweep Width (Hz)	12019.05	Temperature (degree C)	24.999	Acquisition Time (sec)	2.7263



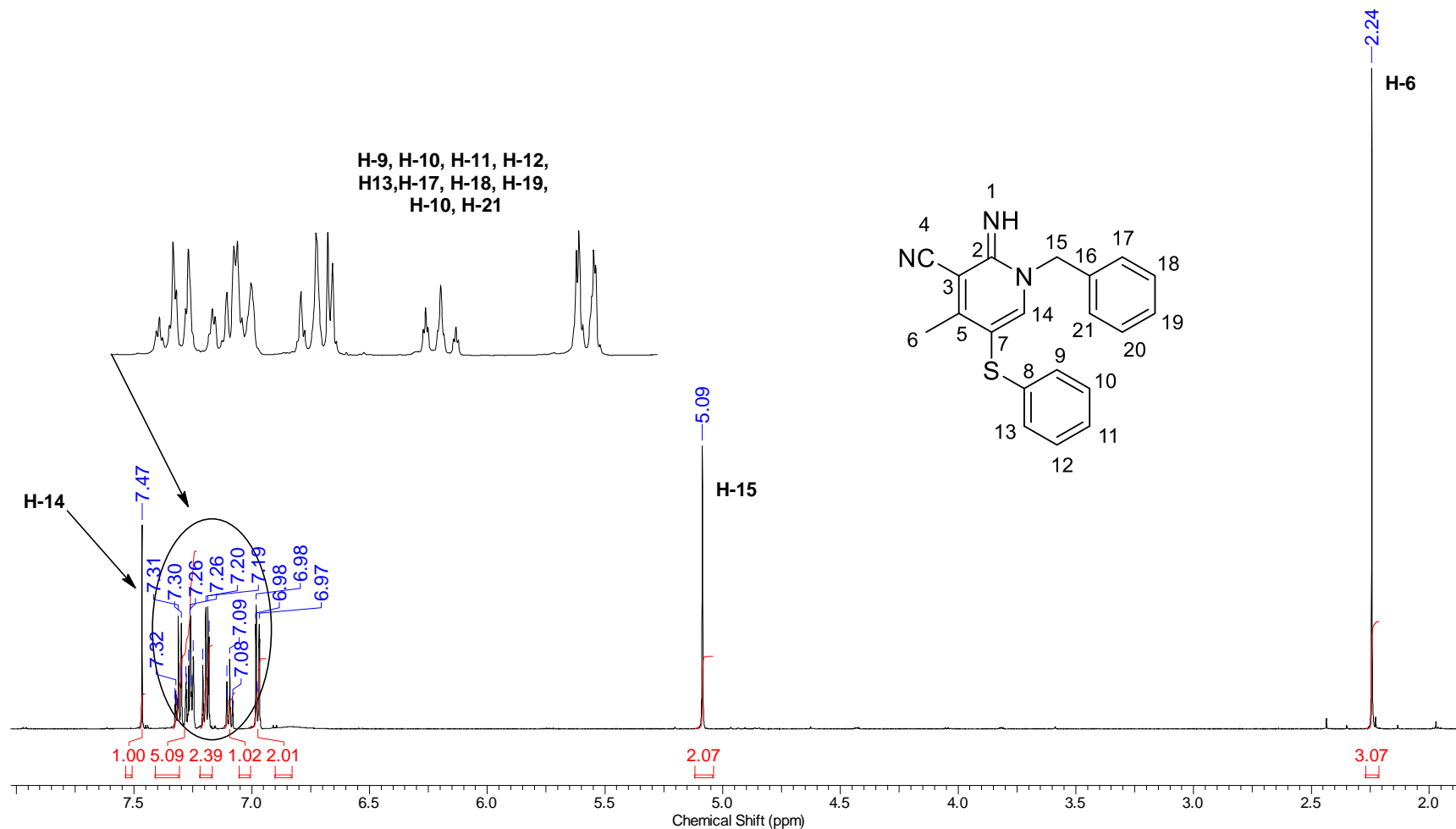
Continuous Conditions Applied to Hazardous Reactions and Fluorophores Synthesis with Photophysics Studies

Frequency (MHz)	150.87	Nucleus	¹³ C	Number of Transients	2500	Origin	spect
Original Points Count	32768	Owner	nmr	Points Count	32768	Pulse Sequence	zgpg30
Receiver Gain	199.73	SW(cyclical) (Hz)	36231.88	Solvent	CDCl ₃	Spectrum Offset (Hz)	15096.2100
Spectrum Type	STANDARD	Sweep Width (Hz)	36230.78	Temperature (degree C)	26.131	Acquisition Time (sec)	0.9044



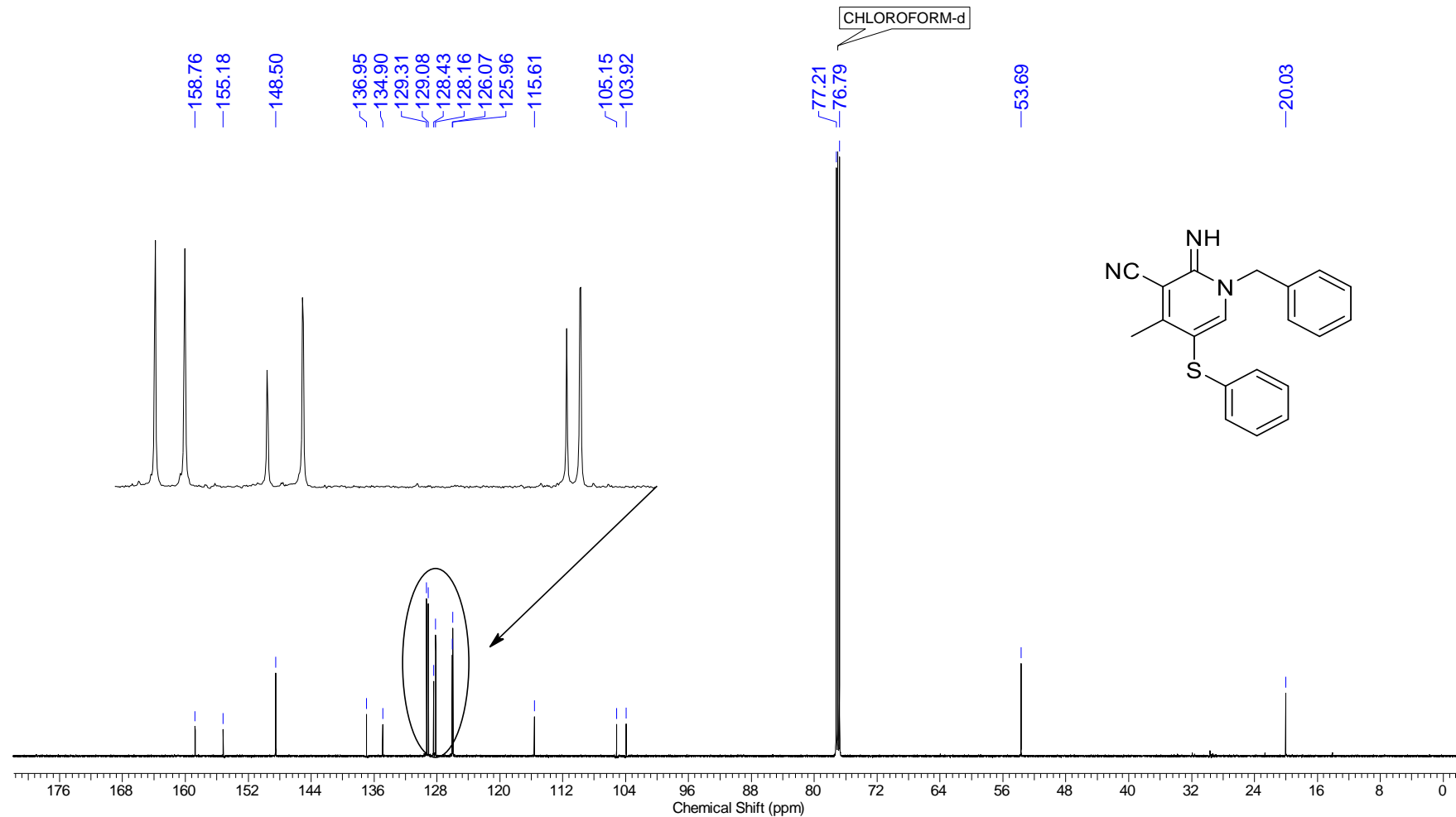
Continuous Conditions Applied to Hazardous Reactions and Fluorophores Synthesis with Photophysics Studies

Nucleus	1H	Number of Transients	16	Origin	spect	Original Points Count	32768
Owner	nmr	Points Count	65536	Pulse Sequence	zg30	Receiver Gain	199.73
SW(cyclical) (Hz)	12019.23	Solvent	CDCl3	Spectrum Offset (Hz)	3693.0540	Spectrum Type	STANDARD
Sweep Width (Hz)	12019.05	Temperature (degree C)	24.998	Acquisition Time (sec)	2.7263	Frequency (MHz)	600.01



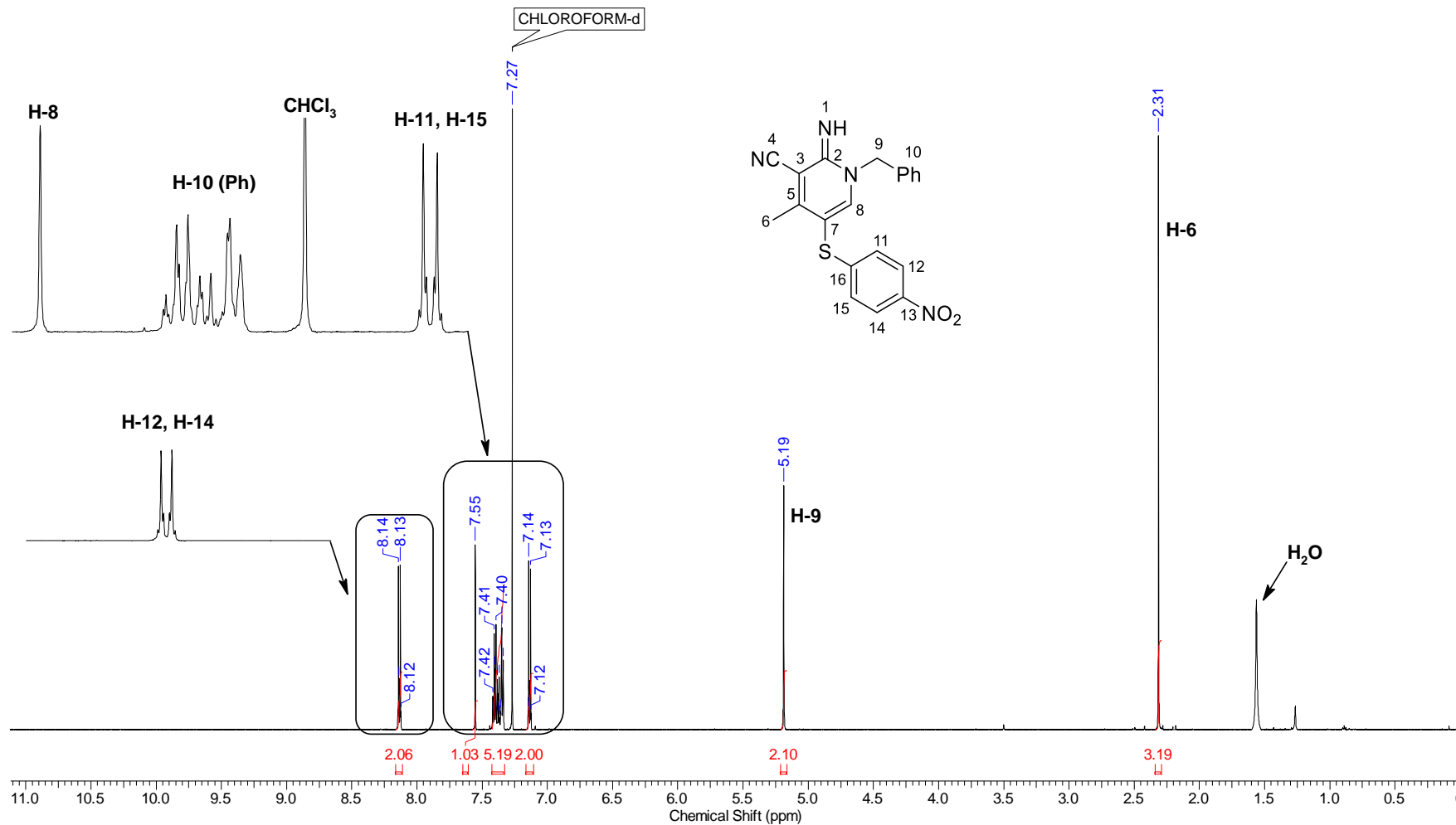
Continuous Conditions Applied to Hazardous Reactions and Fluorophores Synthesis with Photophysics Studies

Nucleus	13C	Number of Transients	2500	Origin	spect	Original Points Count	32768
Owner	nmr	Points Count	32768	Pulse Sequence	zgpg30	Receiver Gain	199.73
SW(cyclical) (Hz)	36231.88	Solvent	BENZENE-d6	Spectrum Offset (Hz)	15092.8926	Spectrum Type	STANDARD
Sweep Width (Hz)	36230.78	Temperature (degree C)	25.270	Acquisition Time (sec)	0.9044	Frequency (MHz)	150.87



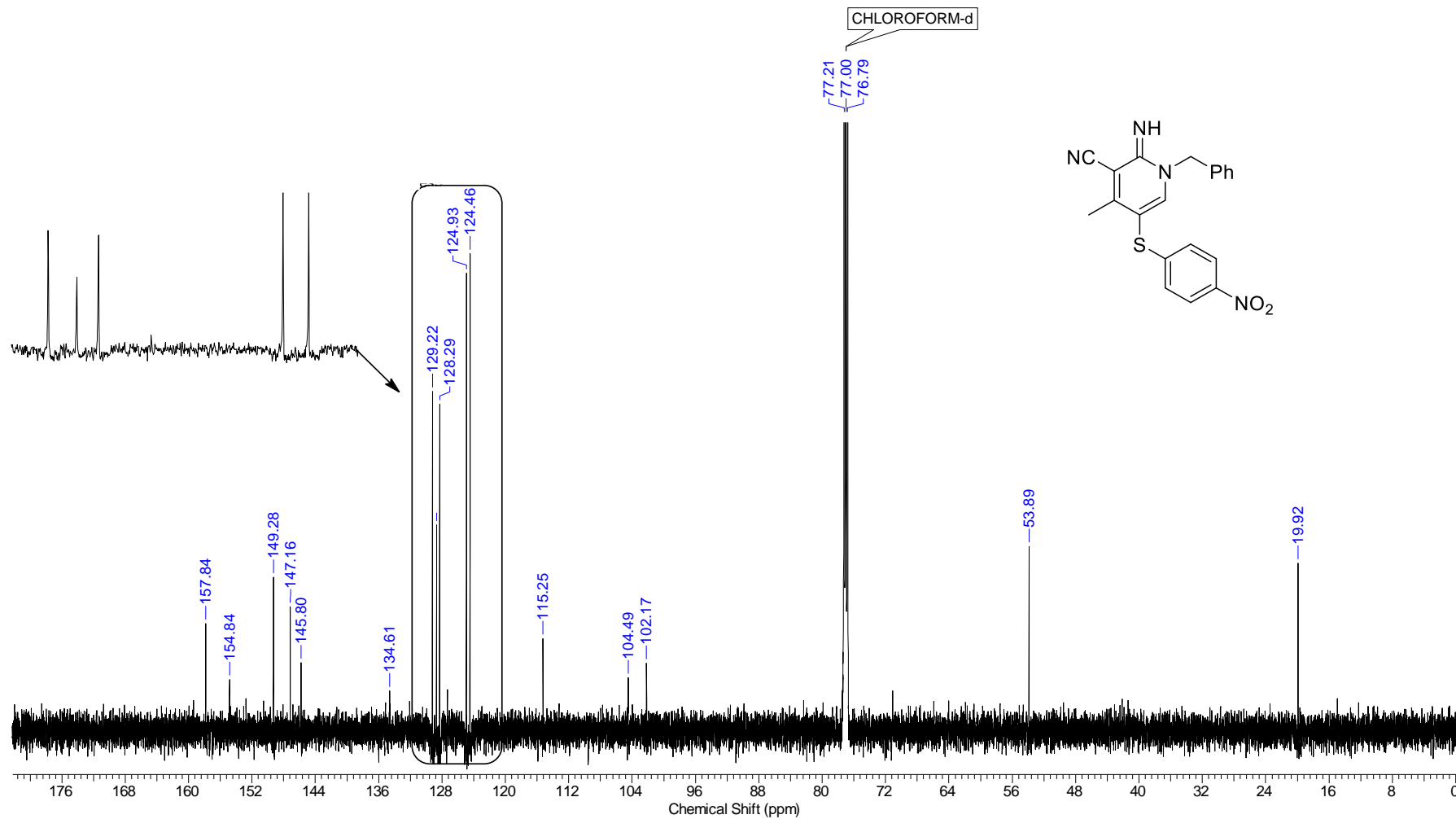
Continuous Conditions Applied to Hazardous Reactions and Fluorophores Synthesis with Photophysics Studies

Nucleus	1H	Number of Transients	16	Origin	spect	Original Points Count	32768
Owner	nmr	Points Count	65536	Pulse Sequence	zg30	Receiver Gain	199.73
SW(cyclical) (Hz)	12019.23	Solvent	CDCl3	Spectrum Offset (Hz)	3695.2903	Spectrum Type	STANDARD
Sweep Width (Hz)	12019.05	Temperature (degree C)	24.998	Acquisition Time (sec)	2.7263	Frequency (MHz)	600.01



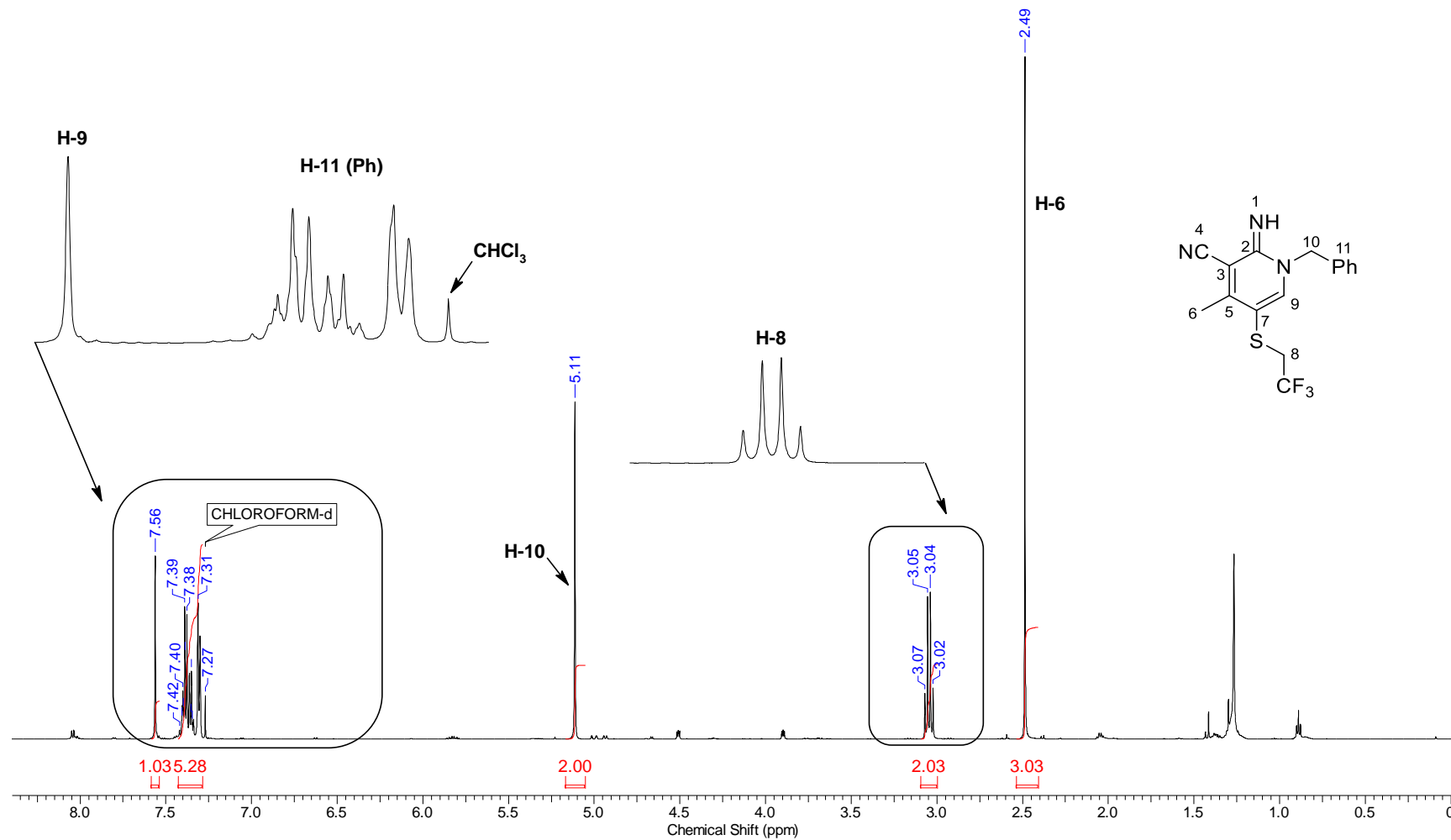
Continuous Conditions Applied to Hazardous Reactions and Fluorophores Synthesis with Photophysics Studies

Nucleus	13C	Number of Transients	2500	Origin	spect	Original Points Count	32768
Owner	nmr	Points Count	32768	Pulse Sequence	zpgq30	Receiver Gain	199.73
SW(cyclical) (Hz)	36231.88	Solvent	CDCl3	Spectrum Offset (Hz)	15097.3164	Spectrum Type	STANDARD
Sweep Width (Hz)	36230.78	Temperature (degree C)	25.395	Acquisition Time (sec)	0.9044	Frequency (MHz)	150.87



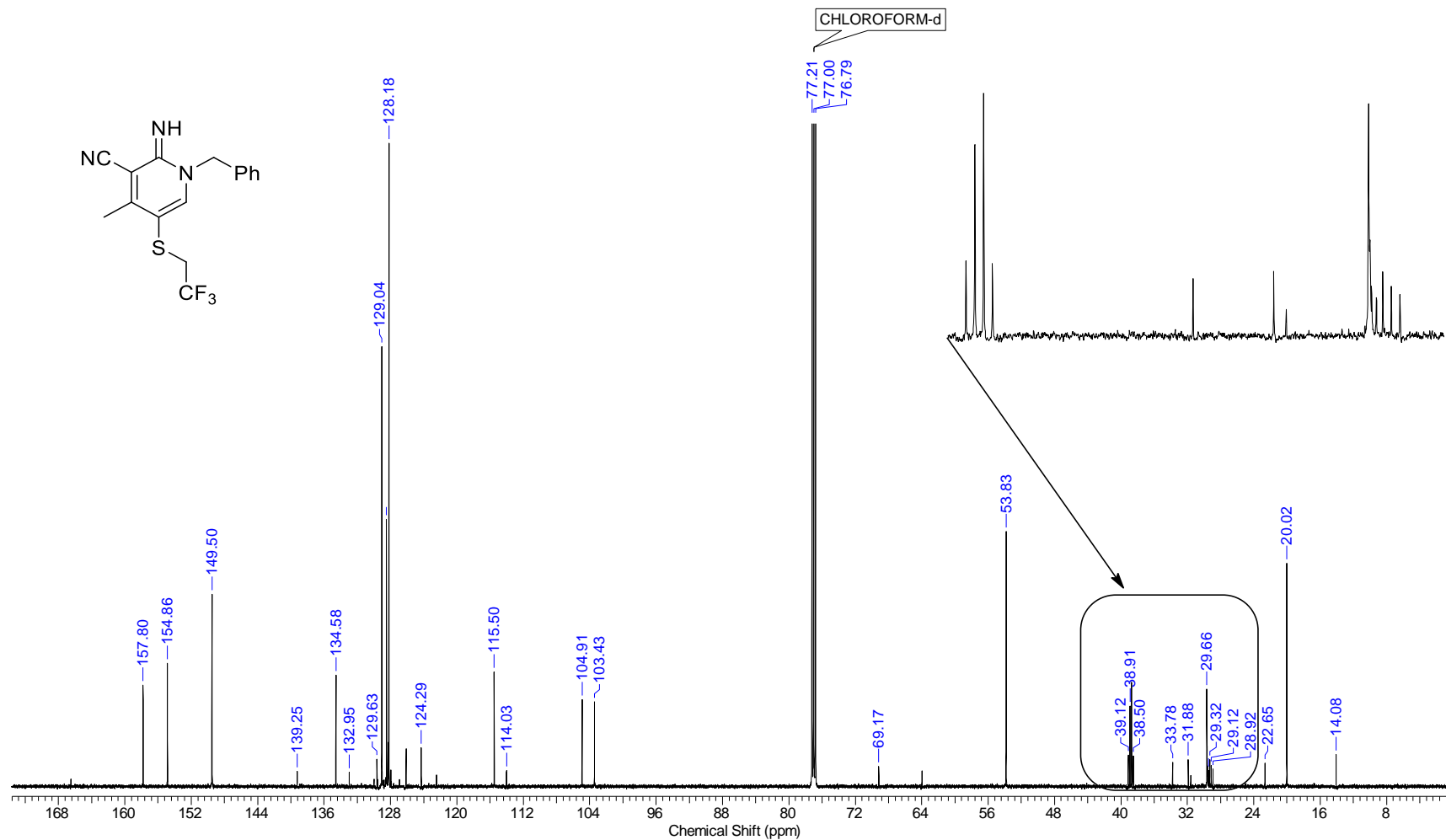
Continuous Conditions Applied to Hazardous Reactions and Fluorophores Synthesis with Photophysics Studies

Frequency (MHz)	600.01	Nucleus	¹ H	Number of Transients	16	Origin	spect
Original Points Count	32768	Owner	nmr	Points Count	65536	Pulse Sequence	zg30
Receiver Gain	106.90	SW(cyclical) (Hz)	12019.23	Solvent	CDCl ₃	Spectrum Offset (Hz)	3695.4736
Spectrum Type	STANDARD	Sweep Width (Hz)	12019.05	Temperature (degree C)	25.000	Acquisition Time (sec)	2.7263

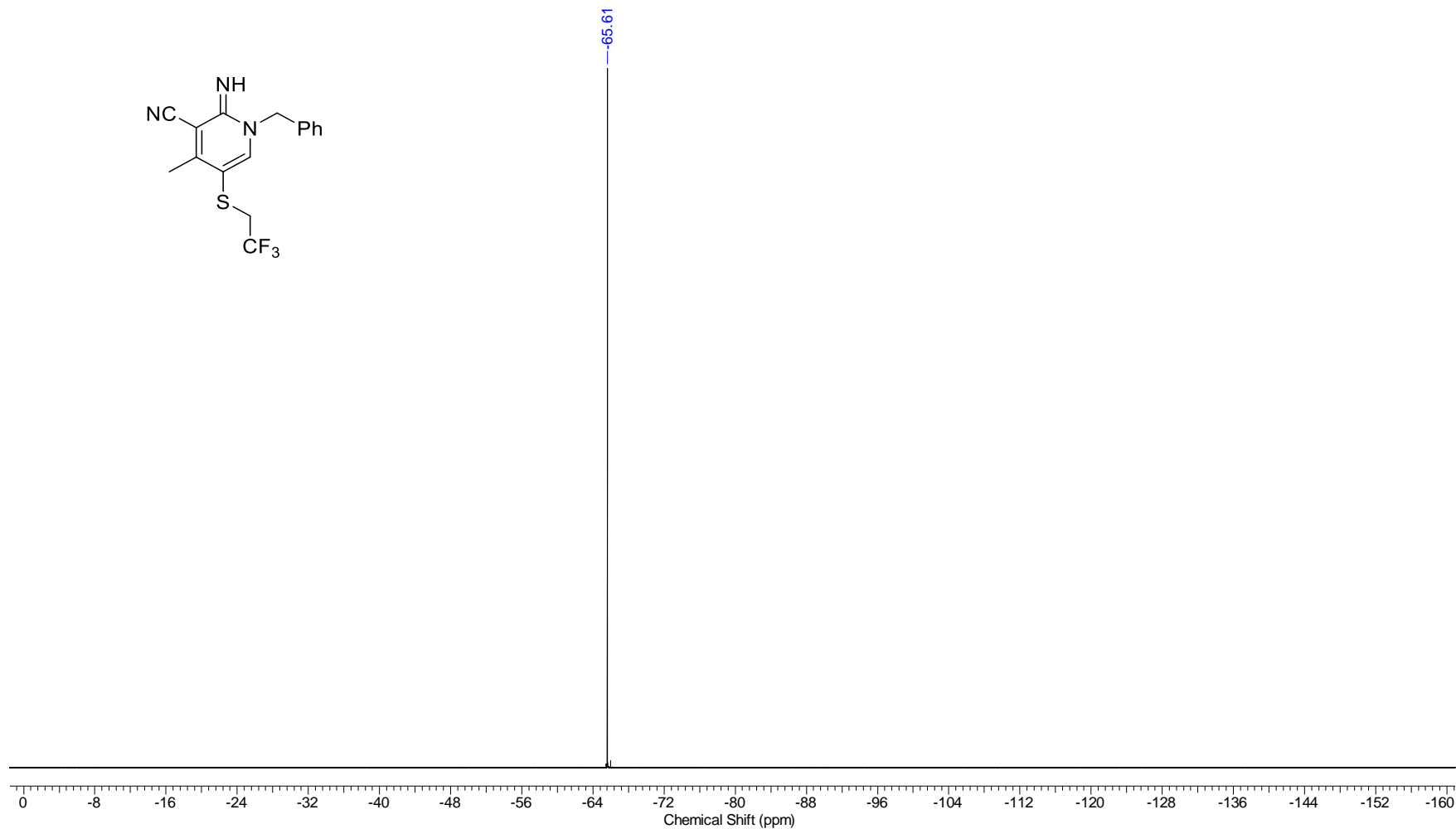
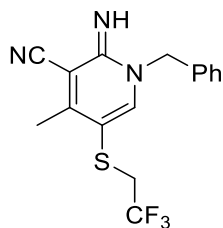


Continuous Conditions Applied to Hazardous Reactions and Fluorophores Synthesis with Photophysics Studies

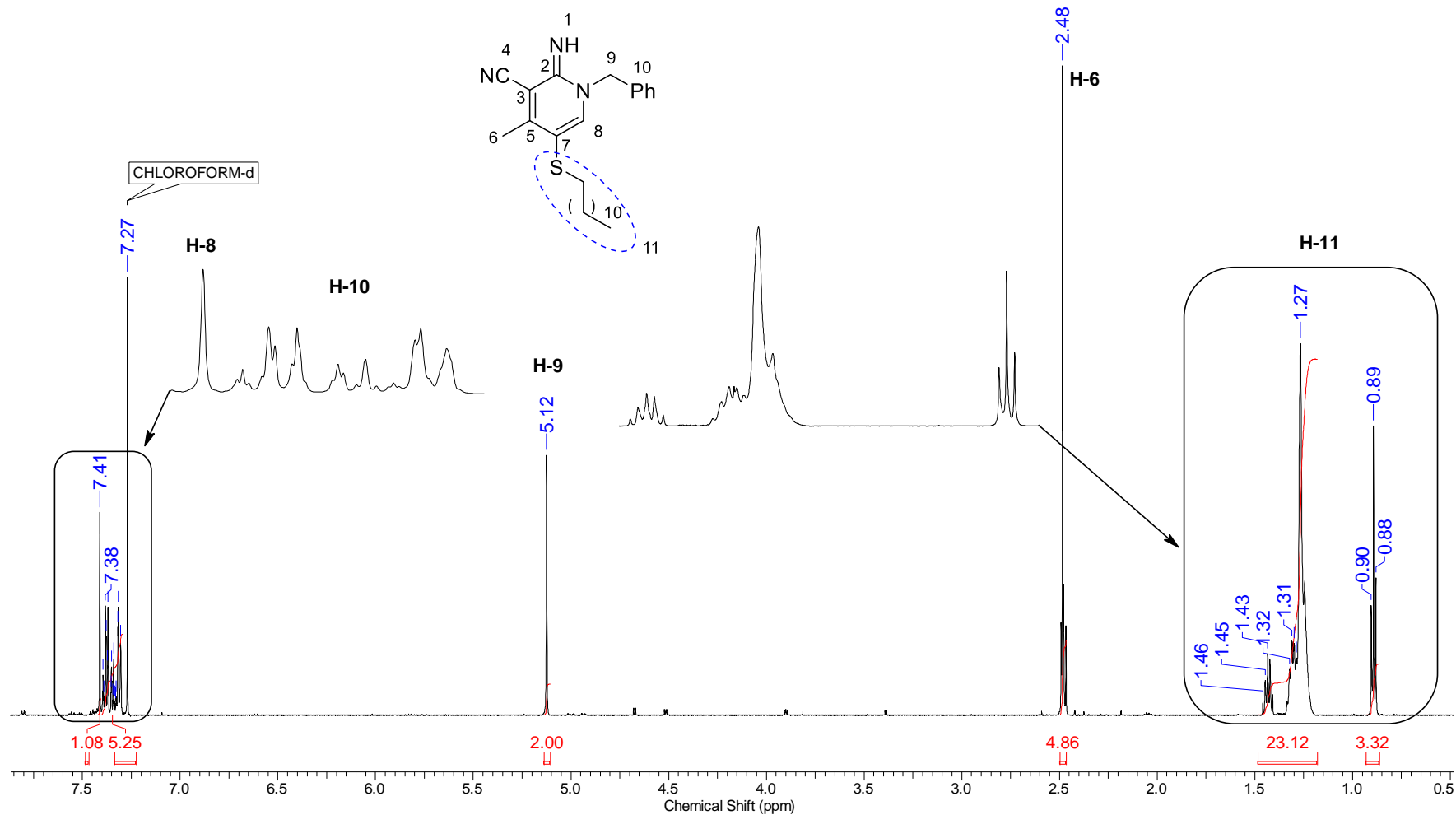
Frequency (MHz)	150.87	Nucleus	¹³ C	Number of Transients	2500	Origin	spect
Original Points Count	32768	Owner	nmr	Points Count	32768	Pulse Sequence	zgpg30
Receiver Gain	199.73	SW(cyclical) (Hz)	36231.88	Solvent	CDCl ₃	Spectrum Offset (Hz)	15079.6250
Spectrum Type	STANDARD	Sweep Width (Hz)	36230.78	Temperature (degree C)	25.343	Acquisition Time (sec)	0.9044



Frequency (MHz)	564.57	Nucleus	19F	Number of Transients	32	Origin	spect
Original Points Count	65536	Owner	nmr	Points Count	65536	Pulse Sequence	zgf Higgins.2
Receiver Gain	199.73	SW(cyclical) (Hz)	133928.58	Solvent	CDCl3	Spectrum Offset (Hz)	-56456.8867
Spectrum Type	STANDARD	Sweep Width (Hz)	133926.53	Temperature (degree C)	23.875	Acquisition Time (sec)	0.4893

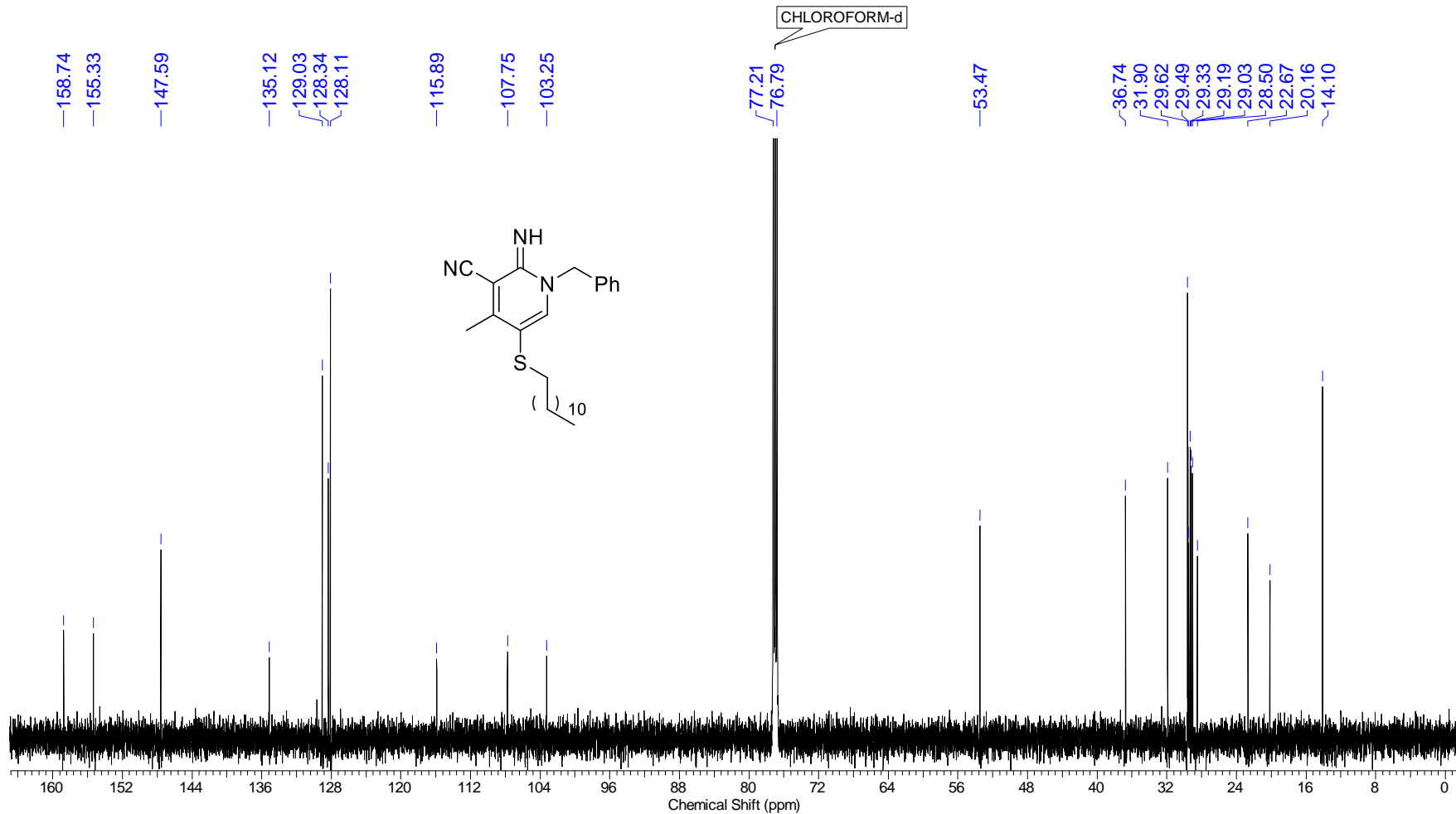


Nucleus	1H	Number of Transients	16	Origin	spect	Original Points Count	32768
Owner	nmr	Points Count	65536	Pulse Sequence	zg30	Receiver Gain	199.73
SW(cyclical) (Hz)	12019.23	Solvent	CDCl3	Spectrum Offset (Hz)	3695.4734	Spectrum Type	STANDARD
Sweep Width (Hz)	12019.05	Temperature (degree C)	24.998	Acquisition Time (sec)	2.7263	Frequency (MHz)	600.01



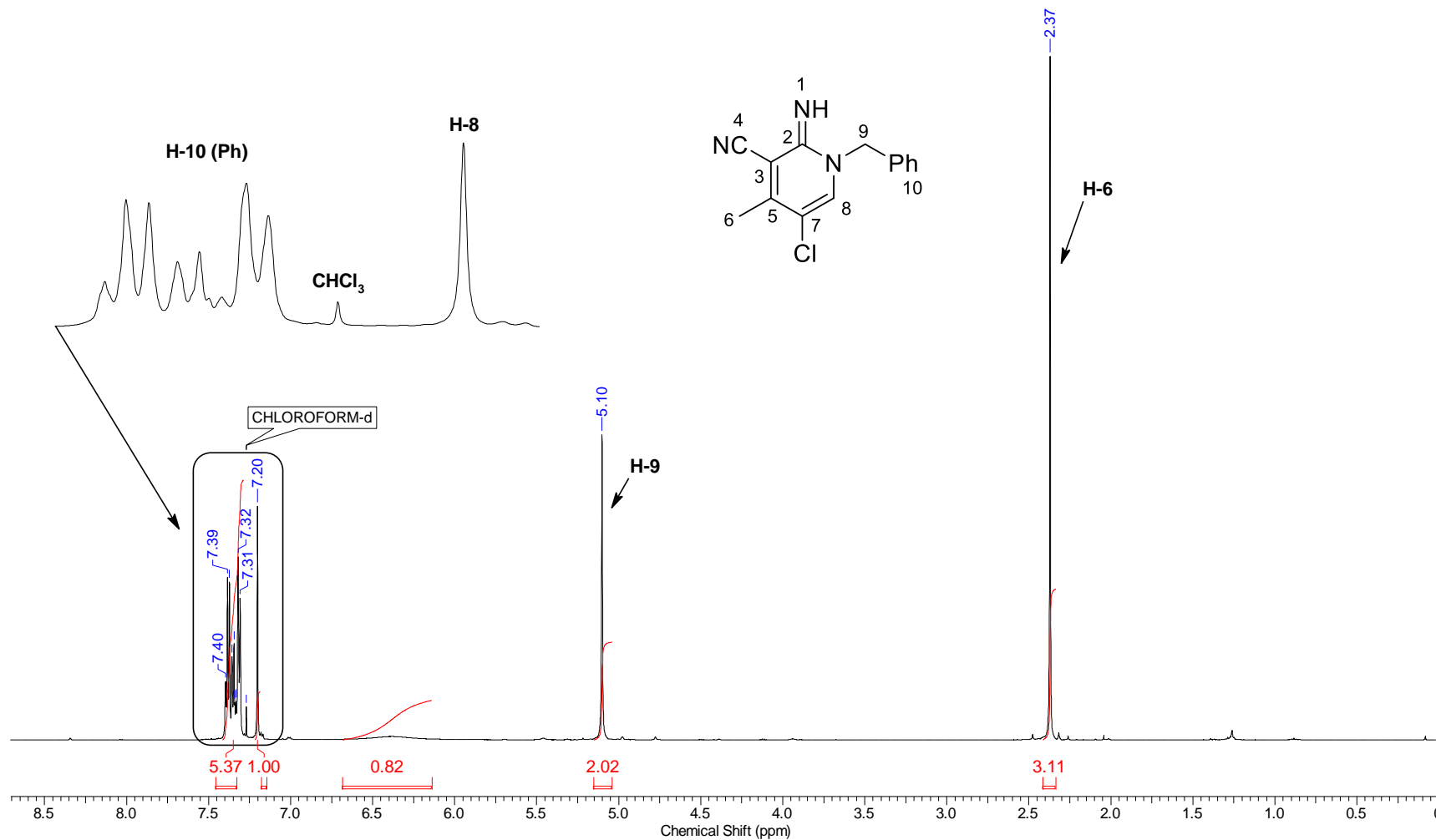
Continuous Conditions Applied to Hazardous Reactions and Fluorophores Synthesis with Photophysics Studies

Nucleus	13C	Number of Transients	1024	Origin	spect	Original Points Count	32768
Owner	nmr	Points Count	32768	Pulse Sequence	zgpg30	Receiver Gain	199.73
SW(cyclical) (Hz)	36231.88	Solvent	CDCI3	Spectrum Offset (Hz)	15084.0479	Spectrum Type	STANDARD
Sweep Width (Hz)	36230.78	Temperature (degree C)	25.333	Acquisition Time (sec)	0.9044	Frequency (MHz)	150.87



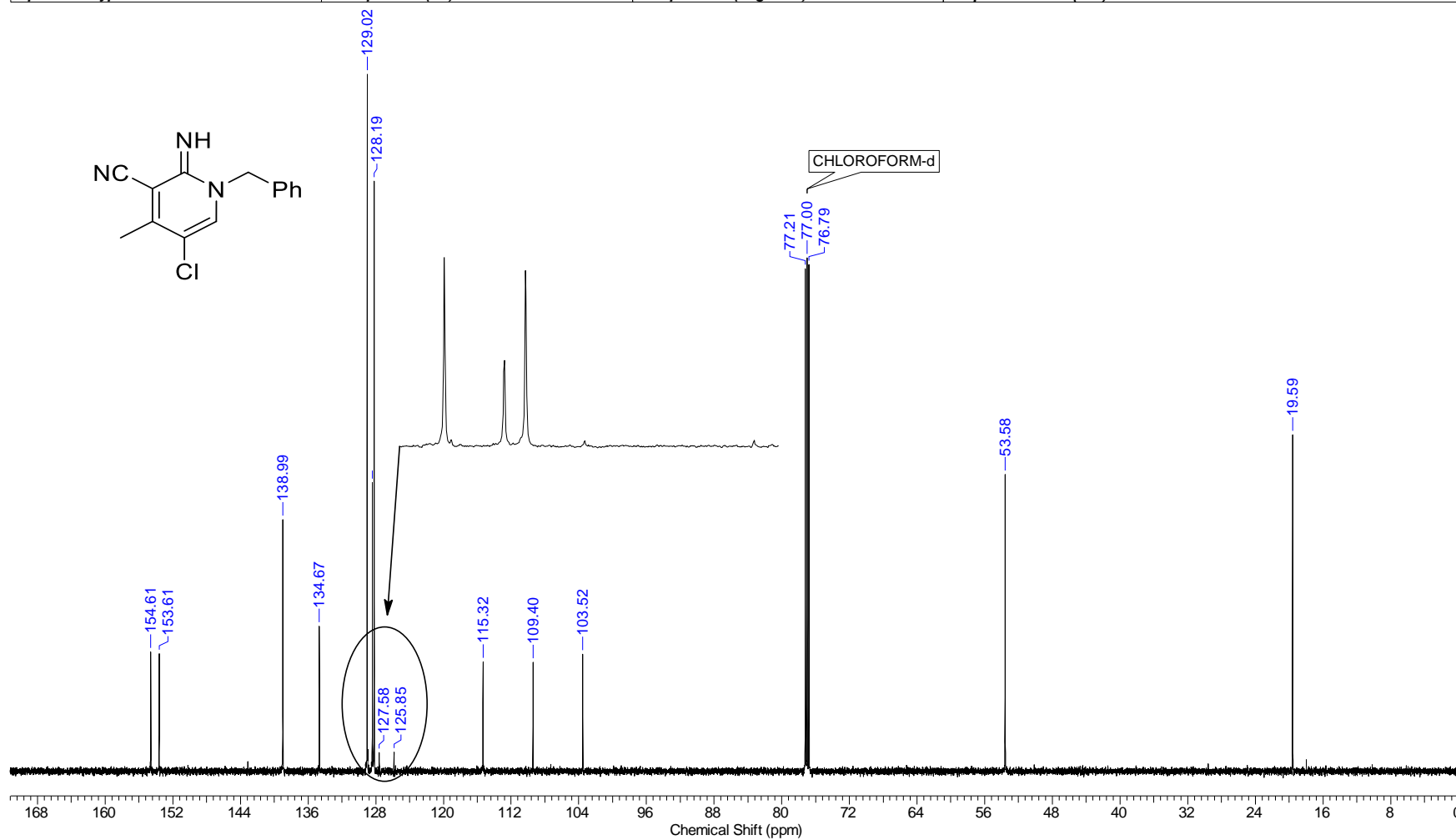
Continuous Conditions Applied to Hazardous Reactions and Fluorophores Synthesis with Photophysics Studies

Frequency (MHz)	600.01	Nucleus	1H	Number of Transients	16	Origin	spect
Original Points Count	32768	Owner	nmr	Points Count	65536	Pulse Sequence	zg30
Receiver Gain	68.55	SW(cyclical) (Hz)	12019.23	Solvent	CDCl3	Spectrum Offset (Hz)	3740.7729
Spectrum Type	STANDARD	Sweep Width (Hz)	12019.05	Temperature (degree C)	23.191	Acquisition Time (sec)	2.7263



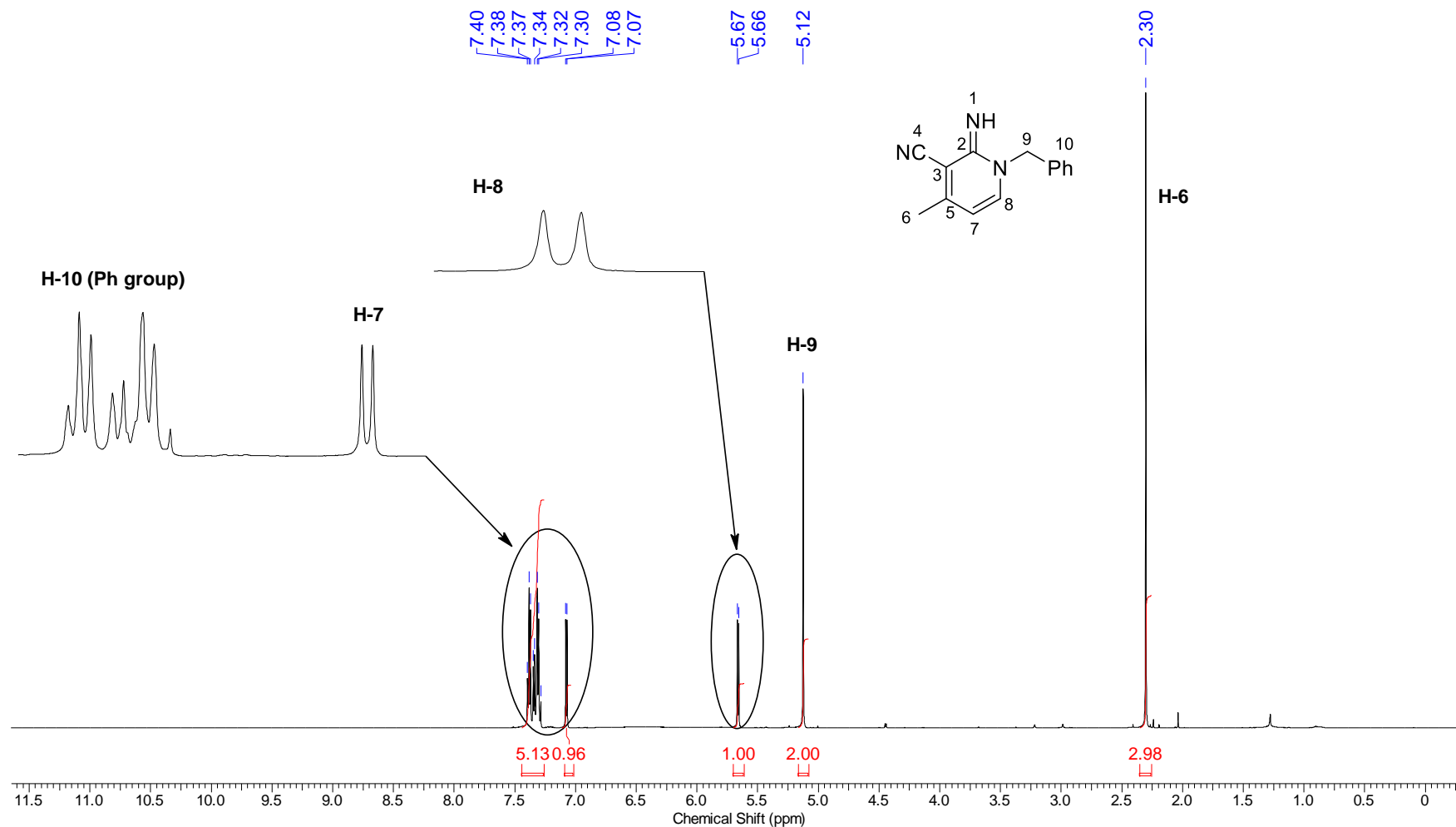
Continuous Conditions Applied to Hazardous Reactions and Fluorophores Synthesis with Photophysics Studies

Frequency (MHz)	150.87	Nucleus	¹³ C	Number of Transients	197	Origin	spect
Original Points Count	32768	Owner	nmr	Points Count	32768	Pulse Sequence	zpgg30
Receiver Gain	199.73	SW(cyclical) (Hz)	36231.88	Solvent	CDCl ₃	Spectrum Offset (Hz)	15079.6250
Spectrum Type	STANDARD	Sweep Width (Hz)	36230.78	Temperature (degree C)	24.951	Acquisition Time (sec)	0.9044

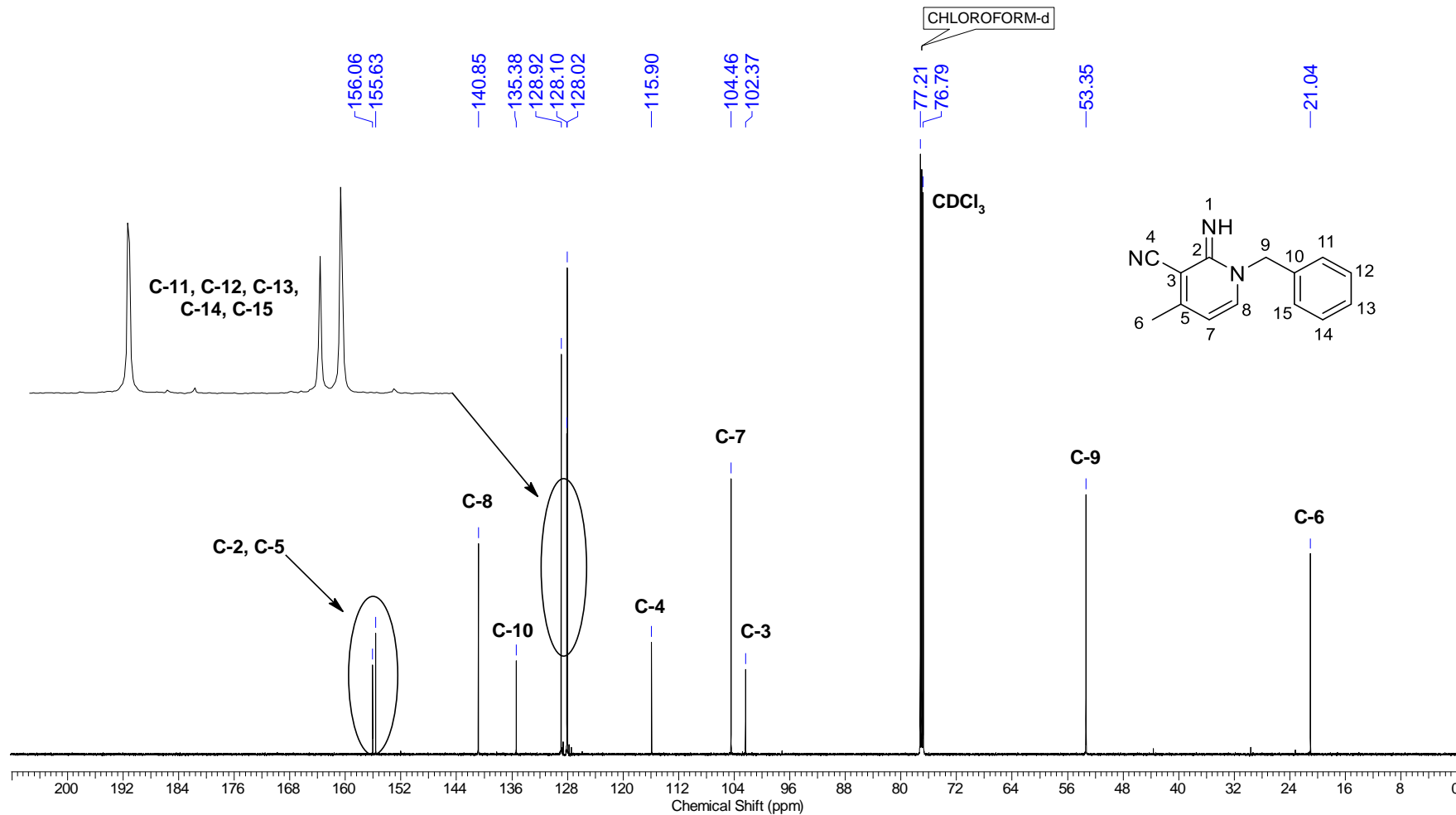


Continuous Conditions Applied to Hazardous Reactions and Fluorophores Synthesis with Photophysics Studies

Nucleus	1H	Number of Transients	16	Origin	spect	Original Points Count	32768
Owner	nmr	Points Count	65536	Pulse Sequence	zg30	Receiver Gain	106.90
SW(cyclical) (Hz)	12019.23	Solvent	CDCl3	Spectrum Offset (Hz)	3705.0303	Spectrum Type	STANDARD
Sweep Width (Hz)	12019.05	Temperature (degree C)	24.998	Acquisition Time (sec)	2.7263	Frequency (MHz)	600.01

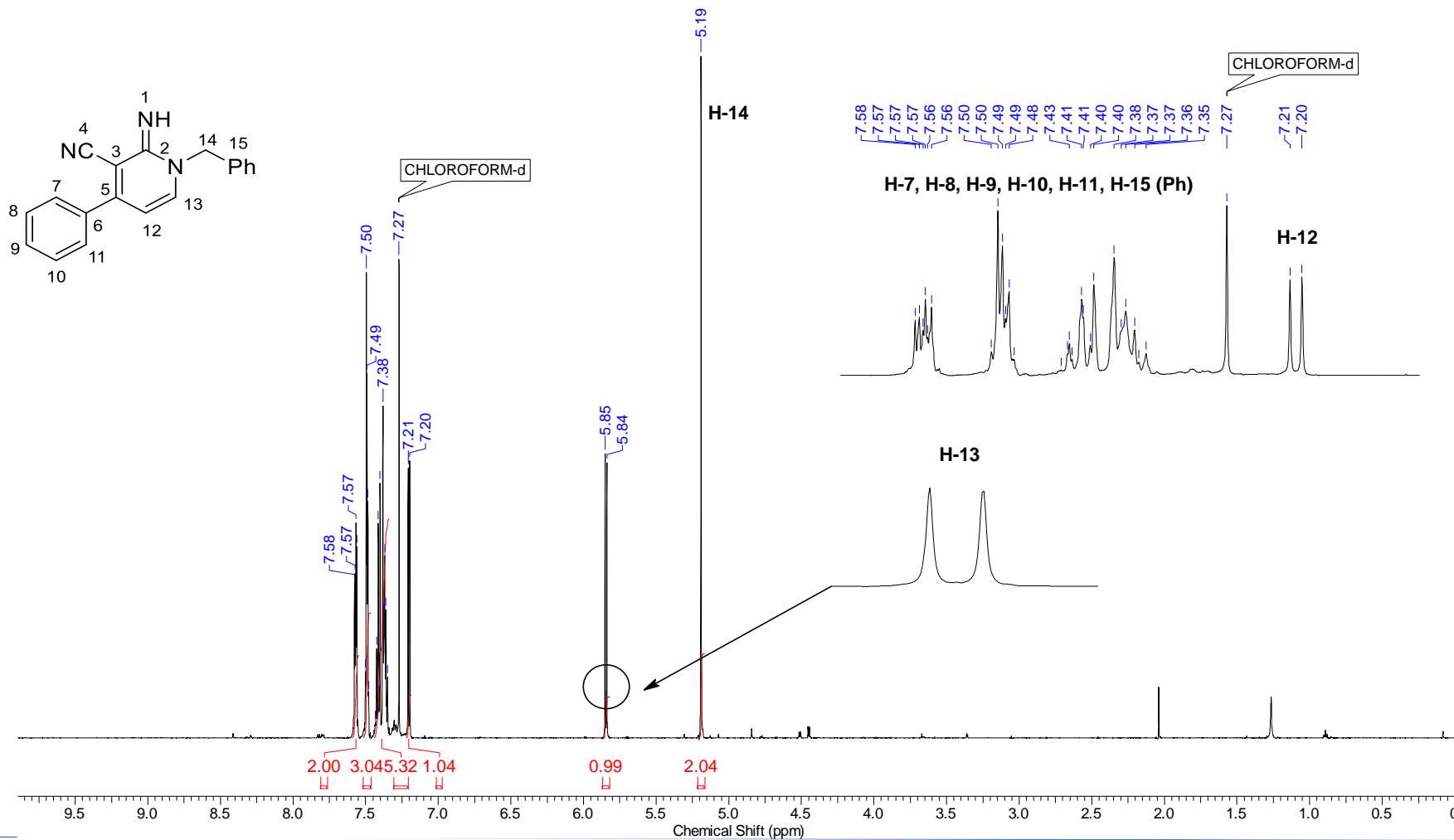


Nucleus	13C	Number of Transients	2500	Origin	spect	Original Points Count	32768
Owner	nmr	Points Count	32768	Pulse Sequence	zgpg30	Receiver Gain	199.73
SW(cyclical) (Hz)	36231.88	Solvent	CDCl3	Spectrum Offset (Hz)	15075.2021	Spectrum Type	STANDARD
Sweep Width (Hz)	36230.78	Temperature (degree C)	25.203	Acquisition Time (sec)	0.9044	Frequency (MHz)	150.87



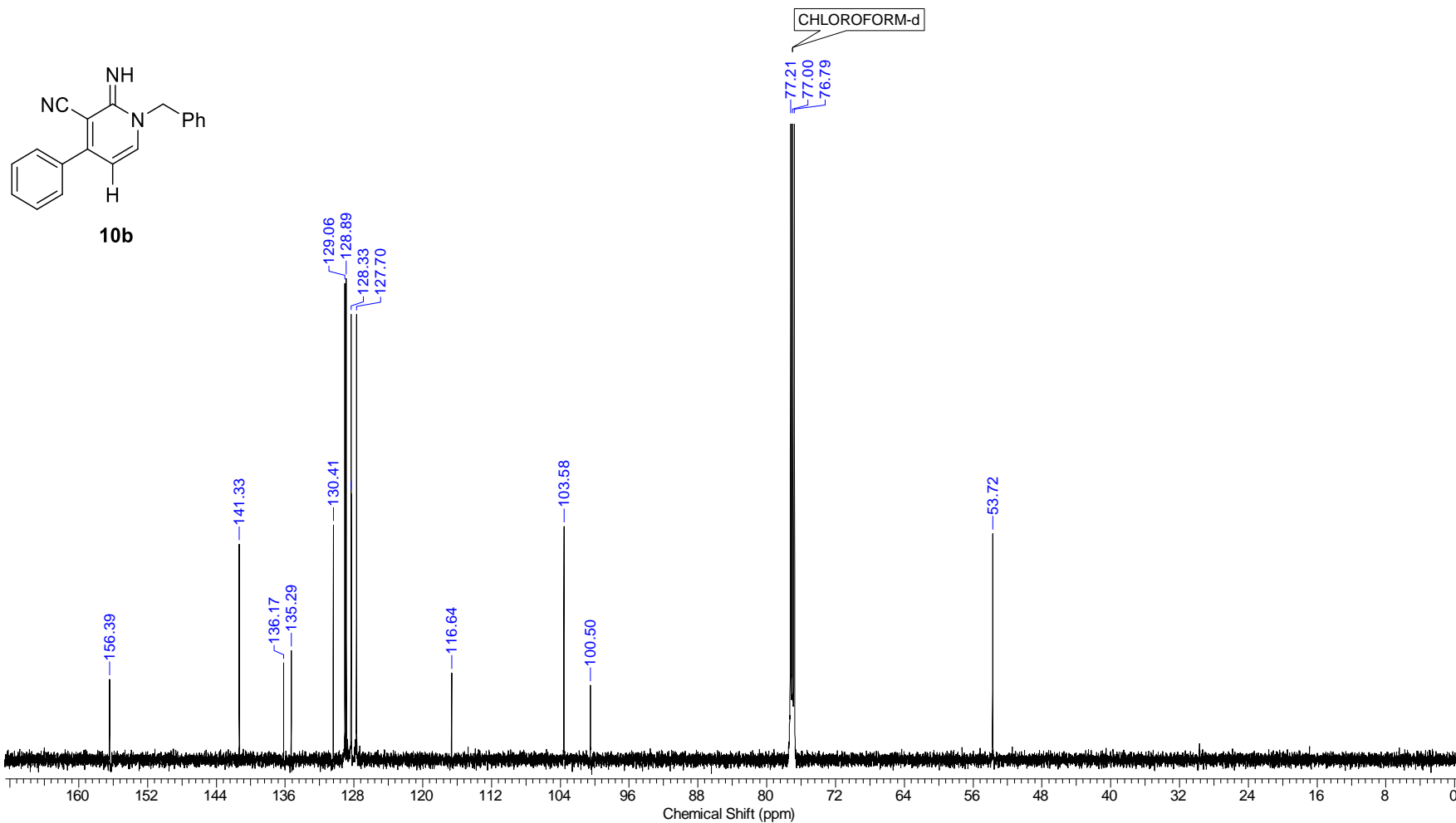
Continuous Conditions Applied to Hazardous Reactions and Fluorophores Synthesis with Photophysics Studies

Frequency (MHz)	600.01	Nucleus	1H	Number of Transients	16	Origin	spect
Original Points Count	32768	Owner	nmr	Points Count	65536	Pulse Sequence	zg30
Receiver Gain	199.73	SW(cyclical) (Hz)	12019.23	Solvent	CDCl3	Spectrum Offset (Hz)	3695.1067
Spectrum Type	STANDARD	Sweep Width (Hz)	12019.05	Temperature (degree C)	24.998	Acquisition Time (sec)	2.7263

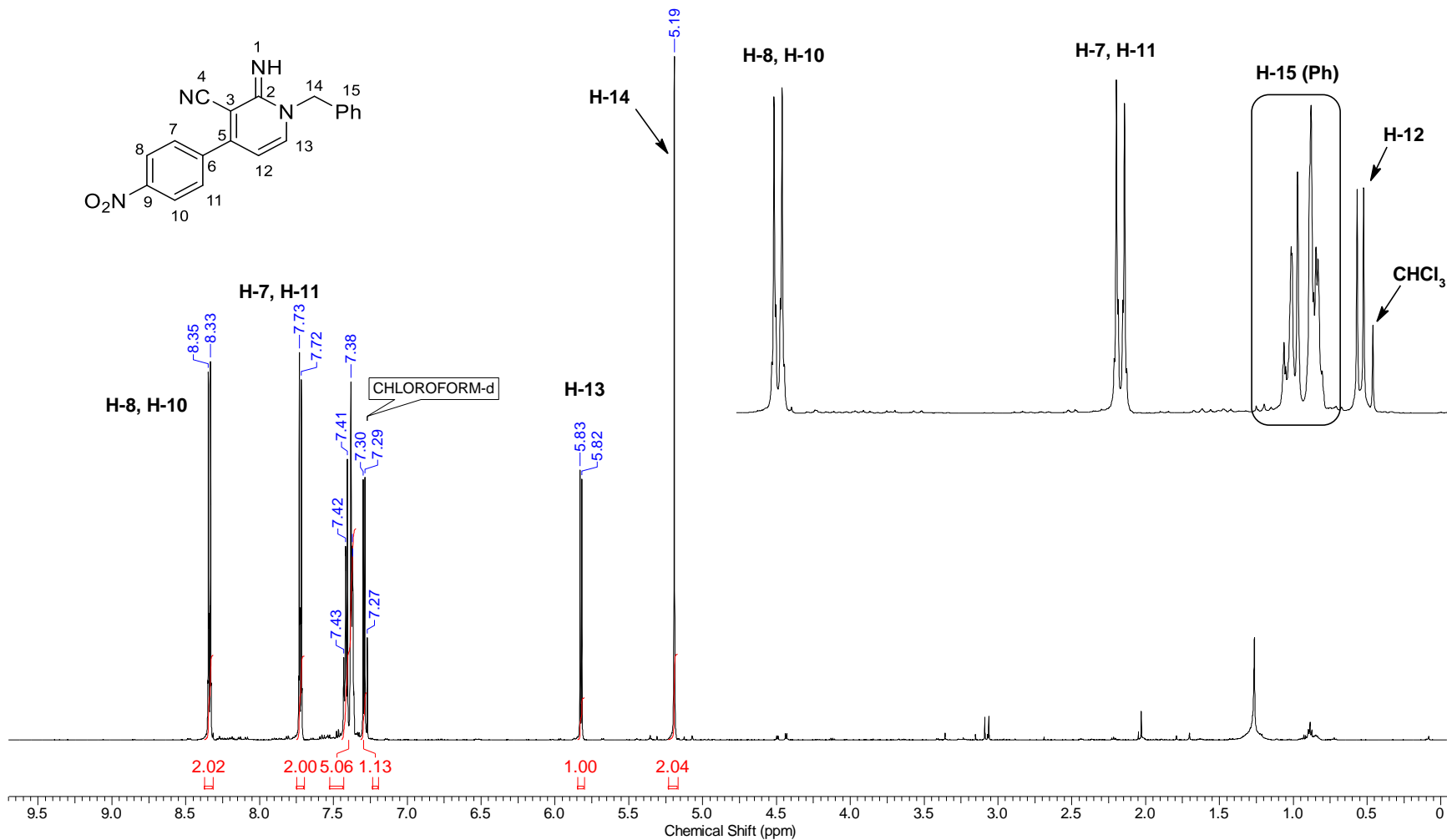


Continuous Conditions Applied to Hazardous Reactions and Fluorophores Synthesis with Photophysics Studies

Frequency (MHz)	150.87	Nucleus	¹³ C	Number of Transients	2500	Origin	spect
Original Points Count	32768	Owner	nmr	Points Count	32768	Pulse Sequence	zgpg30
Receiver Gain	199.73	SW(cyclical) (Hz)	36231.88	Solvent	CDCl ₃	Spectrum Offset (Hz)	15096.2100
Spectrum Type	STANDARD	Sweep Width (Hz)	36230.78	Temperature (degree C)	25.734	Acquisition Time (sec)	0.9044

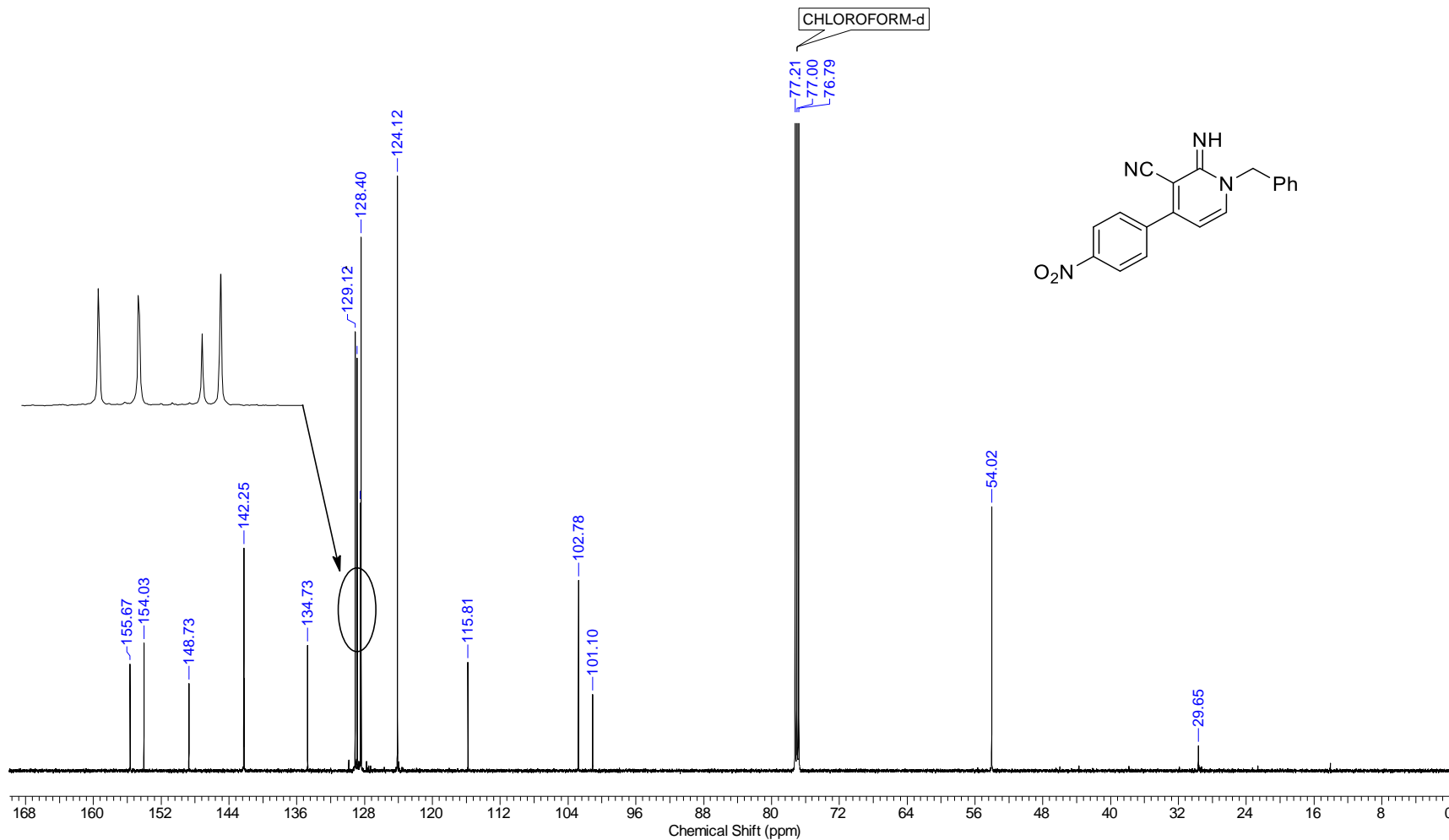


Frequency (MHz)	600.01	Nucleus	1H	Number of Transients	16	Origin	spect
Original Points Count	32768	Owner	nmr	Points Count	65536	Pulse Sequence	zg30
Receiver Gain	135.67	SW(cyclical) (Hz)	12019.23	Solvent	CDCl3	Spectrum Offset (Hz)	3695.2900
Spectrum Type	STANDARD	Sweep Width (Hz)	12019.05	Temperature (degree C)	24.998	Acquisition Time (sec)	2.7263



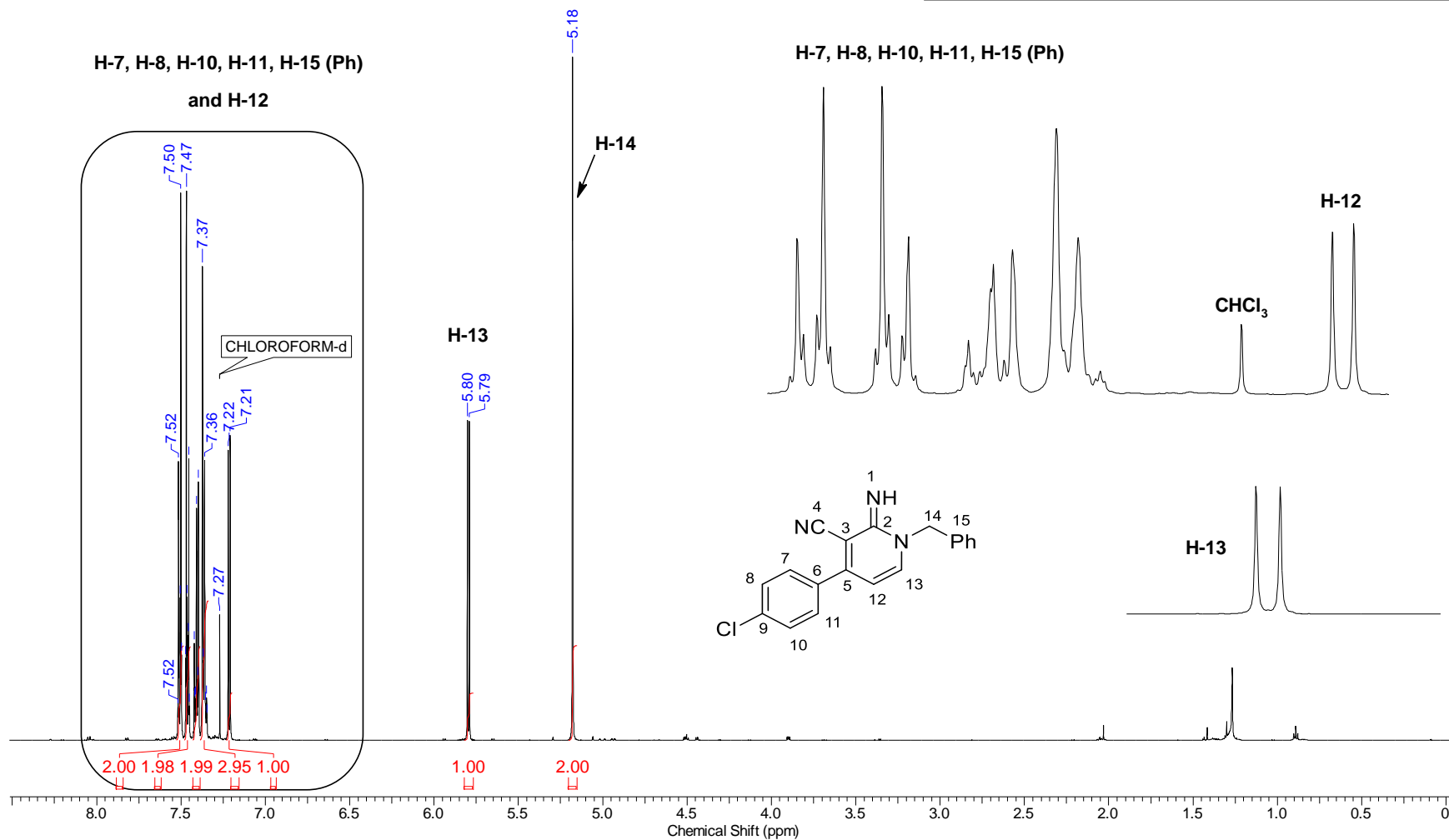
Continuous Conditions Applied to Hazardous Reactions and Fluorophores Synthesis with Photophysics Studies

Frequency (MHz)	150.87	Nucleus	¹³ C	Number of Transients	2500	Origin	spect
Original Points Count	32768	Owner	nmr	Points Count	32768	Pulse Sequence	zgpg30
Receiver Gain	199.73	SW(cyclical) (Hz)	36231.88	Solvent	CDCl ₃	Spectrum Offset (Hz)	15077.4131
Spectrum Type	STANDARD	Sweep Width (Hz)	36230.78	Temperature (degree C)	25.348	Acquisition Time (sec)	0.9044



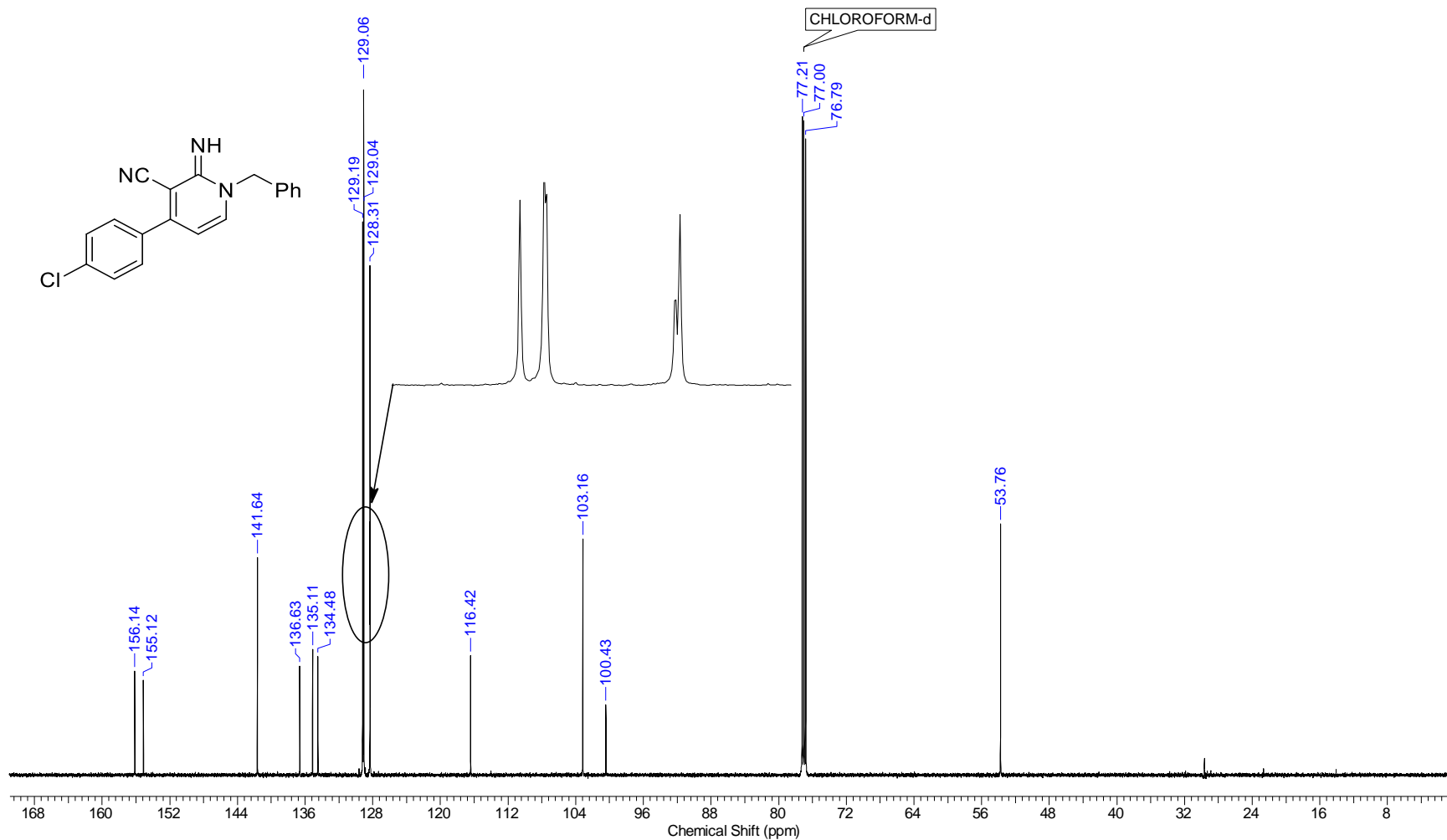
Continuous Conditions Applied to Hazardous Reactions and Fluorophores Synthesis with Photophysics Studies

Frequency (MHz)	600.01	Nucleus	1H	Number of Transients	16	Origin	spect
Original Points Count	32768	Owner	nmr	Points Count	65536	Pulse Sequence	zg30
Receiver Gain	157.38	SW(cyclical) (Hz)	12019.23	Solvent	CDCl3	Spectrum Offset (Hz)	3695.4734
Spectrum Type	STANDARD	Sweep Width (Hz)	12019.05	Temperature (degree C)	24.998	Acquisition Time (sec)	2.7263



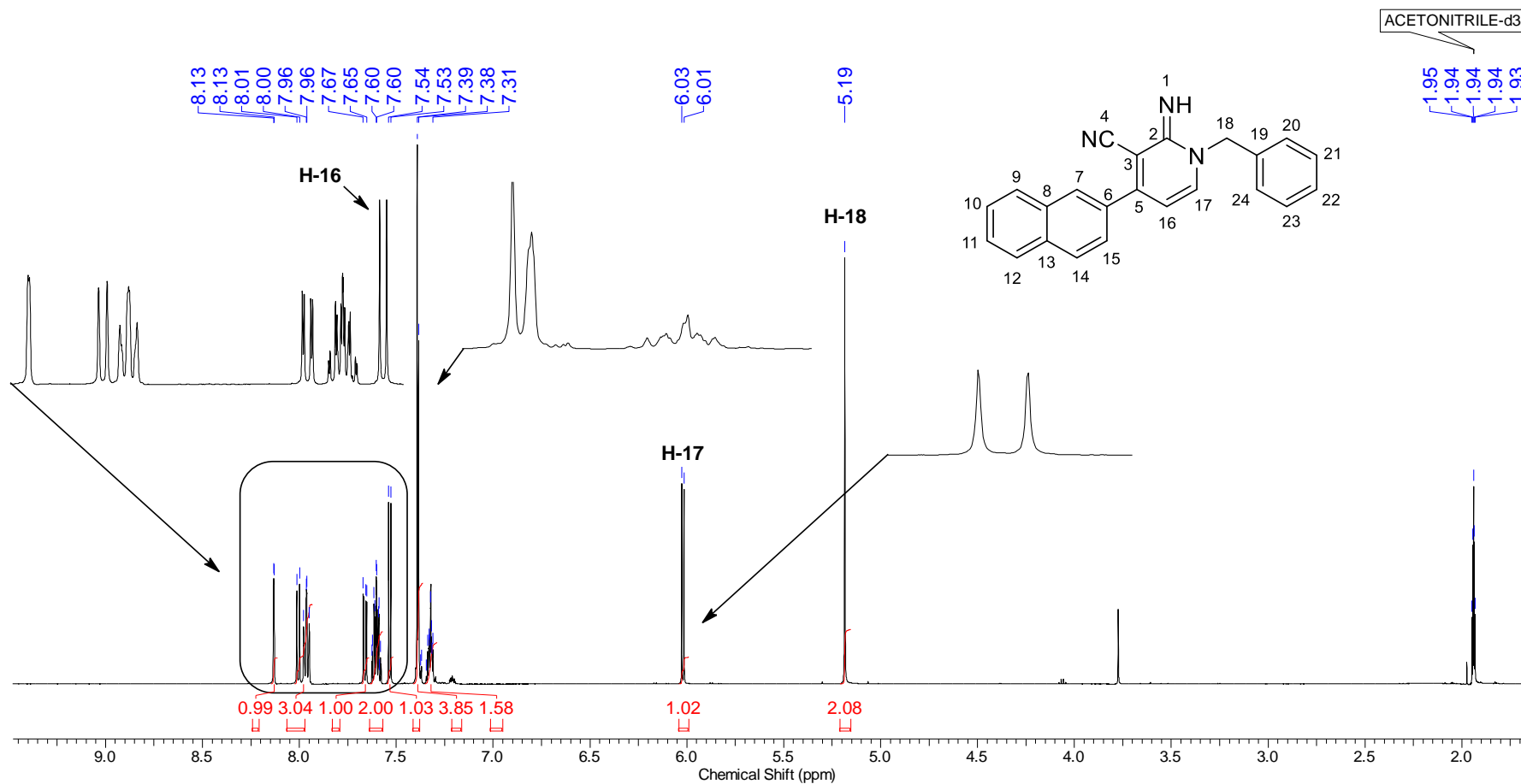
Continuous Conditions Applied to Hazardous Reactions and Fluorophores Synthesis with Photophysics Studies

Frequency (MHz)	150.87	Nucleus	¹³ C	Number of Transients	2500	Origin	spect
Original Points Count	32768	Owner	nmr	Points Count	32768	Pulse Sequence	zgpg30
Receiver Gain	199.73	SW(cyclical) (Hz)	36231.88	Solvent	CDCl ₃	Spectrum Offset (Hz)	15090.6826
Spectrum Type	STANDARD	Sweep Width (Hz)	36230.78	Temperature (degree C)	25.353	Acquisition Time (sec)	0.9044

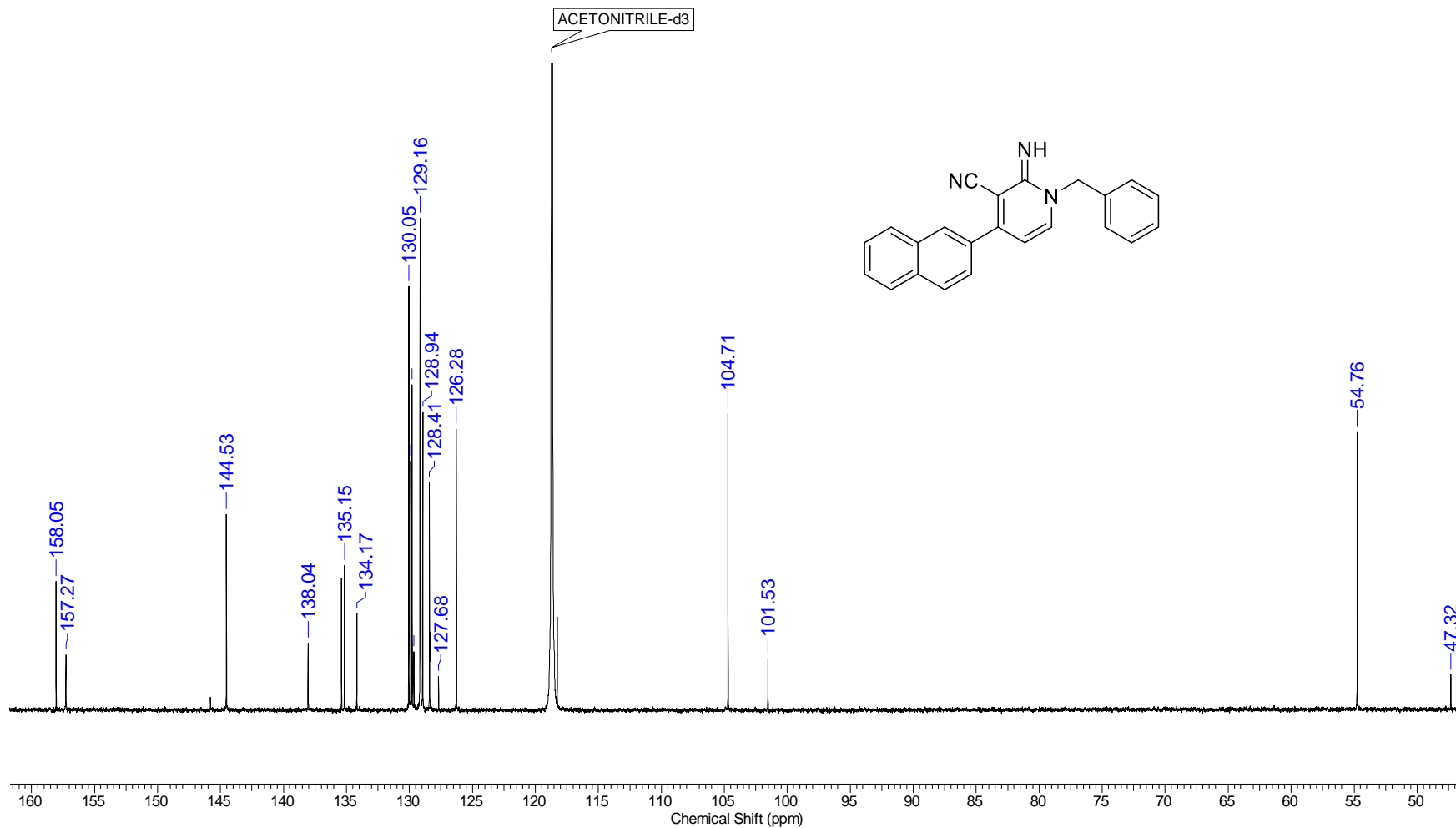


Continuous Conditions Applied to Hazardous Reactions and Fluorophores Synthesis with Photophysics Studies

Nucleus	1H	Number of Transients	16	Origin	spect	Original Points Count	32768
Owner	nmr	Points Count	65536	Pulse Sequence	zg30	Receiver Gain	157.38
SW(cyclical) (Hz)	12019.23	Solvent	ACETONITRILE-d3	Acquisition Time (sec)	2.7263	Spectrum Offset (Hz)	3688.0371
Spectrum Type	STANDARD	Sweep Width (Hz)	12019.05	Temperature (degree C)	24.999	Frequency (MHz)	600.01

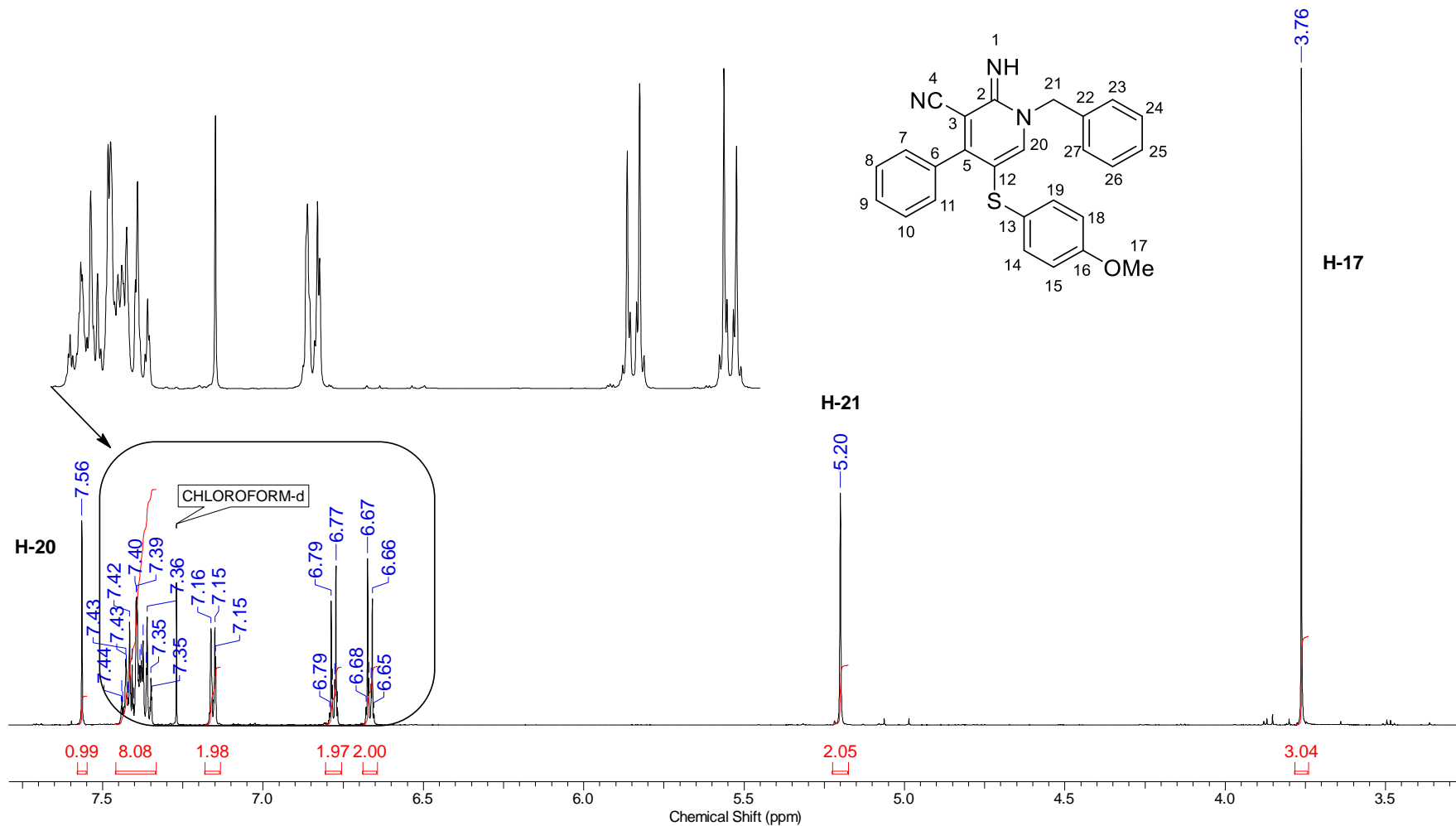


Nucleus	13C	Number of Transients	2500	Origin	spect	Original Points Count	32768
Owner	nmr	Points Count	32768	Pulse Sequence	zgpg30	Receiver Gain	199.73
SW(cyclical) (Hz)	36231.88	Solvent	ACETONITRILE-d3	Spectrum Offset (Hz)	15293.5693	Spectrum Type	STANDARD
Sweep Width (Hz)	36230.78	Temperature (degree C)	25.371	Acquisition Time (sec)	0.9044	Frequency (MHz)	150.87

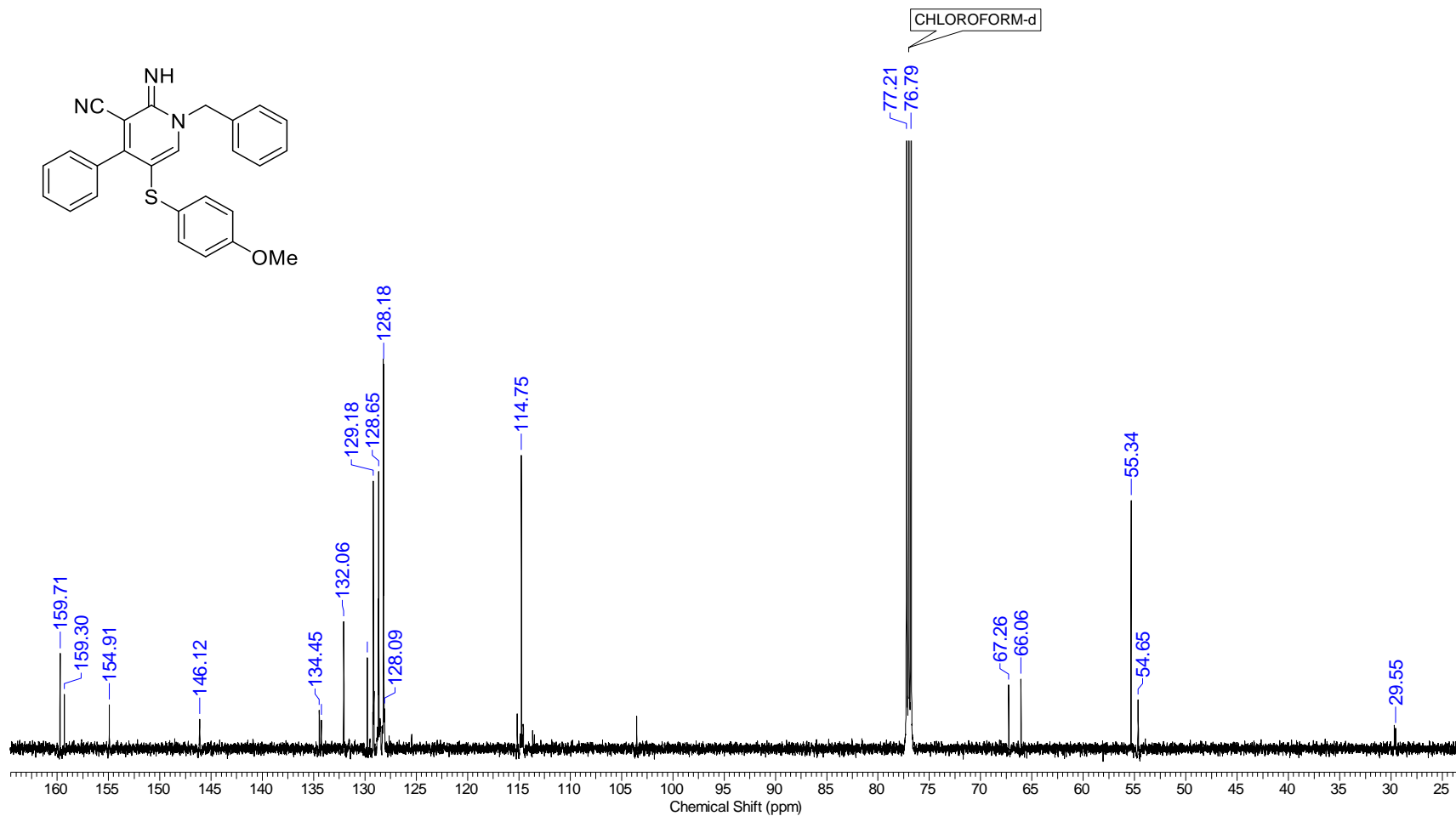


Continuous Conditions Applied to Hazardous Reactions and Fluorophores Synthesis with Photophysics Studies

Nucleus	1H	Number of Transients	16	Origin	spect	Original Points Count	32768
Owner	nmr	Points Count	65536	Pulse Sequence	zg30	Receiver Gain	199.73
SW(cyclical) (Hz)	12019.23	Solvent	CDCl3	Spectrum Offset (Hz)	3743.5234	Spectrum Type	STANDARD
Sweep Width (Hz)	12019.05	Temperature (degree C)	24.997	Acquisition Time (sec)	2.7263	Frequency (MHz)	600.01

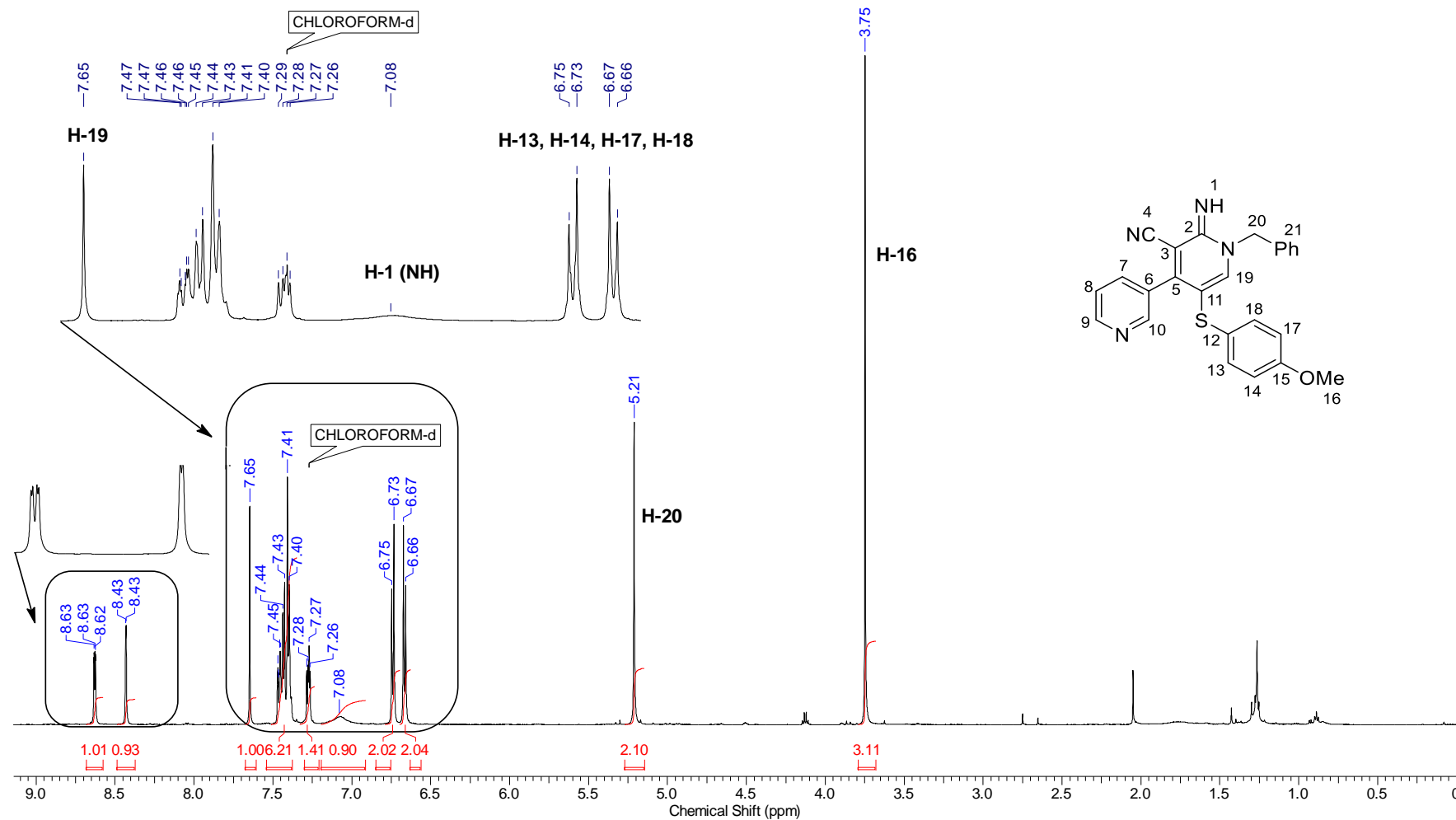


Nucleus	13C	Number of Transients	2500	Origin	spect	Original Points Count	32768
Owner	nmr	Points Count	32768	Pulse Sequence	zgpg30	Receiver Gain	199.73
SW(cyclical) (Hz)	36231.88	Solvent	CDCl3	Spectrum Offset (Hz)	15094.0000	Spectrum Type	STANDARD
Sweep Width (Hz)	36230.78	Temperature (degree C)	25.480	Acquisition Time (sec)	0.9044	Frequency (MHz)	150.87



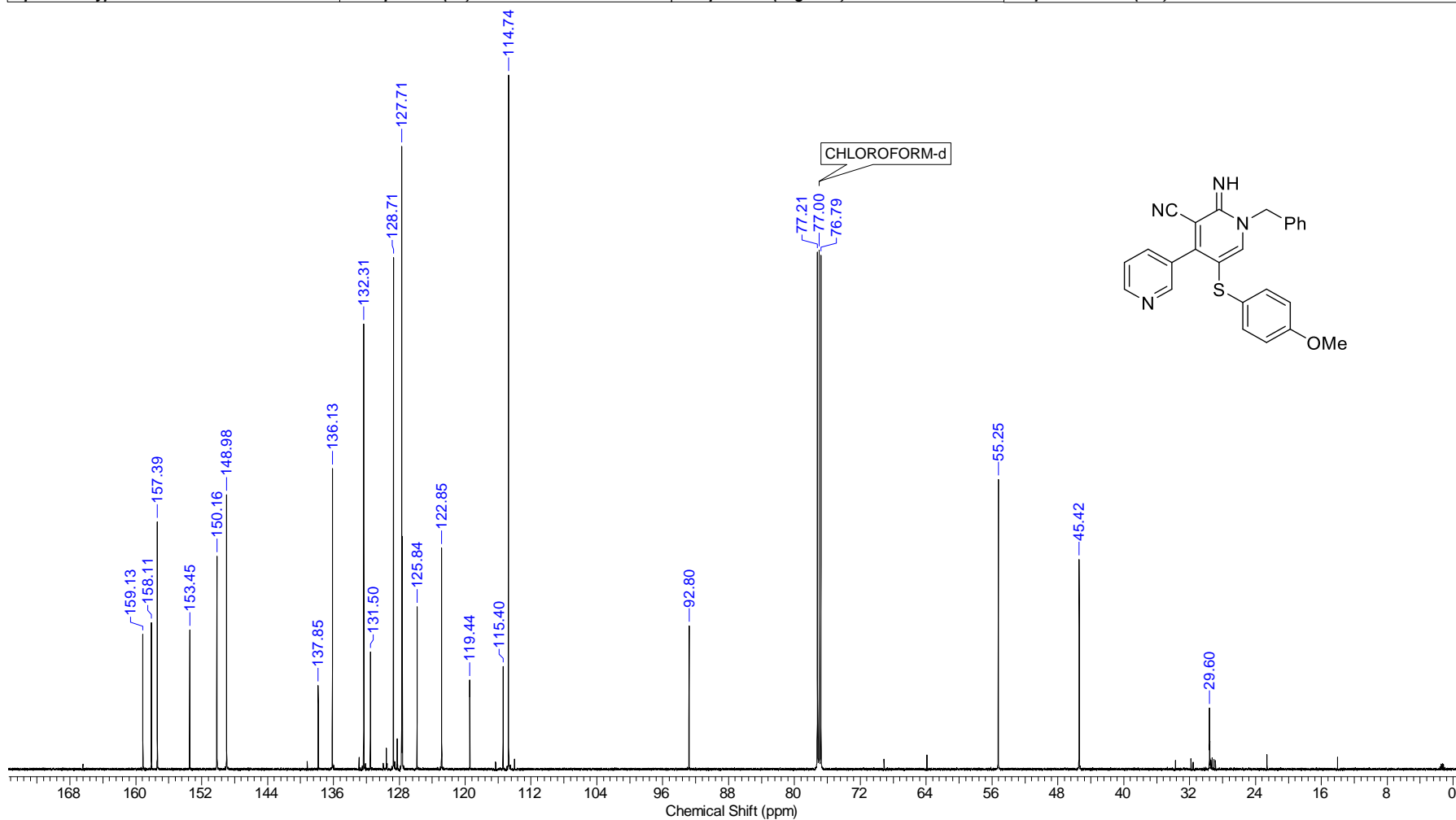
Continuous Conditions Applied to Hazardous Reactions and Fluorophores Synthesis with Photophysics Studies

Frequency (MHz)	600.01	Nucleus	1H	Number of Transients	16	Origin	spect
Original Points Count	32768	Owner	nmr	Points Count	65536	Pulse Sequence	zg30
Receiver Gain	157.38	SW(cyclical) (Hz)	12019.23	Solvent	CDCl3	Spectrum Offset (Hz)	3743.3403
Spectrum Type	STANDARD	Sweep Width (Hz)	12019.05	Temperature (degree C)	24.999	Acquisition Time (sec)	2.7263



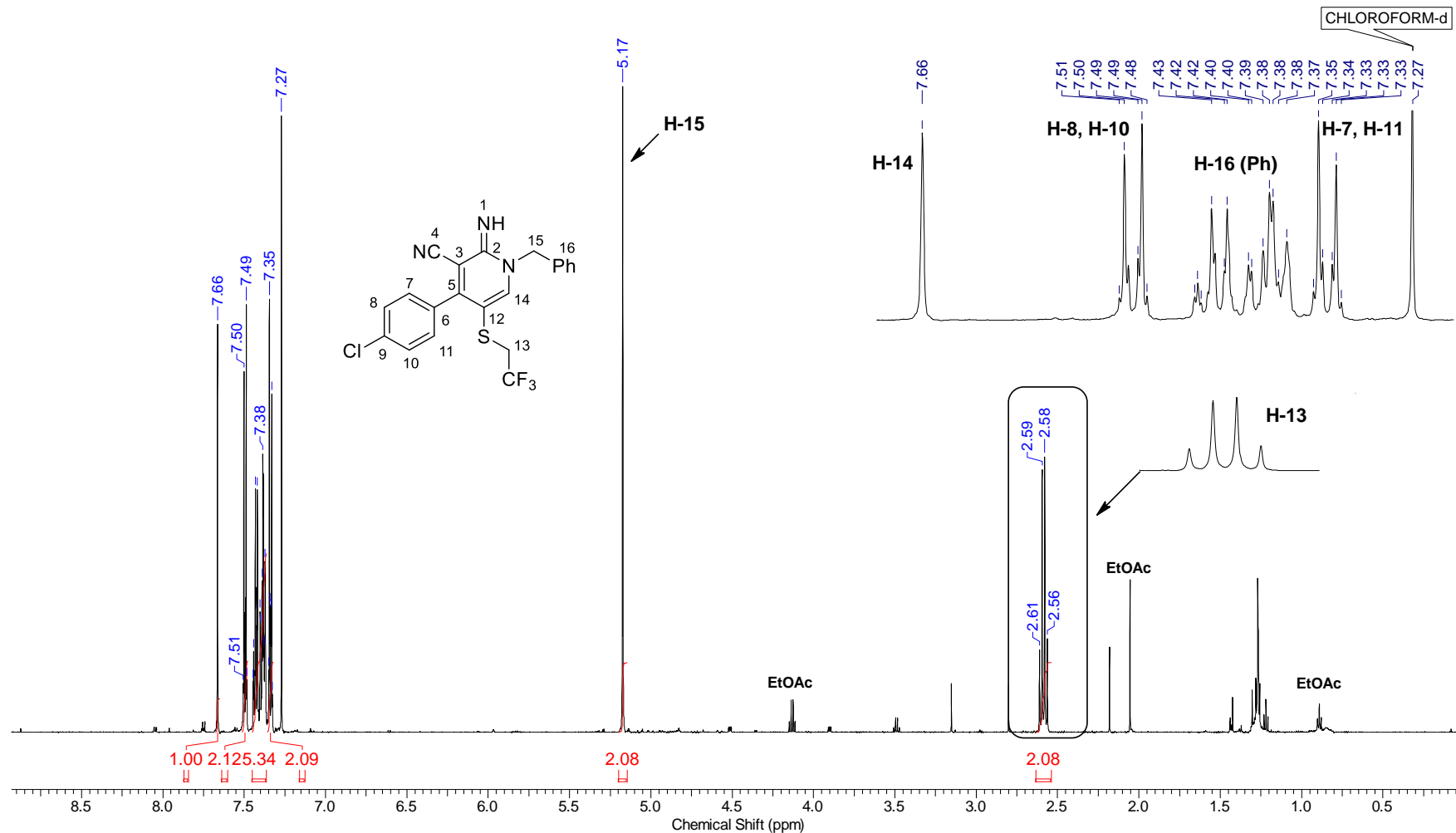
Continuous Conditions Applied to Hazardous Reactions and Fluorophores Synthesis with Photophysics Studies

Frequency (MHz)	150.87	Nucleus	¹³ C	Number of Transients	2500	Origin	spect
Original Points Count	32768	Owner	nmr	Points Count	32768	Pulse Sequence	zpgg30
Receiver Gain	199.73	SW(cyclical) (Hz)	36231.88	Solvent	CDCl ₃	Spectrum Offset (Hz)	15069.6738
Spectrum Type	STANDARD	Sweep Width (Hz)	36230.78	Temperature (degree C)	25.437	Acquisition Time (sec)	0.9044



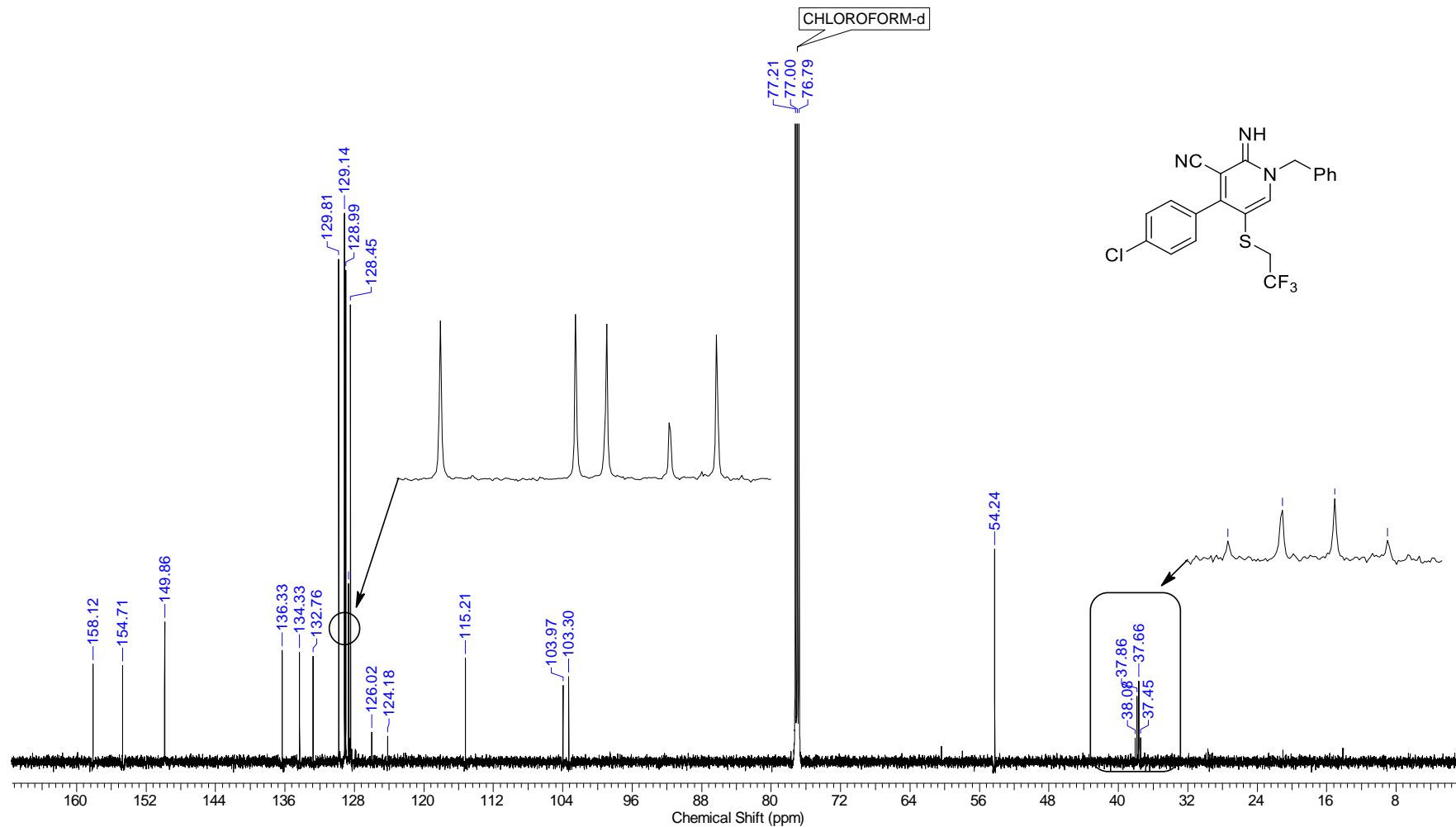
Continuous Conditions Applied to Hazardous Reactions and Fluorophores Synthesis with Photophysics Studies

Frequency (MHz)	600.01	Nucleus	¹ H	Number of Transients	16	Origin	spect
Original Points Count	32768	Owner	nmr	Points Count	65536	Pulse Sequence	zg30
Receiver Gain	199.73	SW(cyclical) (Hz)	12019.23	Solvent	CDCl ₃	Spectrum Offset (Hz)	3743.7070
Spectrum Type	STANDARD	Sweep Width (Hz)	12019.05	Temperature (degree C)	24.997	Acquisition Time (sec)	2.7263



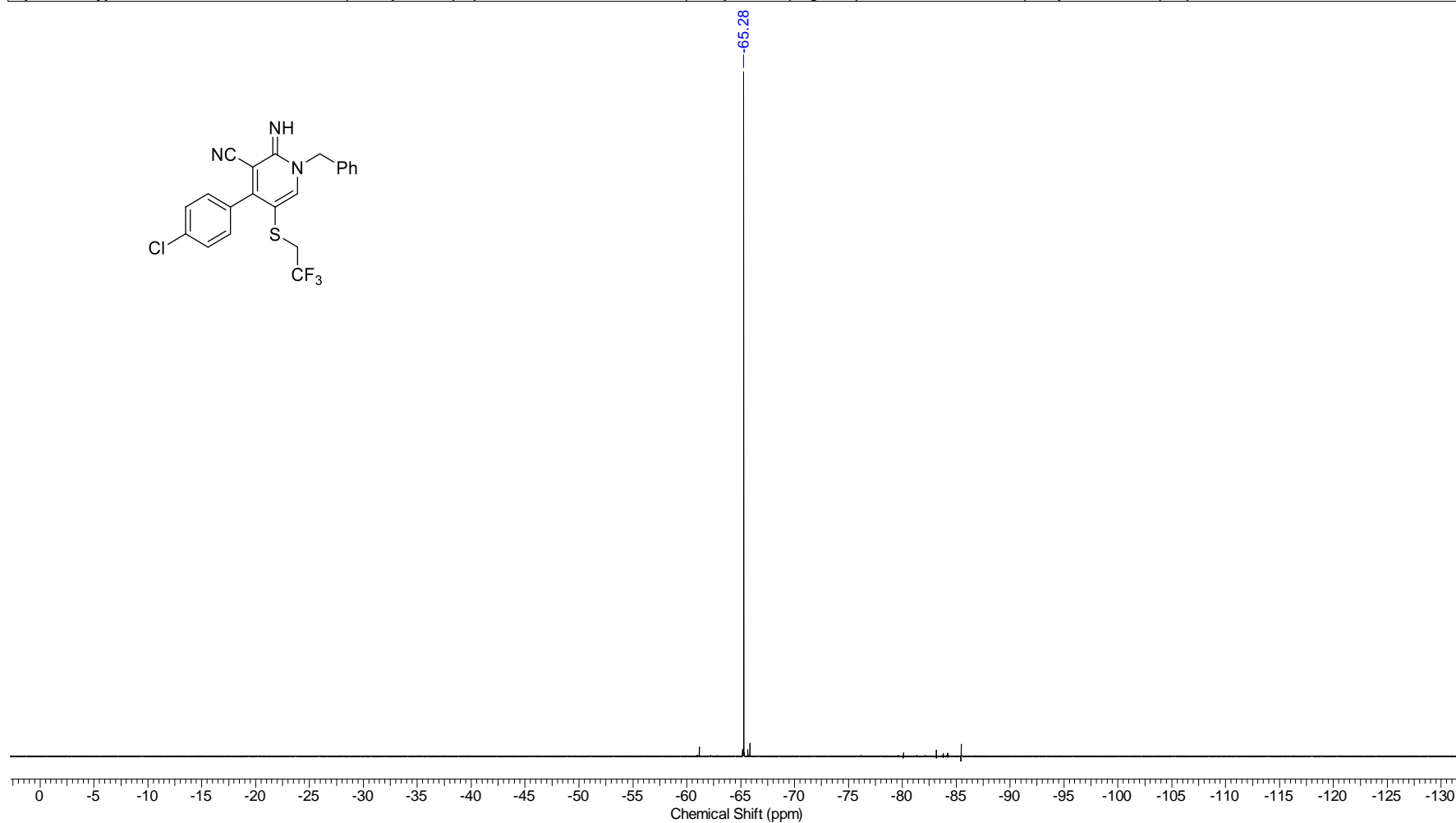
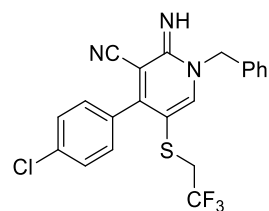
Continuous Conditions Applied to Hazardous Reactions and Fluorophores Synthesis with Photophysics Studies

Frequency (MHz)	150.87	Nucleus	¹³ C	Number of Transients	2500	Origin	spect
Original Points Count	32768	Owner	nmr	Points Count	32768	Pulse Sequence	zpgpg30
Receiver Gain	199.73	SW(cyclical) (Hz)	36231.88	Solvent	CDCl ₃	Spectrum Offset (Hz)	15095.1055
Spectrum Type	STANDARD	Sweep Width (Hz)	36230.78	Temperature (degree C)	25.541	Acquisition Time (sec)	0.9044

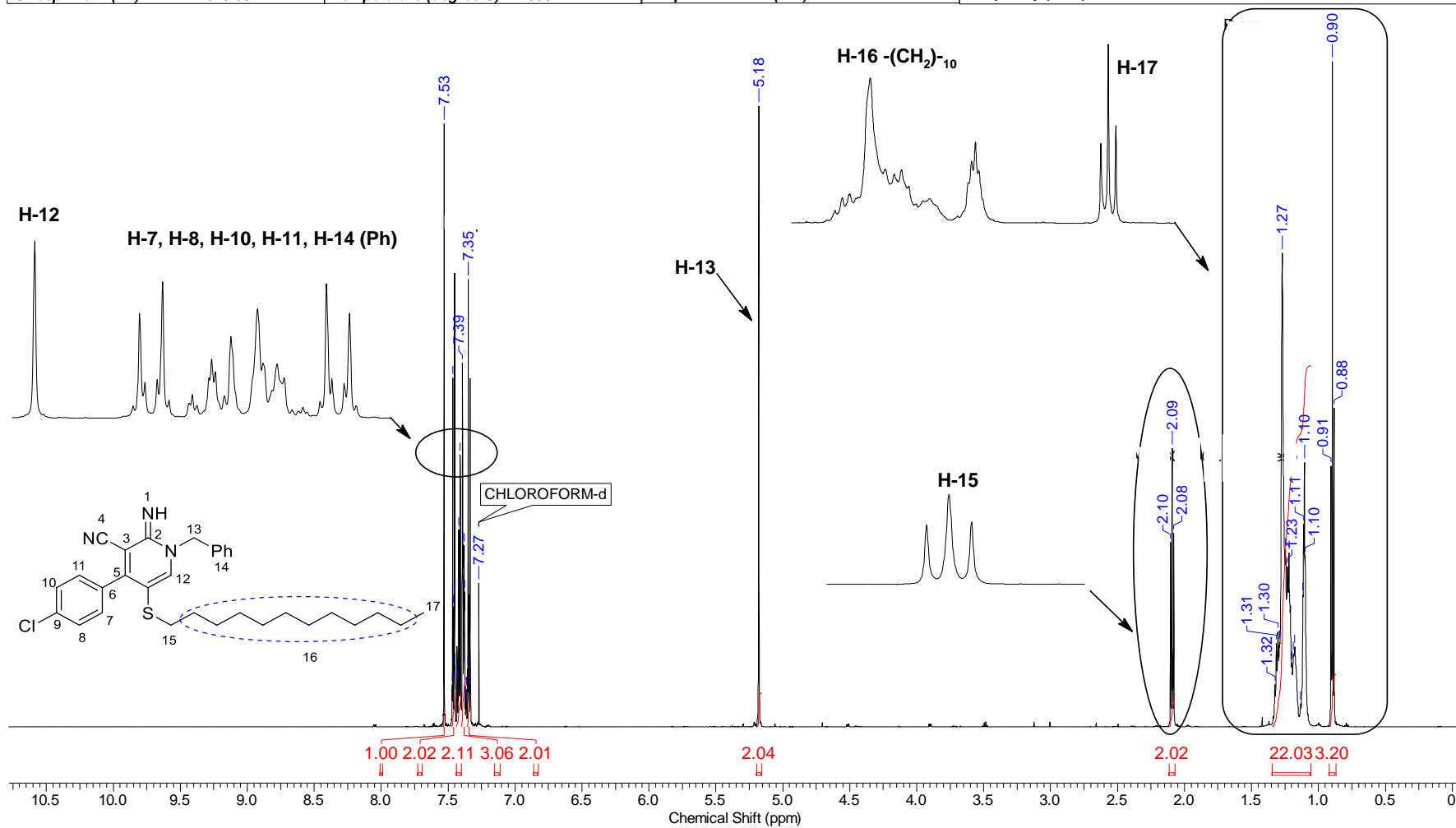


Continuous Conditions Applied to Hazardous Reactions and Fluorophores Synthesis with Photophysics Studies

Frequency (MHz)	564.57	Nucleus	¹⁹ F	Number of Transients	16	Origin	spect
Original Points Count	65536	Owner	nmr	Points Count	65536	Pulse Sequence	zgfhighn.2
Receiver Gain	199.73	SW(cyclical) (Hz)	133928.58	Solvent	CDCl ₃	Spectrum Offset (Hz)	-56456.8867
Spectrum Type	STANDARD	Sweep Width (Hz)	133926.53	Temperature (degree C)	25.191	Acquisition Time (sec)	0.4893

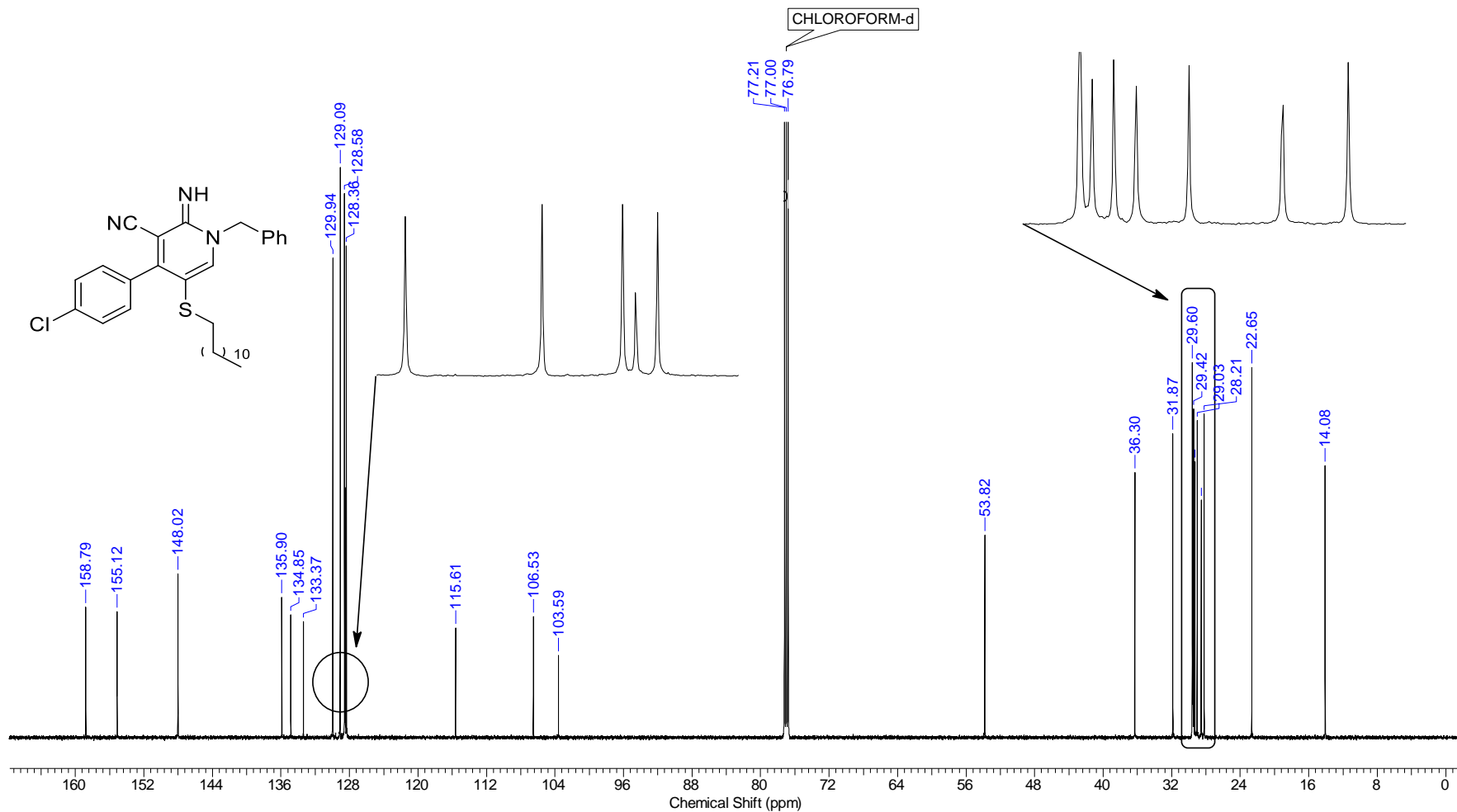


Nucleus	1H	Number of Transients	16	Origin	spect	Original Points Count	32768
Owner	nmr	Points Count	65536	Pulse Sequence	zg30	Receiver Gain	78.64
SW(cyclical) (Hz)	12019.23	Solvent	CDCl3	Spectrum Offset (Hz)	3743.5237	Spectrum Type	STANDARD
Sweep Width (Hz)	12019.05	Temperature (degree C)	24.998	Acquisition Time (sec)	2.7263	Frequency (MHz)	600.01

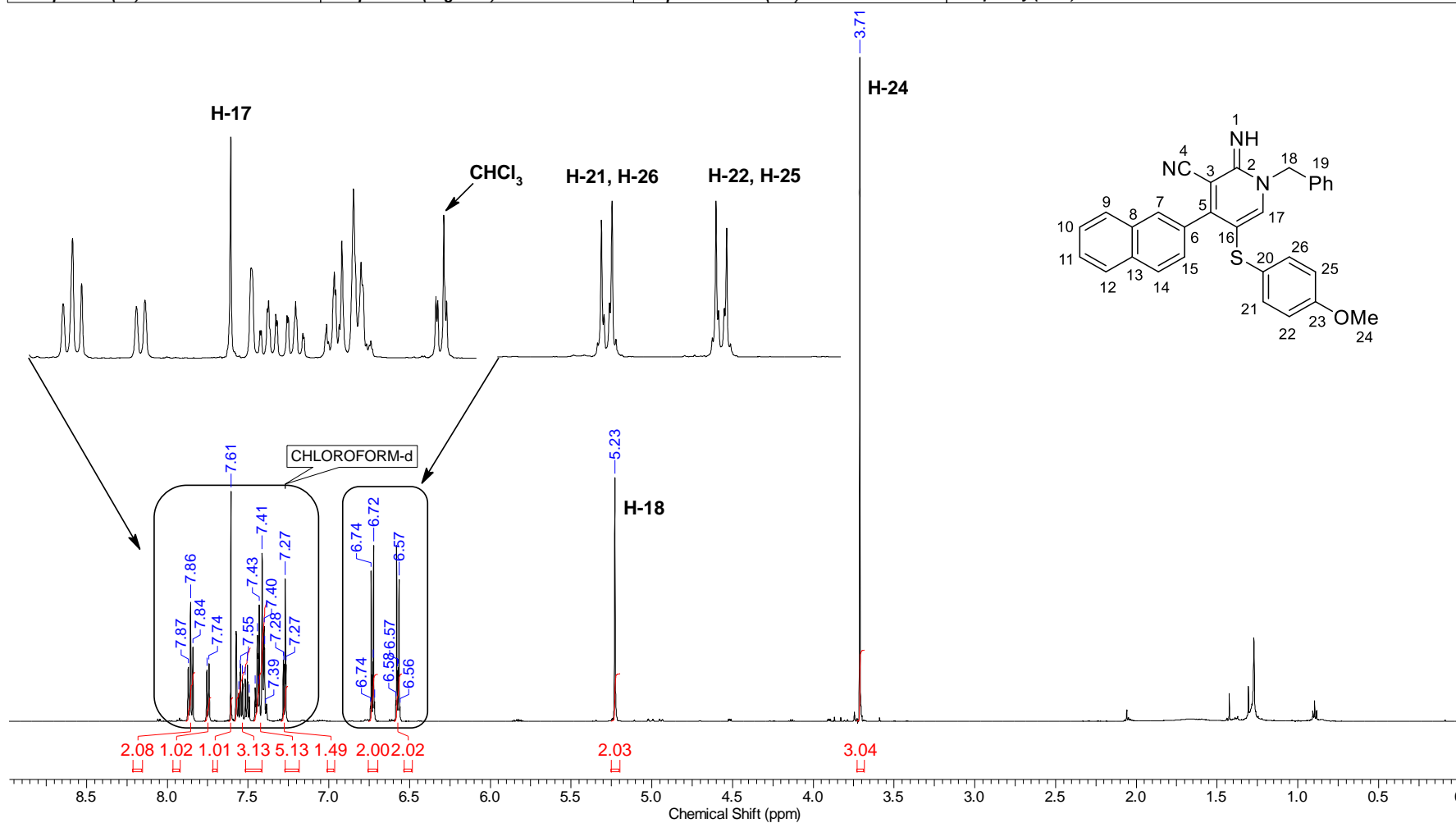


Continuous Conditions Applied to Hazardous Reactions and Fluorophores Synthesis with Photophysics Studies

Nucleus	13C	Number of Transients	2500	Origin	spect	Original Points Count	32768
Owner	nmr	Points Count	32768	Pulse Sequence	zgpg30	Receiver Gain	199.73
SW(cyclical) (Hz)	36231.88	Solvent	CDCl3	Spectrum Offset (Hz)	15090.6826	Spectrum Type	STANDARD
Sweep Width (Hz)	36230.78	Temperature (degree C)	25.249	Acquisition Time (sec)	0.9044	Frequency (MHz)	150.87

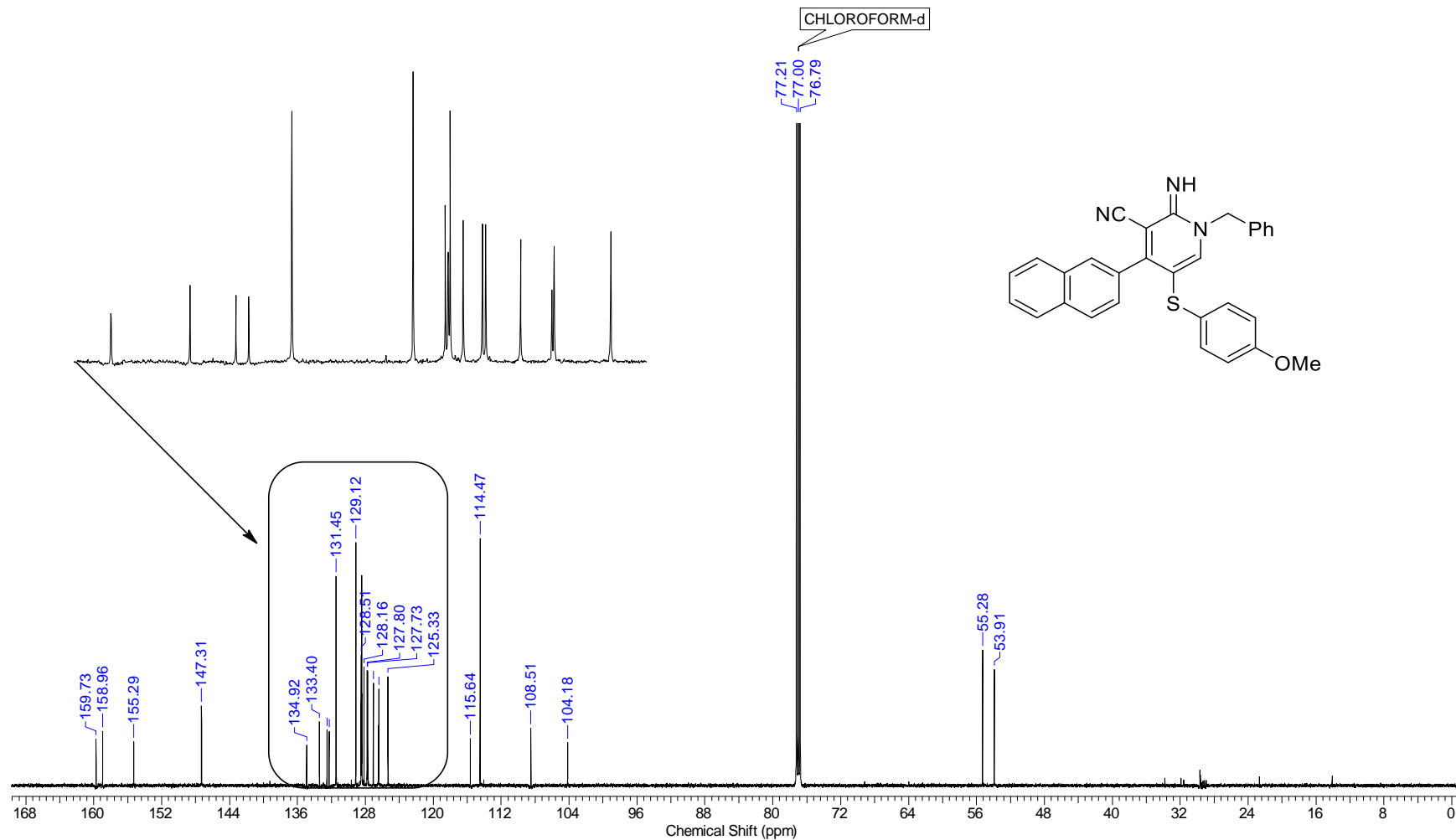


Nucleus	1H	Number of Transients	16	Origin	spect	Original Points Count	32768
Owner	nmrsu	Points Count	65536	Pulse Sequence	zg30	Receiver Gain	125.31
SW(cyclical) (Hz)	12019.23	Solvent	CDCl3	Spectrum Offset (Hz)	3695.2937	Spectrum Type	STANDARD
Sweep Width (Hz)	12019.05	Temperature (degree C)	23.219	Acquisition Time (sec)	2.7263	Frequency (MHz)	599.96



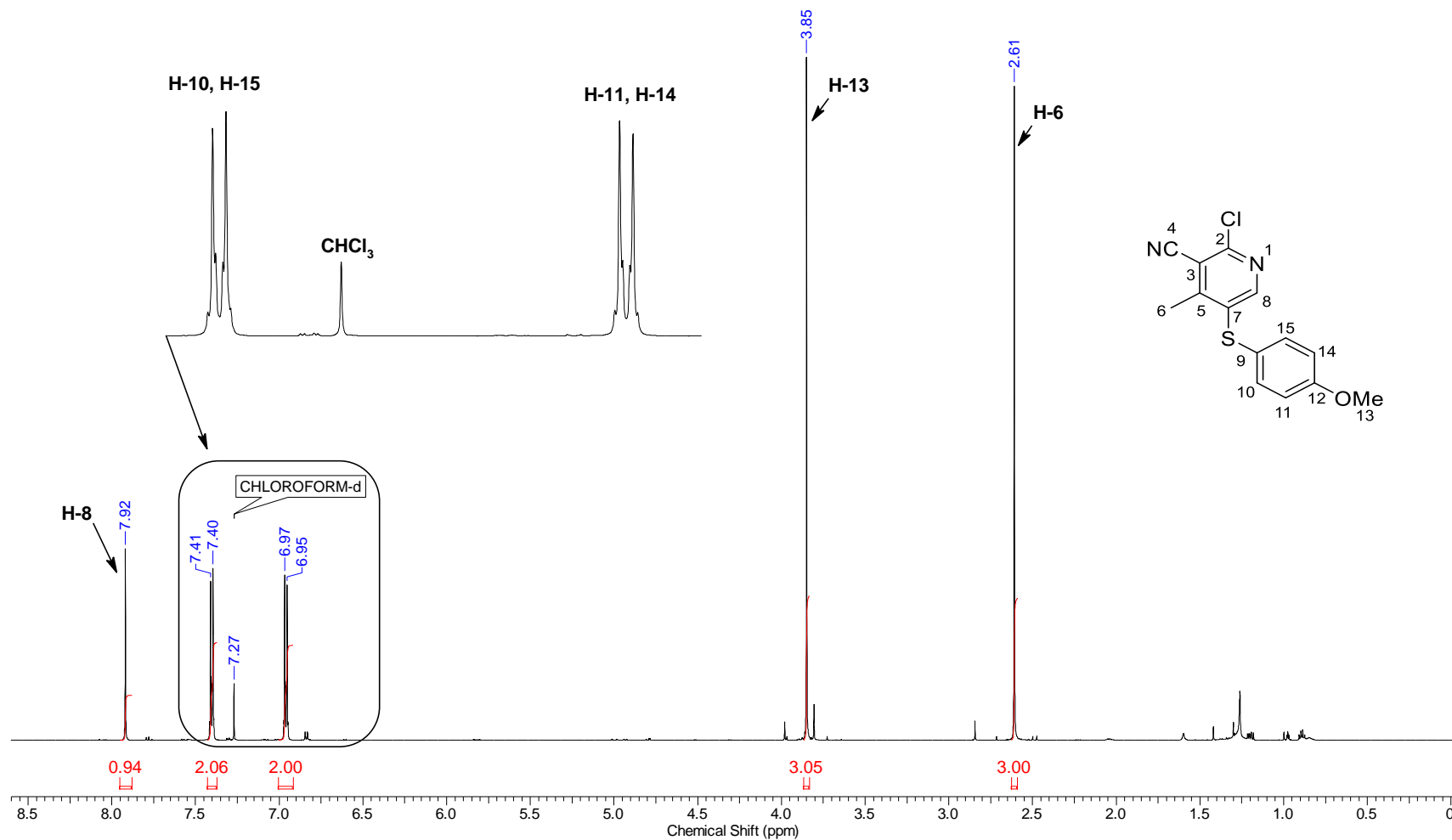
Continuous Conditions Applied to Hazardous Reactions and Fluorophores Synthesis with Photophysics Studies

Frequency (MHz)	150.87	Nucleus	¹³ C	Number of Transients	2500	Origin	spect
Original Points Count	32768	Owner	nmr	Points Count	32768	Pulse Sequence	zgpg30
Receiver Gain	199.73	SW(cyclical) (Hz)	36231.88	Solvent	CDCl ₃	Spectrum Offset (Hz)	15080.7305
Spectrum Type	STANDARD	Sweep Width (Hz)	36230.78	Temperature (degree C)	25.565	Acquisition Time (sec)	0.9044

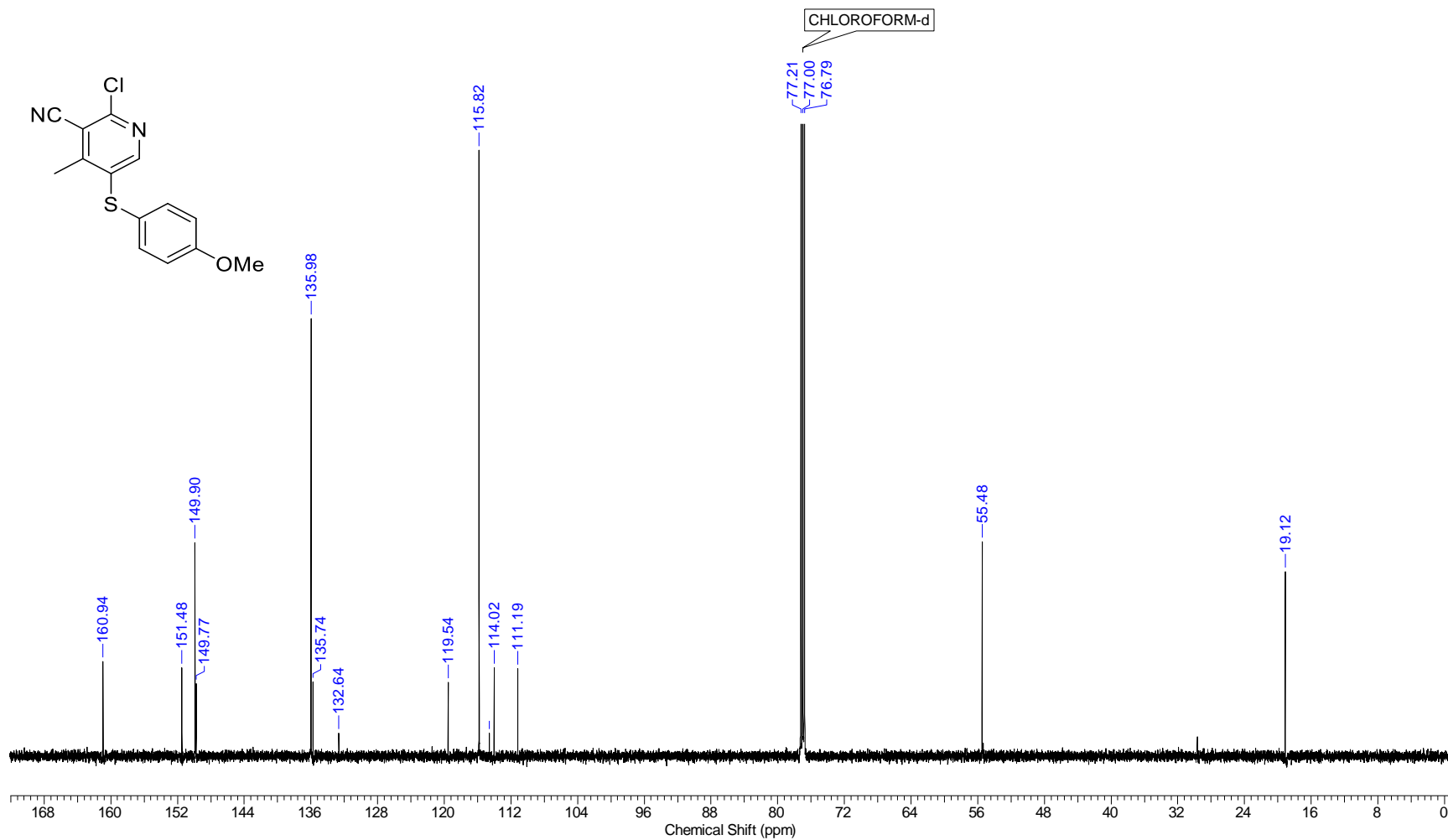


Continuous Conditions Applied to Hazardous Reactions and Fluorophores Synthesis with Photophysics Studies

Frequency (MHz)	600.01	Nucleus	¹ H	Number of Transients	16	Origin	spect
Original Points Count	32768	Owner	nmsu	Points Count	65536	Pulse Sequence	zg30
Receiver Gain	176.24	SW(cyclical) (Hz)	12019.23	Solvent	CDCl ₃	Spectrum Offset (Hz)	3743.5237
Spectrum Type	STANDARD	Sweep Width (Hz)	12019.05	Temperature (degree C)	23.508	Acquisition Time (sec)	2.7263

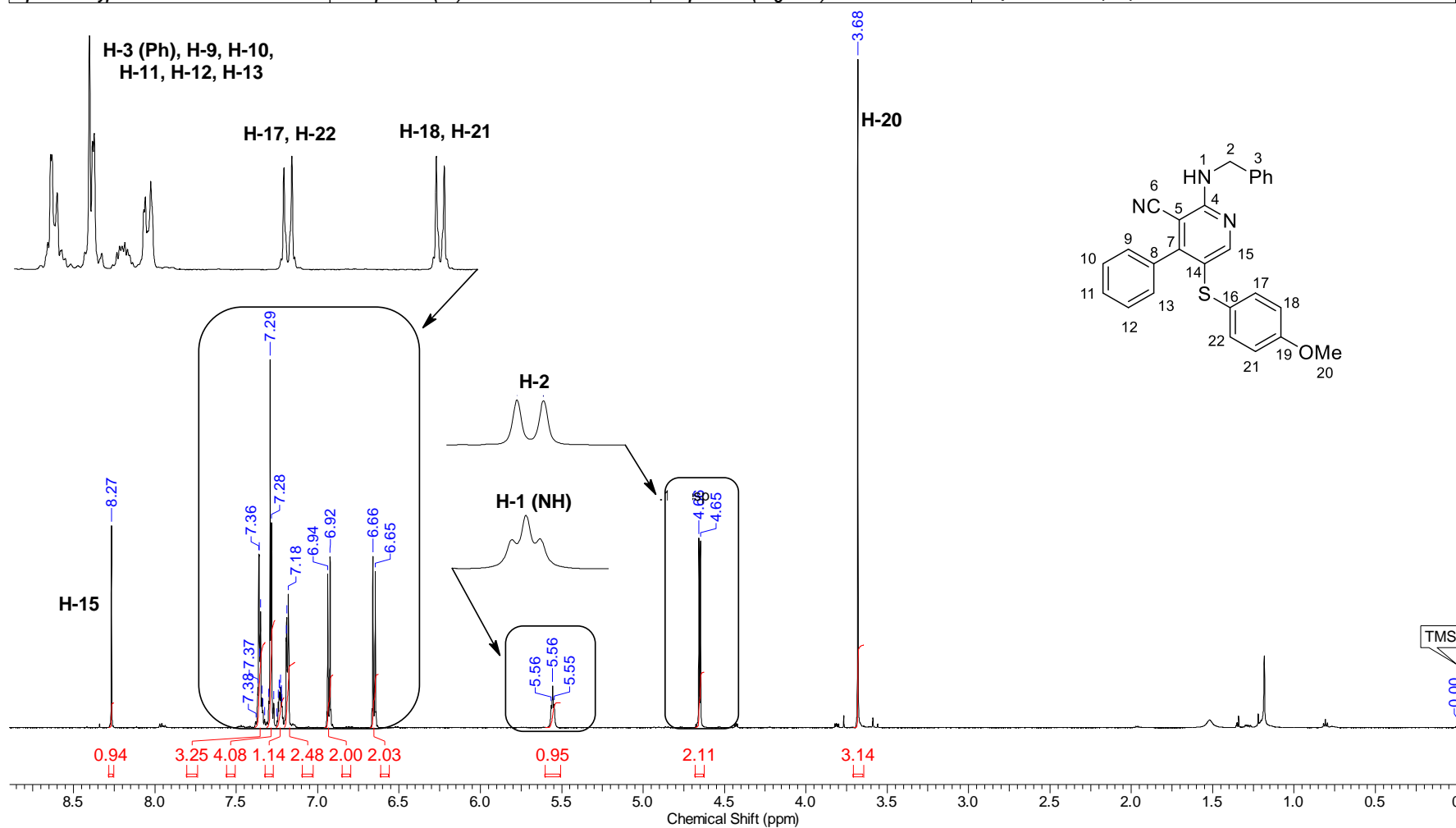


Frequency (MHz)	150.87	Nucleus	¹³ C	Number of Transients	256	Origin	spect
Original Points Count	32768	Owner	nrmrsu	Points Count	32768	Pulse Sequence	zgpg30
Receiver Gain	199.73	SW(cyclical) (Hz)	36231.88	Solvent	CDCl ₃	Spectrum Offset (Hz)	15094.0000
Spectrum Type	STANDARD	Sweep Width (Hz)	36230.78	Temperature (degree C)	25.109	Acquisition Time (sec)	0.9044



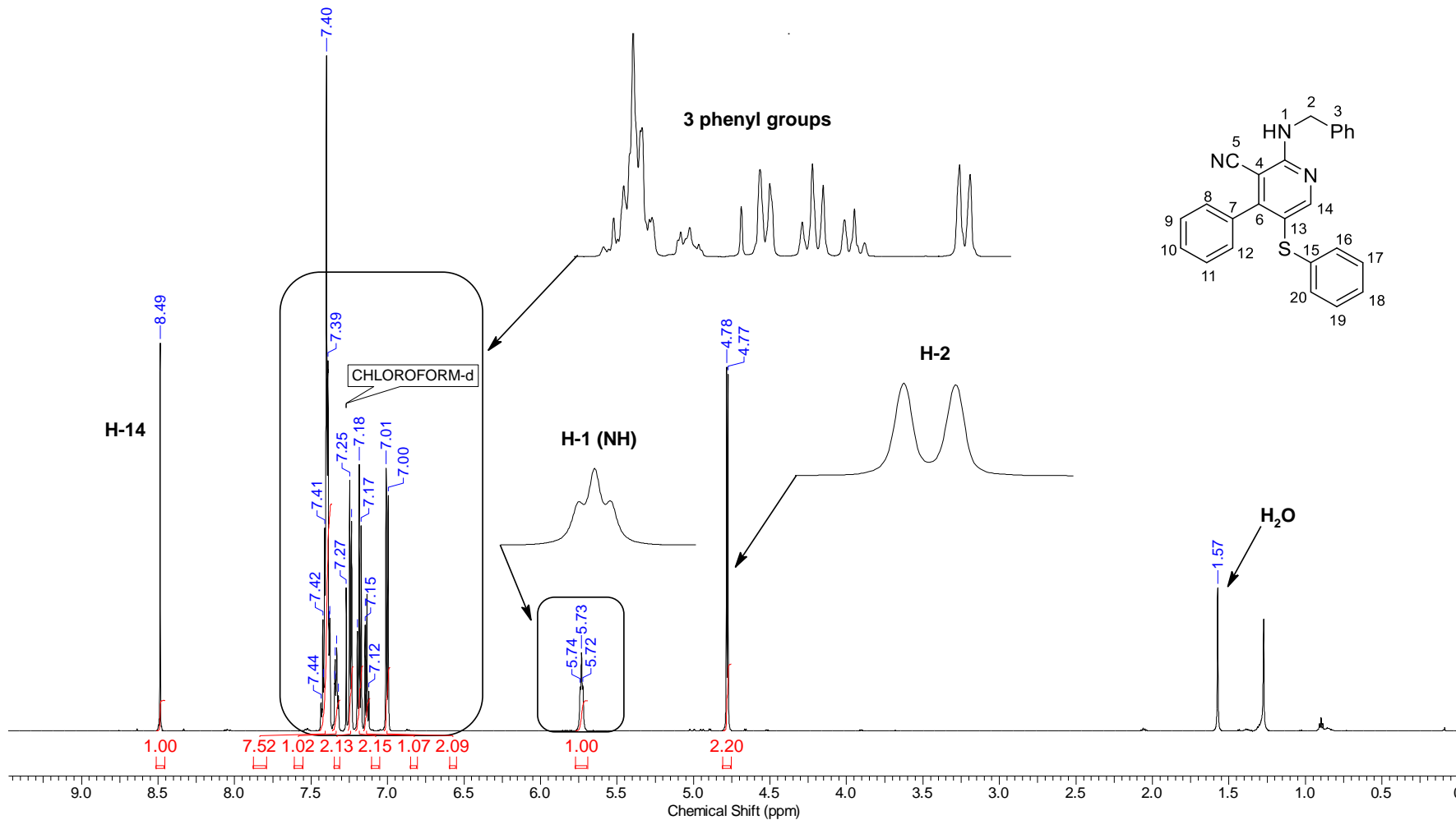
Continuous Conditions Applied to Hazardous Reactions and Fluorophores Synthesis with Photophysics Studies

Frequency (MHz)	600.01	Nucleus	1H	Number of Transients	16	Origin	spect
Original Points Count	32768	Owner	nmsu	Points Count	65536	Pulse Sequence	zg30
Receiver Gain	176.24	SW(cyclical) (Hz)	12019.23	Solvent	CDCl3	Spectrum Offset (Hz)	3641.1101
Spectrum Type	STANDARD	Sweep Width (Hz)	12019.05	Temperature (degree C)	23.625	Acquisition Time (sec)	2.7263



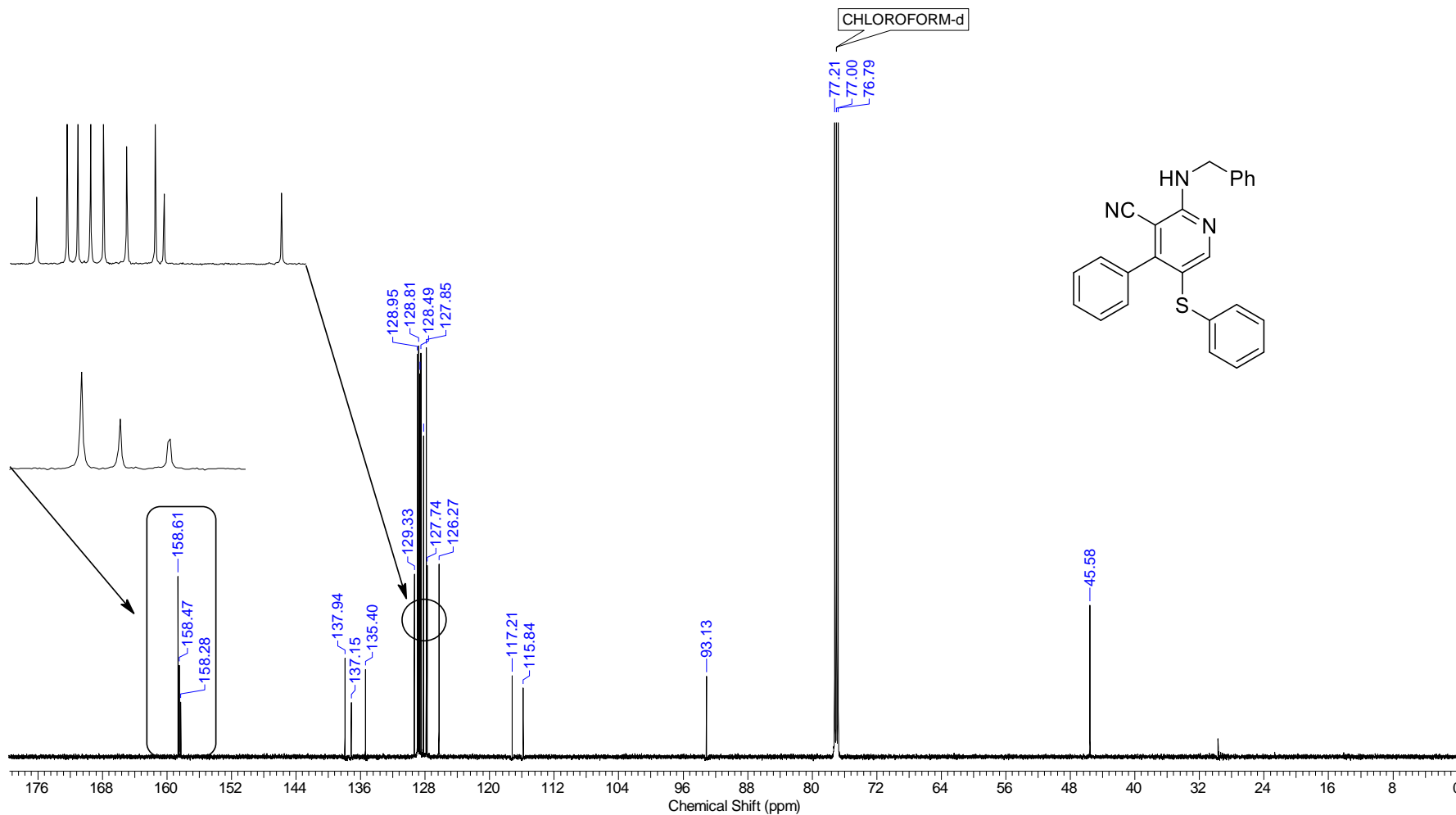
Continuous Conditions Applied to Hazardous Reactions and Fluorophores Synthesis with Photophysics Studies

Frequency (MHz)	600.01	Nucleus	1H	Number of Transients	16	Origin	spect
Original Points Count	32768	Owner	nmrsu	Points Count	65536	Pulse Sequence	zg30
Receiver Gain	199.73	SW(cyclical) (Hz)	12019.23	Solvent	CDCl3	Spectrum Offset (Hz)	3695.1067
Spectrum Type	STANDARD	Sweep Width (Hz)	12019.05	Temperature (degree C)	23.594	Acquisition Time (sec)	2.7263



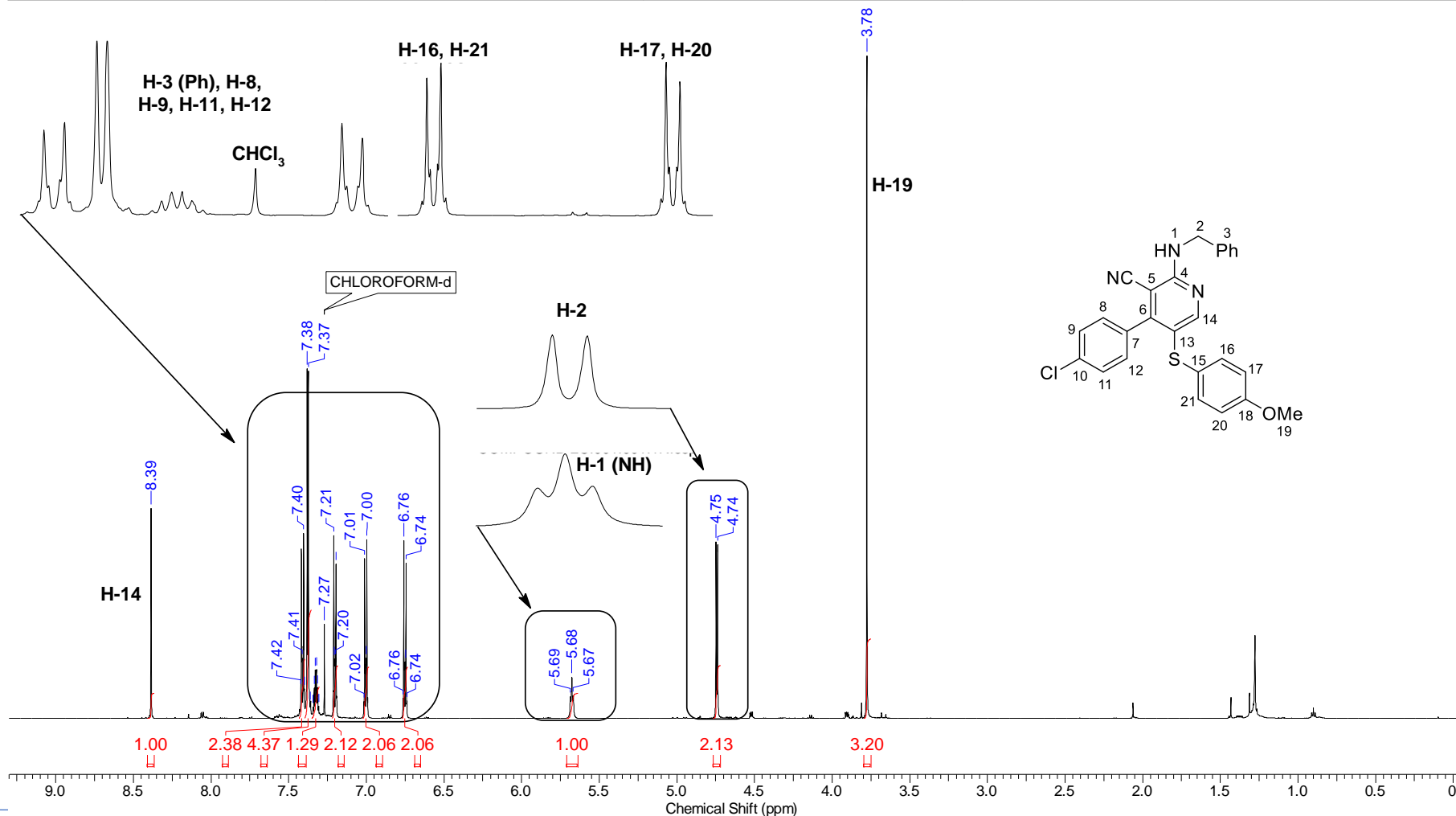
Continuous Conditions Applied to Hazardous Reactions and Fluorophores Synthesis with Photophysics Studies

Nucleus	13C	Number of Transients	2500	Origin	spect	Original Points Count	32768
Owner	nmsu	Points Count	32768	Pulse Sequence	zgpg30	Receiver Gain	199.73
SW(cyclical) (Hz)	36231.88	Solvent	CDCl3	Spectrum Offset (Hz)	15081.8369	Spectrum Type	STANDARD
Sweep Width (Hz)	36230.78	Temperature (degree C)	25.310	Frequency (MHz)	150.87	Acquisition Time (sec)	0.9044



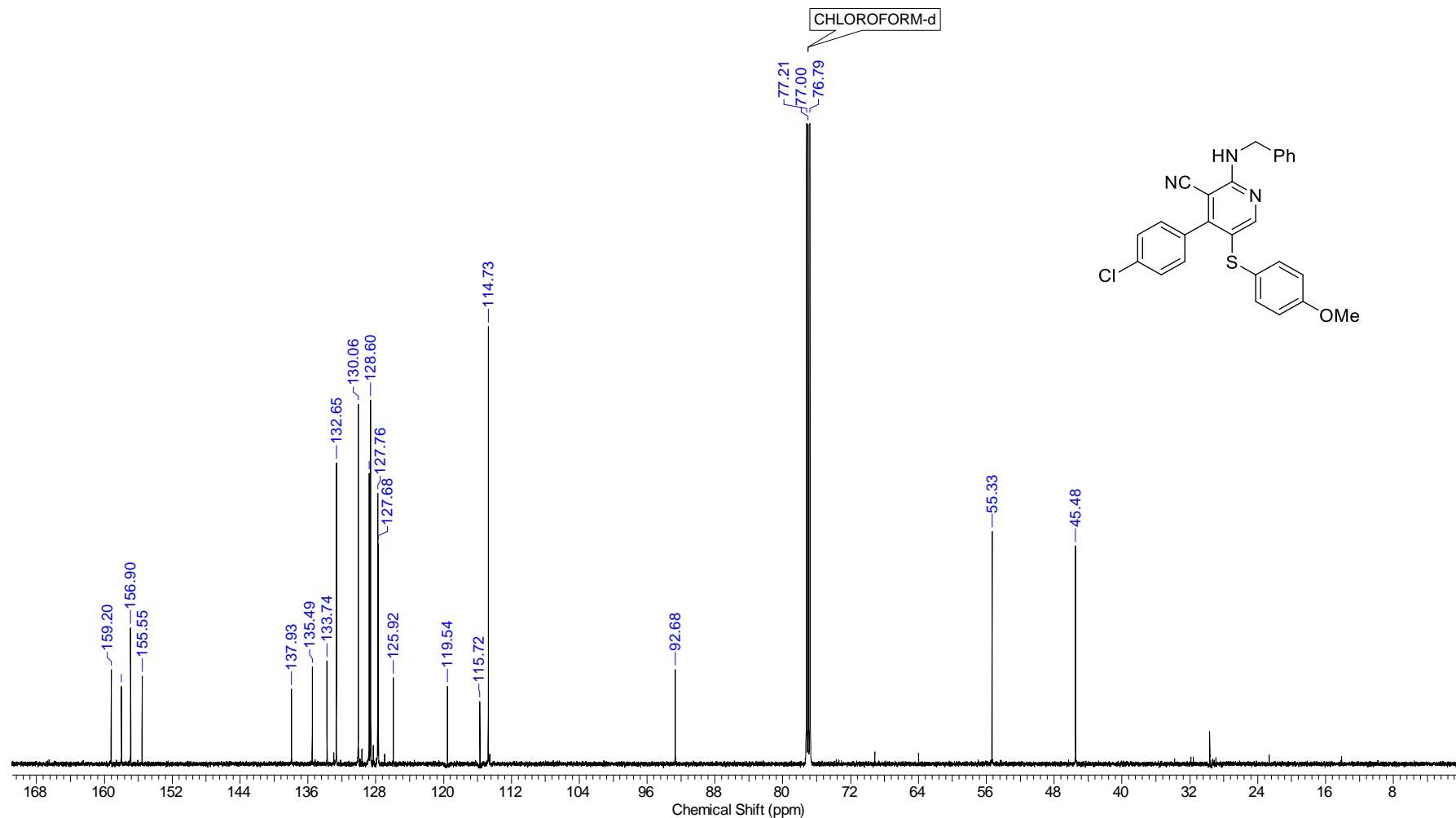
Continuous Conditions Applied to Hazardous Reactions and Fluorophores Synthesis with Photophysics Studies

Frequency (MHz)	599.96	Nucleus	1H	Number of Transients	16	Origin	spect
Original Points Count	32768	Owner	nmrsu	Points Count	65536	Pulse Sequence	zq30
Receiver Gain	71.41	SW(cyclical) (Hz)	12019.23	Solvent	CDCl3	Spectrum Offset (Hz)	3695.2937
Spectrum Type	STANDARD	Sweep Width (Hz)	12019.05	Temperature (degree C)	23.343	Acquisition Time (sec)	2.7263



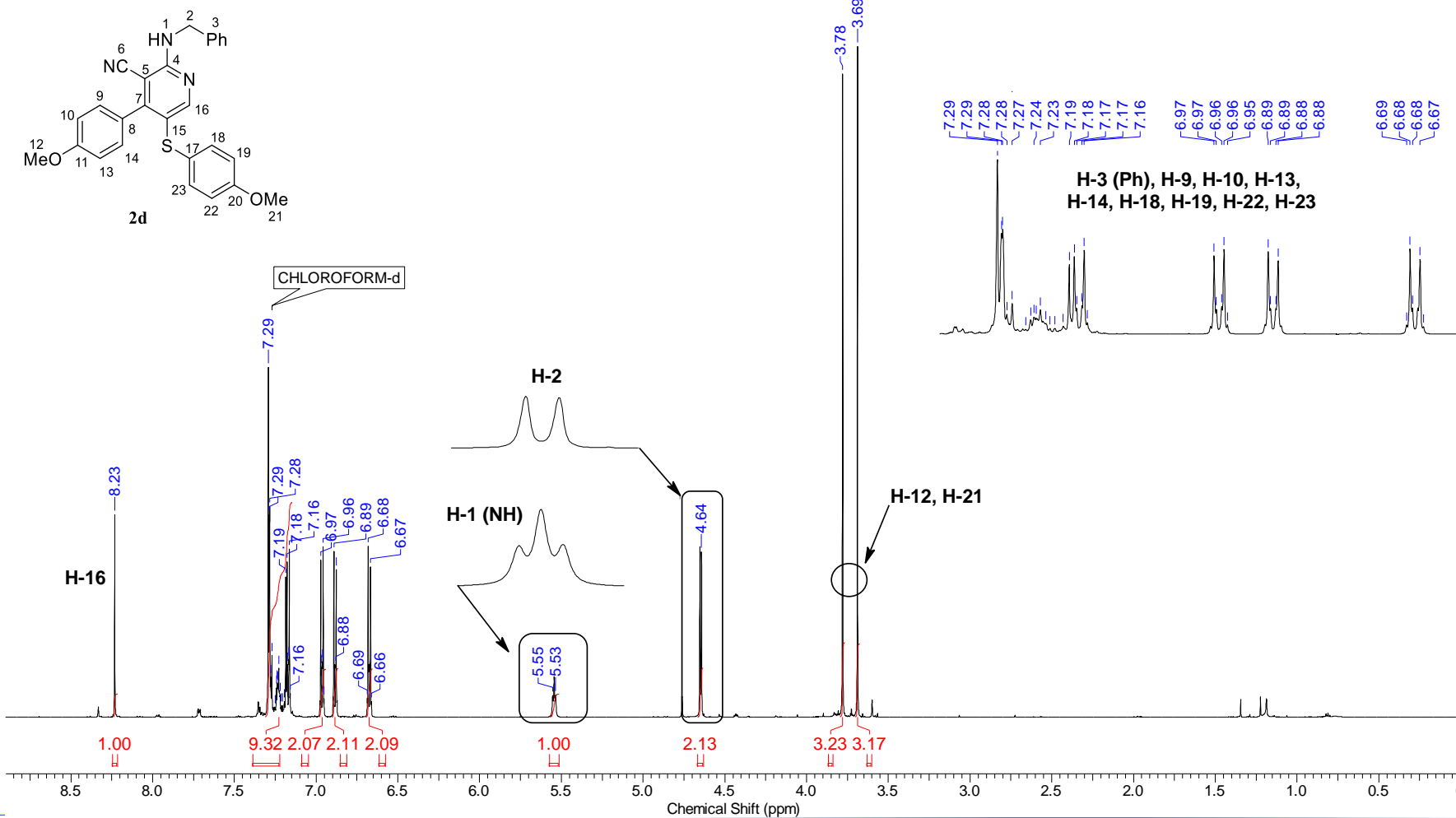
Continuous Conditions Applied to Hazardous Reactions and Fluorophores Synthesis with Photophysics Studies

Nucleus	13C	Number of Transients	2500	Origin	spect	Original Points Count	32768
Owner	nmsu	Points Count	32768	Pulse Sequence	zgpg30	Receiver Gain	194.75
SW(cyclical) (Hz)	36231.88	Solvent	CDCl3	Spectrum Offset (Hz)	15075.3408	Spectrum Type	STANDARD
Sweep Width (Hz)	36230.78	Temperature (degree C)	23.490	Frequency (MHz)	150.86	Acquisition Time (sec)	0.9044



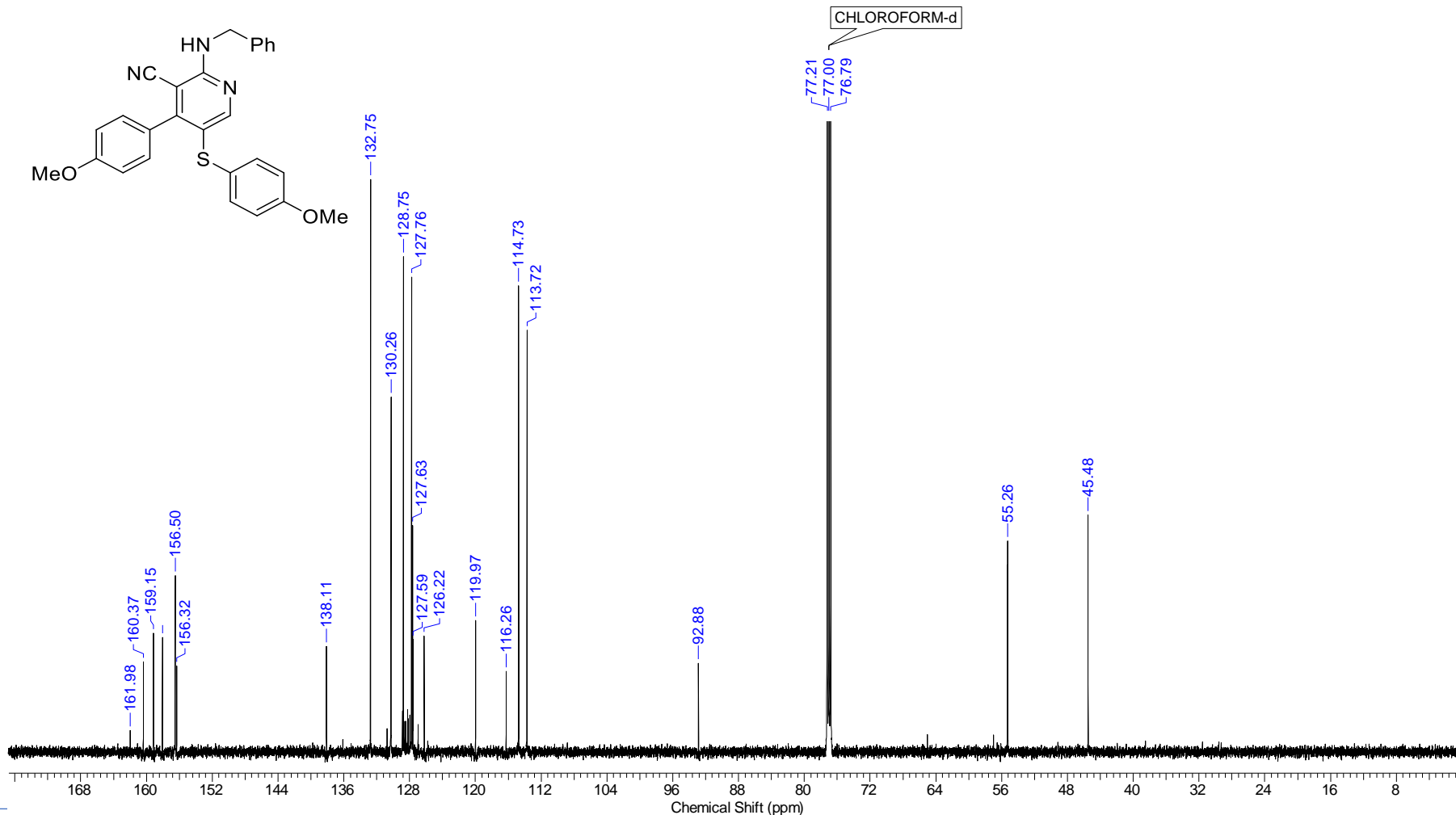
Continuous Conditions Applied to Hazardous Reactions and Fluorophores Synthesis with Photophysics Studies

Frequency (MHz)	599.96	Nucleus	1H	Number of Transients	16	Origin	spect
Original Points Count	32768	Owner	nmrsu	Points Count	65536	Pulse Sequence	zg30
Receiver Gain	110.56	SW(cyclical) (Hz)	12019.23	Solvent	CDCl3	Spectrum Offset (Hz)	3644.6758
Spectrum Type	STANDARD	Sweep Width (Hz)	12019.05	Temperature (degree C)	23.324	Acquisition Time (sec)	2.7263



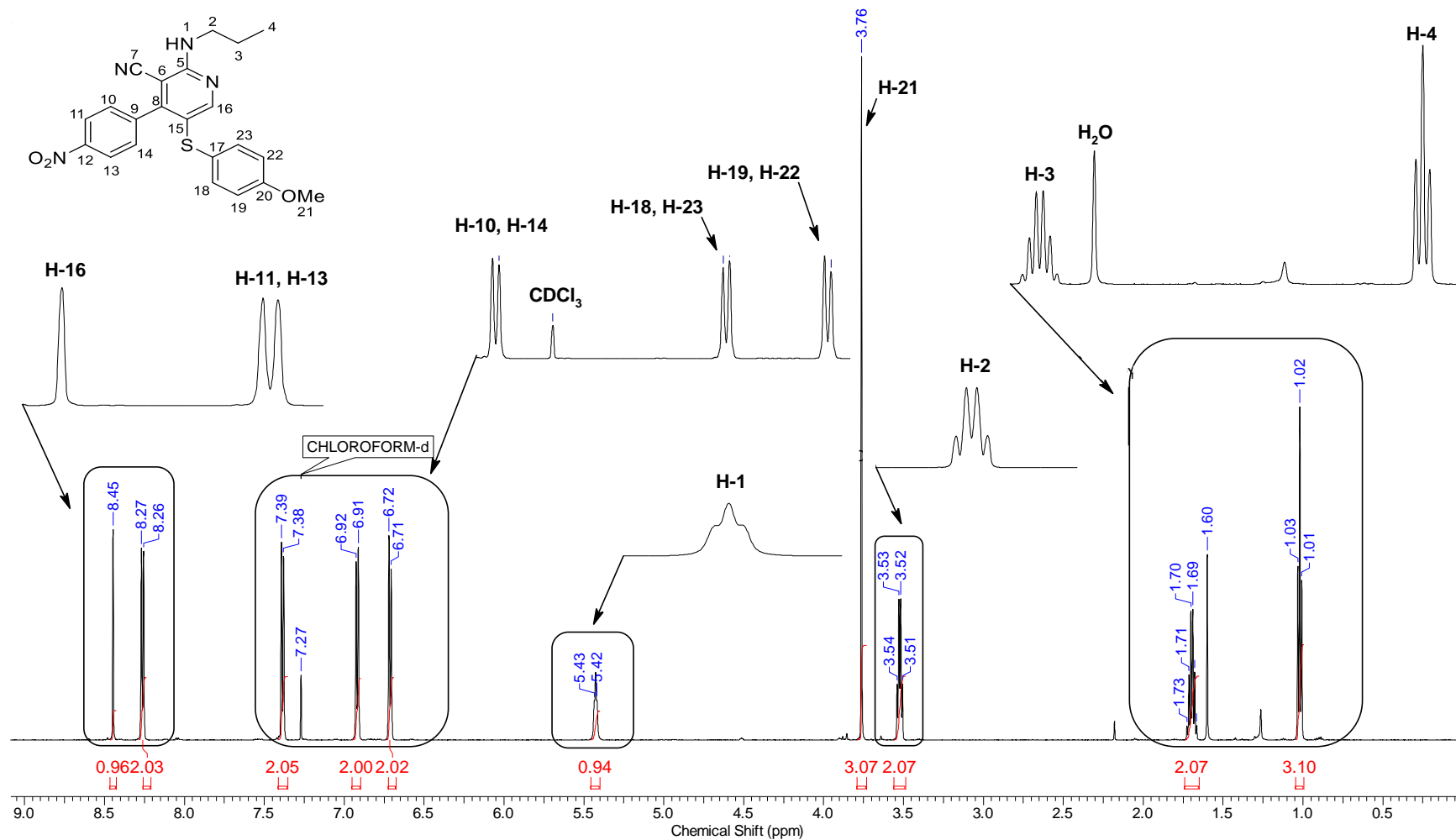
Continuous Conditions Applied to Hazardous Reactions and Fluorophores Synthesis with Photophysics Studies

Nucleus	13C	Number of Transients	2500	Origin	spect	Original Points Count	32768
Owner	nmrsu	Points Count	32768	Pulse Sequence	zpgpg30	Receiver Gain	194.75
SW(cyclical) (Hz)	36231.88	Solvent	CDCl3	Spectrum Offset (Hz)	15078.6563	Spectrum Type	STANDARD
Sweep Width (Hz)	36230.78	Temperature (degree C)	23.455	Frequency (MHz)	150.86	Acquisition Time (sec)	0.9044



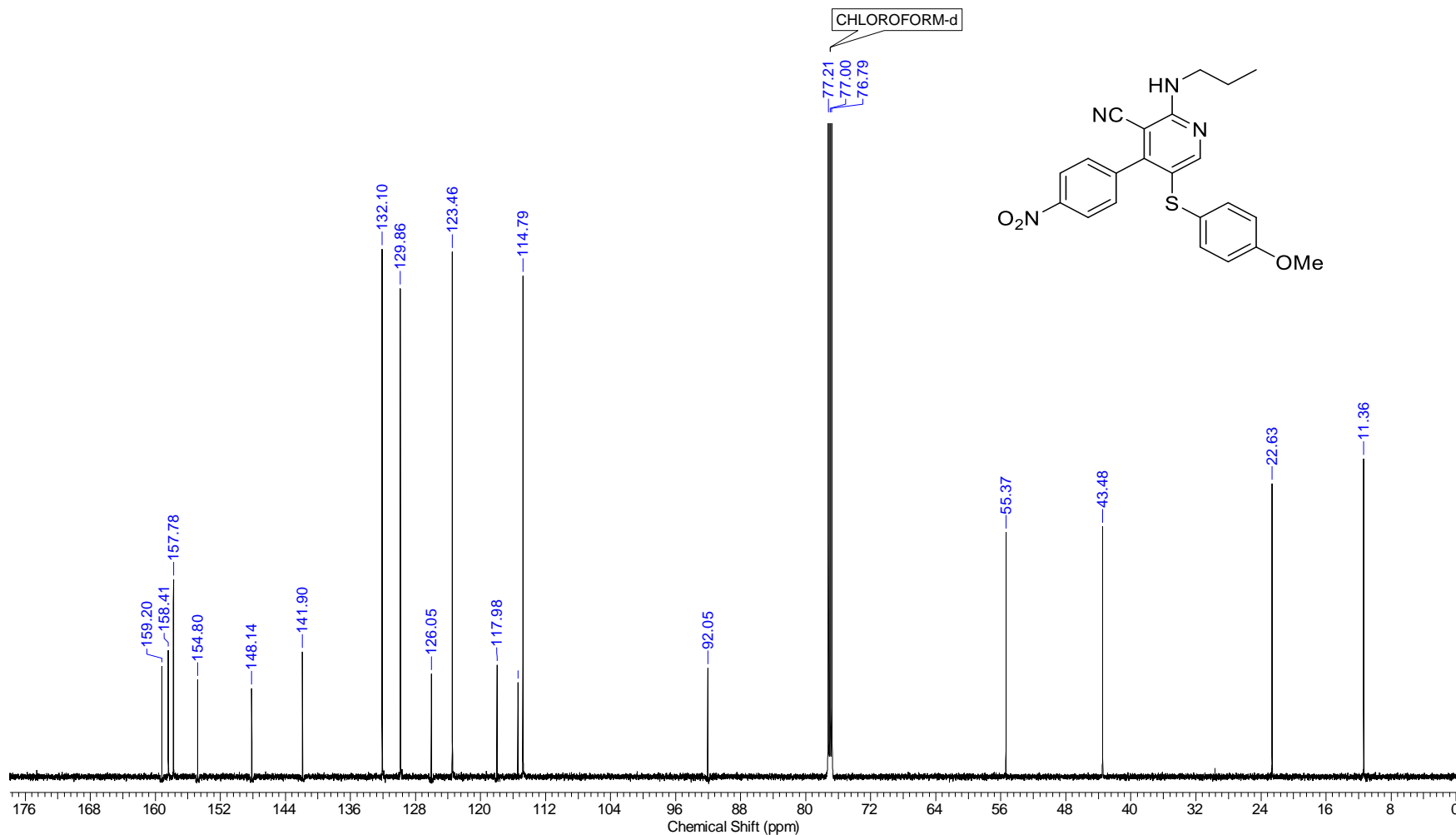
Continuous Conditions Applied to Hazardous Reactions and Fluorophores Synthesis with Photophysics Studies

Frequency (MHz)	600.01	Nucleus	1H	Number of Transients	16	Origin	spect
Original Points Count	32768	Owner	nmsu	Points Count	65536	Pulse Sequence	zg30
Receiver Gain	176.24	SW(cyclical) (Hz)	12019.23	Solvent	CDCl3	Spectrum Offset (Hz)	3695.4729
Spectrum Type	STANDARD	Sweep Width (Hz)	12019.05	Temperature (degree C)	23.551	Acquisition Time (sec)	2.7263



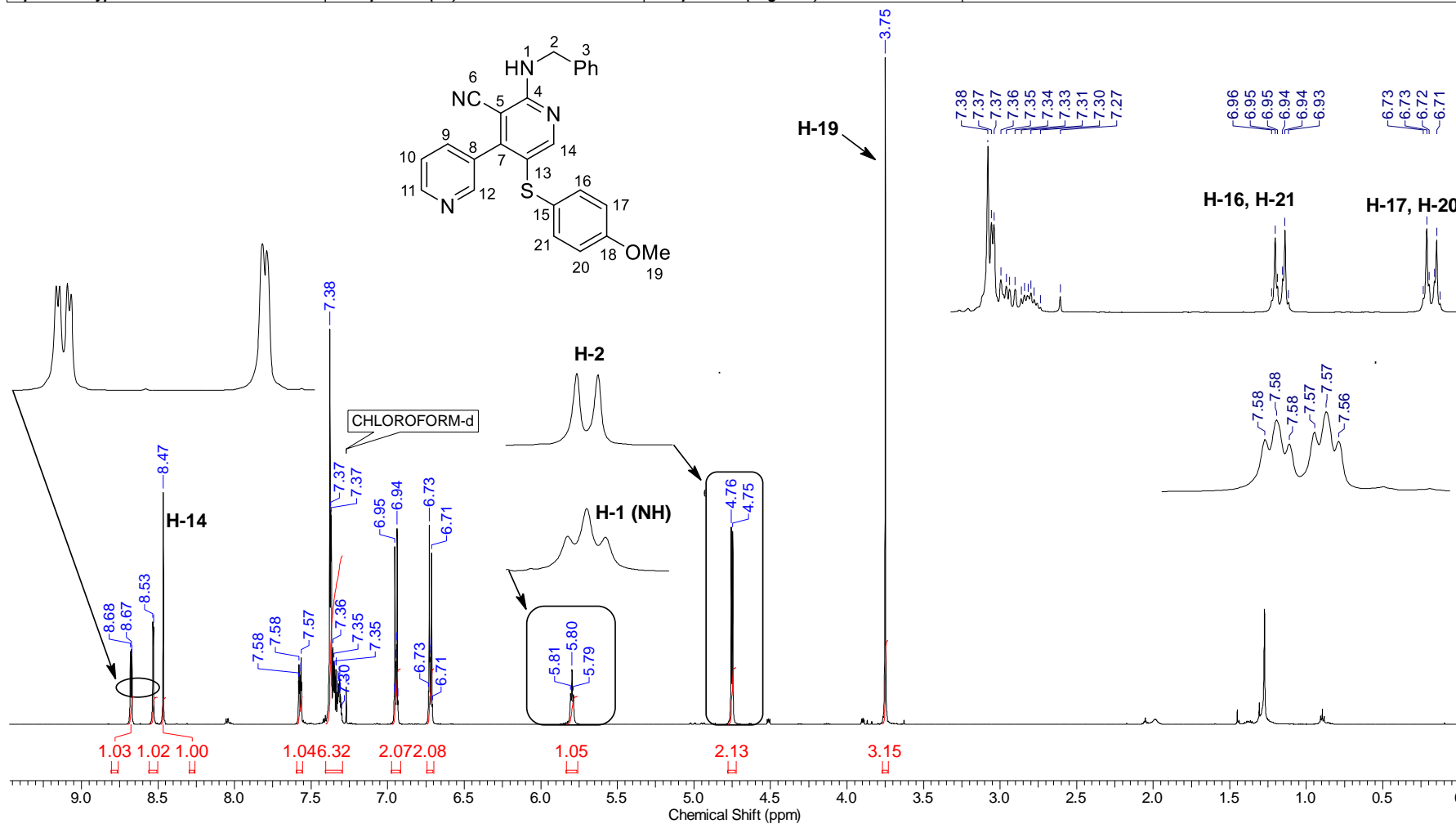
Continuous Conditions Applied to Hazardous Reactions and Fluorophores Synthesis with Photophysics Studies

Frequency (MHz)	150.87	Nucleus	13C	Number of Transients	2048	Origin	spect
Original Points Count	32768	Owner	nmsu	Points Count	32768	Pulse Sequence	zgpg30
Receiver Gain	199.73	SW(cyclical) (Hz)	36231.88	Solvent	CDCl3	Spectrum Offset (Hz)	15081.8369
Spectrum Type	STANDARD	Sweep Width (Hz)	36230.78	Temperature (degree C)	25.316	Acquisition Time (sec)	0.9044



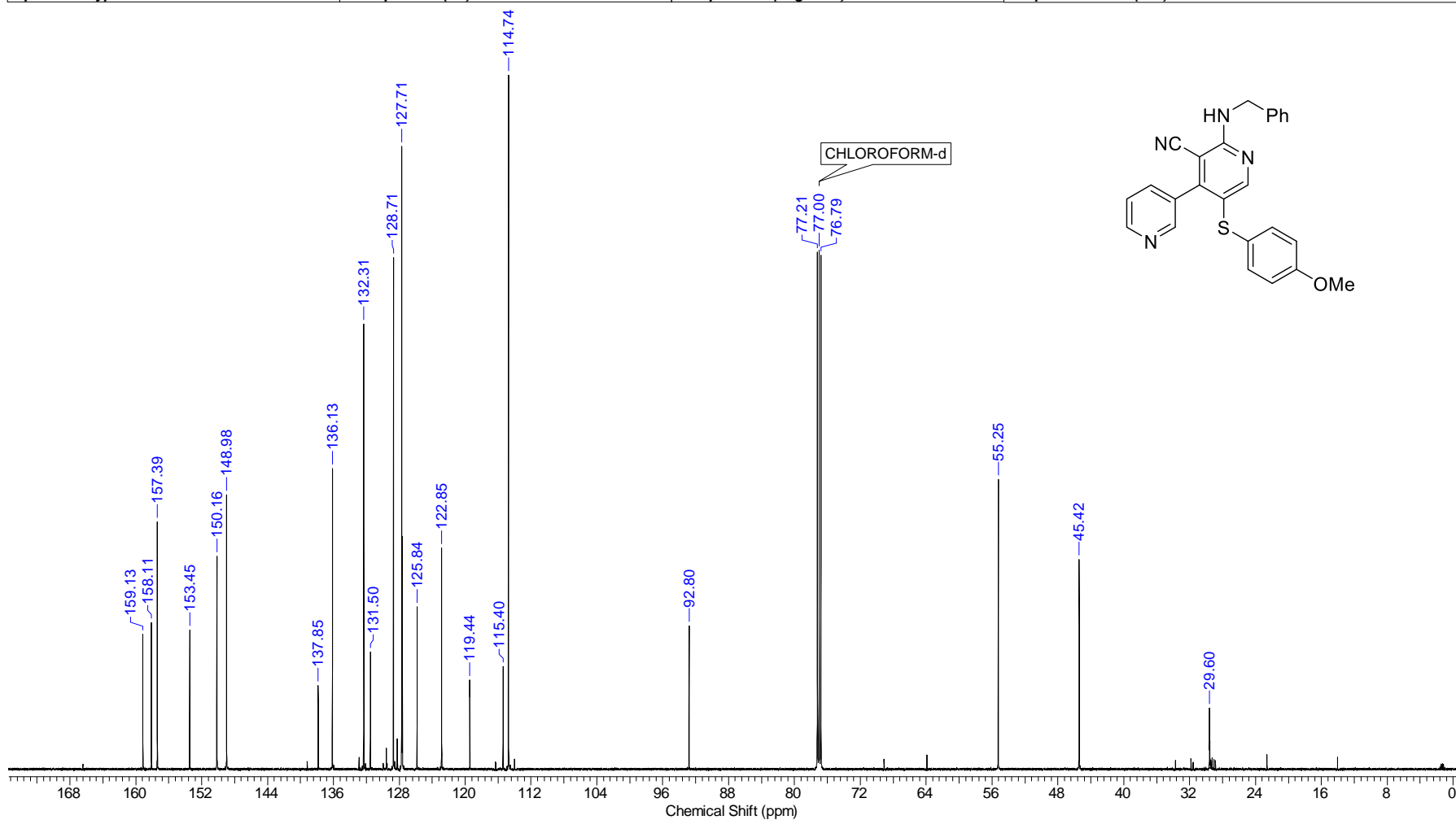
Continuous Conditions Applied to Hazardous Reactions and Fluorophores Synthesis with Photophysics Studies

Frequency (MHz)	599.96	Nucleus	1H	Number of Transients	16	Origin	spect
Original Points Count	32768	Owner	nmrsu	Points Count	65536	Pulse Sequence	zg30
Receiver Gain	30.85	SW(cyclical) (Hz)	12019.23	Solvent	CDCl3	Spectrum Offset (Hz)	3695.2937
Spectrum Type	STANDARD	Sweep Width (Hz)	12019.05	Temperature (degree C)	23.230	Acquisition Time (sec)	2.7263



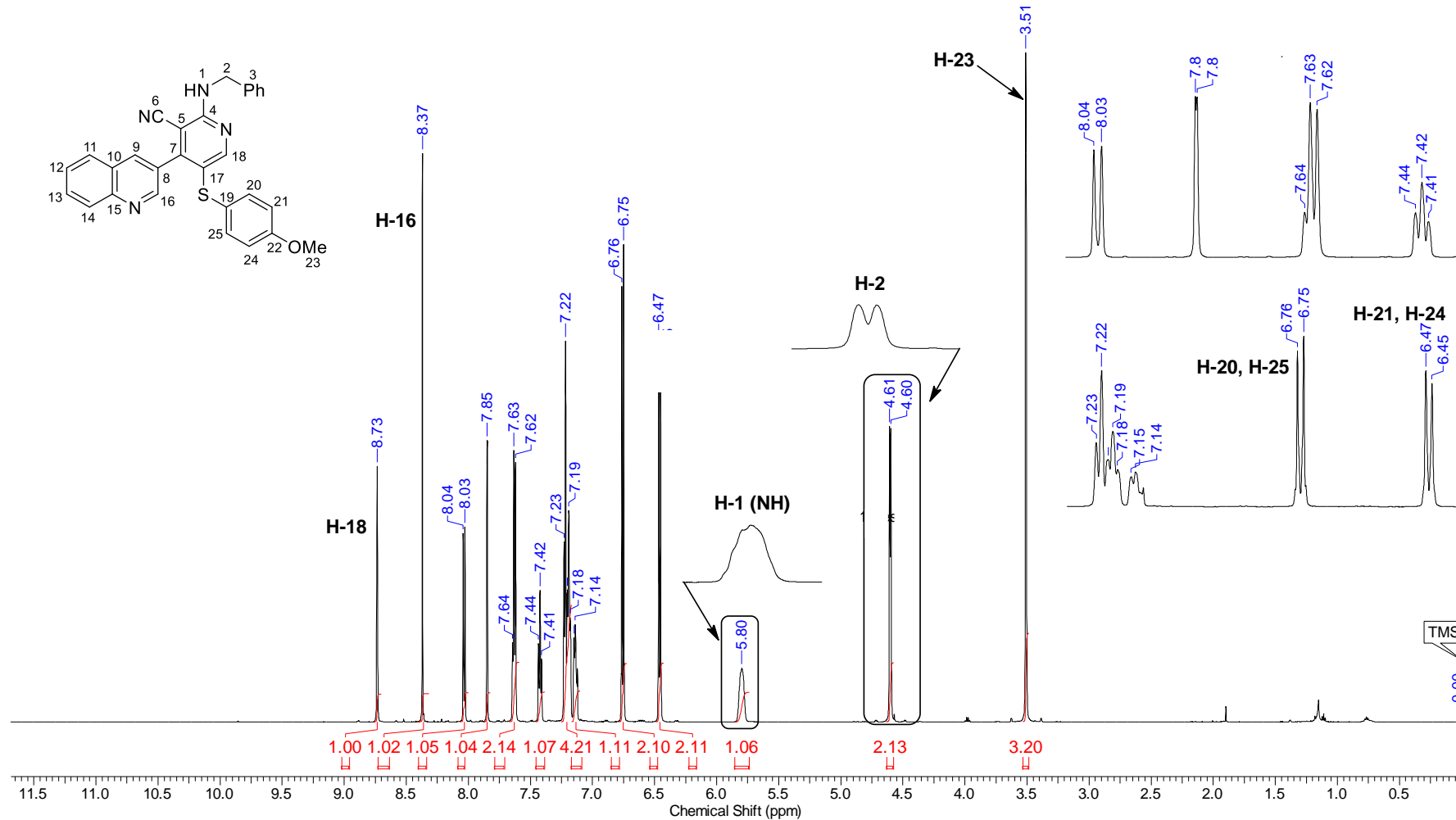
Continuous Conditions Applied to Hazardous Reactions and Fluorophores Synthesis with Photophysics Studies

Frequency (MHz)	150.87	Nucleus	¹³ C	Number of Transients	2500	Origin	spect
Original Points Count	32768	Owner	nmr	Points Count	32768	Pulse Sequence	zpgg30
Receiver Gain	199.73	SW(cyclical) (Hz)	36231.88	Solvent	CDCl ₃	Spectrum Offset (Hz)	15069.6738
Spectrum Type	STANDARD	Sweep Width (Hz)	36230.78	Temperature (degree C)	25.437	Acquisition Time (sec)	0.9044



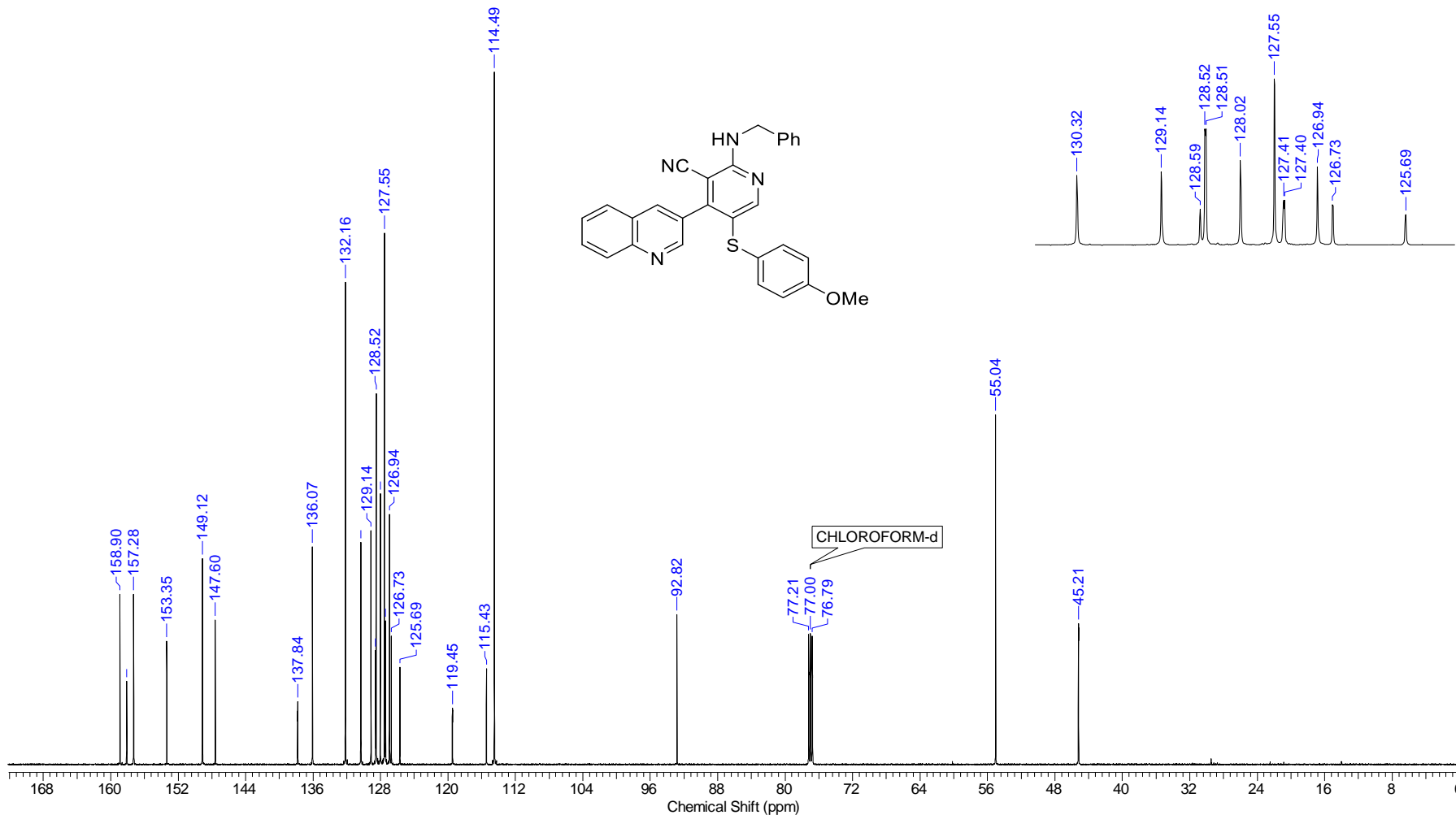
Continuous Conditions Applied to Hazardous Reactions and Fluorophores Synthesis with Photophysics Studies

Frequency (MHz)	600.01	Nucleus	1H	Number of Transients	16	Origin	spect
Original Points Count	32768	Owner	nmrsu	Points Count	65536	Pulse Sequence	zg30
Receiver Gain	31.31	SW(cyclical) (Hz)	12019.23	Solvent	CDCl3	Spectrum Offset (Hz)	3605.7141
Spectrum Type	STANDARD	Sweep Width (Hz)	12019.05	Temperature (degree C)	23.259	Acquisition Time (sec)	2.7263



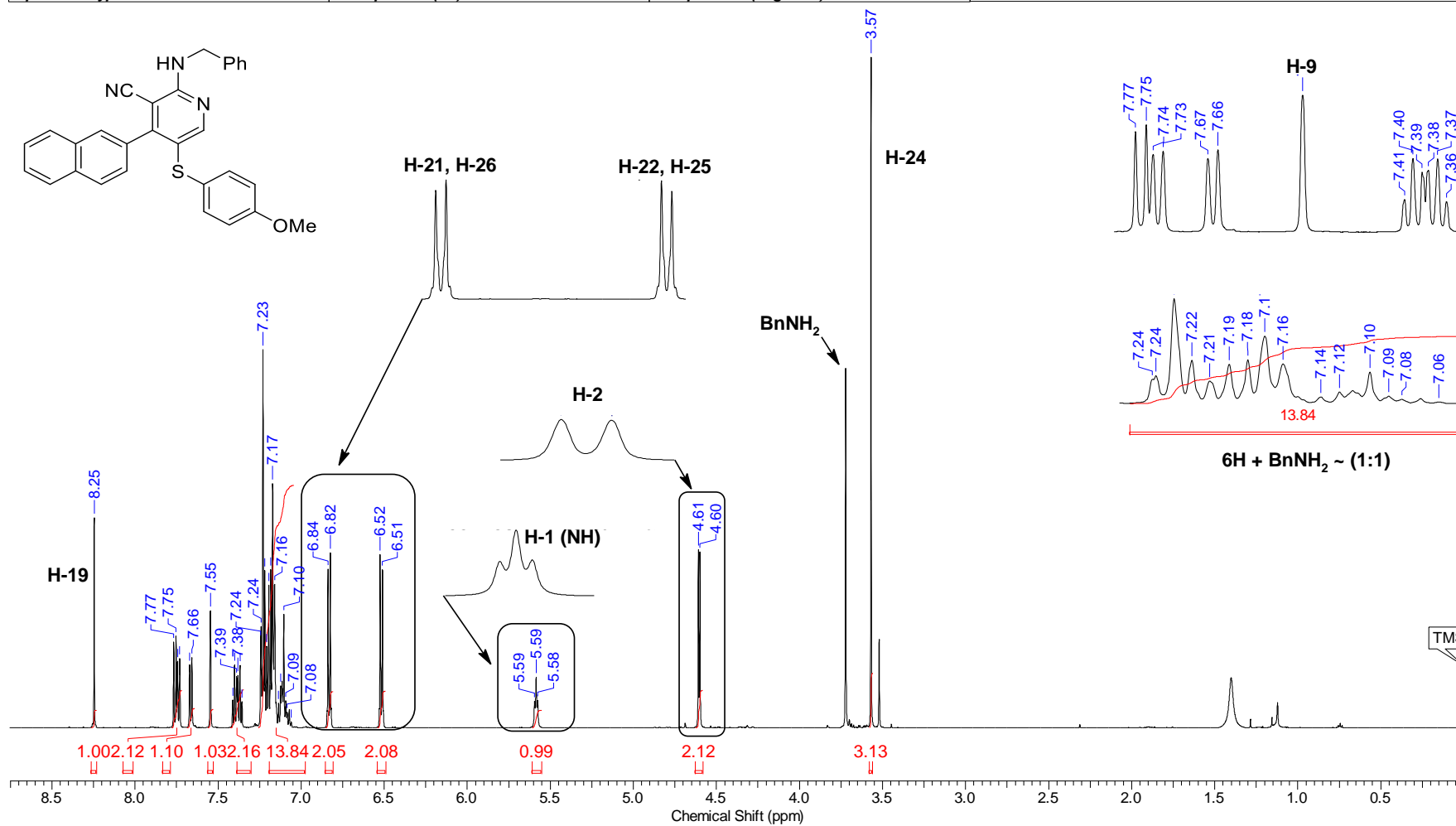
Continuous Conditions Applied to Hazardous Reactions and Fluorophores Synthesis with Photophysics Studies

Nucleus	13C	Number of Transients	2500	Origin	spect	Original Points Count	32768
Owner	nmsu	Points Count	32768	Pulse Sequence	zgpg30	Receiver Gain	199.73
SW(cyclical) (Hz)	36231.88	Solvent	CDCl3	Spectrum Offset (Hz)	15044.2432	Spectrum Type	STANDARD
Sweep Width (Hz)	36230.78	Temperature (degree C)	25.275	Acquisition Time (sec)	0.9044	Frequency (MHz)	150.87

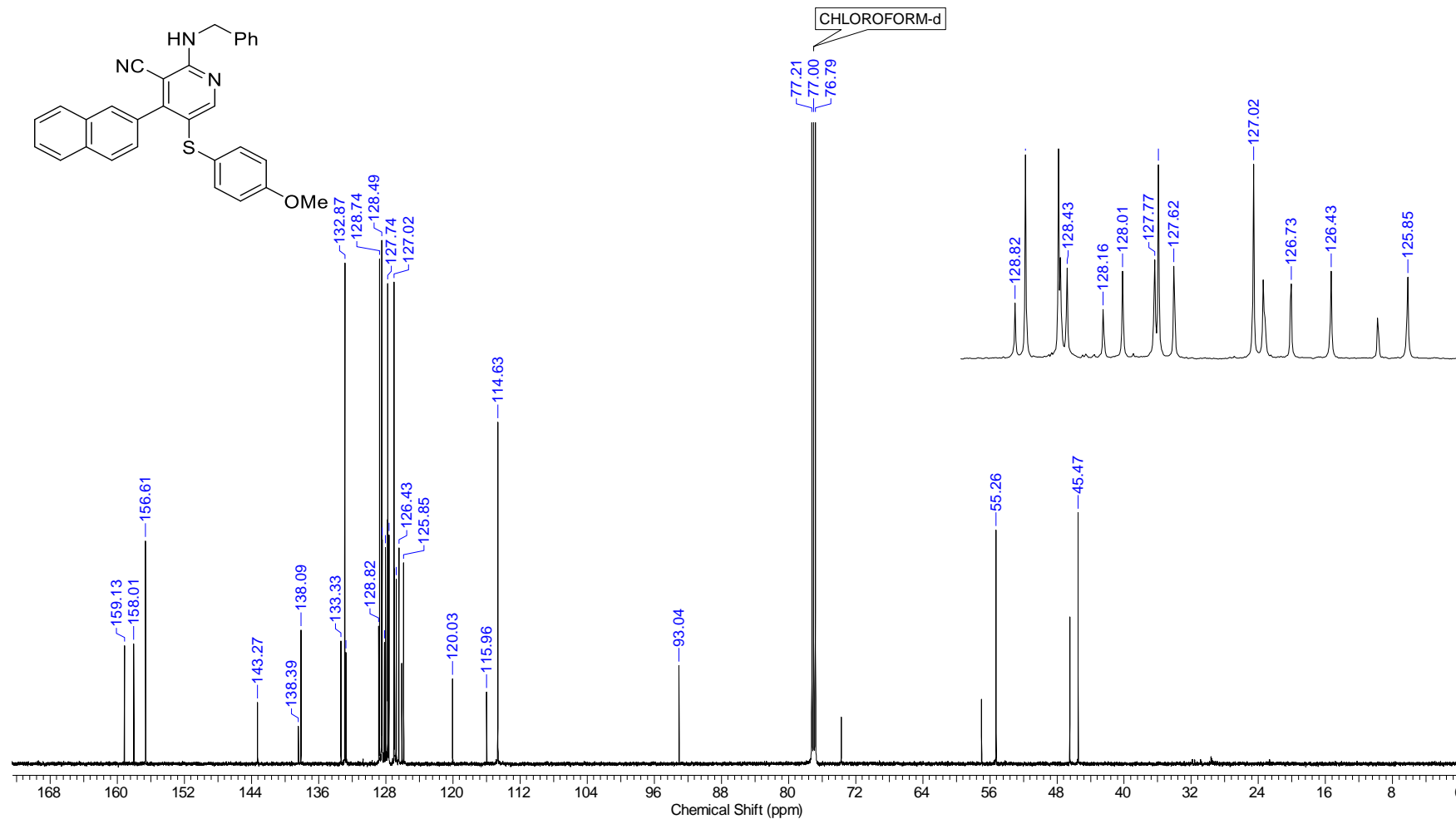


Continuous Conditions Applied to Hazardous Reactions and Fluorophores Synthesis with Photophysics Studies

Frequency (MHz)	600.01	Nucleus	¹ H	Number of Transients	16	Origin	spect
Original Points Count	32768	Owner	nmsu	Points Count	65536	Pulse Sequence	zg30
Receiver Gain	89.69	SW(cyclical) (Hz)	12019.23	Solvent	CDCl ₃	Spectrum Offset (Hz)	3595.9939
Spectrum Type	STANDARD	Sweep Width (Hz)	12019.05	Temperature (degree C)	23.248	Acquisition Time (sec)	2.7263

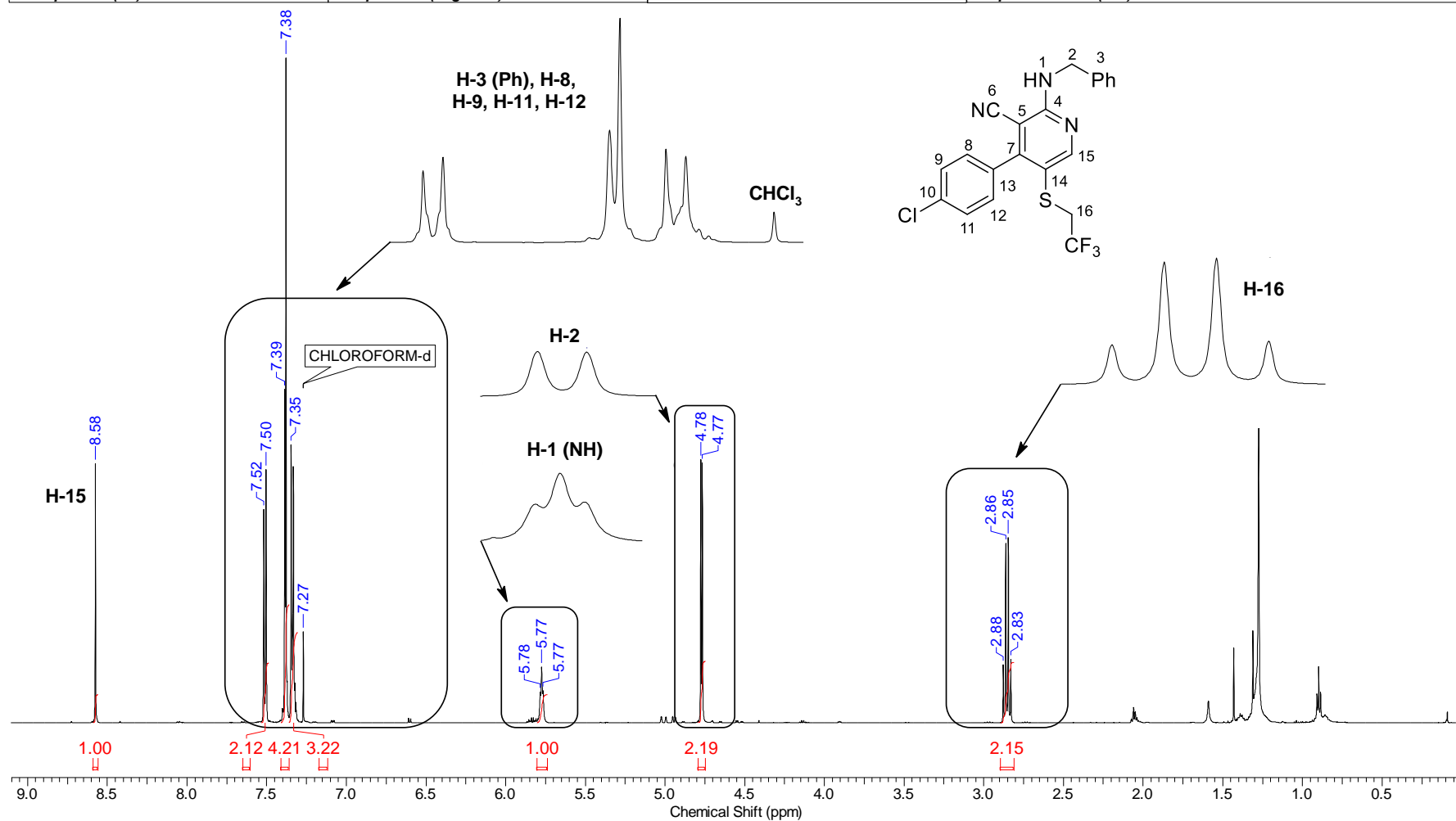


Nucleus	13C	Number of Transients	2500	Origin	spect	Original Points Count	32768
Owner	nrmrsu	Points Count	32768	Pulse Sequence	zgpgg30	Receiver Gain	199.73
SW(cyclical) (Hz)	36231.88	Solvent	CDCl3	Spectrum Offset (Hz)	15075.2021	Spectrum Type	STANDARD
Sweep Width (Hz)	36230.78	Temperature (degree C)	25.390	Acquisition Time (sec)	0.9044	Frequency (MHz)	150.87



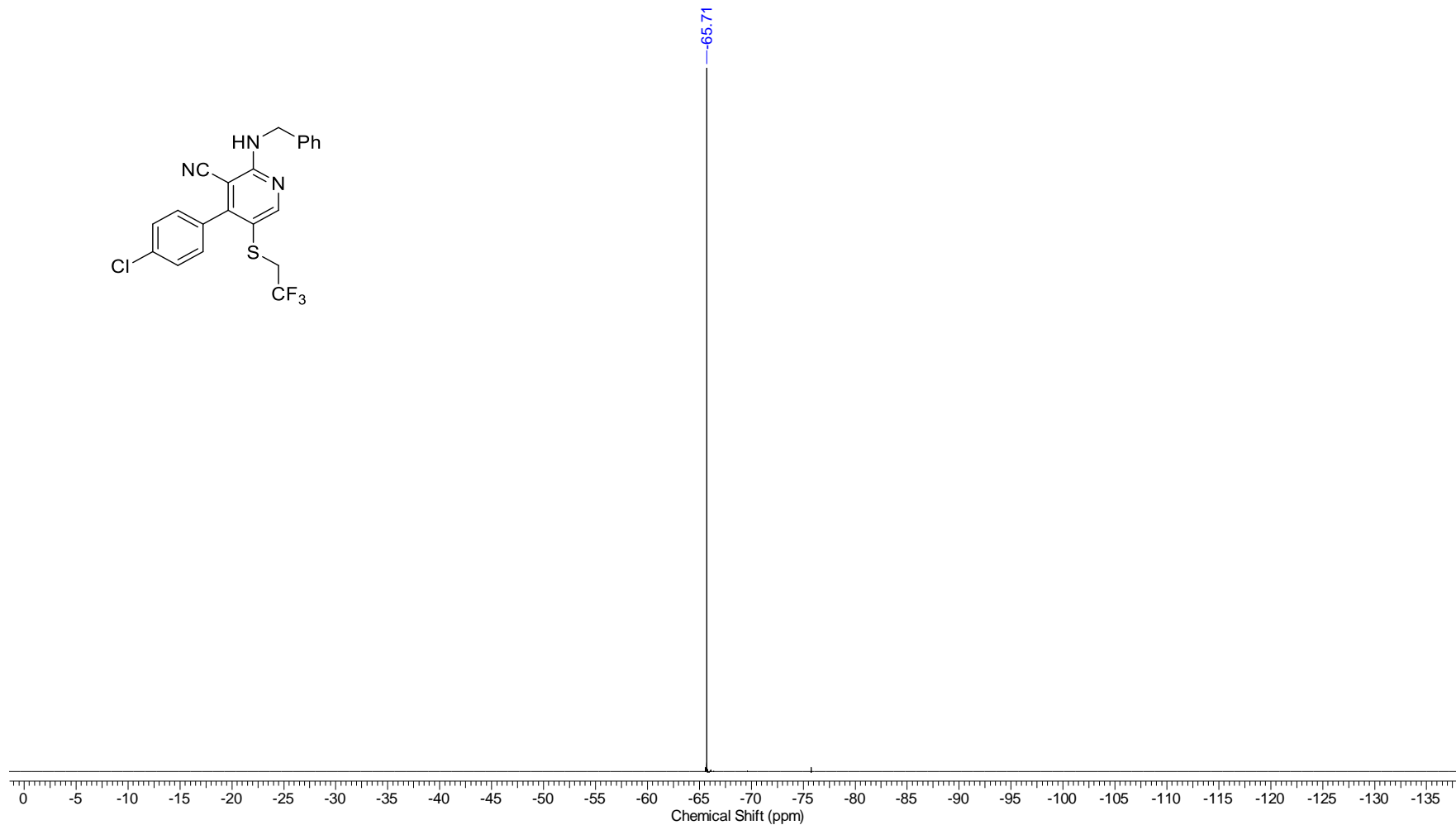
Continuous Conditions Applied to Hazardous Reactions and Fluorophores Synthesis with Photophysics Studies

Nucleus	1H	Number of Transients	16	Origin	spect	Original Points Count	32768
Owner	nmrsu	Points Count	65536	Pulse Sequence	zg30	Receiver Gain	120.50
SW(cyclical) (Hz)	12019.23	Solvent	CDCl3	Spectrum Offset (Hz)	3695.4736	Spectrum Type	STANDARD
Sweep Width (Hz)	12019.05	Temperature (degree C)	23.258	Frequency (MHz)	600.01	Acquisition Time (sec)	2.7263



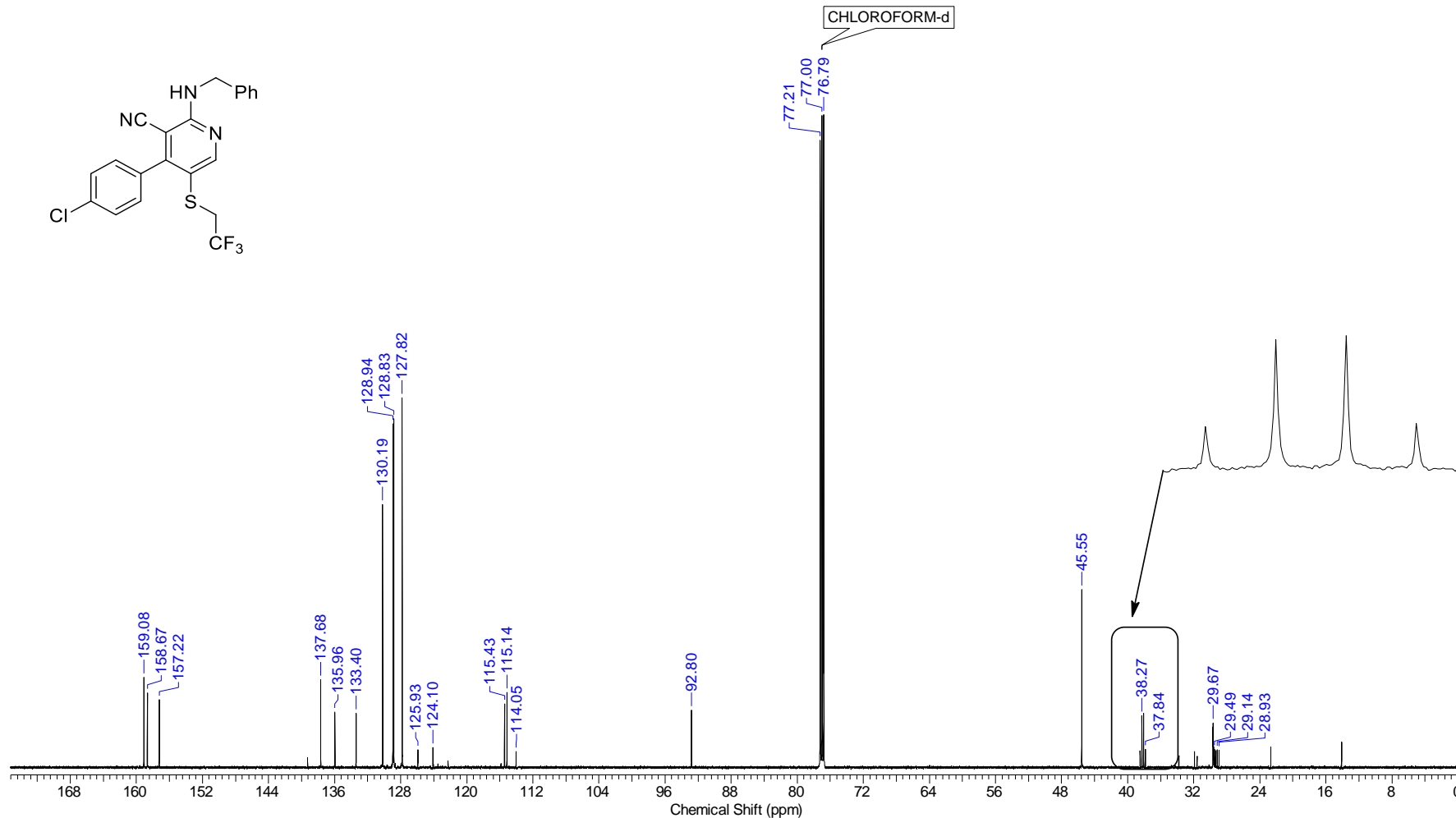
Continuous Conditions Applied to Hazardous Reactions and Fluorophores Synthesis with Photophysics Studies

Nucleus	19F	Number of Transients	32	Origin	spect	Original Points Count	65536
Owner	nmsu	Points Count	65536	Pulse Sequence	zgfhiggn.2	Receiver Gain	199.73
SW(cyclical) (Hz)	133928.58	Solvent	CDCI3	Spectrum Offset (Hz)	-56456.8867	Spectrum Type	STANDARD
Sweep Width (Hz)	133926.53	Temperature (degree C)	23.721	Frequency (MHz)	564.57	Acquisition Time (sec)	0.4893



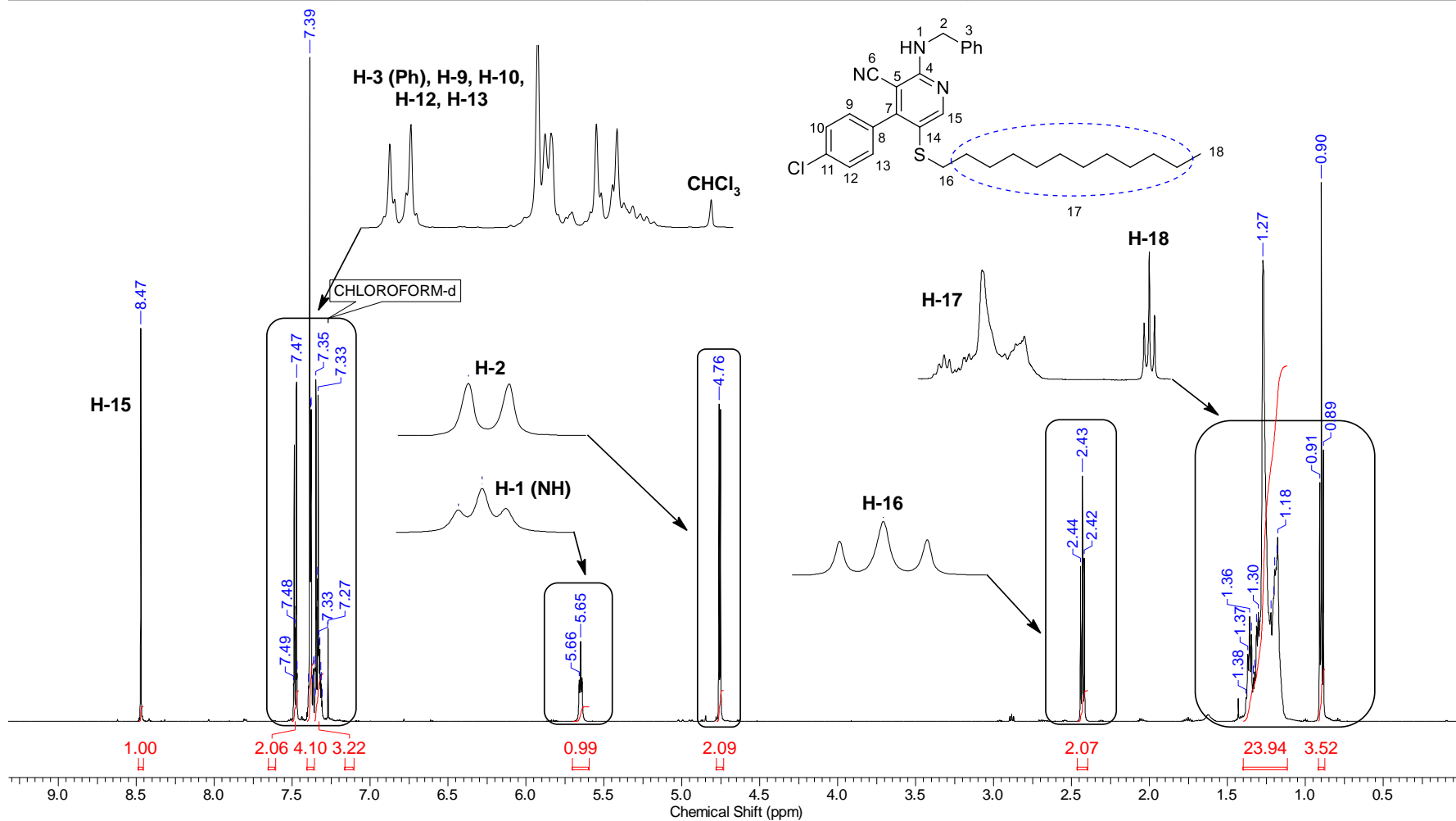
Continuous Conditions Applied to Hazardous Reactions and Fluorophores Synthesis with Photophysics Studies

Nucleus	13C	Number of Transients	2500	Origin	spect	Original Points Count	32768
Owner	nmsu	Points Count	32768	Pulse Sequence	zgpg30	Receiver Gain	199.73
SW(cyclical) (Hz)	36231.88	Solvent	CDCl3	Spectrum Offset (Hz)	15080.7305	Spectrum Type	STANDARD
Sweep Width (Hz)	36230.78	Temperature (degree C)	25.343	Frequency (MHz)	150.87	Acquisition Time (sec)	0.9044



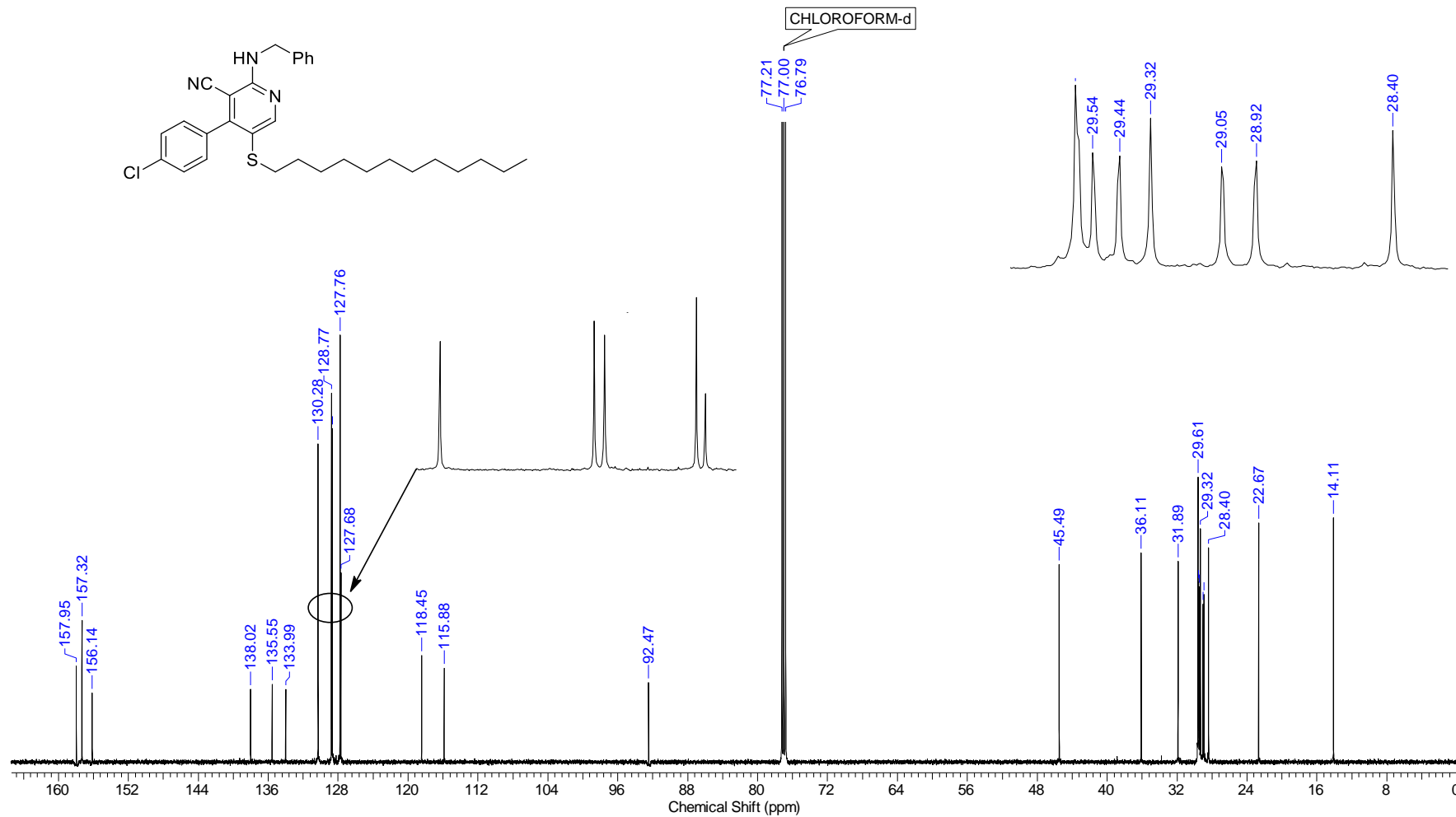
Continuous Conditions Applied to Hazardous Reactions and Fluorophores Synthesis with Photophysics Studies

Frequency (MHz)	599.96	Nucleus	¹ H	Number of Transients	16	Origin	spect
Original Points Count	32768	Owner	nmrsu	Points Count	65536	Pulse Sequence	zg30
Receiver Gain	30.85	SW(cyclical) (Hz)	12019.23	Solvent	CDCl ₃	Spectrum Offset (Hz)	3695.2930
Spectrum Type	STANDARD	Sweep Width (Hz)	12019.05	Temperature (degree C)	23.104	Acquisition Time (sec)	2.7263



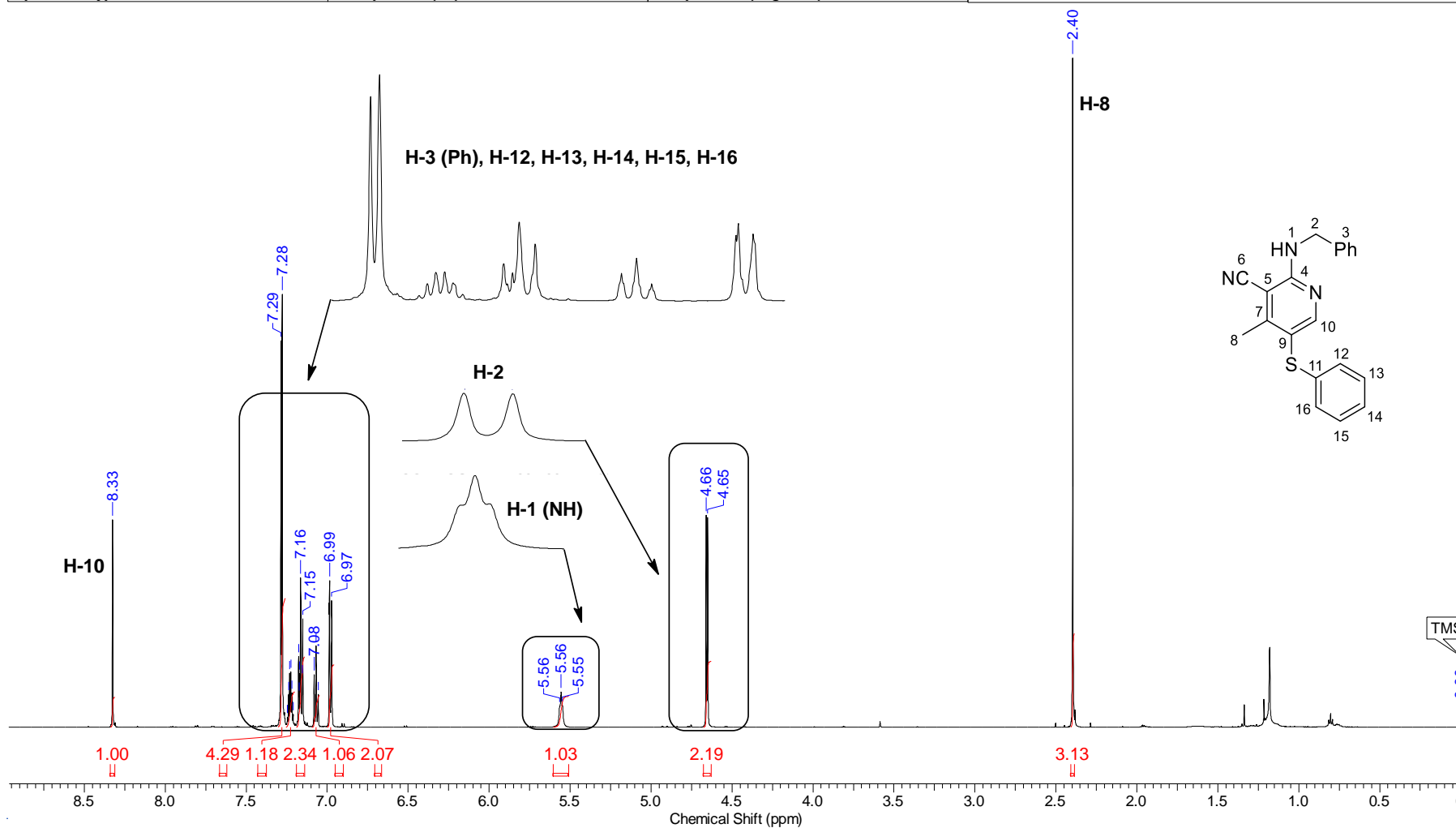
Continuous Conditions Applied to Hazardous Reactions and Fluorophores Synthesis with Photophysics Studies

Nucleus	13C	Number of Transients	2500	Origin	spect	Original Points Count	32768
Owner	nmsu	Points Count	32768	Pulse Sequence	zgpg30	Receiver Gain	194.75
SW(cyclical) (Hz)	36231.88	Solvent	CDCl3	Spectrum Offset (Hz)	15077.5518	Spectrum Type	STANDARD
Sweep Width (Hz)	36230.78	Temperature (degree C)	23.437	Frequency (MHz)	150.86	Acquisition Time (sec)	0.9044



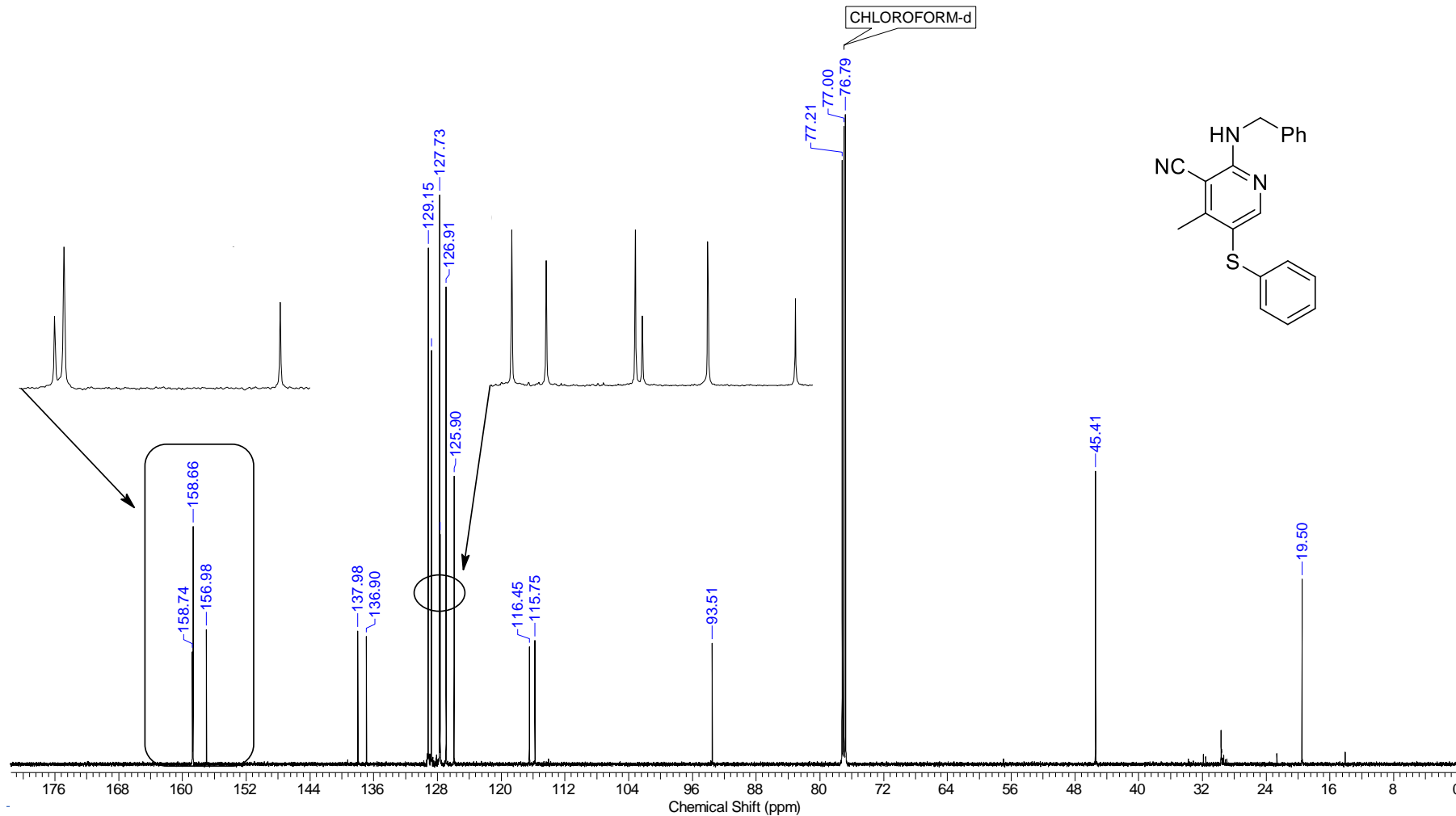
Continuous Conditions Applied to Hazardous Reactions and Fluorophores Synthesis with Photophysics Studies

Frequency (MHz)	599.96	Nucleus	¹ H	Number of Transients	16	Origin	spect
Original Points Count	32768	Owner	nmr-su	Points Count	65536	Pulse Sequence	zg30
Receiver Gain	63.39	SW(cyclical) (Hz)	12019.23	Solvent	CDCl ₃	Spectrum Offset (Hz)	3634.8745
Spectrum Type	STANDARD	Sweep Width (Hz)	12019.05	Temperature (degree C)	23.083	Acquisition Time (sec)	2.7263



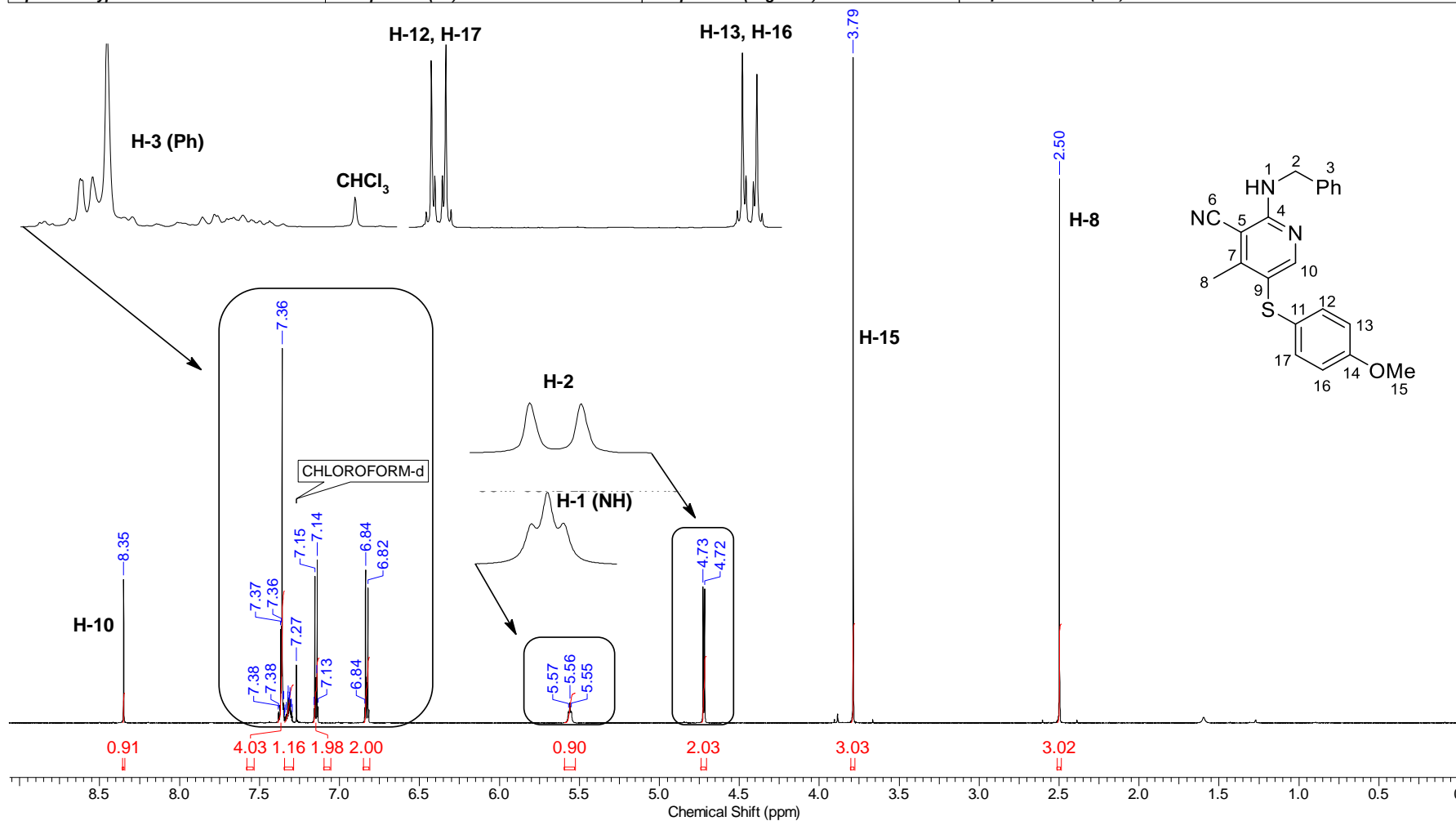
Continuous Conditions Applied to Hazardous Reactions and Fluorophores Synthesis with Photophysics Studies

Nucleus	13C	Number of Transients	2500	Origin	spect	Original Points Count	32768
Owner	nmrslu	Points Count	32768	Pulse Sequence	zgpg30	Receiver Gain	194.75
SW(cyclical) (Hz)	36231.88	Solvent	CDCl3	Spectrum Offset (Hz)	15074.2344	Spectrum Type	STANDARD
Sweep Width (Hz)	36230.78	Temperature (degree C)	23.409	Frequency (MHz)	150.86	Acquisition Time (sec)	0.9044



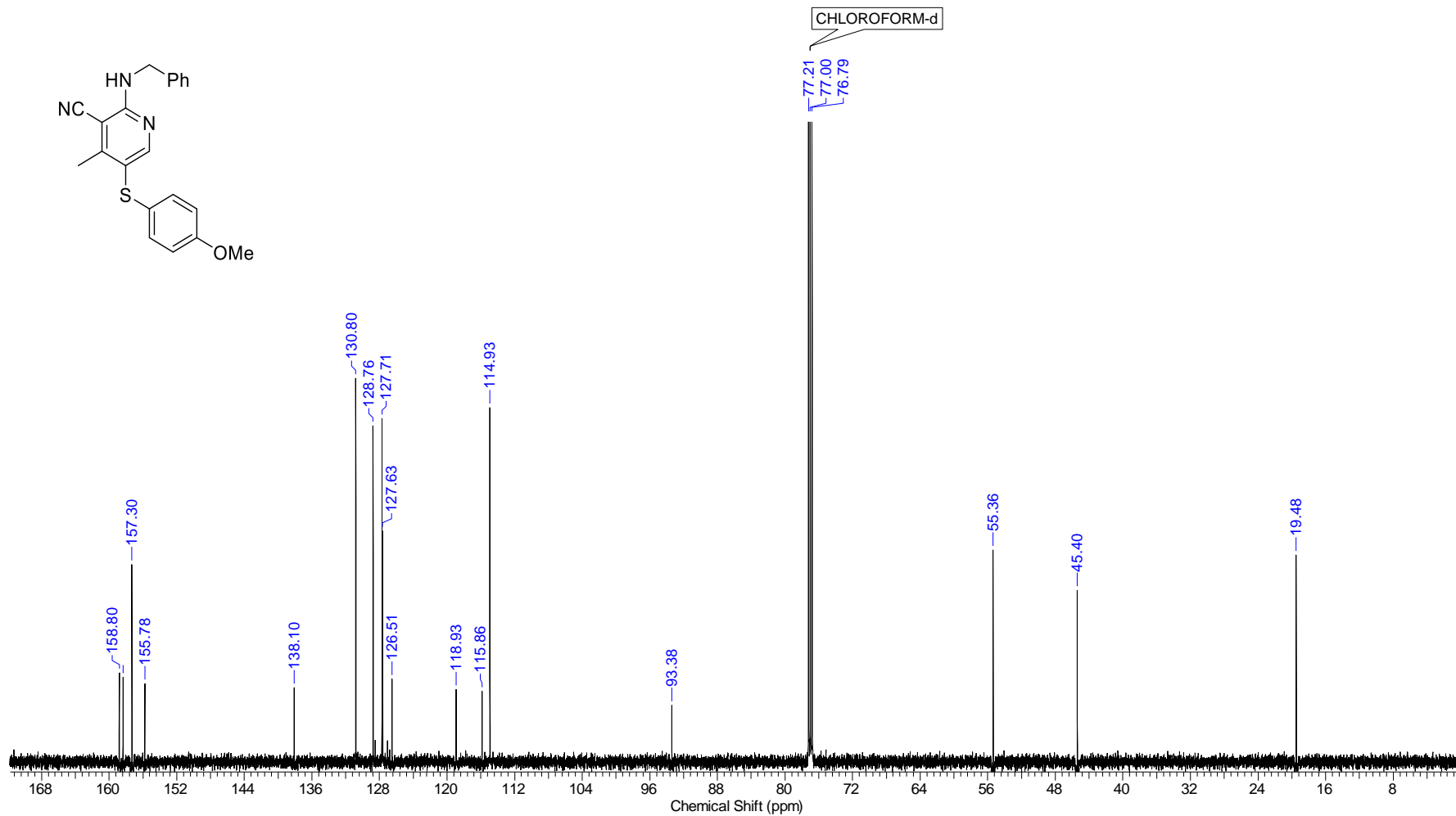
Continuous Conditions Applied to Hazardous Reactions and Fluorophores Synthesis with Photophysics Studies

Frequency (MHz)	600.01	Nucleus	1H	Number of Transients	16	Origin	spect
Original Points Count	32768	Owner	nmrsu	Points Count	65536	Pulse Sequence	zg30
Receiver Gain	176.24	SW(cyclical) (Hz)	12019.23	Solvent	CDCl3	Spectrum Offset (Hz)	3695.4729
Spectrum Type	STANDARD	Sweep Width (Hz)	12019.05	Temperature (degree C)	23.373	Acquisition Time (sec)	2.7263



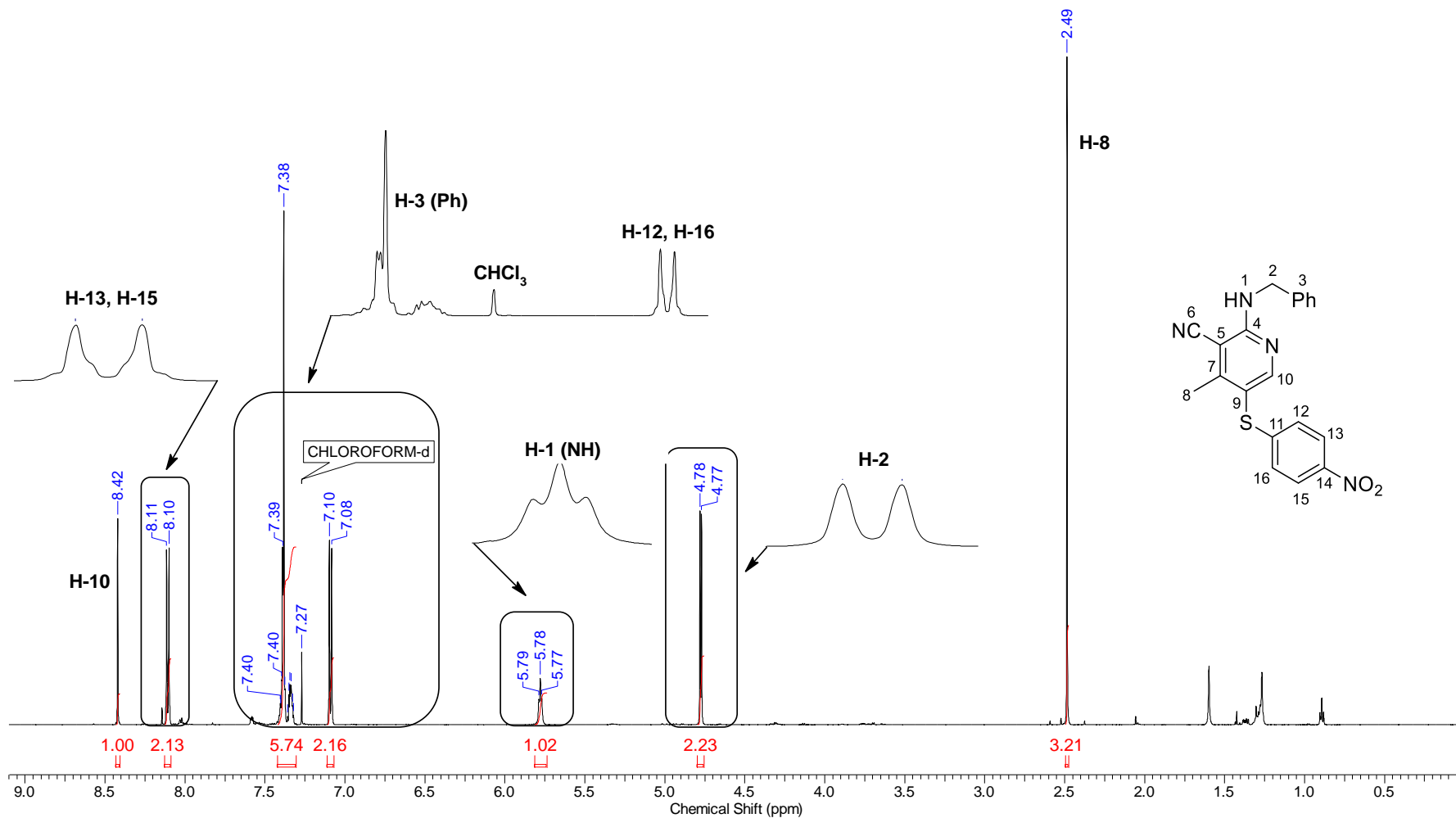
Continuous Conditions Applied to Hazardous Reactions and Fluorophores Synthesis with Photophysics Studies

Nucleus	13C	Number of Transients	128	Origin	spect	Original Points Count	32768
Owner	nmrsl	Points Count	32768	Pulse Sequence	zgpg30	Receiver Gain	199.73
SW(cyclical) (Hz)	36231.88	Solvent	CDCl3	Spectrum Offset (Hz)	15080.7305	Spectrum Type	STANDARD
Sweep Width (Hz)	36230.78	Temperature (degree C)	24.028	Frequency (MHz)	150.87	Acquisition Time (sec)	0.9044



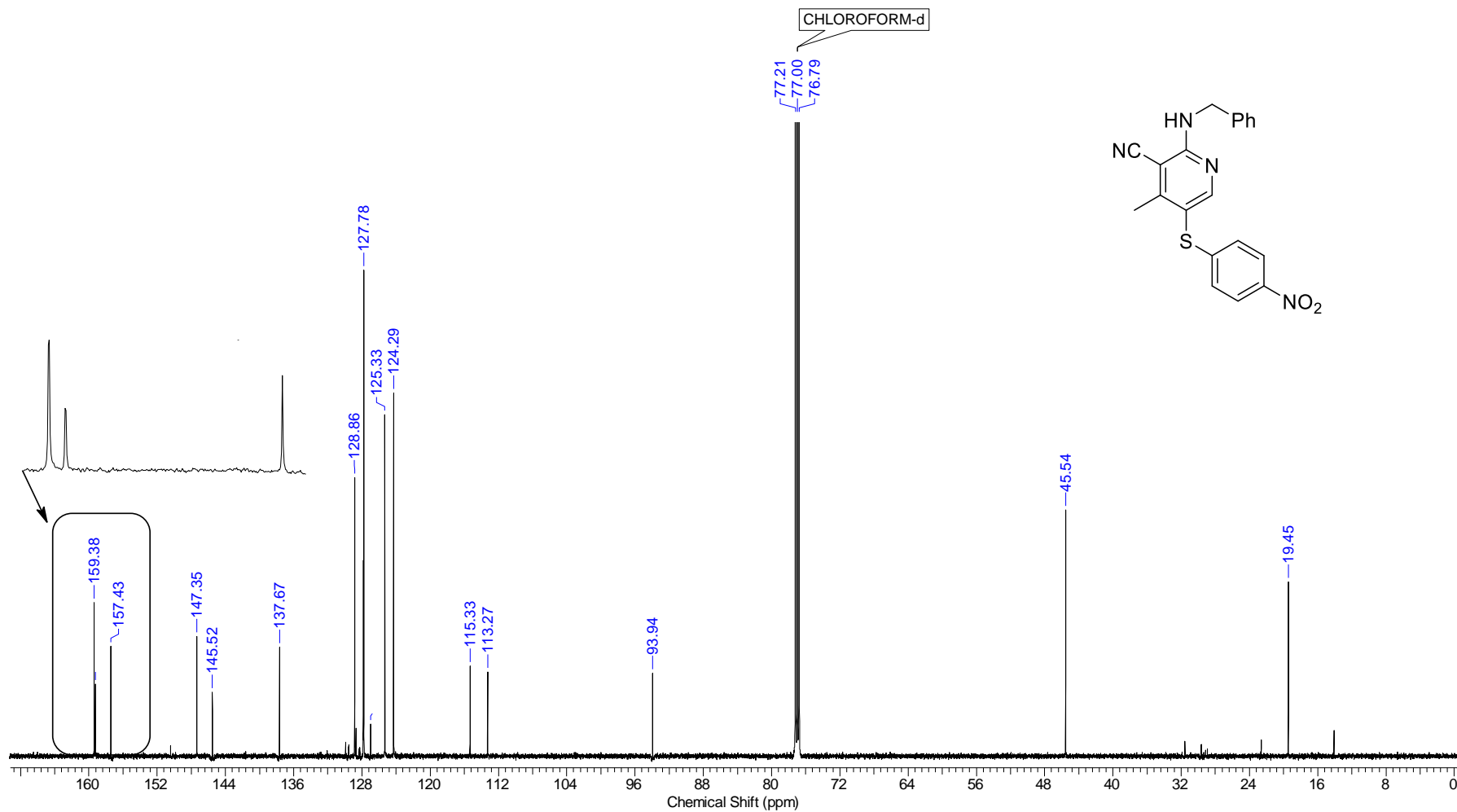
Continuous Conditions Applied to Hazardous Reactions and Fluorophores Synthesis with Photophysics Studies

Frequency (MHz)	600.01	Nucleus	1H	Number of Transients	16	Origin	spect
Original Points Count	32768	Owner	nmsu	Points Count	65536	Pulse Sequence	zg30
Receiver Gain	199.73	SW(cyclical) (Hz)	12019.23	Solvent	CDCl3	Spectrum Offset (Hz)	3695.6567
Spectrum Type	STANDARD	Sweep Width (Hz)	12019.05	Temperature (degree C)	23.216	Acquisition Time (sec)	2.7263



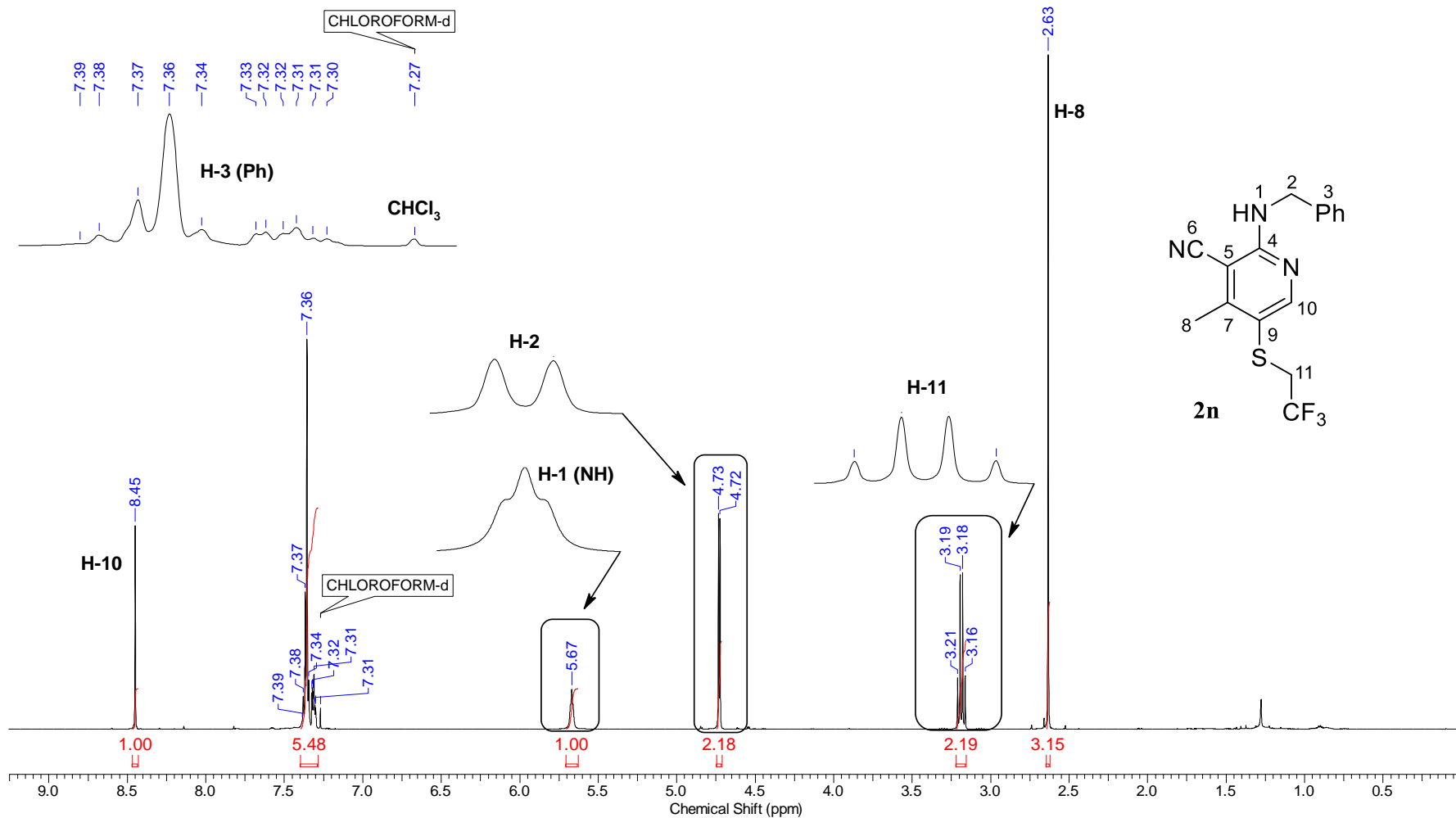
Continuous Conditions Applied to Hazardous Reactions and Fluorophores Synthesis with Photophysics Studies

Nucleus	13C	Number of Transients	2500	Origin	spect	Original Points Count	32768
Owner	nmsu	Points Count	32768	Pulse Sequence	zgpg30	Receiver Gain	199.73
SW(cyclical) (Hz)	36231.88	Solvent	CDCl3	Spectrum Offset (Hz)	15081.8369	Spectrum Type	STANDARD
Sweep Width (Hz)	36230.78	Temperature (degree C)	25.457	Frequency (MHz)	150.87	Acquisition Time (sec)	0.9044



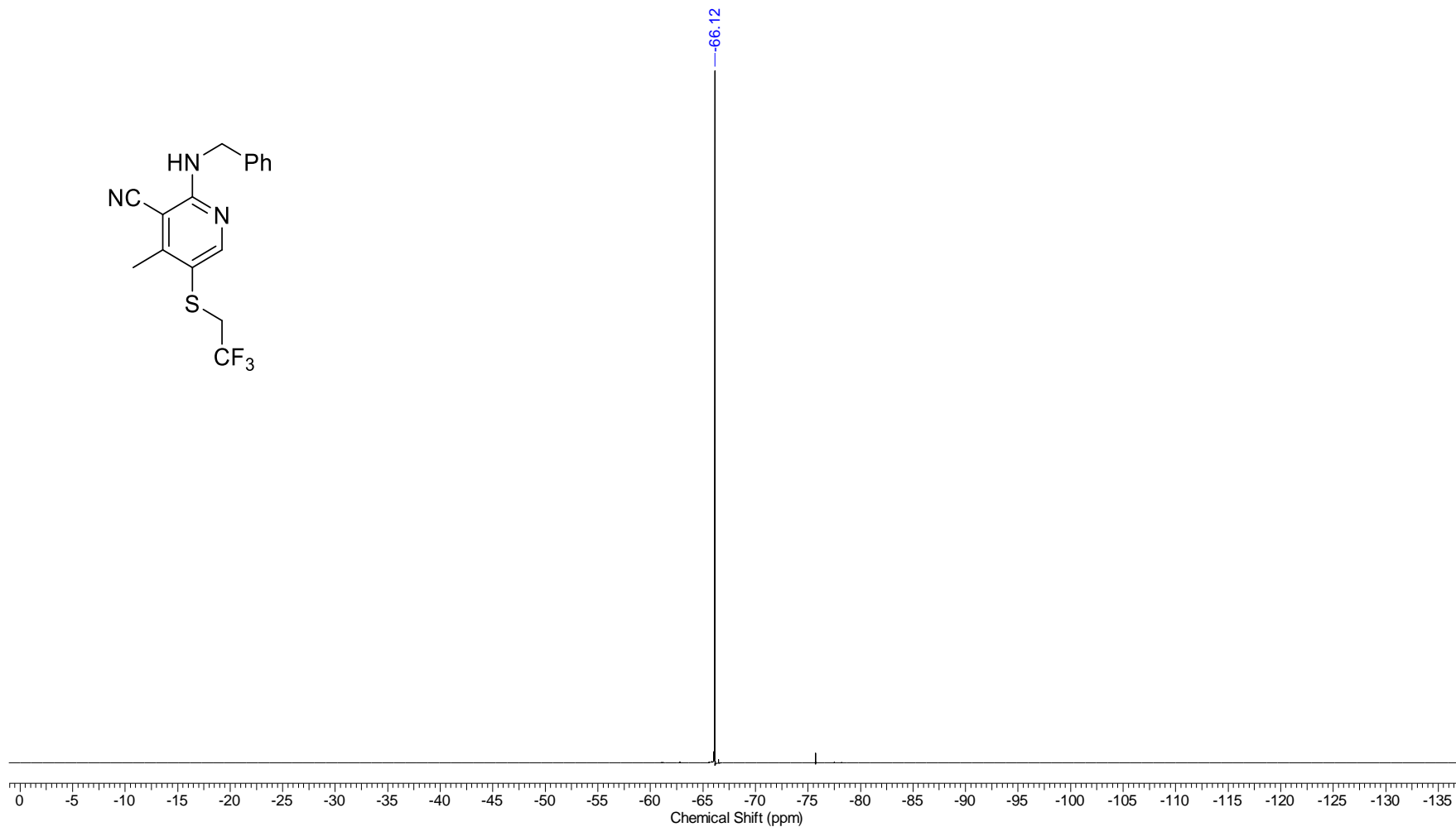
Continuous Conditions Applied to Hazardous Reactions and Fluorophores Synthesis with Photophysics Studies

Frequency (MHz)	600.01	Nucleus	1H	Number of Transients	16	Origin	spect
Original Points Count	32768	Owner	nmsu	Points Count	65536	Pulse Sequence	zg30
Receiver Gain	89.69	SW(cyclical) (Hz)	12019.23	Solvent	CDCl3	Spectrum Offset (Hz)	3695.6567
Spectrum Type	STANDARD	Sweep Width (Hz)	12019.05	Temperature (degree C)	23.591	Acquisition Time (sec)	2.7263



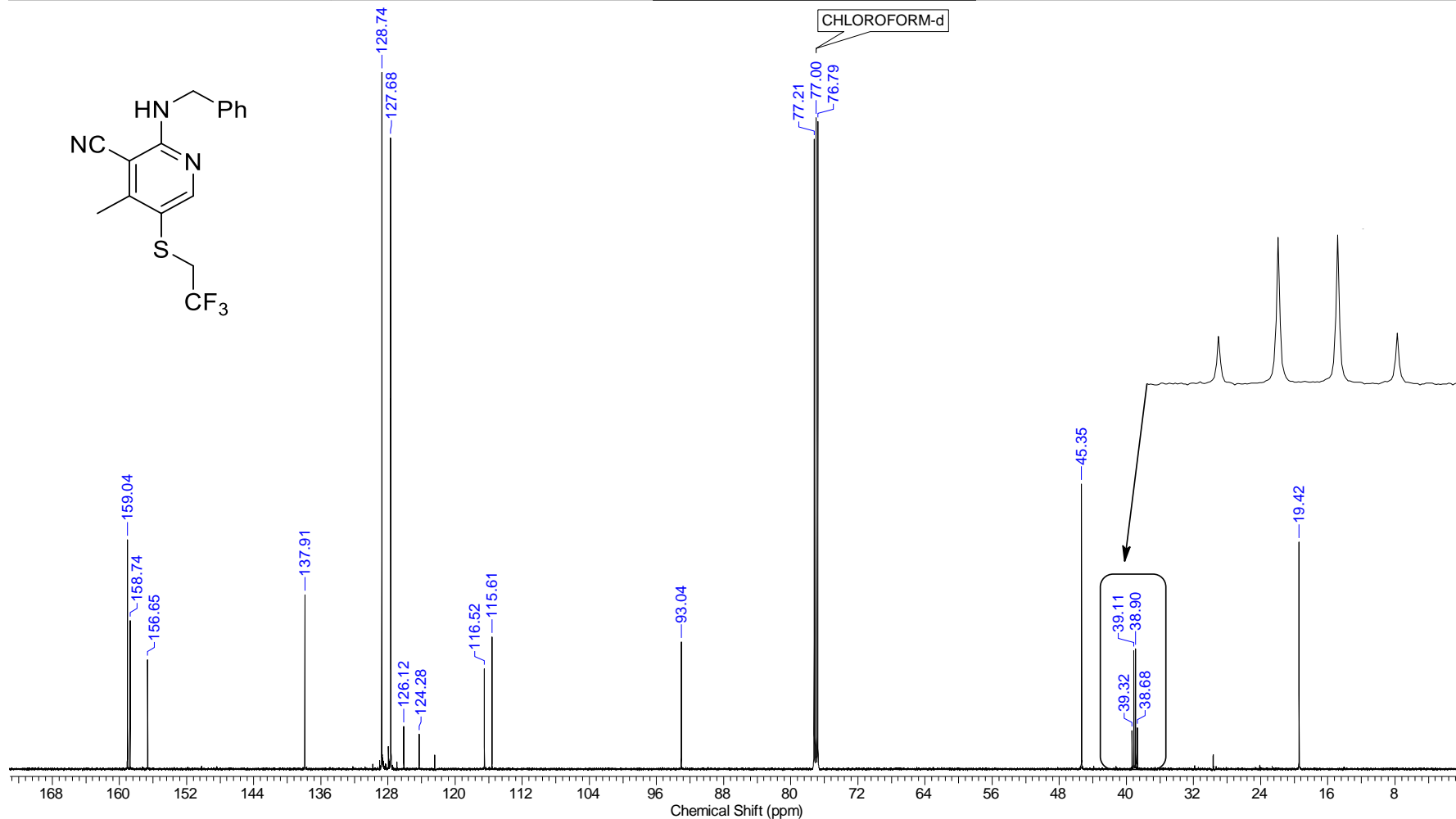
Continuous Conditions Applied to Hazardous Reactions and Fluorophores Synthesis with Photophysics Studies

Nucleus	19F	Number of Transients	32	Origin	spect	Original Points Count	65536
Owner	nmsu	Points Count	65536	Pulse Sequence	zgfhiggn.2	Receiver Gain	199.73
SW(cyclical) (Hz)	133928.58	Solvent	CDCl3	Spectrum Offset (Hz)	-56456.8867	Spectrum Type	STANDARD
Sweep Width (Hz)	133926.53	Temperature (degree C)	24.042	Frequency (MHz)	564.57	Acquisition Time (sec)	0.4893



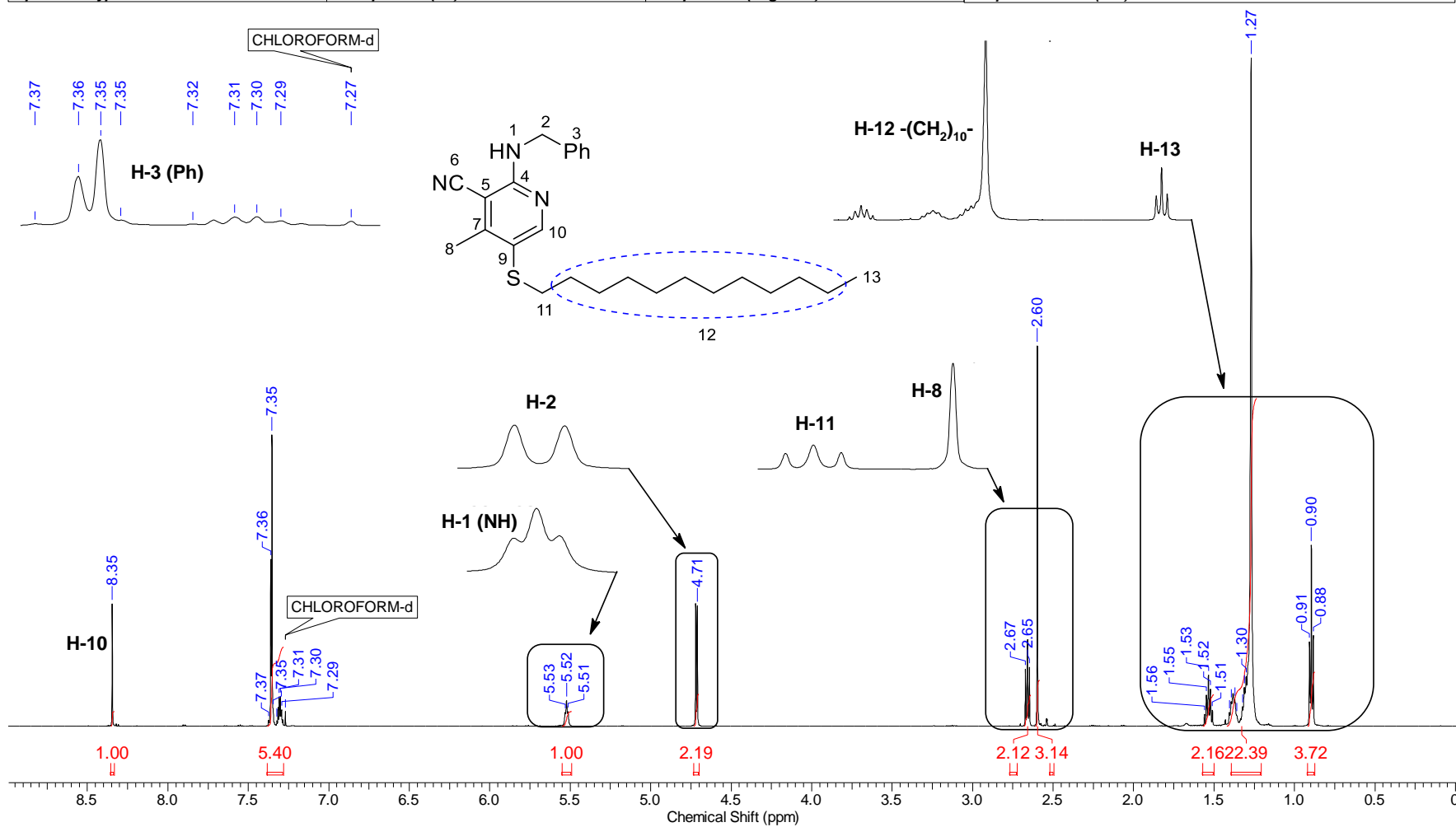
Continuous Conditions Applied to Hazardous Reactions and Fluorophores Synthesis with Photophysics Studies

Nucleus	13C	Number of Transients	2500	Origin	spect	Original Points Count	32768
Owner	nmrsu	Points Count	32768	Pulse Sequence	zgpg30	Receiver Gain	199.73
SW(cyclical) (Hz)	36231.88	Solvent	CDCl3	Spectrum Offset (Hz)	15077.4131	Spectrum Type	STANDARD
Sweep Width (Hz)	36230.78	Temperature (degree C)	25.309	Frequency (MHz)	150.87	Acquisition Time (sec)	0.9044



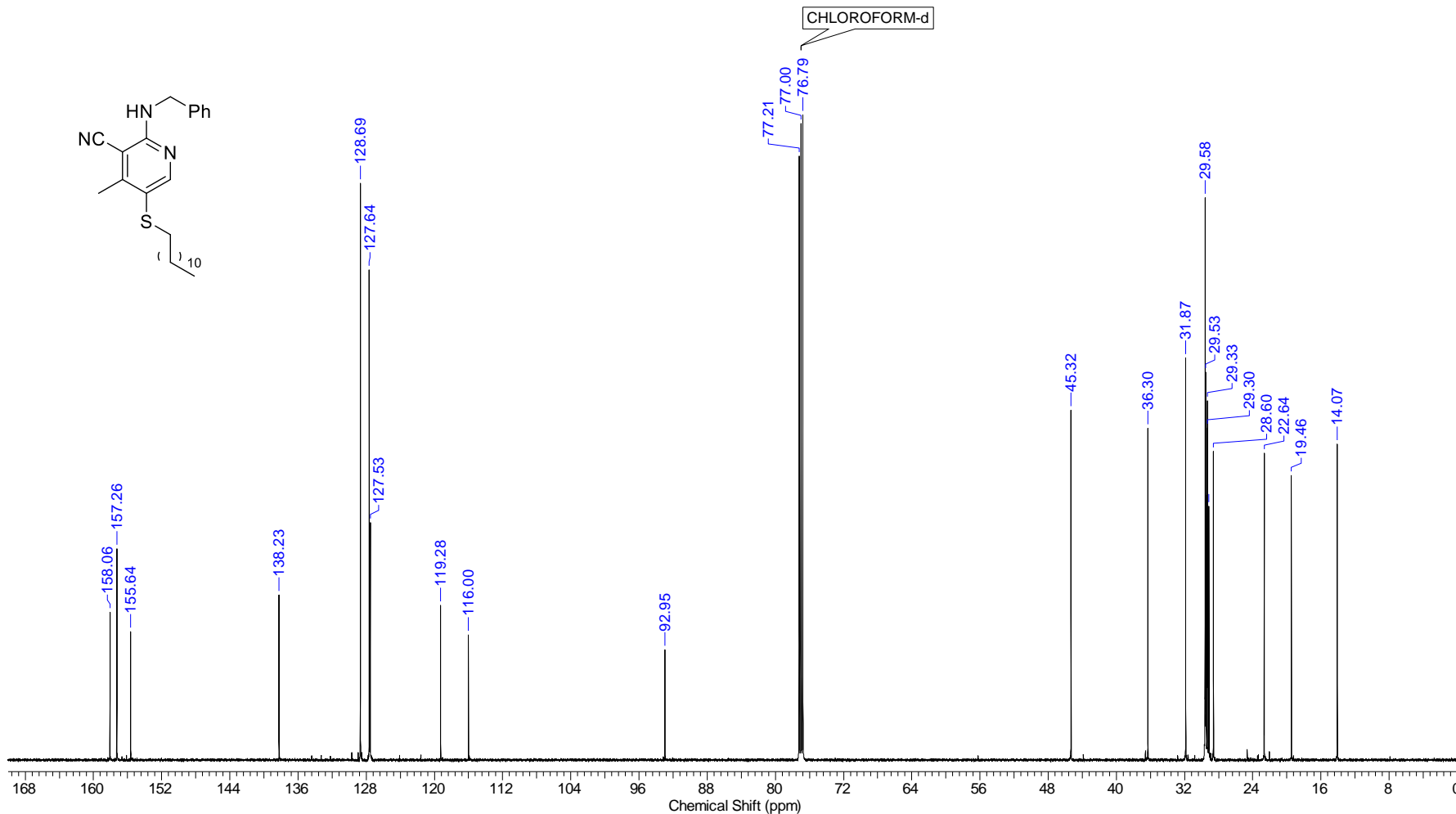
Continuous Conditions Applied to Hazardous Reactions and Fluorophores Synthesis with Photophysics Studies

Frequency (MHz)	600.01	Nucleus	1H	Number of Transients	16	Origin	spect
Original Points Count	32768	Owner	nmrsu	Points Count	65536	Pulse Sequence	zg30
Receiver Gain	31.31	SW(cyclical) (Hz)	12019.23	Solvent	CDCl3	Spectrum Offset (Hz)	3695.4729
Spectrum Type	STANDARD	Sweep Width (Hz)	12019.05	Temperature (degree C)	23.587	Acquisition Time (sec)	2.7263



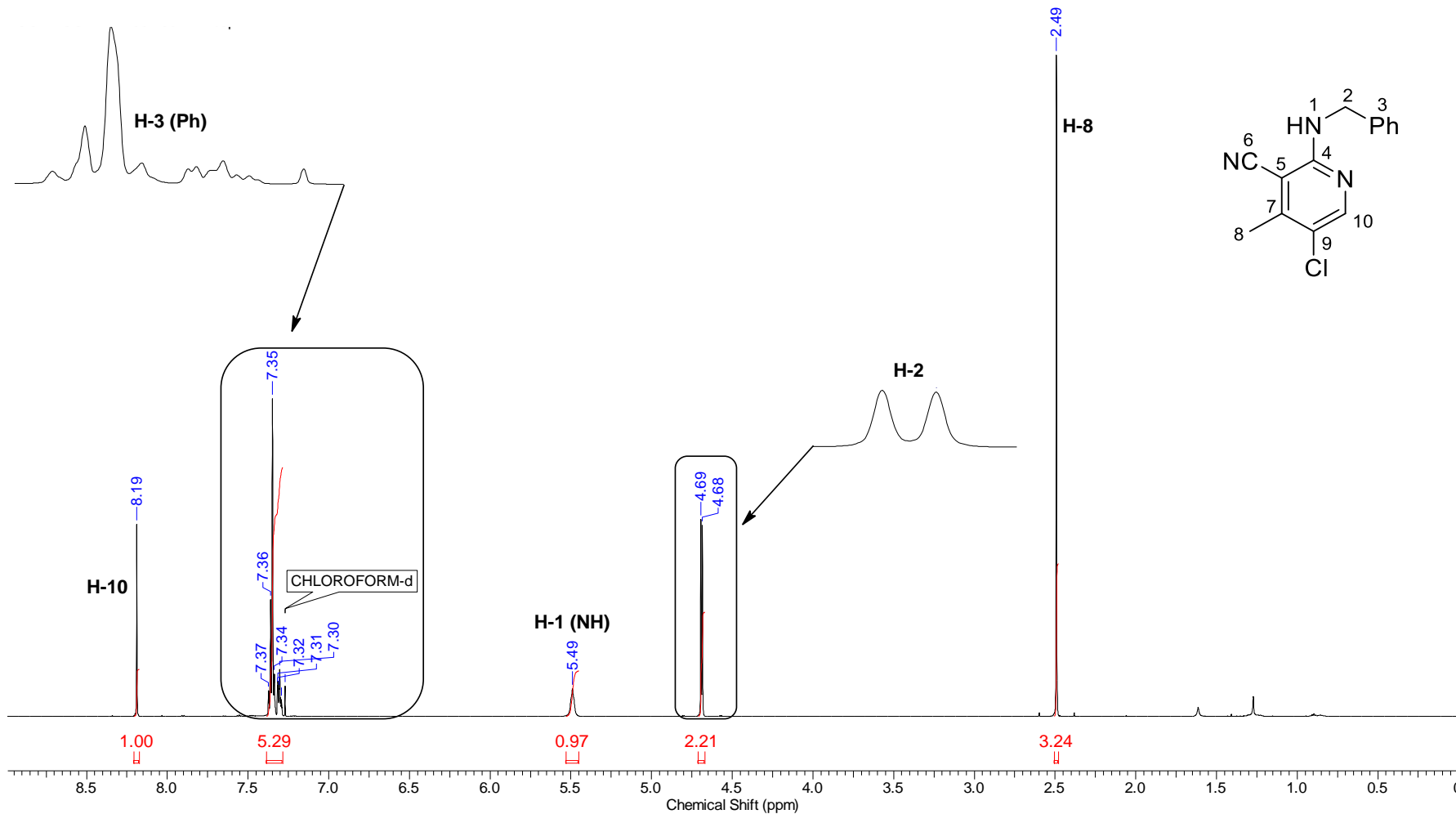
Continuous Conditions Applied to Hazardous Reactions and Fluorophores Synthesis with Photophysics Studies

Nucleus	13C	Number of Transients	2500	Origin	spect	Original Points Count	32768
Owner	nmrsl	Points Count	32768	Pulse Sequence	zgpg30	Receiver Gain	199.73
SW(cyclical) (Hz)	36231.88	Solvent	CDCl3	Spectrum Offset (Hz)	15077.4131	Spectrum Type	STANDARD
Sweep Width (Hz)	36230.78	Temperature (degree C)	25.263	Acquisition Time (sec)	0.9044	Frequency (MHz)	150.87



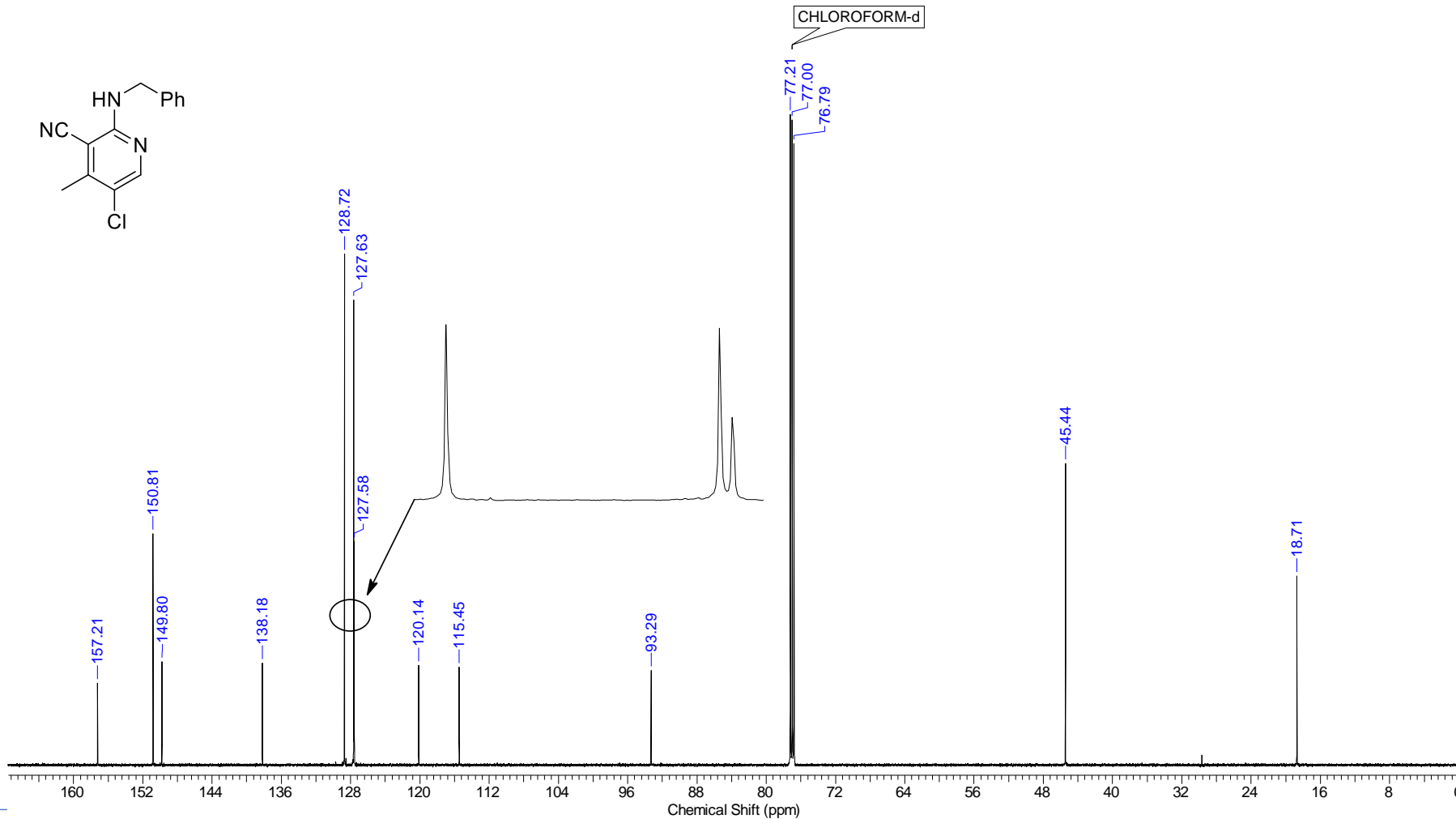
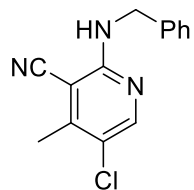
Continuous Conditions Applied to Hazardous Reactions and Fluorophores Synthesis with Photophysics Studies

Frequency (MHz)	600.01	Nucleus	¹ H	Number of Transients	16	Origin	spect
Original Points Count	32768	Owner	nmsu	Points Count	65536	Pulse Sequence	zg30
Receiver Gain	135.67	SW(cyclical) (Hz)	12019.23	Solvent	CDCl ₃	Spectrum Offset (Hz)	3695.6567
Spectrum Type	STANDARD	Sweep Width (Hz)	12019.05	Temperature (degree C)	23.571	Acquisition Time (sec)	2.7263



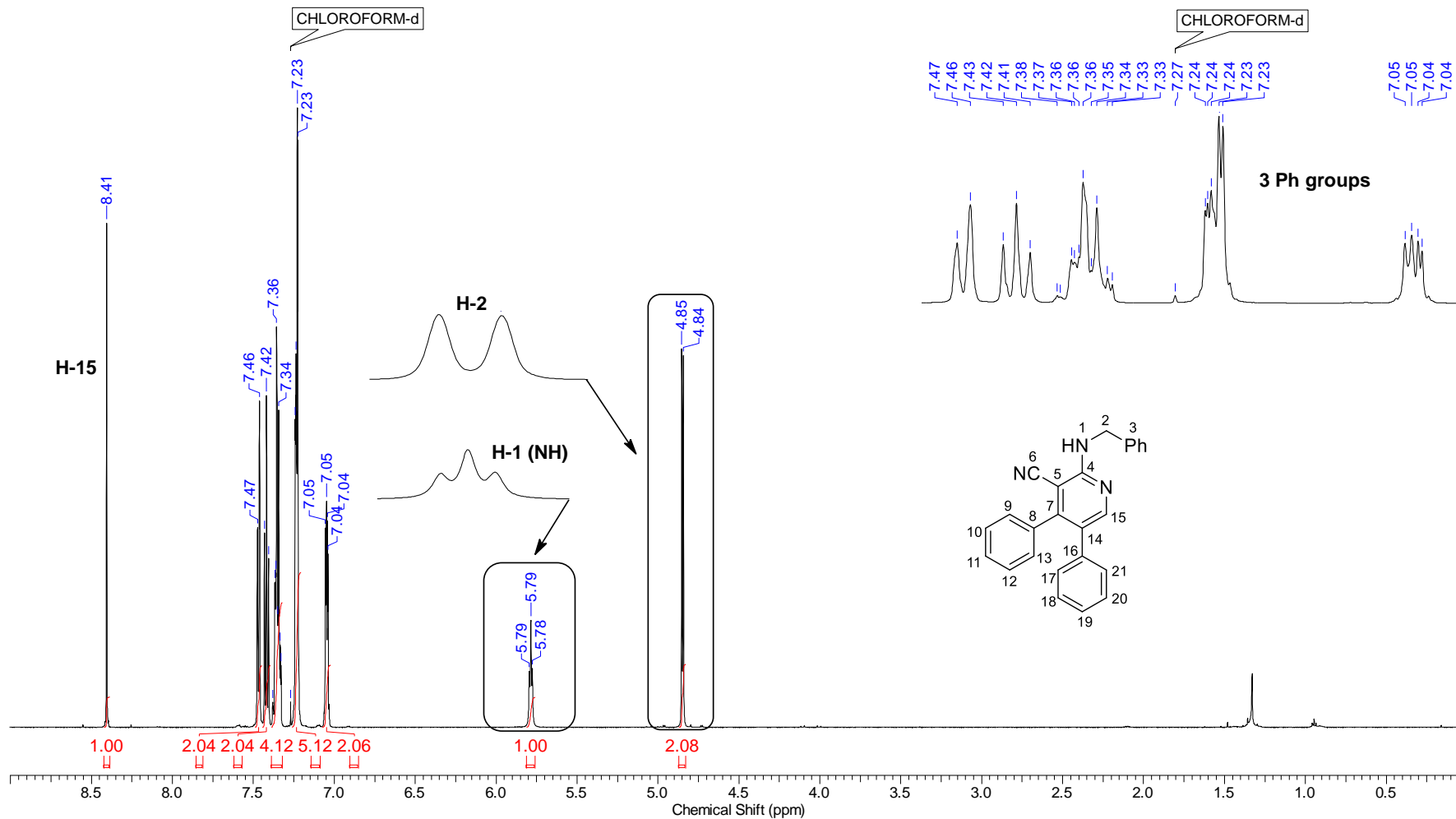
Continuous Conditions Applied to Hazardous Reactions and Fluorophores Synthesis with Photophysics Studies

Nucleus	13C	Number of Transients	2500	Origin	spect	Original Points Count	32768
Owner	nmrsu	Points Count	32768	Pulse Sequence	zpgg30	Receiver Gain	199.73
SW(cyclical) (Hz)	36231.88	Solvent	CDCl3	Spectrum Offset (Hz)	15080.7305	Spectrum Type	STANDARD
Sweep Width (Hz)	36230.78	Temperature (degree C)	25.337	Frequency (MHz)	150.87	Acquisition Time (sec)	0.9044



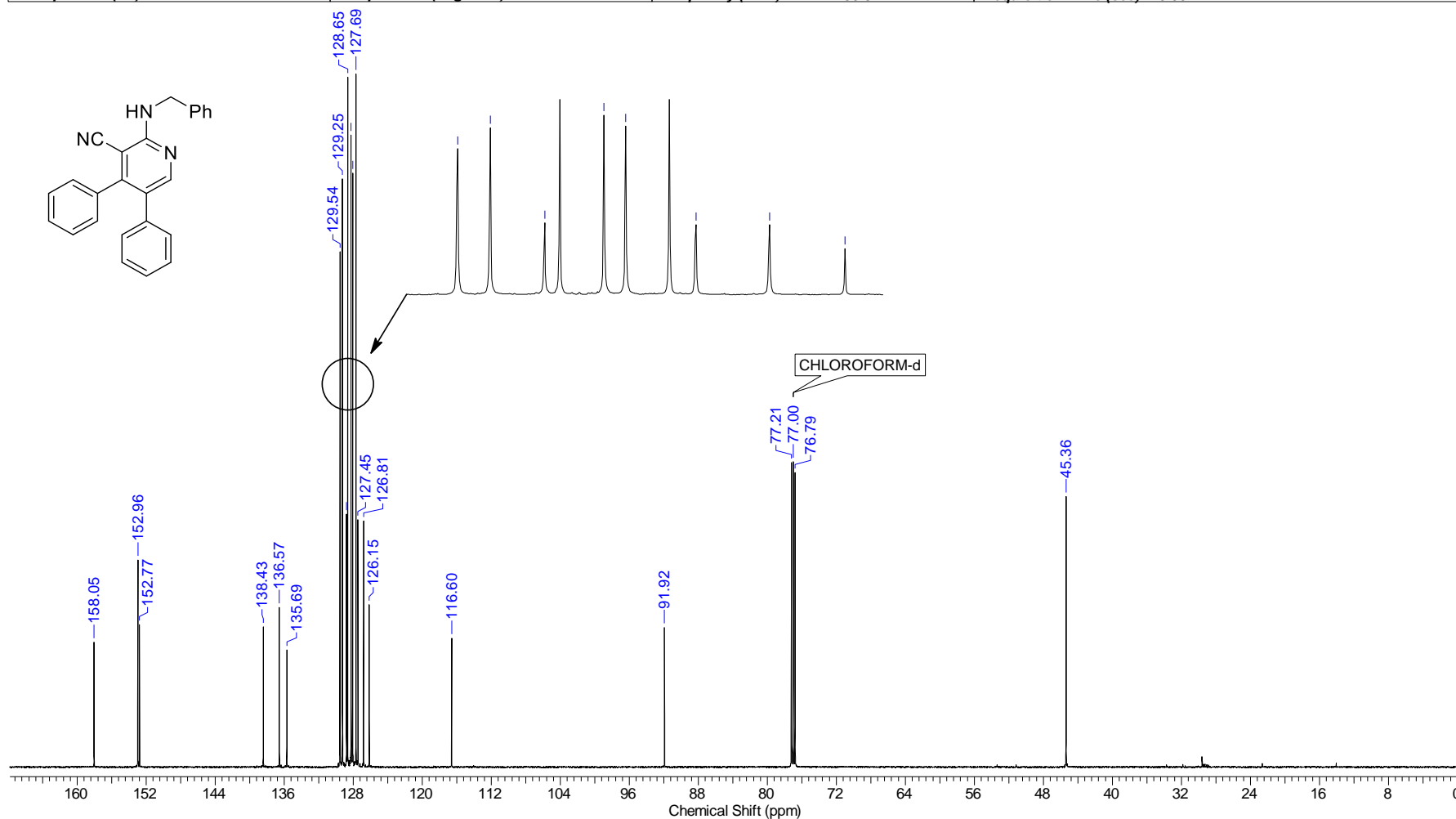
Continuous Conditions Applied to Hazardous Reactions and Fluorophores Synthesis with Photophysics Studies

Frequency (MHz)	600.01	Nucleus	1H	Number of Transients	16	Origin	spect
Original Points Count	32768	Owner	nmsu	Points Count	65536	Pulse Sequence	zg30
Receiver Gain	31.31	SW(cyclical) (Hz)	12019.23	Solvent	CDCl3	Spectrum Offset (Hz)	3695.6575
Spectrum Type	STANDARD	Sweep Width (Hz)	12019.05	Temperature (degree C)	23.553	Acquisition Time (sec)	2.7263



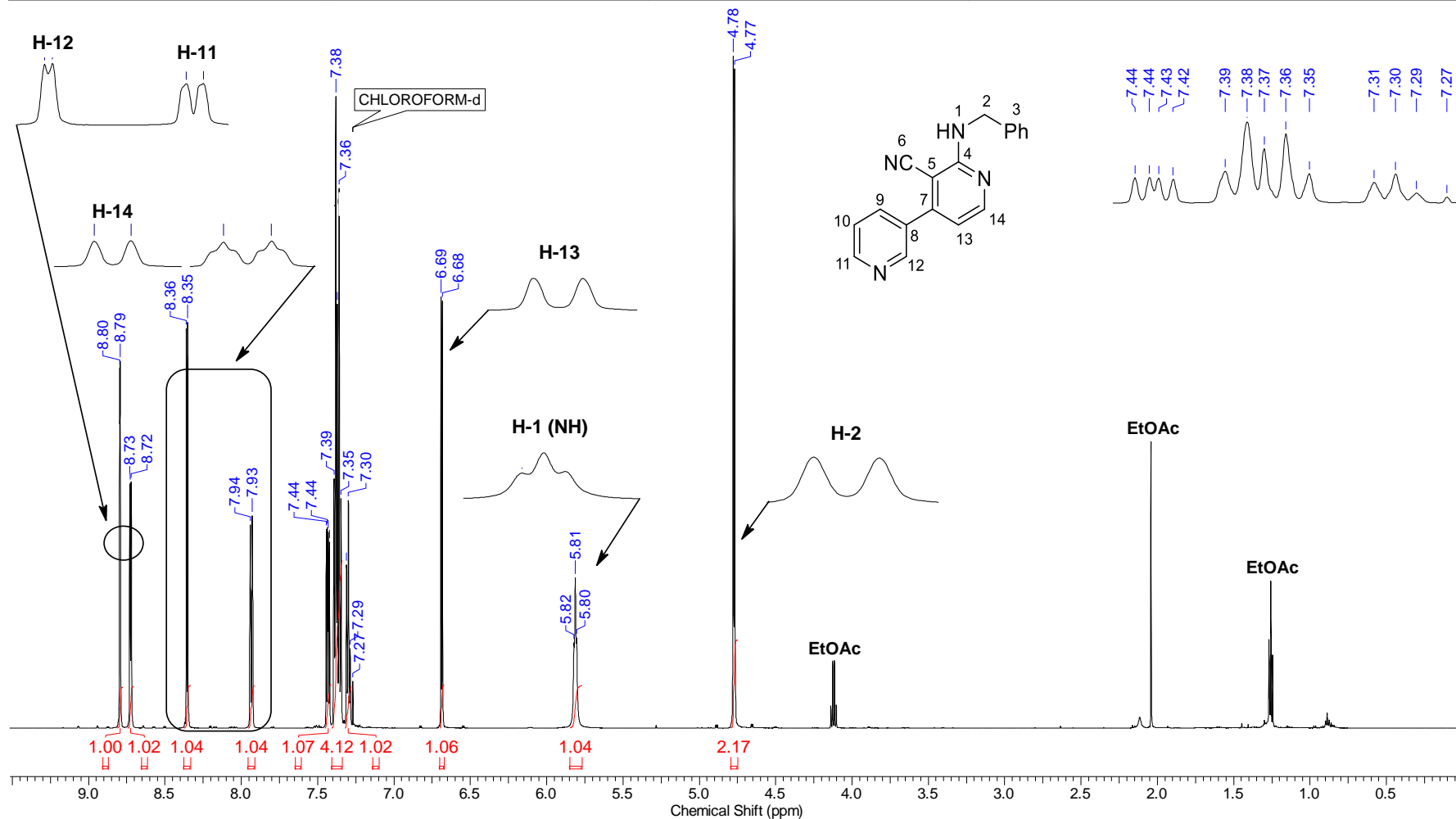
Continuous Conditions Applied to Hazardous Reactions and Fluorophores Synthesis with Photophysics Studies

Nucleus	13C	Number of Transients	2500	Origin	spect	Original Points Count	32768
Owner	nmsu	Points Count	32768	Pulse Sequence	zgpg30	Receiver Gain	199.73
SW(cyclical) (Hz)	36231.88	Solvent	CDCl3	Spectrum Offset (Hz)	15061.9326	Spectrum Type	STANDARD
Sweep Width (Hz)	36230.78	Temperature (degree C)	25.358	Frequency (MHz)	150.87	Acquisition Time (sec)	0.9044



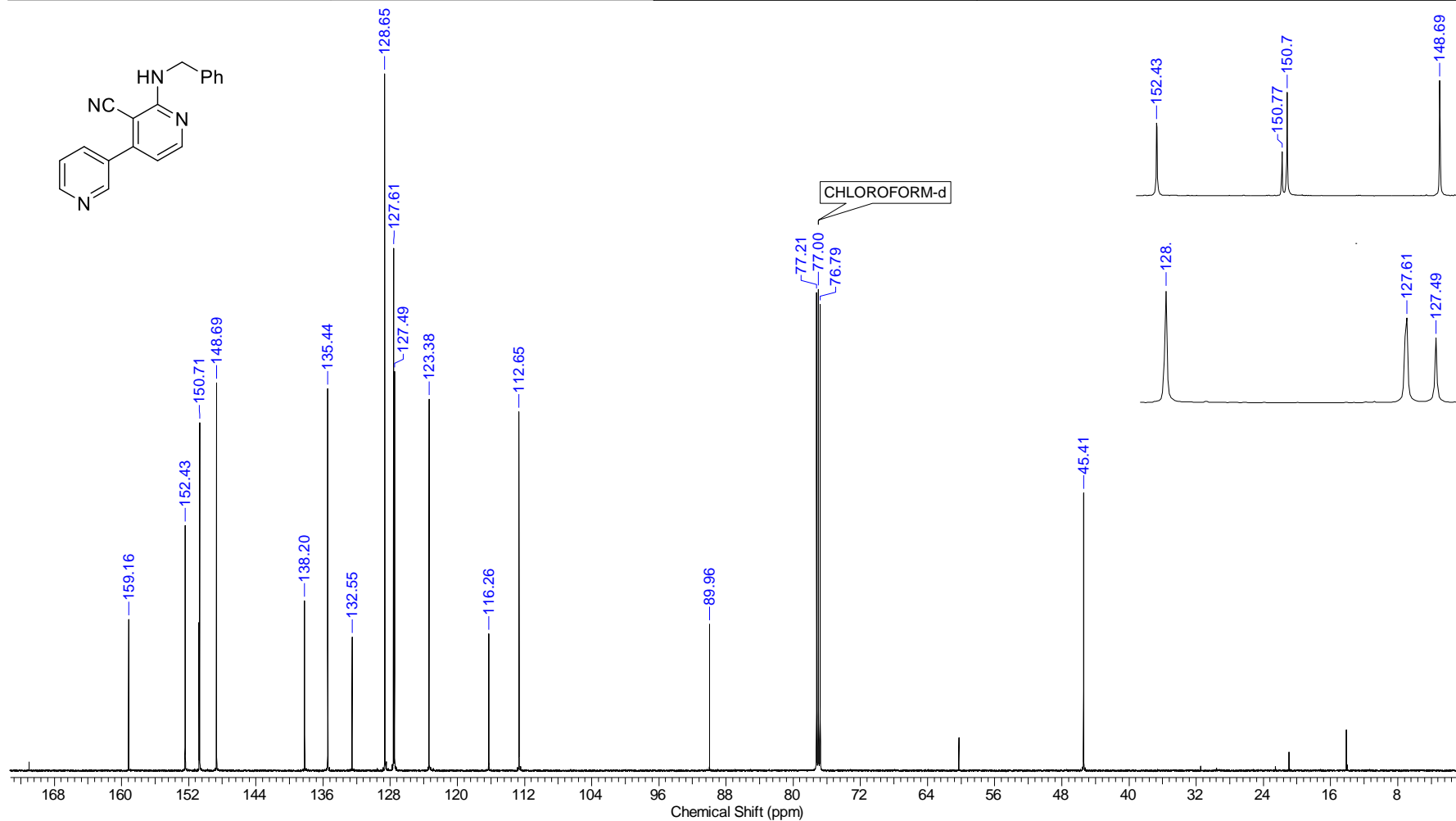
Continuous Conditions Applied to Hazardous Reactions and Fluorophores Synthesis with Photophysics Studies

Frequency (MHz)	600.01	Nucleus	¹ H	Number of Transients	16	Origin	spect
Original Points Count	32768	Owner	nmrsu	Points Count	65536	Pulse Sequence	zg30
Receiver Gain	68.55	SW(cyclical) (Hz)	12019.23	Solvent	CDCl ₃	Spectrum Offset (Hz)	3695.4729
Spectrum Type	STANDARD	Sweep Width (Hz)	12019.05	Temperature (degree C)	24.167	Acquisition Time (sec)	2.7263



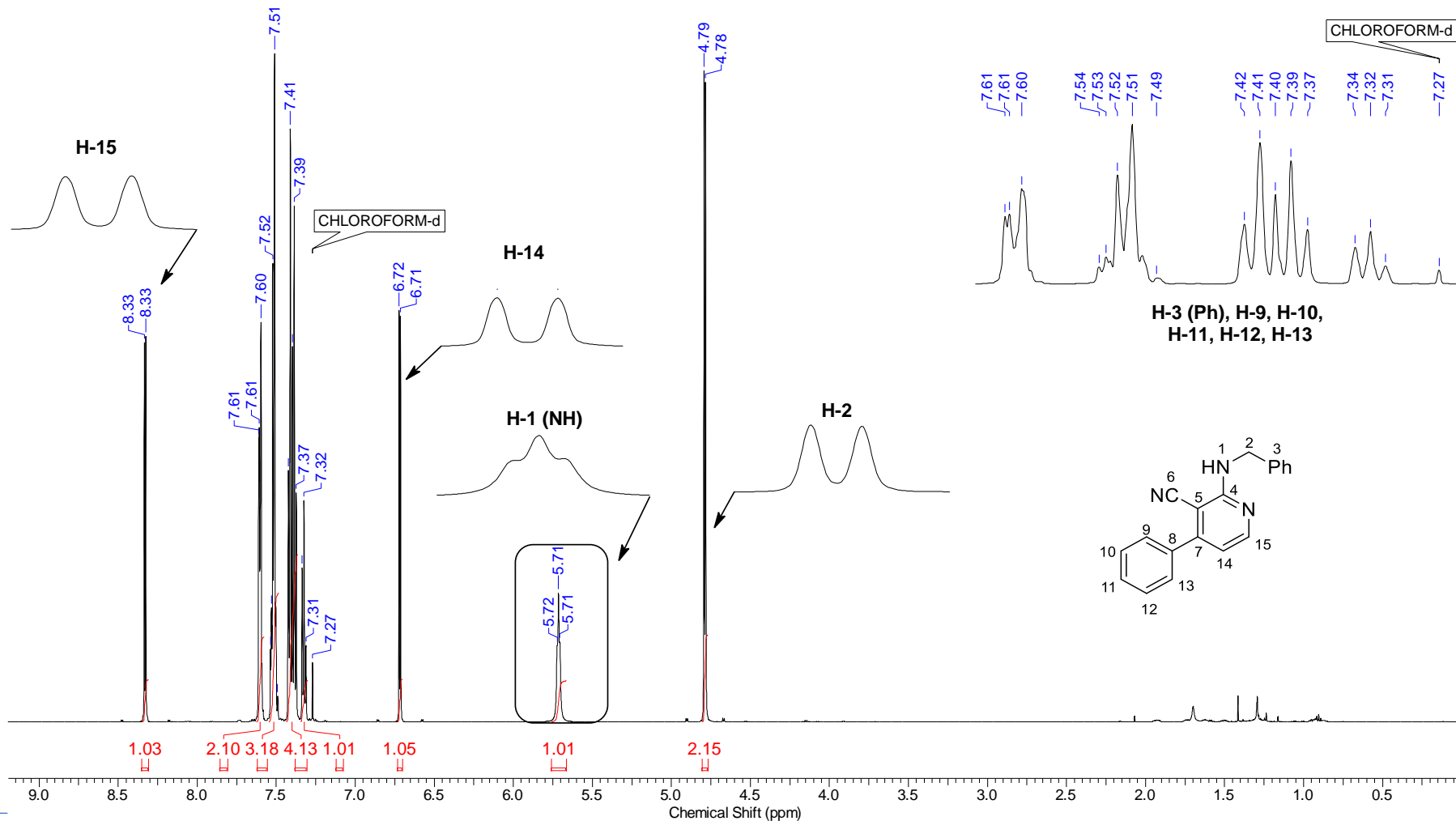
Continuous Conditions Applied to Hazardous Reactions and Fluorophores Synthesis with Photophysics Studies

Nucleus	13C	Number of Transients	2500	Origin	spect	Original Points Count	32768
Owner	nmsu	Points Count	32768	Pulse Sequence	zgpg30	Receiver Gain	199.73
SW(cyclical) (Hz)	36231.88	Solvent	CDCl3	Spectrum Offset (Hz)	15068.5674	Spectrum Type	STANDARD
Sweep Width (Hz)	36230.78	Temperature (degree C)	25.554	Frequency (MHz)	150.87	Acquisition Time (sec)	0.9044



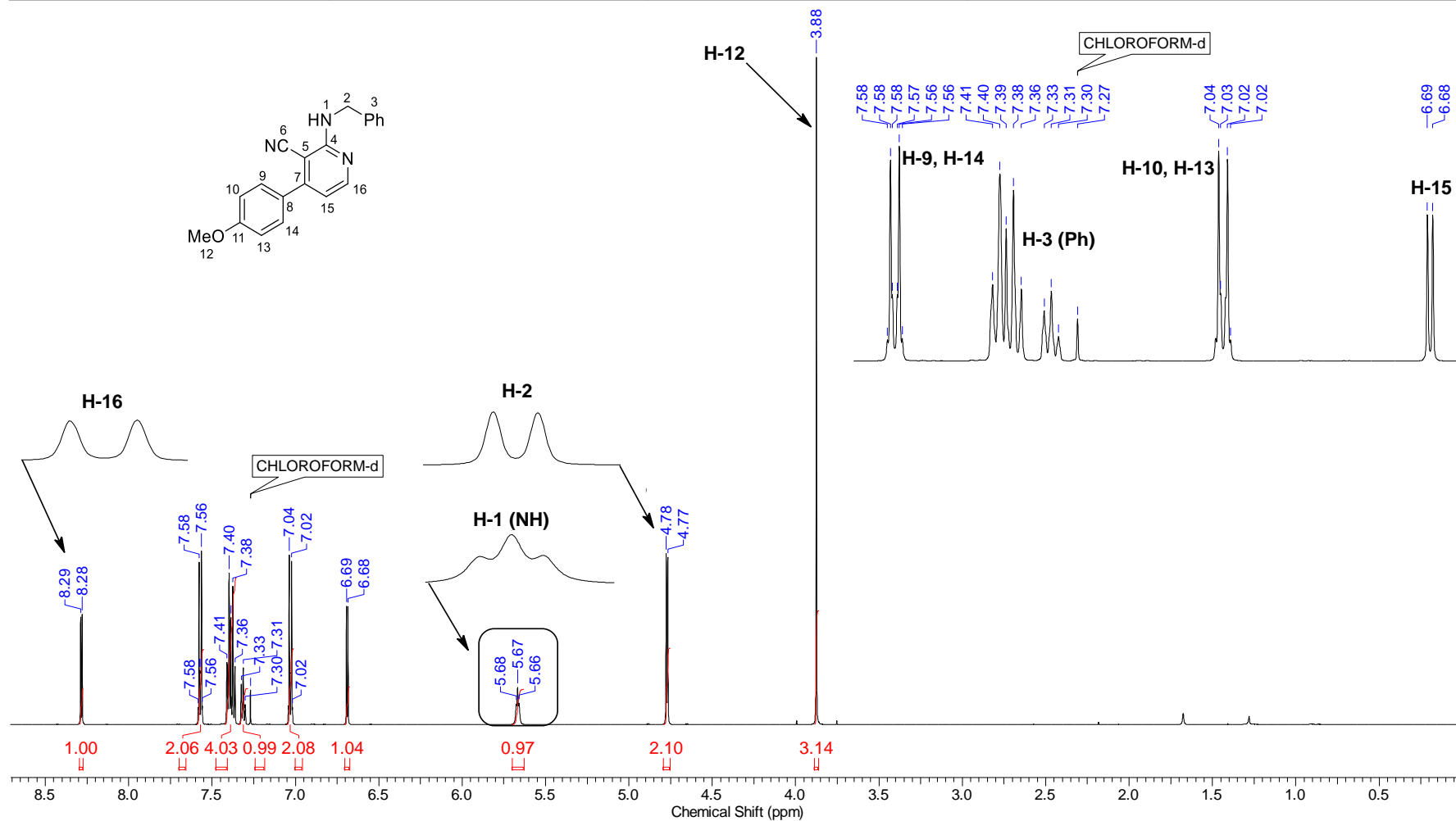
Continuous Conditions Applied to Hazardous Reactions and Fluorophores Synthesis with Photophysics Studies

Frequency (MHz)	600.01	Nucleus	1H	Number of Transients	16	Origin	spect
Original Points Count	32768	Owner	nmrsu	Points Count	65536	Pulse Sequence	zg30
Receiver Gain	78.64	SW(cyclical) (Hz)	12019.23	Solvent	CDCl3	Spectrum Offset (Hz)	3695.6567
Spectrum Type	STANDARD	Sweep Width (Hz)	12019.05	Temperature (degree C)	23.547	Acquisition Time (sec)	2.7263



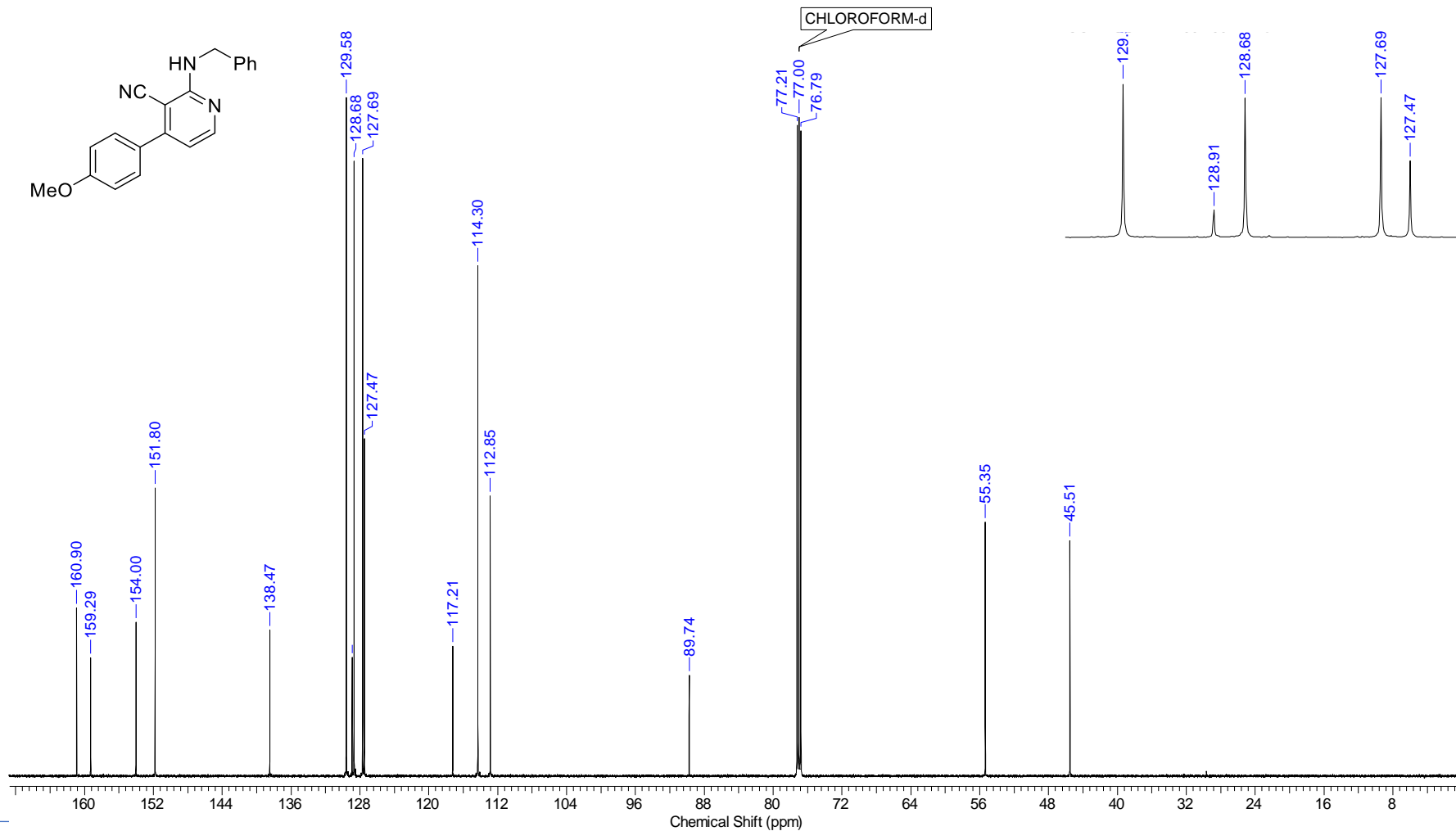
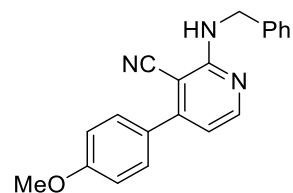
Continuous Conditions Applied to Hazardous Reactions and Fluorophores Synthesis with Photophysics Studies

Frequency (MHz)	600.01	Nucleus	¹ H	Number of Transients	16	Origin	spect
Original Points Count	32768	Owner	nmsu	Points Count	65536	Pulse Sequence	zg30
Receiver Gain	99.50	SW(cyclical) (Hz)	12019.23	Solvent	CDCl ₃	Spectrum Offset (Hz)	3695.4729
Spectrum Type	STANDARD	Sweep Width (Hz)	12019.05	Temperature (degree C)	23.609	Acquisition Time (sec)	2.7263



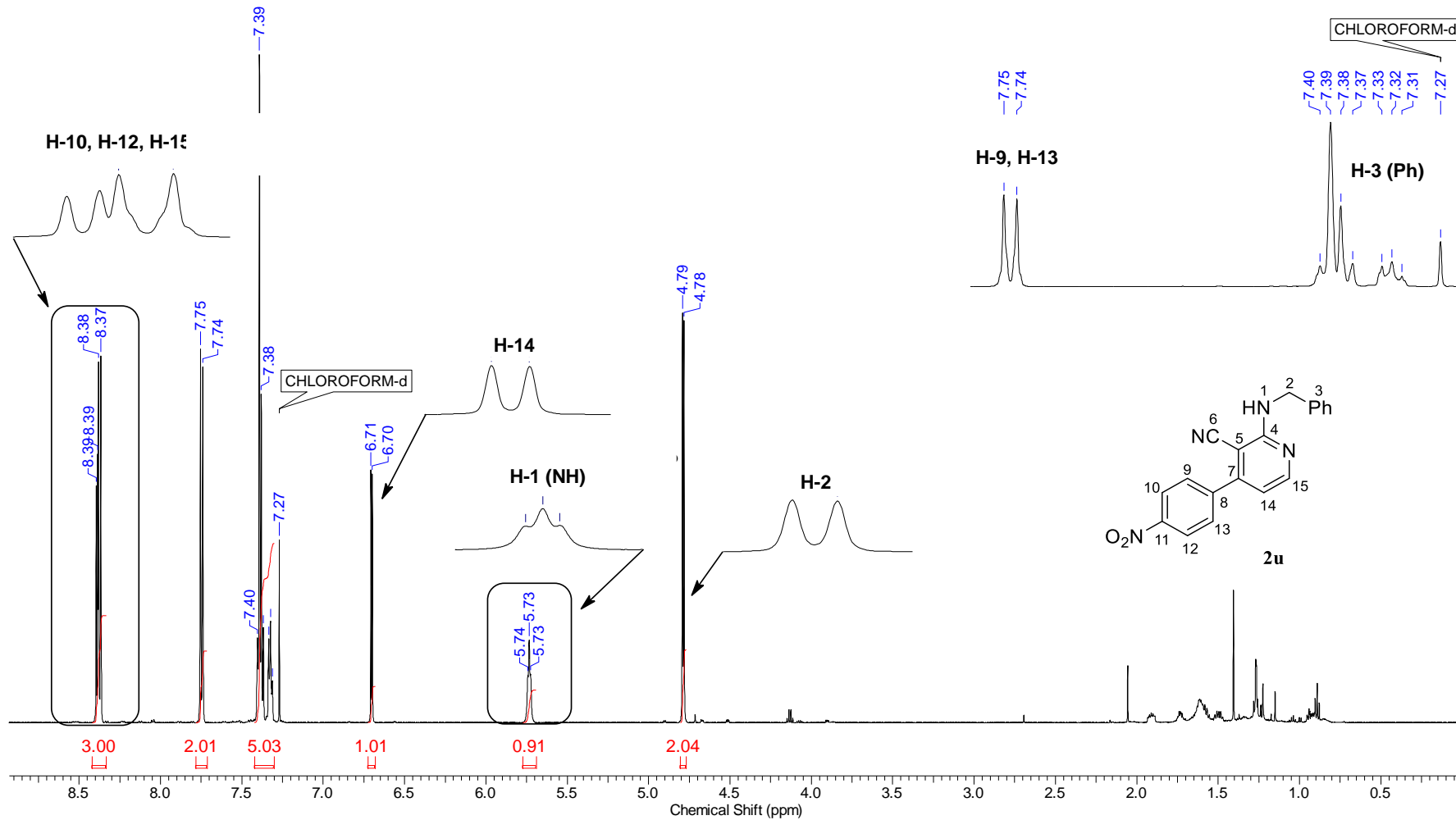
Continuous Conditions Applied to Hazardous Reactions and Fluorophores Synthesis with Photophysics Studies

Nucleus	13C	Number of Transients	2500	Origin	spect	Original Points Count	32768
Owner	nmrsl	Points Count	32768	Pulse Sequence	zgpg30	Receiver Gain	199.73
SW(cyclical) (Hz)	36231.88	Solvent	CDCl3	Spectrum Offset (Hz)	15076.3086	Spectrum Type	STANDARD
Sweep Width (Hz)	36230.78	Temperature (degree C)	25.349	Frequency (MHz)	150.87	Acquisition Time (sec)	0.9044

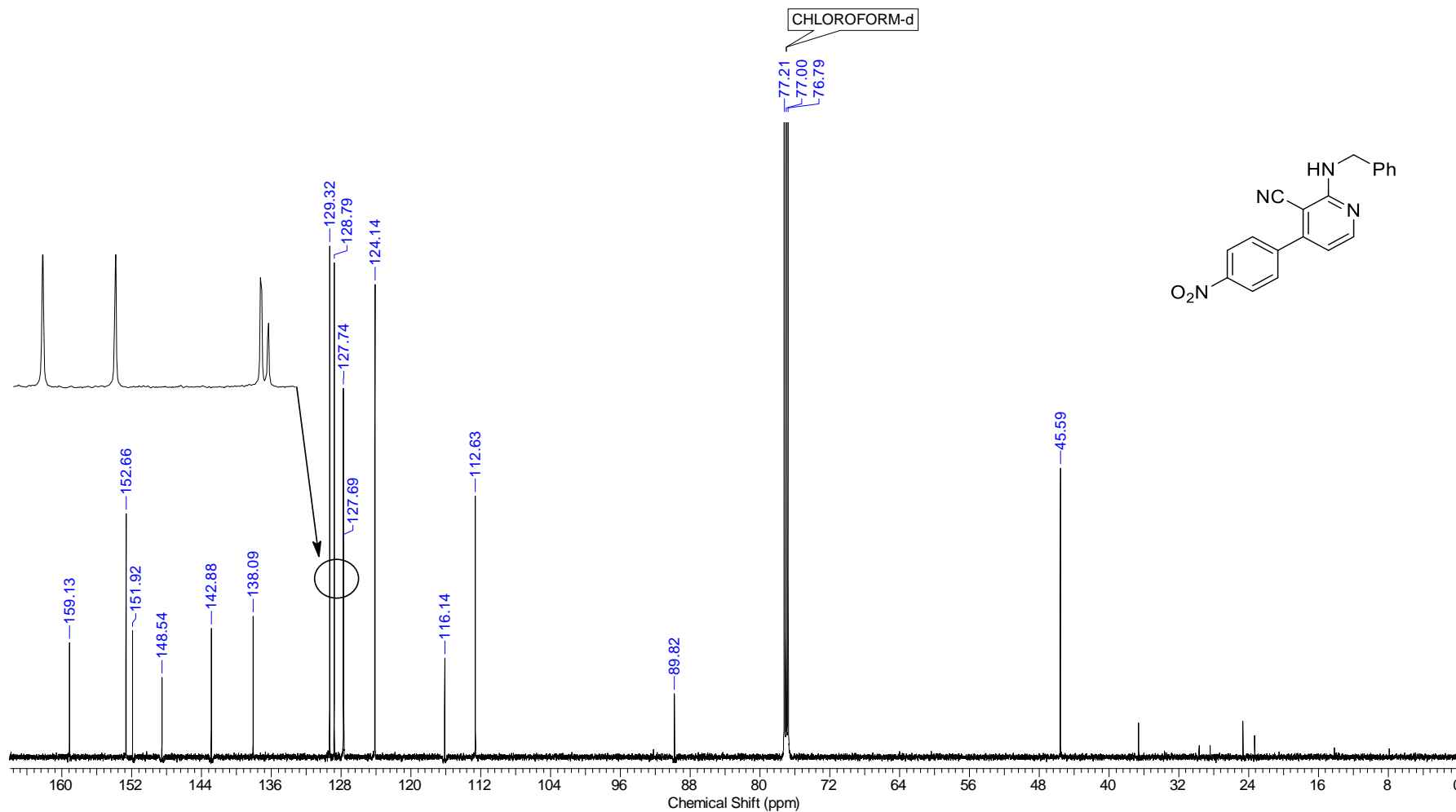


Continuous Conditions Applied to Hazardous Reactions and Fluorophores Synthesis with Photophysics Studies

Frequency (MHz)	600.01	Nucleus	1H	Number of Transients	16	Origin	spect
Original Points Count	32768	Owner	nmrsu	Points Count	65536	Pulse Sequence	zg30
Receiver Gain	199.73	SW(cyclical) (Hz)	12019.23	Solvent	CDCl3	Spectrum Offset (Hz)	3695.4729
Spectrum Type	STANDARD	Sweep Width (Hz)	12019.05	Temperature (degree C)	23.299	Acquisition Time (sec)	2.7263



Nucleus	13C	Number of Transients	2500	Origin	spect	Original Points Count	32768
Owner	nmsu	Points Count	32768	Pulse Sequence	zgpg30	Receiver Gain	199.73
SW(cyclical) (Hz)	36231.88	Solvent	CDCl3	Spectrum Offset (Hz)	15082.9424	Spectrum Type	STANDARD
Sweep Width (Hz)	36230.78	Temperature (degree C)	25.251	Frequency (MHz)	150.87	Acquisition Time (sec)	0.9044



Continuous Conditions Applied to Hazardous Reactions and Fluorophores Synthesis with Photophysics Studies

6. References

- ¹ Bogdan, A. R.; Dombrowski, A. W. *J. Med. Chem.* **2019**, *62*, 14, 6422–6468.
- ² (a) Lau, S.-H.; Galván, A.; Merchant, R. R.; Battilocchio, C.; Souto, J. A.; Berry, M. B.; Ley, S. V. *Org. Lett.* **2015**, *17*, 3218–3221. (b) Baumann, M.; Baxendale, I. R. *Synlett* **2016**, *27*, 159–163.
- ³ (a) Tsubogo, T.; Oyamada, H.; Kobayashi, S. *Nature*, **2015**, *520*, 329–332. (b) Battilocchio, C.; Feist, F.; Hafner, A.; Simon, M.; Tran, D. N.; Allwood, D. M.; Blakemore, D. C.; Ley, S. V. *Nature Chemistry* **2016**, *8*, 360–367.
- ⁴ (a) O'Brien, M.; Baxendale, I. R.; Ley, S. V. *Org. Lett.* **2010**, *12*, 1596–1598. (b) Mastronardi, F.; Gutmann, B.; Kappe, C. O. *Org. Lett.* **2013**, *15*, 5590–5593.
- ⁵ Deadman, B. J.; Browne, D. L.; Baxendale, I. R.; Ley, S. V. *Chem. Eng. Technol.* **2015**, *38*, 259–264.
- ⁶ (a) Su, Y.; Kuijpers, K.; Hessel, V.; Noël, T. *React. Chem. Eng.* **2016**, *1*, 73–81. (b) Baumann, M.; Baxendale, I. R. *React. Chem. Eng.* **2016**, *1*, 147–150.
- ⁷ (a) Ouchi, T.; Battilocchio, C.; Hawkins, J. M.; Ley, S. V. *Org. Process Res. Dev.* **2014**, *18*, 1560–1566. (b) Ouchi, T.; Mutton, R. J.; Rojas, V.; Fitzpatrick, D. E.; Cork, D. G.; Battilocchio, C.; Ley, S. V. *ACS Sustainable Chem. Eng.* **2016**, *4*(4), 1912–1916.
- ⁸ (a) Wiles, C.; Watts, P. *Eur. J. Org. Chem.* **2008**, 1655–1671. (b) Roberge, D. M.; Zimmermann, B.; Rainone, F.; Gottsponer, M.; Eyholzer, M.; Kockmann, N. *Org. Process Res. Dev.* **2008**, *12*, 905–910. (c) Geyer, K.; Gustafsson, T.; Seeberger, P. H. *Synlett* **2009**, *15*, 2382–2391. (d) Newman, S. G.; Jensen, K. F. *Green Chem.* **2013**, *15*, 1456–1472. (e) Baxendale, I. R. *J. Chem. Technol. Biotechnol.* **2013**, *88*, 519–552. (f) Ley, S. V. *Angew. Chem. Int. Ed.* **2018**, *57*, 2–4. (g) Akwi, F. M.; Watts, P. *Chem. Commun.* **2018**, *54*, 13894–13928.
- ⁹ (a) Kockmann, N.; Roberge, D. M. *Chem. Eng. Technol.* **2009**, *32*(11), 682–1694. (b) Booker-Milburn, K. *Nature Chemistry* **2012**, *4*, 433–435. (c) Tucker, J. W.; Zhang, Y.; Jamison, T. F.; Stephenson, C. R. J. *Angew. Chem. Int. Ed.* **2012**, *51*, 4144–4147. (d) Wegner, J.; Ceylan, S.; Kirschning, A. *Adv. Synth. Catal.* **2012**, *354*, 17–57. (e) McQuade, D. T.; Seeberger, P. H. *J. Org. Chem.* **2013**, *78*, 6384–6389. (f) Gutmann, B.;

Cantillo, D.; Kappe, C. O. *Angew. Chem. Int. Ed.* **2015**, *54*, 6688–6728. (g) Cambié, D.; Bottecchia, C.; Straathof, N. J. W.; Hessel, V.; Noël, T. *Chem. Rev.* **2016**, *116*, 10276–10341. (h) Noël, T. *Photochemical Processes in Continuous-flow Reactors: From Engineering Principles to Chemical Applications*, World Scientific Publishing Company, **2017**.

¹⁰ Plutschack, M. B.; Pieber, B.; Gilmore, K.; Seeberger, P. H. *Chem. Rev.* **2017**, *117*, 11796–11893.

¹¹ (a) Smith, J. M.; Van Ness, H. C. (1959). *Introduction to Chemical Engineering Thermodynamics* (2nd ed.). McGraw-Hill. p. 34. (b) Zemansky, M. W.; Van Ness, H. C. (1966). *Basic Engineering Thermodynamics*. McGraw-Hill. p. 244.

¹² (a) Poechlauer, P.; Braune, S.; Dielemans, B.; Kaptein, B.; Obermüller, R.; Thathagar, M. *Chimica Oggi/Chemistry Today* **2012**, *30* (4). (b) Movsisyan, M.; Delbeke, E. I. P.; Berton, J. K. E. T.; Battilocchio, C.; Ley, S. V.; Stevens, C. V. *Chem. Soc. Rev.* **2016**, *45*, 4892–4928. (c) Rahman, M. T., Wirth T. (2018) Safe Use of Hazardous Chemicals in Flow. In: Sharma U., Van der Eycken E. (eds) *Flow Chemistry for the Synthesis of Heterocycles*. Topics in Heterocyclic Chemistry, vol. 56, Springer, pp 343–373.

¹³ (a) Hunter, S. M.; Susanne, F.; Whitten, R.; Hartwig, T.; Schilling, M. *Tetrahedron*, **2018**, *74*, 3176–3182. (b) Colella, M.; Nagaki, A.; Luisi, R. *Chem. Eur. J.* **2019**, *26*, 19–32.

¹⁴ (a) Deadman, B. J.; Collins, S. G.; Maguire, A. R. *Chem. Eur. J.* **2015**, *21*, 2298–2308. (b) Hock, K. J.; Koenigs, R. M. *Chem. Eur. J.* **2018**, *24*, 10571–10583. (c) Rullière, P.; Benoit, G.; Allouche, E. M. D.; Charette, A. B. *Angew. Chem. Int. Ed.* **2018**, *57*, 57775782.

¹⁵ (a) Oger, N.; Grogneca, E. L.; Felpin, F.-X. *Org. Chem. Front.* **2015**, *2*, 590–614. (b) Hu, T.; Baxendale, I. R.; Baumann, M. *Molecules* **2016**, *21*(7), 918.

¹⁶ Löb, P.; Löwe, H.; Hessel, V. *J. Fluorine Chem.* **2004**, *125*(11), 1677–1694.

¹⁷ Razzaq, T.; Kappe, C. O. *Chem. Asian J.* **2010**, *5*, 1274–1289.

¹⁸ (a) Hessel, V.; Kralisch, D.; Krtschil, U. *Energy Environ. Sci.* **2008**, *1*, 467–478. (b) Illg, T.; Löb, P.; Hessel, V. *Bioorg. Med. Chem.* **2010**, *18*, 3707–3719. (c) Hessel, V.; Krakisch, D.; Kockmann, N.; Noël, T.; Wang, Q. *ChemSusChem* **13**, *6*, 746–789. (d) Stouten, S. C.; Noël, T.; Wang, Q.; Hessel, V. *Aust. J. Chem.* **2013**, *66*, 121–130.

- ¹⁹ (a) Hessel, V.; Löl, P.; Löwe, H. *Curr. Org. Chem.* **2005**, *9*, 765–787. (b) Hessel, V. *Chem. Eng. Technol.* **2009**, *32*, 1655–1681.
- ²⁰ (a) Hessel, V.; Cortese, B.; De Croon, M. H. J. M. *Chem. Eng. Sci.* **2011**, *66*, 1426–1448. (b) Hessel, V.; Kralischn, D.; Kockmann, N. (2015) *Novel Process Windows: Innovative Gates to Intensified and Sustainable Chemical Processes* Weinheim: Wiley-VCH Verlag GmbH & Co., 344.
- ²¹ Trommsdorf, H. *Ann. Chem. Pharm.* **1834**, *11*, 190–207.
- ²² Natarajan A.; Tsai, C. K.; Khan, S. I.; McCarren, P.; Houk, K. N.; Garcia-Garibay, M. *A. J. Am. Chem. Soc.* **2007**, *129*, 32, 9846–9847
- ²³ Sima, J. *Acta Chimica Slovaca* **2017**, *10*(2), 84–90.
- ²⁴ Cannizzaro, S. ; Sestini, F. *Gazzetta Chimica Italiana* **1873**, *3*, 241–251.
- ²⁵ (a) Albini, A.; Fagnoni, M. *Green Chem.* **2004**, *6*, 1 (b) Albini, A.; Fagnoni, M. *ChemSusChem* **2008**, *1*, 63–66.
- ²⁶ Ciamician, G. *Science* **1912**, *36*, 385–394.
- ²⁷ (a) Cambié, D.; Zhao, F.; Hessel, H.; Debije, M. G.; Noël, T. *Angew. Chem., Int. Ed.* **2017**, *56*, 1050–1054. (b) Zhao, F.; Cambie, D.; Hessel, V.; Debije, M. G.; Noël, T. *Green Chem.* **2018**, *20*, 2459–2464. (c) Cambié, D.; Noël, T. *Topics in Current Chemistry* **2018**, *376*, 45.
- ²⁸ (a) Palmisano, G.; Augugliaro, V.; Pagliaro, M.; Palmisano, L. *Chem. Commun.* **2007**, 3425–3437. (b) Narayanam, J. M. R. ; Stephenson, C. R. J. *Chem. Soc. Rev.* **2011**, *40*, 102–113. (c) Prier, C. K.; Rankic, D. A.; MacMillan, D. W. C. *Chem. Rev.* **2013**, *113*, 5322. (d) Stephenson, C. R. J. *Acc. Chem. Res.* **2015**, *48*, 1474 (e) Nicewicz, D. A. *Chem. Rev.* **2016**, *116*, 10075. (f) von Wangelin, A. J. *Acc. Chem. Res.* **2016**, *49*, 2316. (g) Yoon, T. P. *Chem. Rev.* **2016**, *116*, 10035. (h) MacMillan, D. W. C. *Nat. Chem. Rev.* **2017**, *1*, 1. (i) Buzzetti, L.; Crisenza, G. E. M. *Angew. Chem. Int. Ed.* **2019**, *58*(12), 3730–3747.
- ²⁹ Nicewicz, D. ; MacMillan, D. W. C. *Science* **2008**, *322*, 77–80.
- ³⁰ Ischay, M. A. ; Anzovino, M. E. ; Du, J. ; Yoon, T. P. *J. Am. Chem. Soc.* **2008**, *130*, 12886–12887.
- ³¹ Narayanam, J. M. R.; Tucker, J. W. ; Stephenson, C. R. J. *J. Am. Chem. Soc.* **2009**, *131*, 8756–8757.
- ³² Su, Y.; Straathof, N. J. W.; Hessel, V.; Noël, T. *Chem. Eur. J.* **2014**, *20*, 10562–10589.

- ³³ (a) Knowles, J. P.; Elliott, L. D.; Booker-Milburn, K. I. *Beilstein J. Org. Chem.* **2012**, *8*, 2025–2052. (b) Gilmore, K.; Seeberger, P. H. *Chem. Rec.* **2014**, *14*(3), 410–418. (c) Politano, F.; Oksdath-Mansilla, G. *Org. Process Res. Dev.* **2018**, *22*(9), 1045–1062. (d) Sambiagio, C.; Noël, T. *Trends in Chemistry* **2019**, *2*(2), 92–106.
- ³⁴ Jensen, K. F. *Chem. Eng. Sci.* **2001**, *56*, 293–303.
- ³⁵ Sterk, D.; Jukic, M.; Casar, Z. *Org. Process. Res. Dev.* **2013**, *17*, 145–151.
- ³⁶ Oelgemöller, M.; Shvydkiv, O. *Molecules* **2011**, *16*, 7522–7550.
- ³⁷ Pinho, V. D., Miranda, L. S. M.; de Souza, R. O. M. A. *Rev. Virtual Quim.* **2015**, *7*, 144–164.
- ³⁸ (a) Knowles, J. P.; Elliott, L. D.; Booker-Milburn, K. I. *Beilstein J. Org. Chem.* **2012**, *8*, 2025–2052. (b) Elliott, L. D.; Knowles, J. P.; Koovits, P. J.; Maskill, K. G.; Ralph, M. J.; Lejeune, G.; Edwards, L. J.; Robinson, R. I.; Clemens, I. R.; Cox, B.; Pascoe, D. D.; Koch, G.; Eberle, M.; Berry, M. B.; Booker-Milburn, K. I. *Chem. Eur. J.* **2014**, *20*, 15226–15232.
- ³⁹ Lévesque, F.; Seeberger, P. H. *Angew. Chem., Int. Ed.* **2012**, *51*, 1706–1709.
- ⁴⁰ Beatty, J. W.; Stephenson, C. R. J. *J. Am. Chem. Soc.* **2014**, *136*, 10270–10273.
- ⁴¹ Berton, M.; de Souza, J. M.; Abdiaj, I.; McQuade, D. T.; Snead, D. R. *J. Flow Chem.* **2020**, *10*, 73–92.
- ⁴² Schenck, G. O.; Ziegler, K. *Naturwissenschaften* **1944**, *32*, 157.
- ⁴³ (a) Schenck, G. O. *Angew. Chem.* **1952**, *64*, 12–23. (b) Foote, C. S.; Wexler, S. *J. Am. Chem. Soc.* **1964**, *86*, 3879–3880. (c) Foote, C. S.; Wexler, S. *J. Am. Chem. Soc.* **1964**, *86*, 3880–3881. (d) Foote, C. S.; Valentine, J. S.; Greenberg, A.; Liebman, J. F. *Active Oxygen in Chemistry*, Chapman & Hall, London, Vol.2, 1st ed., **1995**.
- ⁴⁴ (a) Ghogare, A. A.; Greer, A. *Chem. Rev.* **2016**, *116*, 9994–10034. (b) Griesbeck, A. G.; Sillner, S.; Kleczka, M. Singlet oxygen as a reagent in Organic Synthesis. *Singlet Oxygen: Applications in Biosciences and Nanosciences*, RSC Publishing, **2016**, *1*, 369–392.
- ⁴⁵ Adam, W.; Saha-Möller, C. R.; Schambony, S. B.; Schmid, K. S.; Wirth, T. *Photochem. Photobiol.* **1999**, *70*(4), 476–483.
- ⁴⁶ Fritzsche, M. *Compt. Rend.* **1867**, *64*, 1035.
- ⁴⁷ Kautsky, H.; de Bruijin, N. *Naturwissenschaften* **1931**, *19*, 1043.
- ⁴⁸ Schenck, G.O.; Ziegler, K. *Naturwissenschaften* **1944**, *32*, 157.

- ⁴⁹ Jensen, F.; Ogilby, P. R. *Angew. Chem. Int. Ed.* **2005**, *44*, 6268–6268.
- ⁵⁰ (a) MacDonald, I. J.; Dougherty, T. J. *J. Porphyrins Phthalocyanines* **2001**, *5*, 105–129
(b) Dolmans, D. E. J. G. J.; Fukumura, D.; Jain, R. K. *Nat. Rev. Cancer* **2003**, *3*, 380–387. (c) Kwiatkowski, S.; Knap, B.; Przystupski, D.; Saczko, J.; Kędzierska, E.; Knap-Czop, K.; Kotlińska, J.; Michel, O.; Kotowski, K.; Kulbacka, J. *Biomed. Pharmacother.* **2018**, *106*, 1098–1107. (d) Mansoori, B.; Mohammadi, A.; Doustvandi, M. A.; Mohammadnejad, F.; Kamari, F.; Gjerstorff, M. F.; Baradaran, B.; Hamblin, M. R. *Photodiagn. Photodyn.* **2019**, *26*, 395–404.
- ⁵¹ (a) Piotrowska, A.; Bartnik, E. *Postepy Biochem.* **2014**, *60*(2), 240–247. (b) Santos, A. L.; Sinha, S.; Lindner, A. B. *Oxid. Med. Cell. Longev.* **2018**.
- ⁵² (a) Trost, B. M. *Science* **1991**, *254*, 1471–1477. (b) Trost, B. M. *Angew. Chem. Int. Ed. Engl.* **1995**, *34*, 259–281. (c) Pace, A.; Clennan, E. L. *Tetrahedron* **2005**, *61*, 6665–6691. (d) Greer, A. *Acc. Chem. Res.* **2006**, *39*(11), 797–804.
- ⁵³ (a) Frimer, A. A. *Chem. Rev.* **1979**, *79*, 359–387. (b) Schweitzer, C.; Schmidt, R. *Chem. Rev.* **2003**, *103*(5), 1685–1758.
- ⁵⁴ (a) Frimer, A. A. *Singlet Oxygen Physical-Chemical Aspects*, Vol. 1, CRC Press, 1985.
(b) Krukiewicz, K. *CHEMIK* **2011**, *65*(11), 1190–1192.
- ⁵⁵ (a) Uchoa, A. F.; de Oliveira, K. T.; Baptista, M. S.; Bortoluzzi, A. J.; Iamamoto, Y.; Serra, O. A. *J. Org. Chem.* **2011**, *76*, 8824–8832. (b) Carvalho, C. M. B.; Brocksom, T. J.; de Oliveira, K. T. *Chem. Soc. Rev.* **2013**, *42*, 3302–3317. (c) Carvalho, C. M. B.; Fujita, M. A.; Brocksom, T. J.; de Oliveira, K. T. *Tetrahedron* **2013**, *69*, 9986–9993. (d) dos Santos, F. A. B.; Uchoa, A. F.; Baptista, M. S.; Iamamoto, Y.; Serra, O. A.; Brocksom T. J.; de Oliveira, K. T. *Dyes Pigm.* **2013**, *99*, 402–411. (e) Menezes, J. C. J. M. D. S.; Faustino, M. A. F.; de Oliveira, K. T.; Uliana, M. P.; Ferreira, V. F.; Hackbarth, S.; Röder, B.; Tasso, T. T.; Furuyama, T.; Kobayashi, N.; Silva, A. M. S.; Neves M. G. P. M. S.; Cavaleiro, J. A. S. *Chem. Eur. J.* **2014**, *20*, 13644–13655. (f) Momo, P. B.; Pavani, C.; Baptista, M. S.; Brocksom, T. J.; de Oliveira, K. T. *Eur. J. Org. Chem.* **2014**, 4536–4547. (g) Uliana, M. P.; Pires, L.; Pratavieira, S.; Brocksom, T. J.; de Oliveira, K. T.; Bagnato V. S.; Kurachi, C. *Photochem. Photobiol. Sci.* **2014**, *13*, 1137–1145.
- ⁵⁶ (a) Kavarnos, G. J.; Turro N. J. *Chem. Rev.* **1986**, *86*, 401–449. (b) Fagnoni, M.; Dondi, D.; Ravelli, D.; Albini, A. *Coord. Chem. Rev.* **2007**, *107*, 2725–2756.

- ⁵⁷ (a) Knowles, J. P.; Elliott, L.D.; Booker-Milburn, K. I. *Beilstein J. Org. Chem.* **2012**, *8*, 2025–2052. (b) Su, Y.; Straathof, N. J. W.; Hessel, V.; Noël, T. *Chem. Eur. J.* **2014**, *20*, 10562–10589.
- ⁵⁸ (a) Bourne, R. A.; Han, X.; Poliakoff, M.; George, M. W. *Angew. Chem. Int. Ed.* **2009**, *48*, 5322–5325. (b) Lévesque, F.; Seeberger, P. H. *Org. Lett.* **2011**, *13*(19), 5008–5011. (c) Kopetzki, D.; Lévesque, F.; Seeberger, P. H. *Chem. Eur. J.* **2013**, *19*, 5450–5456. (d) Ushakov, D. B.; Gilmore, K.; Kopetzki, D.; McQuade, D. T.; Seeberger, P. H. *Angew. Chem. Int. Ed.* **2014**, *53*, 557–561. (e) Heugebaert, T. S. A.; Stevens, C. V.; Kappe, C. O. *ChemSusChem*, **2015**, *8*, 1648–1651. (f) de Oliveira, K. T.; Miller, L. Z.; McQuade, D. T. *RSC Adv.* **2016**, *6*, 12717–12725. (g) Hone, C. A.; Roberge, D. M.; Kappe, C. O. *ChemSusChem* **2016**, *9*, 1–11. (h) Kouridaki, A.; Huvaere, K. *React. Chem. Eng.* **2017**, *2*, 590–597. (i) Konga, C. J.; Fishera, D.; Desai, B. K.; Yanga, Y.; Ahmada, S.; Beleckia, K.; Gupton, B. F. *Bioorg Med Chem.* **2017**, *25*, 6203–6208.
- ⁵⁹ Yaremenko, I. A.; Vil', V. A.; Demchuk, D. V.; Terent'ev, A. O. *Beilstein J. Org. Chem.* **2016**, *12*, 1647–1748.
- ⁶⁰ Kelly, D. R.; Bansal, H.; Morgan, J. J. G. *Tetrahedron Lett.* **2002**, *43*, 9331–9333.
- ⁶¹ Wiegand, C.; Herdtweck, E.; Bach, T. *Chem. Commun.* **2012**, *48*, 10195–10197.
- ⁶² Staben, S. T.; Linghu, X.; Toste, F. D. *J. Am. Chem. Soc.* **2006**, *128*(39), 12658–12659.
- ⁶³ Kornblum, N.; DeLaMare, H. E. *J. Am. Chem. Soc.* **1951**, *73*, 880–881.
- ⁶⁴ Seebach, D. *Angew. Chem. Int. Ed.* **1979**, *18*(4), 239–258.
- ⁶⁵ Gupton, B. F.; McQuade, D. T. *Org. Process Res. Dev.* **2019**, *23*, 711–715.
- ⁶⁶ (a) Bang, L. M.; Scott, L. J. *Drugs* **2003**, *63*, 2413–2424. (b) Vasconcelos, T. R. A.; Ferreira, M. L.; Gonçalves, R. S. B.; Da Silva, E. T.; De Souza, M. V. N. *J. Sulfur Chem.* **2008**, *29*(5), 559–571. (c) Nelson, M.; Schiavone, M. *Int. J. Clin. Pract.* **2004**, *58*(5), 504–510. (d) Quercia, R.; Perno, C. -F.; Koteff, J.; Moore, K.; McCoig, C.; St. Clair, M.; Kuritzkes, D. *JAIDS* **2018**, *78*(2), 125–135.
- ⁶⁷ (a) Doong, S. L.; Tasi, C. H.; Schinazi, R. F.; Liotta, D. C.; Cheng, Y. C. *Proc. Natl. Acad. Sci. U.S.A.* **1991**, *88*, 8495–8499. (b) Coates, J. A.; Cammack, N.; Jenkinson, H. J.; Mutton, I. M.; Pearson, B. A.; Storer, R.; Cameron, J. M.; Penn, C. R. *Antimicrob. Agent Chemother.* **1992**, *36*, 733–739. (c) Chang, C. N.; Doong, S. L.; Zhou, J. H.; Beach, J. W.; Jeong, L. S.; Chu, C. K.; Tasi, C. H.; Cheng, Y. C. *J. Biol. Chem.* **1992**, *267*, 13938–13942.

- ⁶⁸ (a) Doong, S. L.; Tasi, C. H.; Schinazi, R. F.; Liotta, D. C.; Cheng, Y. C. *Proc. Natl. Acad. Sci. U.S.A.* **1991**, *88*, 8495–8499. (b) Coates, J. A.; Cammack, N.; Jenkinson, H. J.; Mutton, I. M.; Pearson, B. A.; Storer, R.; Cameron, J. M.; Penn, C. R. *Antimicrob. Agent Chemother.* **1992**, *36*, 733–739. (c) Chang, C. N.; Doong, S. L.; Zhou, J. H.; Beach, J. W.; Jeong, L. S.; Chu, C. K.; Tasi, C. H.; Cheng, Y. C. *J. Biol. Chem.* **1992**, *267*, 13938–13942.
- ⁶⁹ Chu, C. K.; Beach, W. J.; Jeong, L. S.; Choi, B. G.; Comer, F. I.; Alves, A. J.; Schinazi, R. F. *J. Org. Chem.* **1991**, *56*, 6503–6505.
- ⁷⁰ Cousins, R. P.; Mahmoudian, M.; Youds, P. M. *Tetrahedron: Asymmetry* **1995**, *6*, 393–396. (b) Milton, J.; Brand, S.; Jones, M. F.; Rayner, C. M. *Tetrahedron: Asymmetry* **1995**, *6*(8), 1903–1906.
- ⁷¹ Belleau, B.; Nguyen-Ba, N. 2-substituted-5-substituted-1,3-oxathiolanes with antiviral properties 1991, US Patent 5,047,407.
- ⁷² Balzarini, J.; Naesens, L.; De Clercq, E. *Curr. Opin. Microbiol.* **1998**, *1*(5), 535–546.
- ⁷³ (a) Humber, D. C.; Jones, M. F.; Payne, J. J.; Ramsay, M. V.; Zacharie, B. *Tetrahedron Lett.* **1992**, *33*, 4625–4628. (b) Mahmoudian, M.; Baines, B. S.; Drake, C. S.; Hale, R. S.; Jones, P.; Piercy, J. E.; Montgomery, D. S.; Purvis, I. J.; Storer, R. *Enzyme Microb. Technol.* **1993**, *15*, 749–755; (c) Storer, R.; Clemens, I. R.; Lamont, B.; Noble, S. A.; Williamson, C.; Belleau, B. *Nucleosides Nucleotides* **1993**, *12*, 225–236. (d) Milton, J.; Brand, S.; Jones, M. F.; Raynor, C. M. *Tetrahedron: Asymmetry* **1995**, *6*, 1903–1906. (e) Li, J.; Lain-xun, G.; Meng-xian, D. *Synth. Commun.* **2002**, *32*, 2355–2359. (f) D’Alonzo, D.; Guaragna, A. Stereoselective Methods in the Synthesis of Bioactive Oxathiolane and Dioxolane Nucleosides. In *Chemical Synthesis of nucleosides*, Merino, P., Ed.; John Wiley & Sons Inc., New Jersey 2013; Vol. 1; p. 727. (g) Lapponia, M. J.; Riveroa, C. W.; Zinnia, M. A.; Britosa, C. N.; Trelles, J. A. *J. Mol. Catal. B Enzym.* **2016**, *133*, 218–233. (h) D’Alonzo, D.; De Fenza, M.; Palumbo, G.; Romanucci, V.; Zarrelli, A.; Di Fabio, G.; Guaragna, A. *Synthesis* **2017**, *49*, 998–1008. (i) Akhtar, R.; Yousaf, M.; Zahoor, A. F.; Naqvi, S. A. R.; Abbas, N. *Phosphorus Sulfur* **2017**, *192*(9), 989–1001.
- ⁷⁴ (a) Beach, J. W.; Jeong, L. S.; Alves, A. J.; Pohl, D.; Kim, H. O.; Chang, C. N.; Doong, S. L.; Schinazi, R. F.; Cheng, Y.-C.; Chu, C. K. *J. Org. Chem.* **1992**, *57*, 2217–2219. (b) Jeong, L. S.; Schinazi, R. F.; Beach, J. W.; Kim, H. O.; Nampalli, S.; Shanmuganathan, K.; Alves, A. J.; McMillan, A.; Chu, C. K. *J. Med. Chem.* **1993**, *36*, 181–185.

- ⁷⁵ (a) Li, J.-Z.; Gao, L.-X.; Ding, M.-X. *Synth. Commun.* **2002**, *32*, 2355–2359. (b) Roy, B. N.; Singh, G. P.; Srivastava, D.; Jadhav, H. S.; Saini, M. B.; Aher, U. P. *Org. Process Res. Dev.* **2009**, *13*, 450–455.
- ⁷⁶ Hu, L.; Schaufelberger, F.; Zhang, Y.; Ramström, O. *Chem. Commun.* **2013**, *49*, 10376–10378.
- ⁷⁷ (a) Hoong, L. K.; Strange, L. E.; Liotta, D. C.; Koszalka, G. W.; Burns, C. L.; Schinazi, R. F. *J. Org. Chem.* **1992**, *57*, 5563–5565. (b) Milton, J.; Brand, S.; Jones, M. F.; Rayner, C. M. *Tetrahedron Lett.* **1995**, *36*, 6961–6964. (c) Milton, J.; Brand, S.; Jones, M. F.; Rayner, C. M. *Tetrahedron: Asymmetry* **1995**, *6*(8), 1903–1906.
- ⁷⁸ (a) Wilson, L. J.; Hager, M. W.; El-Kattan, Y. A.; Liotta, D. C. *Synthesis* **1995**, 1465–1479. (b) Romeo, G.; Chiacchio, U.; Corsaro, A.; Merino, P. *Chem. Rev.* **2010**, *110*, 3337–3370.
- ⁷⁹ (a) Goodyear, M. D.; Hill, M. L.; West, J. P.; Whitehead, A. J. *Tetrahedron Lett.* **2005**, *46*, 8535–8538. (b) Richhariya, S.; Singh, K.; Prasad, M. PCT Int. Appl. WO2007077505 A2, 2007. (c) dos Santos Pinheiro, E.; Antunes, O. A. C.; Fortunak, J. M. D. *Antiviral Res.* **2008**, *79*, 143–165.
- ⁸⁰ (a) Mansour, T.; Jin, H.; Tse, A. H. L.; Siddiqui, M. A. PCT Int. Appl. WO 92/20669, 1992. (b) Jin, H.; Siddiqui, A.; Evans, C. A.; Tse, A.; Mansour, T. S.; Goodyear, M. D.; Ravenscroft, P.; Beels, C. D. *J. Org. Chem.* **1995**, *60*, 2621–2623.
- ⁸¹ (a) Caso, M. F.; D’Alonzo, D.; D’Errico, S.; Palumbo, G.; Guaragna, A. *Org. Lett.* **2015**, *17*(11), 2626–2629. (b) Mandala, D.; Watts, P. *ChemistrySelect* **2017**, *2*, 1102–1105. (c) Mandala, D.; Chada, S.; Watts, P. *Org. Biomol. Chem.* **2017**, *15*, 3444–3454.
- ⁸² (a) Polyzos, A.; O’Brien, M.; Petersen, T. P.; Baxendale, I. R.; Ley, S. V. *Angew. Chem. Int. Ed.* **2011**, *50*, 1190–1193. (b) Cranwell, P. B.; O’Brien, M.; Browne, D. L.; Koos, P.; Polyzos, A.; Peña-López, M.; Ley, S. V. *Org. Biomol. Chem.* **2012**, *10*, 5774–5779. (c) Mercadante, M. A.; Leadbeater, N. E. *Green Process. Synth.* **2012**, *1*, 499–507. (d) Pastre, J. C.; Browne, D. L.; O’Brien, M.; Ley, S. V. *Org. Process Res. Dev.* **2013**, *17*, 1183–1191. (e) Brzozowski, M.; O’Brien, M.; Ley, S. V.; Polyzos, A. *Acc. Chem. Res.* **2015**, *48*(2), 349–362. (f) Mallia, C. J.; Baxendale, I. R. *Org. Process Res. Dev.* **2016**, *20*(2), 327–360.
- ⁸³ Momo, P. B.; Belleste, B. S.; Brocksom, T. J.; de Souza, R. O. M. A.; de Oliveira, K. T. *RSC Adv.* **2015**, *5*, 84350–84355.

- ⁸⁴ (a) Takakis, I. M.; Agosta, W. C. *J. Org. Chem.* **1978**, *43*, 1952–1957. (b) Adam, W.; Balci, M. *J. Am. Chem. Soc.* **1979**, *101*, 7542–7547. (c) Dahnke, K. R.; Paquette, L. A. *Org. Synth* **1993**, *71*, 181–188. (d) Mete, E.; Altundas, R.; Seçen, H. *Turk. J. Chem.* **2003**, *27*, 145–153. (e) Zhang, Z.; Song, Q-P.; Wang, G-W.; Luh, T-Y. *ARKIVOC* **2009**, *7*, 229–236.
- ⁸⁵ (a) Chung, S.-K.; Kwon, Y.-U.; Shin, J.-H.; Chang, Y.-T.; Lee, C.; Shin, B.-G.; Kim, K.-C.; Kim, M.-J. *J. Org. Chem.* **2002**, *67*(16), 5626–5637. (b) Durantie, E.; Huwiler, S.; Leroux, J.-C.; Castagner, B. *Org. Lett.* **2016**, *18* (13), 3162–3165. (c) Pavlovic, I.; Thakora, D. T.; Jessen, H. J. *Org. Biomol. Chem.* **2016**, *14*(24), 5559–5562. (d) Zhong, C.; You, C.; Wei, P.; Zhang, Y.-H. *P. ACS Catal.* **2017**, *7*(9), 5992–5999.
- ⁸⁶ Yeom, C.-E.; Kim, H. W.; Lee, S. Y.; Kim, B. M. *Synlett* **2007**, *38*(19), 146–150.
- ⁸⁷ (a) Adams, W. R.; Trecker, D. J. *Tetrahedron* **1971**, *27*, 2631–2637. (b) Matsumoto, M.; Dobashi, S.; Kuroda, K.; Kondo, K. *Tetrahedron* **1985**, *41*, 2147–2154.
- ⁸⁸ (a) Kondo, K.; Matsumoto, M. *Tetrahedron Lett.* **1976**, *48*, 4363–4366. (b) Ono, K.; Nakagawa, M.; Nishida, A. *Angew. Chem. Int. Ed.* **2004**, *43*, 2020–2023. (c) Griesbeck, A. G.; Kiff, A.; Kleczka, M. *Adv. Synth. Catal.* **2014**, *356*, 2839–2845. (d) Saito, N.; Saito, K.; Shiro, M.; Sato, Y. *Org. Lett.* **2011**, *13*(10), 2718–2728. (e) Eske, A.; Goldfus, B.; Griesbeck, A. G.; Kiff, A.; Kleczka, M.; Leven, M.; Neudörfl, J.-M.; Vollmer, M. *J. Org. Chem.*, **2014**, *79*(4), 1818–1829.
- ⁸⁹ Lee, R. J.; Lindley, M. R.; Pritchard, G. J.; Kimber, M. C. *Chem. Commun.* **2017**, *53*, 6327–6330.
- ⁹⁰ Goodyear, M.D.; Dwyer, P.O.; Hill, M.L.; Whitehead, A.J.; Hornby, R.; Hallet, P. Process for the Diastereoselective Synthesis of Nucleoside Analogues, US6051709, **2000**.
- ⁹¹ Rozwadowska, M. D.; Sulima, A.; Gzella, A. *Tetrahedron Asymmetry* **2002**, *13*, 2329–2333.
- ⁹² Snead, D. R.; McQuade, D. T.; Ahmad, S.; Krack, R.; Stringham, R. W.; Burns, J. M.; Abdiaj, I.; Gopalsamuthiram, V.; Nelson, R. C.; Gupton, B. F. *Org. Process Res. Dev.* **2020**, in press.
- ⁹³ Mandala, D.; Watts, P. Process for producing Lamivudine and Emtricitabine 2019, US Patent App. 16/301,255.
- ⁹⁴ Youn, J.-H.; Herrmann, R. *Synthesis* **1987**, 72–73.

- ⁹⁵ Mettler Toledo/Heat of Reaction. (2020, March 20). Retrieved from https://www.mt.com/int/ar/home/applications/L1_AutoChem_Applications/Process_Safety/heat-of-reaction.html
- ⁹⁶ (a) Lowe, A. B. *Polym. Chem.* **2010**, *1*, 17–36.
- ⁹⁷ (a) de la Mare, P. B. D.; Suzuki, H. *J. Chem. Soc. (C)* **1967**, 1586. (b) Elix, J. A.; Norfolk, S. *Aust. J. Chem.* **1975**, *28*, 1113–1124. (c) Masilamani, D.; Rogić, M. M. *J. Org. Chem.* **1981**, *46*, 4486–4489. (d) Wriede, U.; Fernandez, M.; West, K. F.; Harcourt, D.; Moore, H. W. *J. Org. Chem.* **1987**, *52*, 4485–4489.
- ⁹⁸ Murray, P. R. D.; Browne, D. L.; Pastre, J. C.; Butters, C.; Guthrie, D.; Ley, S. V. *Org. Process Res. Dev.* **2013**, *17*(9), 1192–1208.
- ⁹⁹ Binkley, W. W.; Degering, E. F. *J. Am. Chem. Soc.* **1938**, *60*, 2810–2811.
- ¹⁰⁰ Simon, A.; Kunath, D. *Journal fuer Praktische Chemie (Leipzig)* **1961**, *13*, 205–210.
- ¹⁰¹ Becker, H.; Berger, W.; Domschke, G. *Organicum Practical Handbook of Organic Chemistry*, 1973, Addison-Wesley Pub. Co, 170.
- ¹⁰² Khatinzadeh, G.; Ahmadi, A. N.; Mehdizadeh, A. *Acta Chim. Slov.* **2007**, *54*, 284–286.
- ¹⁰³ Paddock, V. L.; Phipps, R. J.; Conde-Angulo, A.; Blanco-Martin, A.; Giró -Mañas, C.; Martin, L. J.; White, A. J. P.; Spivey, A. L. *J. Org. Chem.* **2011**, *76*, 1483–1486.
- ¹⁰⁴ Harirchian, B.; Bauld, N. L. *J. Am. Chem. Soc.* **1989**, *111*, 1826–1828.
- ¹⁰⁵ Szakonyi, Z.; Sillanpää, R.; Fülöp, F. *Beilstein J. Org. Chem.* **2014**, *10*, 2738–2742.
- ¹⁰⁶ Brichacek, M.; Batory, L. A.; McGrath, N. A.; Njardarson, J. T. *Tetrahedron* **2010**, *66*, 4832–4840.
- ¹⁰⁷ Salamci, E. *Tetrahedron* **2010**, *66*(23), 4010–4015.
- ¹⁰⁸ Kayama, Y.; Oda, M.; Kitahara, Y. *Chem. Lett.* **1974**, *4*, 345–348.
- ¹⁰⁹ Trost, B. M.; Masters, J. T.; Lumba, J.-P.; Fateen, D. *Chem. Sci.* **2014**, *5*, 1354–1360.
- ¹¹⁰ Zhang, Z.; Song, Q.-P.; Wang, G.-W.; Luh, T.-Y. *ARKIVOC* **2009**, *7*, 229–236.
- ¹¹¹ Oda, M.; Kitahara, Y. *Tetrahedron Lett.* **1969**, *10*(38), 3295–3296.
- ¹¹² Matsuzawa, M.; Kakeya, H.; Yamaguchi, J.; Shoji, M.; Onose, R.; Osada, H.; Hayashi, Y. *Chem. Asian J.* **2006**, *1*, 845–851.
- ¹¹³ Saikia, B.; Borah, P.; Barua, N. C. *Green Chem.* **2015**, *17*, 4533–4536.
- ¹¹⁴ Dakin, H. D. *Org. Synth.* **1923**, *3*, 28.
- ¹¹⁵ Klaper, M.; Wessig, P.; Linker, T. *Chem. Commun.* **2016**, *52*, 1210–1213.

- ¹¹⁶ Peixoto, D.; Figueiredo, M.; Malta, G.; Roma-Rodrigues, C.; Baptista, P. V.; Fernandes, A. R.; Barroso, S.; Carvalho, A. L.; Afonso, C. A. M.; Ferreira, L. M.; Branco, P. S. *Eur. J. Org. Chem.* **2018**, 545–549.
- ¹¹⁷ Camaioni, D. M.; Alnajjar, M. S. *J. Org. Chem.* **1985**, *50*, 4461–4465.
- ¹¹⁸ Pozzi, G.; Mercs, L.; Holczknecht, O.; Martimbianco, F.; Fabris, F. *Adv. Synth. Catal.* **2006**, *348*, 1611–1620.
- ¹¹⁹ Trabanco, A. A.; Montalban, A. G.; Rumbles, G.; Barrett, A. G. M.; Hoffman, B. M. *Synlett* **2000**, 1010–1012.
- ¹²⁰ Donohoe, T. J.; Bower, J. F. *Proc. Natl. Acad. Sci. U.S.A.* **2010**, *107*, 3373–3376.
- ¹²¹ Buglioni, L.; Riente, P.; Palomares, E.; Pericàs, M. A. *Eur. J. Org. Chem.* **2017**, 6986–6990.
- ¹²² Huang, G.; Lu, L.; Jianga, H.; Yin, B. *Chem. Commun.* **2017**, *53*, 12217–12220.
- ¹²³ Campaigne, E.; Foye, W. O. *J. Org. Chem.* **1952**, *17* (10), 1405–1412.
- ¹²⁴ Wang, C.-M.; Song, D.; Xia, P.-J.; Wang, J.; Xiang, H.-Y.; Yang, H. *Chem. Asian J.* **2018**, *13*(3), 271–274.
- ¹²⁵ Chalikidi, P. N.; Uchuskin, M. G.; Trushkov, I. V.; Abaev, V. T.; Serdyuk, O. V. *Synlett* **2018**, *29*(5), 571–575.
- ¹²⁶ Schaefer, J. *J. Org. Chem.* **1960**, *25*(11), 2027–2027.
- ¹²⁷ V. Balzani, P. Ceroni, A. *Juris Photochemistry and Photophysics*, 2014, Wiley.
- ¹²⁸ Atkins, P. W. *Physical Chemistry*, Oxford University Press, 1994, 591.
- ¹²⁹ Acuña, A. U.; Amat-Guerri, F. *Springer Ser. Fluoresc.* **2008**, *4*, 3–20.
- ¹³⁰ Jameson, D. M. *Introduction to Fluorescence*, 2014, 1st ed. CRC Press.
- ¹³¹ (a) Clarke, E. D. *Ann. Philos.* **1819**, *14*, 34–36. (b) Brewster, D. *Trans. R. Soc. Edinburgh* **1834**, *12*(2), 538–545. (c) Herschel, J. *Philos. Trans. R. Soc. Lond.* **1845**, *135*, 143–145. (d) Herschel, J. *Philos. Trans. R. Soc. Lond.* **1845**, *135*, 147–153.
- ¹³² Haüy, *Traité de Minéralogie*, 2nd ed., Paris, France: Bachelier and Huzard, 1822, vol. 1, p. 512.
- ¹³³ Stokes, G. G. *Philos. Trans. R. Soc. Lond.* **1853**, *143*, 385–396.
- ¹³⁴ Stokes, G. G. *Philosophical Transactions of the Royal Society of London* **1852**, *142*, 463–562.
- ¹³⁵ (a) Stephens, D. J.; Allan, V. J. *Science* **2003**, *300*, 82–86. (b) Lichtman, J. W.; Conchello, J. A. *Nat. Methods* **2005**, *2*, 910–919. (c) Medintz, I. L.; Uyeda, H. T.;

Goldman, E. R.; Mattoussi, H. *Nat. Mater.* **2005**, *4*, 435–446. (d) Stennett, E. M. S.; Ciuba, M. A.; Levitus, M. *Chem. Soc. Rev.* **2014**, *43*, 1057–1075.

¹³⁶ Longstreet, A. R.; Chandler, R. R.; Banerjee, T.; Miller, L. Z.; Hanson, K.; McQuade, D. T. *Photochem. Photobiol. Sci.* **2017**, *16*, 455–458.

¹³⁷ (a) Longstreet, A. R.; Opalka, S. M.; Campbell, B. S.; Gupton, B. F.; McQuade, D. T. *Beilstein J. Org. Chem.* **2013**, *9*, 2570–2578; (b) Verghese, J.; Kong, C. G.; Rivalti, D.; Yu, E. C.; Krack, R.; Alcázar, J.; Manley, J. B.; McQuade, D. T.; Ahmad, S.; Belecki, K.; Gupton, B. F. *Green Chem.* **2017**, *19*, 2986–2991.

¹³⁸ Stocks, M. J.; Cheshire, D. R.; Reynolds, R. *Org. Lett.* **2004**, *17*, 2969–2971.

¹³⁹ De Kimpe, N.; Schamp, N. *Org. Prep. Proced. Int.* **1981**, *13*, 241–313. (b) Duhamel, L.; Duhamel, P.; Poirier, J. M. *Tetrahedron Lett.* **1973**, *43*, 4237–4240.

¹⁴⁰ Longstreet, A. R.; Rivalti, D.; McQuade, D. T. *J. Org. Chem.* **2015**, *80*, 8583–8596.

¹⁴¹ (a) Granik, V. G.; Grizik, S. I.; Soloveva, N. P.; Anisimova, O. S.; Sheinker, Y. N. *Zh. Org. Khim.* **1984**, *20*, 673. (b) Mittelbach, M.; Kastner, G.; Junek, H. *Arch. Pharm.* **1985**, *318*, 481–486. (c) Mittelbach, M. *Monatsh. Chem.* **1987**, *118*, 617–626.

¹⁴² (a) Kiuru, P. and Yli-Kauhaluoma, J. Pyridine and Its Derivatives. In *Heterocycles in Natural Product Synthesis*; Majumdar, K. C.; Chattopadhyay, S. K.; Eds.; Wiley-VCH Verlag GmbH & Co. 2011, 267–297. (b) Altaf, A. A.; Shahzad, A.; Gul, Z.; Rasool, N.; Badshah, A.; Lal, B.; Khan, E. *J. Med. Chem. Drug Discov.* **2015**, *1*, 1–11. (c) Yates, F.; Courts, R. T. and Casy, A. F. In *Pyridine and Its Derivatives*; supplement IV, R. A. Abramovitch ed., Wiley, New York, 1975, 445. (d) Scriven, E. F. V. *Pyridines: from Lab to Production*, 1st ed., Elsevier, Amsterdam, 2013.

¹⁴³ (a) Giam, C. S. In *The Chemistry of Heterocyclic Compounds*; Abramovitch, R. A., Ed.; John Wiley and Sons, Inc.: New York, 1974, Vol. 14, 41. (b) Vorbruggen, H. *Adv. Heterocycl. Chem.* **1990**, *49*, 117–185. (c) Matsumoto, K.; Minatogawa, H.; Munakata, M.; Toda, M.; Tsukube, H. *Tetrahedron Lett.* **1990**, *27*, 3923–3926. (d) Matsumoto, K.; Hashimoto, S.; Otani, S. *J. Chem. Soc. Chem. Commun.* **1991**, 306. (e) McKillop, A.; Boulton, A. J. In *Comprehensive Heterocyclic Chemistry*, Vol. 2; Katritzky, A. R.; Rees, C. W., Eds.; Pergamon Press: New York, **1984**, 67. (f) McKillop, A.; Boulton, A. J. In

Comprehensive Heterocyclic Chemistry, Vol. 2; Katritzky, A. R.; Rees, C. W., Eds.; Pergamon Press: New York, **1984**, 460–463.

¹⁴⁴ (a) Sakurai, A.; Midorikawa, H. *Bull. Chem. Soc. Jpn.* **1968**, *41*, 430–432. (b) Katritzky, A. R.; Belyakov, S. A.; Sorochinsky, A. E.; Henderson, S. A. and Chen, J. *J. Org. Chem.* **1997**, *62*, 6210–6214. (c) Manna, F.; Chimenti, F.; Bolasco, A.; Bizzarri, B.; Filippelli, W.; Filippelli A. and Gagliardi, L. *Eur. J. Med. Chem.* **1999**, *34*, 245–254. (d) Salem, M. A. I.; Madkour, H. M. F.; Soliman, E. S. A. and Mahmoud, N. F. H. *Heterocycles* **2000**, *53*, 1129–1143. (e) Raghukumar, V.; Thirumalai, D.; Ramakrishnan, V. T.; Karunakarac, V. and Ramamurthy, P. *Tetrahedron* **2003**, *59*, 3761–3768. (f) Tu, S.; Jiang, B.; Zhang, Y.; Jia, R.; Zhang, J.; Yao, C. and Shi, F. *Org. Biomol. Chem.* **2007**, *5*, 355–359. (g) Han Z. G.; Miao, C. B.; Shi, F.; Ma, N.; Zhang, G. and Tu, S. *J. Comb. Chem.* **2010**, *12*, 16–19. (h) Wan, Y.; Yuan, R.; Zhang, F. R.; Pang, L. L.; Ma, R.; Yue, C. H.; Lin, W.; Bo, R. C. and Wu, H. *Synth. Commun.* **2011**, *41*, 2997–3015. (i) Khaksar, S. and Yaghoobi, M. *J. Fluorine Chem.* **2012**, *142*, 41–44. (j) Tang, J.; Wang, L.; Yao, Y.; Zhang, L. and Wang, W. *Tetrahedron Lett.* **2011**, *52*, 509–511. (l) Dissanayake, A. A.; Staples, R. J. and Odom, A. L. *Adv. Synth. Catal.* **2014**, *356*, 1811–1822.

¹⁴⁵ (a) Farhanullah, F.; Agarwal, N.; Goel, A.; Ram, V. J. *J. Org. Chem.* **2003**, *68*, 2983–2985. (b) Goel, A.; Singh, F. V.; Sharon, A. and Maulikb, P. R. *Synlett* **2005**, *4*, 623–626.

¹⁴⁶ (a) Schmidt, R. R. *Chem. Ber.* **1965**, *98*, 3892–3901. (b) Ege, G.; Frey, H. O.; Schuck, E. *Synthesis* **1979**, 376–378. (c) Villemin, D.; Belhadj, Z.; Cheikh, N.; Choukchou-Braham, N.; Bar, N.; Lohier, J.-F. *Tetrahedron Lett.* **2013**, *54*, 1664–1668.

¹⁴⁷ (a) Kuehne, M. E. *J. Org. Chem.* **1963**, *28*, 2124–2128. (b) Cook, G. A. *Enamines: Synthesis, Structure and Reactions*, **1969**, Marcel Dekker: New York, 148–149. (c) Bogdanowicz-Szwed, K.; Kawasek, B.; Lieb, M. J. *Fluor. Chem.* **1987**, *35*, 317–327. (d) Kovregin, A. N.; Sizov, A. Y.; Ermolov, A. F. *Russ. Chem. Bull. Int. Ed.* **2001**, *50*, 1645–1647. (e) Siry, S. A.; Ogurok, V. M.; Shermolovich, Y. G. *J. Fluor. Chem.* **2014**, *168*, 137–143. (f) Tucker, J. W.; Chenard, L.; Young, J. M. *ACS Comb. Sci.* **2015**, *17*, 653–657.

¹⁴⁸ (a) Peterson, S. W.; Williams, J. M. *J. Am. Chem. Soc.* **1966**, *20*, 2866–2868. (b) Schmid, G. H. *Can. J. Chem.* **1968**, *46*, 3757–3758. (c) Mueller, W. H. *Angew. Chem. Int. Ed.* **1969**, *8*, 482–492. (d) Kühle, E. *Synthesis* **1971**, 617–638. (e) Schmidt, G.

- H.; Garrat, D. G. *The Chemistry of Double Bonded Functional Groups*, Ed. S. Patai, Ch. 9, 1977. (f) Abu-Yousef, I. A.; Hynes, R. C.; Harpp, D. N. *Tetrahedron Lett.* **1993**, *34*, 4289–4292. (g) Abu-Yousef, I. A.; Harpp, D. N. *Sulfur Reports* **2003**, *24*, 255–282. (h) Smit, W. A.; Gromova, A. V.; Yagodkina, E. A. *Mendeleev Commun.* **2003**, *13*, 21–23. (i) Smit, W. A.; Yagodkin, E. A.; Zatonsky, G. V. *Russ. Chem. Bull. Int. Ed.* **2005**, *54*, 743–747.
- ¹⁴⁹ Longstreet, A. R.; Jo, M.; Chandler, R. R.; Hanson, K.; Zhan, N.; Hrudka, J. J.; Mattoussi, H.; Shatruck, M.; McQuade, D. T. *J. Am. Chem. Soc.* **2014**, *136*, 15493–15496.
- ¹⁵⁰ Shaw, P. E.; Burn, P. L. *Phys. Chem. Chem. Phys.* **2017**, *19*, 29714–29730.
- ¹⁵¹ Hong, Y.; Lamab, J. W. Y. and Tang, B. Z. *Chem. Soc. Rev.* **2011**, *40*, 5361–5388.
- ¹⁵² Shaw, P. E.; Burn, P. L. *Phys. Chem. Chem. Phys.* **2017**, *19*, 29714–29730.
- ¹⁵³ (a) Hong, Y.; Lam, J. W. Y.; Tang, B. Z. *Chem. Soc. Rev.* **2011**, *40*, 5361–5388. (b) Chen, Y.; Lam, J. W. Y.; Kwok, R. T. K.; Liu, B.; Zhong, Tang, B. Z. *Mater. Horiz.* **2019**, *6*, 428–433. (c) Jimenez, E. R.; Rodríguez, H. *J. Mater. Sci.* **2020**, *55*, 1366–1387.
- ¹⁵⁴ Xue, D.; Chen, Y.-C.; Cui, X.; Wang, Q.-W.; Zhu, J.; Deng, J.-G. *J. Org. Chem.* **2005**, *70*, 3584–3591.
- ¹⁵⁵ Longstreet, A. R.; Campbell, B.; Gupton, B. F.; McQuade, D. T. *Org. Lett.* **2013**, *15*, 20, 5298–5301.